

THE TOTAL SYNTHESIS OF
DRAGMACIDINS D AND F

Thesis by

Neil Kamal Garg

In Partial Fulfillment of the Requirements for the

Degree of

Doctor of Philosophy

CALIFORNIA INSTITUTE OF TECHNOLOGY

Pasadena, California

2005

(Defended March 17, 2005)

© 2005

Neil Kamal Garg

All Rights Reserved

To my family

ACKNOWLEDGEMENTS

First of all, I would like to thank my thesis advisor, Professor Brian Stoltz, for his support and enthusiasm over the past few years. Looking back, I was pretty lucky that Brian even let me join his lab in the first place. Brian knew I had little synthetic experience but still decided to take me into his group. He spent an enormous amount of time working with me that first summer getting me up to speed on lab technique and teaching me how to be an experimentalist. Learning synthesis from Brian first-hand in the early years was certainly one of the most fun and valuable experiences I had in graduate school. Over the more recent years, Brian has continued to be a role model, mentor, and friend to me. Being a part of the Stoltz group has been a great honor. Although I am sad to be leaving, I am looking forward to the future and will enjoy watching the lab develop during the upcoming years.

The other members of my thesis committee have been a true pleasure to interact with. Professor David Tirrell, the chair of my committee, could be the most well-organized person I have ever met. He heads the chemistry department, maintains his own research laboratory and, somehow, still finds time to read over candidacy reports and research proposals with a fine-toothed comb. Professor David MacMillan has also been incredibly supportive. He has provided me with scientific insight numerous times, particularly during my candidacy and proposal exams. I will always appreciate his willingness to share equipment and closely interact with our lab (MOM meetings, etc.), especially during the early days. Although Professor Peter Dervan is the newest member of my committee, I have already gotten to know him quite well. Sitting in on his bioorganic class this past year was a great learning experience for me. Most of all, I value his highly interactive teaching style and the philosophical discussions he promotes.

My undergraduate chemistry teachers also deserve special thanks. My roots as a researcher come from Professor Marc Walters at NYU. He was always full of sound advice and was able to foster a great learning environment for undergraduate students; Kev Adjemian, Steven Damo, and Ray Doss were a blast to work with. I also must thank

Professor Yorke Rhodes for his sound advice over the years. His love for organic chemistry and teaching was truly inspiring.

During my time at Caltech I have had the privilege of working closely with many people. Dr. Richmond Sarpong (a.k.a., sars) arrived in Pasadena in November 2000. He crashed on my sofa for a little while, used my deodorant, and bought a BMW to impress the ladies. Although he pounded me at the ping pong table and on the tennis court, I can grow a thicker beard than he can. I have photos to prove it. As far as lab work goes, Richmond is an exceptional chemist, the best of the best. I was lucky enough to work with him on the dragmacidin D project for nearly two years. In 2003, Dan Caspi (a.k.a., caspo, monk) joined team dragmacidin and, together, he and I worked on dragmacidin F. Dan brought a lot of great ideas and discoveries to the project, which made working together exciting at all times. Outside of the lab, Dan has become a close friend of mine. He's a pretty funny guy too. I once overheard a conversation he was having with a worker at Jamba Juice—'You see, they're enantiomers,' he said. It was a nice try Caspo, but she was too smart for that line. I am indebted to Richmond and Dan for their work on the dragmacidins, but more importantly, for their friendship over the past few years.

I would like to collectively thank the Stoltz group for making our laboratory a great working environment. There are also a number of people whom I would like to acknowledge individually: the original members of the group: Sarah Spessard, Jeremy May, and Eric Ferreira for being a part of the lab in the early days—especially Jeremy whom I have stayed close friends with over the years; Uttam Tambar for his sound advice; J.T. Mohr, Mike Krout, and Dan Caspi for good times at the Taco Truck; everyone in 204 Church for keeping things exciting on a daily basis (yes, that includes you, Roizen); Haiming Zhang, Sekar Govindasamy, and Taichi Kano for their knowledge and encouragement. I am also grateful to all of my labmates who have proofread sections of this thesis: Dan Caspi, Jeremy May, Mike Krout, J.T. Mohr, David Ebner, Ernie Cruz, Uttam Tambar, Ryan McFadden, Eric Ferreira, and Eric Ashley. The last person in the Stoltz lab whom I would like to thank individually is Raissa Trend, my baymate for the past few years. I am grateful to Raissa for just about all of the items listed above, but especially for her support, encouragement, and friendship. Raissa's skills as a scientist and

critical thinker are outstanding. I've learned so much from her, and I will really miss working with her.

The Dervan lab has been like a second home to me. The students are exceptionally talented and kind, and not a single one of them has ever refused to lend a hand my way. Their willingness to share equipment and their expertise in handling polar compounds were crucial to the drarmacidin project. Special thanks go to Raymond Doss, Michael Marques, Shane Foister, Victor Rucker, Ryan Stafford, James Puckett, Adam Kerstien, Sanchez, Ben Edelson, Bogdan Olenyuk, and Eric Fechter. I've known Ray since freshman year at NYU, where he earned the nickname, 'the mailman.' Yes, he always delivers.

The list of people I would like to thank goes on and on. The MacMillan lab has also been extremely helpful, particularly when we got started. I have many fond memories from those days, especially from time spent with my indole counterpart Joel Austin (a.k.a., jdogg). From the Grubbs group, JP Morgan, Arnab Chatterjee, Andrew Waltman, and Brian Connell were incredibly helpful. I've had many great conversations with Jon Owen in the Bercaw group, and his assistance with the 500 has been invaluable. From the Dougherty group, I must thank James Petersson for all that he has taught me. I am also indebted to Chris Lacenere from the Quake lab for introducing me to the world of the biologique. I would also like to thank Tara Suntok from the Chan lab for running bioassays and Jeremy Weaver from the Gray group for obtaining circular dichroism spectra on multiple occasions.

The staff at Caltech is superb. For facilities, I would like to thank Scott Ross in the NMR lab. If you've ever heard Scott talk about NMR, you know he's the best in the business. He's a great teacher, and his passion for his work is incredible. Mona Shahgholi (Caltech) and John Greaves (UC Irvine) are acknowledged for their assistance in obtaining mass spectral data. I would also like to thank Larry Henling and Mike Day for solving several crystal structures for the drarmacidin project. I am indebted to Tom Dunn for everything he has helped with over the years, especially with regards to Hg3. I'd like to thank Rick Gerhart and Mike Roy for many great conversations. I've also enjoyed time spent with the guys in the chemistry stockroom, Joe Drew, Moises Renteria, and Terry

James, especially the trips to Lee's Hoagie House. Lynne Martinez and Linda Syme have always been good to me. And where would we all be without Dian Buchness?

This thesis certainly would not have been possible without the love and encouragement of my family and friends. My mom and dad have always been incredibly compassionate, and my brother Bobby and his wife Biraj have been equally caring. Finally, I want to give my deepest thanks to my fiancée Lindsey. She has been my best friend for many years and, without her, I would have had a tough time making it through graduate school. Her patience, love, and support mean the world to me.

ABSTRACT

The dragmacidins are an emerging class of bis(indole) natural products isolated from deep-water marine organisms. Although there has been a substantial effort to prepare the simple piperazine dragmacidins, little synthetic work has been done in the area of the pyrazinone-containing family members, dragmacidins D, E, and F. These compounds are particularly interesting due to their complex structures and broad range of biological activity.

A highly convergent strategy to access dragmacidin D has been developed. In this approach, sequential halogen-selective Suzuki couplings were used to assemble the carbon scaffold of the natural product. After executing a highly optimized sequence of final events, the first completed total synthesis of dragmacidin D was achieved.

An enantiodivergent strategy for the total chemical synthesis of both (+)- and (–)-dragmacidin F from a single enantiomer of quinic acid has been developed and successfully implemented. Although unique, the synthetic routes to these antipodes share a number of key features, including novel reductive isomerization reactions, Pd(II)-mediated oxidative carbocyclization reactions, halogen-selective Suzuki couplings, and high-yielding late-stage Neber rearrangements.

The formal total syntheses of dragmacidin B, *trans*-dragmacidin C, and dihydrohamacanthin A are described. In addition, preliminary studies involving a novel approach for the preparation of dragmacidin E are reported.

TABLE OF CONTENTS

Dedication.....	iii
Acknowledgements	iv
Abstract.....	viii
Table of Contents	ix
List of Figures	xvi
List of Schemes	xxiv
List of Tables	xxvii
List of Abbreviations.....	xxviii

CHAPTER ONE: The Dragmacidins: A Family of Biologically

Active Marine Alkaloids.....	1
1.1 Introduction.....	1
1.1.1 Bis(indole) Alkaloids.....	1
1.1.2 The Dragmacidins	3
1.2 Biological Activity of the Pyrazinone- Containing Dragmacidins.....	3
1.2.1 Inhibitors of Protein Phosphatases.....	3
1.2.1.1 Activity of Dragmacidins	3
1.2.1.2 About Protein Phosphatases	4
1.2.2 Inhibitors of Neural Nitric Oxide Synthase	5
1.2.2.1 Activity of Dragmacidins	5
1.2.2.2 About Nitric Oxide Synthase	5
1.2.2.3 Aminoimidazoles as Inhibitors	6
1.2.3 Miscellaneous Biological Activity.....	6
1.2.3.1 Cytotoxicity	6

1.2.3.2 Antiviral and Anti-Inflammatory Properties	7
1.3 Biosynthesis of Dragmacidins	7
1.3.1 Biosynthesis of Piperazine Dragmacidins and Dragmacidin D	7
1.3.2 Biosynthesis of Dragmacidins E and F	8
1.4 Synthetic Studies Relating to the Pyrazinone- Containing Dragmacidins	10
1.4.1 Jiang's Approach to the Pyrazinone Core	10
1.4.2 Horne's Approach to the Pyrazinone Core	10
1.4.3 Jiang's Approach to the Aminoimidazole Segment of Dragmacidin D	11
1.4.4 Jiang's Second Generation Approach to the Pyrazinone Core.	12
1.5 Conclusion	13
1.6 Notes and References	14
CHAPTER TWO: The Total Synthesis of Dragmacidin D	19
2.1 Background	19
2.1.1 Introduction	19
2.1.2 Retrosynthetic Analysis of Dragmacidin D	20
2.2 The Cyclocondensation Approach to Access the Bis(indole) Framework	21

2.3 The Metal-Mediated Strategy to Construct the Bis(indole) Framework	23
2.3.1 The Development of Suitable Conditions for Selective Cross-Couplings	24
2.3.2 Synthesis of Pyrazine and Bromoindole Fragments.....	26
2.3.3 Synthesis of the 3,4,7-Trisubstituted Indole Fragment	27
2.3.4 Construction of the Fully Substituted Bis(indole)pyrazinone core	28
2.4 End-Game Studies	29
2.4.1 End-Game Strategy 1	29
2.4.2 End-Game Strategy 2	30
2.4.3 End-Game Strategy 3: The Total Synthesis of Dragmacidin D	31
2.4.4 Subtleties of Late-Stage Manipulations	34
2.5 An Asymmetric Route to Dragmacidin D	35
2.6 Conclusion	36
2.7 Experimental Section.....	37
2.7.1 Materials and Methods	37
2.7.2 Preparative Procedures	39
2.8 Notes and References	69
APPENDIX ONE: Synthetic Summary for Dragmacidin D (5)	77

APPENDIX TWO: Spectra Relevant to Chapter Two	80
---	----

CHAPTER THREE: The Total Synthesis of (+)- and (-)-

Dragmacidin F	131
3.1 Background	131
3.1.1 Introduction.....	131
3.1.2 Retrosynthetic Analysis of Dragmacidin F.....	132
3.2 The Total Synthesis of (+)-Dragmacidin F.....	133
3.2.1 Synthesis of Cyclization Substrates	133
3.2.2 Constructing the [3.3.1] Bicycle	137
3.2.3 Assembling the Carbon Skeleton of Dragmacidin F.....	139
3.2.4 End-Game Studies	140
3.2.4.1 End-Game Strategy 1	141
3.2.4.2 End-Game Strategy 2	141
3.2.4.3 End-Game Strategy 3: The Total Synthesis of (+)-Dragmacidin F	142
3.3 The Absolute Stereochemistry of the Pyrazinone-Containing Dragmacidins	145
3.4 The Total Synthesis of (-)-Dragmacidin F	147
3.4.1 An Enantiodivergent Strategy for the Preparation of (-)-Dragmacidin F	147
3.4.2 The Development and Investigation of a Reductive Isomerization Reaction	149

3.4.3 Constructing the [3.3.1] Bicycle en Route to (–)-Dragmacidin F	152
3.4.4 End-Game Studies	153
3.4.4.1 End-Game Strategy 1	153
3.4.4.2 End-Game Strategy 2: Rh-Mediated Allylic Isomerization and the Total Synthesis of (–)-Dragmacidin F	154
3.5 Conclusion	159
3.6 Experimental Section.....	160
3.6.1 Materials and Methods	160
3.6.2 Preparative Procedures	162
3.7 Notes and References	213
APPENDIX THREE: Synthetic Summary for (+)- and (–)-Dragmacidin F (7)	223
APPENDIX FOUR: Spectra Relevant to Chapter Three.....	227
APPENDIX FIVE: The Formal Total Synthesis of Dragmacidin B, <i>trans</i> -Dragmacidin C, and <i>cis</i> - and <i>trans</i> -Dihydrohamacanthin A	310
A5.1 Introduction.....	310

A5.2 The Formal Total Synthesis of Dragmacidin B and <i>trans</i> -Dragmacidin C	311
A5.3 The Formal Total Synthesis of <i>cis</i> - and <i>trans</i> -Dihydrohamacanthin A	313
A5.4 Conclusion	315
A5.5 Experimental Section	316
A5.5.1 Materials and Methods	316
A5.5.2 Preparative Procedures	316
A5.6 Notes and References	319
APPENDIX SIX: A Strategy for the Preparation of Dragmacidin E	321
A6.1 Background	321
A6.1.1 Introduction	321
A6.1.2 Retrosynthetic Analysis of Dragmacidin E	321
A6.2 Model Systems: The Facile Synthesis of Bis(indole)-1,2,4-Triazinones	323
A6.3 An Alternative Strategy to Access Bis(indole)triazines	326
A6.4 Conclusion	327
A6.5 Experimental Section	328
A6.5.1 Materials and Methods	328

A6.5.2 Preparative Procedures	329
A6.6 X-Ray Crystallography Reports	335
A6.6.1 X-Ray Crystallographic Report for <i>p</i> -Triazinone 187	335
A6.6.2 X-Ray Crystallographic Report for <i>m</i> -Triazinone 188	348
A6.6.3 X-Ray Crystallographic Report for Allyl Triazinone 193	356
A6.7 Notes and References	364
APPENDIX SEVEN: Notebook Cross-Reference	366
Comprehensive Bibliography	369
Index	388
About the Author.....	393

LIST OF FIGURES

CHAPTER ONE

Figure 1.1.1	Representative bis(indole) alkaloids	1
Figure 1.1.2	The dragmacidin alkaloids	2
Figure 1.2.1	Protein phosphatases and kinases.....	4

CHAPTER TWO

Figure 2.1.1	The pyrazinone-containing dragmacidins	19
Figure 2.3.1	The design of suitable substrates for cross-coupling	26
Figure 2.4.1	¹ H NMR comparison spectra of dragmacidin D (5); natural vs. synthetic	33
Figure 2.4.2	Fluorescence of late-stage compounds.....	34

APPENDIX ONE

Figure A1.1	The synthesis of indolylpyrazine 73	78
Figure A1.2	The synthesis of boronic ester 62	78
Figure A1.3	The synthesis of dragmacidin D (5)	79

APPENDIX TWO

Figure A2.1	¹ H NMR (300 MHz, DMSO- <i>d</i> ₆) of compound 52a	81
Figure A2.2	Infrared spectrum (thin film/NaCl) of compound 52a	82
Figure A2.3	¹³ C NMR (75 MHz, DMSO- <i>d</i> ₆) of compound 52a	82
Figure A2.4	¹ H NMR (300 MHz, acetone- <i>d</i> ₆) of compound 53a	83
Figure A2.5	Infrared spectrum (thin film/NaCl) of compound 53a	84
Figure A2.6	¹³ C NMR (75 MHz, acetone- <i>d</i> ₆) of compound 53a	84
Figure A2.7	¹ H NMR (300 MHz, DMSO- <i>d</i> ₆) of compound 22a	85
Figure A2.8	Infrared spectrum (thin film/NaCl) of compound 22a	86
Figure A2.9	¹³ C NMR (125 MHz, DMSO- <i>d</i> ₆) of compound 22a	86

Figure A2.10	^1H NMR (300 MHz, CDCl_3) of compound 63	87
Figure A2.11	Infrared spectrum (KBr pellet) of compound 63	88
Figure A2.12	^{13}C NMR (75 MHz, CDCl_3) of compound 63	88
Figure A2.13	^1H NMR (300 MHz, CDCl_3) of compound 91	89
Figure A2.14	Infrared spectrum (thin film/ NaCl) of compound 91	90
Figure A2.15	^{13}C NMR (75 MHz, CDCl_3) of compound 91	90
Figure A2.16	^1H NMR (300 MHz, $\text{DMSO}-d_6$) of compound 65	91
Figure A2.17	^1H NMR (300 MHz, CDCl_3) of compound 67	92
Figure A2.18	Infrared spectrum (thin film/ NaCl) of compound 67	93
Figure A2.19	^{13}C NMR (75 MHz, CDCl_3) of compound 67	93
Figure A2.20	^1H NMR (300 MHz, CDCl_3) of compound 68	94
Figure A2.21	Infrared spectrum (thin film/ NaCl) of compound 68	95
Figure A2.22	^{13}C NMR (75 MHz, CDCl_3) of compound 68	95
Figure A2.23	^1H NMR (300 MHz, CDCl_3) of compound 70	96
Figure A2.24	Infrared spectrum (thin film/ NaCl) of compound 70	97
Figure A2.25	^{13}C NMR (75 MHz, CDCl_3) of compound 70	97
Figure A2.26	^1H NMR (300 MHz, CDCl_3) of compound 72	98
Figure A2.27	Infrared spectrum (thin film/ NaCl) of compound 72	99
Figure A2.28	^{13}C NMR (75 MHz, CDCl_3) of compound 72	99
Figure A2.29	^1H NMR (300 MHz, CDCl_3) of compound 92	100
Figure A2.30	Infrared spectrum (thin film/ NaCl) of compound 92	101
Figure A2.31	^{13}C NMR (75 MHz, CDCl_3) of compound 92	101
Figure A2.32	^1H NMR (300 MHz, CDCl_3) of compound 93	102
Figure A2.33	Infrared spectrum (thin film/ NaCl) of compound 93	103
Figure A2.34	^{13}C NMR (75 MHz, CDCl_3) of compound 93	103
Figure A2.35	^1H NMR (300 MHz, C_6D_6) of compound 62	104
Figure A2.36	^1H NMR (300 MHz, CDCl_3) of compound 73	105
Figure A2.37	Infrared spectrum (thin film/ NaCl) of compound 73	106
Figure A2.38	^{13}C NMR (125 MHz, CDCl_3) of compound 73	106
Figure A2.39	^1H NMR (300 MHz, CDCl_3) of compound 74	107

Figure A2.40	Infrared spectrum (thin film/NaCl) of compound 74	108
Figure A2.41	^{13}C NMR (125 MHz, CDCl_3) of compound 74	108
Figure A2.42	^1H NMR (500 MHz, CDCl_3) of compound 75	109
Figure A2.43	Infrared spectrum (thin film/NaCl) of compound 75	110
Figure A2.44	^{13}C NMR (125 MHz, CDCl_3) of compound 75	110
Figure A2.45	^1H NMR (300 MHz, CDCl_3) of compound 76	111
Figure A2.46	Infrared spectrum (thin film/NaCl) of compound 76	112
Figure A2.47	^{13}C NMR (125 MHz, CDCl_3) of compound 76	112
Figure A2.48	^1H NMR (500 MHz, CDCl_3) of compound 77	113
Figure A2.49	Infrared spectrum (thin film/NaCl) of compound 77	114
Figure A2.50	^{13}C NMR (125 MHz, CDCl_3) of compound 77	114
Figure A2.51	^1H NMR (500 MHz, CDCl_3) of compound 78	115
Figure A2.52	Infrared spectrum (thin film/NaCl) of compound 78	116
Figure A2.53	^{13}C NMR (125 MHz, CDCl_3) of compound 78	116
Figure A2.54	^1H NMR (300 MHz, CDCl_3) of compound 80	117
Figure A2.55	^1H NMR (500 MHz, CD_3OD) of compound 81	118
Figure A2.56	^1H NMR (500 MHz, CDCl_3) of compound 82	119
Figure A2.57	Infrared spectrum (thin film/NaCl) of compound 82	120
Figure A2.58	^{13}C NMR (125 MHz, CDCl_3) of compound 82	120
Figure A2.59	^1H NMR (300 MHz, acetone- d_6) of compound 83	121
Figure A2.60	Infrared spectrum (thin film/NaCl) of compound 83	122
Figure A2.61	^{13}C NMR (125 MHz, acetone- d_6) of compound 83	122
Figure A2.62	^1H NMR (500 MHz, CD_3OD) of compound 84	123
Figure A2.63	Infrared spectrum (thin film/NaCl) of compound 84	124
Figure A2.64	^{13}C NMR (125 MHz, CD_3OD) of compound 84	124
Figure A2.65	^1H NMR (600 MHz, CD_3OD) of dragmacidin D (5).....	125
Figure A2.66	Infrared spectrum (thin film/NaCl) of dragmacidin D (5).....	126
Figure A2.67	^{13}C NMR (125 MHz, CD_3OD) of dragmacidin D (5).....	126
Figure A2.68	^1H NMR (300 MHz, CDCl_3) of compound 86	127
Figure A2.69	Infrared spectrum (thin film/NaCl) of compound 86	128

Figure A2.70	^{13}C NMR (75 MHz, CDCl_3) of compound 86	128
Figure A2.71	^1H NMR (300 MHz, CDCl_3) of compound 88	129
Figure A2.72	Infrared spectrum (thin film/ NaCl) of compound 88	130
Figure A2.73	^{13}C NMR (125 MHz, CDCl_3) of compound 88	130

CHAPTER THREE

Figure 3.1.1	Dragmacidin F (7).....	131
Figure 3.3.1	^1H NMR comparison spectra of dragmacidin F (7); (–)-natural vs. (+)-synthetic	146
Figure 3.3.2	Absolute stereochemical configurations for dragmacidins D (5), E (6), and F (7)	147
Figure 3.4.1	Rational design of reductive isomerization substrate 130	151
Figure 3.4.2	^1H NMR comparison spectra of (–)-dragmacidin F (7); natural vs. synthetic	158

APPENDIX THREE

Figure A3.1	The synthesis of boronic ester 97	224
Figure A3.2	The synthesis of (+)-dragmacidin F (7)	225
Figure A3.3	The synthesis of (–)-dragmacidin F (7).....	226

APPENDIX FOUR

Figure A4.1	^1H NMR (300 MHz, CDCl_3) of compound 146	228
Figure A4.2	Infrared spectrum (thin film/ NaCl) of compound 146	229
Figure A4.3	^{13}C NMR (75 MHz, CDCl_3) of compound 146	229
Figure A4.4	^1H NMR (300 MHz, CD_3OD) of compound 147	230
Figure A4.5	Infrared spectrum (thin film/ NaCl) of compound 147	231
Figure A4.6	^{13}C NMR (75 MHz, CD_3OD) of compound 147	231
Figure A4.7	^1H NMR (300 MHz, CDCl_3) of compound 103	232
Figure A4.8	Infrared spectrum (thin film/ NaCl) of compound 103	233
Figure A4.9	^{13}C NMR (75 MHz, CDCl_3) of compound 103	233

Figure A4.10	^1H NMR (300 MHz, CDCl_3) of compound 105	234
Figure A4.11	Infrared spectrum (thin film/ NaCl) of compound 105	235
Figure A4.12	^{13}C NMR (75 MHz, CDCl_3) of compound 105	235
Figure A4.13	^1H NMR (300 MHz, CDCl_3) of compound 106	236
Figure A4.14	Infrared spectrum (thin film/ NaCl) of compound 106	237
Figure A4.15	^{13}C NMR (75 MHz, CDCl_3) of compound 106	237
Figure A4.16	^1H NMR (300 MHz, CDCl_3) of compound 104	238
Figure A4.17	Infrared spectrum (thin film/ NaCl) of compound 104	239
Figure A4.18	^{13}C NMR (75 MHz, CDCl_3) of compound 104	239
Figure A4.19	^1H NMR (300 MHz, CDCl_3) of compound 109	240
Figure A4.20	Infrared spectrum (thin film/ NaCl) of compound 109	241
Figure A4.21	^{13}C NMR (75 MHz, CDCl_3) of compound 109	241
Figure A4.22	^1H NMR (300 MHz, CDCl_3) of compound 151	242
Figure A4.23	Infrared spectrum (thin film/ NaCl) of compound 151	243
Figure A4.24	^{13}C NMR (75 MHz, CDCl_3) of compound 151	243
Figure A4.25	^1H NMR (300 MHz, CDCl_3) of compound 99	244
Figure A4.26	Infrared spectrum (thin film/ NaCl) of compound 99	245
Figure A4.27	^{13}C NMR (75 MHz, CDCl_3) of compound 99	245
Figure A4.28	^1H NMR (300 MHz, CDCl_3) of compound 153	246
Figure A4.29	Infrared spectrum (thin film/ NaCl) of compound 153	247
Figure A4.30	^{13}C NMR (75 MHz, CDCl_3) of compound 153	247
Figure A4.31	^1H NMR (300 MHz, CDCl_3) of compound 100	248
Figure A4.32	Infrared spectrum (thin film/ NaCl) of compound 100	249
Figure A4.33	^{13}C NMR (75 MHz, CDCl_3) of compound 100	249
Figure A4.34	^1H NMR (300 MHz, CDCl_3) of compound 98	250
Figure A4.35	^1H NMR (300 MHz, C_6D_6) of compound 98	251
Figure A4.36	Infrared spectrum (thin film/ NaCl) of compound 98	252
Figure A4.37	^{13}C NMR (75 MHz, C_6D_6) of compound 98	252
Figure A4.38	^1H NMR (300 MHz, CDCl_3) of compound 110	253
Figure A4.39	^1H NMR (300 MHz, C_6D_6) of compound 110	254

Figure A4.40	Infrared spectrum (thin film/NaCl) of compound 110	255
Figure A4.41	^{13}C NMR (75 MHz, CDCl_3) of compound 110	255
Figure A4.42	^1H NMR (300 MHz, C_6D_6) of compound 154	256
Figure A4.43	Infrared spectrum (thin film/NaCl) of compound 154	257
Figure A4.44	^{13}C NMR (75 MHz, C_6D_6) of compound 154	257
Figure A4.45	^1H NMR (300 MHz, C_6D_6) of compound 111	258
Figure A4.46	Infrared spectrum (thin film/NaCl) of compound 111	259
Figure A4.47	^{13}C NMR (75 MHz, C_6D_6) of compound 111	259
Figure A4.48	^1H NMR (300 MHz, C_6D_6) of compound 155	260
Figure A4.49	Infrared spectrum (thin film/NaCl) of compound 155	261
Figure A4.50	^{13}C NMR (75 MHz, C_6D_6) of compound 155	261
Figure A4.51	^1H NMR (300 MHz, C_6D_6) of compound 97	262
Figure A4.52	Infrared spectrum (thin film/NaCl) of compound 97	263
Figure A4.53	^{13}C NMR (75 MHz, C_6D_6) of compound 97	263
Figure A4.54	^1H NMR (300 MHz, CDCl_3) of compound 112	264
Figure A4.55	Infrared spectrum (thin film/NaCl) of compound 112	265
Figure A4.56	^{13}C NMR (75 MHz, CDCl_3) of compound 112	265
Figure A4.57	^1H NMR (300 MHz, CDCl_3) of compound 113	266
Figure A4.58	Infrared spectrum (thin film/NaCl) of compound 113	267
Figure A4.59	^{13}C NMR (75 MHz, CDCl_3) of compound 113	267
Figure A4.60	^1H NMR (300 MHz, C_6D_6) of compound 117	268
Figure A4.61	Infrared spectrum (thin film/NaCl) of compound 117	269
Figure A4.62	^{13}C NMR (125 MHz, C_6D_6) of compound 117	269
Figure A4.63	^1H NMR (600 MHz, CD_3OD) of compound 118	270
Figure A4.64	Infrared spectrum (thin film/NaCl) of compound 118	271
Figure A4.65	^{13}C NMR (125 MHz, CD_3OD) of compound 118	271
Figure A4.66	^1H NMR (300 MHz, CDCl_3) of compound 119	272
Figure A4.67	Infrared spectrum (thin film/NaCl) of compound 119	273
Figure A4.68	^{13}C NMR (75 MHz, CDCl_3) of compound 119	273
Figure A4.69	^1H NMR (600 MHz, CD_3OD) of compound 123	274

Figure A4.70	^1H NMR (300 MHz, CD_3OD) of compound 120	275
Figure A4.71	Infrared spectrum (thin film/ NaCl) of compound 120	276
Figure A4.72	^{13}C NMR (75 MHz, CD_3OD) of compound 120	276
Figure A4.73	^1H NMR (300 MHz, CD_3OD) of compound 124	277
Figure A4.74	Infrared spectrum (thin film/ NaCl) of compound 124	278
Figure A4.75	^{13}C NMR (75 MHz, CD_3OD) of compound 124	278
Figure A4.76	^1H NMR (600 MHz, CD_3OD) of (+)-dragmacidin F (7)	279
Figure A4.77	Infrared spectrum (thin film/ NaCl) of (+)-dragmacidin F (7).....	280
Figure A4.78	^{13}C NMR (125 MHz, CD_3OD) of (+)-dragmacidin F (7)	280
Figure A4.79	^1H NMR (300 MHz, CDCl_3) of compound 128	281
Figure A4.80	Infrared spectrum (thin film/ NaCl) of compound 128	282
Figure A4.81	^{13}C NMR (75 MHz, CDCl_3) of compound 128	282
Figure A4.82	^1H NMR (300 MHz, C_6D_6) of compound 159	283
Figure A4.83	Infrared spectrum (thin film/ NaCl) of compound 159	284
Figure A4.84	^{13}C NMR (75 MHz, C_6D_6) of compound 159	284
Figure A4.85	^1H NMR (300 MHz, C_6D_6) of compound 131	285
Figure A4.86	Infrared spectrum (thin film/ NaCl) of compound 131	286
Figure A4.87	^{13}C NMR (75 MHz, C_6D_6) of compound 131	286
Figure A4.88	^1H NMR (300 MHz, C_6D_6) of compound 132	287
Figure A4.89	Infrared spectrum (thin film/ NaCl) of compound 132	288
Figure A4.90	^{13}C NMR (75 MHz, C_6D_6) of compound 132	288
Figure A4.91	^1H NMR (300 MHz, C_6D_6) of compound 130	289
Figure A4.92	Infrared spectrum (thin film/ NaCl) of compound 130	290
Figure A4.93	^{13}C NMR (75 MHz, C_6D_6) of compound 130	290
Figure A4.94	^1H NMR (300 MHz, C_6D_6) of compound 126	291
Figure A4.95	Infrared spectrum (thin film/ NaCl) of compound 126	292
Figure A4.96	^{13}C NMR (75 MHz, C_6D_6) of compound 126	292
Figure A4.97	^1H NMR (300 MHz, C_6D_6) of compound 127	293
Figure A4.98	Infrared spectrum (thin film/ NaCl) of compound 127	294

Figure A4.99	^{13}C NMR (75 MHz, C_6D_6) of compound 127	294
Figure A4.100	^1H NMR (300 MHz, C_6D_6) of compound 133	295
Figure A4.101	Infrared spectrum (thin film/ NaCl) of compound 133	296
Figure A4.102	^{13}C NMR (75 MHz, C_6D_6) of compound 133	296
Figure A4.103	^1H NMR (300 MHz, C_6D_6) of compound 136	297
Figure A4.104	Infrared spectrum (thin film/ NaCl) of compound 136	298
Figure A4.105	^{13}C NMR (75 MHz, C_6D_6) of compound 136	298
Figure A4.106	^1H NMR (500 MHz, C_6D_6) of compound 134	299
Figure A4.107	Infrared spectrum (thin film/ NaCl) of compound 134	300
Figure A4.108	^{13}C NMR (125 MHz, C_6D_6) of compound 134	300
Figure A4.109	^1H NMR (300 MHz, C_6D_6) of compound 137	301
Figure A4.110	Infrared spectrum (thin film/ NaCl) of compound 137	302
Figure A4.111	^{13}C NMR (75 MHz, C_6D_6) of compound 137	302
Figure A4.112	^1H NMR (300 MHz, C_6D_6) of compound 138	303
Figure A4.113	Infrared spectrum (thin film/ NaCl) of compound 138	304
Figure A4.114	^{13}C NMR (125 MHz, C_6D_6) of compound 138	304
Figure A4.115	^1H NMR (300 MHz, C_6D_6) of compound 139	305
Figure A4.116	Infrared spectrum (thin film/ NaCl) of compound 139	306
Figure A4.117	^{13}C NMR (75 MHz, C_6D_6) of compound 139	306
Figure A4.118	^1H NMR (300 MHz, C_6D_6) of compound 144	307
Figure A4.119	Infrared spectrum (thin film/ NaCl) of compound 144	308
Figure A4.120	^{13}C NMR (125 MHz, C_6D_6) of compound 144	308
Figure A4.121	^1H NMR (600 MHz, CD_3OD) of (–)-dragmacidin F (7)	309

APPENDIX FIVE

Figure A5.1.1	Dragmacidins B (3), <i>trans</i> -dragmacidin C (4), and dihydrohamacanthin A (164).....	310
---------------	--	-----

APPENDIX SIX

Figure A6.1.1	Dragmacidin E (6)	321
---------------	----------------------------------	-----

LIST OF SCHEMES

CHAPTER ONE

Scheme 1.2.1	Mechanism of nitric oxide synthase.....	6
Scheme 1.3.1	Biosynthesis of diketopiperazines	7
Scheme 1.3.2	Proposed biosynthesis of dragmacidins 1-5	8
Scheme 1.3.3	Proposed biosynthesis of dragmacidins 6-7	9
Scheme 1.4.1	Jiang's approach to bis(indole)pyrazinones	10
Scheme 1.4.2	Horne's approach to bis(indole)pyrazinones	11
Scheme 1.4.3	Jiang's approach to the aminoimidazole segment of dragmacidin D (5).....	12
Scheme 1.4.4	Jiang's second approach to bis(indole)pyrazinones.....	13

CHAPTER TWO

Scheme 2.1.1	Retrosynthetic analysis of dragmacidin D (5)	21
Scheme 2.2.1	Synthesis of cyclocondensation fragments 52a and 53a	22
Scheme 2.2.2	Preparation of bis(indole)pyrazinones 22a and 22b via a cyclocondensation approach.....	23
Scheme 2.3.1	Model studies to prepare bis(indole)pyrazines	25
Scheme 2.3.2	Synthesis of coupling fragments 63 and 54b	27
Scheme 2.3.3	Synthesis of 3,4,7-trifunctionalized indole 62	28
Scheme 2.3.4	Synthesis of bis(indole)pyrazine 74 via halogen- selective cross-coupling sequence.....	29
Scheme 2.4.1	End-game strategy 1	30
Scheme 2.4.2	End-game strategy 2	31
Scheme 2.4.3	End-game strategy 3 and the total synthesis of dragmacidin D (5)	32
Scheme 2.5.1	An asymmetric route to dragmacidin D (5)	35

Scheme 2.5.2	Sn(II)-promoted racemization of 84	36
--------------	---	----

CHAPTER THREE

Scheme 3.1.1	Retrosynthetic analysis of dragmacidin D (7)	133
Scheme 3.2.2	Functionalization of quinic acid and π -allyl reduction studies	135
Scheme 3.2.3	Reductive isomerization of lactone 103	136
Scheme 3.2.4	Synthesis of cyclization substrates 99 and 100	136
Scheme 3.2.5	Intramolecular Heck reaction to prepare 98	137
Scheme 3.2.6	Pd(II) oxidative cyclization to prepare 98	139
Scheme 3.2.7	Synthesis of the carbon scaffold of dragmacidin F (7)	140
Scheme 3.2.8	Synthesis of ketone 113	141
Scheme 3.2.9	Unsuccessful α -nitration attempts	141
Scheme 3.2.10	An unexpected Favorskii rearrangement	142
Scheme 3.2.11	Neber rearrangement/deprotection sequence	143
Scheme 3.2.12	Detailed mechanism of Neber rearrangement	144
Scheme 3.2.13	The total synthesis of (+)-dragmacidin F (7)	145
Scheme 3.4.1	An enantiodivergent strategy for the preparation of (+)- and (–)-dragmacidin F (7)	148
Scheme 3.4.2	Critical reductive isomerization experiments	150
Scheme 3.4.3	Elaboration of (–)-quinic acid to 126	152
Scheme 3.4.4	Construction of [3.3.1] bicycle 133	153
Scheme 3.4.5	End-game strategy 1 and desilylation experiments	154
Scheme 3.4.6	End-game strategy 2 and Rh-mediated allylic isomerization studies	155
Scheme 3.4.7	Mechanism of Rh-mediated allylic isomerization	156
Scheme 3.4.8	The total synthesis of (–)-dragmacidin F (7)	157

APPENDIX FIVE

Scheme A5.2.1	Retrosynthetic analysis of dragmacidin B (3) and <i>trans</i> -dragmacidin C (4)	311
Scheme A5.2.2	The formal total synthesis of dragmacidin B (3) and <i>trans</i> -dragmacidin C (4)	312
Scheme A5.3.1	Retrosynthetic analysis of dihydrohamacanthins A (164) and B (169).....	313
Scheme A5.3.2	The formal total synthesis of <i>cis</i> - and <i>trans</i> - dihydrohamacanthin A (164b)	314

APPENDIX SIX

Scheme A6.1.1	Retrosynthetic analysis of dragmacidin E (6).....	322
Scheme A6.2.1	The synthesis of amidrazone 185	323
Scheme A6.2.2	The synthesis of triazinones 187 and 188	324
Scheme A6.2.3	The synthesis of bis(methyl)triazinones 191 and 192	325
Scheme A6.2.4	The synthesis of allyl triazinones 193	325
Scheme A6.2.5	Attempted aromatization of triazinones	326
Scheme A6.3.1	A cross-coupling approach to access bis(indole)triazines	327

LIST OF TABLES

CHAPTER TWO

Table 2.5.1	Optimization of Asymmetric Hydrogenation	35
-------------	--	----

APPENDIX SEVEN

Table A7.1	Compounds Appearing in Chapter 2.....	366
Table A7.2	Compounds Appearing in Chapter 3.....	367

LIST OF ABBREVIATIONS

$[\alpha]_D$	specific rotation at wavelength of sodium D line
Ac	acetyl, acetate
app.	apparent
aq.	aqueous
atm	atmosphere
Bn	benzyl
Boc	<i>tert</i> -butyloxycarbonyl
br	broad
Bu	butyl
<i>n</i> -Bu	butyl
<i>t</i> -Bu	<i>tert</i> -Butyl
<i>c</i>	concentration for specific rotation measurements
°C	degrees Celsius
calc'd	calculated
CCDC	Cambridge Crystallographic Data Centre
CDI	1,1'-carbonyldiimidazole
CI	chemical ionization
Cy	cyclohexyl
d	doublet
dba	dibenzylideneacetone
dppb	1,4-bis(diphenylphosphino)butane
dec	decomposition
DMAP	4-dimethylaminopyridine
DMF	<i>N,N</i> -dimethylformamide
DMSO	dimethyl sulfoxide
EC ₅₀	50% effective concentration
ee	enantiomeric excess
eNOS	endothelial nitric oxide synthase
equiv	equivalent
ESI	electrospray ionization
Et	ethyl
FAB	fast atom bombardment

g	gram(s)
gCOSY	gradient-selected Correlation Spectroscopy
h	hour(s)
HIV	human immunodeficiency virus
HRMS	high resolution mass spectroscopy
HPLC	high performance liquid chromatography
HSV	herpes simplex virus
h ν	light
Hz	hertz
iNOS	inducible nitric oxide synthase
IR	infrared (spectroscopy)
<i>J</i>	coupling constant
λ	wavelength
L	liter
m	multiplet or milli
<i>m</i>	meta
<i>m/z</i>	mass to charge ratio
μ	micro
Me	methyl
MHz	megahertz
min	minute(s)
mol	mole(s)
mp	melting point
Ms	methanesulfonyl (mesyl)
MS	molecular sieves
nbd	norbornadiene
NBS	<i>N</i> -bromosuccinimide
NMO	<i>N</i> -methylmorpholine <i>N</i> -oxide
NMR	nuclear magnetic resonance
NOE	Nuclear Overhauser Effect
NOESY	Nuclear Overhauser Enhancement Spectroscopy
NOS	nitric oxide synthase
nNOS	neural nitric oxide synthase
[O]	oxidation
<i>p</i>	para

PDC	pyridinium dichromate
Ph	phenyl
pH	hydrogen ion concentration in aqueous solution
PhH	benzene
ppm	parts per million
PP	protein phosphatase
Pr	propyl
<i>i</i> -Pr	isopropyl
pyr	pyridine
q	quartet
rt	room temperature
R_f	retention factor
s	singlet or strong
SEM	(trimethylsilyl)ethoxymethyl
t	triplet
TBAF	tetrabutylammonium fluoride
TBS	<i>tert</i> -butyldimethylsilyl
Tf	trifluoromethanesulfonyl (trifyl)
TFA	trifluoroacetic acid
THF	tetrahydrofuran
TIPS	triisopropylsilyl
TLC	thin layer chromatography
TMS	trimethylsilyl
Tr	triphenylmethyl (trityl)
Ts	<i>p</i> -toluenesulfonyl (tosyl)
UV	ultraviolet
w	weak

CHAPTER ONE

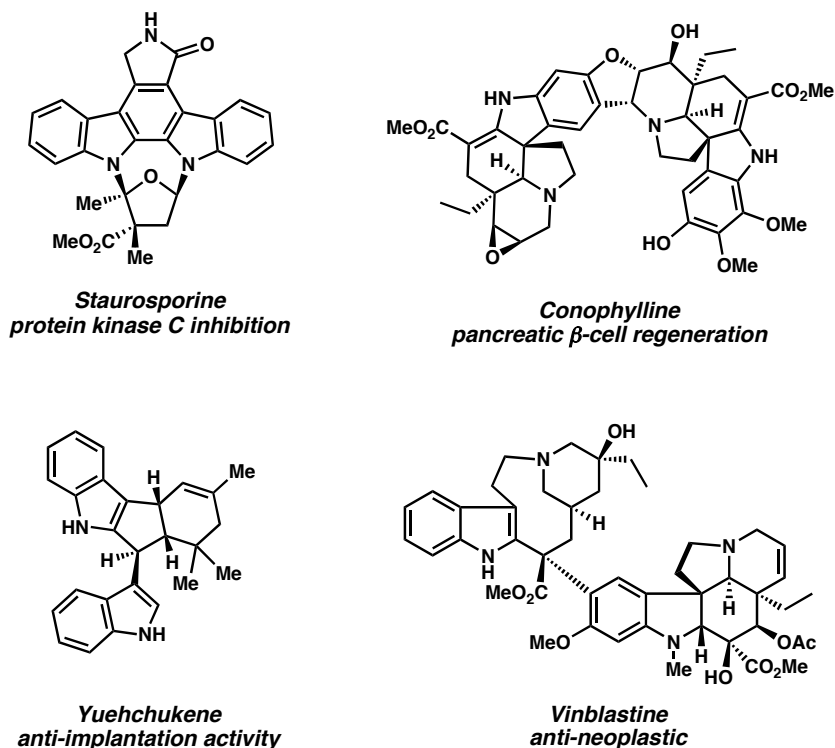
The Dragmacidins: A Family of Biologically Active Marine Alkaloids

1.1 Introduction

1.1.1 Bis(indole) Alkaloids

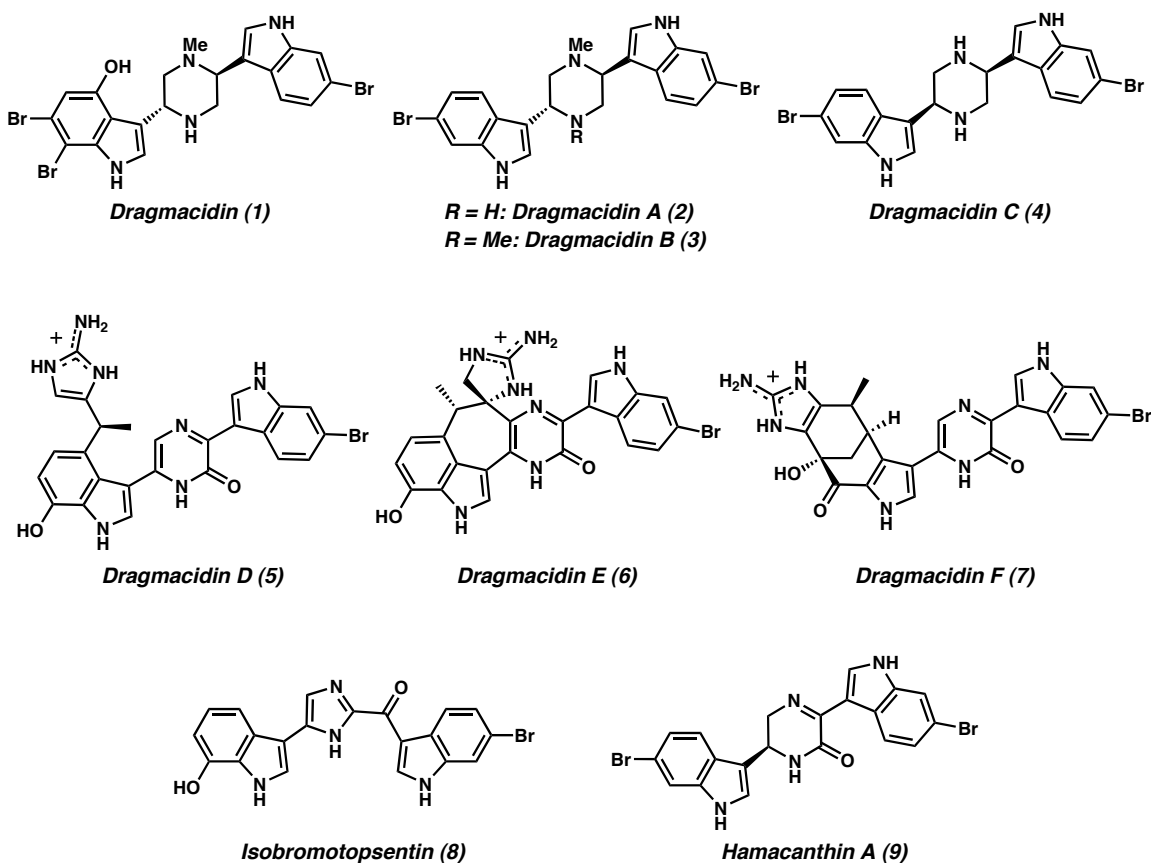
Over the past several decades, the search for natural products in marine and terrestrial environments has led to the discovery of a number of biologically active bis(indole) alkaloids.¹ These compounds, as well as their unnatural analogs, have shown promise as leads for the development of novel therapeutics. Several representative bis(indole) compounds are shown below in Figure 1.1.1.²

Figure 1.1.1



Although many bis(indole) alkaloids have been found in nature, relatively few have been discovered in marine environments.³ Of those, the dragmacidins have received considerable attention from the scientific community over the past decade due to their broad range of biological activity and complex structures (**1-7**, Figure 1.1.2).^{4,5} Several closely related bis(indole) natural products have been discovered in similar environments, such as the topsentins (e.g., **8**)^{4b,6} and the hamacanthins (e.g., **9**).⁷

Figure 1.1.2



1.1.2 The Dragmacidins

The dragmacidins are an emerging class of novel bis(indole) natural products isolated from the deep-water marine sponges *Dragmacidon*, *Halicortex*, *Spongisorites*, and *Hexadella*, and the tunicate *Didemnum candidum*. The four dragmacidins initially identified (**1-4**) contain a piperazine linker and display modest antifungal, antiviral, and cytotoxic activities.^{4a-c} However, our interest in these natural products was piqued by the structurally complex pyrazinone-containing family members, dragmacidins D (**5**), E (**6**), and F (**7**).^{4d-g} Although the relative stereochemistry of **1-7** was known, at the onset of our investigations, the absolute stereochemistry of **1-7** had not been established.

1.2 Biological Activity of Pyrazinone-Containing Dragmacidins

The following section describes the wide range of biological activity associated with the pyrazinone-containing dragmacidins, D (**5**), E (**6**), and F (**7**). Preliminary studies suggest that these compounds are interesting from a biological standpoint and are therefore attractive targets for total synthesis. Synthetic routes to the pyrazinone dragmacidins could facilitate the production of sufficient quantities of material needed for advanced biological studies.

1.2.1 Inhibitors of Protein Phosphatases

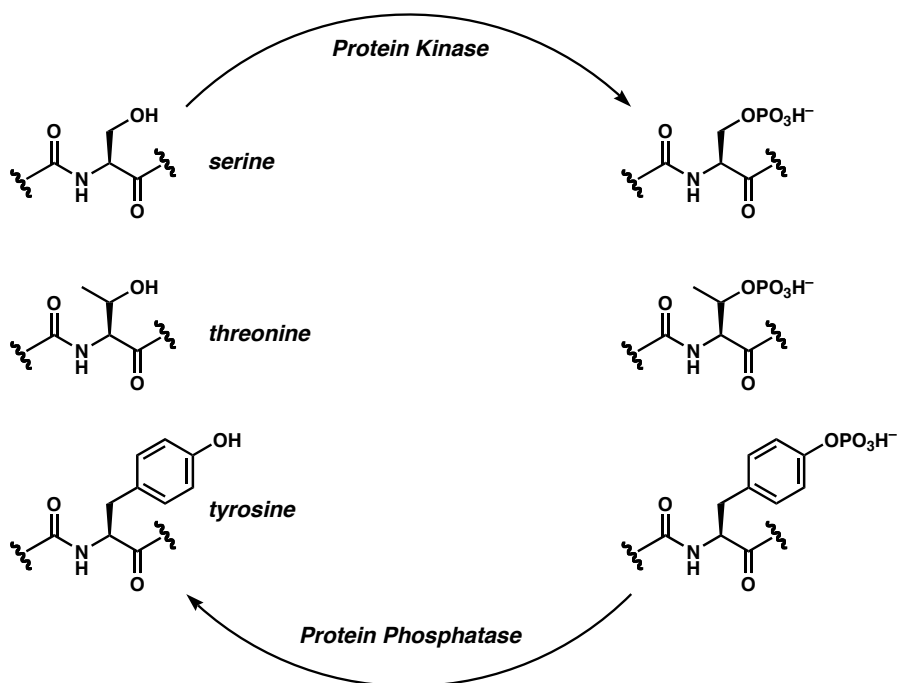
1.2.1.1 Activity of Dragmacidins

In 1998, Capon et al. reported that dragmacidins D (**5**) and E (**6**) are potent inhibitors of serine-threonine protein phosphatases (PP).^{4e} In addition, preliminary testing showed that dragmacidin D (**5**) selectively inhibited PP1 over the PP2A isozyme.

1.2.1.2 About Protein Phosphatases

The reversible phosphorylation of proteins containing serine, threonine, and tyrosine residues is widely recognized as a mechanism by which many cellular events are regulated (Figure 1.2.1).⁸ While phosphorylation is catalyzed by protein kinases, dephosphorylation is carried out by protein phosphatases. To date, many phosphatase enzymes have been discovered; however, discerning which phosphatase is responsible for controlling particular cellular pathways has remained an elusive goal. In particular, distinguishing the action of the PP1 and PP2A isozymes has been extremely difficult. Ultimately, the discovery of small molecules that display selective PP inhibition could help elucidate the mechanism of many physiological processes including cell division, gene expression, neurotransmission, and muscle contraction.^{8c}

Figure 1.2.1



1.2.2 Inhibitors of Neural Nitric Oxide Synthase

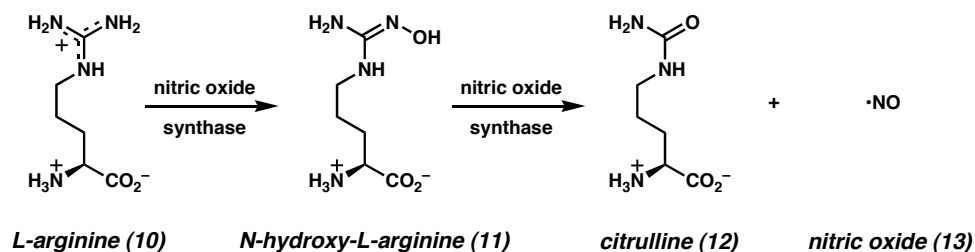
1.2.2.1 Activity of Dragmacidins

Dragmacidin D (**5**) has also been shown to selectively inhibit neural nitric oxide synthase (nNOS) in the presence of inducible nitric oxide synthase (iNOS).⁹ The ability to efficiently prepare dragmacidin D, and related derivatives thereof, could be extremely valuable for the discovery of novel drugs that target neurodegenerative disorders.

1.2.2.2 About Nitric Oxide Synthase

The production of nitric oxide (NO) in the human body is known to be associated with the regulation of a number of physiological properties.¹⁰ NO (**13**) arises from the decomposition of L-arginine (**10**) by an enzyme known as nitric oxide synthase (NOS) (**10** → **11** → **12** + **13**, Scheme 1.2.1). This enzyme occurs in three main isoforms: a) inducible NOS (iNOS), which generates NO during the immune response where NO acts as a cytotoxic molecule, b) endothelial NOS (eNOS), which produces NO for vasodilatation, and c) neuronal NOS (nNOS), which provides NO involved in neuronal physiology. Although NO provides many beneficial functions, the overproduction of NO in the brain has been linked to a number of neurodegenerative disorders. Thus, the ability to selectively inhibit nNOS may be useful for the treatment of related illnesses, including Alzheimer's, Parkinson's, and Huntington's diseases.¹¹

Scheme 1.2.1



1.2.2.3 Aminoimidazoles as Inhibitors

Compounds bearing aminoimidazole functionality are an attractive class of NOS inhibitors since, when protonated, they resemble the guanidinium system present in arginine (**10**).¹² Therefore, the aminoimidazole moiety of dragmacidin D (**5**) could potentially be responsible for its reported NOS activity through competitive inhibition. It is possible that the other aminoimidazole-containing dragmacidins (**6** and **7**) could display similar activity, although studies in this area have not appeared in the literature.

1.2.3 Miscellaneous Biological Activity

1.2.3.1 Cytotoxicity

Many bis(indole) compounds discovered in nature have shown promise as leads in the search for new anti-cancer medicines. Although its mechanism of action is not known, dragmacidin D (**5**) shows cytotoxicity against several human lung tumor cell lines.^{4d} Dragmacidins E (**6**) and F (**7**), on the other hand, have not yet been evaluated for anti-neoplastic activity.

1.2.3.2 Antiviral and Anti-Inflammatory Properties

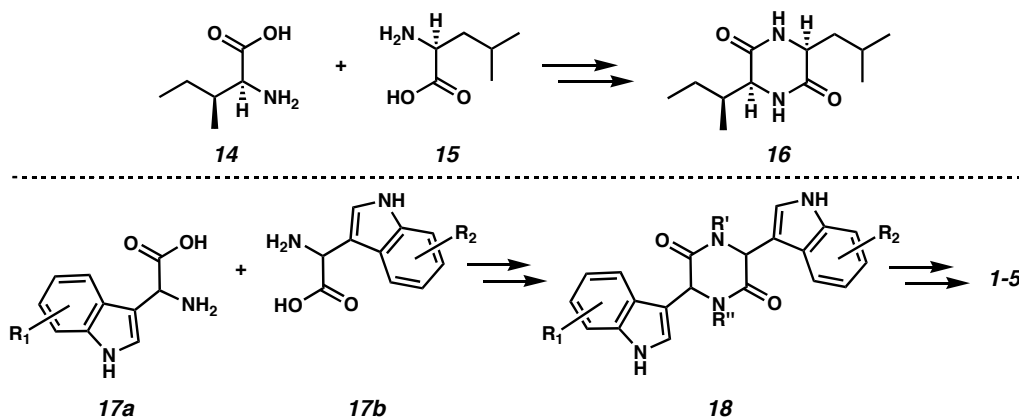
Dragmacidin F (**7**) is reported to exhibit in vitro antiviral activity against herpes simplex virus (HSV-I; $EC_{50} = 95.8$ mM) and human immunodeficiency virus (HIV-I; $EC_{50} = 0.91$ mM).^{4f} In addition, dragmacidins D (**5**) and F (**7**) display anti-inflammatory activity in resiniferatoxin-induced inflammation of the mouse ear.^{13,4g}

1.3 Biosynthesis of Dragmacidins

1.3.1 Biosynthesis of Piperazine Dragmacidins and Dragmacidin D

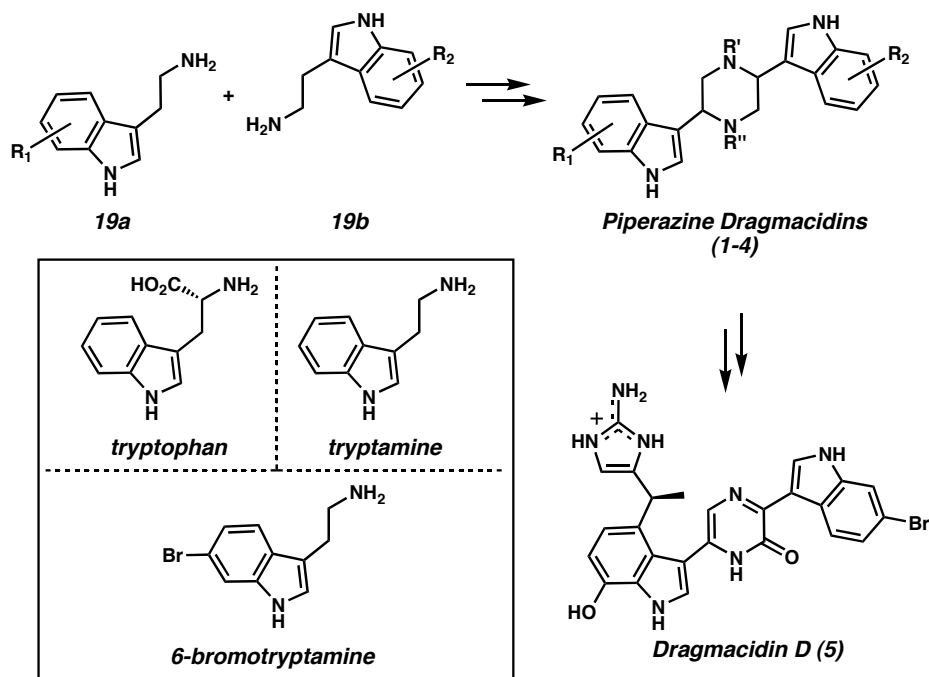
The biosynthesis of the dragmacidins has not been studied in detail.¹⁴ However, in the 1960s, MacDonald and co-workers examined the origin of simple diketopiperazine natural products.¹⁵ It was found that disubstituted piperazine derivatives could form via the condensation of two amino acids, L-isoleucine and L-leucine (**14** + **15** → **16**, Scheme 1.3.1). Based on this work, one could propose that the dragmacidins arise by a related pathway (**17a** + **17b** → **18** → **1-5**). However, the necessary indole-containing amino acids (**17a** and **17b**) for this biosynthesis are not known to be naturally occurring.

Scheme 1.3.1



Tryptophan and tryptamine (Scheme 1.3.2), on the other hand, are both commonly found in nature. In fact, 6-bromotryptamine was found in the same marine sponge from which dragmacidin C was isolated.^{4c} It seems plausible that the dragmacidins could be biosynthetically derived from building blocks of this type (i.e., **19a** and **19b**). Various oxidations could take place before or after the dimerization event occurs,¹⁶ eventually leading to formation of the piperazine dragmacidins (**1-4**). These molecules, or a related derivative, could perhaps be biosynthetically transformed into dragmacidin D (**5**).

Scheme 1.3.2

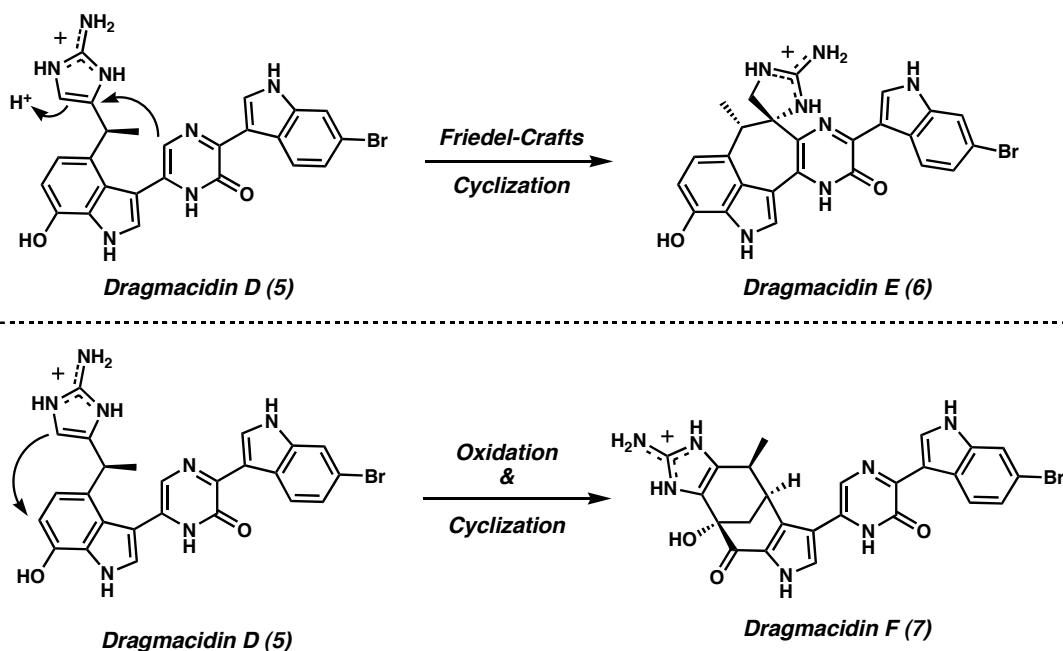


1.3.2 Biosynthesis of Dragmacidins E and F

Dragmacidins D, E, and F are likely biosynthetically related.^{4f} Of the possible biosynthetic scenarios, most probable is that dragmacidins E (**6**) and F (**7**) are derived by

cyclization of either dragmacidin D (**5**) or a closely related congener (Scheme 1.3.3). For example, dragmacidins D and E are isomers that differ by a single C–C bond. In nature, it is likely that a Friedel-Crafts cyclization between the pyrazinone and aminoimidazole groups of dragmacidin D occurs in order to construct the seven-membered ring of dragmacidin E (i.e., **5** \rightarrow **6**). Dragmacidins D (**5**) and F (**7**) also differ in connectivity by one C–C bond; however, in this case, there is also a difference in oxidation state between the two natural products. Thus, oxidative dearomatization with concomitant cyclization could facilitate the formation of the unique polycyclic framework present in dragmacidin F (i.e., **5** \rightarrow **7**). Related oxidation pathways for tryptophan derivatives have been observed in nature.¹⁷

Scheme 1.3.3



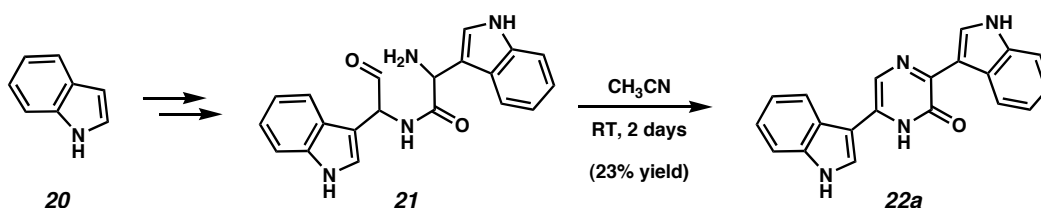
1.4 Synthetic Studies Relating to the Pyrazinone-Containing Dragmacidins

At the onset of our studies, there was a single report related to the synthesis of the pyrazinone-containing dragmacidins (**5-7**) by Jiang and Gu.^{5g} Although the authors claimed to have prepared the bis(indole)pyrazinone scaffold of **5** and **6**, this work was clearly erroneous but was never retracted.¹⁸

1.4.1 Jiang's Approach to the Pyrazinone Core

In 2000, shortly after we began work in the area of the dragmacidin natural products, Jiang and co-workers reported a successful synthetic route to the bis(indole)pyrazinone core of dragmacidins D and E (Scheme 1.4.1).^{5h} Their strategy involved the elaboration of indole (**20**) to bis(indole)amide **21** via a series of functional group manipulations. Then, in the final step, intramolecular condensation of amide **21** produced pyrazinone **22a** in 23% yield. Although Jiang's route produced the desired bis(indole) core (**22a**), it is lengthy and hampered by low yields.

Scheme 1.4.1

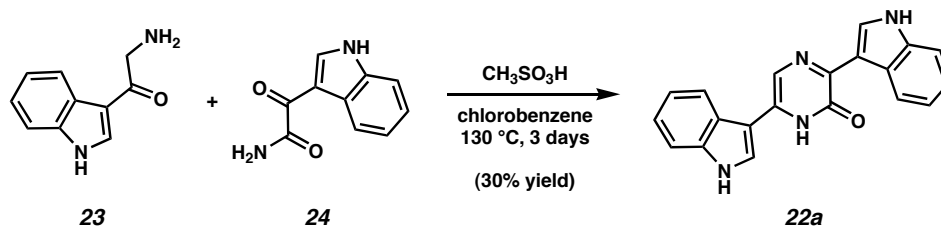


1.4.2 Horne's Approach to the Pyrazinone Core

In 2002, during the course of our own investigations, a convergent strategy for constructing pyrazinone **22a** was reported by Horne (Scheme 1.4.2).^{5j} Upon exposure to

methanesulfonic acid at 130 °C, aminoketone **23** underwent a cyclocondensation reaction with ketoamide **24** to afford the desired product **22a** in 30% yield. Further work in this area using substituted indoles has yet to be reported.

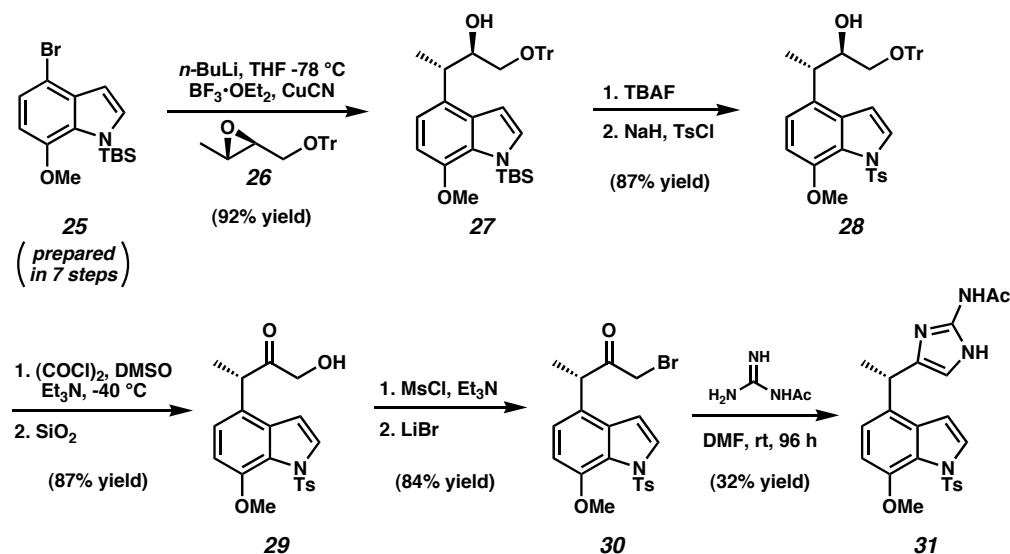
Scheme 1.4.2



1.4.3 Jiang's Approach to the Aminoimidazole Segment of Dragmacidin D

Concurrent with our own work, in 2002 Jiang described a synthesis of the aminoimidazole segment of dragmacidin D.⁵¹ The 4,7-disubstituted indole (**25**) was prepared in 7 steps from commercially available compounds via a Leimgruber-Batcho indole synthesis (Scheme 1.4.3).^{19,20} Subsequent metallation and quenching with epoxide **26** afforded alcohol **27** in good yield. After manipulations of the indole nitrogen protecting group (**27** → **28**), the 2° alcohol was oxidized, and the trityl group was removed to produce hydroxyketone **29**. Elaboration to bromide **30**, followed by exposure to acetylguanidine for 4 days, installed the desired aminoimidazole segment (**31**) in 32% yield. At the time of Jiang's publication, our group had already independently prepared **31** and determined that it was not a productive route to dragmacidin D (see Chapter 2, reference 33).

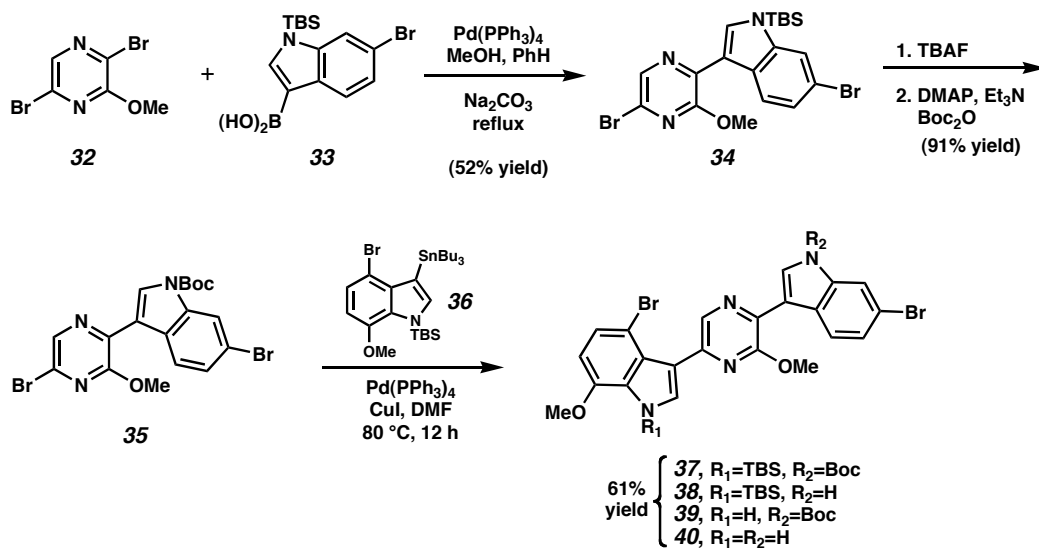
Scheme 1.4.3



1.4.4 Jiang's Second Generation Approach to the Pyrazinone Core

Following our publication describing the first total synthesis of dragmacidin D, Jiang reported a similar approach to construct the core of the natural product in the form of a bis(indole)pyrazine (Scheme 1.4.4).^{5k} First, dibromopyrazine **32** was cross-coupled with boronic acid **33** to afford indolopyrazine **34**. After switching protecting groups on the indole nitrogen (**34** → **35**), indolopyrazine **35** was coupled with stannane **36** to produce a mixture of pyrazine products (**37-40**) in 61% combined yield. An account describing the elaboration of **37-40** to the natural product (**5**) has yet to appear in the literature.

Scheme 1.4.4



1.5 Conclusion

The dragmacidin alkaloids are a unique class of molecules that are interesting from both a biological and structural standpoint. Although there has been synthetic work aimed at the piperazine dragmacidins (**1-4**), the pyrazinone-containing dragmacidins, D (**5**), E (**6**), and F (**7**), have received little attention from the synthetic community. Ultimately, synthetic routes to these natural products could be extremely valuable in the search for new medicines.

1.6 Notes and References

- (1) (a) Blunt, J. W.; Copp, B. R.; Munro, M. H. G.; Northcote, P. T.; Prinsep, M. R. *Nat. Prod. Rep.* **2004**, *21*, 1-49. (b) Aygün, A.; Pindur, U. *Curr. Med. Chem.* **2003**, *10*, 1113-1127. (c) Faulkner, D. J. *Nat. Prod. Rep.* **2002**, *19*, 1-48. (d) Pindur, U.; Lemster, T. *Curr. Med. Chem.* **2001**, *8*, 1681-1698.
- (2) (a) For staurosporine, see: Omura, S.; Iwai, Y.; Hirano, A.; Nakagawa, A.; Awaya, J.; Tsuchiya, H.; Takahashi, Y.; Masuma, R. *J. Antibiot.* **1977**, *30*, 275-289. (b) For conophylline, see: Kam, T.-S.; Pang, H.-S.; Lim, T.-M. *Org. Biomol. Chem.* **2003**, *1*, 1292-1297. (c) For yuehchukene, see: Kong, Y. C.; Cheng, K. F.; Cambie, R. C.; Waterman, P. G. *J. Chem. Soc., Chem. Commun.* **1985**, 47-48. (d) For vinblastine, see: Noble, R. L.; Beer, C. T.; Cutts, J. H. *Ann. N.Y. Acad. Sci.* **1958**, *76*, 882-894.
- (3) (a) Yang, C.-G.; Huang, H.; Jiang, B. *Curr. Org. Chem.* **2004**, *8*, 1691-1720. (b) Jin, Z. *Nat. Prod. Rep.* **2003**, *20*, 584-605. (c) Hibino, S.; Choshi, T. *Nat. Prod. Rep.* **2002**, *19*, 148-180. (d) Sasaki, S.; Ehara, T.; Sakata, I.; Fujino, Y.; Harada, N.; Kimura, J.; Nakamura, H.; Maeda, M. *Bioorg. Med. Chem. Lett.* **2001**, *11*, 583-585.
- (4) For the isolation of the piperazine-containing drarmacidins, see: (a) Kohmoto, S.; Kashman, Y.; McConnell, O. J.; Rinehart, K. L., Jr.; Wright, A.; Koehn, F. *J. Org. Chem.* **1988**, *53*, 3116-3118. (b) Morris, S. A.; Andersen, R. J. *Tetrahedron* **1990**,

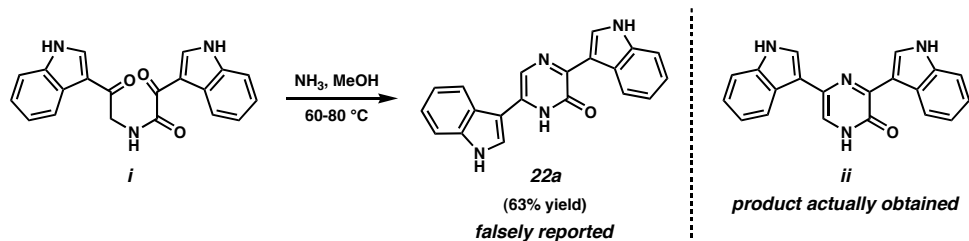
46, 715-720. (c) Fahy, E.; Potts, B. C. M.; Faulkner, D. J.; Smith, K. *J. Nat. Prod.* **1991**, *54*, 564-569. For the isolation of the pyrazinone-containing dragmacidins, see: (d) Wright, A. E.; Pomponi, S. A.; Cross, S. S.; McCarthy, P. *J. Org. Chem.* **1992**, *57*, 4772-4775. (e) Capon, R. J.; Rooney, F.; Murray, L. M.; Collins, E.; Sim, A. T. R.; Rostas, J. A. P.; Butler, M. S.; Carroll, A. R. *J. Nat. Prod.* **1998**, *61*, 660-662. (f) Cutignano, A.; Bifulco, G.; Bruno, I.; Casapullo, A.; Gomez-Paloma, L.; Riccio, R. *Tetrahedron* **2000**, *56*, 3743-3748. (g) Wright, A. E.; Pomponi, S. A.; Jacobs, R. S. PCT Int. Appl. WO 9942092, August 26, 1999.

- (5) For synthetic work aimed toward the piperazine-containing dragmacidins, see: (a) Jiang, B.; Smallheer, J. M.; Amaral-Ly, C.; Wuonola, M. A. *J. Org. Chem.* **1994**, *59*, 6823-6827. (b) Whitlock, C. R.; Cava, M. P. *Tetrahedron Lett.* **1994**, *35*, 371-374. (c) Kawasaki, T.; Enoki, H.; Matsumura, K.; Ohyama, M.; Inagawa, M.; Sakamoto, M. *Org. Lett.* **2000**, *2*, 3027-3029. (d) Miyake, F. Y.; Yakushijin, K.; Horne, D. A. *Org. Lett.* **2000**, *2*, 3185-3187. (e) Yang, C.-G.; Wang, J.; Tang, X.-X.; Jiang, B. *Tetrahedron: Asymmetry* **2002**, *13*, 383-394. (f) Kawasaki, T.; Ohno, K.; Enoki, H.; Umemoto, Y.; Sakamoto, M. *Tetrahedron Lett.* **2002**, *43*, 4245-4248. For studies targeting dragmacidins D, E, or F, see: (g) Jiang, B.; Gu, X.-H. *Bioorg. Med. Chem.* **2000**, *8*, 363-371. (h) Jiang, B.; Gu, X.-H. *Heterocycles* **2000**, *53*, 1559-1568. (i) Yang, C.-G.; Wang, J.; Jiang, B. *Tetrahedron Lett.* **2002**, *43*, 1063-1066. (j) Miyake, F. Y.; Yakushijin, K.; Horne, D. A. *Org. Lett.* **2002**, *4*, 941-943. (k) Yang, C.-G.; Liu, G.; Jiang, B. *J. Org. Chem.* **2002**, *67*, 9392-9396.

- (6) For the isolation of topsentin natural products, see: (a) Bartik, K.; Braekman, J.-C.; Daloze, D.; Stoller, C.; Huysecom, J.; Vendevyver, G.; Ottinger, R. *Can. J. Chem.* **1987**, *65*, 2118-2121. (b) Tsujii, S.; Rinehart, K. L.; Gunasekera, S. P.; Kashman, Y.; Cross, S. S.; Lui, M. S.; Pomponi, S. A.; Diaz, M. C. *J. Org. Chem.* **1988**, *53*, 5446-5453. (c) Murray, L. M.; Lim, T. K.; Hooper, J. N. A.; Capon, R. J. *Aust. J. Chem.* **1995**, *48*, 2053-2058. (d) Shin, J.; Seo, Y.; Cho, K. W.; Rho, J.-R.; Sim, C. J. *J. Nat. Prod.* **2000**, *62*, 647-649.
- (7) For the isolation of hamacanthins and dihydrohamacanthins, see: (a) Gunasekera, S. P.; McCarthy, P. J.; Kelly-Borges, M. *J. Nat. Prod.* **1994**, *57*, 1437-1441. (b) Casapullo, A.; Bifulco, G.; Bruno, I.; Riccio, R. *J. Nat. Prod.* **2000**, *63*, 447-451.
- (8) For reviews regarding protein phosphatases, see: (a) McCluskey, A.; Sim, A. T. R.; Sakoff, J. A. *J. Med. Chem.* **2002**, *45*, 1151-1175. (b) Burke, T. R.; Zhang, Z.-Y. *Biopolymers* **1998**, *47*, 225-241. (c) Sheppeck, J. E.; Gauss, C.-M.; Chamberlin, A. R. *Bioorg. Med. Chem.* **1997**, *5*, 1739-1750.
- (9) Longley, R. E.; Isbrucker, R. A.; Wright, A. E. U.S. Patent 6,087,363, July 11, 2000.
- (10) (a) Kerwin, J. F., Jr.; Lancaster, J. R., Jr.; Feldman, P. L. *J. Med. Chem.* **1995**, *38*, 4343-4362. (b) Schmidt, H. H. W.; Walter, U. *Cell* **1994**, *78*, 919-925. (c) Mocada, S.; Palmer, R. M. J.; Higgs, E. A. *Pharmacol. Rev.* **1991**, *43*, 109-142.

- (11) (a) Marletta, M. A. *J. Med. Chem.* **1994**, *37*, 1899-1907. (b) Molina, J. A.; Jimenez-Jimenez, F. J.; Orti-Pareja, M.; Navarro, J. A. *Drugs Aging* **1998**, *12*, 251-259. (c) Thorns, V.; Hansen, L. M. *Exp. Neurol.* **1998**, *150*, 14-20.
- (12) (a) Ulhaq, S.; Naylor, M. A.; Chinje, E. C.; Threadgill, M. D.; Stratford, I. J. *Anti-Cancer Drug Des.* **1997**, *12*, 61-65. (b) Aoki, S.; Ye, Y.; Higuchi, K.; Takashima, A.; Tanaka, Y.; Kitagawa, I.; Kobayashi, M. *Chem. Pharm. Bull.* **2001**, *49*, 1372-1374.
- (13) Jacobs, R. S.; Pomponi, S.; Gunasekera, S.; Wright, A. PCT Int. Appl. WO 9818466, May 7, 1998.
- (14) For a review regarding the biosynthesis of indole alkaloids derived from plants, see: Kutney, J. P. *Nat. Prod. Rep.* **1990**, *7*, 85-103.
- (15) (a) MacDonald, J. C. *J. Biol. Chem.* **1961**, *236*, 512-514. (b) Leete, E.; Bjorklund, J. A.; Reineccius, G. A.; Chen, T.-B. *Spec. Publ.-R. Soc. Chem.* **1992**, *95*, 75-95.
- (16) For a review regarding the biosynthesis of halogenated marine natural products, see: Butler, A.; Carter-Franklin, J. N. *Nat. Prod. Rep.* **2004**, *21*, 180-188.
- (17) McIntire, W. S.; Wemmer, D. E.; Chistoserdov, A.; Lidstrom, M. E. *Science* **1991**, *252*, 817-824.

- (18) Jiang reported the synthesis of bis(indole)pyrazinone **22a** by the amination/cyclization of **i**. It is likely that *m*-substituted product **ii** actually formed during this reaction. See reference 5h.



- (19) For the Leimgruber-Batcho indole synthesis, see: Batcho, A. D.; Leimgruber, W. *Org. Synth.* **1985**, 63, 214-225, and references therein.
- (20) We also explored a Leimgruber-Batcho route to 4,7-disubstituted indoles. See Chapter 2, section 2.3.3 and references 22 and 28.

CHAPTER TWO

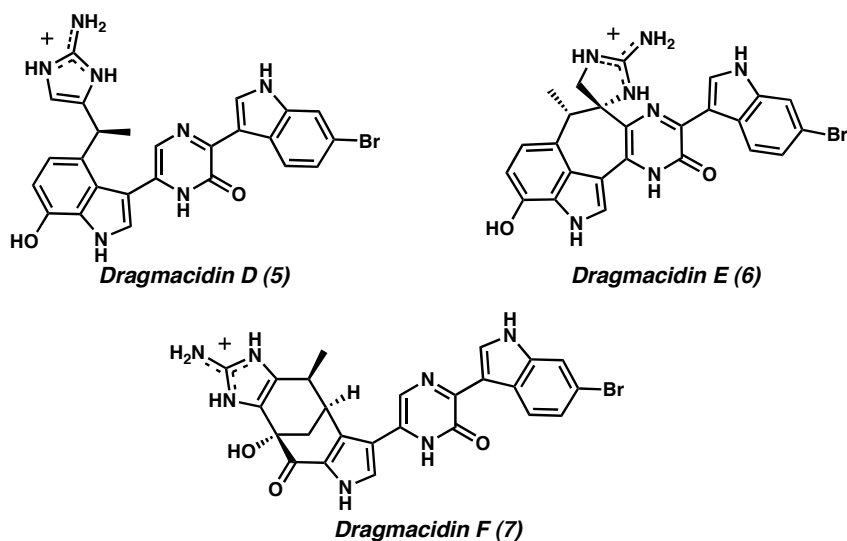
The Total Synthesis of Dragmacidin D[†]

2.1 Background

2.1.1 Introduction

In 2000, the pyrazinone-containing dragmacidins, namely, dragmacidins D, E, and F, were selected as formidable synthetic targets for our laboratory (Figure 2.1.1).¹ Initially, we chose to pursue the total synthesis of dragmacidin D (**5**),^{1a,b} predominantly because it was believed to be the biosynthetic precursor to dragmacidins E (**6**) and F (**7**).^{1c} In addition, **5** appeared to be the simplest of the pyrazinone-containing family members. Thus, we hoped to develop a strategy for the preparation of dragmacidin D (**5**) that would be amenable to the synthesis of the other complex dragmacidin natural products.²

Figure 2.1.1



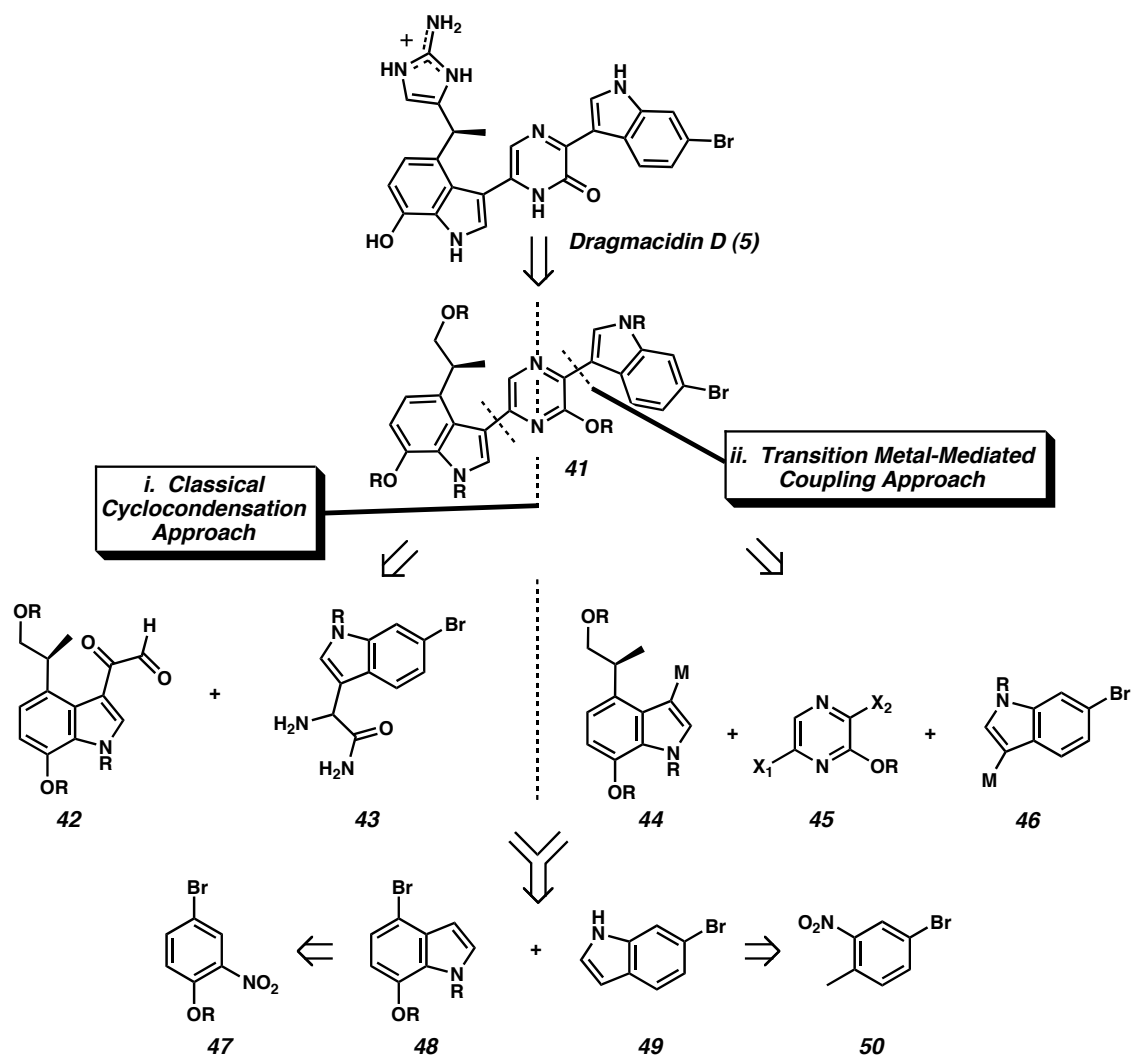
[†] This work was performed in collaboration with Dr. Richmond Sarpong, a postdoctoral scholar in the Stoltz group.

When considering the structure of dragmacidin D (**5**), several synthetic challenges become apparent. Dragmacidin D possesses a total of seven nitrogen atoms, three of which are incorporated in the aminoimidazole moiety, while two are within the pyrazinone core. The compound contains an unusual bis(indole) architecture featuring a 3,4,7-trisubstituted indole and a 3,6-disubstituted indole. Both of these indole substitution patterns are known to be synthetically challenging targets.³ It was predicted that dragmacidin D, as well as many of its synthetic precursors, would be highly polar, extremely reactive, and perhaps difficult to handle in a laboratory setting.

2.1.2 Retrosynthetic Analysis of Dragmacidin D

Two retrosynthetic strategies for the synthesis of dragmacidin D are presented in Scheme 2.1.1. As a critical maneuver, we chose to introduce the aminoimidazole moiety at a late stage in the synthesis in order to facilitate the handling of key precursors. Thus, disconnection of the aminoimidazole in the natural product (**5**) provided ether **41**. We then targeted **41** through two complementary routes: *i*) a classical cyclocondensation approach⁴ and *ii*) a more modern transition metal-mediated cross-coupling approach.⁵ In approach *i*, the pyrazinone system would be constructed through the linkage of two functionalized indole units (**42** + **43**), while in route *ii*, the dragmacidin core was envisioned to arise by a stepwise three-component coupling sequence (**44** + **45** + **46**). Both routes relied on the same indole building blocks (**48** and **49**), which were readily available from simple aromatic starting materials **47** and **50**, respectively.

Scheme 2.1.1

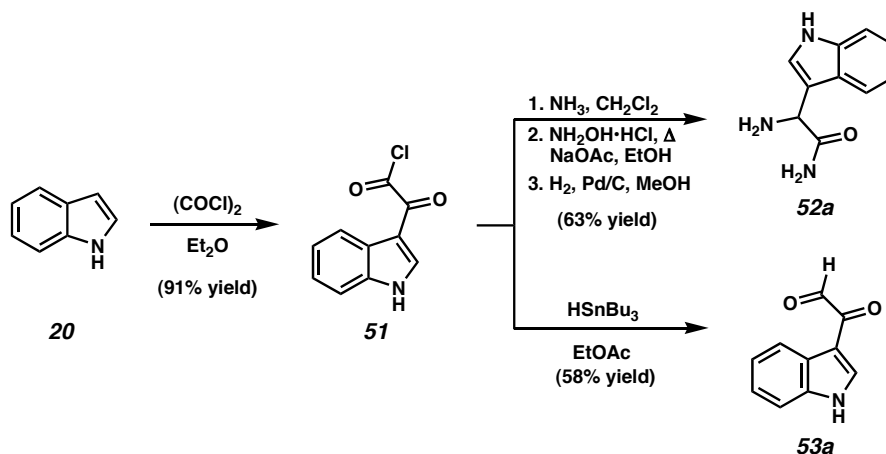


2.2 The Cyclocondensation Approach to Access the Bis(indole) Framework

Our initial efforts toward the total synthesis of dragmacidin D (**5**) focused on the cyclocondensation approach (i). A model system for the preparation of the pyrazinone core (i.e., **22a**) was explored. Treatment of indole (**20**) with oxalyl chloride produced **51** in high yield (Scheme 2.2.1).⁶ This compound was then employed as a common intermediate for the synthesis of the unsubstituted coupling fragments **52a** and **53a**. The synthesis of aminoamide **52a** proceeded via elaboration of **51** by a sequence involving: a)

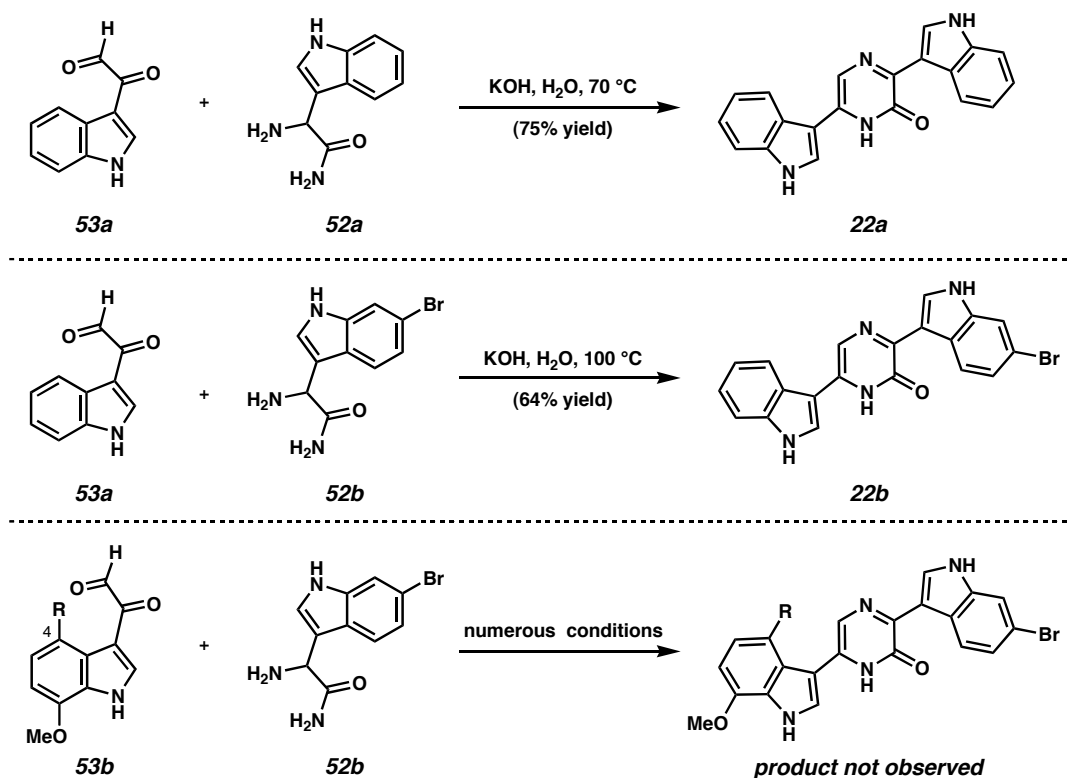
amidation using ammonia, b) oxime formation, and c) reduction using hydrogen, catalyzed by palladium on carbon. Ketoaldehyde **53a** was prepared directly by reduction of **51** with tributyltin hydride.⁷

Scheme 2.2.1



With the key fragments in hand, we investigated the viability of the cyclocondensation reaction (Scheme 2.2.2). Upon exposure to heated aqueous potassium hydroxide, compounds **52a** and **53a** underwent smooth conversion to the desired pyrazinone **22a** in good yield, as the only observed product of the reaction. Under similar conditions, bromide **52b**⁸ also participated in the pyrazinone-forming reaction (**53a** + **52b** \rightarrow **22b**). However, under our optimized conditions, as well as a variety of others (Bronsted acids and bases, Lewis acids), we were unable to effect cyclocondensative coupling with any C(4)-substituted ketoaldehyde derivative (i.e., **53b**).⁹

Scheme 2.2.2



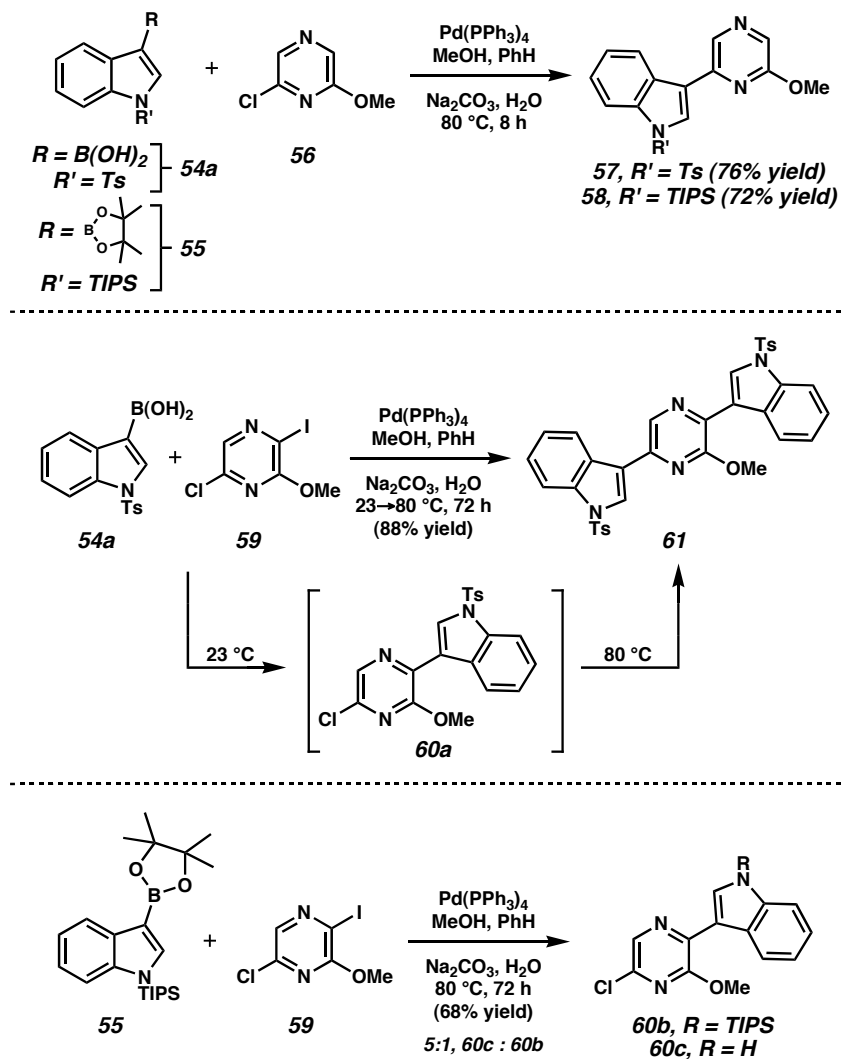
2.3 The Metal-Mediated Strategy to Construct the Bis(indole) Framework

We turned our attention to the alternative retrosynthetic strategy, the transition metal-catalyzed cross-coupling route *ii*. The ability to carry the 6-bromoindole moiety directly through the reaction sequence would be critical for the success of our plan. The synthesis clearly became an issue of strategy involving not only the exact order of the coupling reactions, but also the specific identity of each substrate involved. The appropriate selection of halides, metals, and protecting groups would be crucial. We thus turned our attention toward experiments that would delineate suitable conditions for coupling.

2.3.1 The Development of Suitable Conditions for Selective Cross-Couplings

We initially surveyed a variety of coupling reactions involving model indoles and various halogenated pyrazine derivatives in order to assess the relative reactivity of such systems as well as the suitability of the protective groups on the indole nitrogen. It was quickly established that halogenated pyrazines are highly reactive toward palladium-mediated couplings to metalated indoles. Furthermore, the oxidative addition of palladium(0) to pyrazinyl halides is more facile than to simple aromatic halides.¹⁰ For example, reaction of borylated indoles **54a** and **55** with readily available chloropyrazine **56**¹¹ proceeded smoothly at 80 °C under standard Suzuki conditions to afford coupled products **57** and **58** (Scheme 2.3.1). Under identical conditions, simple aryl chlorides do not readily participate in such couplings.¹² Additionally, treatment of chloriodopyrazine **59** with 2 equiv of indole **54a** at 23 °C produced indolylpyrazine **60a** exclusively, while raising the temperature to 80 °C resulted in the formation of the bis(indole)pyrazine **61**. A more surprising development was observed upon treatment of pyrazine **59** with an excess of silylated boronic ester **55** (2.3 equiv) at 80 °C. Under these conditions, exclusively monocoupled product was obtained as a mixture of silylated and desilylated compounds (**60b** and **60c**). This difference in reactivity points to a remote electronic effect of the indole protecting group on the activation of the intermediate chloroindolylpyrazine (**60**) toward coupling.

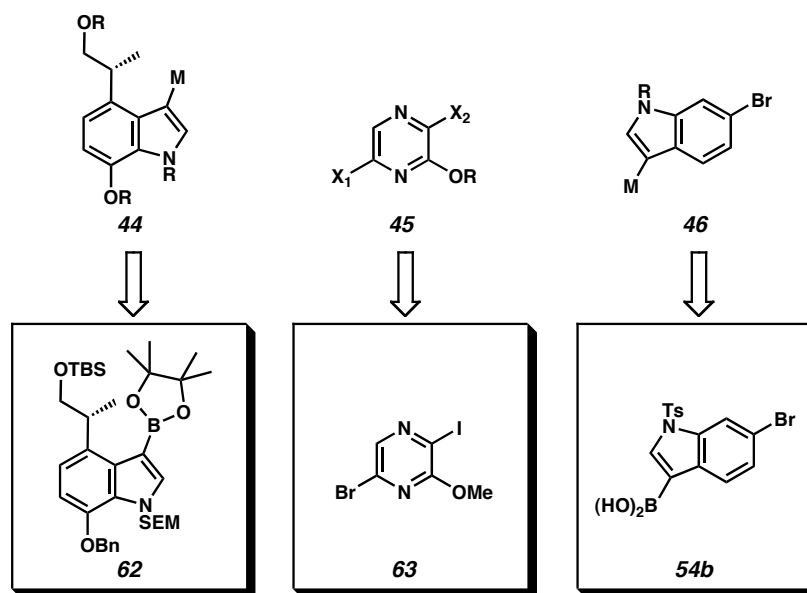
Scheme 2.3.1



Having conducted these simple experiments, we began to identify appropriate substitution patterns for building blocks **44**, **45**, and **46** (Figure 2.3.1). It was immediately clear that the use of Suzuki couplings would be favorable due to our success in the model systems. Thus, boron substituents were employed as the metal species for both indole substrates (**44** and **46**). In addition, the protecting groups for indoles **44** and **46** were chosen in a manner that optimized orthogonality with respect to deprotection, which would facilitate control during late-stage manipulations. In particular, the *N*-

protecting groups were very carefully selected. The SEM group¹³ of **62** was considered ideal due to its marked stability and electron-donating nature, while the Ts group of **54b** was preferred mainly because of its success in the model system studies. Perhaps the most important decision was the selection of halogens X_1 and X_2 of pyrazine **45**. Although chloriodopyrazine **59** was utilized in the model systems described above, it was believed that replacing the chloride with a bromide would allow for better position selectivity.¹⁴ Thus, bromiodopyrazine **63** was selected as the key synthetic fragment. We then proceeded to develop rapid syntheses of the three essential pieces (**62**, **63**, and **54b**).

Figure 2.3.1

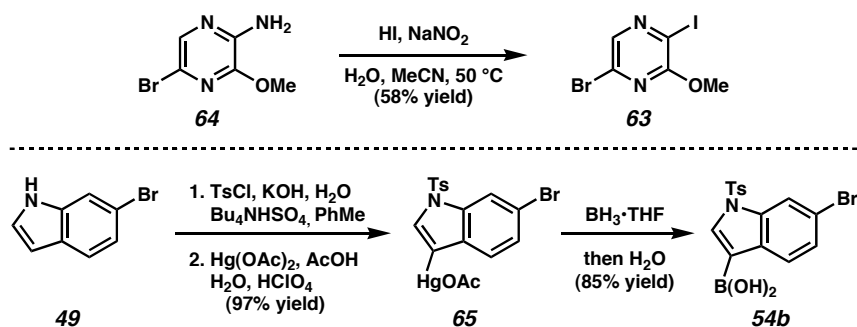


2.3.2 Synthesis of Pyrazine and Bromoindole Fragments

The key differentially halogenated pyrazine fragment **63** was readily prepared via iodide displacement of the in situ prepared diazonium salt of aminopyrazine **64**¹⁵

(Scheme 2.3.2).¹⁶ Bromoindole boronic acid derivative **54b** was synthesized from parent indole **49**¹⁷ by protection of the indole nitrogen,¹⁸ treatment with mercuric acetate, and reaction of the resulting organomercurial (**65**) with borane•THF complex followed by hydrolytic work-up (82% yield, 3 steps).¹⁹

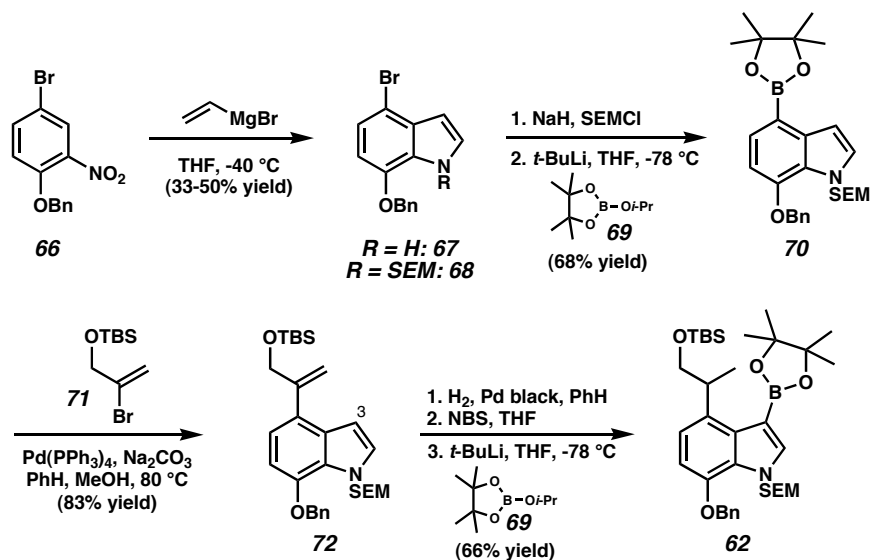
Scheme 2.3.2



2.3.3 Synthesis of the 3,4,7-Trisubstituted Indole Fragment

The 3,4,7-trisubstituted indole fragment (**62**) was synthesized by the Bartoli indolization reaction (Scheme 2.3.3).²⁰ Treatment of nitroaromatic **66**²¹ with vinyl Grignard produced the highly functionalized indole **67** directly. Although the yield of this reaction was variable and modest, we were able to prepare **67** on multigram scale.²² Following protection of the indole nitrogen by a 2-(trimethylsilyl)ethoxymethyl (SEM) group (**67** → **68**),¹³ halogen-metal exchange and trapping with dioxaborolane reagent **69** produced metalloindole **70**.²³ Suzuki coupling of **70** with the known vinyl bromide **71**,²⁴ smoothly provided olefin **72**.²⁵ Final conversion of **72** to the coupling fragment **62** was accomplished using a sequence involving selective hydrogenation of the terminal olefin,²⁶ bromination at the C(3) position,²⁷ and halogen-metal exchange/trapping with the dioxaborolane reagent (**69**).²⁸

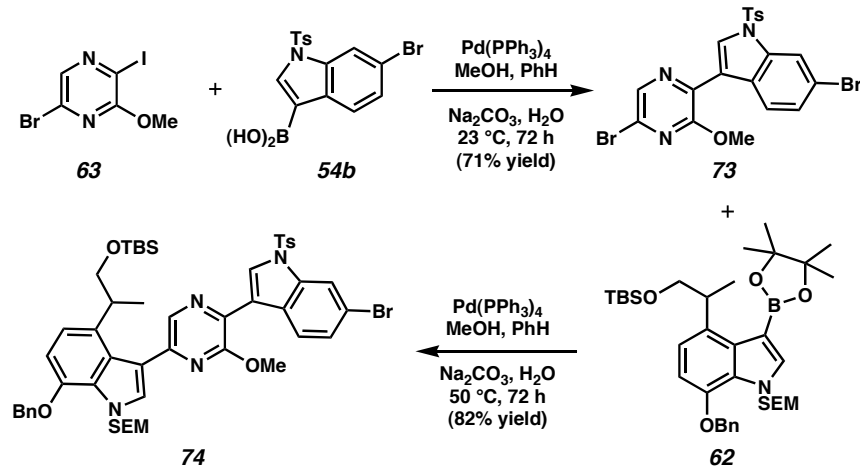
Scheme 2.3.3



2.3.4 Construction of the Fully Substituted Bis(indole)pyrazinone Core

With the appropriate fragments in hand (**62**, **63**, and **54b**), the critical three-component coupling reaction sequence was explored. Suzuki coupling of dihalopyrazine **63** and indole **54b** proceeded selectively to afford the coupled indolylpyrazine **73** (Scheme 2.3.4). In the second Suzuki coupling of dibromide **73** with boronic ester **62**, we were delighted to find that the desired bis(indole)pyrazine **74** formed in good yield and with complete selectivity for coupling of the pyrazinyl bromide in the presence of the indolyl bromide. Precise temperature control was critical for the success of both coupling reactions (23 °C and 50 °C, respectively). Importantly, the selectivity of the second Suzuki reaction depended not only on temperature, but also on the exact identity of each coupling substrate. In fact, varying protective groups on the indole nitrogen in **54a** had a dramatic effect on halide reactivity, as competitive coupling of the indolyl bromide occurred when electron-donating *N*-protective groups were employed.

Scheme 2.3.4



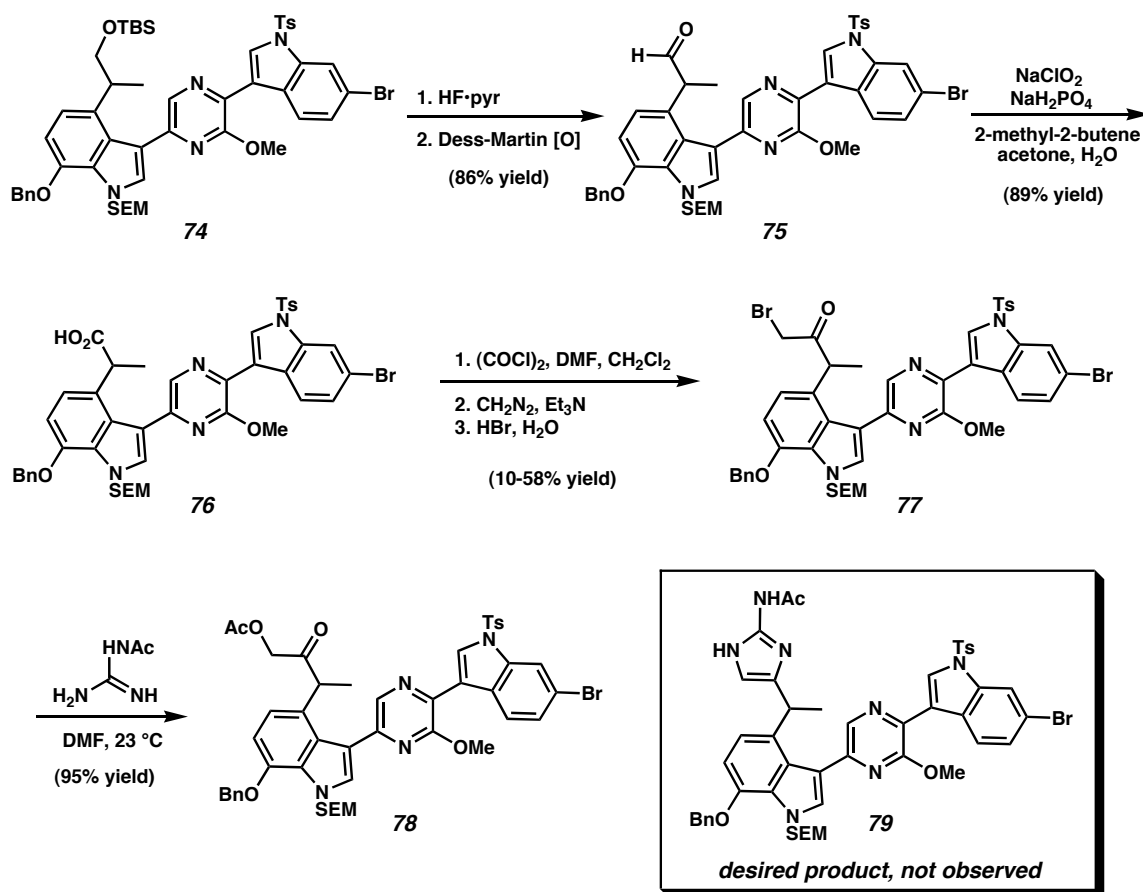
2.4 End-Game Studies

2.4.1 End-Game Strategy 1

Having established a viable route to the core structure of dragmacidin D (**5**), we focused our efforts on completing the natural product synthesis. Selective cleavage of the silyl ether in **74**,²⁹ followed by Dess-Martin oxidation³⁰ furnished aldehyde **75**, which was further oxidized to its carboxylic acid derivative **76** (Scheme 2.4.1). Conversion of **76** to bromoketone **77** was accomplished by an Arndt-Eistert-type homologation, followed by treatment with aqueous HBr. The extreme sensitivity of the intermediate acid chloride was particularly troublesome and required that the diazomethane used in the reaction sequence be dried thoroughly over both potassium hydroxide and sodium metal immediately before use.³¹ In addition, chemical yields for this homologation varied to a large extent and caused substantial material throughput problems. Nonetheless, with bromide **77** in hand, we explored installation of the aminoimidazole functionality. Reaction of bromide **77** with acetylguanidine in DMF was anticipated to produce aminoimidazole **79** based on model studies.^{32,33} However, the only product observed in

the reaction was acetoxyketone **78**, in quantitative yield. Although a variety of guanidine sources, solvents, and temperatures were explored to promote the synthesis of aminoimidazole **79**, all of our efforts resulted in the formation of the same undesired product (**78**).

Scheme 2.4.1

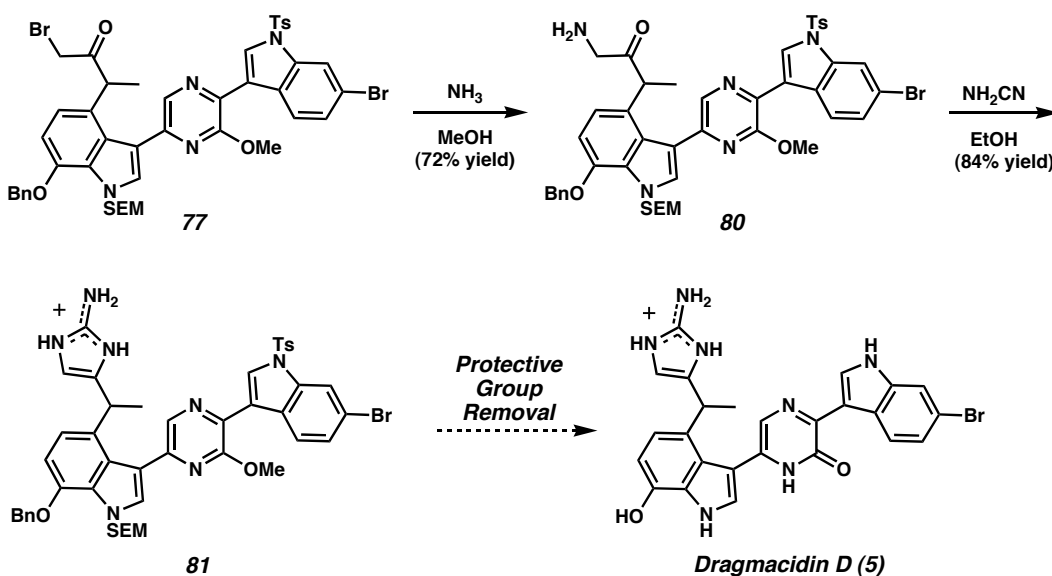


2.4.2 End-Game Strategy 2

Through our studies it was observed that nucleophilic displacement of the alkyl bromide in **77** was actually a facile process. Thus, we considered an alternative end-game strategy that would exploit this reactivity (Scheme 2.4.2). Treatment of **77** with

ammonia afforded aminoketone **80** which, in turn, underwent facile condensation with cyanamide to produce the desired aminoimidazole product (**81**).³⁴ At this point, all that remained in order to complete the total synthesis of dragmacidin D (**5**) was the removal of the four protective groups from **81**. Despite several months of experimentation, our efforts to complete the total synthesis of (**5**) were accompanied by decomposition of the aminoimidazole moiety, which was exceptionally unstable to the basic conditions needed to remove the protective groups that we had strategically chosen (*vide supra*).

Scheme 2.4.2

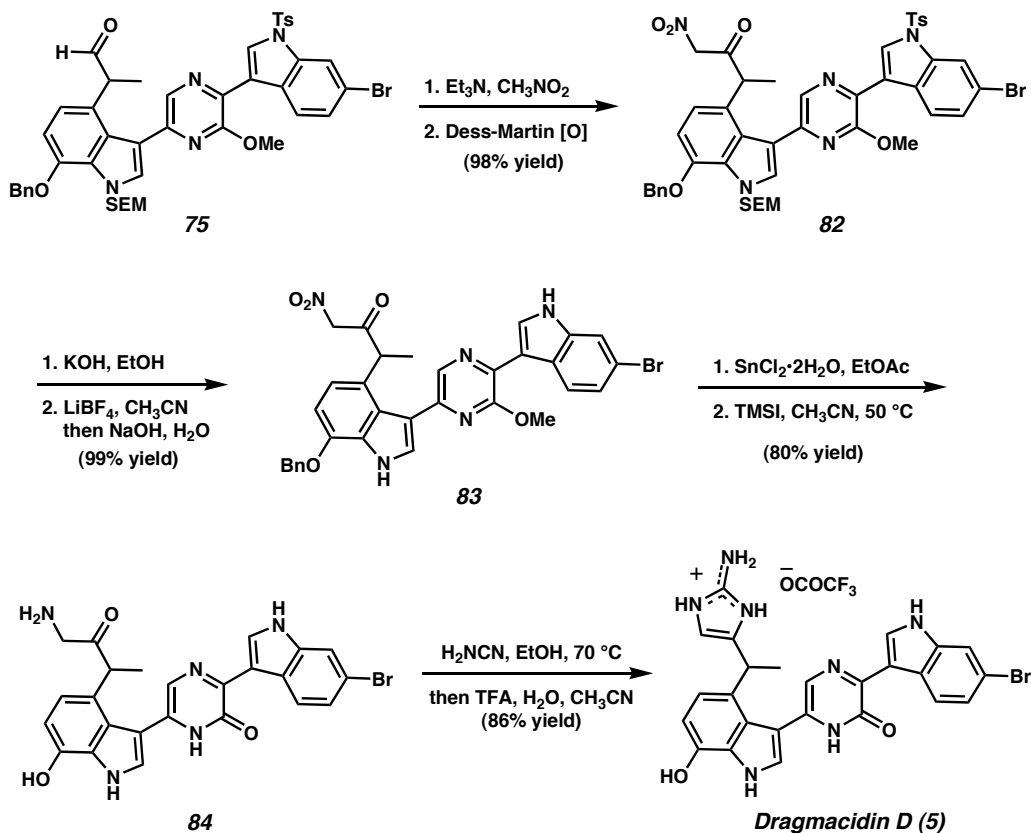


2.4.3 End-Game Strategy 3: The Total Synthesis of Dragmacidin D

The possibility of installing the aminoimidazole as the last step of the total synthesis, after the full deprotection of a late-stage intermediate, was explored next. In addition, we sought an alternative one-carbon homologation reaction in place of the unreliable Arndt-Eistert sequence. After extensive experimentation, we found that

nitromethane addition³⁵ to aldehyde **75** and subsequent oxidation produced **82** in high yield (Scheme 2.4.3).³⁶ Deoxygenated ethanolic potassium hydroxide facilitated removal of the *N*-tosyl group,³⁷ while lithium tetrafluoroborate followed by aqueous sodium hydroxide effected complete hydrolysis of the SEM group (**82** → **83**). Reduction of nitroketone **83** with stannous chloride,³⁸ then cleavage of the benzyl and methyl ethers with iodotrimethylsilane, revealed fully deprotected aminoketone **84**.³⁹ Final installation of the aminoimidazolium unit occurred by treatment of **84** with cyanamide followed by trifluoroacetic acid workup to produce the natural product (**5**) in 86% yield. Synthetic dragmacidin D (**5**) was spectroscopically identical to samples obtained from natural sources (Figure 2.4.1).

Scheme 2.4.3



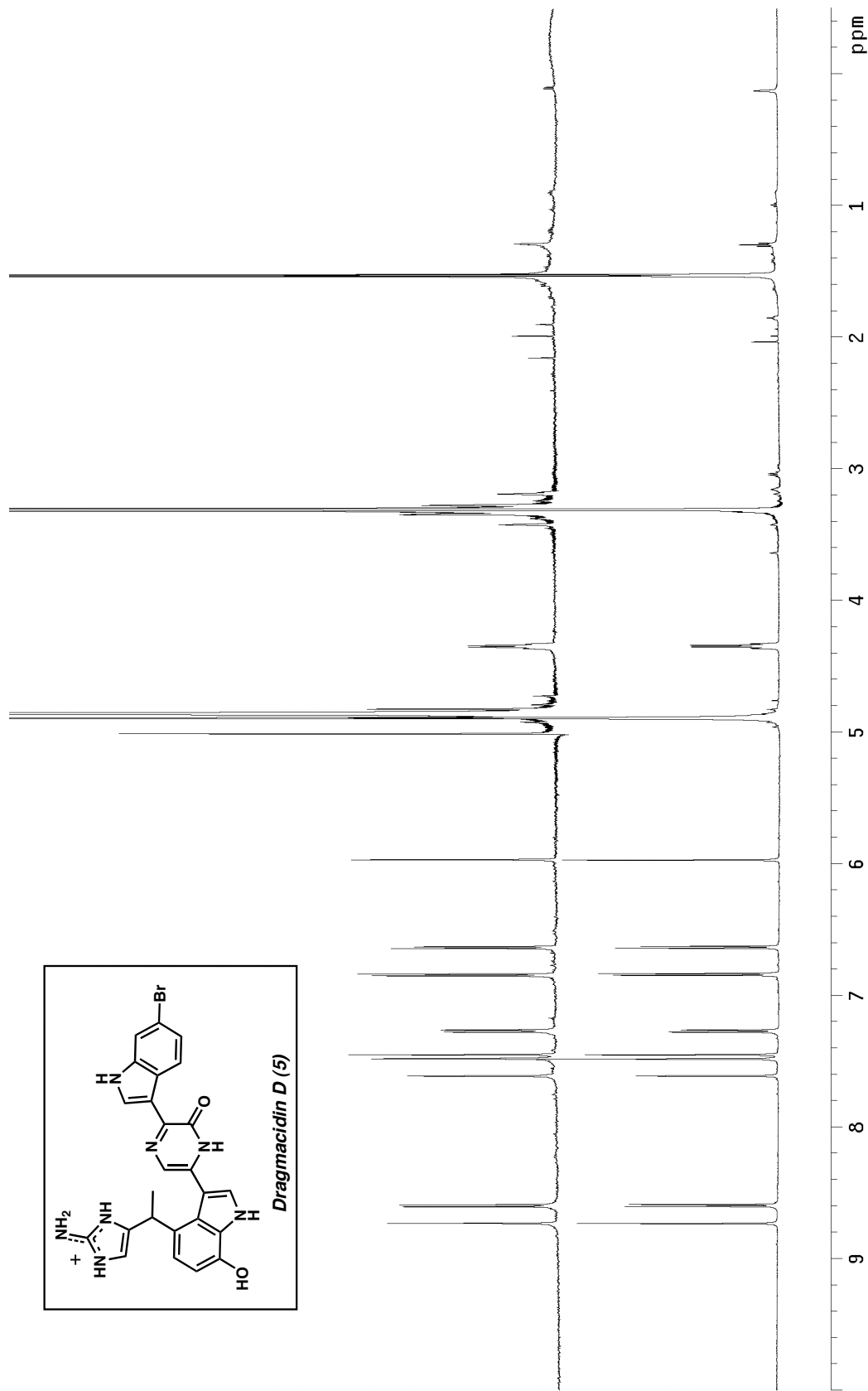


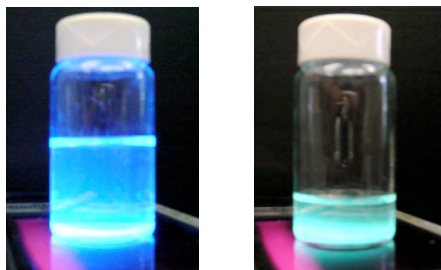
Figure 2.4.1 ¹H NMR (600 MHz, CD₃OD) of Dragmacidin D (5); natural (top) and synthetic (bottom).

2.4.4 Subtleties of Late-Stage Manipulations

The exact order of final synthetic events presented herein was essential for the completion of dragmacidin D. In particular, intermediates **82** through **84** were highly labile when treated under a variety of other conditions. For example, attempts to reduce nitroketone **82** or to remove the SEM group prior to detosylation resulted in substantial nonspecific decomposition. Likewise, efforts to deprotect **83** prior to reduction of the nitro group led to decomposition of the nitroketone moiety. Finally, reversing the order of the final two steps (i.e., aminoimidazole formation followed by treatment with TMSI) afforded only a low yield of dragmacidin D (ca. 5%).

Also noteworthy is the brilliant fluorescent nature of most of the bis(indole) pyrazine/pyrazinone intermediates. By shining longwave UV light from a benchtop UV lamp ($\lambda = 365$ nm), we were able to monitor and isolate extremely small amounts of compounds in large quantities of solvent during necessary reversed-phase chromatography (i.e., ca. 1 mg/30-50 mL solvent). Two typical examples that demonstrate the fluorescent behavior of these compounds are shown below (Figure 2.4.2).⁴⁰

Figure 2.4.2



2.5 An Asymmetric Route to Dragmacidin D

With the racemic synthesis of dragmacidin D (**5**) completed, our attention turned to the development of an asymmetric route to the natural product. It was envisioned that the stereocenter present in **5** could arise from an asymmetric hydrogenation⁴¹ of **87**, a compound prepared readily from **68** via Fu-modified Stille coupling⁴² with **85**⁴³ followed by saponification (Scheme 2.5.1). Dr. Richmond Sarpong investigated the ruthenium-catalyzed asymmetric reduction of **87** by varying several reaction parameters including solvent, pressure, temperature, and additive effects (Table 2.5.1). Ultimately, hydrogenation of **87** in the presence of chiral ruthenium complex **89** under optimized conditions (78 atm of hydrogen, at -10 °C in MeOH) resulted in the formation of enantioenriched carboxylic acid **88** in 90% ee.

Scheme 2.5.1

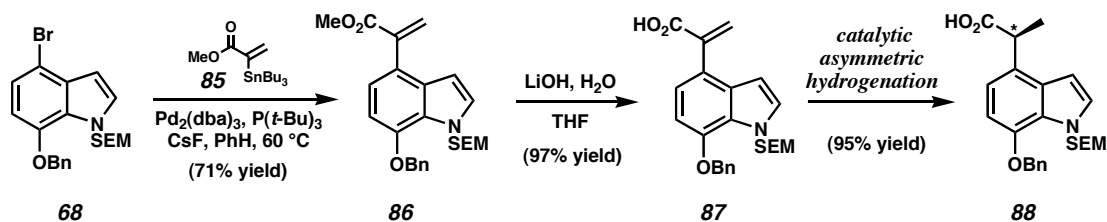
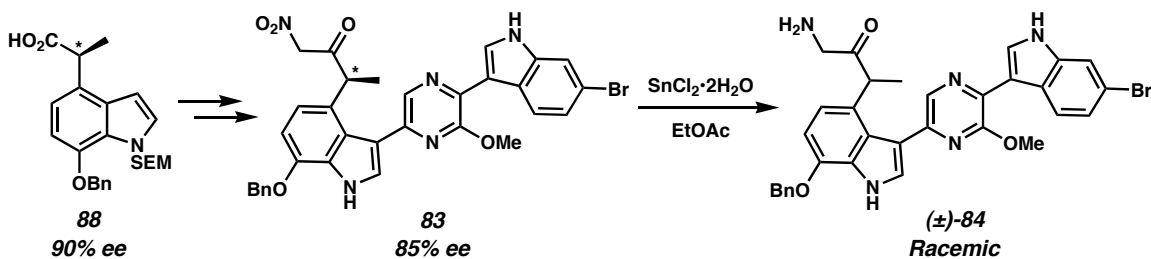


Table 2.5.1

catalyst	solvent	temp	additive	H ₂ pressure	time	conversion	ee
 89	MeOH	25 °C	—	30 atm	14 h	100%	83%
	MeOH/ CH ₂ Cl ₂ (1:1)	25 °C	—	30 atm	14 h	100%	59%
	CH ₂ Cl ₂	25 °C	—	30 atm	14 h	40%	0%
	MeOH	25 °C	Et ₃ N (1 equiv)	30 atm	14 h	100%	80%
	MeOH	5 °C	Et ₃ N (1 equiv)	30 atm	72 h	100%	86%
	MeOH	5 °C	—	30 atm	72 h	100%	87%
	MeOH	-10 °C	—	78 atm	72 h	100%	90%

Carboxylic acid **88** could be elaborated to nitroketone **83** without substantial loss in enantiomeric excess (Scheme 2.5.2). However, upon Sn(II)-promoted reduction to aminoketone **84**, racemization occurred. Alternative conditions to access enantiopure **84** were explored but were also unsuccessful at promoting reduction without epimerization of the benzylic α -keto stereocenter. The enantiopurity of natural dragmacidin D (**5**) is also somewhat uncertain. During the first isolation of **5**, no optical rotation could be detected.^{1a} Subsequently, a very small rotation value was reported ($[\alpha]_D +12^\circ$ (c 0.95, EtOH)).^{1b} Nonetheless, an asymmetric total synthesis of dragmacidin D remains an elusive goal.

Scheme 2.5.2



2.6 Conclusion

In summary, we have completed the first total synthesis of the important bis(indole) alkaloid dragmacidin D (**5**). The concise route that we have developed (longest linear sequence of 17 steps from **66**) relies on a series of halogen-selective Suzuki couplings and a meticulous late-stage sequence to complete the natural product synthesis.

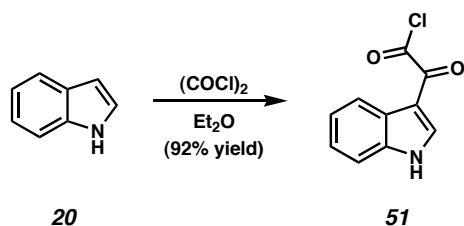
2.7 Experimental Section

2.7.1 Materials and Methods

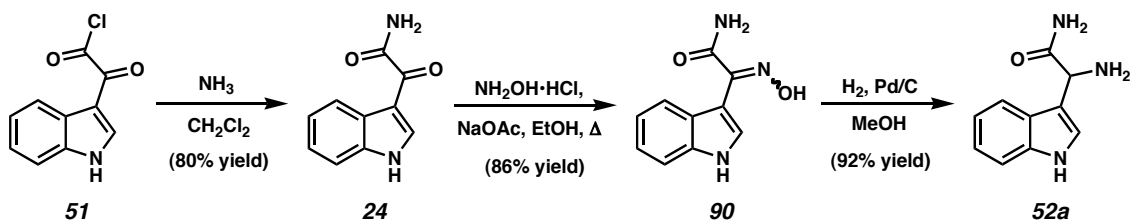
Unless stated otherwise, reactions were performed in flame-dried glassware under a nitrogen or argon atmosphere using dry, deoxygenated solvents. All other commercially obtained reagents were used as received. Solvents were dried by passage through an activated alumina column under argon. Reaction temperatures were controlled by an IKA Mag temperature modulator. Thin-layer chromatography (TLC) was performed using E. Merck silica gel 60 F254 precoated plates (0.25 mm) and visualized using a combination of UV, anisaldehyde, ceric ammonium molybdate, and potassium permanganate staining. ICN Silica gel (particle size 0.032-0.063 mm) was used for flash chromatography. Disposable Sep-Pak C₁₈ Vac Cartridges were purchased from Waters and used for all reversed-phase filtrations. HPLC analysis was performed on a Beckman Gold system using a Rainin C₁₈, Microsorb MV, 5 μ m, 300 x 4.6 mm reversed-phased column in 0.1% (w/v) TFA with acetonitrile/H₂O as eluent and a flow rate of 1.0 ml/min, gradient elution of 1.25% acetonitrile/min. Preparatory reversed-phase HPLC was performed on a Beckman HPLC with a Waters DeltaPak 25 x 100 mm, 100 mm C₁₈ column equipped with a guard, 0.1% (w/v) TFA with acetonitrile/H₂O as eluent, and gradient elution of 0.50% acetonitrile/min. For all reversed-phase purifications, H₂O (18M Ω) was obtained from a Millipore MiliQ water purification system and TFA from Halocarbon, Inc. ¹H and ¹³C NMR spectra were recorded on either a Varian Mercury 300 (at 300 MHz and 75 MHz, respectively), Varian Mercury 500 (at 500 MHz and 125 MHz, respectively), or on a Varian Mercury 600 (600 MHz for proton only) spectrometer and are reported relative to Me₄Si (δ 0.0). Data for ¹H NMR spectra

are reported as follows: chemical shift (δ ppm), multiplicity, coupling constant (Hz), and integration. Data for ^{13}C NMR spectra are reported in terms of chemical shift. IR spectra were recorded on a Perkin Elmer Paragon 1000 spectrometer and are reported in frequency of absorption (cm^{-1}). UV spectra were measured on a Hewlett-Packard Model 8452A diode array spectrophotometer. High resolution mass spectra were obtained from the UC Irvine Mass Spectral Facility. Chiral HPLC was performed on a Chiralcel AD column (4.6 mm x 25 cm) obtained from Daicel Chemical Industries, Ltd.

2.7.2 Preparative Procedures



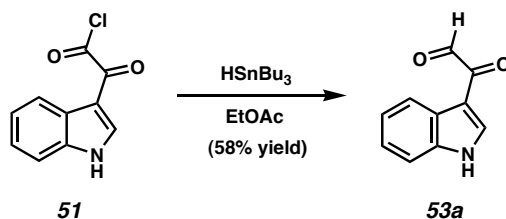
Glyoxal chloride 51. To a solution of indole **20** (20.0 g, 171 mmol) in anhydrous Et₂O (340 mL) at 0 °C, was added oxalyl chloride (17.3 mL, 198 mmol) dropwise over 30 min. The reaction mixture was stirred at 0 °C for 3 h, then allowed to warm to 23 °C over 1 h. The resulting yellow crystals were collected by filtration, washed with anhydrous Et₂O (100 mL), and dried under vacuum to yield **51** (32.52 g, 92% yield), which was used without further purification.



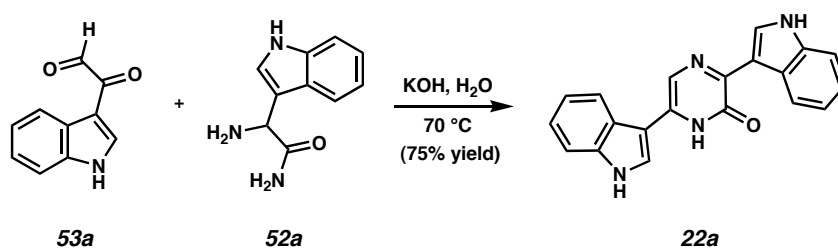
Aminoamide 52a. Gaseous ammonia was bubbled through a suspension of **51** (12.4 g, 59.7 mmol) in CH₂Cl₂ (300 mL) for 10 min. After stirring for 30 min, the solvent was removed under reduced pressure. Addition of H₂O (600 mL) was followed by extraction of the resulting heterogeneous mixture with EtOAc (2 x 600 mL). The combined organic layers were washed with brine (300 mL), dried over magnesium sulfate, and evaporated under reduced pressure to afford the crude amide **24** (9.0 g, 80% yield), which was used without further purification.

To a suspension of **24** (500 mg, 5.32 mmol) in CH₃OH (7.8 mL) was added hydroxylamine hydrochloride (2.0 g, 39.9 mmol) in H₂O (3.8 mL) and sodium acetate (1.64 g, 39.9 mmol) in H₂O (3.8 mL). The resulting heterogeneous mixture was heated under reflux for 10 h and allowed to cool to 23 °C. The solvent was removed under reduced pressure, and the remaining crude residue was extracted with EtOAc (3 x 20 mL). The combined organic layers were washed with brine (20 mL) and dried over sodium sulfate. After removal of solvent under reduced pressure, the crude residue was purified by flash chromatography (3:1 CH₂Cl₂/hexanes eluent) to afford oxime **90** (454 mg, 86% yield), which was used without further purification.

To a solution of **90** (4.07g, 20 mmol) in CH₃OH in a stainless steel bomb was added 10% palladium on charcoal (450 mg). The bomb was then purged with hydrogen and pressurized to 450 psi. After stirring for 14 h at 23 °C, the palladium on carbon was removed via filtration, and the solvent was removed under reduced pressure. Passage through a plug of celite (CH₃OH eluent) afforded the desired aminoamide **52a** (3.5 g, 92% yield) as a yellow oil: *R_f* 0.10 (5:1 EtOAc:CH₃OH); ¹H NMR (300 MHz, DMSO-*d*₆) δ 10.93 (s, 1H), 7.71 (d, *J* = 7.7 Hz, 1H), 7.43 (s, 1H), 7.33 (d, *J* = 7.7 Hz, 1H), 7.23 (s, 1H), 7.07-6.93 (comp. m, 3H), 4.56 (s, 1H), 2.38 (br s, 2H); ¹³C NMR (75 MHz, DMSO-*d*₆) δ 175.9, 136.2, 125.7, 122.8, 120.9, 119.5, 118.2, 116.2, 111.3, 52.5; IR (film) 3176, 1660, 1592 cm⁻¹; HRMS-NH₃Cl (*m/z*): [M + H]⁺ calc'd for C₁₀H₁₂N₃O, 190.0980; found, 190.0978.

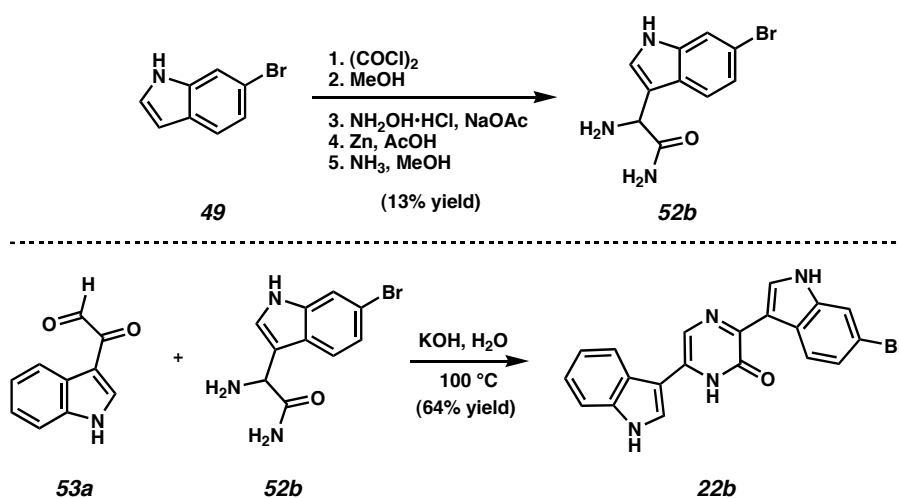


Ketoaldehyde 53a. To a suspension of **51** (22.0 g, 106 mmol) in EtOAc (106 mL) at 0 °C, was added a solution of tributyltin hydride (28.5 mL, 106 mmol) in EtOAc (158 mL). The reaction mixture was stirred at 0 °C for 30 min, warmed to 23 °C, then stirred for an additional 15 h. Hexanes (150 mL) was added, and the resulting yellow powder was collected by filtration. Washing with copious amounts of hexanes (1 L) and drying under vacuum, gave ketoaldehyde **53a** (10.6 g, 58% yield): R_f 0.76 (13:7 CHCl₃:CH₃OH); ¹H NMR (300 MHz, acetone-*d*₆) δ 9.54 (s, 1H), 8.65 (s, 1H), 8.36-8.33 (comp. m, 1H), 7.61-7.58 (comp. m, 1H), 7.33-7.29 (comp. m, 2H); ¹³C NMR (75 MHz, acetone-*d*₆) δ 192.9, 183.2, 138.1, 125.3, 124.6, 124.1, 123.5, 123.1, 113.6, 113.3; IR (film) 3117, 1628, 1580, 1518, 1234 cm⁻¹; HRMS-NH₃Cl (*m/z*): [M + H]⁺ calc'd for C₁₀H₈NO₂, 174.0555; found, 174.0555.



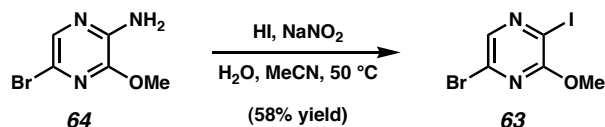
Pyrazinone 22a. To H₂O (17 mL) at 70 °C was added ketoaldehyde **53a** (300 mg, 1.73 mmol) and aminoamide **52a** (321 mg, 1.73 mmol), followed by powdered potassium hydroxide (487 mg, 8.67 mmol). After stirring at 70 °C for 5 h, the reaction mixture was allowed to cool to 23 °C, poured into saturated aq. ammonium chloride (75

mL), and extracted with EtOAc (4 x 75 mL). The combined organic layers were dried briefly over sodium sulfate and concentrated under reduced pressure to afford the desired pyrazinone **22a** (423 mg, 75% yield) as an orange/red solid: R_f 0.57 (5:1 CH_2Cl_2 : CH_3OH); ^1H NMR (300 MHz, $\text{DMSO}-d_6$) δ 12.23 (s, 1H), 11.75 (s, 1H), 11.52 (s, 1H), 8.75 (s, 1H), 8.69 (d, $J = 7.3$ Hz, 1H), 8.11 (d, $J = 2.6$ Hz, 1H), 8.40-7.82 (comp. m, 2H), 7.51-7.45 (comp. m, 2H), 7.25-7.12 (comp. m, 4H); ^{13}C NMR (125 MHz, $\text{DMSO}-d_6$) δ 155.5, 147.2, 136.8, 136.2, 130.1, 126.3, 125.9, 124.1, 122.7, 122.2, 122.0, 120.6, 120.1, 119.7, 112.2, 111.9, 111.6, 106.8; IR (film) 3307, 1633, 1602, 1421 cm^{-1} ; HRMS-ESI (m/z): $[\text{M} + \text{Na}]^+$ calc'd for $\text{C}_{20}\text{H}_{15}\text{N}_4\text{ONa}$, 349.1065; found, 349.1070.

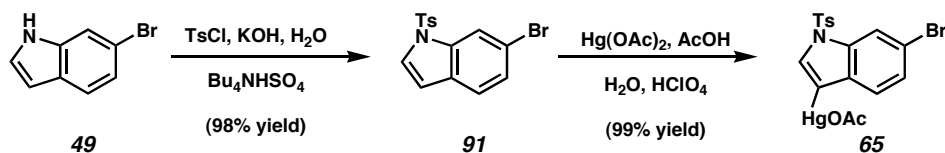


Bromopyrazinone 22b. To a solution of bromoindole **49**¹⁷ (3.4 g, 17.3 mmol) in anhydrous Et_2O (35 mL) at 0 °C was added oxalyl chloride (1.76 mL, 20.1 mmol) dropwise over 30 min. The reaction mixture was stirred at 0 °C for 3 h, then allowed to warm to 23 °C over 1 h. The resulting yellow crystals were collected by filtration, washed with anhydrous Et_2O (15 mL), and dried under vacuum. To a suspension of these crystals at 0 °C in CH_2Cl_2 (70 mL) was added MeOH (2.2 mL, 70 mmol). The reaction

mixture was warmed to 23 °C, stirred for 12 h, and then filtered to collect the product. To this crude material in MeOH (87 mL) was added NaOAc (8.09g, 98.4 mmol) in H₂O (19 mL), followed by NH₂OH•HCl (9.84 g, 98.4 mmol) in H₂O (19 mL). The mixture was heated to 80 °C for 24 h then cooled to 23 °C. After removal of solvent under reduced pressure, the aqueous residue was extracted with EtOAc (3 x 50 mL). The combined organic layers were washed with brine (30 mL) and evaporated in vacuo. The resulting material was purified by flash chromatography (2:1 EtOAc:hexanes eluent) to afford an off-white solid. To this compound in MeOH (84 mL) was added 1 N HCl (84 mL) followed by zinc dust (2.75 g, 42.1 mmol). The reaction mixture was stirred for 10 min and filtered (MeOH eluent). The filtrate was evaporated under reduced pressure to afford an off-white solid that was triturated with CH₂Cl₂, diluted with 1 N NaOH (25 mL), and extracted with CH₂Cl₂ (4 x 50 mL). The combined organic layers were dried over MgSO₄ and evaporated. The residue was dissolved in a saturated solution of NH₃ in MeOH (50 mL) at 23 °C and stirred for 72 h. After removal of solvents under vacuum and trituration with Et₂O, bromoamide **52b** (600 mg, 13% yield, 5 steps) was obtained as an off-white solid. This product was used immediately in the subsequent reaction. To H₂O (1.5 mL) at 100 °C was added ketoaldehyde **53a** (26.2 mg, 0.152 mmol) and bromoamide **52b** (40 mg, 0.152 mmol), followed by powdered potassium hydroxide (43 mg, 0.76 mmol). After stirring at 100 °C for 5 h, the reaction mixture was allowed to cool to 23 °C, poured into saturated aq. ammonium chloride (10 mL), and extracted with EtOAc (4 x 10 mL). The combined organic layers were dried briefly over sodium sulfate and concentrated under reduced pressure to afford known pyrazinone **22b**⁴⁴ (39 mg, 64% yield) as an orange/red solid: R_f 0.52 (7:1 CH₂Cl₂: CH₃OH).



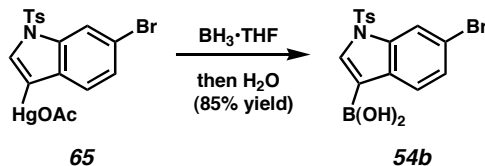
Iodopyrazine 63. To a thick-walled flask charged with **64**¹⁵ (100 mg, 0.49 mmol) was added acetonitrile (1.0 mL), H₂O (1.5 mL), and 48% aq. HI (1.3 mL). The resulting solution was cooled in an ice bath, and a solution of sodium nitrite (600 mg, 8.7 mmol) in H₂O (1.0 mL) was added in a dropwise fashion. The reaction mixture was sealed, allowed to warm to 23 °C, then stirred at 50 °C for 30 h. After cooling, the solution was poured into 20% aq. NaOH and extracted with Et₂O (3 x 20 mL). The combined organic layers were washed with saturated aq. sodium metabisulfite (20 mL) and brine (20 mL), dried over anhydrous sodium sulfate, then evaporated under reduced pressure. The crude product was then dissolved in a CH₂Cl₂/hexanes mixture (1:1) and filtered over silica gel (1:1 CH₂Cl₂:hexanes eluent) to provide iodopyrazine **63** (90 mg, 58% yield) as a white powder: *R_f* 0.52 (1:1 CH₂Cl₂:hexanes); ¹H NMR (300 MHz, CDCl₃) δ 8.07 (s, 1H), 4.05 (s, 3H); ¹³C NMR (75 MHz, CDCl₃) δ 158.8, 139.2, 136.1, 104.4, 56.2; IR (KBr) 1357, 1150 cm⁻¹; HRMS-NH₃Cl (*m/z*): [M]⁺ calc'd for C₅H₄BrIN₂O, 313.8552; found, 313.8553.



Organomercurial 65. To a solution of **49**¹⁷ (4.35 g, 22.2 mmol) in toluene (22 mL) was added tetrabutylammonium hydrogensulfate (520 mg, 1.54 mmol), KOH (50% aq. solution, 28 mL), and a solution of *p*-toluenesulfonyl chloride (5.08 g, 26.6 mmol) in toluene (44 mL). After stirring for 4 h, H₂O (40 mL) was added and the layers separated. The organic layer was washed with H₂O (2 x 20 mL) and brine (20 mL), dried over

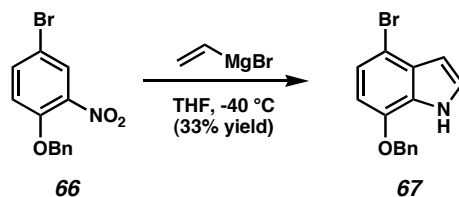
magnesium sulfate, and concentrated under reduced pressure to afford 6-bromo-*N*-tosylindole **91** (7.6 g, 98% yield) as an off-white powder: R_f 0.25 (9:1 hexanes:EtOAc); ^1H NMR (300 MHz, CDCl_3) δ 8.19 (s, 1H), 7.75 (d, $J = 8.2$ Hz, 2H), 7.53 (d, $J = 3.3$ Hz, 1H), 7.33 (comp. m, 2H), 7.21 (d, $J = 7.7$ Hz, 2H), 6.61 (d, $J = 3.3$ Hz, 1H), 2.32 (s, 3H); ^{13}C NMR (75 MHz, CDCl_3) δ 145.5, 135.6, 135.1, 130.2, 129.7, 126.9, 126.8, 122.6, 118.3, 116.7, 108.9, 21.7; IR (film) 1364, 1169 cm^{-1} ; HRMS- NH_3Cl (m/z): $[\text{M}]^+$ calc'd for $\text{C}_{15}\text{H}_{12}\text{BrNO}_2\text{S}$, 348.9772; found, 348.9773.

To a solution of 6-bromo-*N*-tosylindole **91** (7.6 g, 21.7 mmol) in acetic acid (145 mL) was added mercuric acetate (6.92 g, 21.7 mmol). After stirring at 23 °C for 15 min, perchloric acid (5 drops) was added. The mixture was stirred for 24 h, poured into H_2O (200 mL), then filtered. The resulting white solid was washed with copious amounts of H_2O and dried under vacuum for 12 h to afford organomercurial derivative **65** (13.05 g, 99% yield) as an unstable white powder that was used immediately without further purification: R_f 0.57 (2:1 hexanes:EtOAc); ^1H NMR (300 MHz, $\text{DMSO}-d_6$) δ 8.02 (d, $J = 1.1$ Hz, 1H), 7.76 (d, $J = 8.4$ Hz, 2H), 7.71 (d, $J = 8.4$ Hz, 1H), 7.52 (s, 1H), 7.42-7.39 (comp. m, 3H), 2.32 (s, 3H), 1.96 (s, 3H).

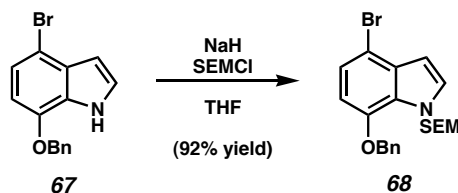


Boronic acid 54b. To a solution of **65** (3.91 g, 6.4 mmol) in THF (128 mL) at 23 °C was added borane (1 M in THF, 32 mL, 32 mmol). The resulting solution was stirred for 1 h, then carefully quenched by the dropwise addition of H_2O (38 mL). After filtration, the organic solvent was evaporated under reduced pressure, and the residue was

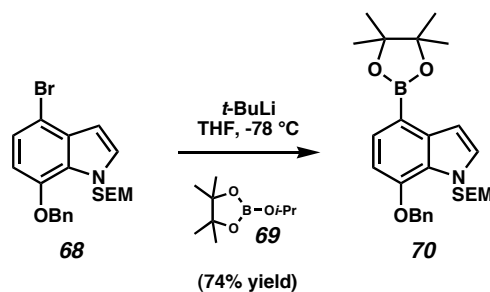
extracted with EtOAc (2 x 60 mL). The combined organic layers were washed with brine (30 mL) and concentrated under reduced pressure. Trituration of the crude product with hexanes (4x) afforded boronic acid **54b** (2.15 g, 85% yield) as an unstable off-white solid that was used immediately without further purification.



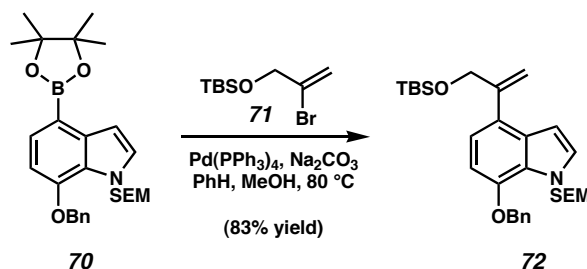
Indole 67. To a solution of **66**²¹ (14.0 g, 45.5 mmol) in THF (455 mL) at -40 °C was added vinylmagnesium bromide (1.0 M in THF, 159 mL, 159 mmol) in a dropwise fashion. The reaction mixture was stirred at -40 °C for 4 h and then poured into a saturated aq. ammonium chloride (350 mL). The reaction mixture was extracted with Et₂O (2 x 200 mL), and the combined organic layers were washed with brine (200 mL), dried over magnesium sulfate, and evaporated under reduced pressure. CH₂Cl₂ (50 mL) was added, and the resulting suspension was filtered over a pad of silica gel topped with celite. Removal of solvent under reduced pressure afforded the crude product as a red oil, which was further purified by flash chromatography (8:1 hexanes:Et₂O eluent) to yield 7-benzyloxy-4-bromoindole **67** (4.54 g, 33% yield) as a yellow oil: *R_f* 0.30 (4:1 hexanes:EtOAc); ¹H NMR (300 MHz, CDCl₃) δ 8.46 (br s, 1H), 7.50-7.40 (comp. m, 5H), 7.20 (d, *J* = 8.2 Hz, 1H), 7.16 (app.t, *J* = 2.7 Hz, 1H), 6.61-6.58 (comp. m, 2H), 5.17 (s, 2H); ¹³C NMR (75 MHz, CDCl₃) δ 145.0, 136.8, 129.7, 128.8, 128.5, 128.1, 126.9, 124.4, 122.6, 106.1, 104.4, 103.4, 70.6; IR (film) 3426, 1228 cm⁻¹; HRMS-NH₃Cl (*m/z*): [M]⁺ calc'd for C₁₅H₁₂BrNO, 301.0101; found, 301.0102.



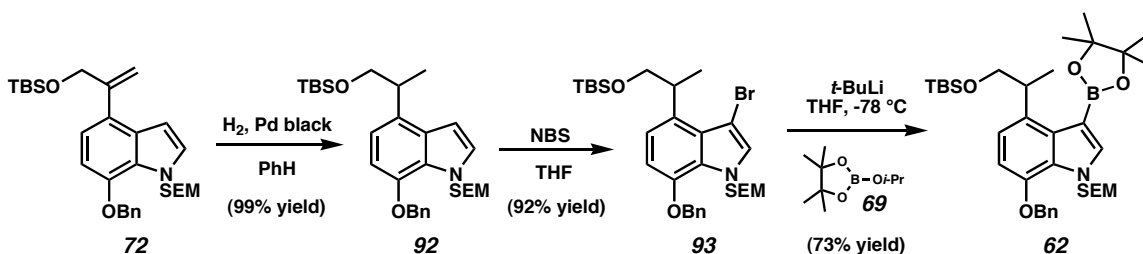
Indole 68. To a stirred suspension of NaH (60% dispersion in mineral oil, 154 mg, 4.0 mmol) in THF (15 mL) at 0 °C was added a solution of **67** (930 mg, 3.08 mmol) in THF (15 mL). The reaction mixture was allowed to warm to 23 °C and stirred for 30 min. The solution was cooled to 0 °C, SEMCl (600 μ L, 3.4 mmol) was added, and the mixture was stirred at 23 °C for 6 h. The reaction mixture was poured into saturated aq. ammonium chloride (20 mL) and extracted with Et₂O (2 x 30 mL). The combined organic layers were washed with brine (20 mL), dried over magnesium sulfate, and evaporated under reduced pressure. The crude residue was purified by flash chromatography (14:1 hexanes:EtOAc eluent) to afford **68** (1.22 g, 92% yield) as a yellow oil: R_f 0.51 (4:1 hexanes:EtOAc); ¹H NMR (300 MHz, CDCl₃) δ 7.53-7.50 (comp. m, 2H), 7.46-7.37 (comp. m, 3H), 7.21 (d, J = 3.3 Hz, 1H), 7.18 (d, J = 8.2 Hz, 1H), 6.63 (d, J = 8.2 Hz, 1H), 6.59 (d, J = 3.3 Hz, 1H), 5.73 (s, 2H), 5.20 (s, 2H), 3.45 (t, J = 8.2 Hz, 2H), 0.84 (t, J = 8.2 Hz, 2H), -0.06 (s, 9H); ¹³C NMR (75 MHz, CDCl₃) δ 146.3, 136.8, 131.6, 129.8, 128.8, 128.3, 127.8, 126.2, 123.0, 106.4, 105.7, 103.6, 77.7, 70.8, 65.5, 17.9, -1.2; IR (film) 1244, 1054 cm⁻¹; HRMS-NH₃Cl (m/z): [M]⁺ calc'd for C₂₁H₂₆BrNO₂Si, 431.0916; found, 431.0919.



Boronic ester 70. To a solution of **68** (3.81 g, 8.8 mmol) in THF (147 mL) at -78 °C was added *t*-BuLi (1.7 M in pentane, 11.4 mL, 19.4 mmol). Following addition, the reaction mixture was stirred for 15 min at -78 °C, then borolane **69** (3.6 mL, 17.6 mmol) was added. The mixture was stirred at -78 °C for 1.5 h, allowed to warm to 23 °C, then quenched with saturated aq. ammonium chloride (75 mL). The layers were separated, and the aqueous portion was extracted with Et₂O (3 x 75 mL). The combined organic layers were washed with brine (100 mL), briefly dried over magnesium sulfate, and evaporated under reduced pressure. The crude residue was purified by flash chromatography (14:1 hexanes:EtOAc eluent) to give boronic ester **70** (3.11 g, 74% yield) as a yellow oil: *R_f* 0.32 (9:1 hexanes:EtOAc); ¹H NMR (300 MHz, CDCl₃) δ 7.67 (d, *J* = 7.7 Hz, 1H), 7.59-7.56 (comp. m, 2H), 7.48-7.39 (comp. m, 3H), 7.25 (d, *J* = 3.3 Hz, 1H), 7.12 (d, *J* = 3.3 Hz, 1H), 6.83 (d, *J* = 7.7 Hz, 1H), 5.81 (s, 2H), 5.28 (s, 2H), 3.49 (t, *J* = 8.2 Hz, 2H), 1.44 (s, 12H), 0.87 (t, *J* = 8.2 Hz, 2H), -0.02 (s, 9H); ¹³C NMR (75 MHz, CDCl₃) δ 149.3, 137.0, 136.5, 129.9, 129.7, 128.7, 128.1, 127.8, 125.2, 105.1, 104.2, 83.2, 77.5, 70.3, 65.2, 25.1, 17.9, -1.3; IR (film) 1371, 1330, 1251 cm⁻¹; HRMS-NH₃Cl (*m/z*): [M]⁺ calc'd for C₂₇H₃₈BNO₄Si, 479.2668; found, 479.2673.



Olefin 72. A solution containing boronic ester **70** (3.17 g, 6.62 mmol) and bromide **71** (3.32 g, 13.2 mmol) in benzene (130 mL), CH₃OH (30 mL), and aq. sodium carbonate (2 M, 11 mL) was deoxygenated by bubbling a stream of argon through the reaction mixture for 5 min. Tetrakis(triphenylphosphine)palladium(0) (1.15 g, 0.99 mmol) was then added and the flask was equipped with a reflux condenser. The mixture was heated to 80 °C for 2 h and allowed to cool to 23 °C. To the reaction vessel was added sodium sulfate (10 g), which was allowed to stand for 30 min. After filtration over a pad of silica gel (CH₂Cl₂ eluent) and concentrating to dryness under reduced pressure, the resulting residue was purified by flash chromatography (1:1 CH₂Cl₂:hexanes eluent) to provide olefin **72** (2.87 g, 83% yield) as a yellow oil: *R_f* 0.53 (9:1 hexanes:EtOAc); ¹H NMR (300 MHz, CDCl₃) δ 7.55-7.53 (comp. m, 2H), 7.46-7.37 (comp. m, 3H), 7.18 (d, *J* = 3.3 Hz, 1H), 6.94 (d, *J* = 7.7 Hz, 1H), 6.74 (d, *J* = 8.2 Hz, 1H), 6.67 (d, *J* = 3.3 Hz, 1H), 5.78 (s, 2H), 5.62 (m, 1H), 5.40 (m, 1H), 5.24 (s, 2H), 4.55 (s, 2H), 3.48 (t, *J* = 8.2 Hz, 2H), 0.99 (s, 9H), 0.85 (t, *J* = 8.2 Hz, 2H), 0.15 (s, 6H), -0.06 (s, 9H); ¹³C NMR (75 MHz, CDCl₃) δ 146.9, 146.3, 137.2, 130.0, 129.3, 128.8, 128.2, 127.8, 126.3, 126.0, 118.9, 111.9, 104.2, 103.0, 77.6, 70.6, 65.6, 65.4, 26.2, 18.7, 18.0, -1.2, -5.1; IR (film) 1250, 1088 cm⁻¹; HRMS-ESI (*m/z*): [M + H]⁺ calc'd for C₃₀H₄₆NO₃Si₂, 524.3016; found, 524.3019.



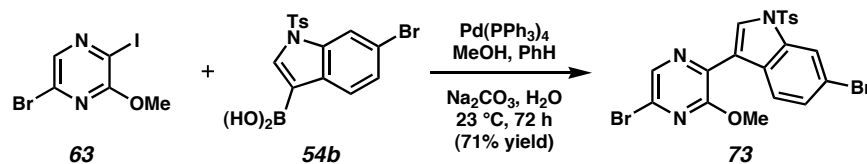
Boronic ester 62. To a solution of olefin **72** (545 mg, 1.04 mmol) in benzene (12 mL), saturated with hydrogen, was added palladium black (35 mg, 0.33 mmol). The reaction vessel was purged with hydrogen and kept under a hydrogen atmosphere (1 atm) with vigorous stirring for 1 h. Palladium black was removed via filtration through a pad of silica gel (benzene eluent) to afford the reduced silyl ether **92** (542 mg, 99% yield) as a yellow oil: R_f 0.53 (9:1 hexanes:EtOAc); ^1H NMR (300 MHz, CDCl_3) δ 7.53–7.50 (comp. m, 2H), 7.43–7.34 (comp. m, 3H), 7.16 (d, $J = 3.3$ Hz, 1H), 6.86 (d, $J = 7.7$ Hz, 1H), 6.71 (d, $J = 7.7$ Hz, 1H), 6.60 (d, $J = 3.3$ Hz, 1H), 5.75 (s, 2H), 5.20 (s, 2H), 3.87 (dd, $J = 9.9$, 4.9 Hz, 1H), 3.62 (app.t, $J = 9.3$ Hz, 1H), 3.45 (t, $J = 8.2$ Hz, 2H), 3.30 (m, 1H), 1.40 (d, $J = 6.6$ Hz, 3H), 0.89 (s, 9H), 0.82 (t, $J = 8.2$ Hz, 2H), 0.00 (s, 6H), -0.09 (s, 9H); ^{13}C NMR (75 MHz, CDCl_3) δ 145.3, 137.3, 130.7, 129.5, 128.8, 128.7, 128.1, 127.8, 125.7, 117.3, 104.4, 101.7, 77.6, 70.6, 69.0, 65.4, 39.1, 26.3, 18.7, 18.0, 17.5, -1.1, -4.99, -5.04; IR (film) 1249, 1076 cm^{-1} ; HRMS-ESI (m/z): $[\text{M} + \text{Na}]^+$ calc'd for $\text{C}_{30}\text{H}_{47}\text{NO}_3\text{Si}_2\text{Na}$, 548.2992; found, 548.2997.

To a solution of the crude silyl ether **92** (270 mg, 0.51 mmol) in THF (5 mL) was added *N*-bromosuccinimide (92.2 mg, 0.51 mmol). After stirring for 5 min, the reaction mixture was poured into a saturated aq. solution of sodium metabisulfite (3 mL), extracted with Et_2O (3 x 2 mL), and dried by passage through a plug of silica gel (Et_2O eluent). After concentrating to dryness under reduced pressure, the crude residue was purified by

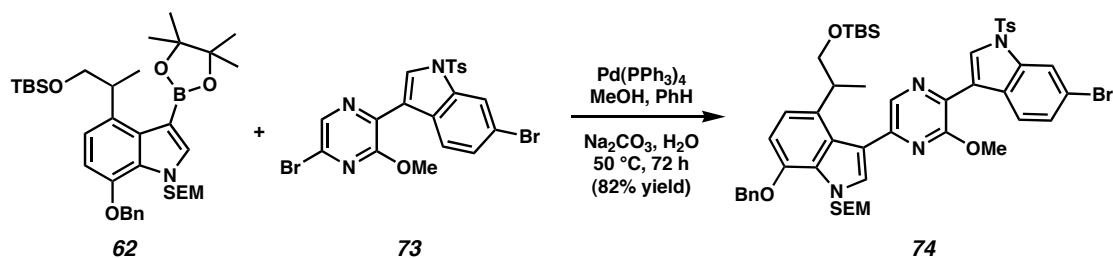
flash chromatography (1:1 CH₂Cl₂:hexanes eluent) to furnish the 3-bromoindole derivative **93** (285 mg, 92% yield) as a yellow oil: *R_f* 0.47 (1:1 CH₂Cl₂:hexanes); ¹H NMR (300 MHz, CDCl₃) δ 7.57-7.54 (comp. m, 2H), 7.49-7.40 (comp. m, 3H), 7.24 (s, 1H), 7.02 (d, *J* = 8.2 Hz, 1H), 6.80 (d, *J* = 7.7 Hz, 1H), 5.77 (d, *J* = 9.9 Hz, 1H), 5.73 (d, *J* = 10.4 Hz, 1H), 5.23 (s, 2H), 4.36 (m, 1H), 4.02 (dd, *J* = 9.6, 4.7 Hz, 1H), 3.65 (dd, *J* = 9.3, 8.3 Hz, 1H), 3.50 (t, *J* = 8.0 Hz, 2H), 1.46 (d, *J* = 7.1 Hz, 3H), 0.96 (s, 9H), 0.89 (t, *J* = 8.0 Hz, 2H), 0.08 (s, 3H), 0.06 (s, 3H), 0.00 (s, 9H); ¹³C NMR (75 MHz, CDCl₃) δ 145.0, 136.9, 130.1, 129.6, 128.7, 128.2, 127.8, 126.1, 125.9, 118.7, 105.2, 90.1, 77.7, 70.7, 69.3, 65.6, 34.7, 26.2, 18.6, 18.0, -1.1, -5.0, -5.1; IR (film) 1250 cm⁻¹; HRMS-ESI (*m/z*): [M + Na]⁺ calc'd for C₃₀H₄₆BrNO₃Si₂Na, 626.2097; found, 626.2079.

To a solution of the 3-bromoindole derivative **93** (2.5 g, 4.1 mmol) in THF (69 mL) at -78 °C was added *t*-BuLi (1.7 M in pentane, 5.4 mL, 9.1 mmol). The reaction mixture was stirred for 15 min at -78 °C and borolane **69** (1.69 mL, 8.3 mmol) was added. The mixture was stirred at -78 °C for 1 h, quenched with saturated aq. ammonium chloride (20 mL), and allowed to warm to 23 °C. The layers were separated, and the aqueous layer was extracted with Et₂O (3 x 50 mL). The combined organic layers were washed with brine (75 mL), briefly dried over magnesium sulfate, and concentrated in vacuo. The crude residue was purified by flash chromatography (14:1 hexanes:EtOAc eluent) to afford boronic ester **62** (1.96 g, 73% yield) as an unstable colorless oil that was used immediately in the coupling reaction that follows: *R_f* 0.38 (9:1 hexanes:EtOAc); ¹H NMR (300 MHz, C₆D₆) δ 7.79 (s, 1H), 7.35 (d, *J* = 7.7 Hz, 1H), 7.20-7.05 (comp. m, 5H), 6.65 (d, *J* = 8.0 Hz, 1H), 5.50 (d, *J* = 10.6 Hz, 1H), 5.46 (d, *J* = 10.3 Hz, 1H), 4.86 (s, 2H), 4.70 (m, 1H), 4.09 (dd, *J* = 9.5, 4.8 Hz, 1H), 3.91 (dd, *J* = 9.5, 7.3 Hz, 1H), 3.28

(t, $J = 7.7$ Hz, 2H), 1.62 (d, $J = 6.6$ Hz, 3H), 1.21 (s, 6H), 1.19 (s, 6H), 0.98 (s, 9H), 0.64 (t, $J = 7.7$ Hz, 2H), 0.00 (s, 3H), -0.01 (s, 3H), -0.19 (s, 9H).



Indolylpyrazine 73. A solution containing iodopyrazine **63** (133 mg, 0.42 mmol) and boronic acid **54b** (200 mg, 0.51 mmol) in benzene (10 mL), CH_3OH (2 mL), and aq. sodium carbonate (2 M, 0.70 mL) was deoxygenated by bubbling a stream of argon through the reaction mixture for 5 min. Tetrakis(triphenylphosphine)palladium(0) (73 mg, 0.06 mmol) was then added, the flask was evacuated, and purged with N_2 . The reaction mixture was stirred at 23 °C for 72 h and quenched by addition of sodium sulfate (500 mg). Filtration over a pad of silica gel (CH_2Cl_2 eluent) and concentration to dryness under reduced pressure, followed by trituration of the remaining residue with Et_2O (3x) and further purification by flash chromatography (CH_2Cl_2 eluent) afforded indolylpyrazine **73** (161 mg, 71% yield) as an off-white powder: R_f 0.13 (3:1 hexanes: CH_2Cl_2); ^1H NMR (300 MHz, CDCl_3) δ 8.52 (d, $J = 8.2$ Hz, 1H), 8.45 (s, 1H), 8.33 (s, 1H), 8.18 (d, $J = 2.2$ Hz, 1H), 7.81 (d, $J = 8.8$ Hz, 2H), 7.43 (dd, $J = 8.5, 2.2$ Hz, 1H), 7.27 (d, $J = 8.8$ Hz, 2H), 4.19 (s, 3H), 2.36 (s, 3H); ^{13}C NMR (125 MHz, CDCl_3) δ 156.5, 145.9, 137.6, 137.0, 135.8, 135.1, 132.7, 130.4, 129.3, 128.2, 127.6, 127.2, 125.2, 119.3, 116.5, 116.1, 55.2, 21.8; IR (film) 1374, 1165 cm^{-1} ; HRMS-ESI (m/z): $[\text{M} + \text{H}]^+$ calc'd for $\text{C}_{20}\text{H}_{16}\text{Br}_2\text{N}_3\text{O}_3\text{S}$, 535.9279; found, 535.9272.



Bis(indole) 74. In a Schlenk flask, a solution containing dibromide **73** (82 mg, 0.15 mmol) and boronic ester **62** (129 mg, 0.20 mmol) in benzene (4 mL), CH₃OH (0.80 mL), and aq. sodium carbonate (2 M, 0.25 mL) was deoxygenated by bubbling a stream of argon through the reaction mixture for 5 min. Tetrakis(triphenylphosphine)palladium(0) (27 mg, 0.02 mmol) was then added, and the flask was evacuated, purged with N₂, and sealed. The reaction mixture was heated to 50 °C for 72 h, cooled to 23 °C, then quenched by addition of sodium sulfate (300 mg). Following filtration through a pad of silica gel (CH₂Cl₂ eluent) and evaporation to dryness in vacuo, the remaining residue was purified by flash chromatography (2:1 CH₂Cl₂:hexanes eluent) to give a crude product, which was further purified by flash chromatography (7:1 hexanes:EtOAc eluent) to afford bis(indole) **74** (122 mg, 82% yield) as a yellow oil: *R_f* 0.2 (9:1 hexanes:EtOAc); ¹H NMR (300 MHz, CDCl₃) δ 8.71 (d, *J* = 8.4 Hz, 1H), 8.52 (s, 1H), 8.50 (s, 1H), 8.27 (d, *J* = 1.8 Hz, 1H), 7.86 (d, *J* = 8.4 Hz, 2H), 7.56–7.38 (comp. m, 7H), 7.28 (d, *J* = 8.4 Hz, 2H), 7.03 (d, *J* = 8.1 Hz, 1H), 6.85 (d, *J* = 8.4 Hz, 1H), 5.84 (s, 2H), 5.25 (s, 2H), 4.25 (s, 3H), 4.07 (m, 1H), 3.62 (dd, *J* = 9.2, 4.4 Hz, 1H), 3.55 (t, *J* = 8.1, 2H), 3.35 (app.t, *J* = 9.2 Hz, 1H), 2.37 (s, 3H), 1.33 (d, *J* = 7.0 Hz, 3H), 0.89 (t, *J* = 8.4 Hz, 2H), 0.69 (s, 9H), -0.04 (s, 9H), -0.16 (s, 3H), -0.28 (s, 3H); ¹³C NMR (125 MHz, CDCl₃) δ 156.1, 145.7, 145.6, 145.4, 137.2, 135.8, 135.6, 135.5, 135.1, 131.3, 130.9, 130.3, 128.8, 128.7, 128.3, 127.8, 127.7, 127.3, 127.1, 127.0,

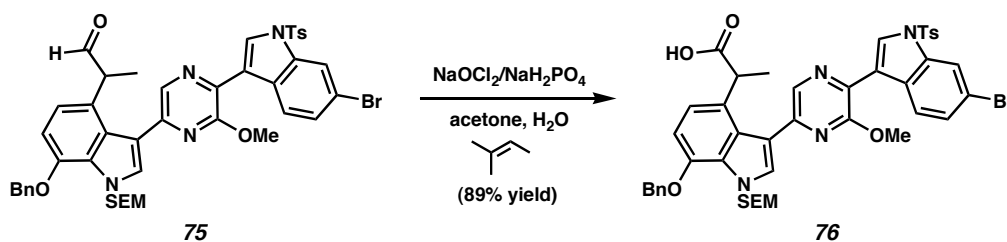
125.5, 119.0, 118.8, 117.3, 116.4, 115.6, 105.5, 78.0, 70.8, 69.2, 65.8, 54.2, 36.8, 25.9, 21.8, 18.2, 18.0, 17.7, -1.2, -5.5, -5.6; IR (film) 1374, 1178, 1087 cm^{-1} ; HRMS-ESI (m/z): $[\text{M} + \text{H}]^+$ calc'd for $\text{C}_{50}\text{H}_{62}\text{BrN}_4\text{O}_6\text{SSi}_2$, 981.3112; found, 981.3097.



Aldehyde 75. To a Falcon tube containing a THF (5 mL) solution of bis(indole) **74** (70 mg, 0.07 mmol) at 0 °C was added HF•pyridine (800 μL) in a dropwise fashion. The reaction mixture was stirred at 0 °C for 1.5 h until the reaction was judged complete by TLC. After dilution of the mixture with Et_2O (10 mL), saturated aq. sodium bicarbonate (10 mL) was added in a dropwise manner at 0 °C. The layers were separated, and the organic portion was further washed with saturated aq. sodium bicarbonate (3 x 10 mL), dried over magnesium sulfate, and concentrated under reduced pressure.

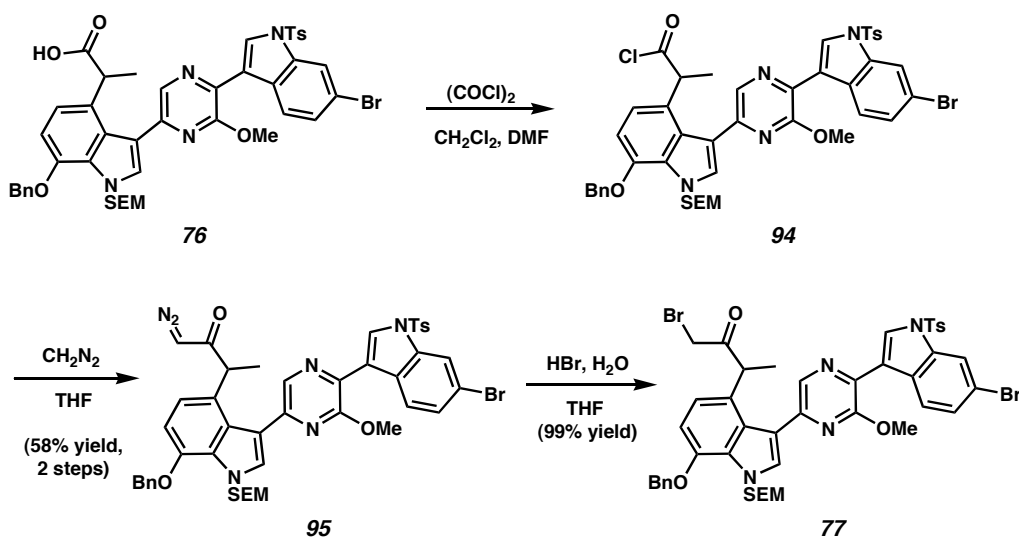
The crude residue prepared above was dissolved in anhydrous CH_2Cl_2 (5 mL), and Dess-Martin periodinane (91 mg, 0.214 mmol) was introduced. The reaction mixture was stirred at 23 °C for 20 min, poured into a saturated aq. solution of sodium bicarbonate/sodium thiosulfate (1:1, 5 mL), and extracted with CH_2Cl_2 (3 x 10 mL). The organic layers were washed with brine (5 mL), dried over magnesium sulfate, and evaporated under reduced pressure to provide the crude product, which was purified by flash chromatography (2:1 hexanes:EtOAc) to furnish aldehyde **75** (53 mg, 86% yield) as a yellow oil: R_f 0.67 (2:1 hexanes:EtOAc); ^1H NMR (500 MHz, CDCl_3) δ 9.73 (s, 1H), 8.69 (d, J = 8.3 Hz, 1H), 8.52 (s, 1H), 8.46 (s, 1H), 8.24 (d, J = 1.5 Hz, 1H), 7.86 (d, J =

8.3 Hz, 2H), 7.56-7.39 (comp. m, 7H), 7.30 (d, $J = 7.8$ Hz, 2H), 6.89 (d, $J = 8.3$ Hz, 1H), 6.83 (d, $J = 8.3$ Hz, 1H), 5.85 (s, 2H), 5.27 (s, 2H), 4.76 (q, $J = 6.8$ Hz, 1H), 4.18 (s, 3H), 3.55 (t, $J = 8.0$ Hz, 2H), 2.39 (s, 3H), 1.37 (d, $J = 6.8$ Hz, 3H), 0.89 (t, $J = 8.0$ Hz, 2H), -0.05 (s, 9H); ^{13}C NMR (125 MHz, CDCl_3) δ 201.9, 156.1, 146.4, 145.7, 144.8, 136.8, 136.2, 135.8, 135.6, 135.0, 131.8, 130.4, 129.1, 128.9, 128.6, 128.5, 128.0, 127.9, 127.5, 127.4, 127.2, 125.4, 124.3, 121.0, 119.1, 116.9, 116.5, 115.2, 105.9, 78.2, 70.9, 66.0, 54.3, 48.5, 21.8, 18.0, 15.0, -1.2; IR (film) 1720, 1374, 1177, 1086 cm^{-1} ; HRMS-ESI (m/z): $[\text{M} + \text{H}]^+$ calc'd for $\text{C}_{44}\text{H}_{46}\text{BrN}_4\text{O}_6\text{SSi}$, 865.2090; found, 865.2103.



Acid 76. A solution of aldehyde **75** (53 mg, 0.061 mmol) in acetone (12 mL) was treated with a saturated solution of NaH_2PO_4 that had been acidified to pH 2 with 1 N HCl (1.4 mL) and cooled to 0 °C. After the addition of 2-methyl-2-butene (32.5 μL , 0.31 mmol), a solution of NaClO_2 (13.9 mg, 0.123 mmol) in H_2O (1.4 mL) was added dropwise over 5 min. The reaction mixture was poured into cold H_2O (2 mL) and extracted with CH_2Cl_2 (2 x 5 mL). The combined organic layers were dried over magnesium sulfate and evaporated to dryness. The crude residue was passed through a short plug of silica gel (EtOAc eluent), and the solvent was evaporated to afford acid **76** (49 mg, 89% yield): R_f 0.22 (2:1 hexanes:EtOAc); ^1H NMR (300 MHz, CDCl_3) δ 8.68 (d, $J = 8.3$ Hz, 1H), 8.52 (s, 1H), 8.44 (s, 1H), 8.23 (d, $J = 1.5$ Hz, 1H), 7.85 (d, $J = 8.3$ Hz, 2H), 7.53-7.37 (comp. m, 7H), 7.28 (d, $J = 9.2$ Hz, 2H), 7.08 (d, $J = 8.3$ Hz, 1H), 6.84 (d,

$J = 8.3$ Hz, 1H), 5.84 (d, $J = 10.3$ Hz, 1H), 5.78 (d, $J = 10.3$ Hz, 1H), 5.24 (s, 2H), 4.86 (q, $J = 6.8$ Hz, 1H), 4.20 (s, 3H), 3.53 (t, $J = 8.3$ Hz, 2H), 2.36 (s, 3H), 1.42 (d, $J = 6.8$ Hz, 3H), 0.86 (t, $J = 8.3$ Hz, 2H), -0.07 (s, 9H); ^{13}C NMR (125 MHz, CDCl_3) δ 178.2, 156.2, 146.2, 145.7, 145.0, 136.9, 136.2, 135.8, 135.7, 135.1, 131.7, 130.4, 129.1, 128.9, 128.6, 128.5, 128.4, 127.9, 127.5, 127.3, 127.2, 126.3, 125.4, 119.8, 119.1, 116.9, 116.5, 114.9, 105.8, 78.1, 70.9, 66.0, 54.5, 40.6, 21.8, 18.4, 18.0, -1.2; IR (film) 2948, 1703, 1373, 1177, 1139, 1088 cm^{-1} ; HRMS-ESI (m/z): $[\text{M} + \text{Na}]^+$ calc'd for $\text{C}_{44}\text{H}_{45}\text{BrN}_4\text{O}_7\text{SSiNa}$, 881.2040; found, 881.2009.

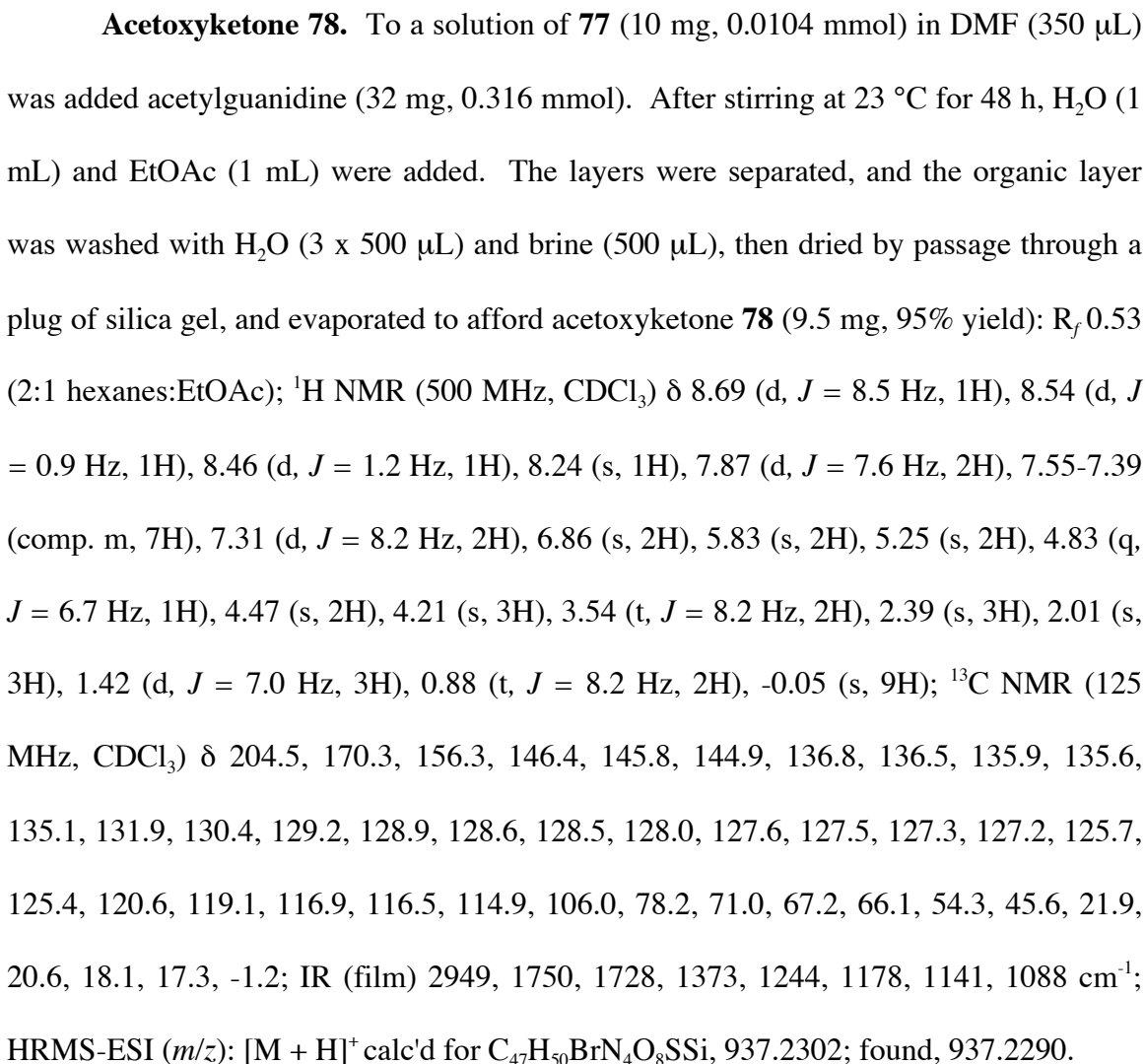


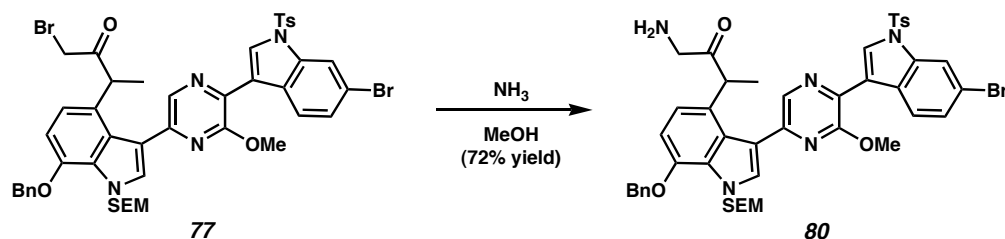
Bromoketone 77. To a solution of **76** (49 mg, 0.0559 mmol) in CH_2Cl_2 (400 mL) at 0 °C was added oxalyl chloride (6.3 μL , 0.0727 mmol), followed by DMF (2 drops). After stirring at 0 °C for 30 min, all solvents were removed in vacuo. The crude acid chloride **94** was allowed to dry under vacuum for an additional 1 h and was used in the next step without further purification.

Note: In the next step, diazomethane was dried by storing the ethereal diazomethane solution over potassium hydroxide pellets. Immediately before use, the diazomethane was further dried over sodium metal for approximately 15 minutes.

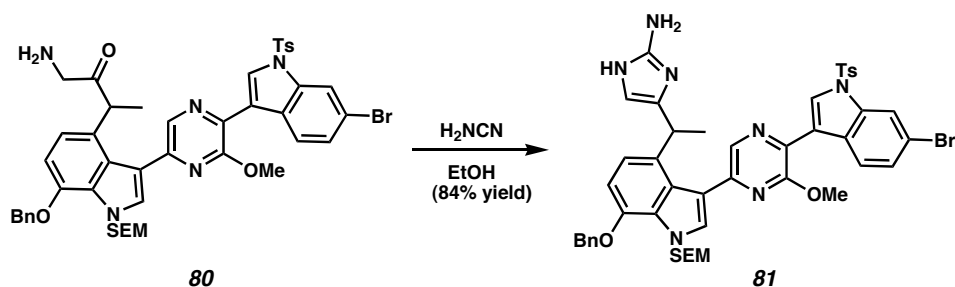
To crude **94** in THF (400 μ L) at 0 $^{\circ}$ C was added an ethereal solution of thoroughly dried diazomethane (1.5 mL) via a flamed glass pipette. The reaction mixture was allowed to warm to 23 $^{\circ}$ C, poured into saturated aq. sodium bicarbonate (1 mL), and extracted with Et₂O (3 x 3 mL). The combined organic layers were dried over magnesium sulfate and evaporated under reduced pressure. The crude residue was purified by flash chromatography (4:1 hexanes:EtOAc eluent) to give diazoketone **95** (29.5 mg, 58% yield) as a yellow oil.

To **95** (19 mg, 0.021 mmol) in THF (2 mL) at 0 $^{\circ}$ C, 48% aq. HBr (3 drops) was added slowly down the walls of the flask. After stirring for 5 min, the reaction mixture was poured into a saturated aq. solution of sodium bicarbonate and extracted with Et₂O (3 x 4 mL). The combined organic layers were dried over magnesium sulfate and evaporated under reduced pressure to afford bromoketone **77** (20 mg, 99% yield) as a yellow oil: R_f 0.68 (2:1 hexanes:EtOAc); ¹H NMR (500 MHz, CDCl₃) δ 8.69 (d, J = 8.6 Hz, 1H), 8.53 (s, 1H), 8.47 (s, 1H), 8.24 (d, J = 1.5 Hz, 1H), 7.87 (d, J = 8.2 Hz, 2H), 7.55-7.38 (comp. m, 7H), 7.31 (d, J = 8.2 Hz, d), 6.85 (d, 2H), 5.83 (s, 2H), 5.25 (s, 2H), 5.01 (q, J = 6.7 Hz, 1H), 4.21 (s, 3H), 3.76 (d, J = 12.8 Hz, 1H), 3.67 (d, J = 13.1 Hz, 1H), 3.55 (t, J = 8.2 Hz, 2H), 2.39 (s, 3H), 1.48 (d, J = 6.7 Hz, 3H), 0.88 (t, J = 8.1 Hz, 2H), -0.052 (s, 9H); ¹³C NMR (125 MHz, CDCl₃) δ 156.3, 146.5, 145.8, 144.8, 136.7, 136.5, 135.8, 135.7, 135.1, 140.0, 130.4, 129.2, 128.9, 128.6, 128.5, 128.0, 127.7, 127.5,





Aminoketone 80. Bromoketone **77** (6 mg, 0.0062 mmol) was dissolved in a saturated solution of ammonia in CH₃OH (1 mL). After stirring for 6 h at 23 °C, the reaction mixture was filtered through a plug of silica gel (CH₃OH eluent), and the solvent was evaporated. The crude residue was then purified by preparative thin layer chromatography (7:1 CH₂Cl₂:CH₃OH) to afford aminoketone **80** (4 mg, 72% yield): *R_f* 0.67 (7:1 CH₂Cl₂:CH₃OH); ¹H NMR (300 MHz, CDCl₃) δ 8.19 (d, 8.8, 1H), 8.53 (s, 1H), 8.46 (s, 1H), 8.23 (s, 1H), 7.85 (d, *J* = 8.4 Hz, 2H), 7.54-7.37 (comp. m, 7H), 7.29 (d, *J* = 8.4 Hz, 2H), 6.84-6.83 (comp. m, 2H), 5.82 (s, 2H), 5.24 (s, 2H), 4.71 (q, *J* = 6.6 Hz, 1H), 4.19 (s, 3H), 3.54 (t, *J* = 8.1 Hz, 2H), 3.31 (d, *J* = 19.3 Hz, 1H), 3.07 (d, *J* = 19.1 Hz, 1H), 2.38 (s, 3H), 1.44 (d, *J* = 7.0 Hz, 3H), 0.87 (t, *J* = 8.1 Hz, 2H), -0.06 (s, 9H).



Aminoimidazole 81. To a solution of aminoketone **80** (7 mg, 0.0078 mmol) in ethanol (700 μL) was added cyanamide (15 mg, 0.36 mmol). The reaction vessel was sealed and heated to 70 °C for 10 h. After cooling to 23 °C, the reaction mixture was

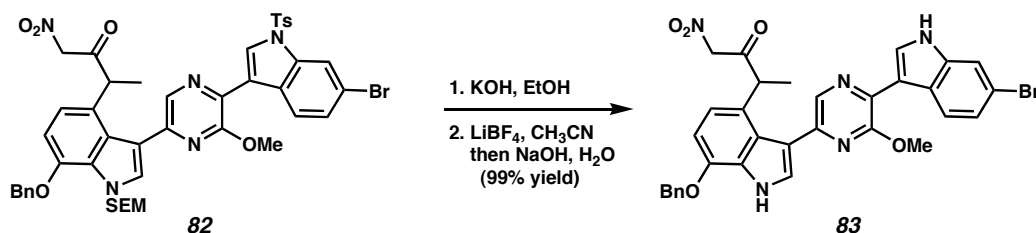
purified by reversed-phase filtration through a Sep-Pak column: first 10% acetonitrile, then 100% acetonitrile to collect the product. After removal of solvent under reduced pressure, **81** (6 mg, 84% yield) was isolated as an orange/red oil: R_f 0.27 (7:1 CH_2Cl_2 : CH_3OH); ^1H NMR (500 MHz, CD_3OD) δ 8.68 (d, J = 8.8 Hz, 1H), 8.52 (s, 1H), 8.38 (s, 1H), 8.16 (d, J = 1.5 Hz, 1H), 7.87 (d, J = 8.1 Hz, 2H), 7.60-7.33 (comp. m, 9H), 6.95 (d, J = 8.4 Hz, 1H), 6.90 (d, J = 8.4 Hz, 1H), 6.10 (s, 1H), 5.85 (s, 2H), 5.28 (s, 2H), 5.09 (q, J = 6.8 Hz, 1H), 4.19 (s, 3H), 3.57 (t, J = 7.9 Hz, 2H), 2.37 (s, 3H), 1.41 (d, J = 7.0 Hz, 3H), 0.82 (t, J = 7.9 Hz, 2H), -0.10 (s, 9H); HRMS-ESI (m/z): $[\text{M} + \text{H}]^+$ calc'd for $\text{C}_{46}\text{H}_{49}\text{BrN}_7\text{O}_5\text{SSi}$, 918.2468; found, 918.2467.



Ketone 82. To aldehyde **75** (20 mg, 0.023 mmol) in nitromethane (1 mL) was added triethylamine (75 μL , 0.54 mmol). The reaction mixture was stirred at 23 $^\circ\text{C}$ for 15 h. The excess nitromethane was removed by evaporation under reduced pressure to afford the crude nitroaldol product, which was used without further purification.

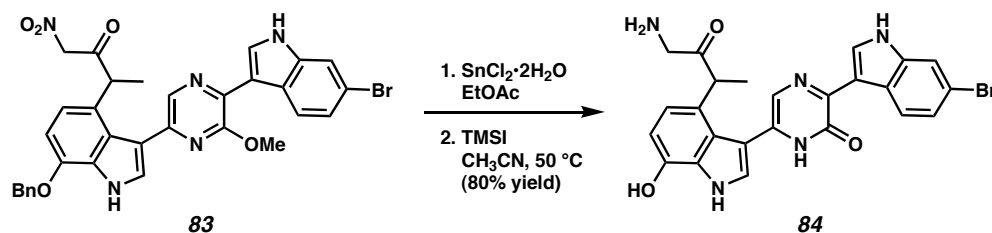
The crude residue was dissolved in anhydrous CH_2Cl_2 (1.5 mL) and treated with Dess-Martin periodinane (15% solution in CH_2Cl_2 , 200 μL , 0.099 mmol). The reaction mixture was stirred at 23 $^\circ\text{C}$ for 5 min and quenched by addition of saturated aq. sodium bicarbonate/sodium thiosulfate (1:1, 2 mL). The layers were separated, and the aqueous layer was extracted with EtOAc (8 x 1 mL). The combined organic layers were washed with brine (2 mL), dried by passage through a plug of silica gel (EtOAc eluent), and

evaporated under reduced pressure to afford ketone **82** (21 mg, 98% yield) as a yellow oil: R_f 0.20 (3:1 hexanes:EtOAc); ^1H NMR (500 MHz, CDCl_3) δ 8.62 (d, $J = 8.3$ Hz, 1H), 8.44 (s, 1H), 8.39 (s, 1H), 8.18 (s, 1H), 7.80 (d, $J = 8.3$ Hz, 2H), 7.49-7.33 (comp. m, 7H), 7.24 (d, $J = 8.3$ Hz, 2H), 6.83 (d, $J = 8.3$ Hz, 1H), 6.81 (d, $J = 7.8$ Hz, 1H), 5.77 (s, 2H), 5.21 (s, 2H), 5.03 (d, $J = 14.6$ Hz, 1H), 4.98 (d, $J = 14.6$ Hz, 1H), 4.90 (q, $J = 6.8$ Hz, 1H), 4.14 (s, 3H), 3.49 (t, $J = 7.8$ Hz, 2H), 2.32 (s, 3H), 1.44 (d, $J = 6.8$ Hz, 3H), 0.82 (t, $J = 8.0$ Hz, 2H), -0.12 (s, 9H); ^{13}C NMR (125 MHz, CDCl_3) δ 197.0, 156.3, 146.9, 145.8, 144.3, 136.9, 136.5, 135.8, 135.6, 135.0, 132.3, 130.4, 129.3, 129.0, 128.6, 128.5, 128.0, 127.6, 127.5, 127.4, 127.2, 125.4, 123.7, 121.0, 119.2, 116.7, 116.5, 114.6, 106.2, 82.2, 78.3, 71.0, 66.2, 54.4, 47.6, 21.8, 18.0, 16.9, -1.2; IR (film) 1732, 1559, 1376, 1178, 1080 cm^{-1} . HRMS-FAB (m/z): $[\text{M} + \text{H}]^+$ calc'd for $\text{C}_{45}\text{H}_{47}\text{BrN}_5\text{O}_8\text{SiSBr}$, 926.2077; found, 926.2080.



gel (EtOAc eluent), and evaporated under reduced pressure to afford the crude detosylated ketone, which was used without further purification.

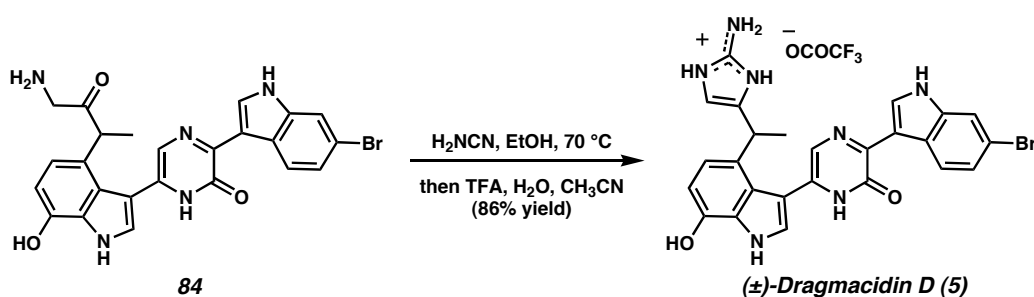
To the crude detosylated ketone prepared above in acetonitrile (3 mL, deoxygenated by sparging with argon for 2 min) and water (30 μ L) was added lithium tetrafluoroborate (120 mg, 0.13 mmol). The reaction vessel was equipped with a reflux condenser and heated to 70 $^{\circ}$ C for 1.5 h. After cooling to 40 $^{\circ}$ C, sodium hydroxide (20% aq., 2 mL) was added. The resulting mixture was stirred for 10 min, allowed to cool to 23 $^{\circ}$ C, quenched with saturated aq. ammonium chloride (2 mL), and extracted with EtOAc (8 x 1 mL). The combined organic layers were washed with brine (2 mL), dried by passage through a plug of silica gel (EtOAc eluent), and evaporated under reduced pressure to afford nitroketone **83** (20.5 mg, 99% yield) as a yellow oil: R_f 0.59 (1:1 hexanes:EtOAc); ^1H NMR (300 MHz, acetone- d_6) δ 11.14 (br s, 1H), 10.86 (br s, 1H), 8.82 (d, J = 8.8 Hz, 1H), 8.54 (s, 1H), 8.43 (m, 1H), 7.75-7.72 (comp. m, 2H), 7.62-7.59 (comp. m, 2H), 7.47-7.30 (comp. m, 4H), 6.95 (d, J = 8.1 Hz, 1H), 6.85 (d, J = 8.1 Hz, 1H), 5.41-5.22 (comp. m, 5H), 4.19 (s, 3H), 1.47 (d, J = 7.0 Hz, 3H); ^{13}C NMR (125 MHz, acetone- d_6) δ 198.7, 156.2, 146.3, 143.6, 139.4, 138.6, 138.3, 136.1, 130.7, 129.4, 129.4, 128.9, 128.8, 128.3, 126.9, 126.8, 125.8, 124.9, 124.2, 120.5, 116.3, 116.0, 115.3, 112.5, 105.1, 83.4, 70.9, 54.1, 47.7, 17.3; IR (film) 3410 (br), 1728, 1697, 1557, 1450 cm^{-1} ; HRMS-ESI (m/z): $[\text{M} + \text{H}]^+$ calc'd for $\text{C}_{32}\text{H}_{27}\text{BrN}_5\text{O}_5$, 640.1196; found, 640.1180.



Aminoketone 84. To a solution of deprotected ketone **83** (5.5 mg, 0.0086 mmol) in EtOAc (600 μL , deoxygenated by bubbling with argon for 1 min), was added $\text{SnCl}_2 \cdot 2\text{H}_2\text{O}$ (30 mg, 0.13 mmol). The reaction vessel was equipped with a reflux condenser and heated at 80 $^\circ\text{C}$ for 3 h. After cooling to 23 $^\circ\text{C}$, the solvent was removed under reduced pressure to leave an orange residue, which was purified by reversed-phase filtration through a Sep-Pak column: first 10% acetonitrile containing 0.1% (w/v) TFA to remove salts, then 90% acetonitrile containing 0.1% (w/v) TFA to collect the crude product. After removal of solvent in vacuo, the compound was filtered through silica gel (5:1 $\text{CH}_2\text{Cl}_2/\text{CH}_3\text{OH}$ eluent) to provide the reduced compound, which was used without further purification.

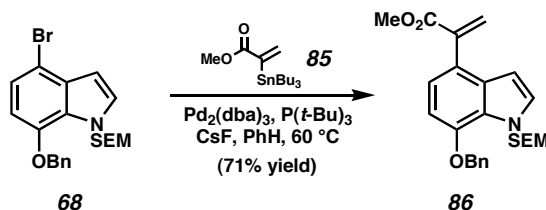
To the crude aminoketone in acetonitrile (700 μL) at 0 $^\circ\text{C}$, in a Schlenk tube, was added iodotrimethylsilane (150 μL , 1.05 mmol). The reaction mixture was heated at 50 $^\circ\text{C}$ for 2 h, cooled to 0 $^\circ\text{C}$, then quenched with saturated aq. sodium metabisulfite. The reaction mixture was purified by reversed-phase filtration through a Sep-Pak column: first 10% acetonitrile containing 0.1% (w/v) TFA to remove salts, then 90% acetonitrile containing 0.1% (w/v) TFA to collect the crude product. After removal of solvent under reduced pressure, the compound was further purified by reversed-phase HPLC. Concentration under reduced pressure provided the fully deprotected aminoketone **84** (3.5 mg, 80% yield) as an orange/red oil: ^1H NMR (500 MHz, CD_3OD) δ 8.75 (s, 1H), 8.60 (d, J = 8.4 Hz, 1H), 7.67 (s, 1H), 7.62 (d, J = 1.7 Hz, 1H), 7.54 (s, 1H), 7.27 (dd, J

= 8.5, 1.8 Hz, 1H), 6.69 (d, J = 8.1 Hz, 1H), 6.63 (d, J = 7.7 Hz, 1H), 4.15 (q, J = 6.9 Hz, 1H), 3.64 (d, J = 1.7 Hz, 2H), 1.44 (d, J = 6.8 Hz, 3H); ^{13}C NMR (125 MHz, CD_3OD) δ 204.4, 157.4, 151.0, 145.3, 139.1, 132.6, 131.7, 129.0, 128.3, 127.7, 126.7, 126.1, 125.6, 124.9, 122.6, 121.0, 117.1, 115.5, 113.7, 108.5, 107.9, 46.8, 17.2; IR (film) 3140 (br), 1671, 1200, 1140 cm^{-1} ; HRMS-ESI (m/z) calc'd for $\text{C}_{24}\text{H}_{21}\text{BrN}_5\text{O}_3$, 506.0828; found, 506.0827.



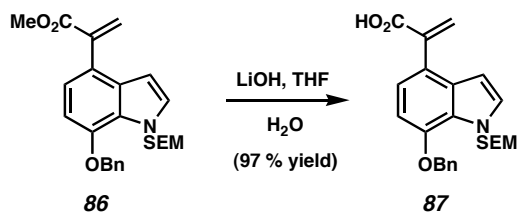
Dragmacidin D (5). To a solution of aminoketone **84** (2 mg, 0.0039 mmol) in ethanol (700 μL , deoxygenated by bubbling with argon for 5 min) was added cyanamide (15 mg, 0.36 mmol). The reaction vessel was purged with argon, sealed, and heated to 70 °C for 3 h. After cooling to 23 °C, the reaction mixture was purified by reversed-phase filtration through a Sep-Pak column: first 10% acetonitrile containing 0.1% (w/v) TFA to remove salts, then 60% acetonitrile containing 0.1% (w/v) TFA to collect the product. After removal of solvent under reduced pressure, dragmacidin D (**5**, 1.8 mg, 86% yield) was isolated as an orange/red oil: ^1H NMR (600 MHz, CD_3OD) δ 8.74 (s, 1H), 8.6 (d, J = 8.7 Hz, 1H), 7.62 (d, J = 1.8 Hz, 1H), 7.49 (s, 1H), 7.46 (s, 1H), 7.27 (dd, J = 8.2, 1.8 Hz, 1H), 6.84 (d, J = 8.2 Hz, 1H), 6.64 (d, J = 7.8 Hz, 1H), 5.98 (s, 1H), 4.35 (q, J = 6.9 Hz, 1H), 1.52 (d, J = 7.3 Hz, 3H); ^{13}C NMR (1645 MHz, CD_3OD) δ 157.1, 150.3, 148.7, 144.8, 139.1, 134.2, 132.4, 132.2, 128.7, 127.9, 127.3, 126.7, 126.3, 125.6, 124.8, 120.2,

117.1, 115.4, 113.7, 110.2, 108.9, 107.3, 33.2, 20.8; IR (film) 3200 (br), 1667, 1204, 1138 cm^{-1} ; UV λ_{max} (EtOH) 216, 274, 389 nm. After addition of 1 drop concentrated HCl to 1 mL cell: λ_{max} (EtOH) 219, 277, 460 nm; HRMS-ESI (m/z): $[\text{M} + \text{H}]^+$ calc'd for $\text{C}_{25}\text{H}_{21}\text{BrN}_7\text{O}_2$, 530.0940; found, 530.0943.

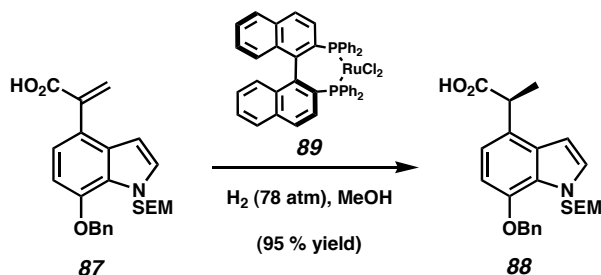


Ester 86. To **68** (50 mg, 0.116 mmol) in a flame-dried Schlenk flask was added tris(dibenzylideneacetone)dipalladium(0) (1.5 mg, 0.0017 mmol), stannane **85** (52 μL , 0.15 mmol), dry cesium fluoride (46 mg, 0.302 mmol), and benzene (1.3 mL), followed by tri-*t*-butylphosphine (0.78 mg, 0.0038 mmol) under an N_2 atmosphere in a dry box. The sealed reaction vessel was then heated at 60 $^\circ\text{C}$ for 14 h. The reaction mixture was cooled to 23 $^\circ\text{C}$ and filtered through a plug of silica gel (EtOAc eluent). After removal of solvent under reduced pressure, the crude product was purified by flash chromatography (4:1 hexanes:EtOAc) to afford **86** (42.6 mg, 71% yield) as a yellow oil: R_f 0.64 (4:1 hexanes:EtOAc); ^1H NMR (300 MHz, CDCl_3) δ 7.54-7.35 (comp. m, 5H), 7.16 (d, J = 3.3 Hz, 1H), 7.00 (d, J = 8.1 Hz, 1H), 6.76 (d, J = 8.1 Hz, 1H), 6.48 (d, J = 1.8 Hz, 1H), 6.41 (d, J = 2.9 Hz, 1H), 5.93 (d, J = 1.8 Hz, 1H), 5.75 (s, 2H), 5.23 (s, 2H), 3.80 (s, 3H), 3.46 (t, J = 8.1 Hz, 2H), 0.83 (t, J = 8.2 Hz, 2H), -0.08 (s, 9H); ^{13}C NMR (75 MHz, CDCl_3) δ 168.2, 146.9, 140.3, 137.0, 130.2, 129.6, 128.8, 128.2, 127.8, 127.3, 125.6, 122.9, 121.3, 104.2, 102.4, 77.6, 70.6, 52.4, 18.0, -1.1; IR (film) 2951, 1724, 1502, 1290,

1258, 1175, 1073 cm^{-1} ; HRMS-ESI (m/z): $[\text{M} + \text{H}]^+$ calc'd for $\text{C}_{25}\text{H}_{32}\text{NO}_4\text{Si}$, 460.1920; found, 460.1913.



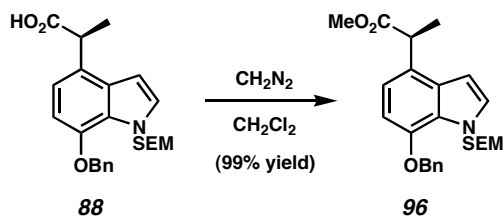
Acid 87. To a solution of **86** (970 mg, 1.88 mmol) in THF (10 mL) and H_2O (2 mL) was added lithium hydroxide monohydrate (394 mg, 9.40 mmol). The resulting solution was heated under reflux to 80 $^{\circ}\text{C}$ for 24 h, then allowed to cool to 23 $^{\circ}\text{C}$. The reaction mixture was diluted with H_2O (5 mL) and extracted with Et_2O (2 x 10 mL). The organic layer was discarded, and the aqueous layer was acidified to pH=2 by the dropwise addition of 6 N HCl at 0 $^{\circ}\text{C}$. After extracting the aqueous layer with CH_2Cl_2 (3 x 20 mL), the combined organic layers were washed with H_2O (10 mL) and brine (10 mL), dried over magnesium sulfate, and evaporated under reduced pressure to yield **87** (919 mg, 97% yield) as a yellow oil, which was used in the subsequent step without further purification.



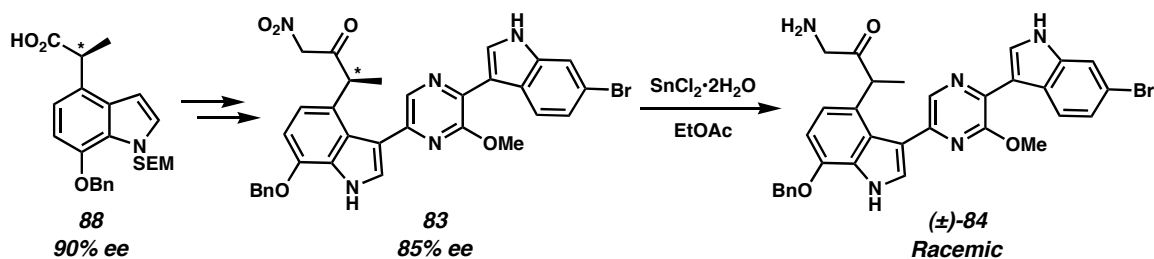
To **87** (578 mg, 1.15 mmol) in a thick-walled glass container under N_2 in a dry box was added dichloro[(*S*)-(-)-2,2'-bis(diphenylphosphino)-1,1'-binaphthyl]ruthenium

(II) (**89**, 46 mg, 0.0576 mmol) and CH₃OH (11.5 mL). The reaction vessel was sealed under nitrogen, removed from the dry box, and placed in a stainless steel bomb, which was purged with argon. After removing the seal of the reaction vessel, the bomb was sealed under an argon atmosphere, cooled to -10 °C over 1 h, then purged and pressurized with H₂ to 1200 psi with vigorous stirring. The H₂ pressure was carefully released after 72 h of stirring, and the reaction vessel was warmed to 23 °C. After filtering the reaction mixture through a plug of celite (CH₃OH eluent), the solvent was evaporated under reduced pressure to yield **88** (550 mg, 95% yield, 90% ee*) as a yellow oil: R_f 0.63 (1:1 hexanes:EtOAc); ¹H NMR (300 MHz, CDCl₃) δ 7.17 (d, *J* = 3.3 Hz, 1H), 6.98 (d, *J* = 8.1 Hz, 1H), 6.73 (d, *J* = 8.1 Hz, 1H), 6.61 (d, *J* = 3.3 Hz, 1H), 5.76 (d, *J* = 10.6 Hz, 1H), 5.72 (d, *J* = 10.3 Hz, 1H), 5.19 (s, 2H), 4.08 (q, *J* = 7.1 Hz, 1H), 3.45 (t, *J* = 8.2 Hz, 2H), 1.60 (d, *J* = 7.0 Hz, 3H), 0.82 (t, *J* = 8.2 Hz, 2H), -0.09 (s, 9H); ¹³C NMR (125 MHz, CDCl₃) δ 180.6, 146.3, 137.2, 130.3, 129.4, 128.8, 128.2, 127.8, 125.9, 124.9, 118.7, 104.6, 101.6, 77.6, 70.6, 65.5, 42.4, 18.0, 17.5, -1.2; IR (film) 2952, 1707, 1503, 1251, 1072 cm⁻¹; HRMS-ESI (*m/z*): [M + Na]⁺ calc'd for C₂₄H₃₁NO₄SiNa, 448.190; found, 448.1918.

The enantiopurity of **88 was determined by derivatization to methyl ester **97** via treatment with diazomethane as described below, followed by chiral HPLC analysis:*



Ester 96. To a sample of **88** (2 mg, 0.004 mmol) in CH_2Cl_2 (1 mL) was added ethereal diazomethane (0.2 M, ca. 1 mL) until a bright green/yellow color persisted. The solvent was removed under reduced pressure to afford ester **96** (2 mg, 99% yield) as a yellow oil. Chiral HPLC was performed on a Chiralcel AD column using 2% *i*-PrOH in hexanes as eluent.

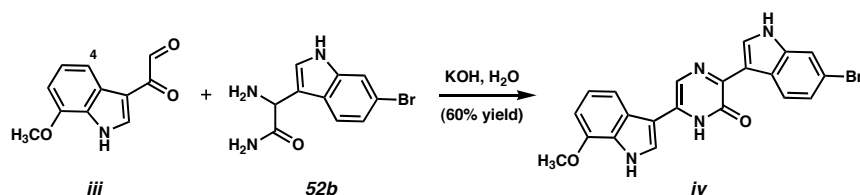


The enantiopurity of **83** was determined by chiral HPLC performed on a Chiralcel AD column using 20% EtOH in hexanes as eluent. The enantiopurity of **84** was determined by chiral HPLC performed on a Chiralcel AD column using 60% EtOH in hexanes as eluent.

2.8 Notes and References

- (1) (a) Wright, A. E.; Pomponi, S. A.; Cross, S. S.; McCarthy, P. *J. Org. Chem.* **1992**, *57*, 4772-4775. (b) Capon, R. J.; Rooney, F.; Murray, L. M.; Collins, E.; Sim, A. T. R.; Rostas, J. A. P.; Butler, M. S.; Carroll, A. R. *J. Nat. Prod.* **1998**, *61*, 660-662. (c) Cutignano, A.; Bifulco, G.; Bruno, I.; Casapullo, A.; Gomez-Paloma, L.; Riccio, R. *Tetrahedron* **2000**, *56*, 3743-3748. (d) Wright, A. E.; Pomponi, S. A.; Jacobs, R. S. PCT Int. Appl. WO 9942092 August 26, 1999.
- (2) Portions of this work have been published, see: Garg, N. K.; Sarpong, R.; Stoltz, B. M. *J. Am. Chem. Soc.* **2002**, *124*, 13179-13184.
- (3) Sundberg, R. J., Ed.; *Indoles*; Academic Press: San Diego, 1996.
- (4) For a reference on biomimetic cyclocondensations to produce pyrazinones, see: Yaylayan, V. A. *J. Agric. Food. Chem.* **1996**, *44*, 2511-2516.
- (5) For comprehensive reviews on transition metal-catalyzed cross-coupling reactions, see: (a) Diederich, F.; Stang, P. J.; Eds.; *Metal-Catalyzed Cross-Coupling Reactions*; Wiley-VCH: Weinheim, 1998. (b) Geissler, H. In *Transition Metals for Organic Synthesis*; Beller, M.; Bolm, C., Eds.; Wiley-VCH: Weinheim, 1998; Chapter 2.10, p 158. (c) Tsuji, J. In *Transition Metal Reagents and Catalysts*; Wiley: Chichester, U.K., 2000; Chapter 3, p 27.

- (6) (a) Kharasch, M. S.; Kane, S. S.; Brown, H. C. *J. Am. Chem. Soc.* **1940**, 62, 2242-2243. (b) Hashem, M. A.; Sultana, I.; Hai, M. A. *Indian J. Chem. Sect. B* **1999**, 38, 789-794.
- (7) (a) Vereshchagin, A. L.; Branskii, O. V.; Semenov, A. A. *Chem. Heterocycl. Compd. (Engl. Transl.)* **1983**, 19, 40-42. (b) Kuivila, H. G. *J. Org. Chem.* **1960**, 25, 284-285.
- (8) Bromide **52b** was prepared in a manner similar to that used for the synthesis of **52a**. See Section 2.7 for details.
- (9) The steric component of C(4) substitution appears to be the determining factor as illustrated by the reaction of **iii** and **52b** to produce pyrazinone **iv** in good yield.

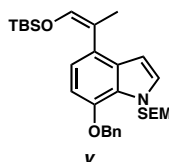


- (10) For an excellent discussion of the cross-coupling chemistry of pyrazines, see: Li, J. J.; Gribble, G. W. In *Palladium in Heterocyclic Chemistry: A Guide for the Synthetic Chemist*; Pergamon: Amsterdam, 2000; pp 355-373.

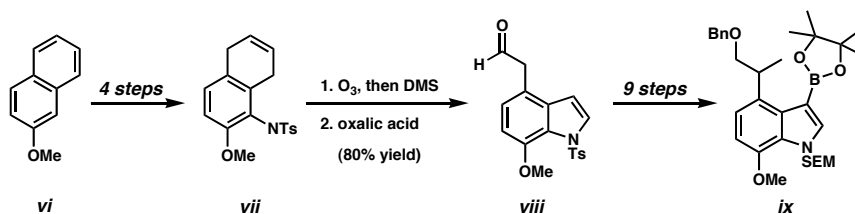
- (11) Turck, A.; Ple, N.; Dognon, D.; Harmoy, C.; Queguiner, G. *J. Heterocycl. Chem.* **1994**, *31*, 1449-1454.
- (12) For a discussion regarding the reactivity of aryl chlorides toward transition-metal complexes, see: Gushin, V. V.; Alper, H. *Chem. Rev.* **1994**, *94*, 1047-1062.
- (13) (a) Edwards, M. P.; Ley, S. V.; Lister, S. G.; Palmer, B. D. *J. Chem. Soc., Chem. Commun.* **1983**, 630-633. (b) Piers, E.; Britton, R.; Andersen, R. J. *J. Org. Chem.* **2000**, *65*, 530-535.
- (14) Pyrazinyl chlorides coupled competitively with the indolylbromide functionality.
- (15) Barlin, G. B. *Aust. J. Chem.* **1983**, *36*, 983-992.
- (16) Zhu, Z.; Moore, J. S. *J. Org. Chem.* **2000**, *65*, 116-123.
- (17) Bromoindole **49** was prepared from **50** by a modified Leimgruber-Batcho synthesis, see: Schumacher, R. W.; Davidson, B. S. *Tetrahedron* **1999**, *55*, 935-942.
- (18) Wenkert, E.; Moeller, P. D.; Piettre, S. R.; McPhail, A. T. *J. Org. Chem.* **1988**, *53*, 3170-3178.

- (19) Zheng, Q.; Yang, Y.; Martin, A. R. *Heterocycles* **1994**, *37*, 1761-1772.
- (20) (a) Bartoli, G.; Palmieri, G.; Bosco, M.; Dalpozzo, R. *Tetrahedron Lett.* **1989**, *30*, 2129-2132. (b) Bosco, M.; Dalpozzo, R.; Bartoli, G.; Palmieri, G.; Petrini, M. *J. Chem. Soc., Perkin Trans. 2* **1991**, *5*, 657-663.
- (21) Benzyl ether **66** is a known compound prepared in a single-step involving benzyl protection of commercially available 4-bromo-2-nitrophenol. See: Auwers, K. *Justus Liebigs Ann. Chem.* **1907**, *357*, 85-94.
- (22) Derivatives of **67** were initially accessed via the Leimgruber-Batcho indole synthesis. These routes took several steps and were low-yielding. For the Leimgruber-Batcho indole synthesis, see: Batcho, A. D.; Leimgruber, W. *Org. Synth.* **1985**, *63*, 214-225. See also references therein.
- (23) Belletete, M.; Beaupre, S.; Bouchard, J.; Blondin, P.; Leclerc, M.; Durocher, G. *J. Phys. Chem. B* **2000**, *104*, 9118-9125.
- (24) Li, K.; Du, W.; Que, N. L.; Liu, H. *J. Am. Chem. Soc.* **1996**, *118*, 8763-8764.

- (25) For general reviews of Suzuki couplings, see: (a) Miyaura, N.; Suzuki, A. *Chem. Rev.* **1995**, 95, 2457-2483. (b) Suzuki, A. *J. Organomet. Chem.* **1999**, 576, 147-168.
- (26) (a) Maki, S.; Okawa, M.; Matsui, R.; Hirano, T.; Niwa, H. *Synlett* **2001**, 10, 1590-1592. (b) In the presence of minor impurities and/or solutions of benzene that were not pre-saturated with H₂, the reaction produced a major byproduct identified as enol ether **v**.



- (27) (a) Ayer, W. A.; Craw, P. A.; Ma, Y. T.; Miao, S. *Tetrahedron* **1992**, 48, 2919-2924. (b) Amat, M.; Hadida, S.; Sathyanarayana, S.; Bosch, J. *J. Org. Chem.* **1994**, 59, 10-11.
- (28) A strategy involving Plieninger indolization was originally employed to prepare fragments related to **62**. Unfortunately, this strategy required 15 steps to access 3,4,7-trisubstituted indoles as summarized below (**vi** → **vii** → **viii** → **ix**). For the Plieninger indole synthesis, see: (a) Plieninger, H.; Suhr, K. *Chem. Ber.* **1956**, 89, 270-278. (b) Maehr, H.; Smallheer, J. *J. Am. Chem. Soc.* **1985**, 107, 2943-2945.



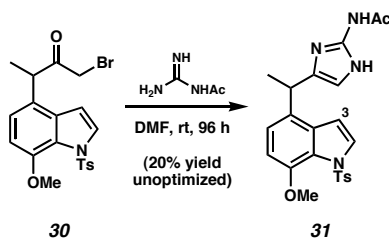
(29) For the cleavage of silyl ethers with HF•pyridine, see: Nicolaou, K. C.; Webber, S. E. *Synthesis* **1986**, 6, 453-461.

(30) Dess, D. B.; Martin, J. C. *J. Org. Chem.* **1983**, 48, 4155-4156.

(31) Arndt, F. *Org. Synth.*, **1943**, Coll. Vol. 2, 165.

(32) Little, T. L.; Webber, S. E. *J. Org. Chem.* **1994**, 59, 7299-7305.

(33) In an early approach, we prepared aminoimidazole **31** as shown below. Attempts to selectively functionalize C(3) of **31** were unsuccessful. Thus, **31** was deemed a non-productive route and was used only for model studies. Soon afterward, a similar approach to synthesize **31** appeared in the literature. See: Yang, C.-G.; Wang, J.; Jiang, B. *Tetrahedron Lett.* **2002**, 43, 1063-1066.



- (34) (a) Lancini, G. C.; Lazzari, E.; Sartori, G. *J. Antibiot.* **1968**, *21*, 387-392. (b) Howes, P. D.; Cleasby, A.; Evans, D. N.; Feilden, H.; Smith, P. W.; Sollis, S. L.; Taylor, N.; Wonacott, A. J. *Eur. J. Med. Chem.* **1999**, *34*, 225-234.
- (35) (a) Luzzio, F. A. *Tetrahedron* **2001**, *57*, 915-945. (b) Ayerbe, M.; Arrieta, A.; Cossio, F. *J. Org. Chem.* **1998**, *63*, 1795-1805.
- (36) Aldehyde **75** was the last compound in the synthesis that was readily purified on preparative scale by silica gel flash chromatography. Although analytical scale purification beyond this point was performed by reversed-phase HPLC or thin layer chromatography on SiO₂, all preparative scale purification was conducted by reversed-phase C₁₈ chromatography. Difficulties associated with the separation of similarly polar compounds by this method necessitated that all reactions in the sequence leading from **75** → **5** be high yielding.
- (37) Gilbert, E. J.; Chisholm, J. D.; Van Vranken, D. L. *J. Org. Chem.* **1999**, *64*, 5670-5676.
- (38) Sakowski, J.; Bohn, M.; Sattler, I.; Dahse, H.; Schlitzer, M. *J. Med. Chem.* **2001**, *44*, 2886-2899.

- (39) Lott, R. S.; Chauhan, V. S.; Virander, S.; Stammer, C. H. *J. Chem. Soc., Chem. Commun.* **1979**, 495-496.
- (40) The compounds depicted in Figure 2.4.2, from left to right, are aldehyde **75** and dragmacidin D (**5**).
- (41) For general reviews of asymmetric hydrogenation, see: (a) Takaya, H.; Ohta, T.; Noyori, R. In *Catalytic Asymmetric Synthesis*; Ojima, I., Ed.; VCH Publishers: New York, 1994; pp 1-39. (b) Noyori, R. In *Asymmetric Catalysis in Organic Synthesis*; Wiley-Interscience: New York, 1994; pp 16-94. (c) Brown, J. M. In *Comprehensive Asymmetric Catalysis*; Jacobsen, E. N.; Pfaltz, A.; Yamamoto, H., Eds.; Springer: Berlin, 1999; Vol. 1, pp 121-195.
- (42) Littke, A. F.; Schwarz, L.; Fu, G. C. *J. Am. Chem. Soc.* **2002**, *124*, 6343-6348.
- (43) Miyake, H.; Yamamura, K. *Chem. Lett.* **1989**, *6*, 981-984.
- (44) Miyake, F. Y.; Yakushijin, K.; Horne, D. A. *Org. Lett.* **2002**, *4*, 941-943.

APPENDIX ONE

Synthetic Summary for Dragmacidin D (5)

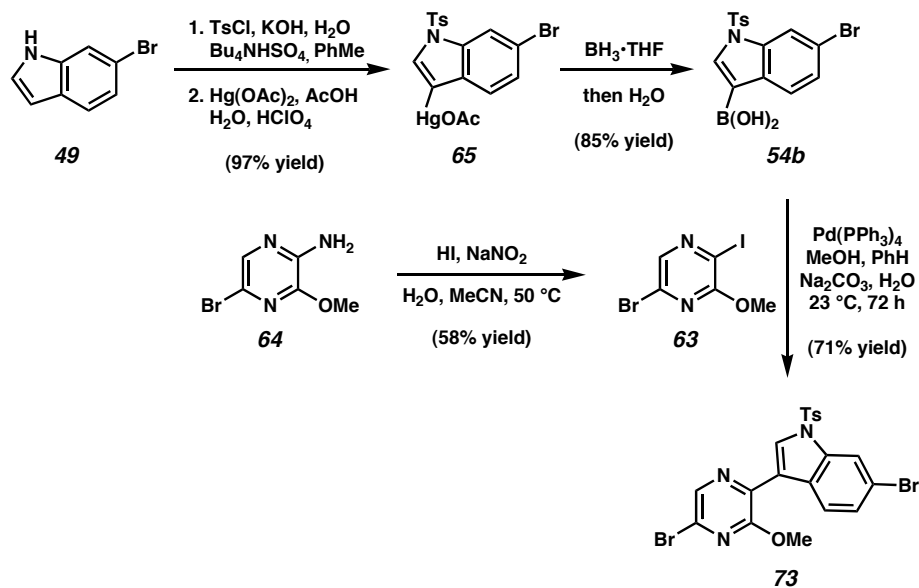
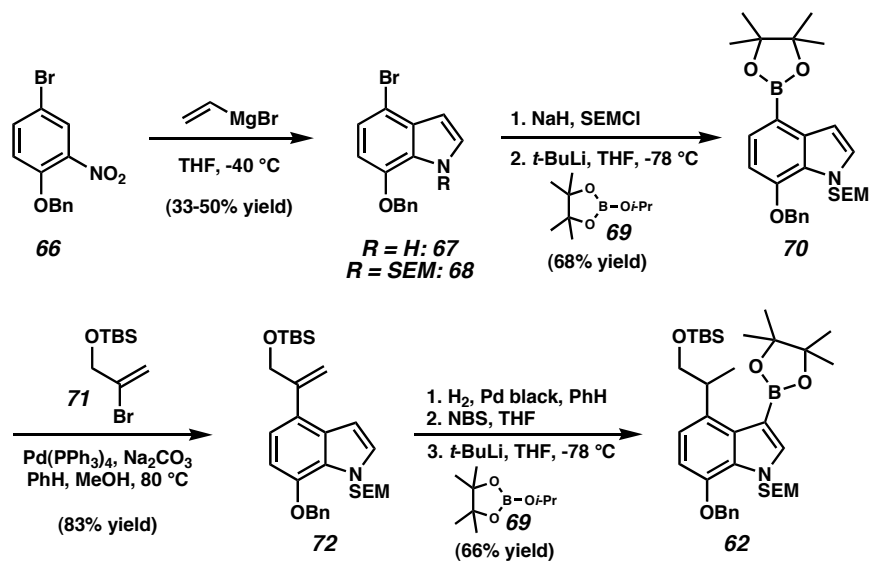
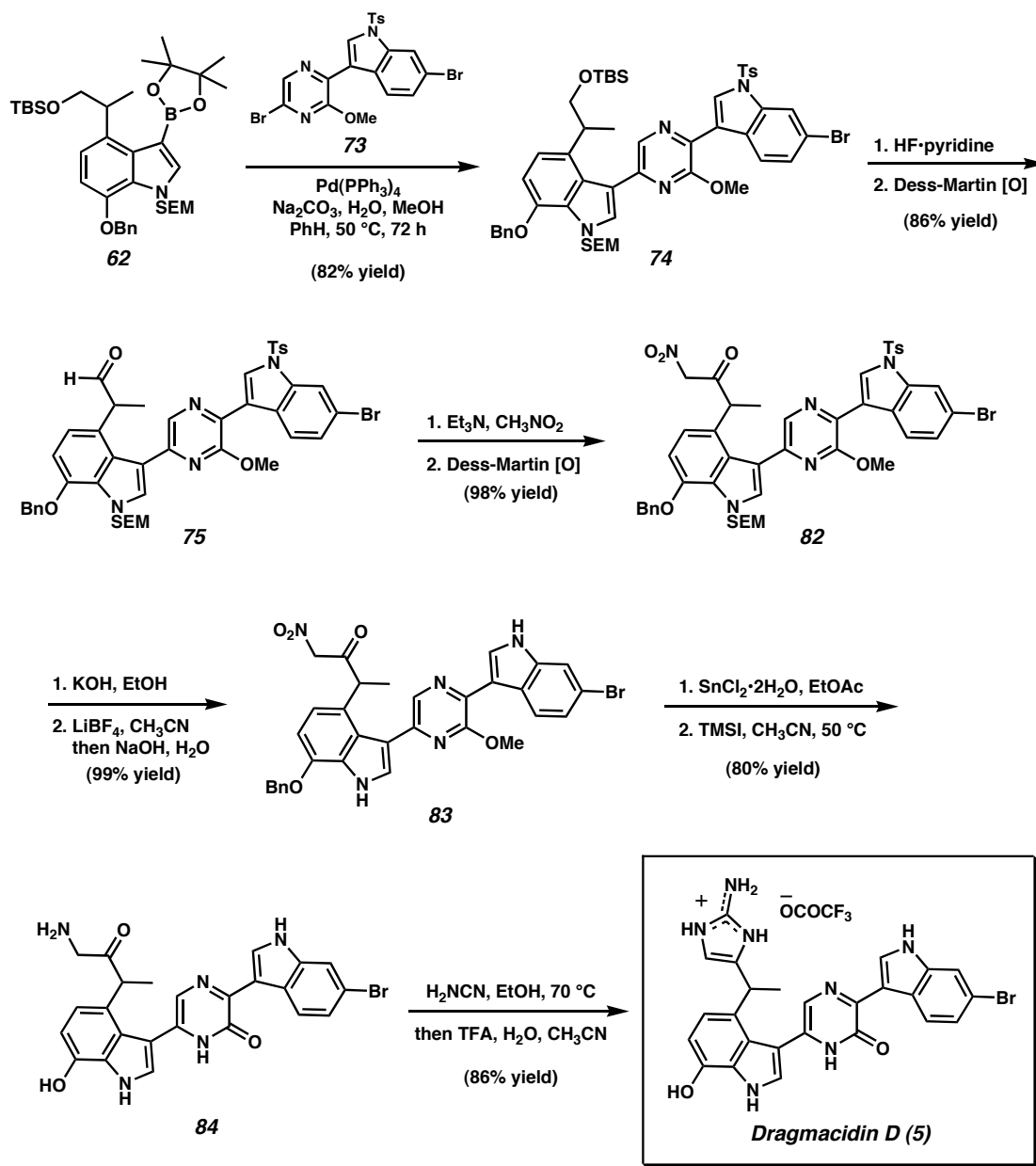
Figure A1.1 The synthesis of indolylpyrazine **73**.Figure A1.2 The synthesis of boronic ester **62**.

Figure A1.3 The synthesis of dragmacidin D (5).



APPENDIX TWO

**Spectra Relevant to Chapter Two:
The Total Synthesis of Dragmacidin D**

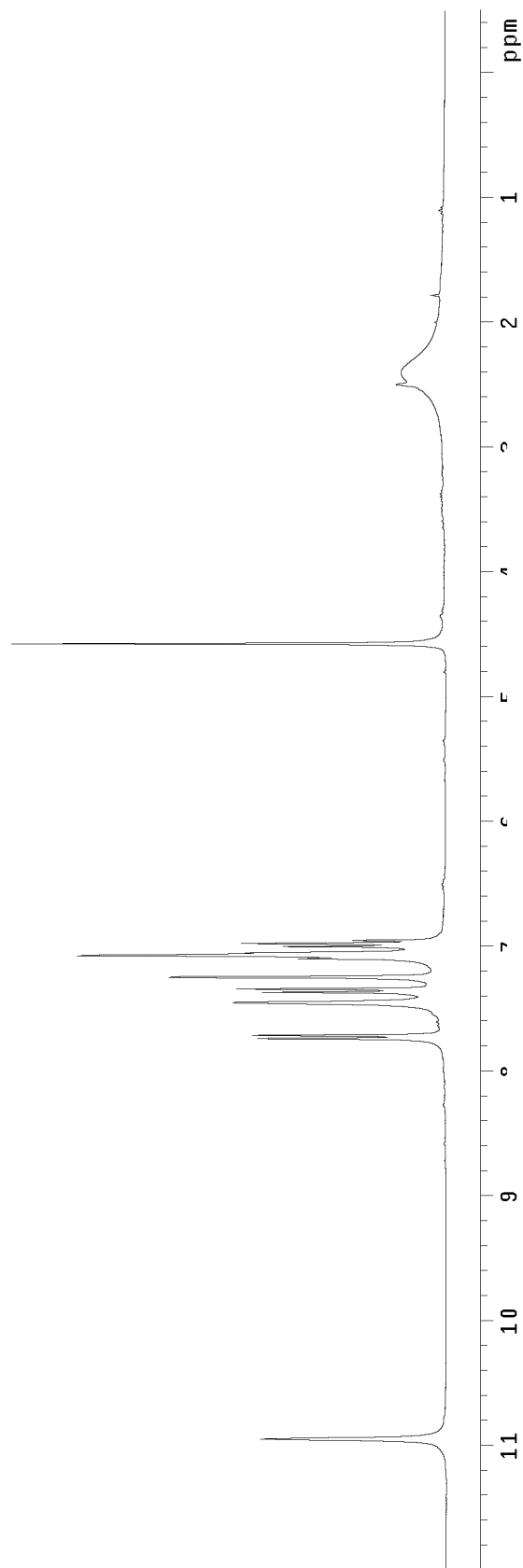
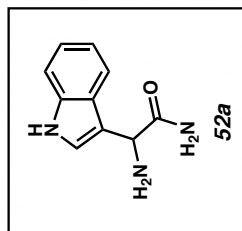


Figure A2.1 ¹H NMR (300 MHz, DMSO-*d*₆) of compound **52a**.



Figure A2.2 Infrared spectrum (thin film/NaCl) of compound **52a**.

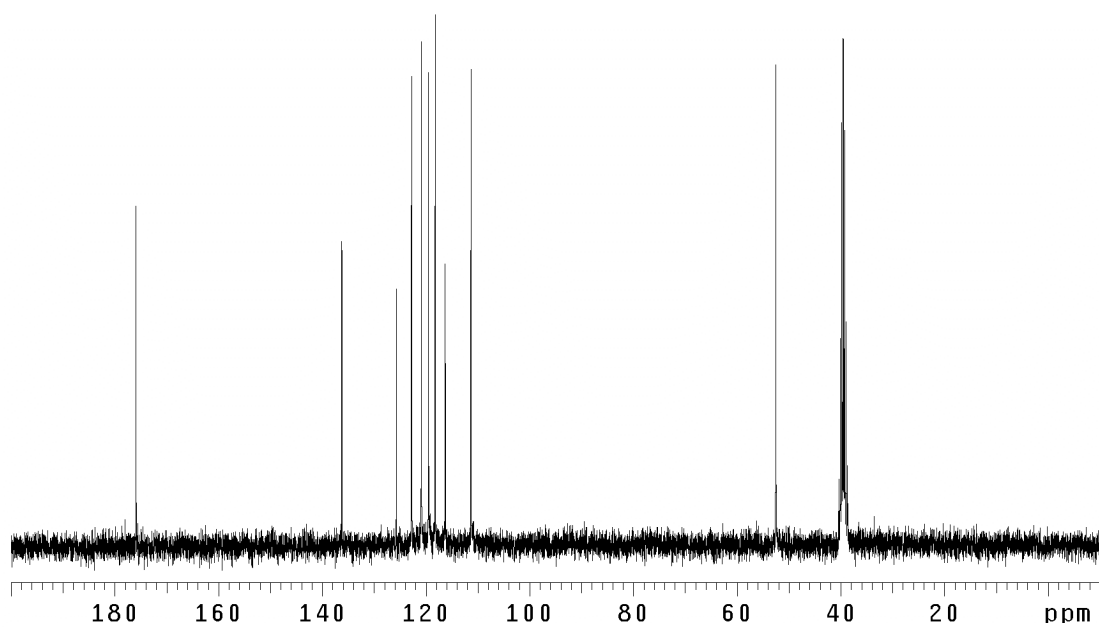


Figure A2.3 ¹³C NMR (75 MHz, DMSO-*d*₆) of compound **52a**.

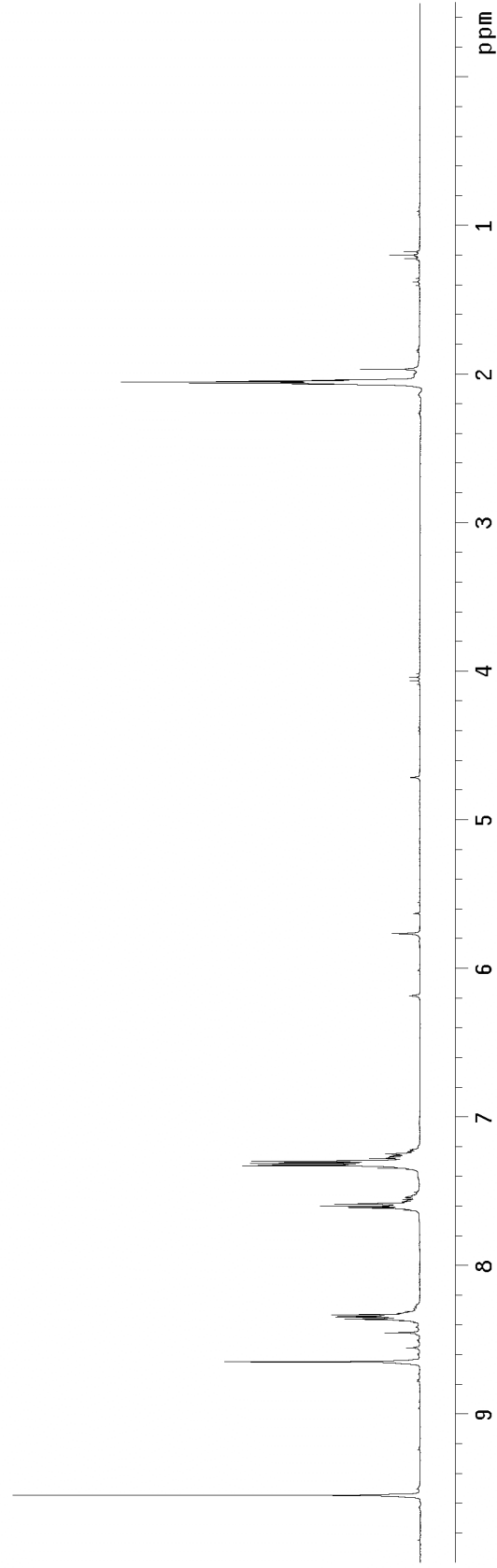
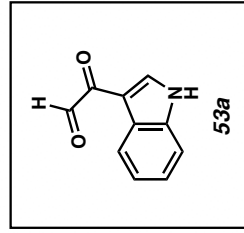


Figure A2.4 ^1H NMR (300 MHz, acetone- d_6) of compound **53a**.

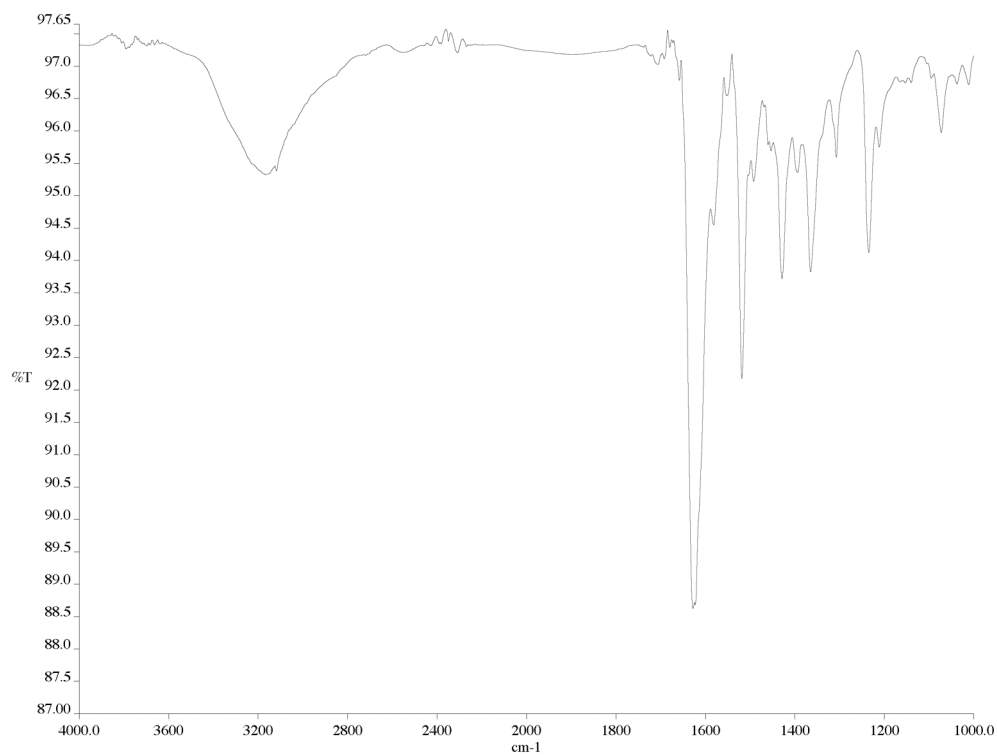


Figure A2.5 Infrared spectrum (thin film/NaCl) of compound **53a**.

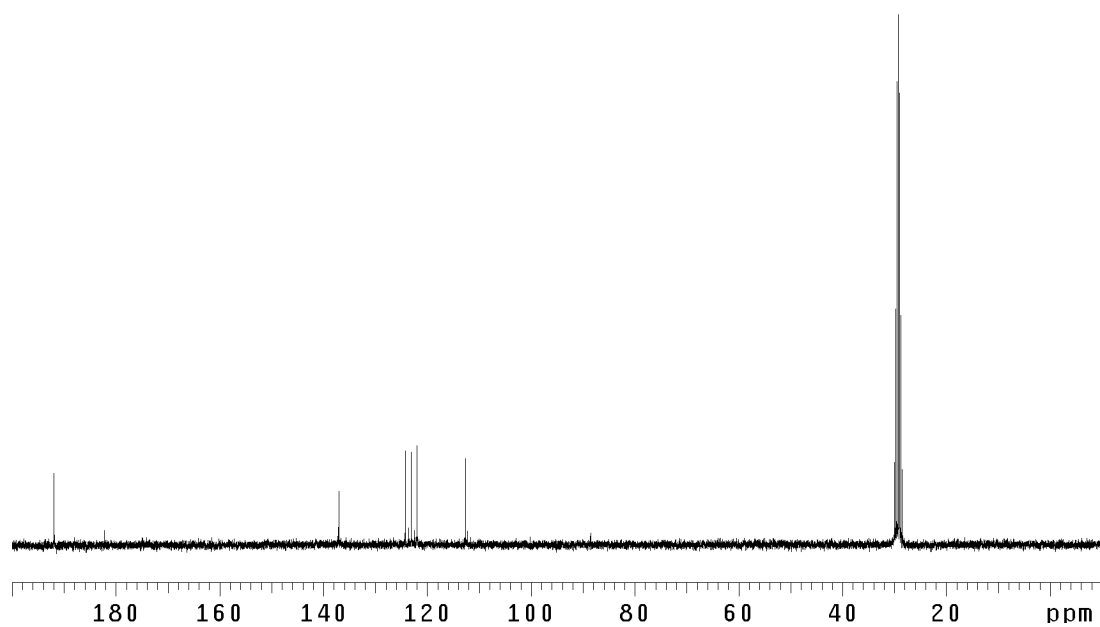


Figure A2.6 ¹³C NMR (75 MHz, acetone-*d*₆) of compound **53a**.

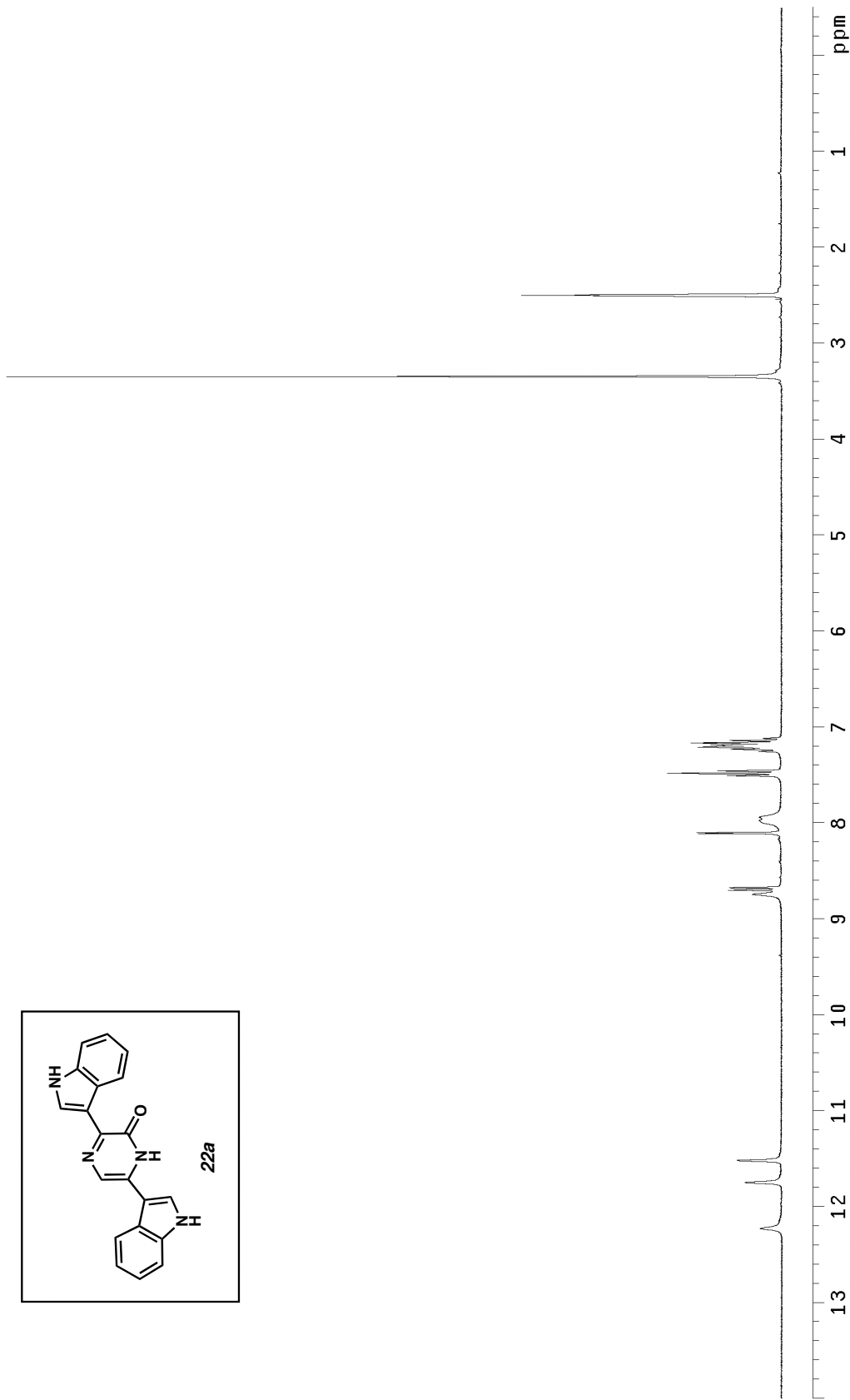
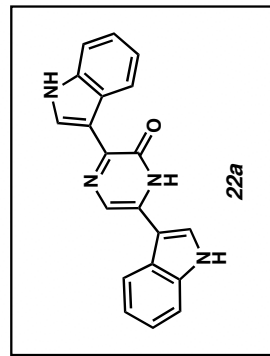


Figure A2.7 ¹H NMR (300 MHz, DMSO-*d*₆) of compound **22a**.



Figure A2.8 Infrared spectrum (thin film/NaCl) of compound **22a**.

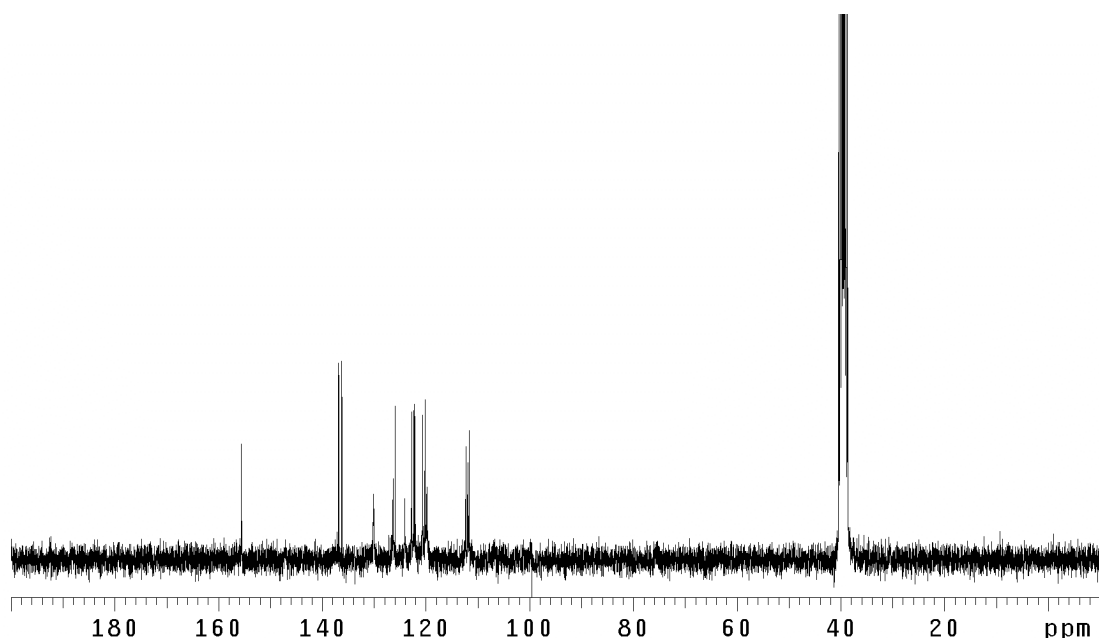


Figure A2.9 ¹³C NMR (125 MHz, DMSO-*d*₆) of compound **22a**.

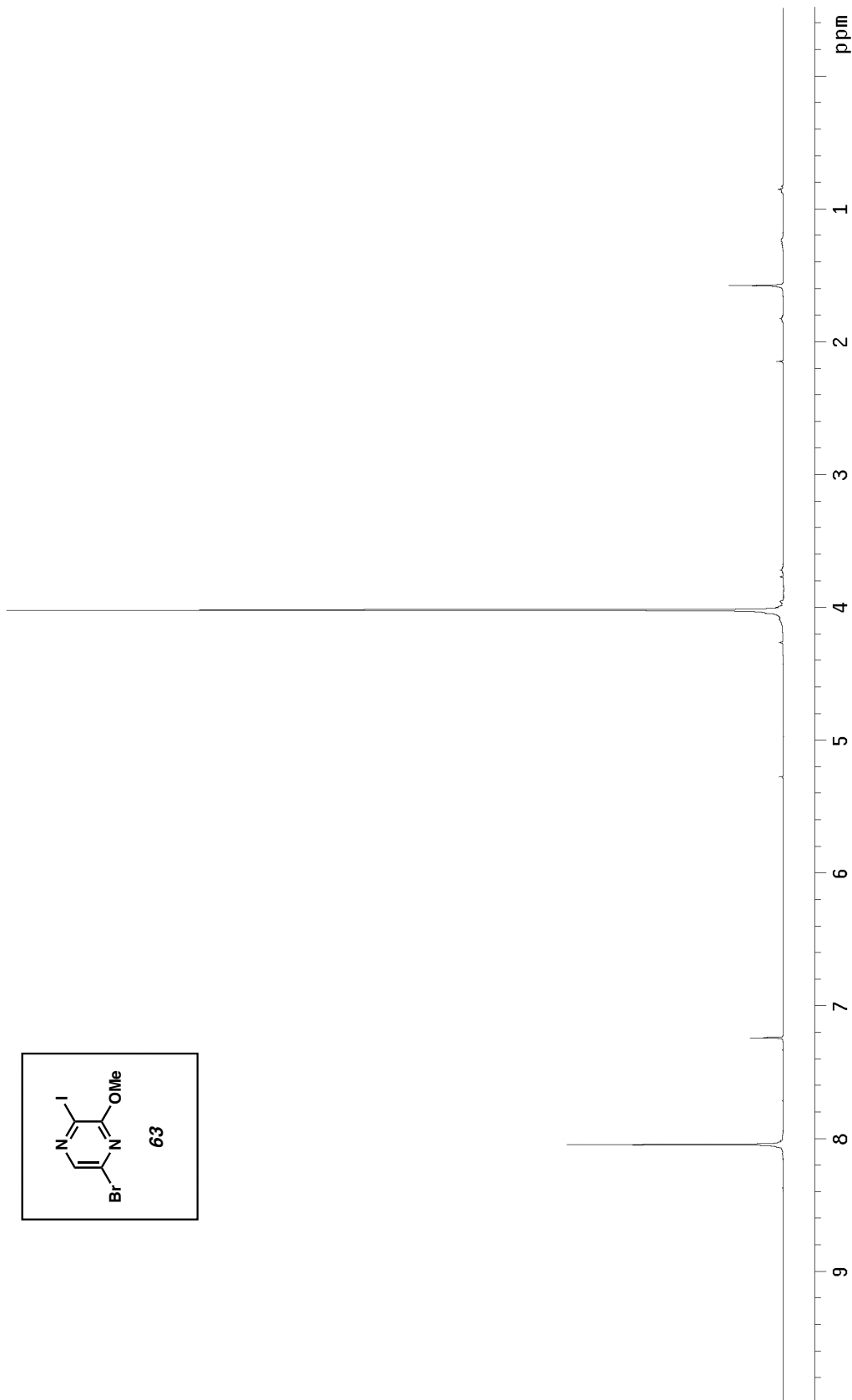
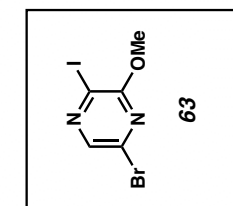


Figure A2.10 ^1H NMR (300 MHz, CDCl_3) of compound **63**.

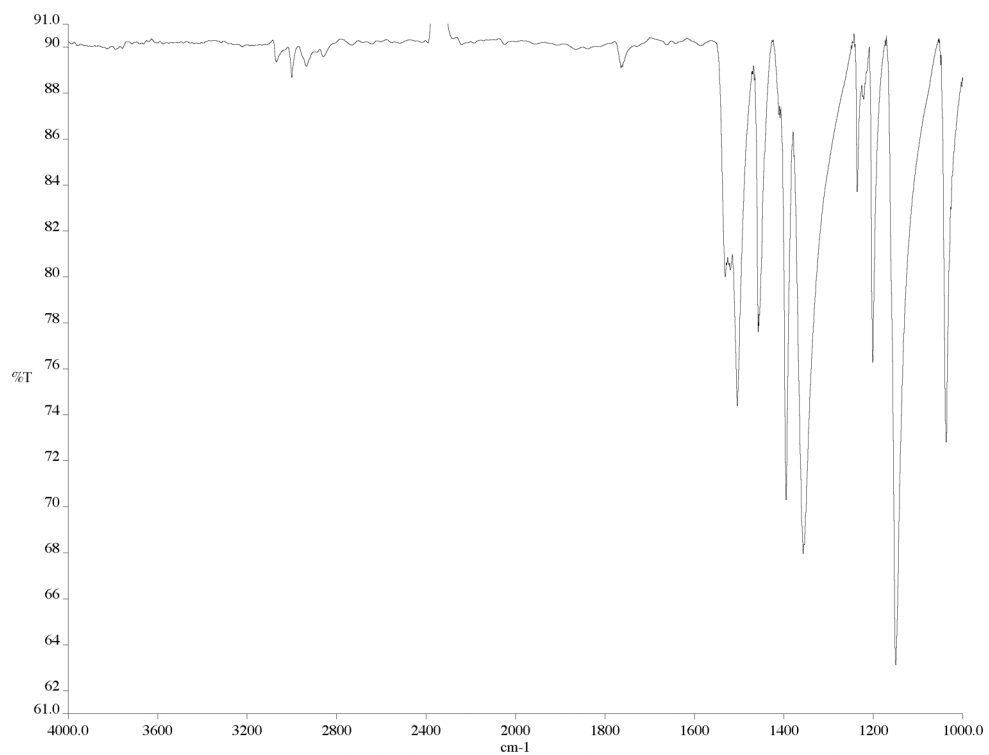


Figure A2.11 Infrared spectrum (KBr pellet) of compound **63**.

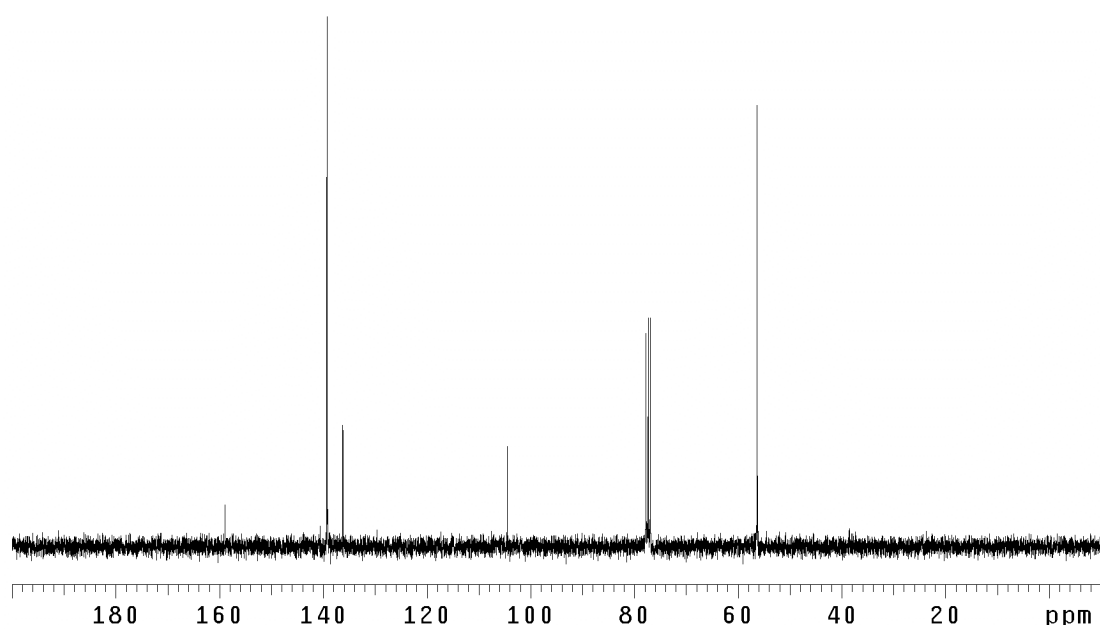


Figure A2.12 ¹³C NMR (75 MHz, CDCl₃) of compound **63**.

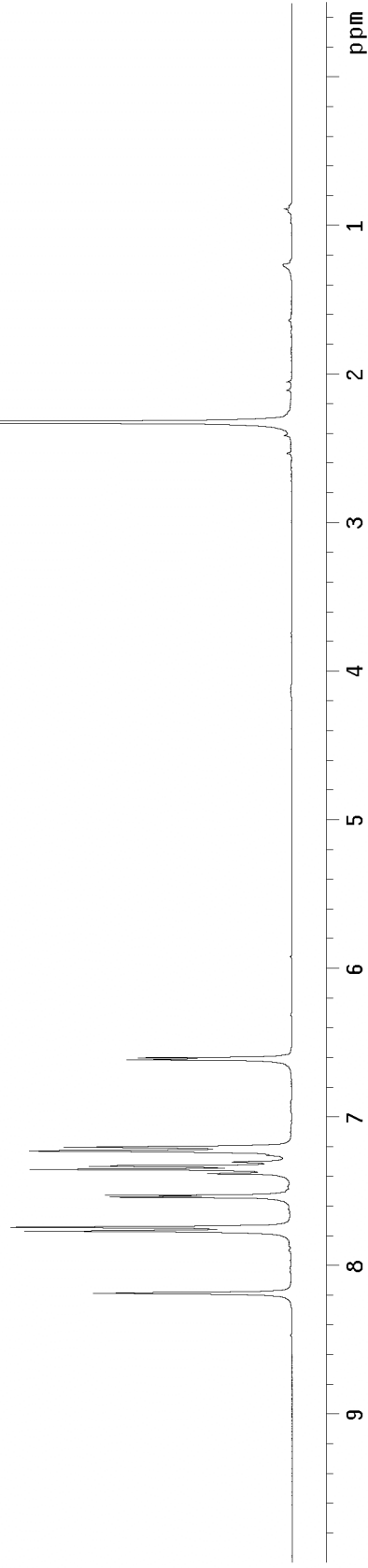
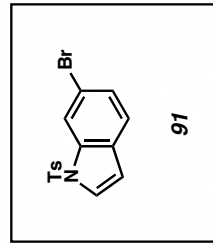


Figure A2.13 ^1H NMR (300 MHz, CDCl_3) of compound **91**.

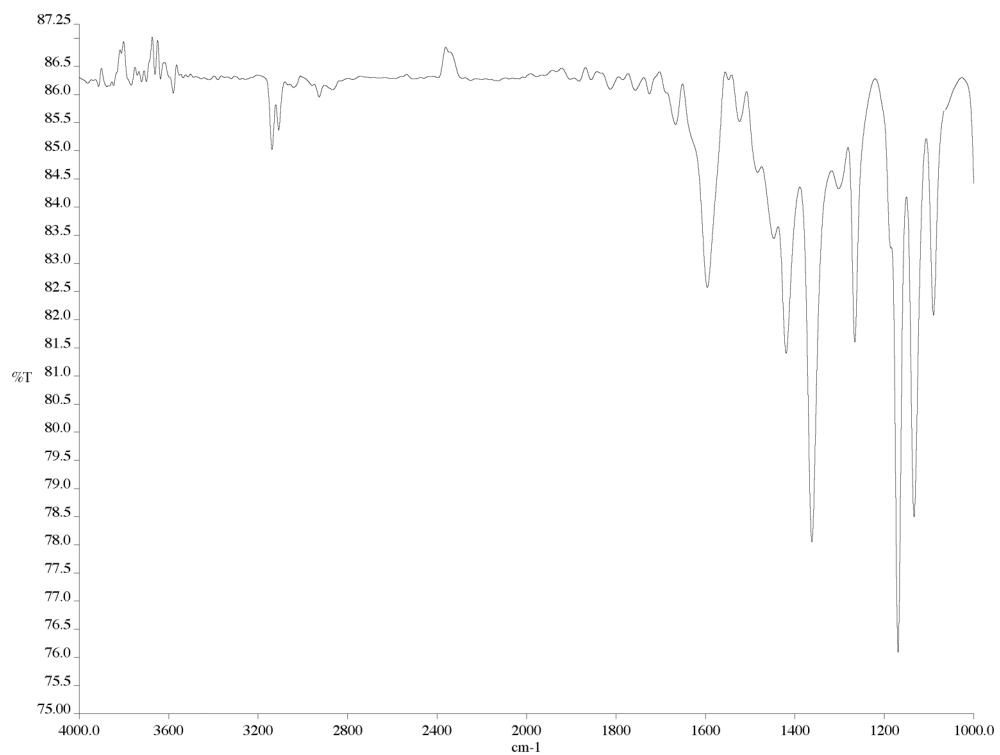


Figure A2.14 Infrared spectrum (thin film/NaCl) of compound **91**.

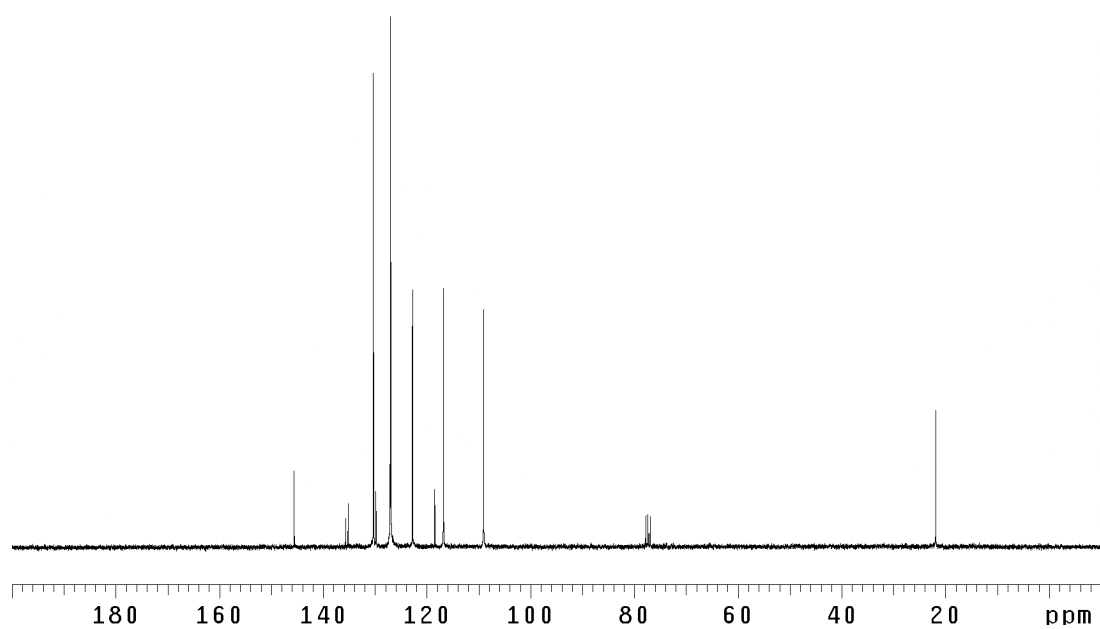


Figure A2.15 ¹³C NMR (75 MHz, CDCl₃) of compound **91**.

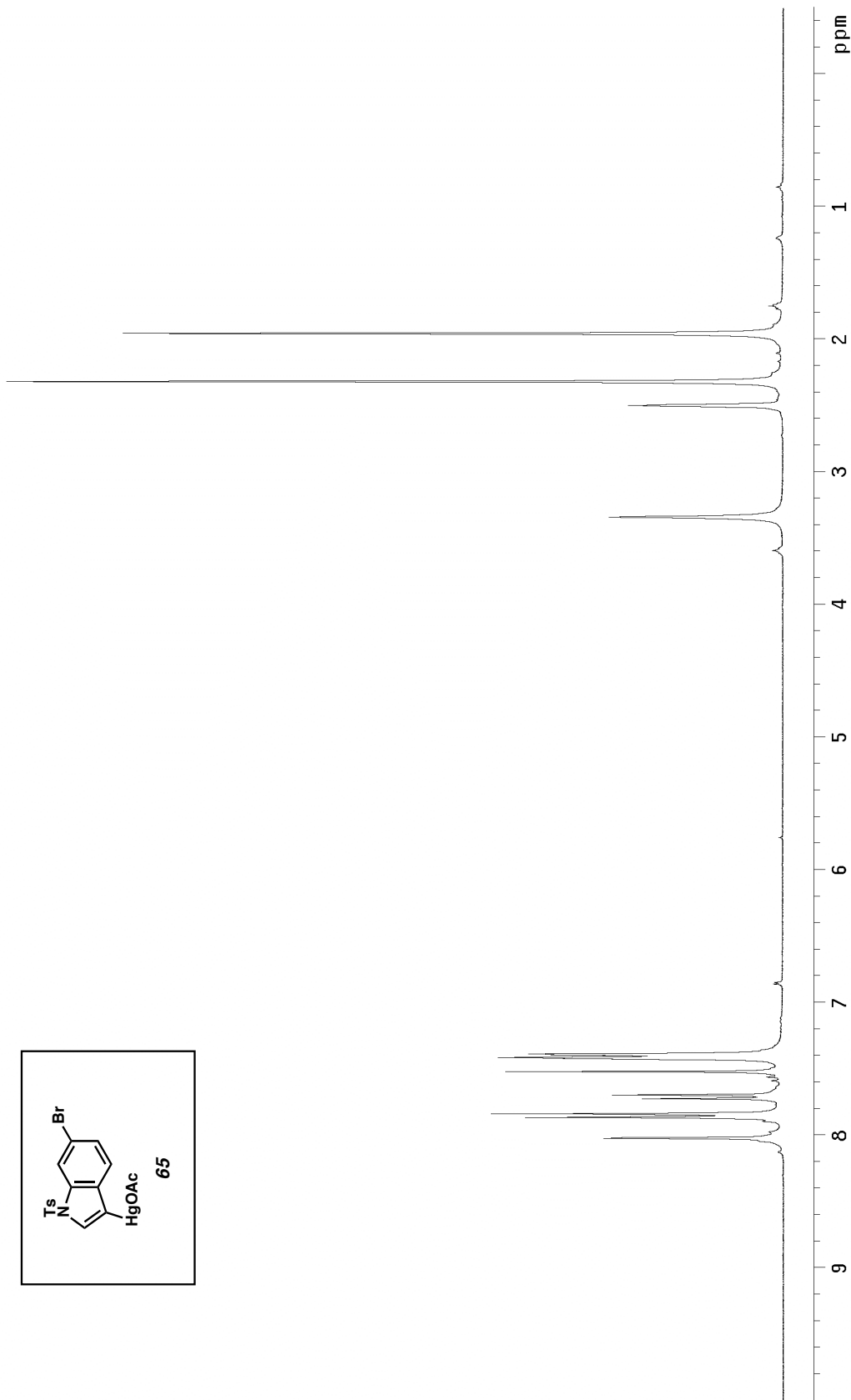


Figure A2.16 ^1H NMR (300 MHz, $\text{DMSO}-d_6$) of compound **65**.

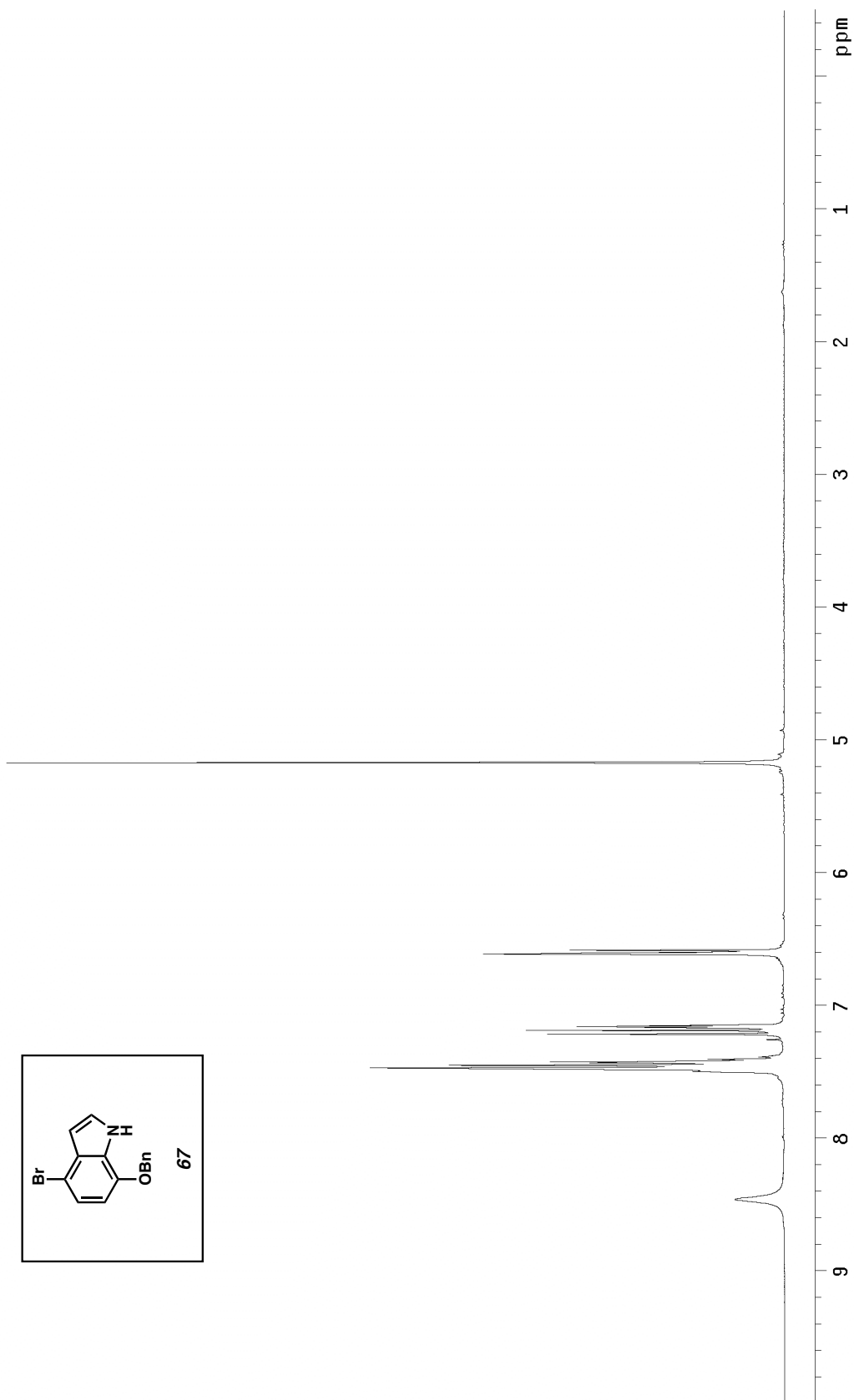
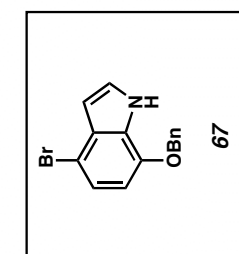


Figure A2.17 ^1H NMR (300 MHz, CDCl_3) of compound **67**.

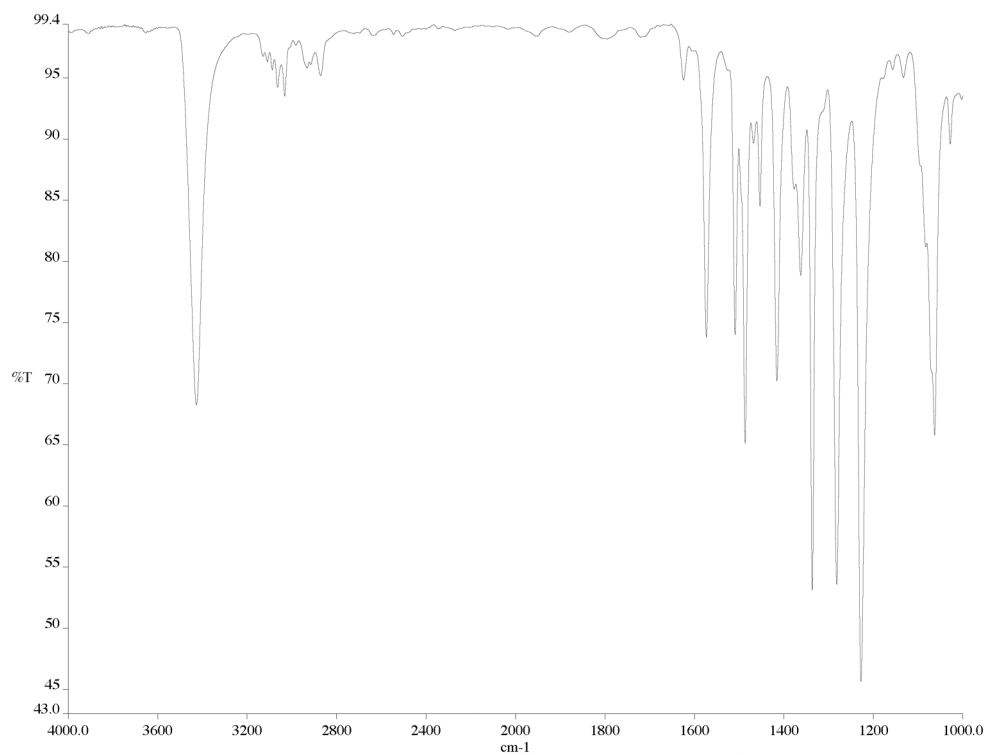


Figure A2.18 Infrared spectrum (thin film/NaCl) of compound **67**.

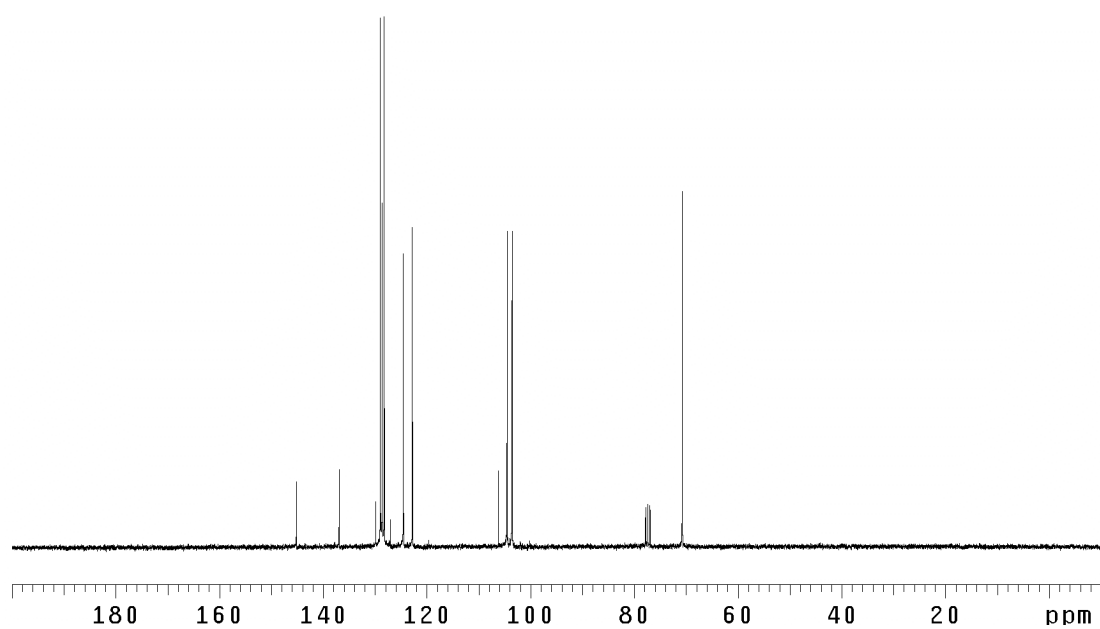


Figure A2.19 ¹³C NMR (75 MHz, CDCl₃) of compound **67**.

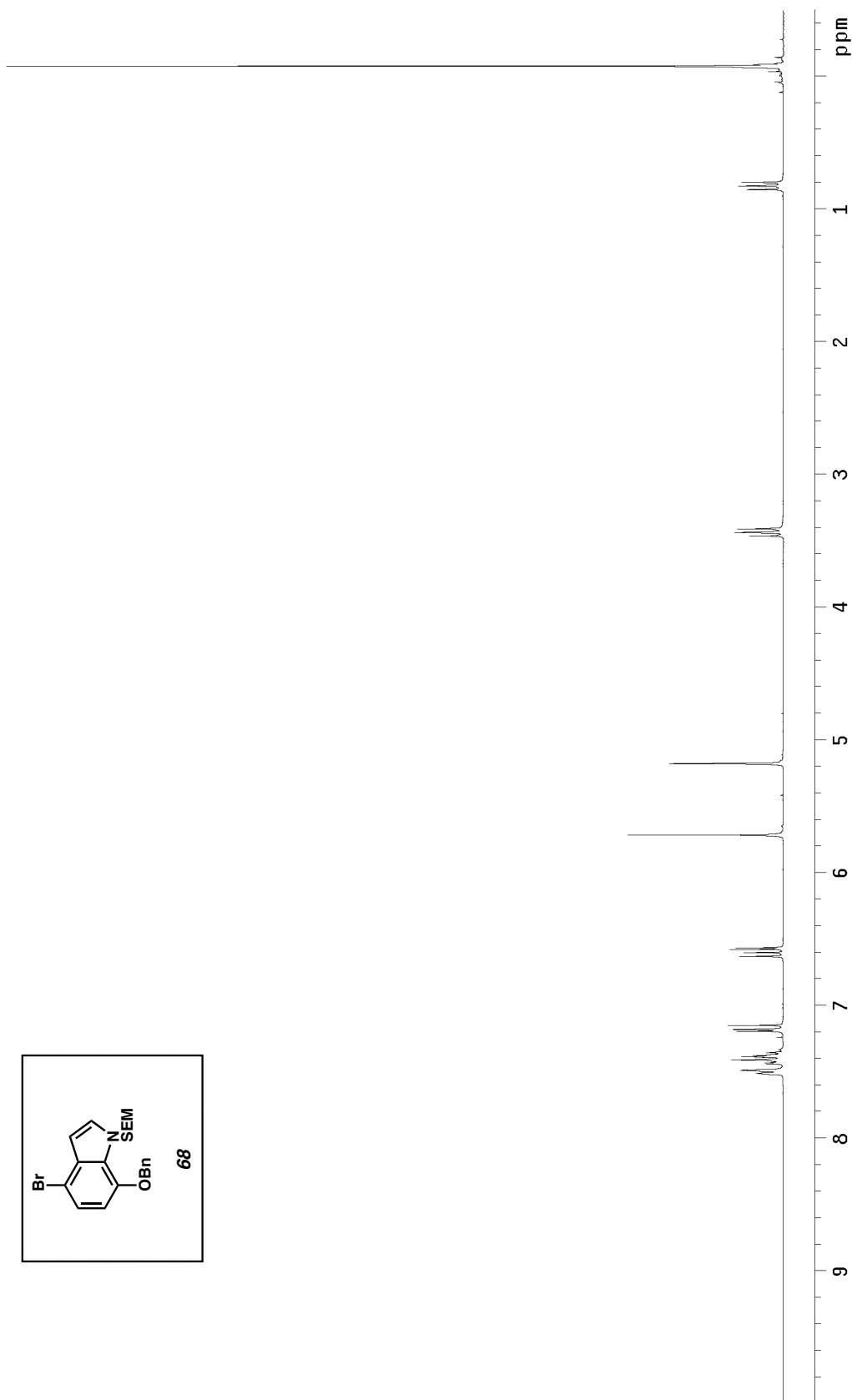
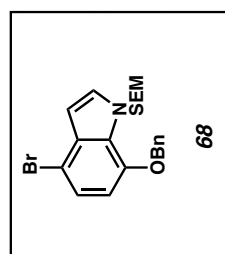


Figure A2.20 ^1H NMR (300 MHz, CDCl_3) of compound **68**.



Figure A2.21 Infrared spectrum (thin film/NaCl) of compound **68**.

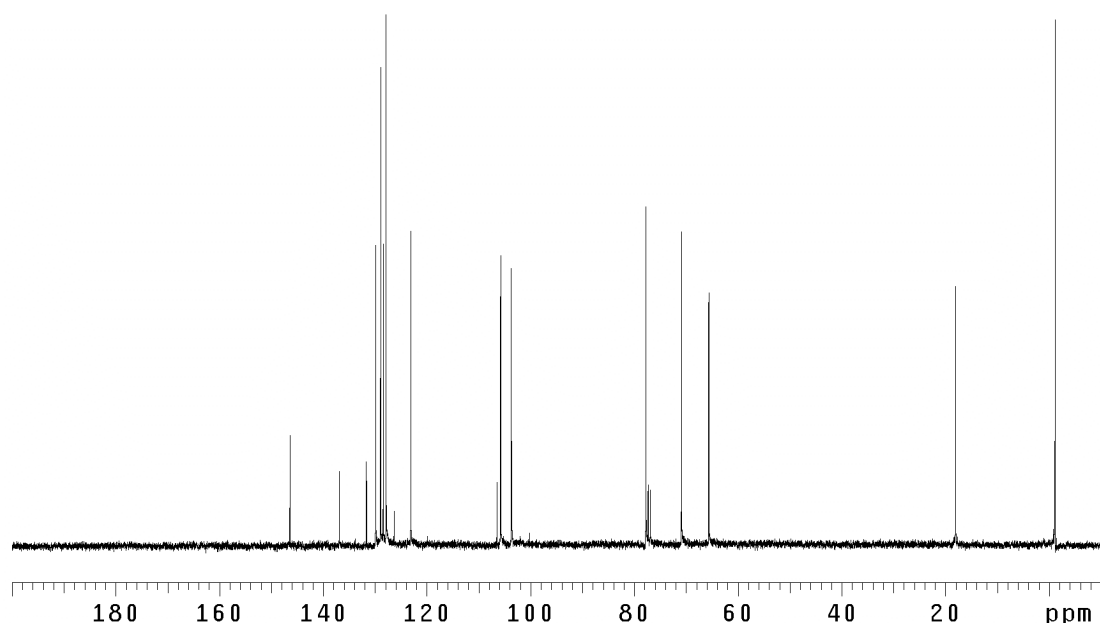


Figure A2.22 ¹³C NMR (75 MHz, CDCl₃) of compound **68**.

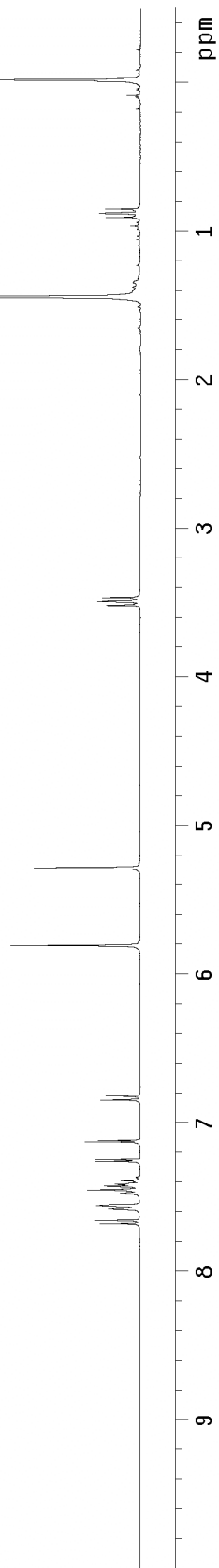
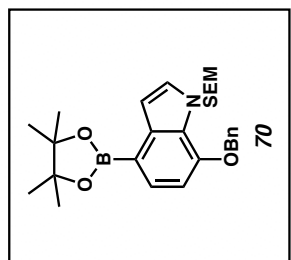


Figure A2.23 ^1H NMR (300 MHz, CDCl_3) of compound **70**.

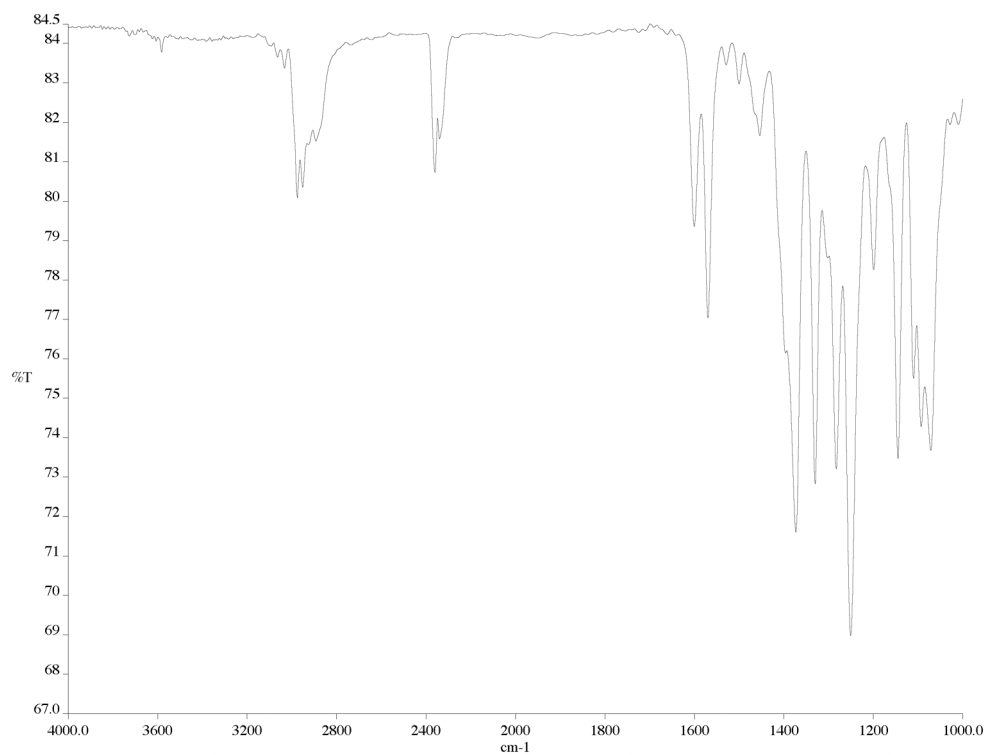


Figure A2.24 Infrared spectrum (thin film/NaCl) of compound **70**.

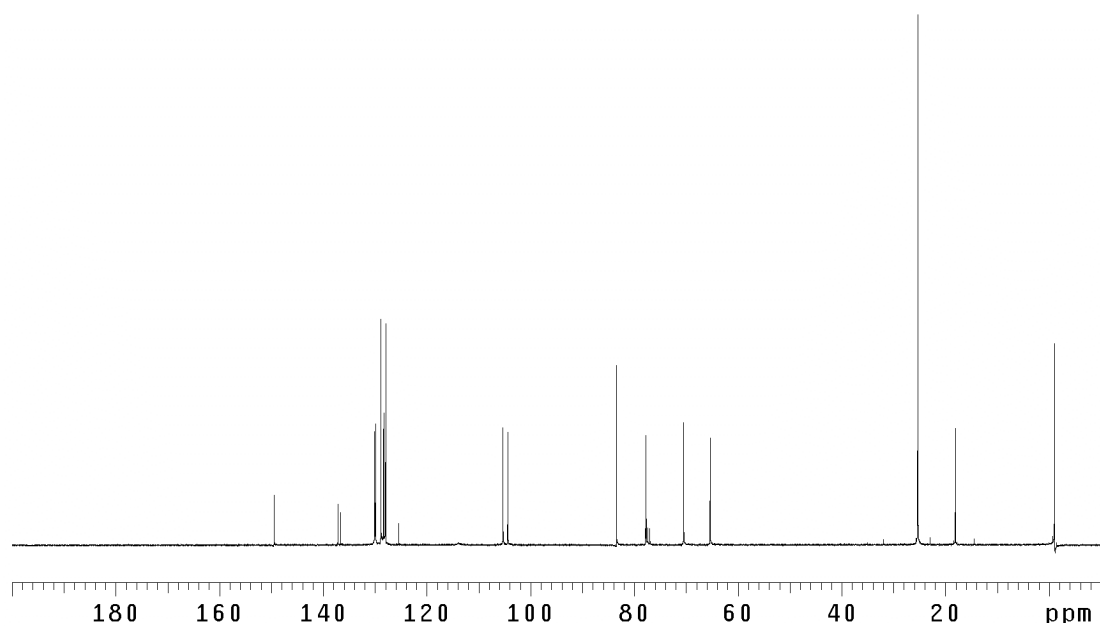


Figure A2.25 ¹³C NMR (75 MHz, CDCl₃) of compound **70**.

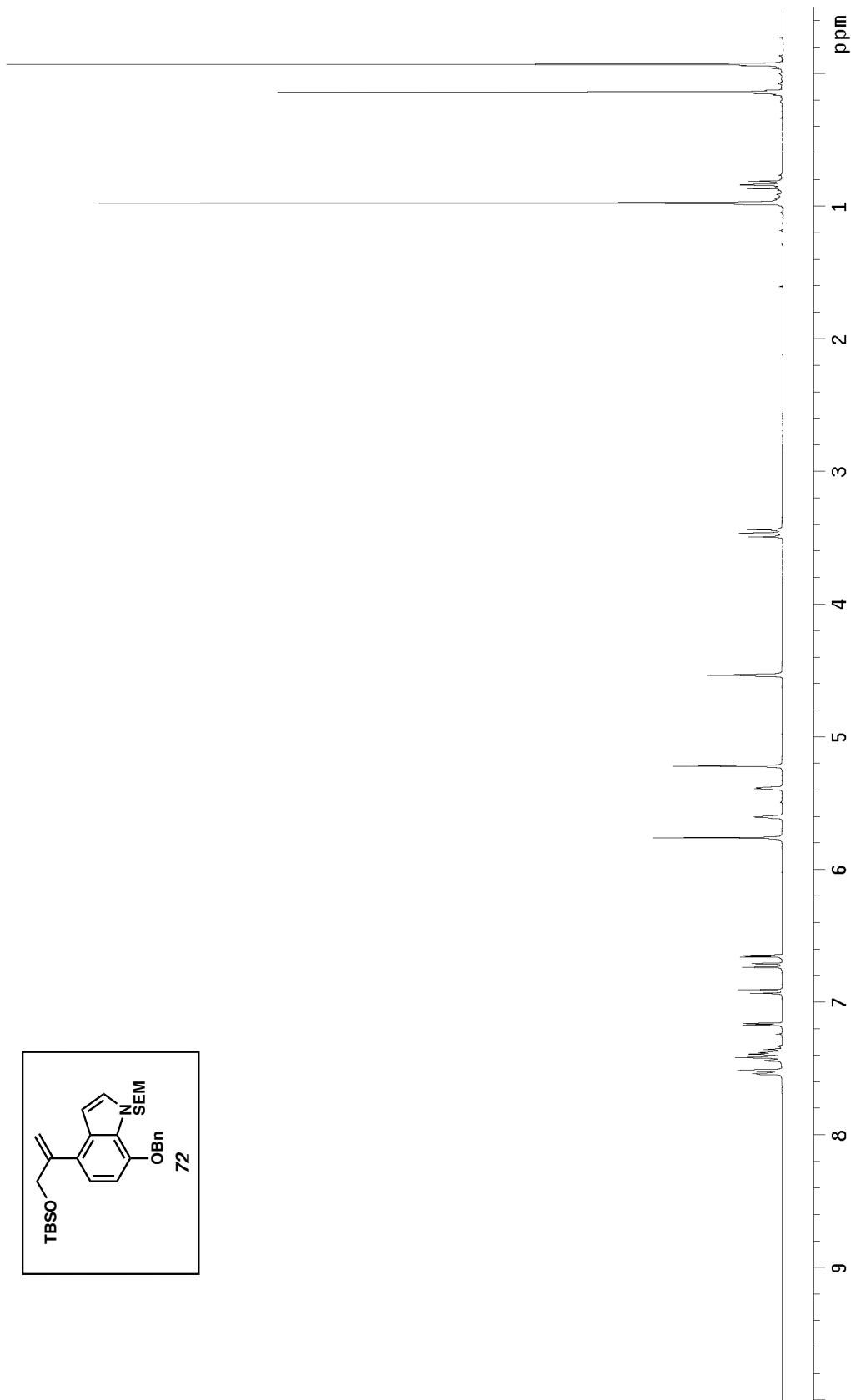
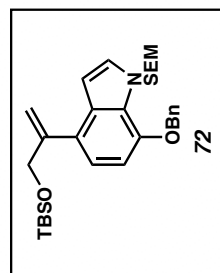


Figure A2.26 ^1H NMR (300 MHz, CDCl_3) of compound **72**.

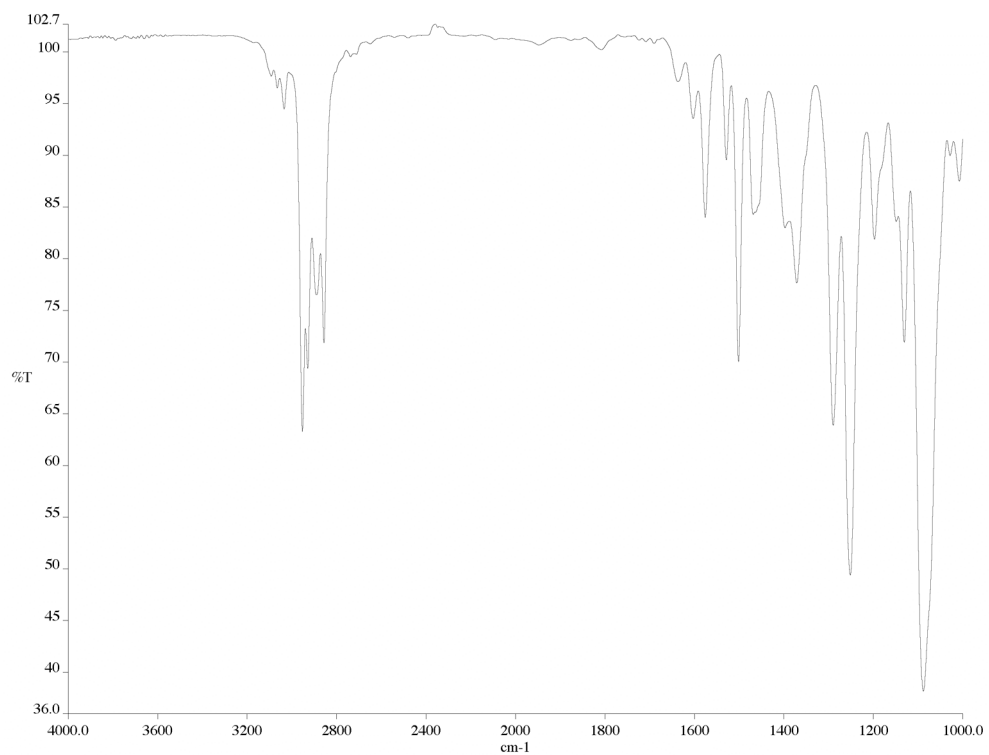


Figure A2.27 Infrared spectrum (thin film/NaCl) of compound **72**.

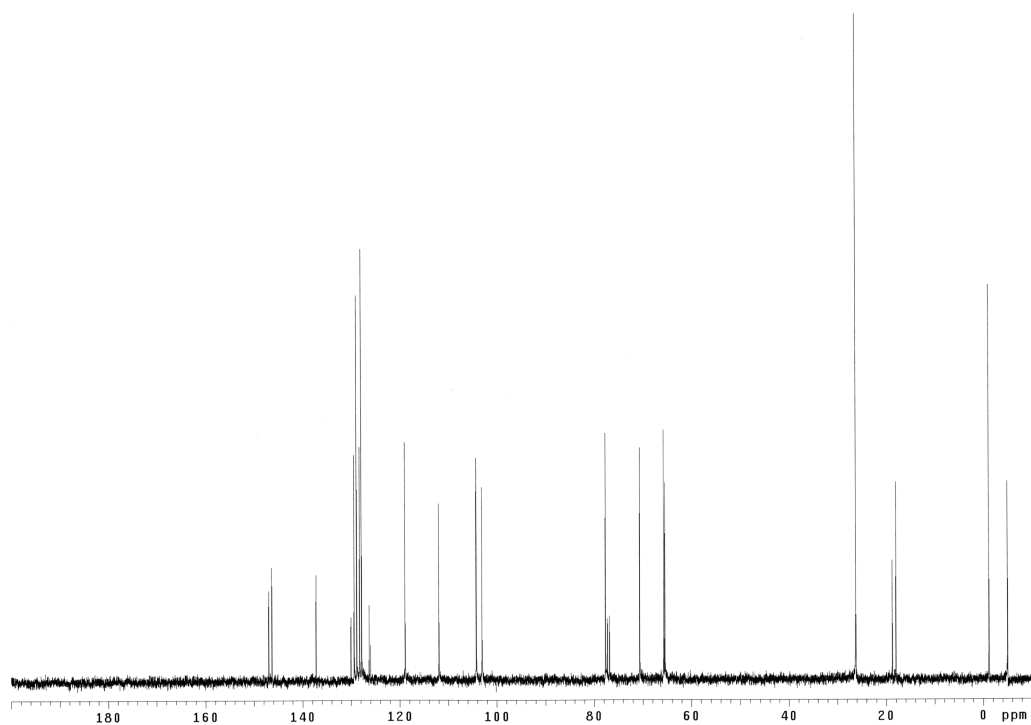


Figure A2.28 ¹³C NMR (75 MHz, CDCl₃) of compound **72**.

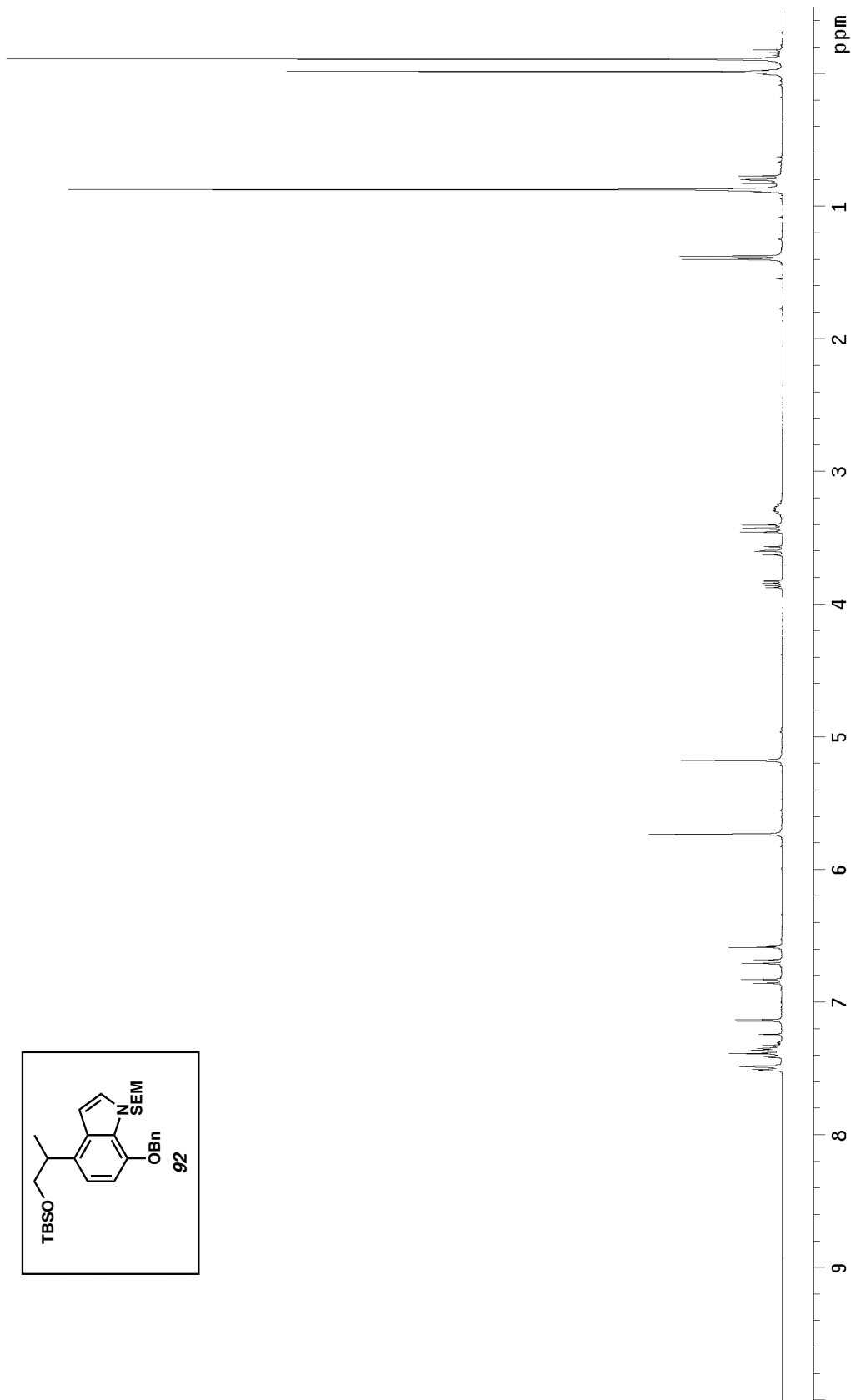
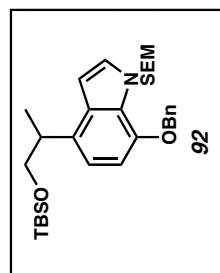


Figure A2.29 ¹H NMR (300 MHz, CDCl₃) of compound **92**.

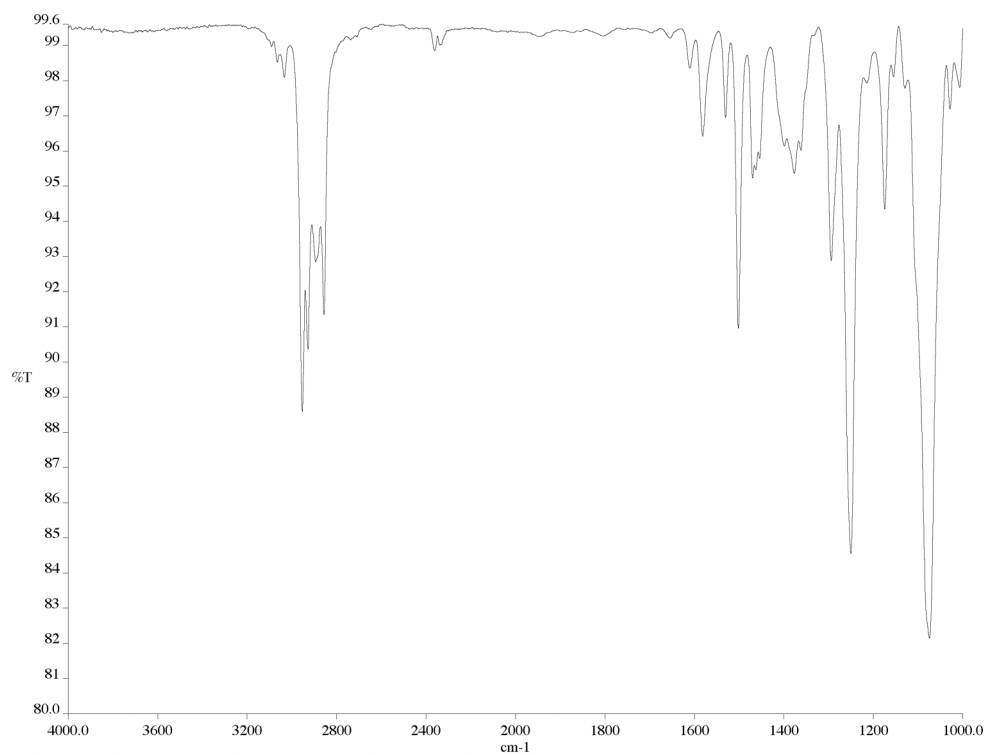


Figure A2.30 Infrared spectrum (thin film/NaCl) of compound **92**.

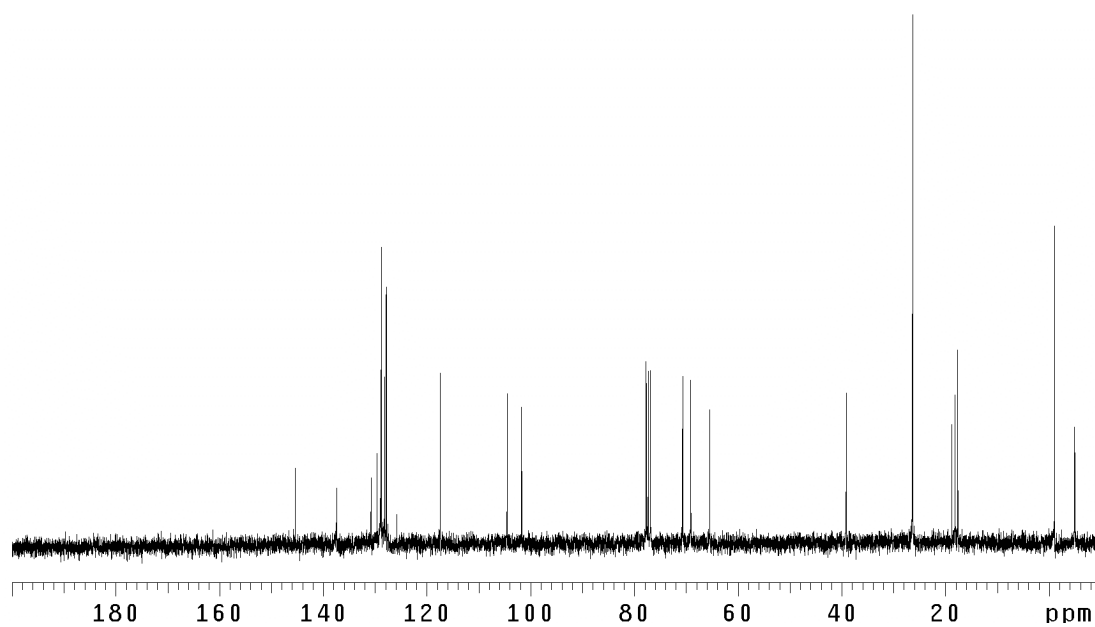


Figure A2.31 ¹³C NMR (75 MHz, CDCl₃) of compound **92**.

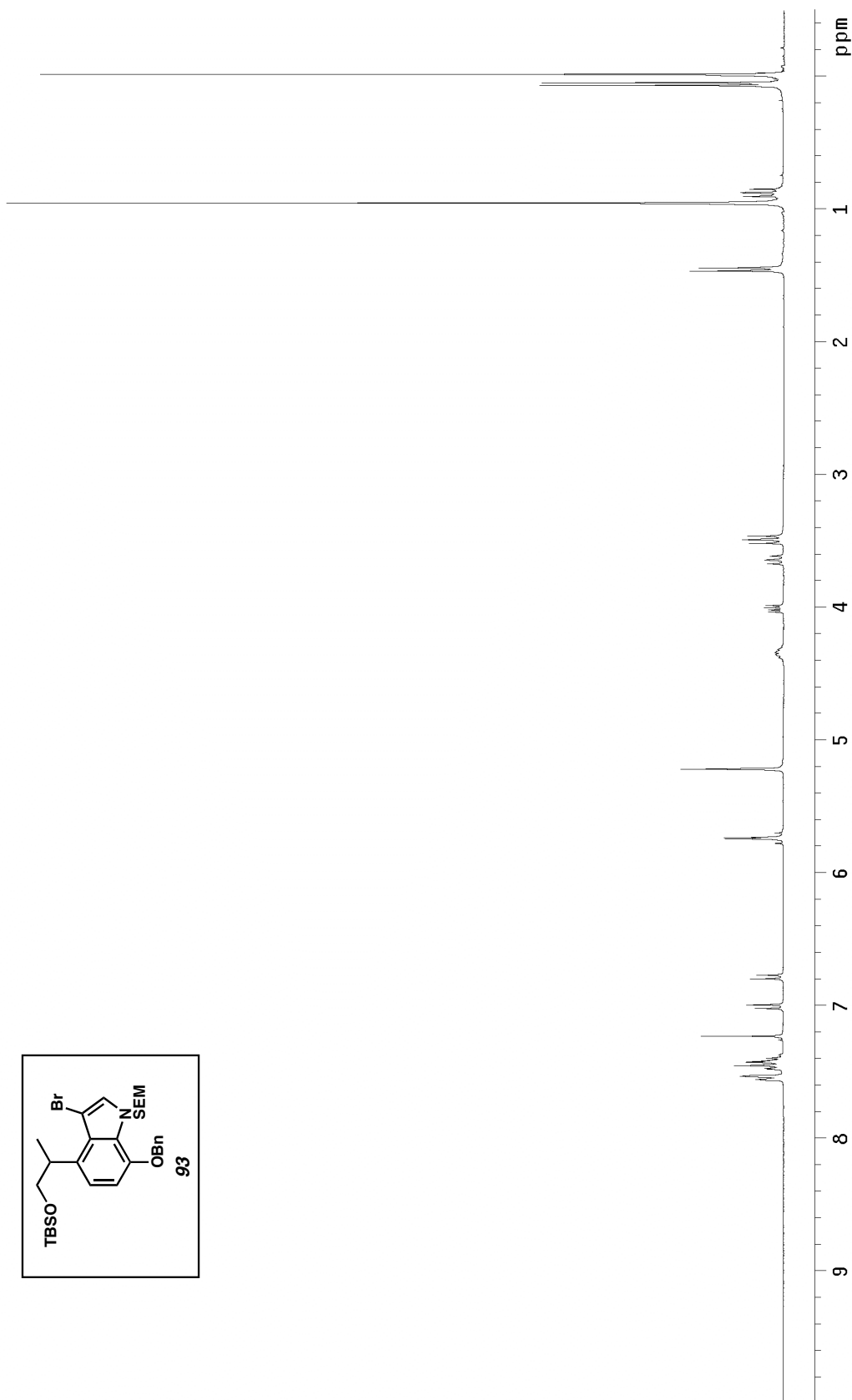
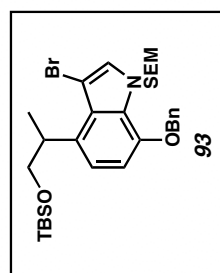


Figure A2.32 ^1H NMR (300 MHz, CDCl_3) of compound **93**.

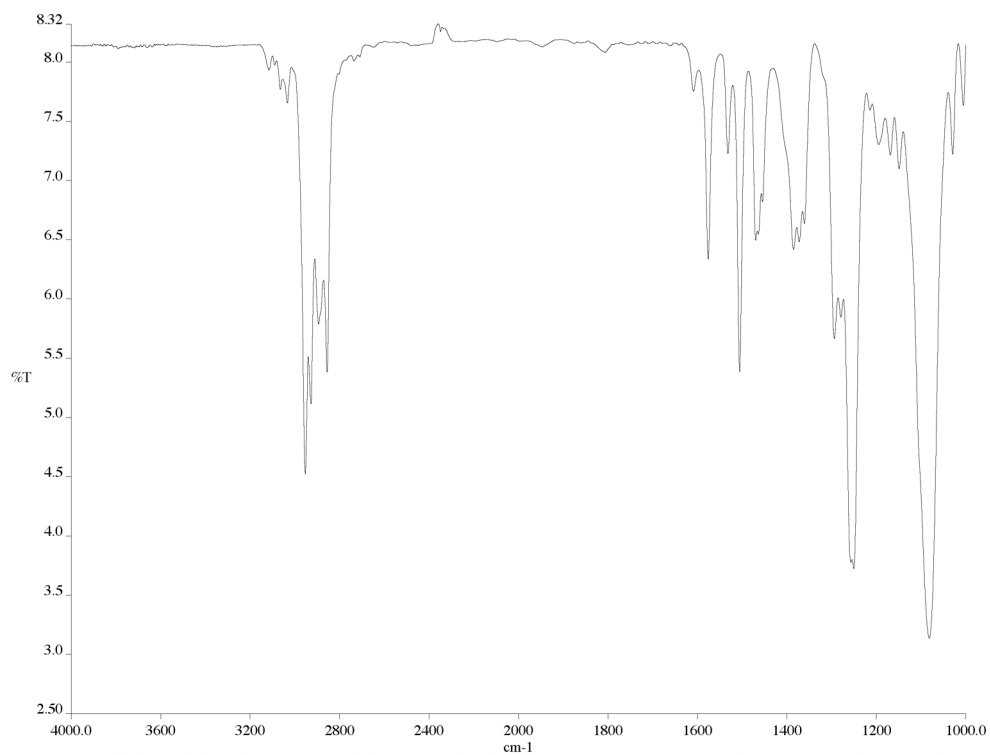


Figure A2.33 Infrared spectrum (thin film/NaCl) of compound **93**.

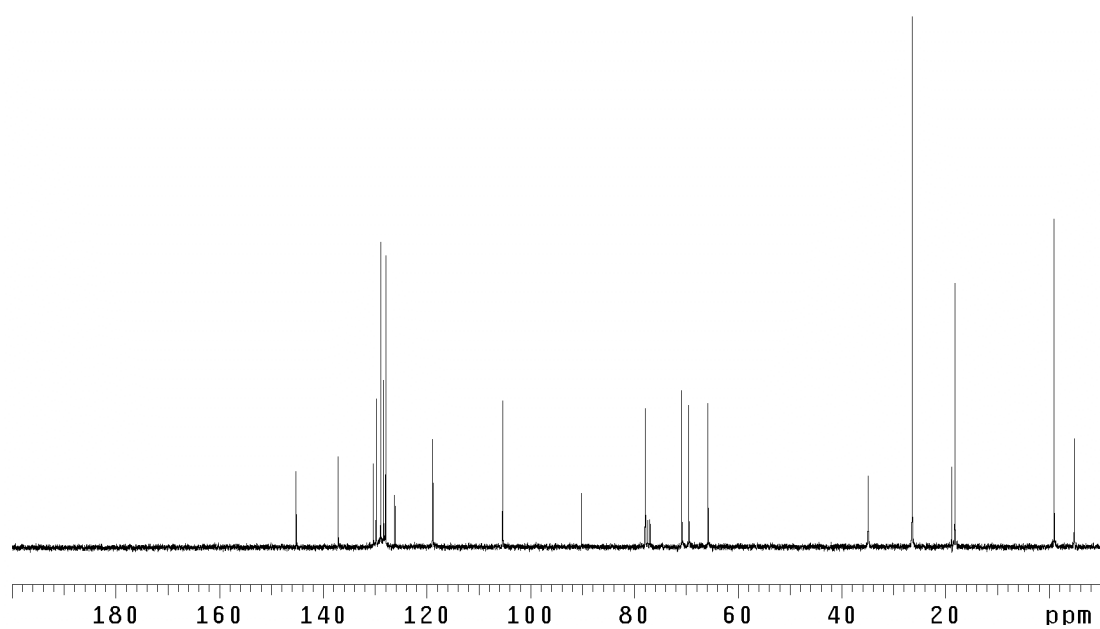


Figure A2.34 ¹³C NMR (75 MHz, CDCl₃) of compound **93**.

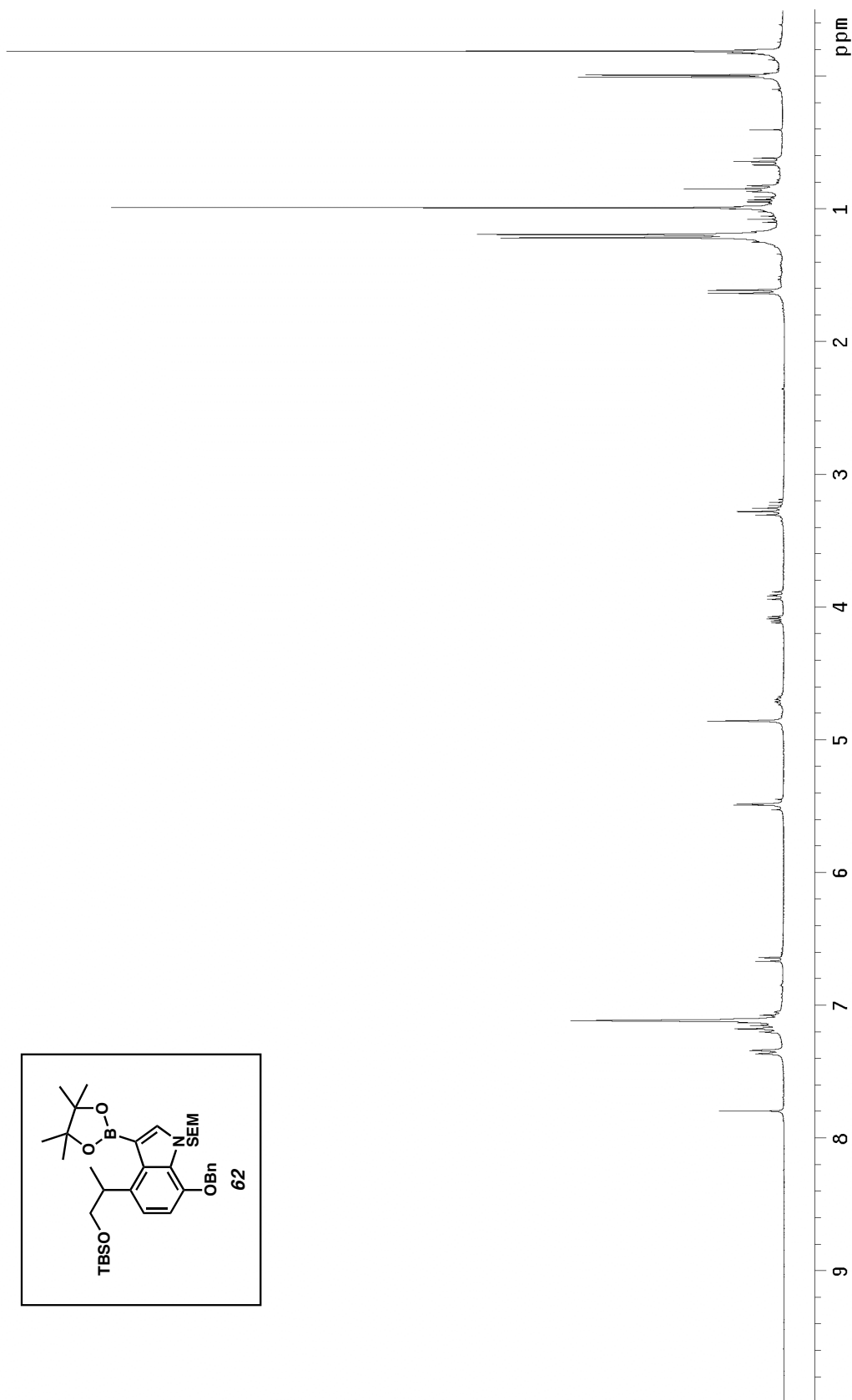
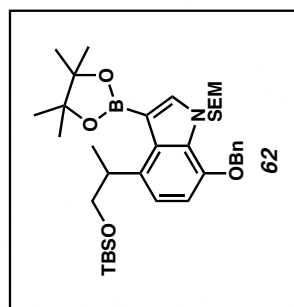


Figure A2.35 ¹H NMR (300 MHz, C₆D₆) of compound **62**.

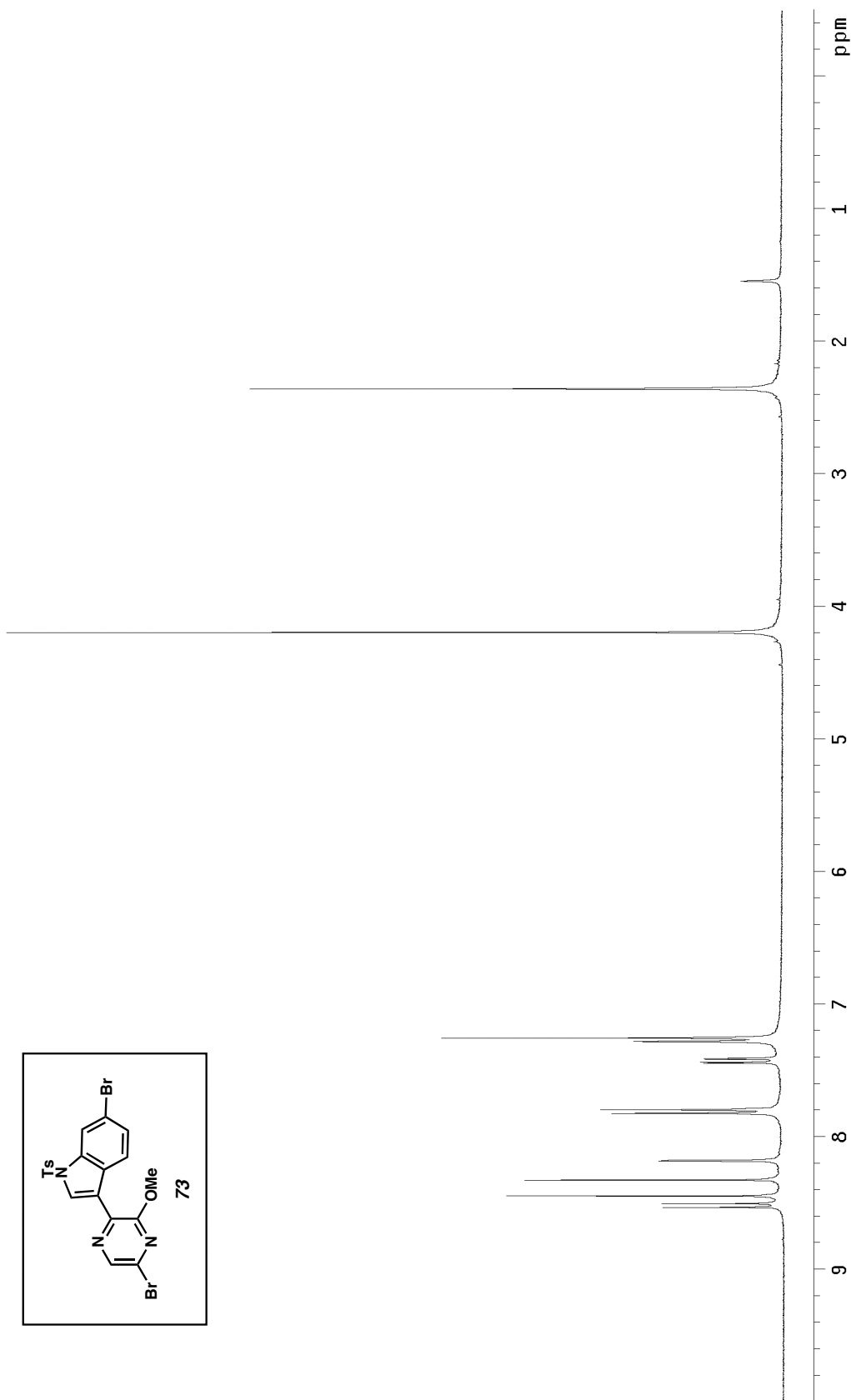
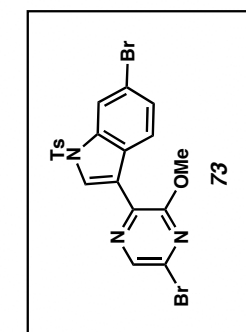


Figure A2.36 ^1H NMR (300 MHz, CDCl_3) of compound **73**.

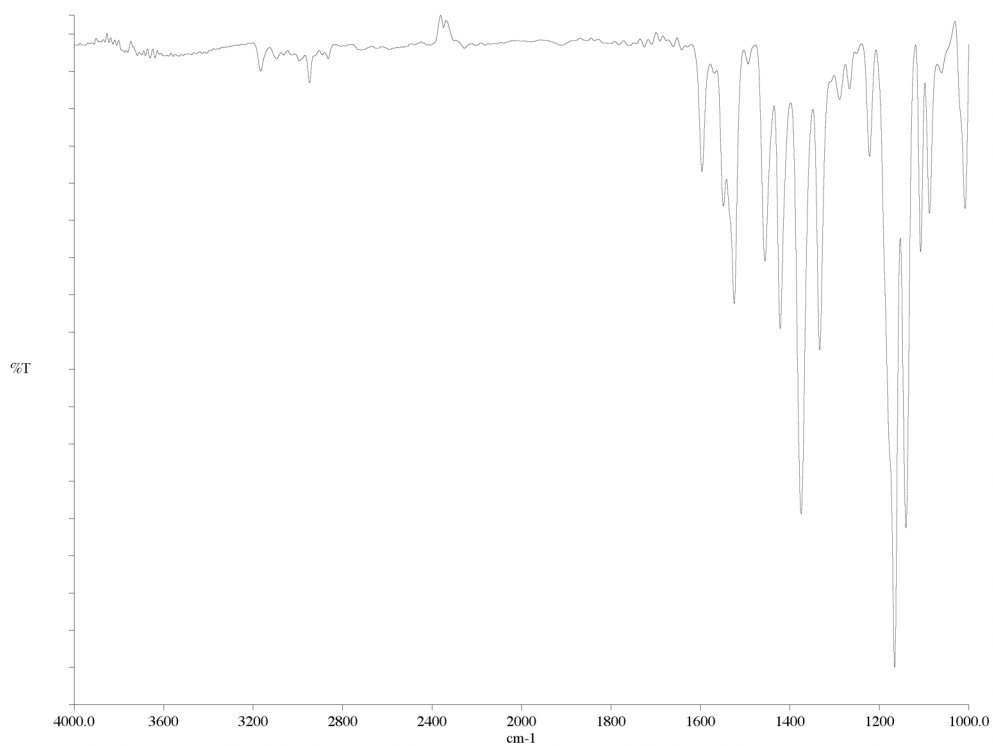


Figure A2.37 Infrared spectrum (thin film/NaCl) of compound **73**.

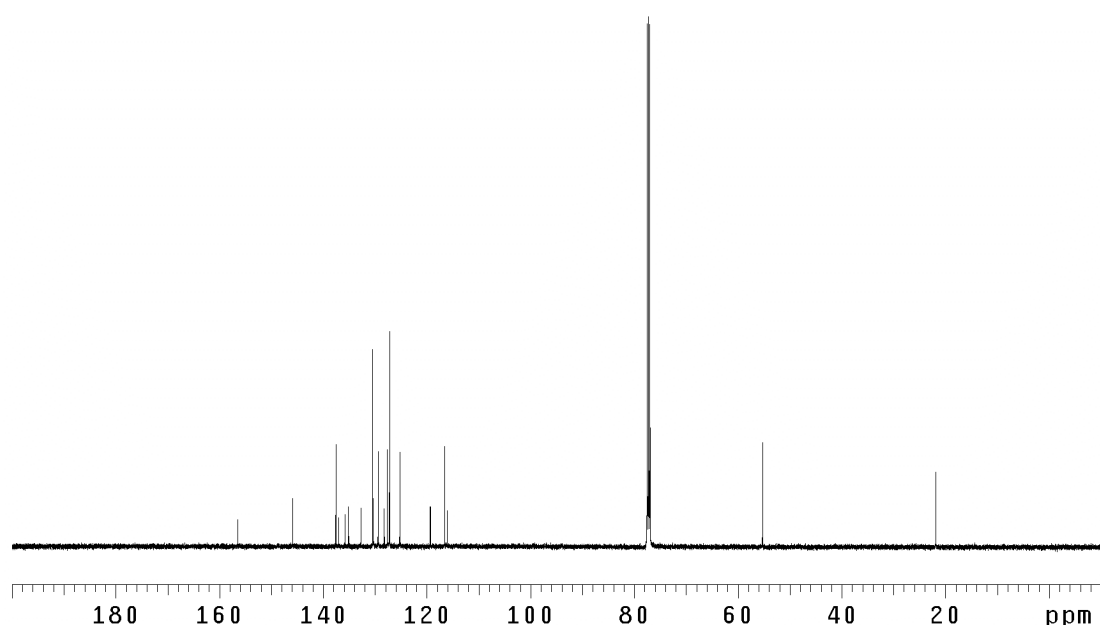


Figure A2.38 ¹³C NMR (125 MHz, CDCl₃) of compound **73**.

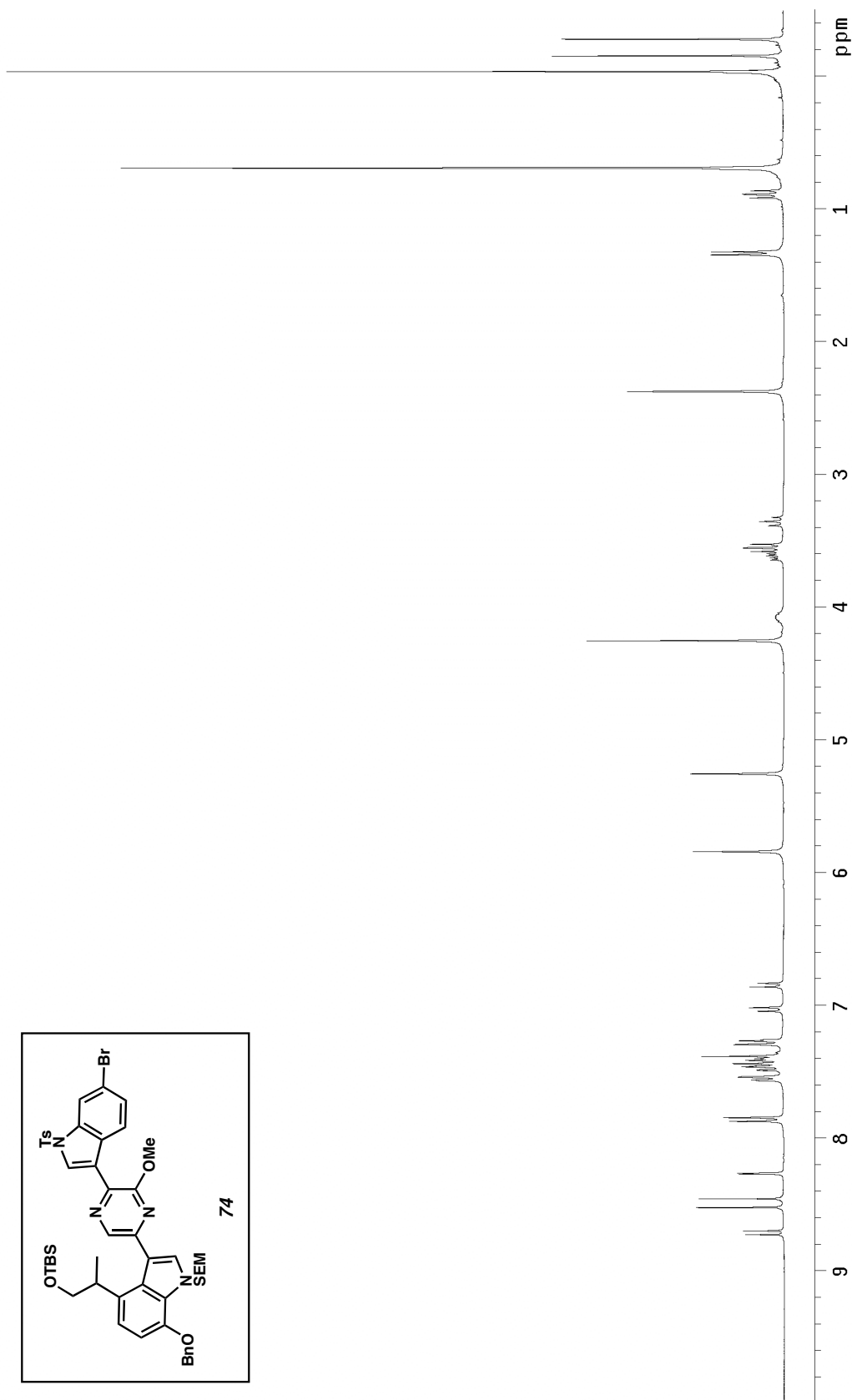
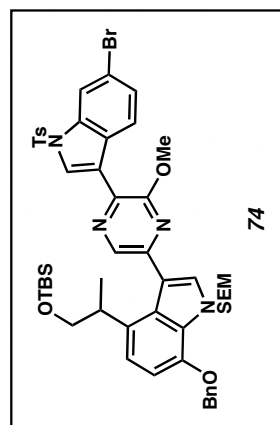


Figure A2.39 ^1H NMR (300 MHz, CDCl_3) of compound **74**.

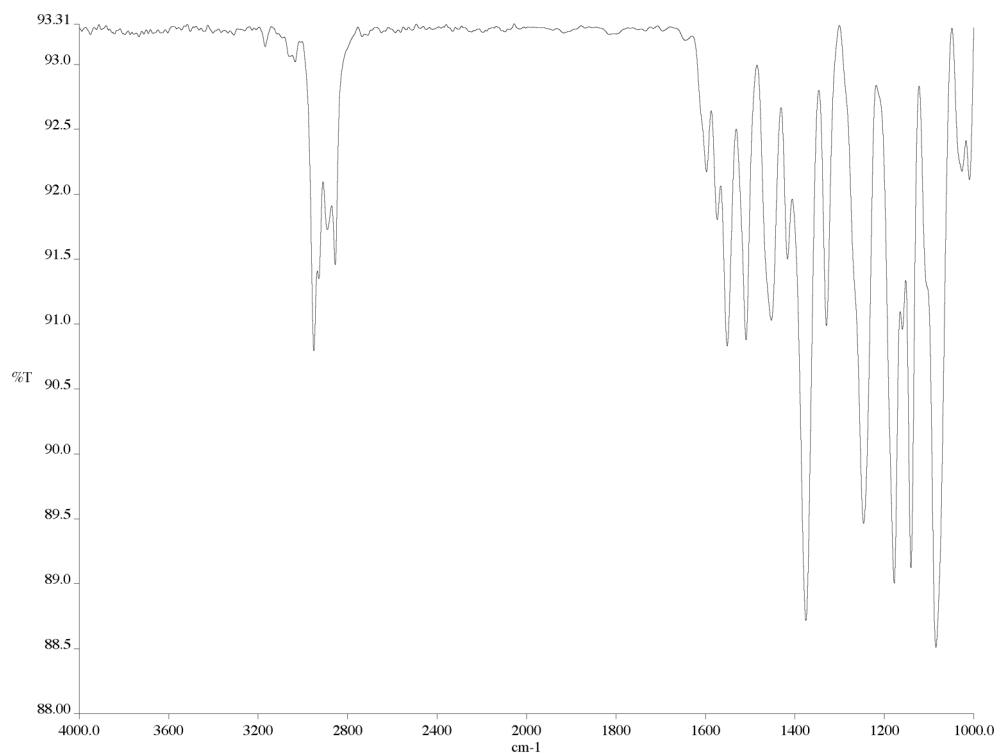


Figure A2.40 Infrared spectrum (thin film/NaCl) of compound **74**.

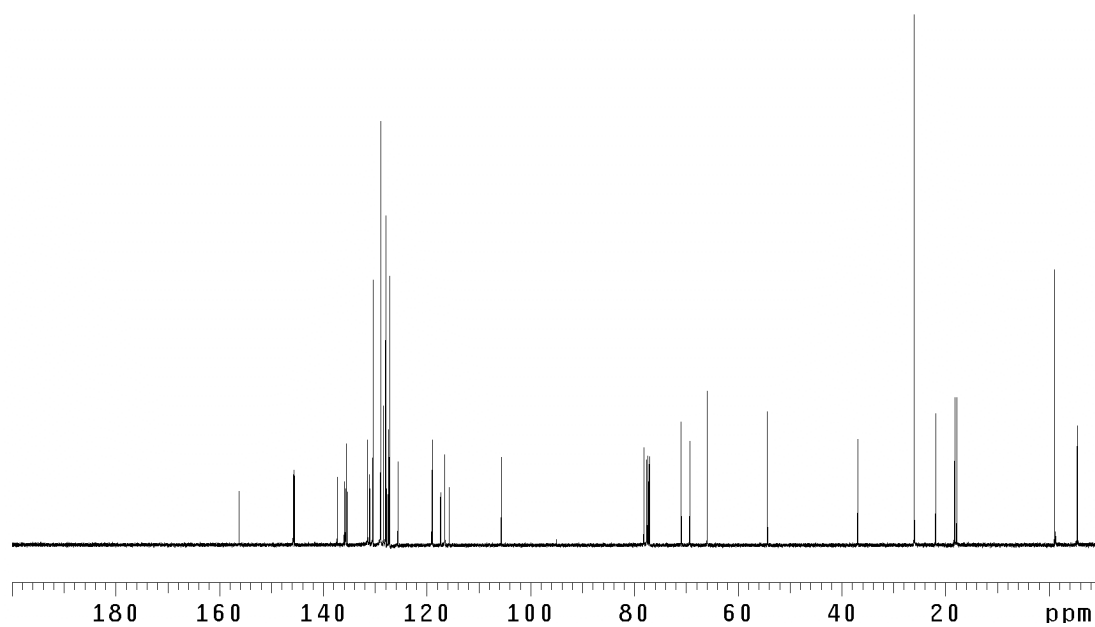


Figure A2.41 ¹³C NMR (125 MHz, CDCl₃) of compound **74**.

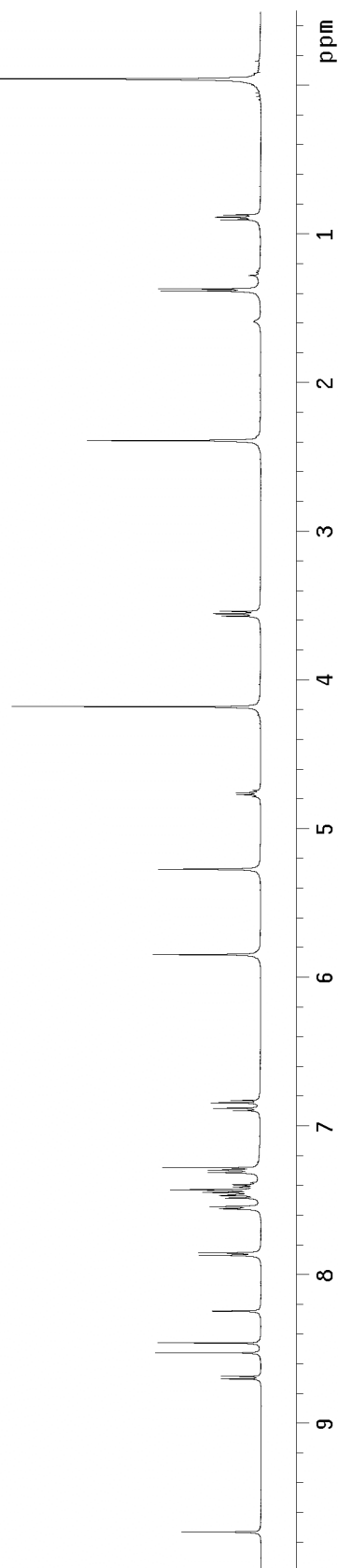
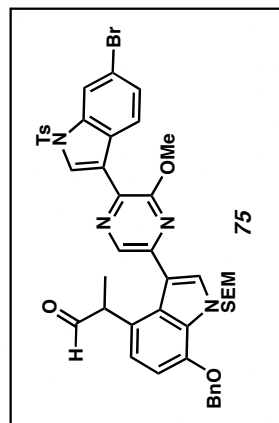


Figure A2.42 ^1H NMR (500 MHz, CDCl_3) of compound **75**.

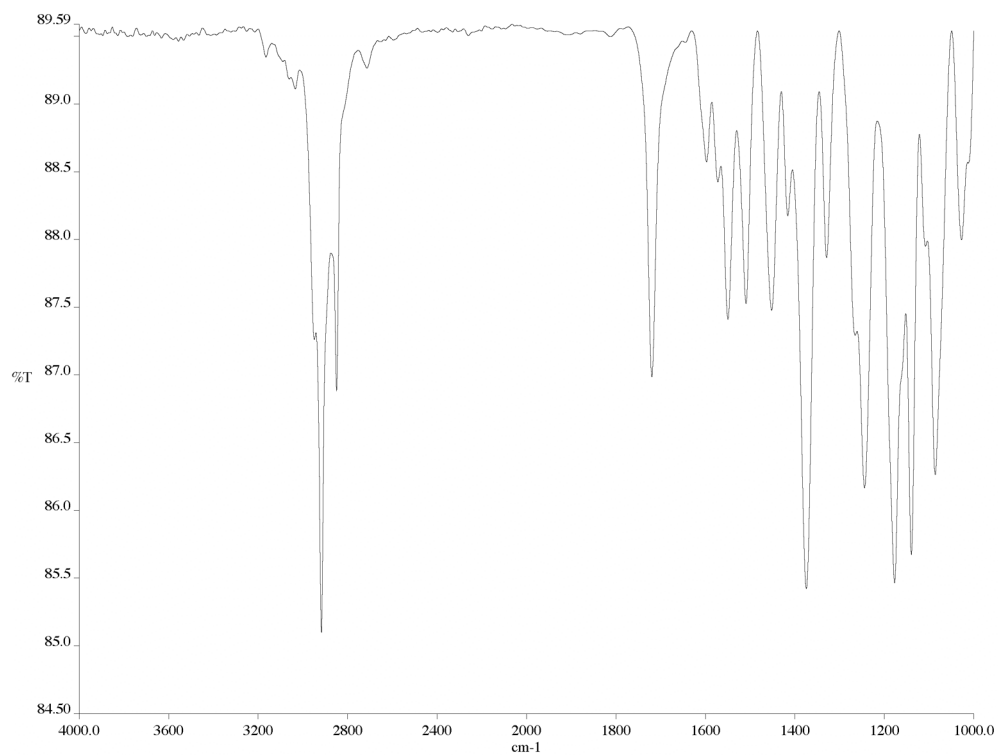


Figure A2.43 Infrared spectrum (thin film/NaCl) of compound **75**.

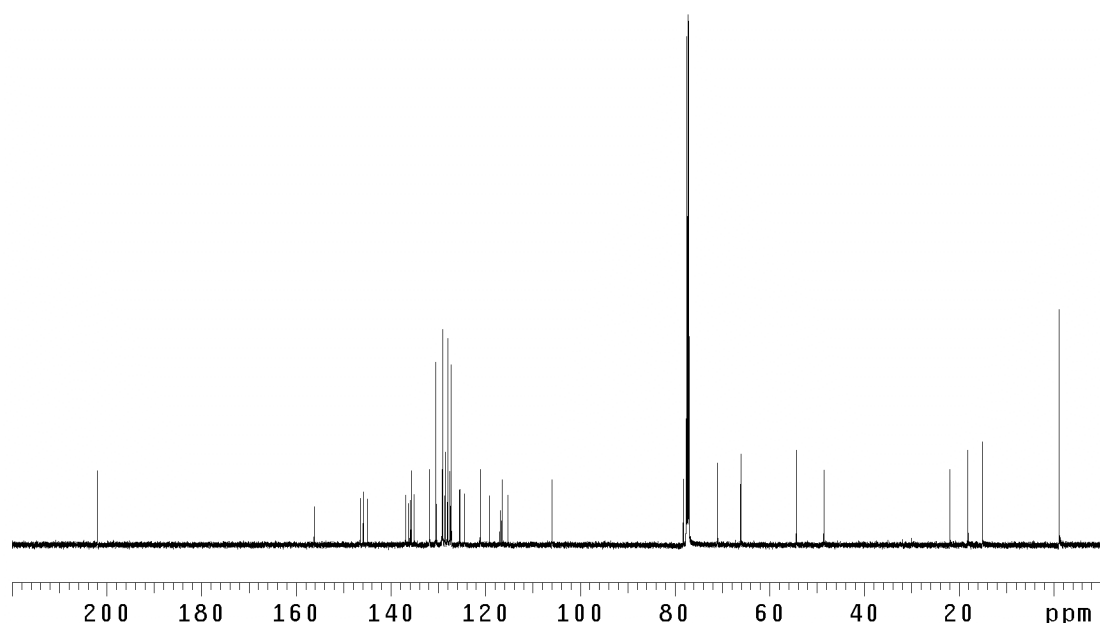


Figure A2.44 ¹³C NMR (125 MHz, CDCl₃) of compound **75**.

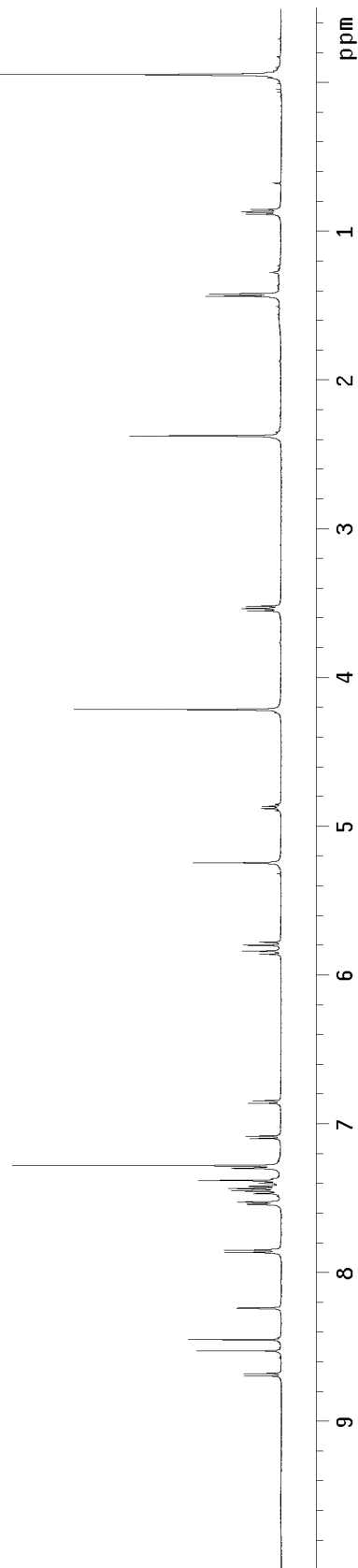
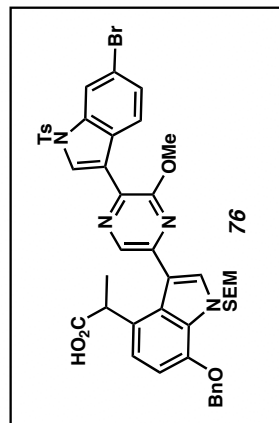


Figure A2.45 ^1H NMR (300 MHz, CDCl_3) of compound **76**.

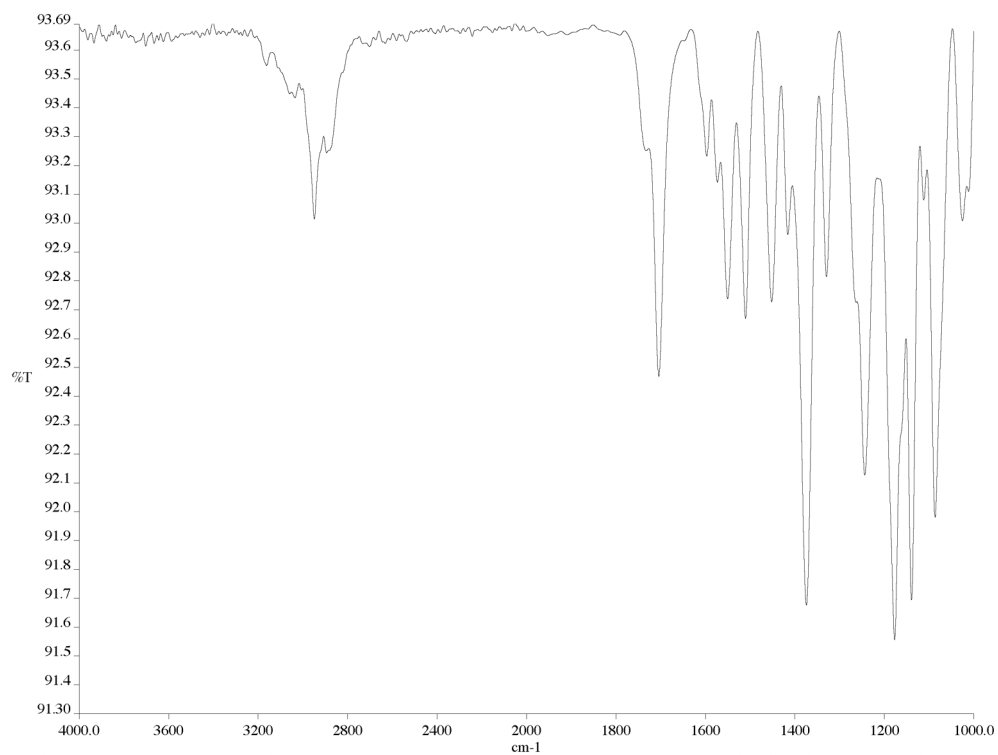


Figure A2.46 Infrared spectrum (thin film/NaCl) of compound **76**.

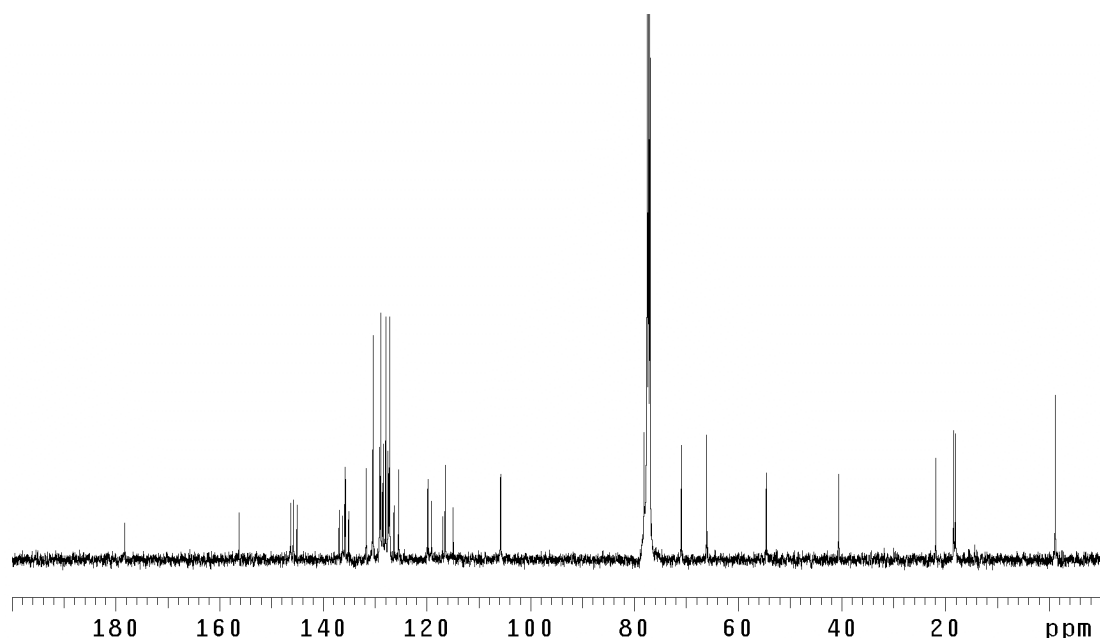


Figure A2.47 ¹³C NMR (125 MHz, CDCl₃) of compound **76**.

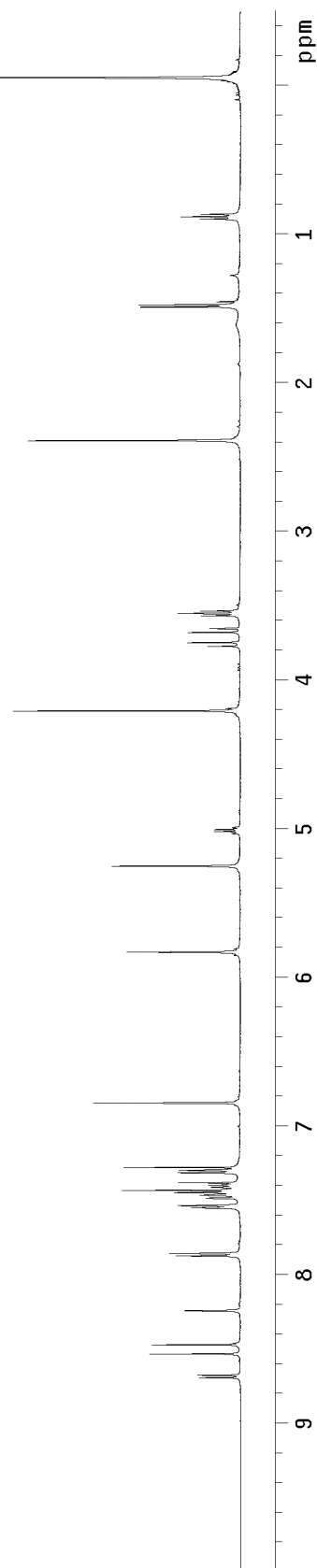
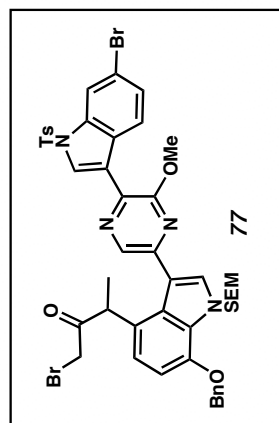


Figure A2.48 ^1H NMR (500 MHz, CDCl_3) of compound 77.

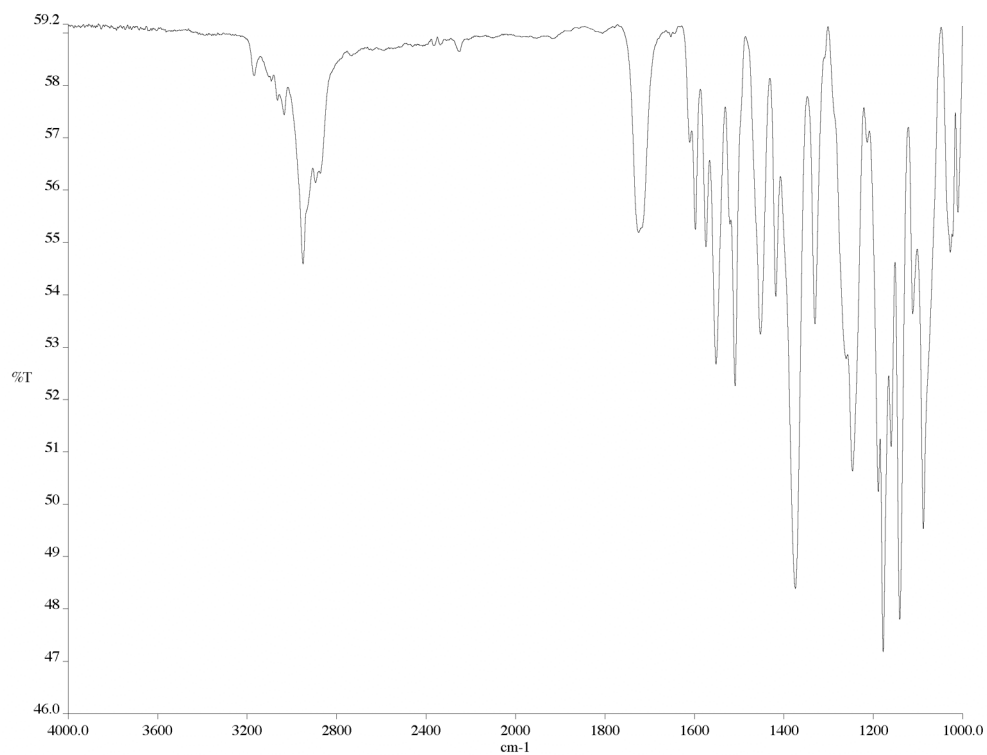


Figure A2.49 Infrared spectrum (thin film/NaCl) of compound **77**.

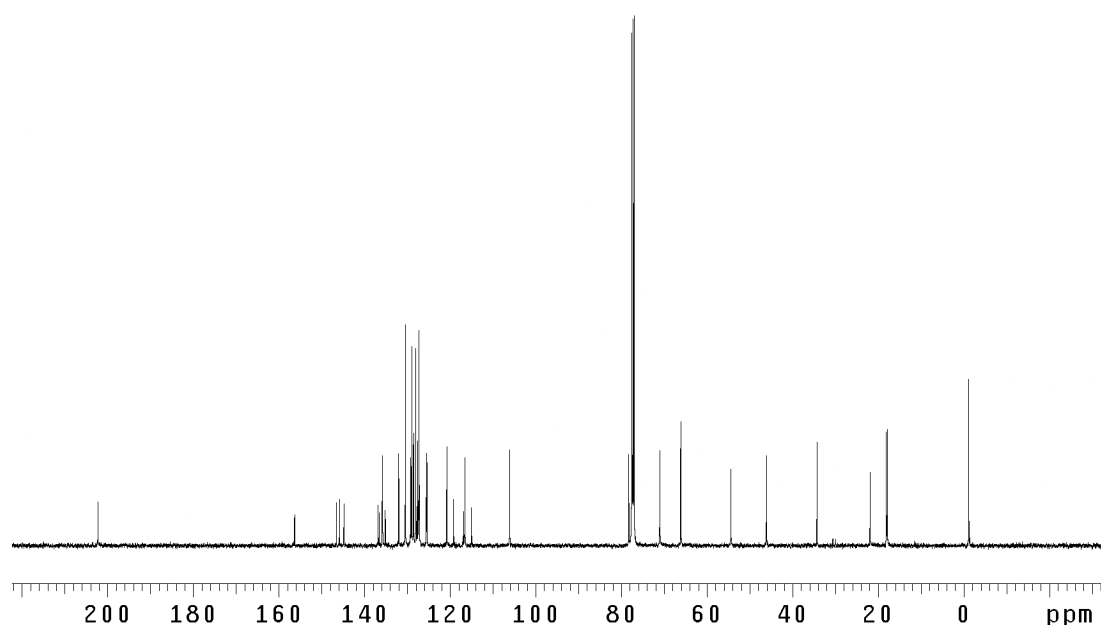


Figure A2.50 ¹³C NMR (125 MHz, CDCl₃) of compound **77**.

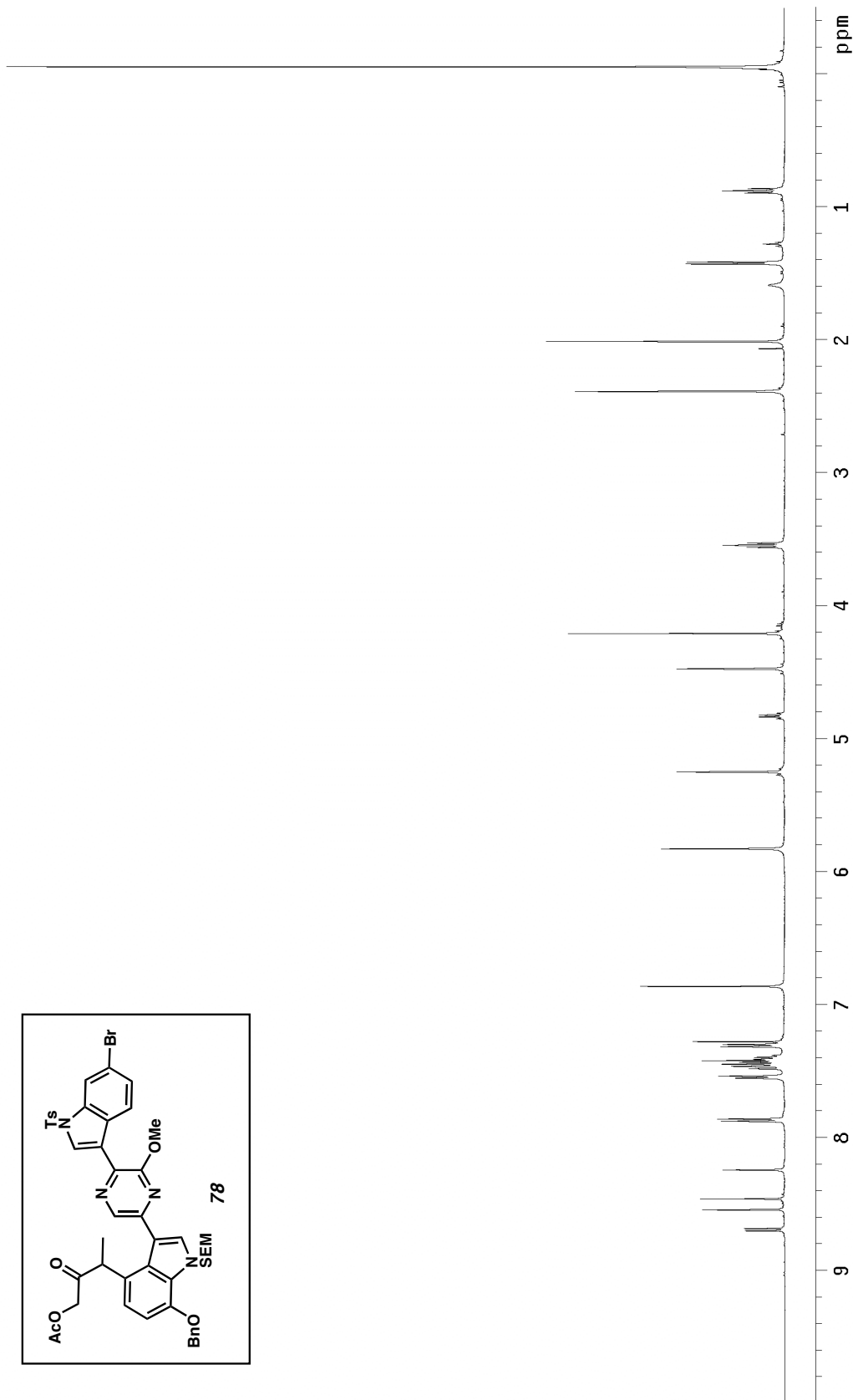
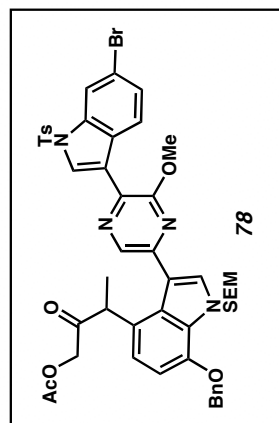


Figure A2.51 ¹H NMR (500 MHz, CDCl₃) of compound **78**.

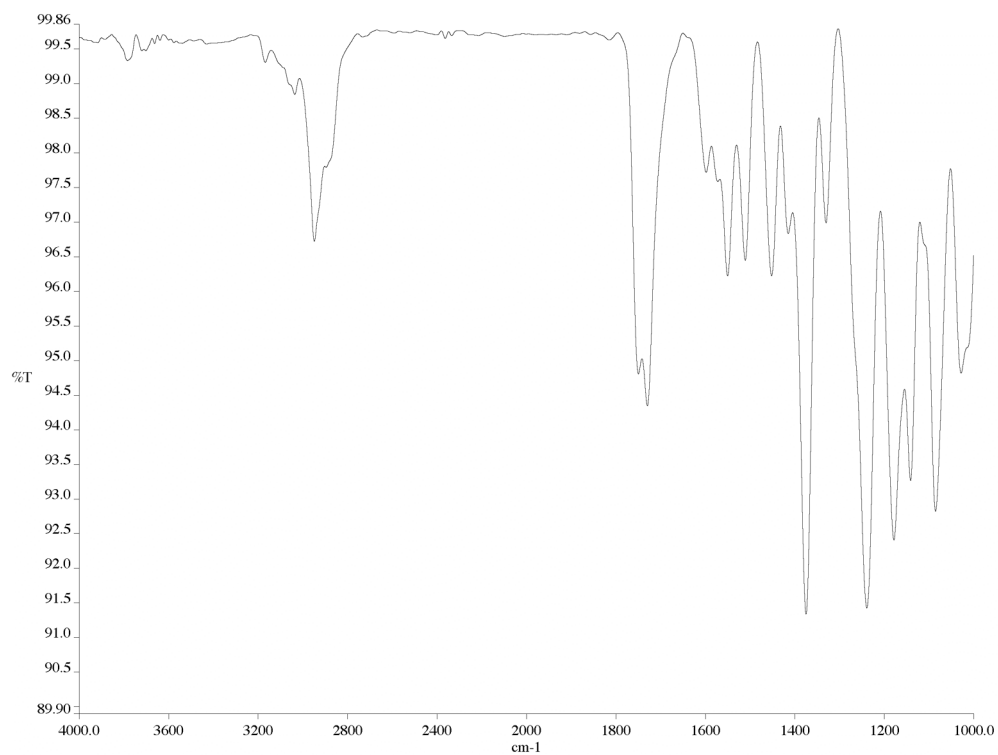


Figure A2.52 Infrared spectrum (thin film/NaCl) of compound **78**.

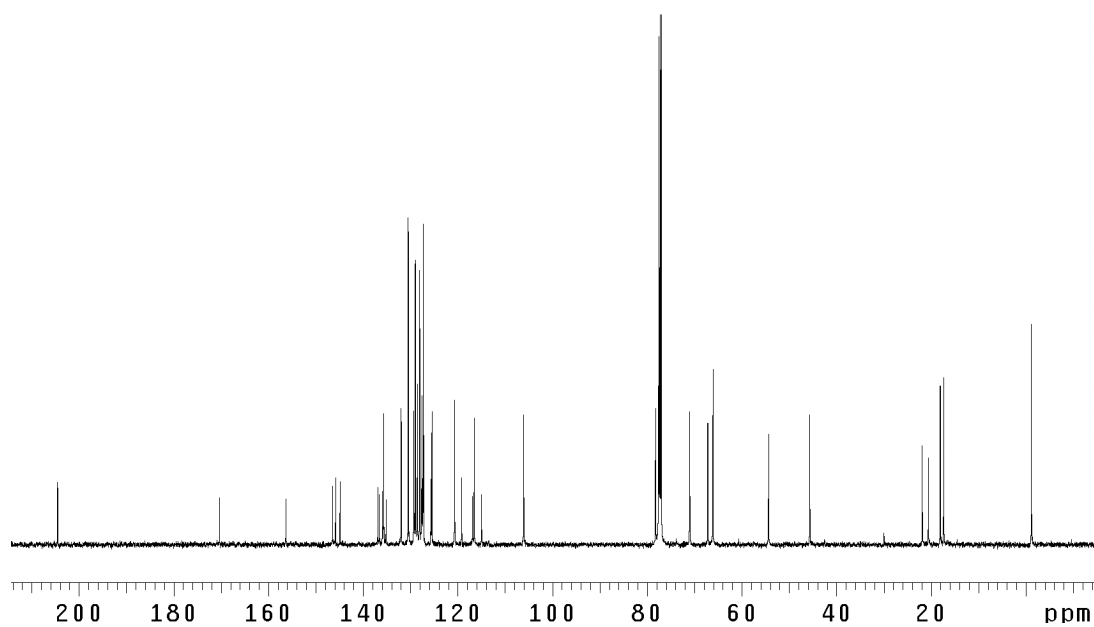


Figure A2.53 ¹³C NMR (125 MHz, CDCl₃) of compound **78**.

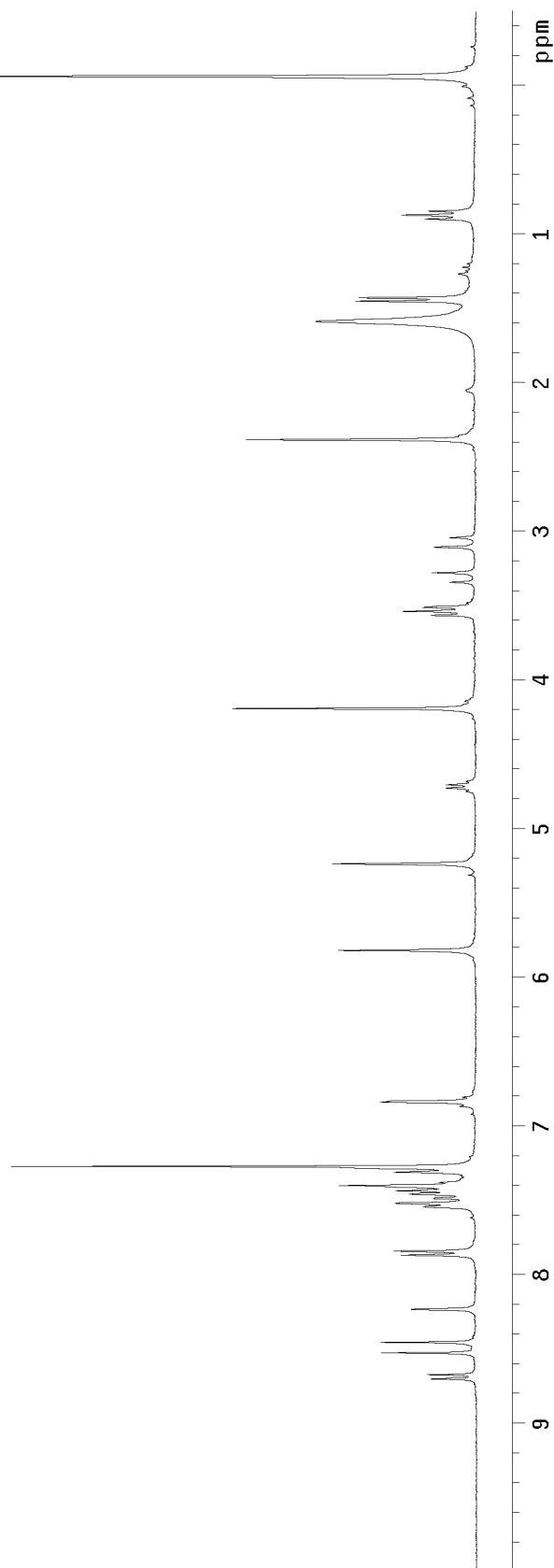
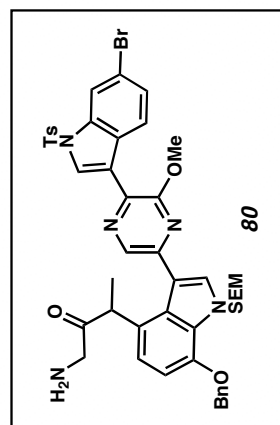


Figure A2.54 ^1H NMR (300 MHz, CDCl_3) of compound **80**.

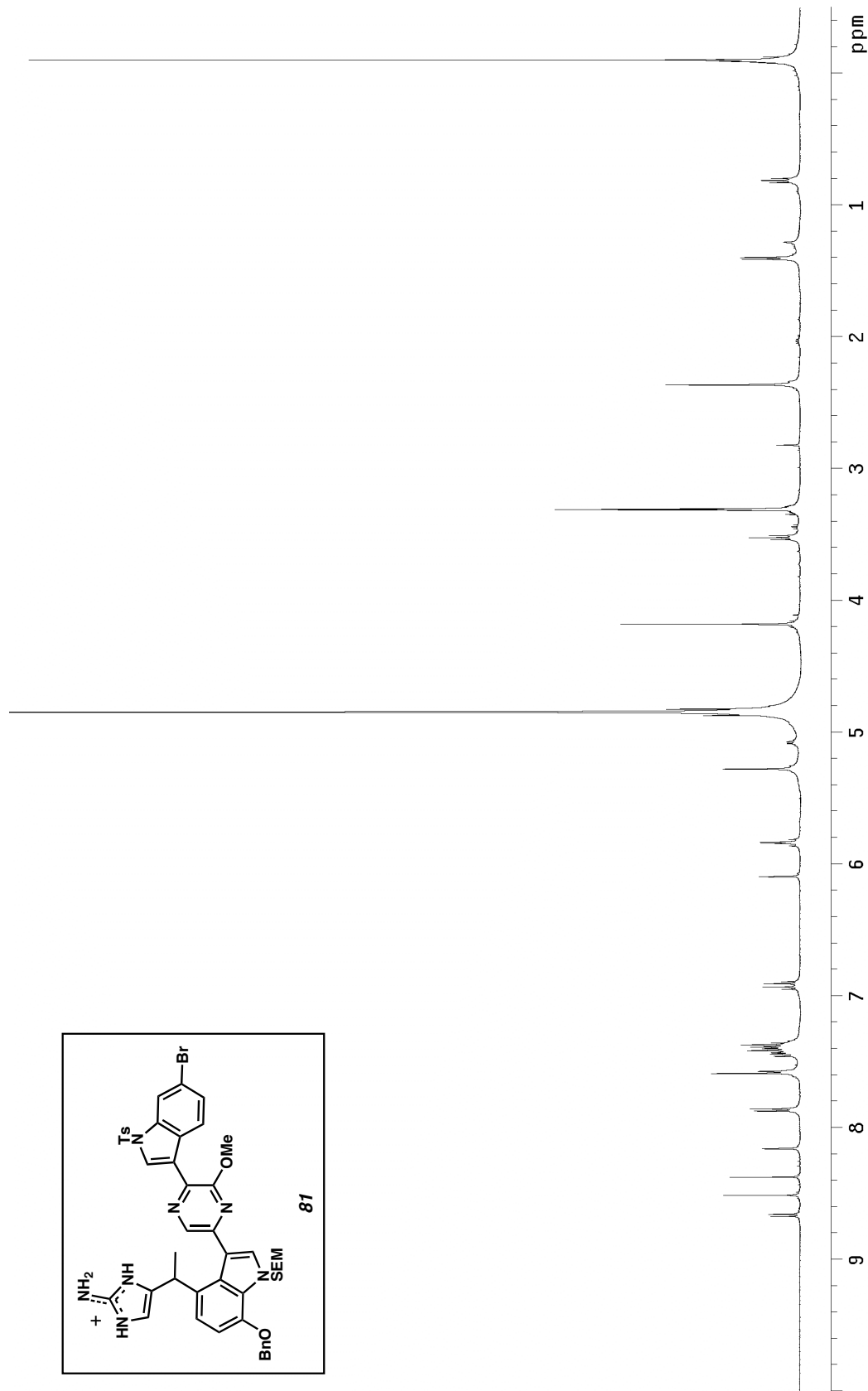


Figure A2.55 ¹H NMR (500 MHz, CD₃OD) of compound **81**.

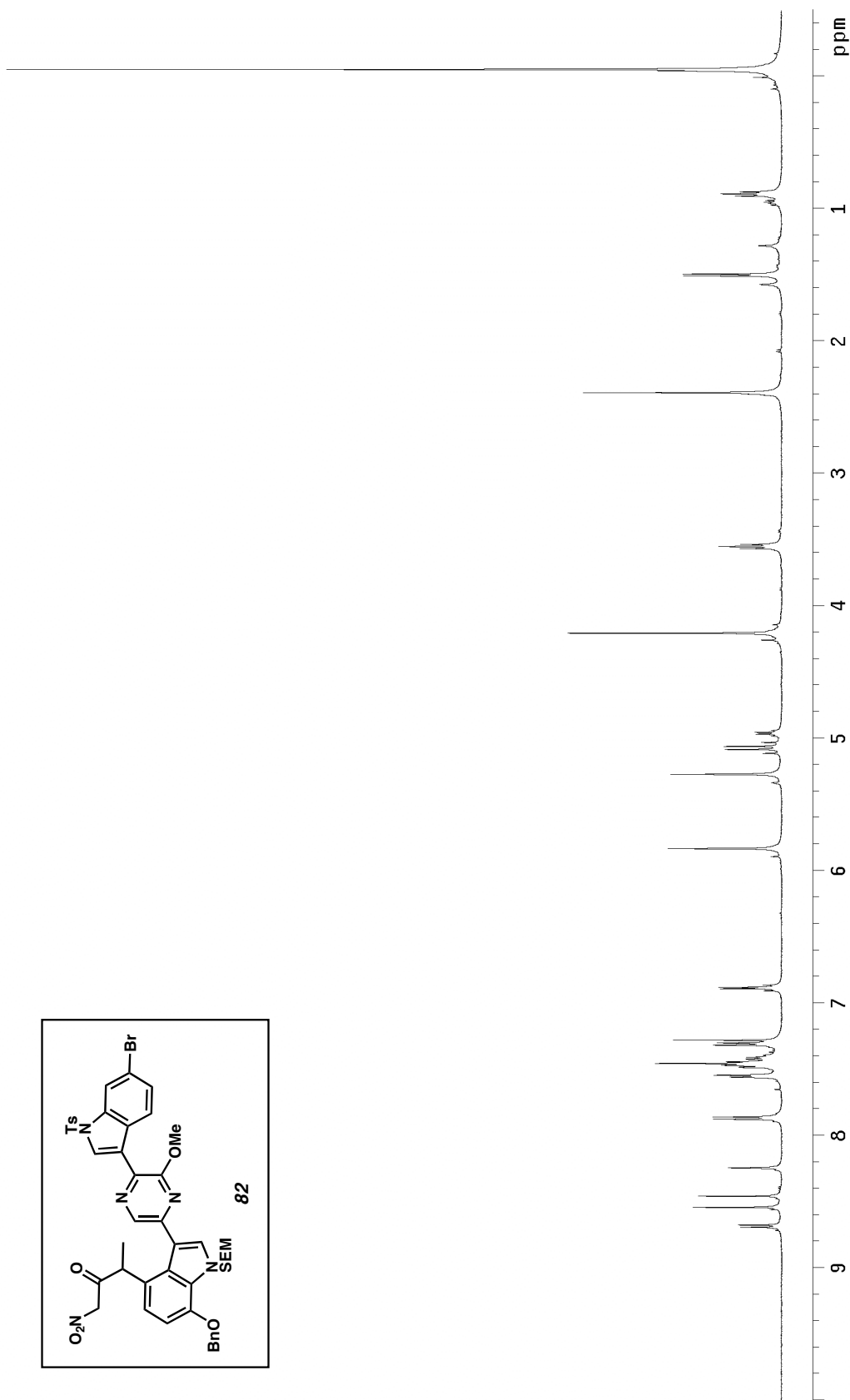
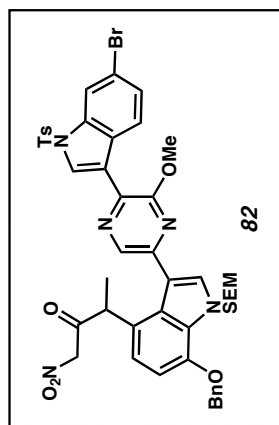


Figure A2.56 ¹H NMR (500 MHz, CDCl₃) of compound **82**.

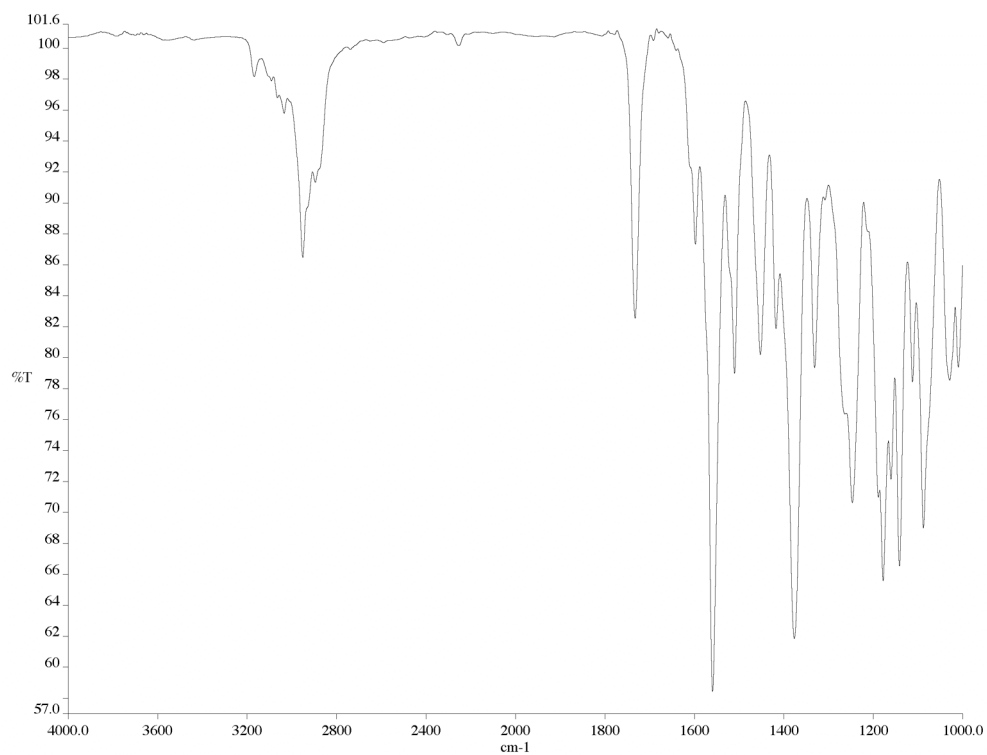


Figure A2.57 Infrared spectrum (thin film/NaCl) of compound **82**.

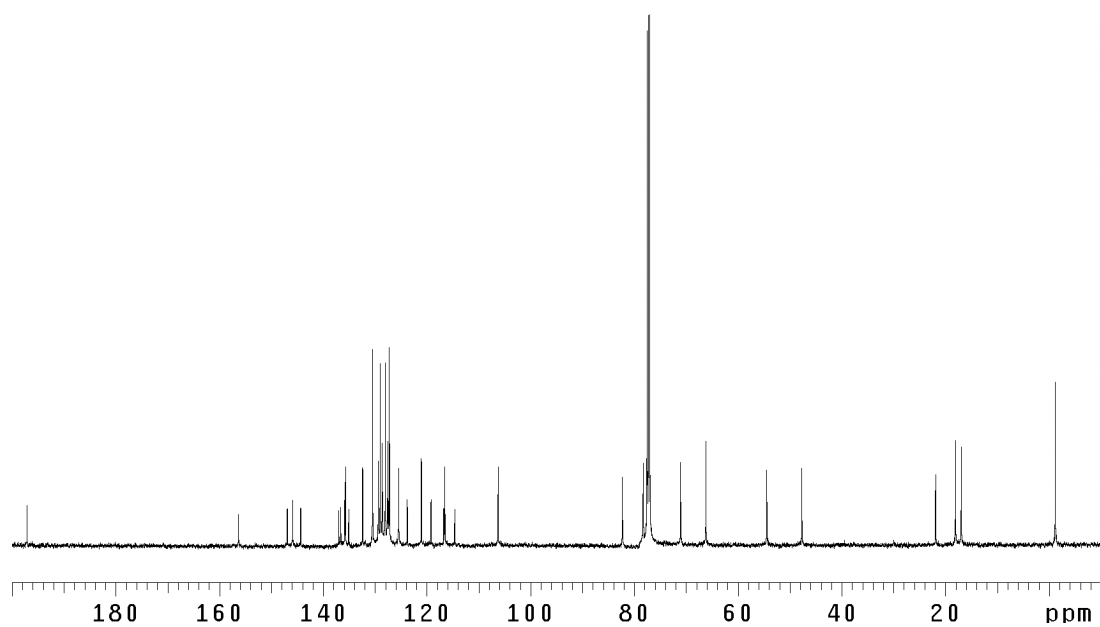


Figure A2.58 ¹³C NMR (125 MHz, CDCl₃) of compound **82**.

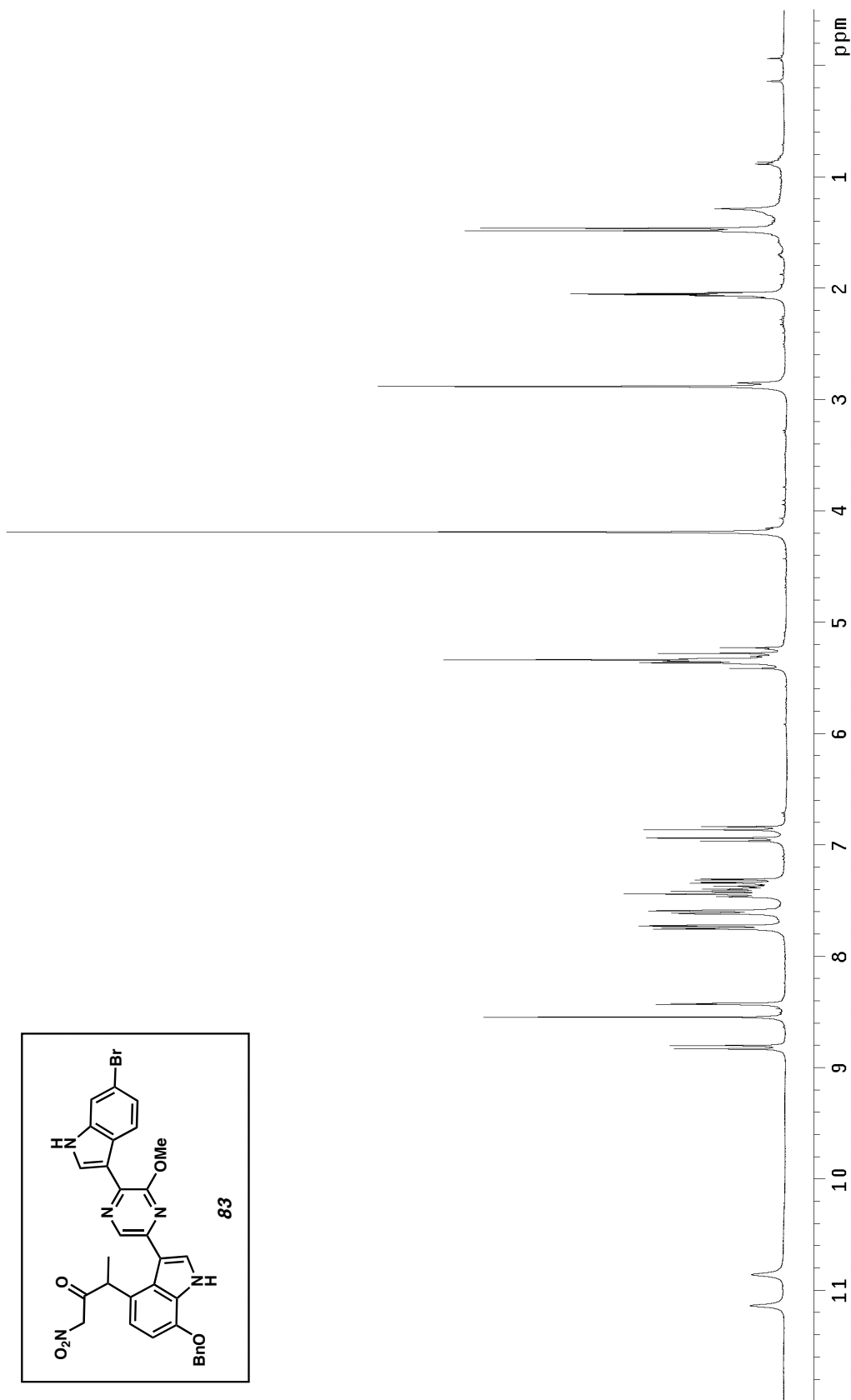
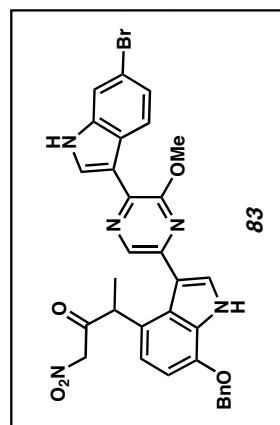


Figure A2.59 ^1H NMR (300 MHz, acetone- d_6) of compound **83**.

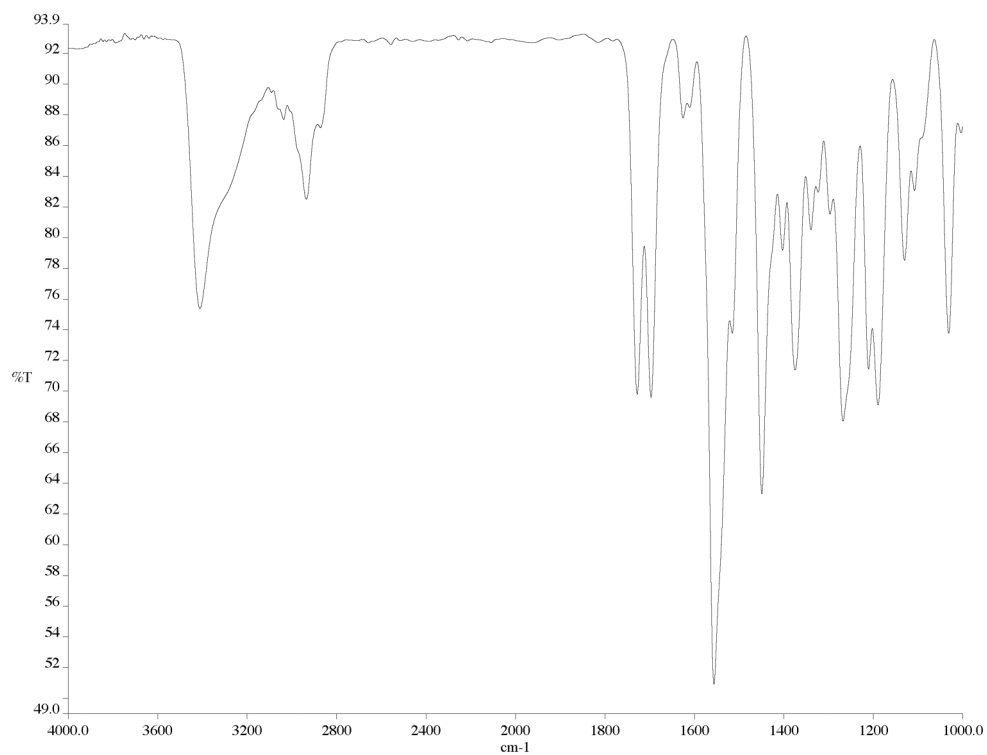


Figure A2.60 Infrared spectrum (thin film/NaCl) of compound **83**.

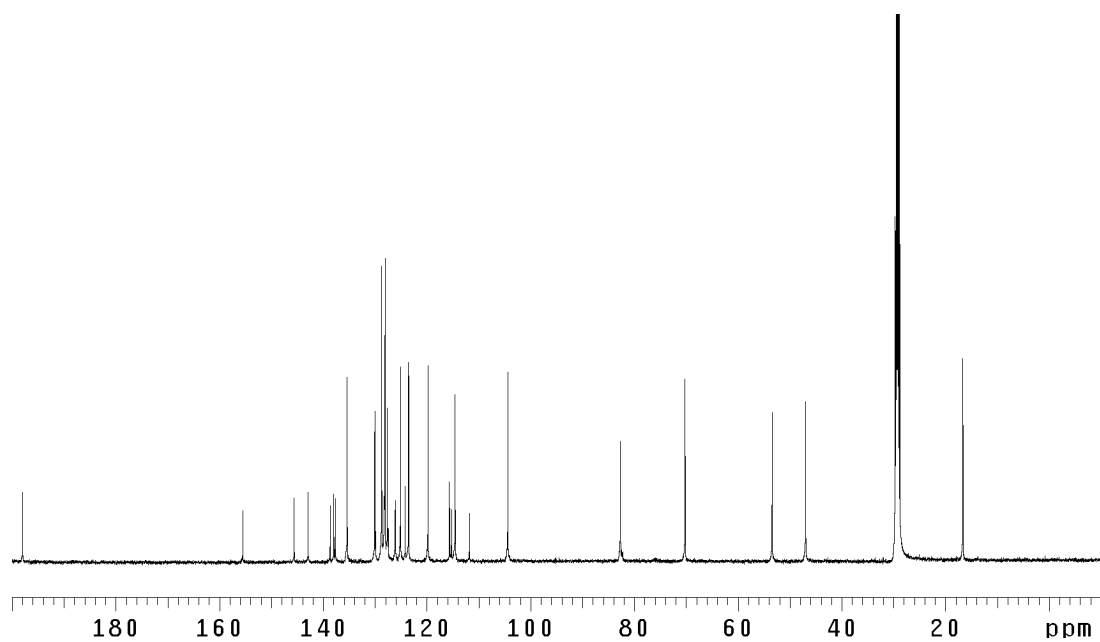


Figure A2.61 ^{13}C NMR (125 MHz, acetone- d_6) of compound **83**.

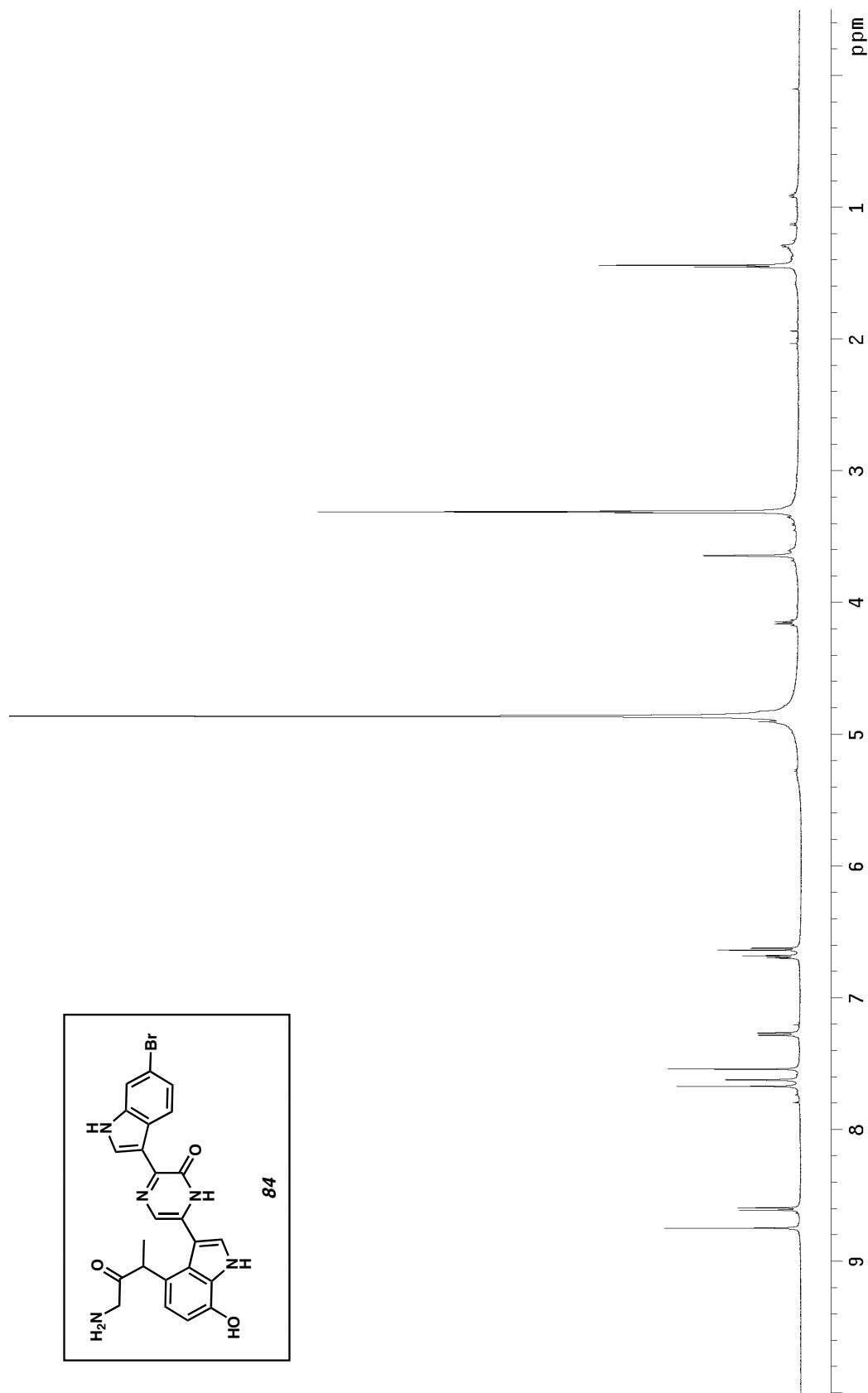
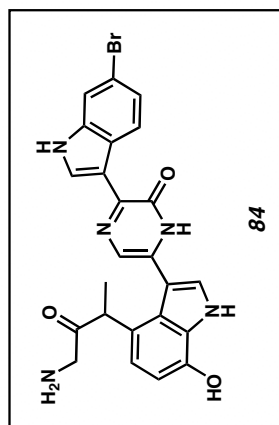


Figure A2.62 ¹H NMR (500 MHz, CD₃OD) of compound **84**.

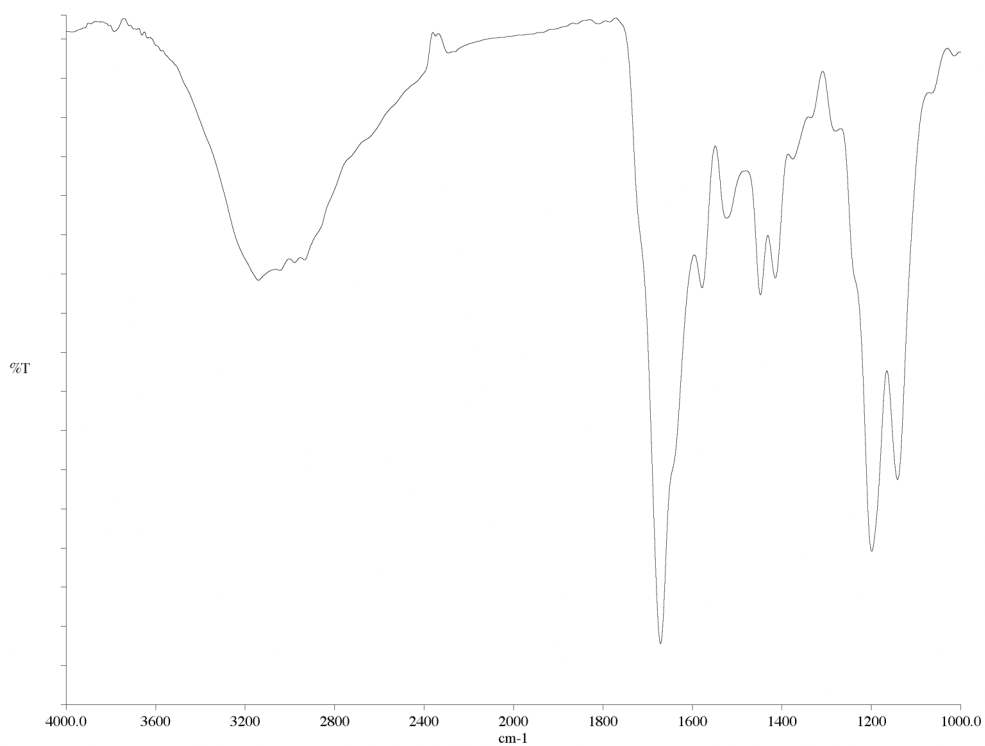


Figure A2.63 Infrared spectrum (thin film/NaCl) of compound **84**.

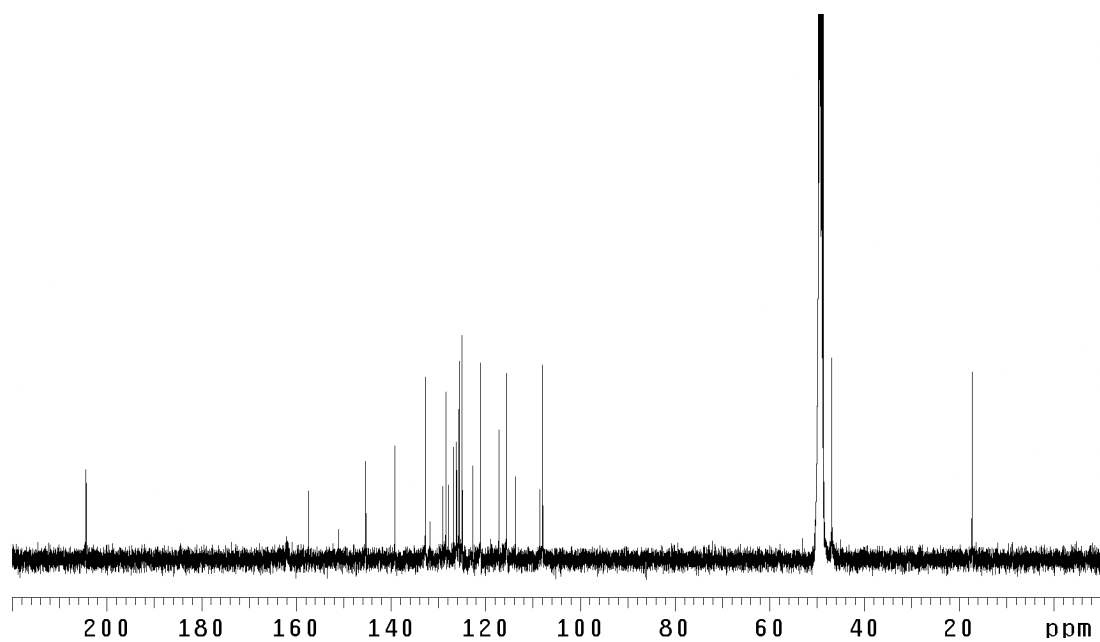


Figure A2.64 ¹³C NMR (125 MHz, CD₃OD) of compound **84**.

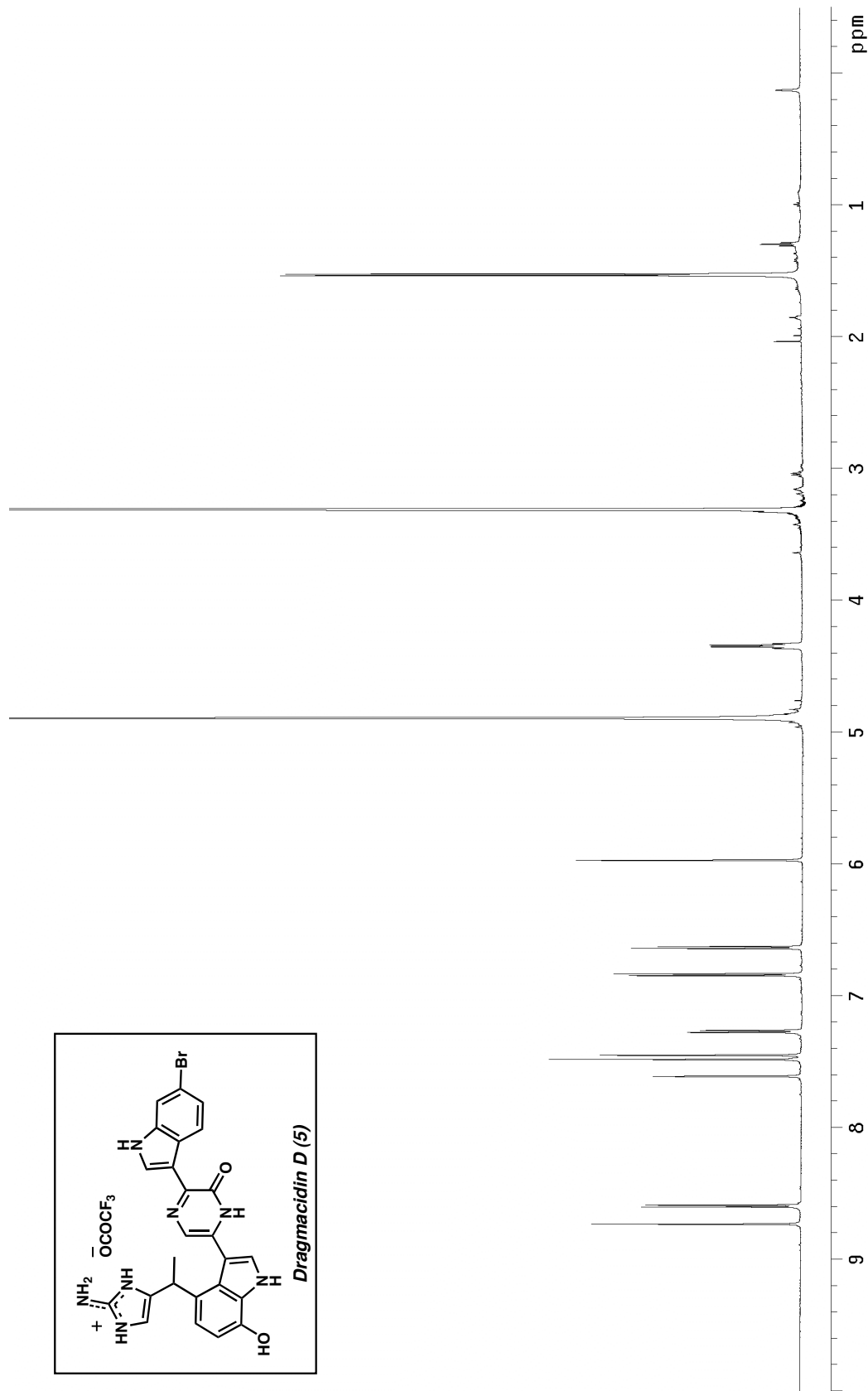


Figure A2.65 ¹H NMR (600 MHz, CD₃OD) of dragmacidin D (5).

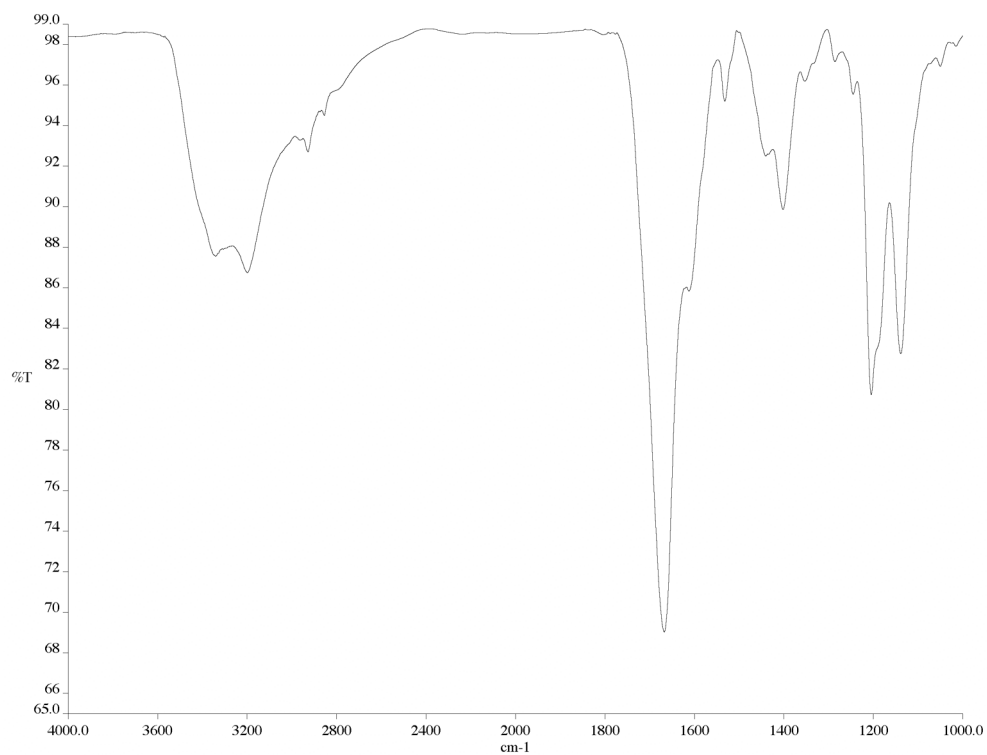


Figure A2.66 Infrared spectrum (thin film/NaCl) of dragmacidin D (**5**).

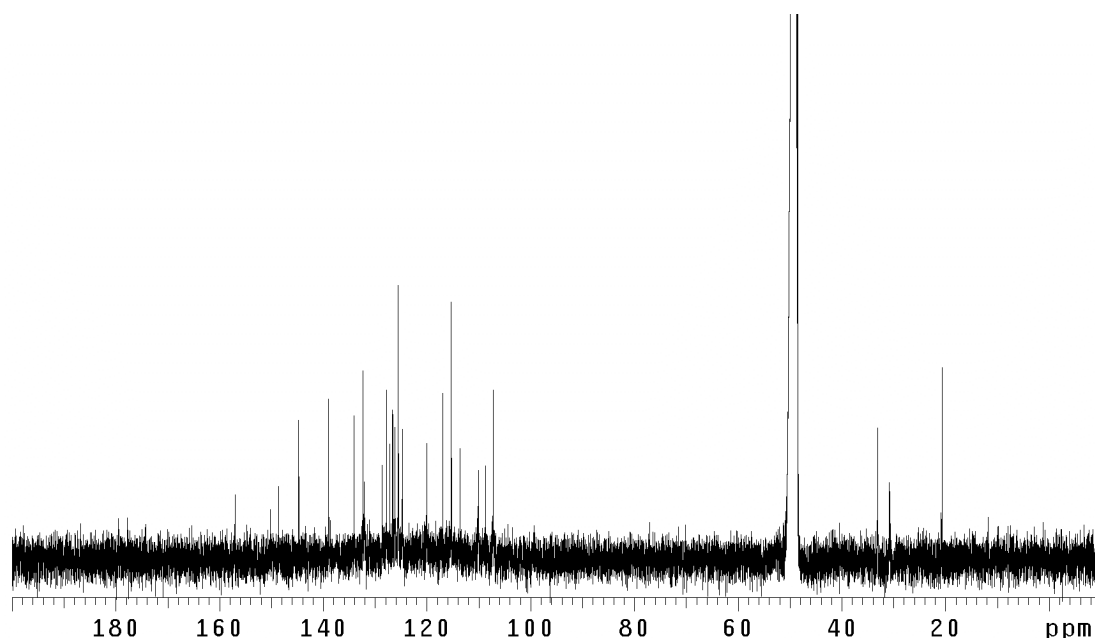


Figure A2.67 ¹³C NMR (125 MHz, CD₃OD) of dragmacidin D (**5**).

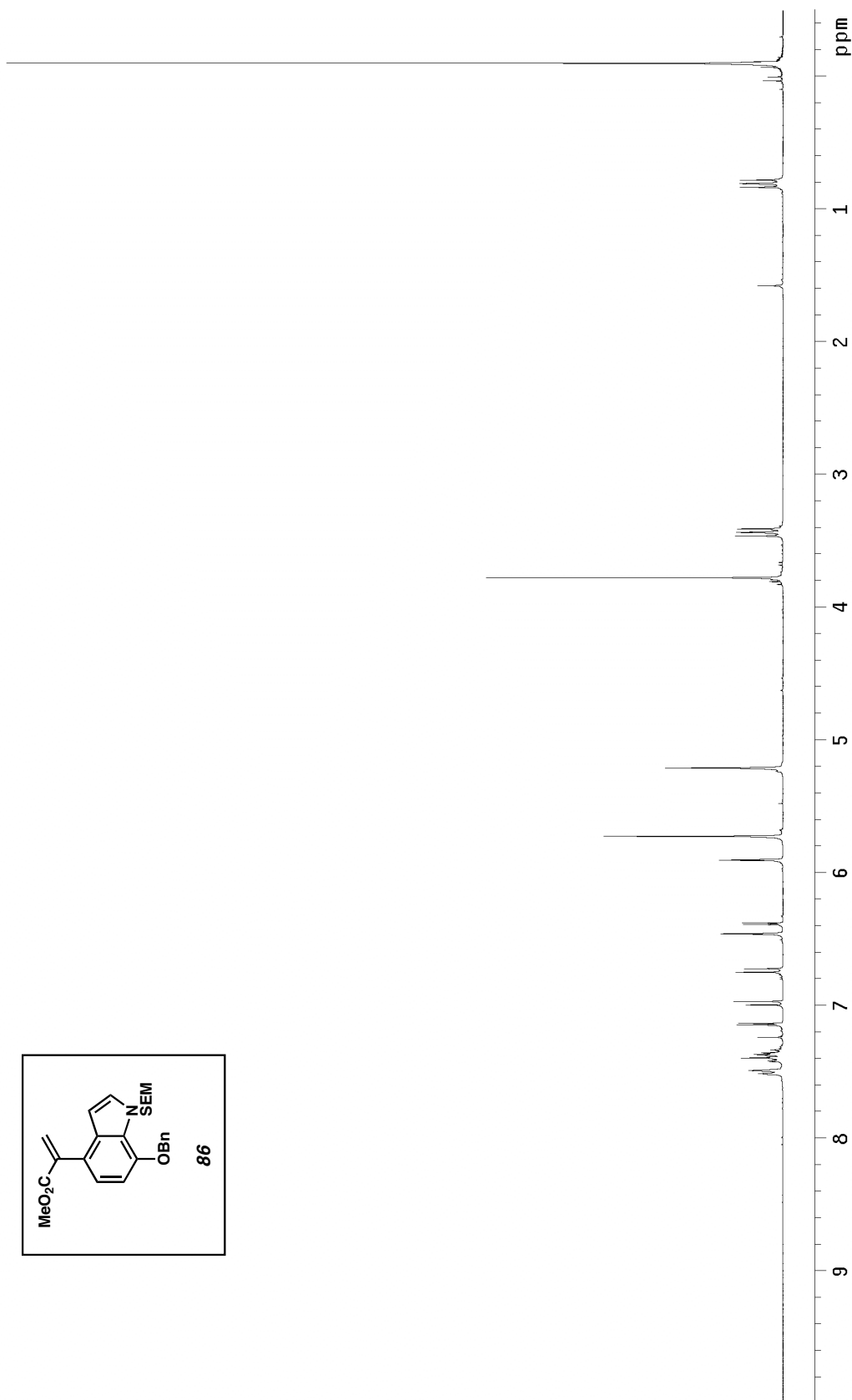
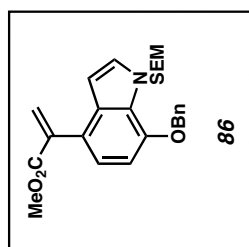


Figure A2.68 ^1H NMR (300 MHz, CDCl_3) of compound **86**.

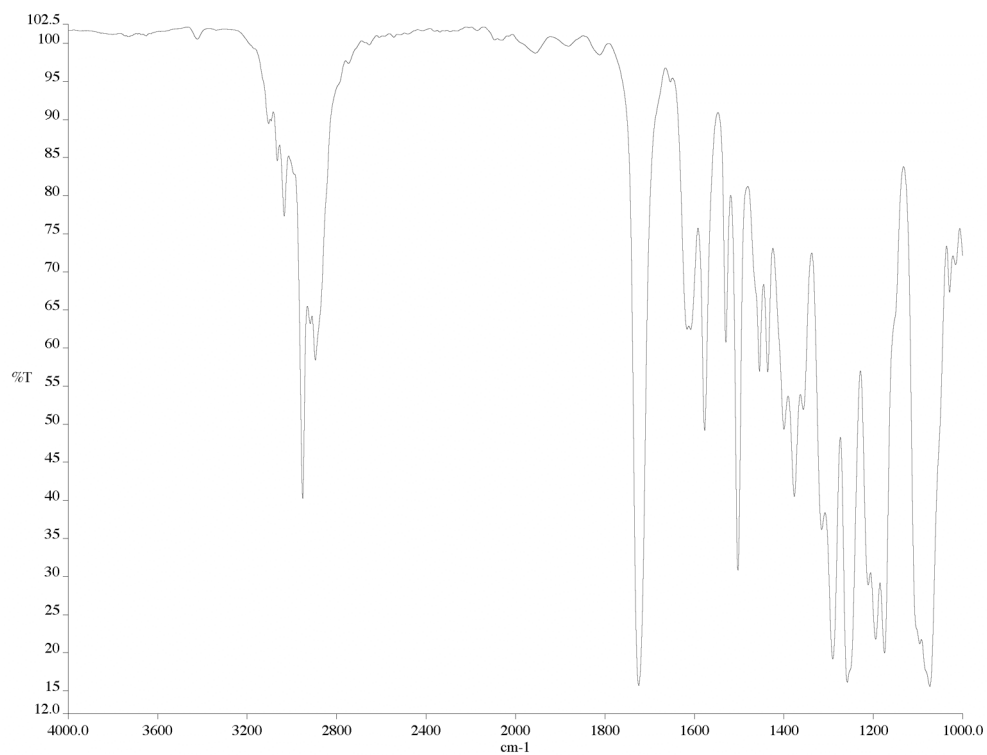


Figure A2.69 Infrared spectrum (thin film/NaCl) of compound **86**.

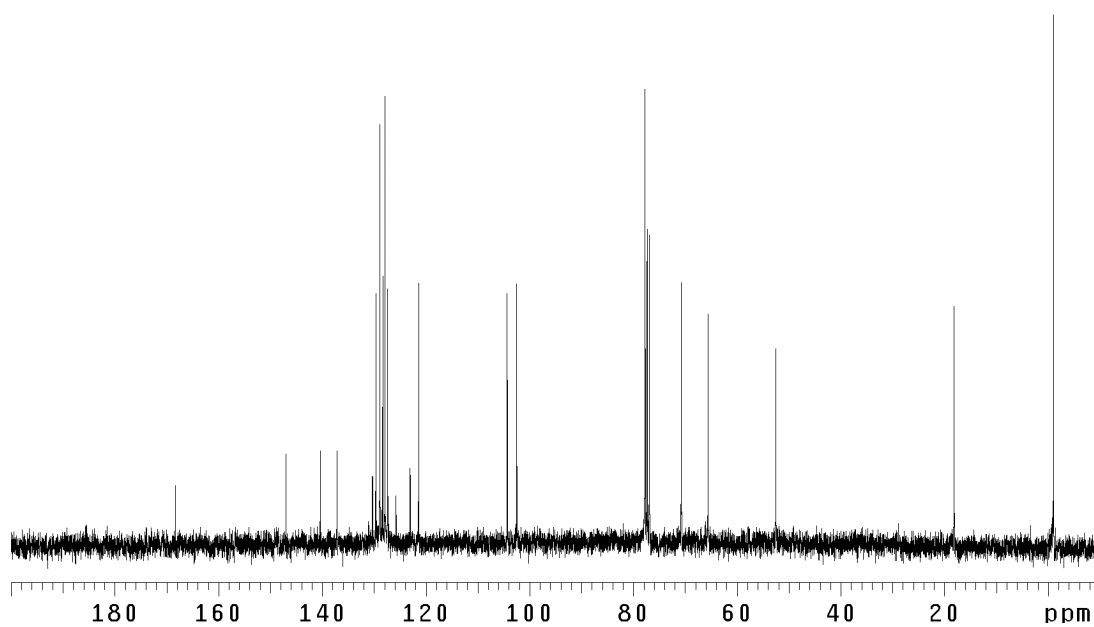


Figure A2.70 ¹³C NMR (75 MHz, CDCl₃) of compound **86**.

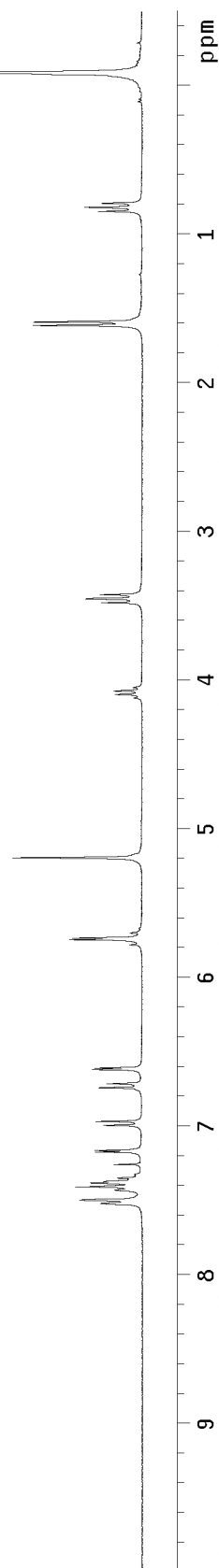
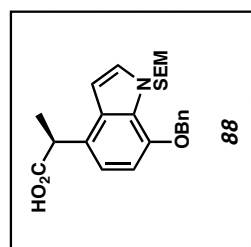


Figure A2.71 ¹H NMR (300 MHz, CDCl₃) of compound **88**.



Figure A2.72 Infrared spectrum (thin film/NaCl) of compound **88**.

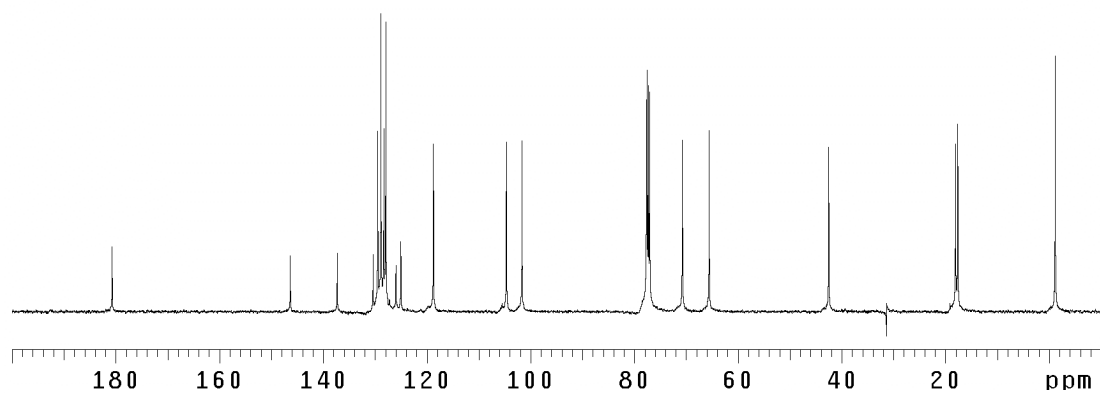


Figure A2.73 ¹³C NMR (125 MHz, CDCl₃) of compound **88**.

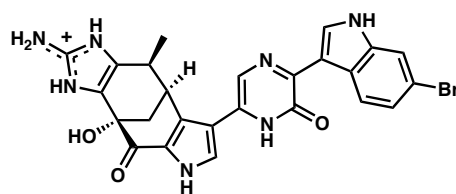
CHAPTER THREE

The Total Synthesis of (+)- and (-)-Dragmacidin F[†]

3.1 Background

3.1.1 Introduction

Having developed a strategy to construct the bis(indole)pyrazinone core of dragmacidin D (**5**, Chapter 2), we set out to extend the scope of our halogen-selective Suzuki coupling methodology to the synthesis of related natural products. We hypothesized that our approach could be amenable to the preparation of the antiviral agent dragmacidin F,¹ which is perhaps the most daunting target of the dragmacidin natural products (Figure 3.1.1).²

Figure 3.1.1*Dragmacidin F (7)*

The antiviral agent dragmacidin F (**7**) possesses a variety of structural features that make it an attractive target for total synthesis. These synthetic challenges include the differentially substituted pyrazinone, the bridged [3.3.1] bicyclic ring system, which is

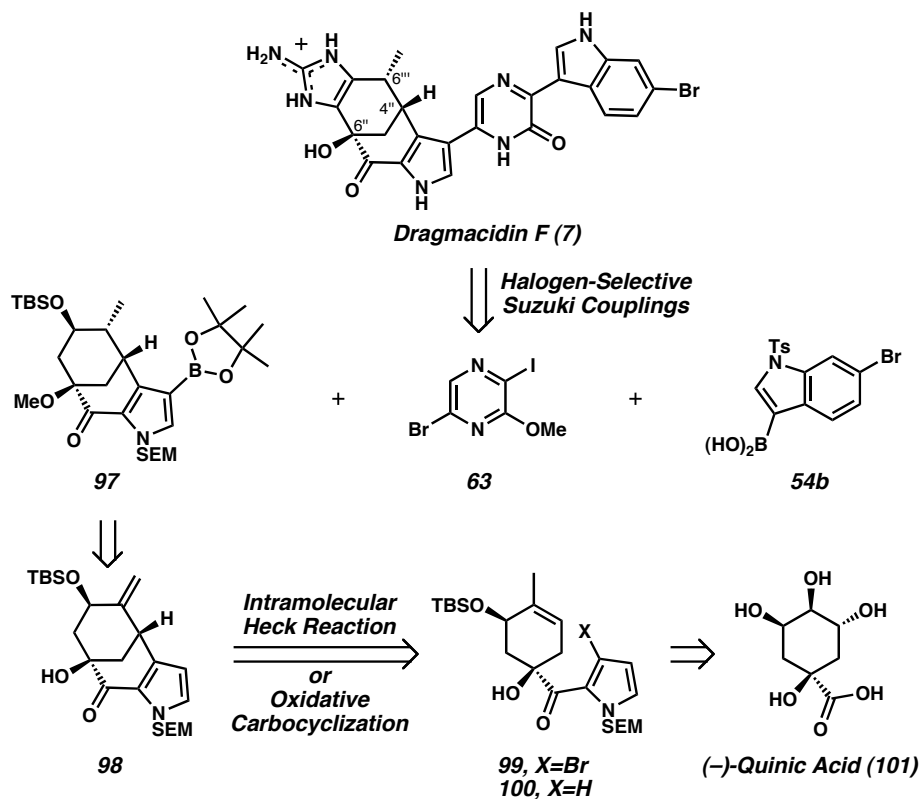
[†] This work was performed in collaboration with Daniel D. Caspi, a graduate student in the Stoltz group.

fused to both the trisubstituted pyrrole and aminoimidazole heterocycles, and the installation and maintenance of the 6-bromoindole fragment.

3.1.2 Retrosynthetic Analysis of Dragmacidin F

Our retrosynthetic analysis for dragmacidin F (**7**) is shown in Scheme 3.1.1. On the basis of our experience with dragmacidin D (**5**), we reasoned that the aminoimidazole moiety would best be incorporated at a late stage in the synthesis. The carbon skeleton of the natural product would then arise via a series of halogen-selective Suzuki cross-coupling reactions (**97** + **63** + **54b**). Pyrazine **63** and indolylboronic acid **54b** were both readily accessible, while pyrroloboronic ester **97** perhaps could be derived from pyrrole-fused bicycle **98**, our key retrosynthetic intermediate. We then targeted bicycle **98** from two related directions: a Pd(0)-mediated intramolecular Heck reaction³ of bromopyrrole **99** and a Pd(II)-promoted oxidative carbocyclization⁴ involving *des*-bromopyrrole **100**. The successful implementation of the latter method was particularly attractive since it is closely aligned with our interest in Pd(II)-catalyzed dehydrogenation reactions.⁵ Both of the cyclization substrates (**99** and **100**) could be prepared from commercially available (–)-quinic acid (**101**).⁶ At the time of this synthetic effort, the absolute stereochemistry of natural dragmacidin F (**7**) was not known; thus, the absolute stereochemistry of our target (**7**) was chosen arbitrarily.

Scheme 3.1.1



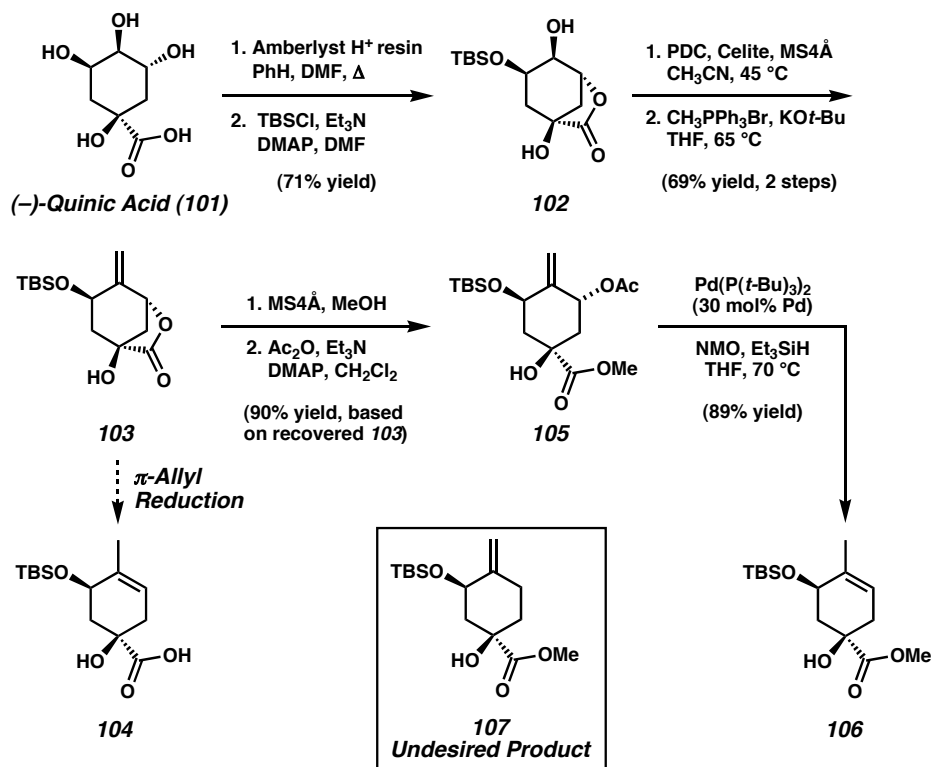
3.2 The Total Synthesis of (+)-Dragmacidin F

3.2.1 Synthesis of Cyclization Substrates

Our synthesis of dragmacidin F (**7**) began with a known two-step protocol involving lactonization and silylation of (–)-quinic acid (**101**) to afford bicyclic lactone **102** (Scheme 3.2.2).⁷ Subsequent oxidation and Wittig olefination of **102** produced exomethylene lactone **103** in good yield. Initially, we envisioned the direct conversion of lactone **103** to unsaturated carboxylic acid **104** by executing a homogeneous Pd(0)-catalyzed π -allyl hydride addition reaction.⁸ Despite considerable experimentation, however, exposure of lactone **103** to a variety of Pd and hydride sources under standard conditions⁸ led to the formation of complex product mixtures. As a result, a more

stepwise approach was tried. Methanolysis of lactone **103** followed by acetylation of the resulting 2° alcohol⁹ gave rise to allylic acetate **105**, another potential substrate for π -allyl reduction chemistry. Although **105** did react under most literature protocols, undesired exocyclic olefin **107** was typically the major product observed. After substantial optimization, we were able to access **106** as the major product by employing stoichiometric $\text{Pd}(\text{P}(t\text{-Bu})_3)_2$ ¹⁰ in the presence of triethylsilane as a reductant. Further refinements designed to facilitate catalysis led to a reduced Pd loading (30 mol%) when *N*-methylmorpholine-*N*-oxide (NMO) was used as an additive.¹¹ Under these conditions, cyclohexene **106** was obtained in 89% yield as a single olefin regioisomer. Unfortunately, this transformation often gave inconsistent results and was particularly sensitive to oxygen, water, and the quality of Et_3SiH . These difficulties coupled with the high catalyst loading resulted in substantial material throughput problems. We therefore sought yet another method to prepare cyclohexene **106** or a closely related derivative thereof (i.e., **104**) in a more facile and preparative manner.

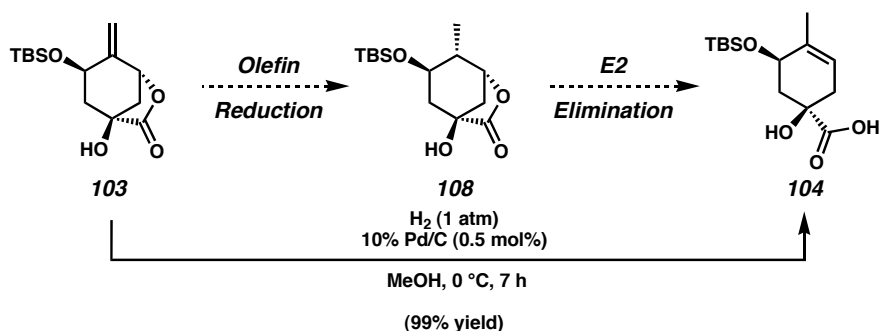
Scheme 3.2.2



In our revised plan, we conceived a two-step route to obtain carboxylic acid **104** via diastereoselective reduction of olefin **103** followed by base-promoted elimination of the carboxylate functionality of **108** (Scheme 3.2.3). Daniel Caspi attempted the first part of this sequence by exposing olefin **103** to standard catalytic hydrogenation conditions (Pd/C, 1 atm H₂). Surprisingly, these conditions led to the production of a compound that was more polar than we expected for simple olefin hydrogenation (i.e., **108**). To our delight, the product was identified as unsaturated carboxylic acid **104**. Under our optimized reaction conditions (0.5 mol% Pd/C, 1 atm H₂, MeOH, 0 °C), essentially quantitative reductive isomerization to **104** was observed. Although the mechanism of

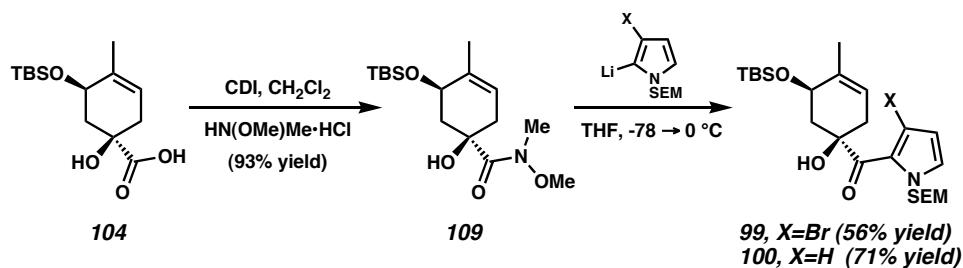
this transformation has not been studied extensively, simple control experiments suggest that stepwise reduction/elimination¹² or π -allyl reduction processes are not operative.¹³

Scheme 3.2.3



With facile access to cyclohexene carboxylic acid **104**, preparation of the key cyclization precursors proceeded without difficulty. Activation of acid **104** with CDI followed by the addition of $\text{HN}(\text{OMe})\text{Me} \cdot \text{HCl}$ afforded Weinreb amide **109** (Scheme 3.2.4). The Weinreb amide functionality was then displaced with the appropriate lithiopyrrole¹⁴ reagent to produce Heck cyclization substrate **99**¹⁵ and oxidative cyclization substrate **100**.

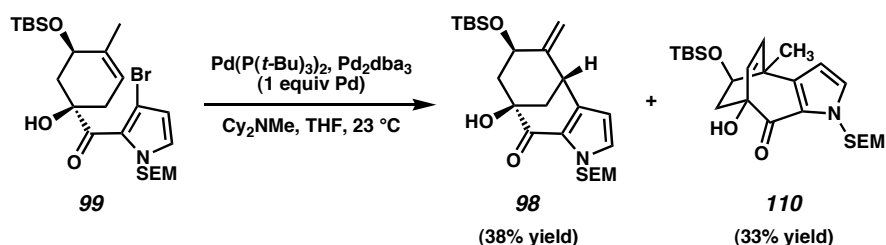
Scheme 3.2.4



3.2.2 Constructing the [3.3.1] Bicycle

Extensive studies were carried out in order to achieve the intramolecular Heck cyclization of bromopyrrole **99**. Attempts to utilize standard procedures were unsuccessful,³ likely due to the thermal instability of the bromopyrrole moiety. However, implementation of the room-temperature conditions developed by Fu¹⁶ provided the desired [3.3.1] bicyclic product (**98**), albeit in low yield (Scheme 3.2.5). Unfortunately, the formation of **98** was hampered by competitive production of [3.2.2] bicycle **110**. Although efforts to optimize temperature, solvent, base, and concentration were not met with success, it was found that increased quantities of Pd improved the ratio of the desired [3.3.1] bicycle (**98**) to the undesired [3.2.2] bicycle (**110**). In addition, the ratio of **98** to **110** decreased over time,¹⁷ suggesting that the active catalytic species varied during the course of the reaction or that selectivity changed as the concentration of $R_3NH^+Br^-$ increased.

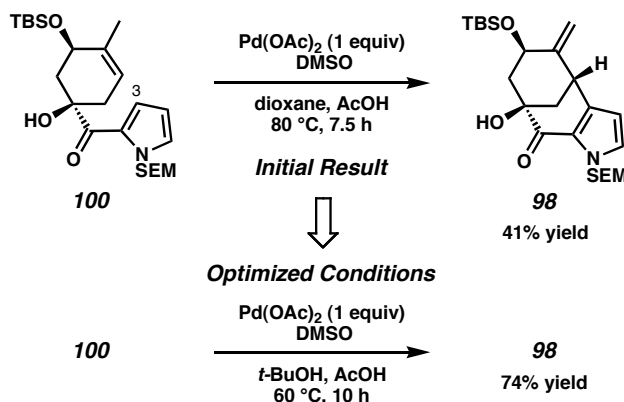
Scheme 3.2.5



Although the Heck reaction was useful for preparing reasonable quantities of bicycle **98**, an alternative and potentially more selective route to **98** was desired. In conjunction with ongoing research in our group,⁵ we turned to the Pd(II)-mediated C-C bond forming approach. In this scenario, C(3)-unsubstituted pyrrole **100** would undergo

intramolecular carbocyclization to afford **98** (Scheme 3.2.6). Initial experimentation revealed that pyridine and ethyl nicotinate were not effective ligands for promoting cyclization in the presence of Pd(OAc)₂.^{5c,d} However, Daniel Caspi found that by using DMSO as a ligand¹⁸ the desired cyclization product could be obtained in modest yield. Subsequent optimization of solvent, temperature, and reaction time led to a set of improved conditions whereby the desired pyrrole-fused bicycle **98** was formed as a single stereo- and regioisomer in 74% yield. Interestingly, these conditions take advantage of a similar solvent mixture employed in Pd cyclization methodology from our laboratory.^{5c,d} This transformation (**100** → **98**) is particularly noteworthy since it results in functionalization of the electronically deactivated and sterically congested C(3) position of acyl pyrrole **100**.^{19,20} Despite our best efforts, we were unable to effect catalytic turnover of Pd with a stoichiometric oxidant in this reaction, presumably due to extensive oxidative decomposition of both the starting material and the desired product.²¹ Nonetheless, the Pd(II)-mediated strategy provided bicycle **98** in nearly twice the isolated yield as the Heck route using equivalent amounts of Pd and obviated the need for polybrominated pyrroles.^{15,22}

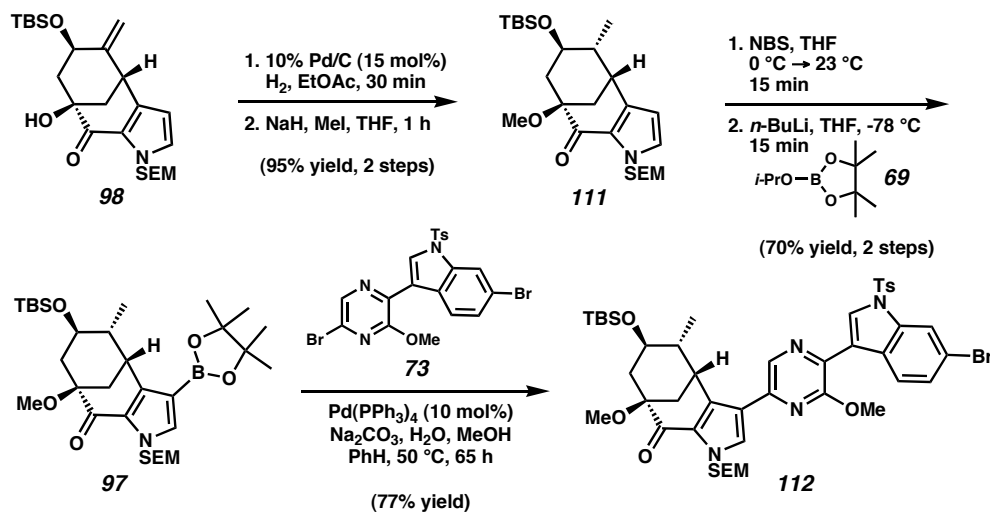
Scheme 3.2.6



3.2.3 Assembling the Carbon Skeleton of Dragmacidin F

With the [3.3.1] bicyclic framework in hand (i.e., **98**), we focused our attention on constructing the full carbon skeleton of dragmacidin F (**112**, Scheme 3.2.7). The final stereocenter present in the natural product was installed via catalytic hydrogenation of olefin **108** and was followed by methylation of the 3° alcohol to produce bis(ether) **111**. The methyl protecting group was selected initially for its robustness⁹ and would presumably allow for the exploration of late-stage chemistry in the form of a model system.²³ Methyl ether **111** was then elaborated via regioselective bromination of the pyrrole and metalation to boronic ester **97**. In the critical halogen-selective Suzuki fragment coupling, pyrroloboronic ester **97** was reacted with dibromide **73** (prepared from **63** + **54b**) under Pd(0) catalysis. By analogy to our dragmacidin D studies, we were pleased to find that at $50\text{ }^\circ\text{C}$, the desired C-C bond forming reaction took place to afford the fully coupled product (**112**) in 77% yield. Importantly, the indolylbromide moiety was maintained under these reaction conditions.

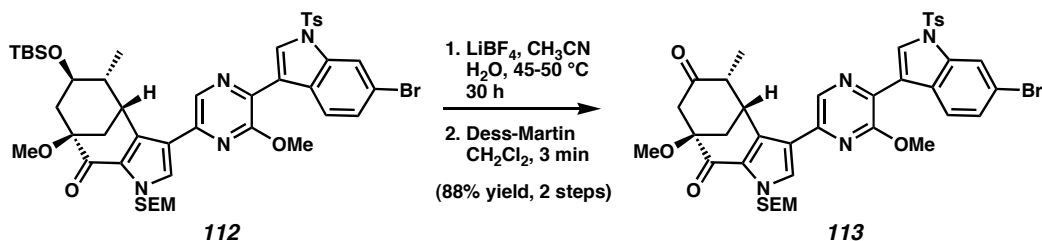
Scheme 3.2.7



3.2.4 End-Game Studies

With the carbon framework completed, few tasks remained in order to finish the total synthesis of dragmacidin F (**7**), namely, removal of all protecting groups and installation of the aminoimidazole unit. Of particular note is the similarity of these synthetic challenges to those encountered in our total synthesis of dragmacidin D (**5**). Not surprisingly, we decided to utilize the methods that were already familiar to us in order to elaborate **112** to the desired natural product (**7**). To this end, we anticipated that the presence of an amino group α to the ketone would allow for eventual introduction of the aminoimidazole moiety. Therefore, selective deprotection of silyl ether **112**, followed by oxidation with Dess-Martin periodinane, produced ketone **113** (Scheme 3.2.8).

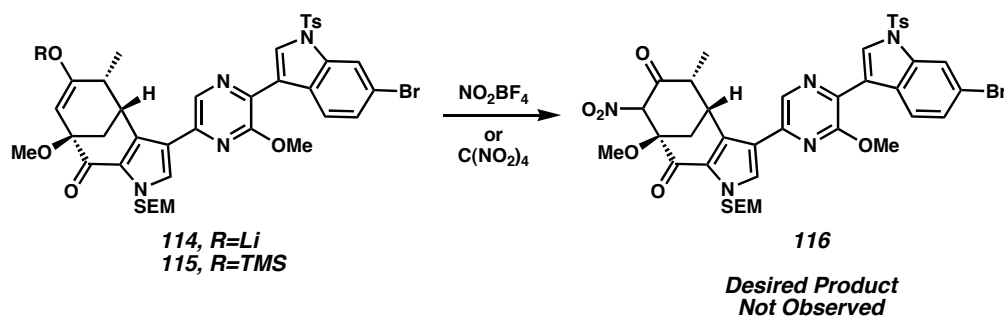
Scheme 3.2.8



3.2.4.1 End-Game Strategy 1

Our first effort to functionalize the ketone α -position involved a nitration strategy to access a compound analogous to an intermediate employed in the dragmacidin D synthesis (Scheme 3.2.9). Both lithium enolate **114** and TMS enol ether **115** were exposed to electrophilic NO_2 sources.²⁴ Unfortunately, in all of these cases, formation of the desired nitroketone product (**116**) was not observed.

Scheme 3.2.9

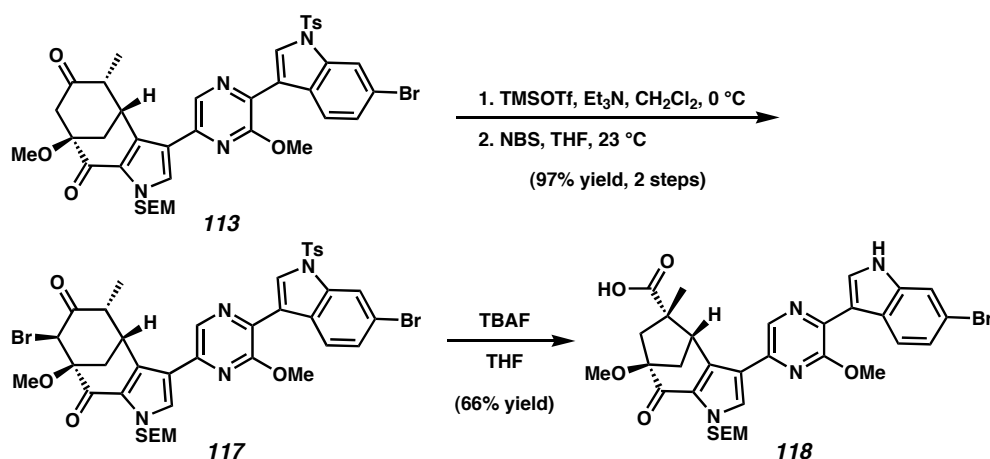


3.2.4.2 End-Game Strategy 2

We then turned to an alternative strategy that would involve installation of an α -amino substituent via nucleophilic displacement of an alkylbromide. Therefore, ketone **113** was treated with TMSOTf and then exposed to NBS to afford bromoketone **117** as a

single diastereomer (Scheme 3.2.10).²⁵ Interestingly, when bromoketone **117** was treated with various nitrogenous nucleophiles, base-promoted rearrangements were observed.²⁶ In fact, reaction of bromide **117** with a basic fluoride anion source (TBAF in THF) gave [3.2.1] bicycle **118** as the major product via a Favorskii rearrangement.²⁷ The utilization of amine bases also led to the formation of related Favorskii products.

Scheme 3.2.10

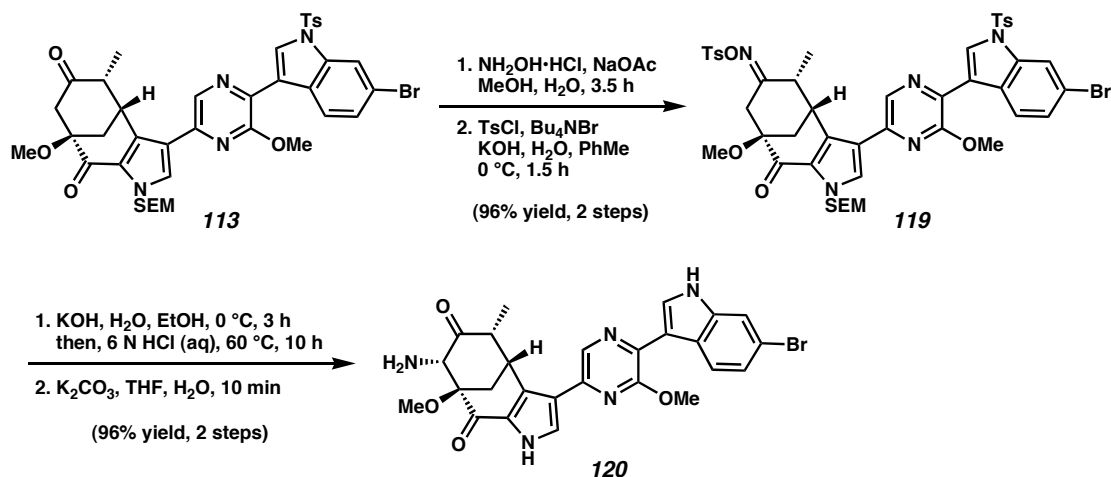


3.2.4.3 End-Game Strategy 3: The Total Synthesis of (+)-Dragmacidin F

With limited options remaining, we became interested in the use of a Neber rearrangement in order to install the necessary α -amino substituent.^{28,29} In this scenario, an activated oxime derivative would undergo alkoxide-promoted rearrangement to furnish an α -aminoketone. Thus, ketone **113** was converted to tosyloxime **119** via standard conditions (Scheme 3.2.11). Gratifyingly, exposure of substrate **119** to aqueous KOH in ethanol led to Neber rearrangement. After optimization, we found that simply exposing tosyloxime **119** to i) KOH, ii) HCl, and iii) K₂CO₃ produced α -aminoketone **120** as a single regio- and stereochemical isomer in excellent yield.^{30,31,32} Furthermore,

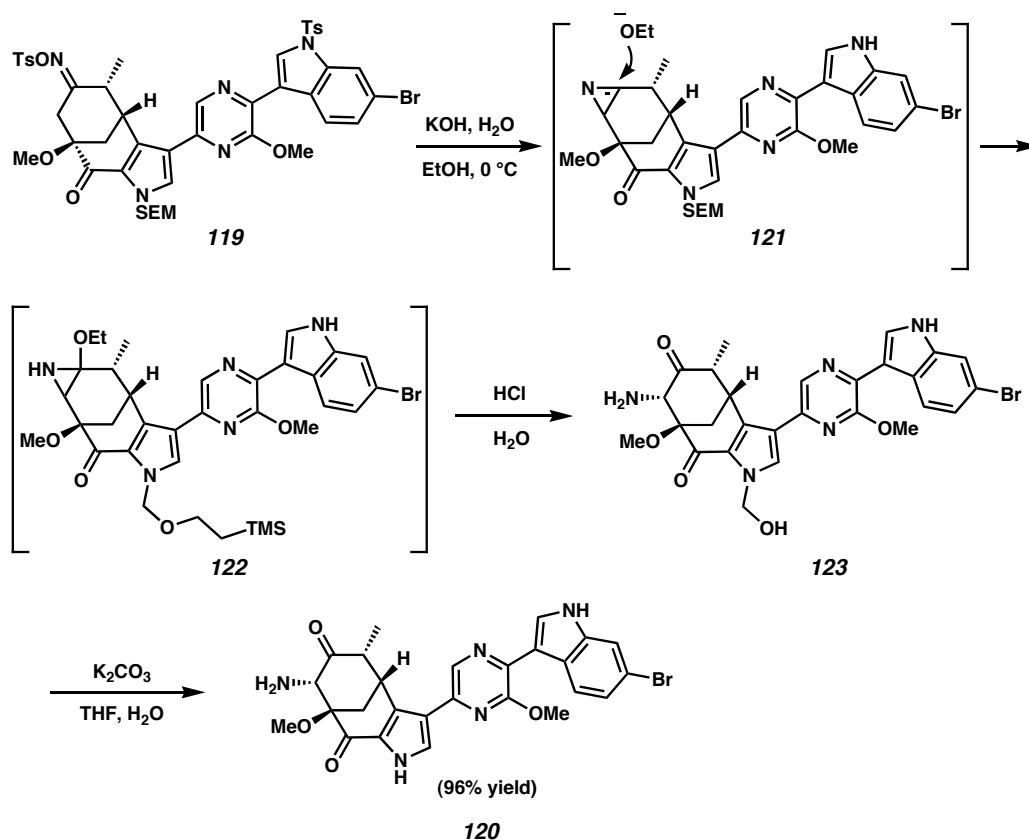
under these reaction conditions, both the tosyl and SEM protective groups were quantitatively removed from their corresponding heterocycles. To the best of our knowledge, this is the first example of a successful Neber rearrangement in the context of natural product synthesis.³³

Scheme 3.2.11



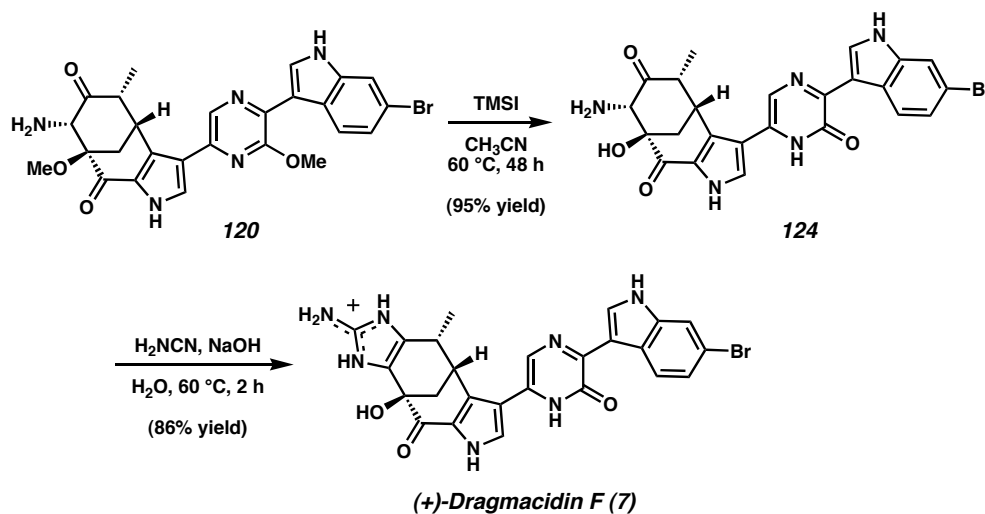
A more detailed look at the possible mechanism of the Neber rearrangement/deprotection sequence is shown in Scheme 3.2.12. Exposure of tosyloxime **119** to KOH in ethanol likely leads to the formation of detosylated azirine **121**, which is attacked by ethoxide to afford ethoxyaziridine **122**.^{29a,34} Following acid-mediated hydrolysis, the aminoketone moiety is installed with concomitant partial cleavage of the SEM protective group (**122** \rightarrow **123**).^{30b,35} Finally, treatment of hemiaminal **123** with K_2CO_3 removes the remaining portion of the SEM group, thus giving rise to the deprotected aminoketone (**120**).

Scheme 3.2.12



In order to unveil the masked pyrazinone functionality, Neber rearrangement product **120** was treated with TMSI at $60\text{ }^\circ\text{C}$ (Scheme 3.2.13).⁹ Fortuitously, both the pyrazinone and the 3° alcohol functionalities were revealed simultaneously (**120** \rightarrow **124**). In the final step of the synthesis, the penultimate aminoketone (**124**) was subjected to cyanamide and aqueous NaOH to produce enantiopure dragmacidin F (**7**).³⁶ Our efficient and enantiospecific route allows access to **7** in 7.8% overall yield in just 21 steps from (–)-quinic acid (**101**).

Scheme 3.2.13



3.3 The Absolute Stereochemistry of the Pyrazinone-Containing Dragmacidins

Synthetic dragmacidin F (**7**) was spectroscopically identical (¹H NMR, ¹³C NMR, IR, UV, HPLC) to a sample obtained from natural sources (Figure 3.3.1),^{1b} with the exception of the sign of rotation (natural: $[\alpha]_D^{25} -159^\circ$ (*c* 0.4, MeOH); synthetic: $[\alpha]_D^{23} +146^\circ$ (*c* 0.45, MeOH)). Thus, our synthesis from (–)-quinic acid (**101**) established, for the first time, the absolute configuration of natural dragmacidin F (**7**) to be (4''*S*, 6''*S*, 6'''*S*) as shown in Figure 3.3.2.³⁷ On the basis of the hypothesis that dragmacidins D, E, and F are biosynthetically related, it is likely that the absolute stereochemical configurations of natural dragmacidins D (**5**) and E (**6**) are (6'''*S*) and (5'''*R*, 6'''*S*), respectively. Having developed a route to the unnatural antipode of dragmacidin F ((+)-**7**), we set out to extend our approach to the total synthesis of (–)-**7**.

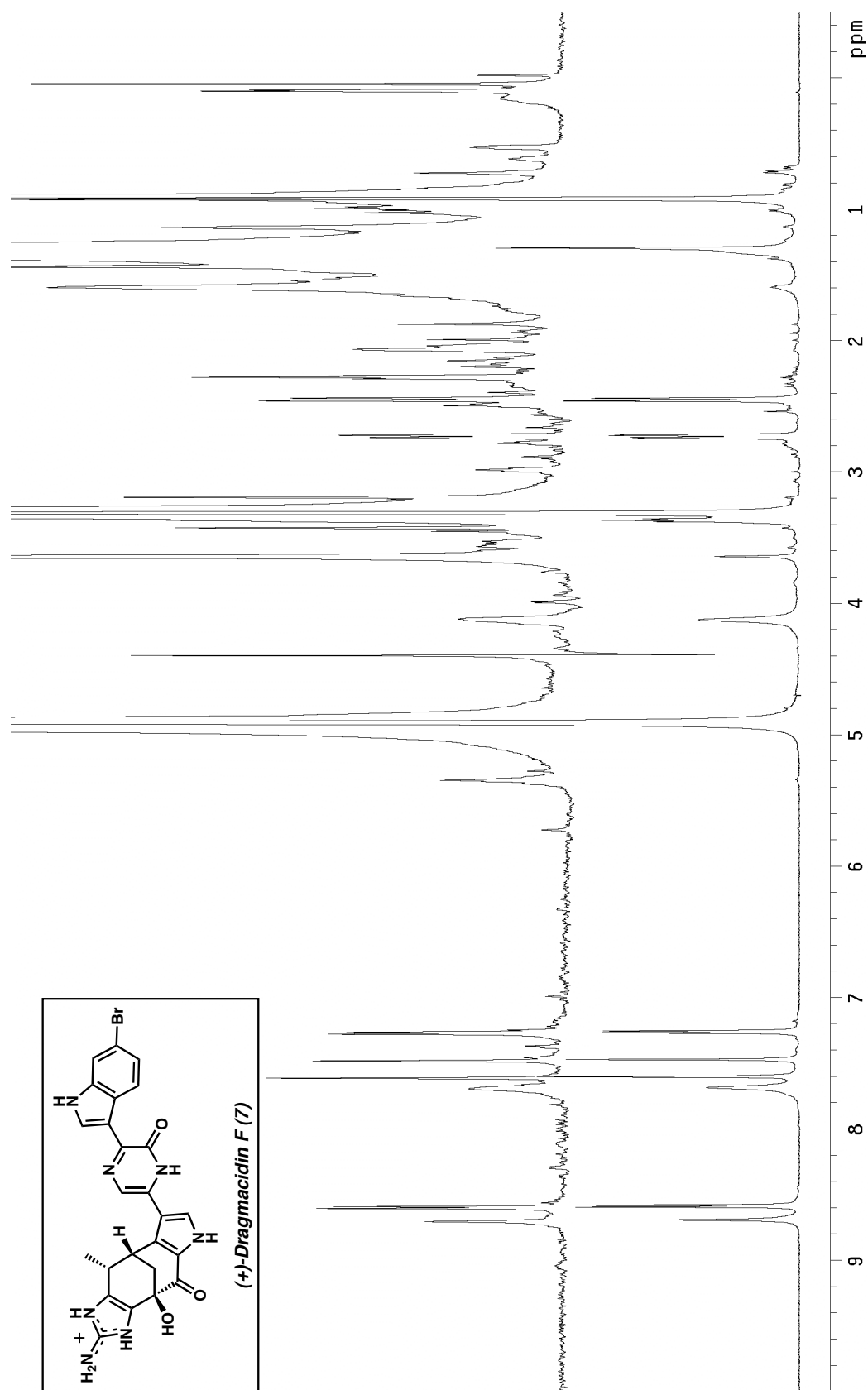
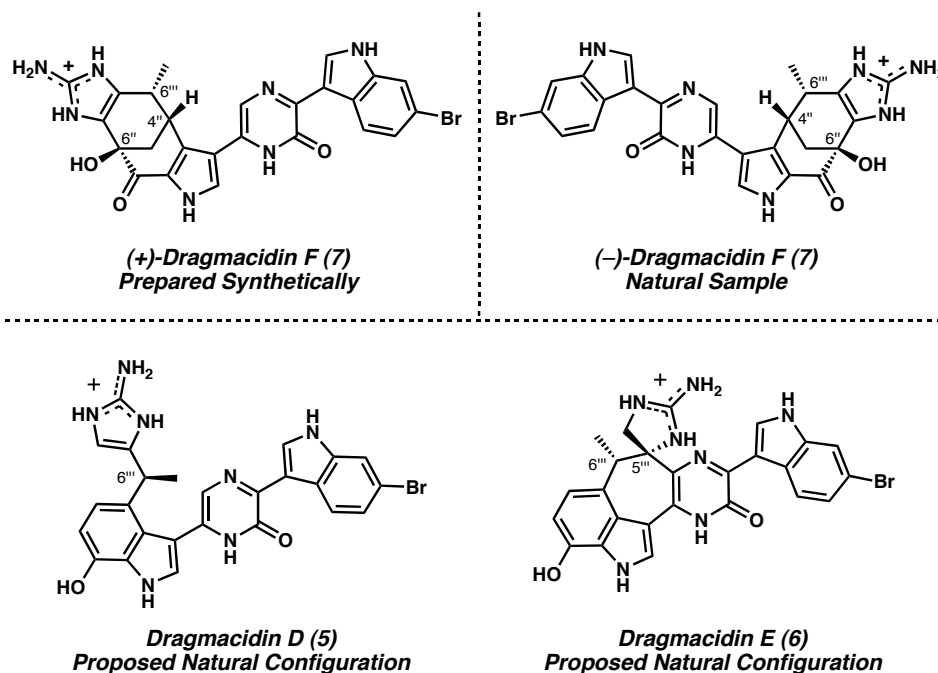


Figure 3.3.1 ^1H NMR (600 MHz, CD_3OD) of dragmacidin F (7); (–)-natural (top) and (+)-synthetic (bottom).

Figure 3.3.2



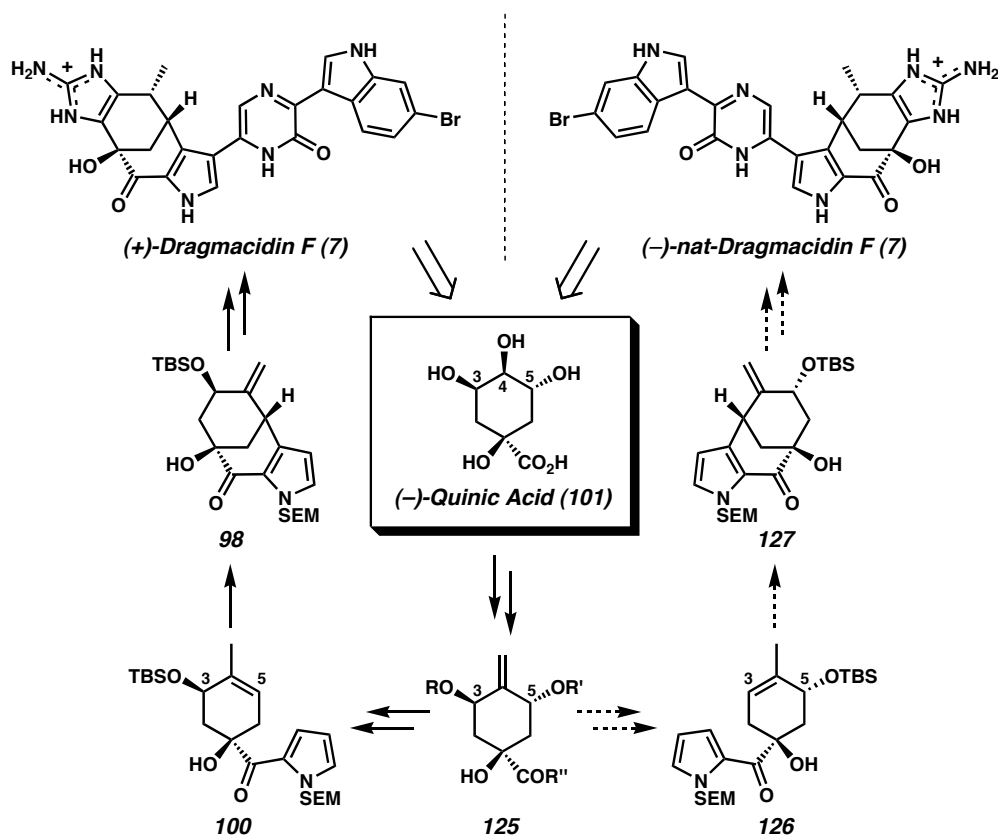
3.4 The Total Synthesis of (–)-Dragmacidin F

3.4.1 An Enantiodivergent Strategy for the Preparation of (–)-Dragmacidin F

As described above, naturally occurring and readily available (–)-quinic acid (**101**)⁶ had served as the starting material for our synthetic approach to (+)-**7**. Unfortunately, the (+)-enantiomer of **101** is not easily accessible,³⁸ and we were confronted with the possibility that our synthesis would not be amenable to the preparation of our new target molecule, (–)-dragmacidin F ((–)-**7**). We reasoned, however, that it might be possible to exploit (–)-quinic acid (**101**) in an enantiodivergent manner that would allow access to both (+)- and (–)-**7** (Scheme 3.4.1).³⁹ For such an approach to succeed, (–)-quinic acid (**101**) would be elaborated via selective manipulation of the C(3), C(4), and C(5) hydroxyl groups to a pseudo- C_2 -symmetric⁴⁰ derivative (**125**) en route to pyrrolocyclohexene **126**, the diastereomer of which (i.e., **100**)

was employed in our synthesis of (+)-**7**. Analogous to our approach to (+)-**7** (i.e., **100** → **98**), we anticipated that **126** could undergo oxidative carbocyclization to afford annulated pyrrole **127**. Bicycle **127** would then be elaborated to (–)-dragmacidin F ((–)-**7**). Of the key transformations outlined in Scheme 15, we were familiar with the Pd-mediated oxidative carbocyclizations and the late-stage manipulations of related compounds; however, the successful preparation of (–)-dragmacidin F ((–)-**7**) would rely heavily on the identification of a suitable quinic acid derivative (**125**), the facile synthesis of that compound, and the rapid conversion of **125** to the requisite cyclization substrate (**126**).

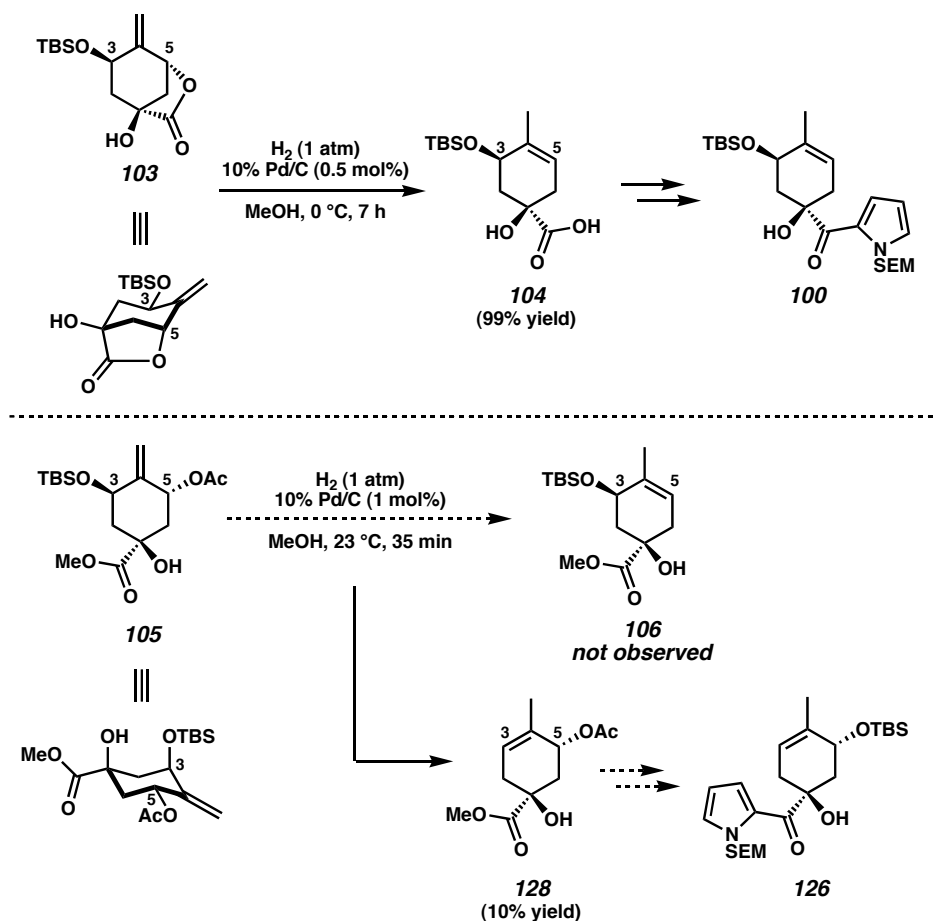
Scheme 3.4.1



3.4.2 The Development and Investigation of a Reductive Isomerization Reaction

Fortunately, potential solutions to these problems had become apparent during our studies of a novel reductive isomerization reaction discovered in our synthesis of (+)-dragmacidin F ((+)-**7**). Two critical results are shown in Scheme 3.4.2. In the first experiment, treatment of lactone **103** with Pd/C and H₂ in methanol at 0 °C furnished carboxylic acid **104** in essentially quantitative yield via reductive loss of the C(5) carboxylate with concomitant olefin migration (i.e., net S_N2' reduction). In the second experiment, a closely related derivative (**105**) was exposed to similar reaction conditions.⁴¹ Surprisingly, the reductive isomerization reaction proceeded with loss of the C(3) silyl ether rather than the C(5) acetate, thus producing small quantities of allylic acetate **128** instead of the anticipated product (**106**).⁴² The observation that (*t*-Bu)Me₂SiO⁻ was preferentially ejected from compound **105** despite the clear superiority of AcO⁻ as a leaving group led us to consider that the C(3) silyl ether moiety was positioned in an axial orientation, thereby facilitating its elimination.⁴³ This preferred conformation of **105** represents a cyclohexane ring-flip with respect to lactone **103**, and thus gives rise to the reductive isomerization product (**128**) possessing a Δ_{3,4} olefin. Importantly, the possibility existed that the unexpected product obtained from this reaction (i.e., **128**) could be converted to cyclization substrate **126** (diastereomeric to **100**).

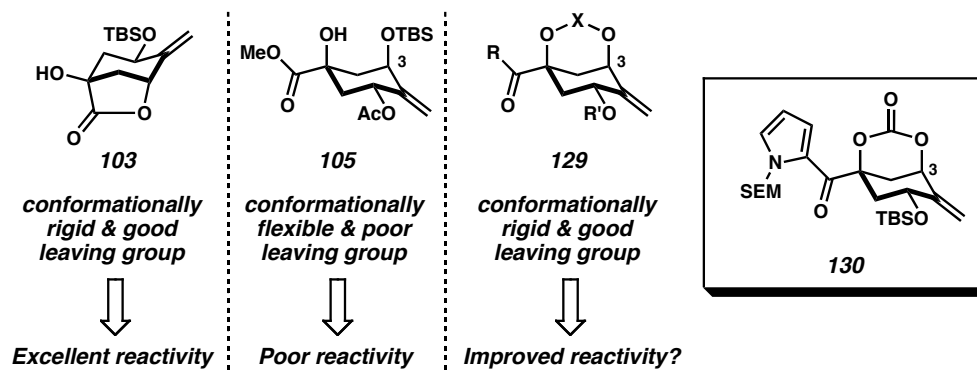
Scheme 3.4.2



Our efforts to optimize the reductive isomerization of **105** to **128** were hampered by competitive hydrogenation of the olefin moiety of **105**, a complication not observed in the high-yielding conversion of **103** to **104**. Although both processes presumably involve the elimination of an axially disposed leaving group,⁴³ we reasoned that the successful conversion of **103** to **104** was due to the carboxylate being conformationally restricted to an axial orientation, while substrate **105** possessed a poorer leaving group ($((t\text{-Bu})\text{Me}_2\text{SiO}^-)$) and was free to adopt alternate conformations (Figure 3.4.1).⁴⁴ We hypothesized that derivatives of **105** containing an axially-locked leaving group at C(3)

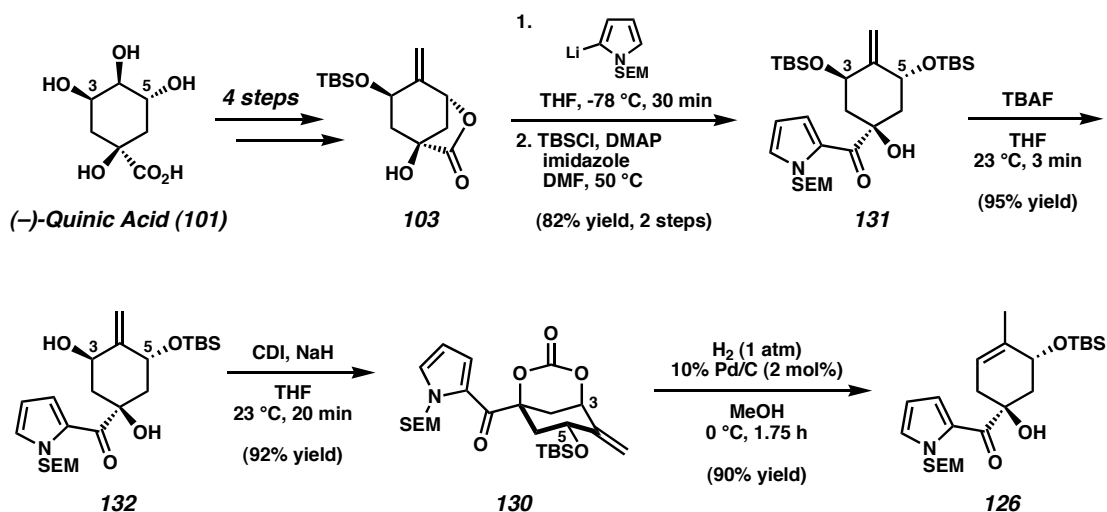
(e.g., **129**) would be more suitable substrates for the reductive isomerization reaction. Thus, carbonate **130** was identified as the key (–)-quinic acid derived intermediate en route to the desired cyclization substrate (**126**) and became the focus of our efforts.

Figure 3.4.1



Our synthesis of carbonate **130** began with bicyclic lactone **103**, a derivative of (–)-quinic acid (**101**) that was used in our total synthesis of (+)-**7** (Scheme 3.4.3). Addition of 2-lithio-SEM-pyrrole¹⁴ followed by TBS protection afforded bis(silylether) **131** in good yield. This pseudo- C_2 -symmetric compound then underwent rapid diastereoselective mono-desilylation upon treatment with TBAF in THF to produce the *syn* 1,3-diol **132**.⁴⁵ Importantly, this desymmetrization proceeded with complete selectivity and allowed us to efficiently differentiate the C(3) and C(5) positions of the cyclohexyl moiety. Diol **132** was smoothly converted to bicyclic carbonate **130** in the presence of CDI, effectively restricting the C(3) substituent to an axial disposition. Gratifyingly, exposure of carbonate **130** to our reductive isomerization conditions (2 mol% Pd/C, H₂, MeOH, 0 °C) led to the selective formation of the desired cyclization substrate (**126**) in 90% yield.⁴⁶

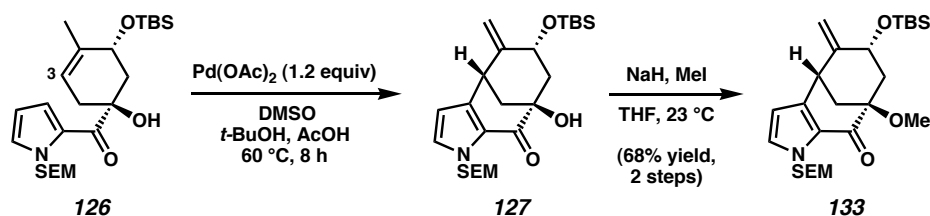
Scheme 3.4.3



3.4.3 Constructing the [3.3.1] Bicycle en Route to (-)-Dragmacidin F

After assembling target substrate **126**, we turned our attention to the key Pd(II)-mediated cyclization reaction (Scheme 3.4.4). Substrate **126** was treated with 1.2 equiv of Pd(OAc)₂ under conditions similar to those described earlier, upon which, the desired pyrrole-fused bicycle (**127**) formed as a single regio- and stereoisomer. Notably, bond formation between the pyrrole functionality and C(3) of **126** occurred even in the presence of the bulky C(5) silyl ether group positioned syn to the acyl pyrrole subunit. Following protection of the 3° alcohol, [3.3.1] bicycle **133** was obtained in 68% yield for the two-step process.

Scheme 3.4.4

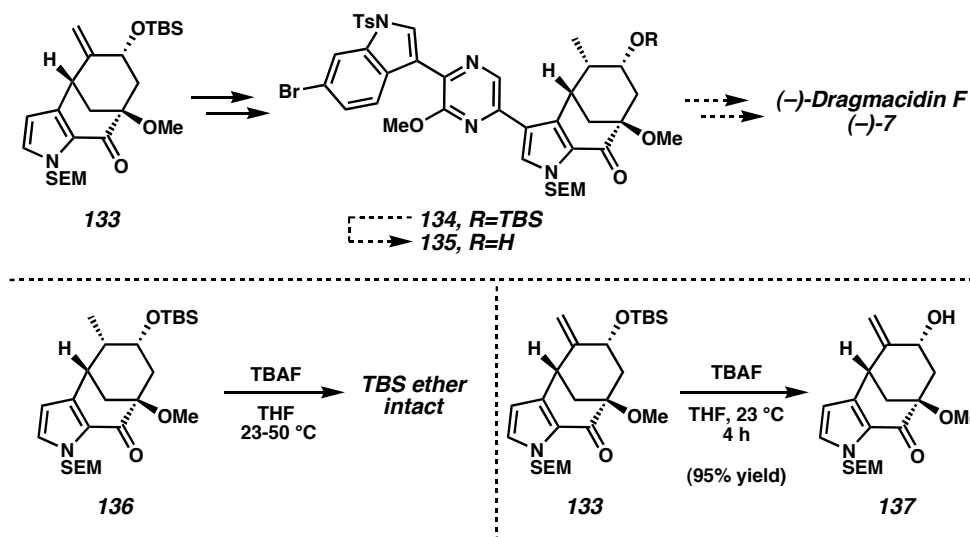


3.4.4 End-Game Studies

3.4.4.1 End-Game Strategy 1

En route to (–)-dragmacidin F, cyclization product **133** was converted to pyrazine **134** (Scheme 3.4.5) by methods similar to those described above.^{30b} Despite the similarity of **134** to its diastereomeric counterpart employed in the synthesis of (+)-**7** (**112**, Scheme 3.2.8), selective desilylation of **134** to afford **135** proved to be difficult. We reasoned that the steric congestion of the axial TBS ether, positioned syn to the methyl stereocenter, was the cause of these problems. In fact, attempted TBS cleavage of parent bicycle **136** was also challenging, even at elevated temperatures.⁴⁷ However, in a critical reaction, the sterically less crowded TBS ether of olefinic substrate **133** underwent smooth and selective cleavage upon treatment with TBAF in THF to afford allylic alcohol **137**. With this result in hand, we conceived of a modified route that would ultimately deliver (–)-**7** in a more convergent manner.

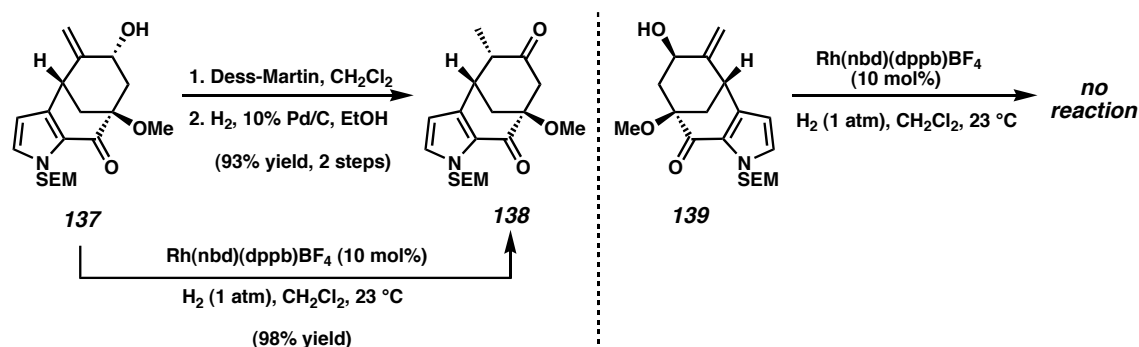
Scheme 3.4.5



3.4.4.2 End-Game Strategy 2: Rh-Mediated Allylic Isomerization and the Total Synthesis of (-)-Dragmacidin F

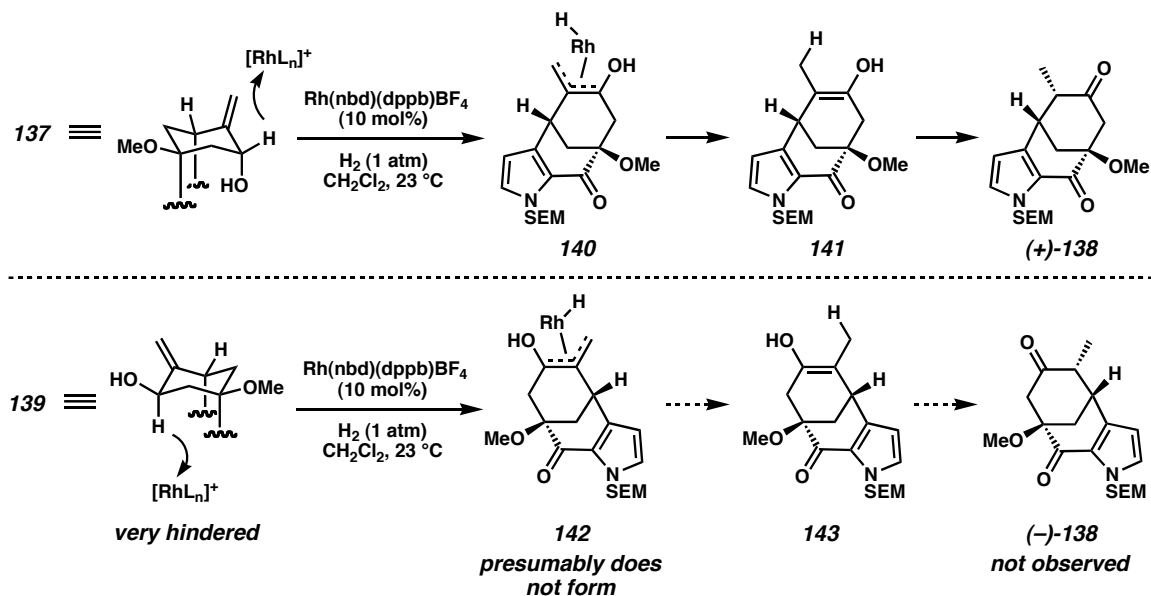
Since allylic alcohol **137** was readily accessible, we chose to employ it as an intermediate in our synthesis. Oxidation of allylic alcohol **137** followed by olefin reduction afforded ketone **138** in good overall yield (Scheme 3.4.6). However, because alcohol **137** and ketone **138** are in the same overall oxidation state, a tandem olefin isomerization/tautomerization process would be more efficient. Upon exposure of alcohol **137** to Brown's cationic rhodium catalyst $\text{Rh}(\text{nbd})(\text{dppb})\text{BF}_4^{48}$ and H_2 , ketone **138** formed directly as a single diastereomer in 98% yield. Interestingly, when diastereomer **139** (closely related to intermediates employed in the synthesis of (+)-dragmacidin F ((+)-**7**)) was subjected to the identical conditions, no reaction took place.

Scheme 3.4.6



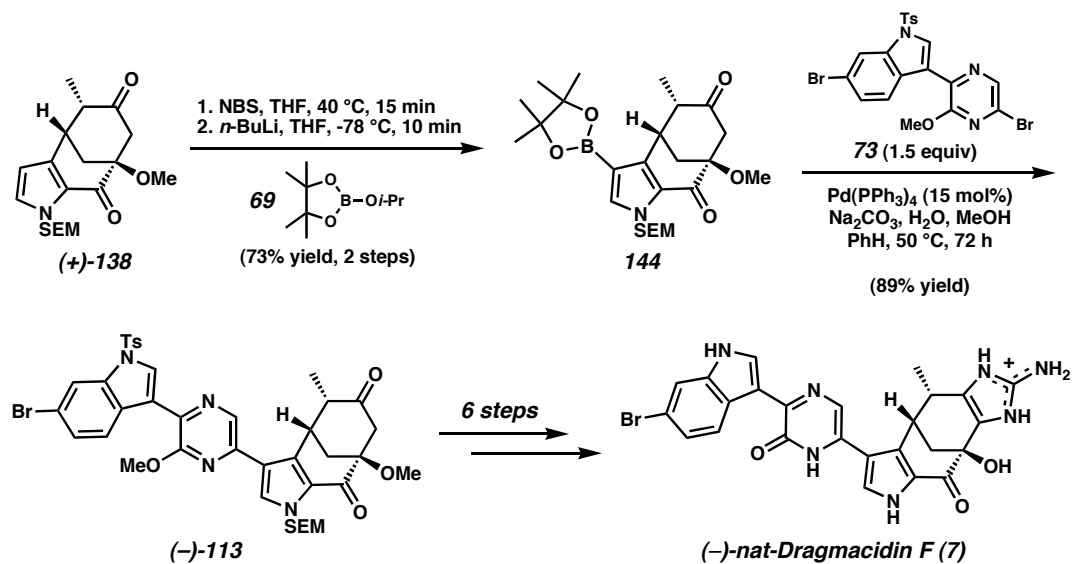
The discrepancy between the two outcomes can be rationalized after examining the mechanism of the Rh-mediated allylic isomerization reaction, which has been studied extensively.^{48b} The process begins by interaction of the cationic rhodium complex with an allylic hydrogen atom to form a π -allyl rhodium complex. In the case of substrate **137**, the allylic proton necessary for isomerization is positioned on the convex face of the bicycle, pointed away from the heterocycle (Scheme 3.4.7). Thus, the π -allyl rhodium intermediate (**140**) can form without difficulty. **140** then undergoes reductive elimination to enol **141**, followed by tautomerization to ketone (+)-**138**. The newly formed stereocenter in **138** is presumably controlled by thermodynamics, as the methyl group rests in an equatorial position. Substrate **139**, in contrast to **137**, possesses an axially disposed allylic proton that is positioned syn to the bicycle. It is likely that this proton is severely hindered, making approach of the large cationic rhodium complex difficult. Thus, isomerization of allylic alcohol **139** to ketone (–)-**138** (via **142** and **143**) does not occur.

Scheme 3.4.7



Elaboration of ketone **(+)-138** to **(-)-7** proceeded with little difficulty. Regioselective bromination and low-temperature metalation of the pyrrole in the presence of two ketones gave rise to boronic ester **144** (Scheme 3.4.8). Subsequent halogen-selective cross-coupling of **144** with dibromide **73** afforded the desired Suzuki adduct **(-)-113** (89% yield), the enantiomer of which had been employed in the synthesis of **(+)-dragmacidin F**. Finally, Suzuki adduct **(-)-113** was converted to **(-)-dragmacidin F** (**(-)-7**) via our previously described six-step protocol (vide supra). Synthetic and natural **(-)-7^{1b}** were spectroscopically identical (Figure 3.4.2), including the sign of optical rotation (natural **(-)-7**: $[\alpha]_{\text{D}}^{25} -159^\circ$ (*c* 0.4, MeOH); synthetic **(-)-7**: $[\alpha]_{\text{D}}^{23} -148^\circ$ (*c* 0.2, MeOH)).^{30b}

Scheme 3.4.8



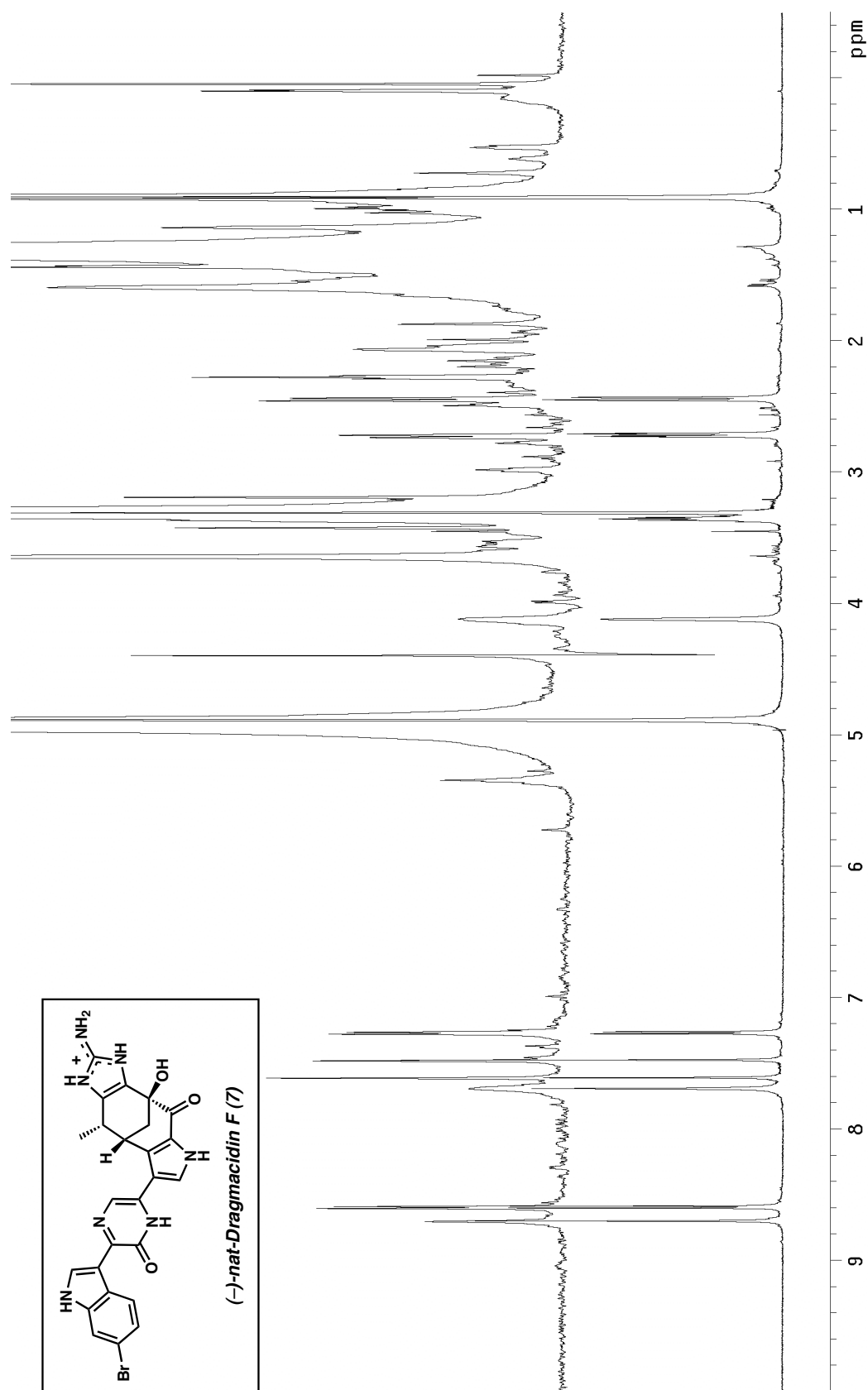


Figure 3.4.2 ^1H NMR (600 MHz, CD_3OD) of *(-)-dragmacidin F (7)*; natural (top) and synthetic (bottom).

3.5 Conclusion

In summary, we have developed an enantiodivergent strategy to access both antipodes of dragmacidin F (**7**) from a single enantiomer of readily available (–)-quinic acid (**101**). Our highly efficient syntheses provide (+)-**7** in 7.8% overall yield and (–)-**7** in 9.3% overall yield beginning from **101**. The routes that we have developed to (+)- and (–)-**7** are concise and feature a number of key transformations, namely: a) highly efficient functionalizations of (–)-**101** to differentiate C(3) and C(5), b) novel reductive isomerization reactions, c) sterically demanding Pd(II)-mediated oxidative carbocyclizations, d) halogen-selective Suzuki cross-coupling reactions, and e) high-yielding late-stage Neber rearrangements. Advanced biological testing of both synthetic antipodes of dragmacidin F is currently underway.

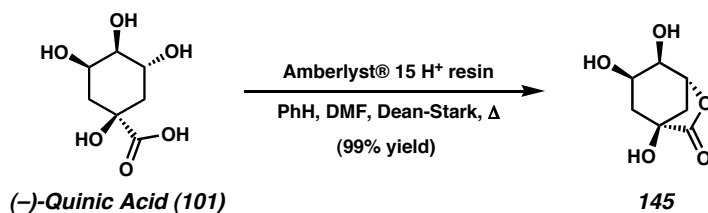
3.6 Experimental Section

3.6.1 Materials and Methods

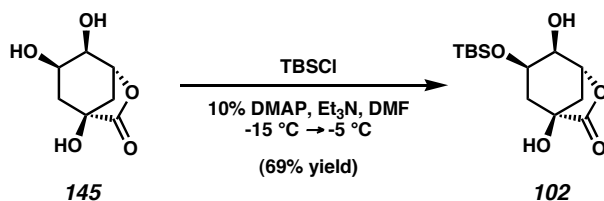
Unless stated otherwise, reactions were conducted in flame-dried glassware under an atmosphere of nitrogen using anhydrous solvents (either freshly distilled or passed through activated alumina columns). All commercially obtained reagents were used as received. Reaction temperatures were controlled using an IKAmag temperature modulator. Thin-layer chromatography (TLC) was conducted with E. Merck silica gel 60 F254 pre-coated plates (0.25 mm) and visualized using a combination of UV, anisaldehyde, ceric ammonium molybdate, and potassium permanganate staining. ICN silica gel (particle size 0.032-0.063 mm) was used for flash column chromatography. Disposable Sep-Pak C₁₈ Vac Cartridges were purchased from Waters and used for all reversed-phase filtrations. HPLC analysis was performed on a Beckman Gold system using a Rainin C₁₈, Microsorb MV, 5 μ m, 300 x 4.6 mm reversed-phased column in 0.1% (w/v) TFA with acetonitrile/H₂O as eluent and a flow rate of 1.0 mL/min, gradient elution of 1.25% acetonitrile/min. Preparatory reversed-phase HPLC was performed on a Beckman HPLC with a Waters DeltaPak 25 x 100 mm, 100 μ m C₁₈ column equipped with a guard, 0.1% (w/v) TFA with acetonitrile/H₂O as eluent, and gradient elution of 0.50% acetonitrile/min. For all reversed-phase purifications, H₂O (18M Ω) was obtained from a Millipore MiliQ water purification system and TFA from Halocarbon, Inc. ¹H NMR spectra were recorded on a Varian Mercury 300 (at 300 MHz), a Varian Inova 500 (at 500 MHz), or a Varian Inova 600 (at 600 MHz) and are reported relative to Me₄Si (δ 0.0). Data for ¹H NMR spectra are reported as follows: chemical shift (δ ppm), multiplicity, coupling constant (Hz), and integration. ¹³C NMR spectra were recorded on

a Varian Mercury 300 (at 75 MHz), or a Varian Inova 500 (at 125 MHz) and are reported relative to Me₄Si (δ 0.0). Data for ¹³C NMR spectra are reported in terms of chemical shift. IR spectra were recorded on a Perkin Elmer Paragon 1000 spectrometer and are reported in frequency of absorption (cm⁻¹). Optical rotations were measured with a Jasco P-1010 polarimeter. High resolution mass spectra were obtained from the California Institute of Technology Mass Spectral Facility.

3.6.2 Preparative Procedures

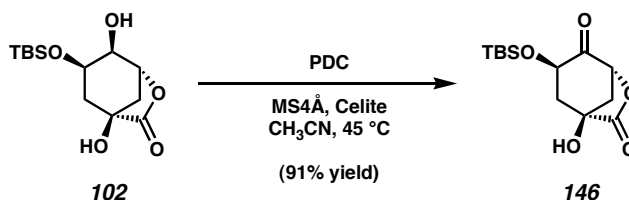


Lactone 145. A mixture of D-(–)-quinic acid (**101**) (50.0 g, 260.2 mmol), Amberlyst® 15 ion-exchange resin (7 g, 35 mmol), benzene (500 mL), and DMF (125 mL) was refluxed under a Dean-Stark trap for 16 h. The reaction mixture was cooled to 23 °C and filtered over a pad of Celite. The filtrate was then evaporated under reduced pressure to afford a thick oil, which was diluted with CH₂Cl₂ (150 mL). Hexanes (250 mL) was added and the resulting mixture was allowed to sit at 23 °C for 2 h. The product was collected by vacuum filtration and was further dried in vacuo to afford lactone **145** (44.9 g, 99% yield) as a white powder. *R_f* 0.40 (3:1 EtOAc:acetone); characterization data for this compound have been previously reported.^{7a}



TBS Lactone 102. To a mixture of lactone **145** (90.0 g, 517 mmol), DMAP (6.31 g, 51.7 mmol), triethylamine (90 mL, 646 mmol), and DMF (345 mL) at –15 °C was added TBSCl (84.9 g, 563 mmol) in 3 equal portions over 30 min. The temperature was maintained between –20 °C and –15 °C during the addition. The reaction mixture was

allowed to warm to $-5\text{ }^{\circ}\text{C}$ over 3 h, quenched by the addition of 5% aq. citric acid (120 mL), and then warmed to $23\text{ }^{\circ}\text{C}$. The solvent was removed in vacuo, and the crude product was diluted with 5% aq. citric acid (350 mL) and extracted with Et_2O (1 x 500 mL, 2 x 400 mL). The combined organic layers were washed with H_2O (2 x 400 mL) and brine (400 mL), dried over MgSO_4 , and evaporated under reduced pressure. The product was triturated with hexanes (750 mL) and collected by vacuum filtration. It was further dried under vacuum to afford TBS lactone **102** (102.8 g, 69% yield) as a dry white solid. R_f 0.48 (1:1 hexanes:EtOAc); R_f 0.28 (2:1 Et_2O :hexanes); characterization data for this compound have been previously reported.^{7b}

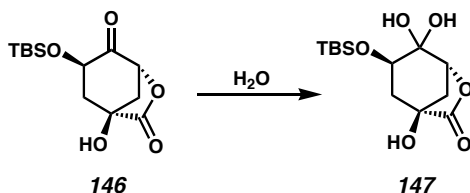


Keto Lactone 146. A mixture of TBS lactone **102** (3.72 g, 12.90 mmol), powdered 4\AA activated molecular sieves (2.79 g), Celite (2.79 g), pyridinium dichromate (12.13 g, 32.2 mmol), and acetonitrile (185 mL) was heated to $45\text{ }^{\circ}\text{C}$ for 24 h. The reaction was allowed to cool to $23\text{ }^{\circ}\text{C}$, and then was filtered over a plug of silica gel topped with Celite (EtOAc eluent). The solvent was removed under reduced pressure to afford a brown oil, which was further purified by passage over a plug of silica gel (1:1 hexanes:EtOAc). Evaporating the solvent in vacuo afforded keto lactone **146** (3.35 g, 91% yield) as a pale yellow oil.

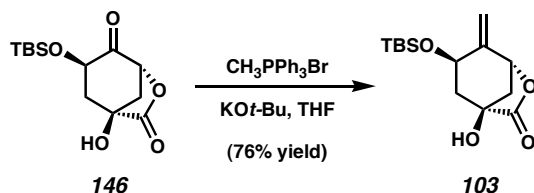
Alternate Procedure. Powdered 4\AA activated molecular sieves (184.6 g) were agitated and flame-dried under vacuum for approximately 30 min until a fine, powder-

like consistency was obtained. Upon cooling to 23 °C, CH₂Cl₂ (540 mL) was introduced, and the slurry was cooled to 0 °C. Freshly prepared pyridinium dichromate⁴⁹ (148.7 g, 395.3 mmol) was added, and the resulting heterogeneous orange mixture was treated with TBS lactone **102** (70.04 g, 242.8 mmol) portionwise over 4 min. After the addition was complete, the reaction was stirred for 5 min and then freshly distilled AcOH (49.0 mL, 856.0 mmol) was added dropwise over a 20 min period. The reaction temperature was maintained at 0 °C for 15 min after the addition was complete, and the mixture was then stirred at 23 °C. After 10 h, the reaction was judged complete by ¹H NMR. The dark mixture was evenly divided into 3 portions, each of which was filtered over a pad of silica gel (10 cm diameter x 7.5 cm height, EtOAc eluent). The filtrates were combined and evaporated in vacuo to afford a dark liquid, and this residue was further coevaporated with toluene (3 x 150 mL). The crude product was diluted in a mixture of hexanes:EtOAc (10:1; 250 mL) and filtered over a pad of powdered Na₂SO₄ to remove insoluble impurities. The filtrate was evaporated, and dried in vacuo, to afford keto lactone **146** (55.27 g, 80% yield) as a brown, waxy solid. This material was used immediately in the next step without further purification. *Unstable to TLC conditions*; ¹H NMR (300 MHz, CDCl₃): δ 4.71 (d, *J* = 6.6 Hz, 1H), 4.52 (dd, *J* = 10.3 Hz, 8.9 Hz, 1H), 2.95 (s, 1H), 2.88-2.79 (m, 1H), 2.57-2.47 (m, 1H), 2.39 (d, *J* = 12.4 Hz, 1H), 2.13 (dd, *J* = 12.4 Hz, 10.5 Hz, 1H), 0.88 (s, 9H), 0.11 (s, 3H), 0.02 (s, 3H); ¹³C NMR (75 MHz, CDCl₃): δ 202.6, 177.4, 79.0, 72.0, 70.6, 43.2, 42.6, 25.8 (3C), 18.5, -4.6, -5.3; IR (film): 3444 (br), 2931, 2858, 1799, 1753, 1254, 1144, 1111 cm⁻¹; HRMS-FAB (*m/z*): [M + H]⁺ calc'd for C₁₃H₂₃O₅Si, 287.1315; found, 287.1316; [α]_D¹⁹ -96.47° (*c* 1.0, C₆H₆).

*NOTE: Exposure of keto lactone **146** to water (e.g., aqueous workup, or prolonged exposure to silica gel) led to the formation of hydrate **147**, as a white powder.*



Unstable to TLC conditions; mp 104-6 °C; ^1H NMR (300 MHz, CD_3OD): δ 4.46 (d, J = 5.8 Hz, 1H), 3.75 (dd, J = 10.7 Hz, 7.0 Hz, 1H), 2.48-2.31 (comp. m, 2H), 2.10-2.00 (m, 1H), 1.76 (app. t, J = 11.4 Hz, 1H), 0.93 (s, 9H), 0.14 (s, 3H), 0.12 (s, 3H); ^{13}C NMR (75 MHz, CD_3OD): δ 179.4, 93.2, 81.8, 73.0, 72.3, 41.5, 40.9, 26.5 (3C), 19.1, -4.3, -4.7; IR (KBr): 3440 (br), 3374 (br), 2929, 2858, 1782, 1256, 1108, 1070 cm^{-1} ; HRMS-CI (m/z): $[\text{M} + \text{H}]^+$ calc'd for $\text{C}_{13}\text{H}_{24}\text{O}_6\text{Si}$, 304.1342; found, 304.1336; $[\alpha]_{\text{D}}^{19}$ -54.29° (c 1.0, MeOH).

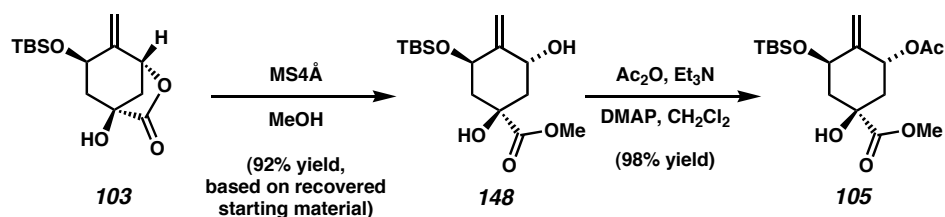


Methylene Lactone 103. To $\text{CH}_3\text{PPh}_3\text{Br}$ (105 mg, 0.293 mmol) in THF (2.8 mL) at 0 °C was added potassium *t*-butoxide (31.3 mg, 0.279 mmol). The mixture was warmed to 23 °C and stirred for an additional 10 min. Keto lactone **146** (40 mg, 0.140 mmol) in THF (1 mL) was added and stirring was continued at 23 °C for 15 min. The reaction mixture was then refluxed for 2 h and cooled to 23 °C. The solvent was removed under reduced pressure, and the residue was partitioned between Et_2O (3 mL)

and brine (1.5 mL). The layers were separated, and the aqueous layer was further extracted with Et₂O (3 x 1 mL). The combined organic layers were washed with brine (1.5 mL), dried by passage over a plug of silica gel (Et₂O eluent, then 2:1 hexanes:EtOAc eluent), and evaporated under reduced pressure. The crude product was purified by flash chromatography (2:1 hexanes:EtOAc) to afford methylene lactone **103** (30 mg, 76% yield) as a white solid.

Alternate Procedure. To CH₃PPh₃Br (82.9 g, 232.1 mmol) in THF (1.10 L) at 23 °C was added potassium *t*-butoxide (23.8 g, 212.1 mmol) in one portion. The mixture was stirred for 2 h, then cooled to 0 °C. Keto lactone **146** (54.5 g, 190.3 mmol) in THF (240 mL) was added dropwise over a 30 min period. The reaction was allowed to warm slowly to 23 °C over 9 h, then quenched by the addition of ice-cold 15% aq. NH₄Cl (500 mL). The solvent was evaporated under reduced pressure, and the residue was partitioned between Et₂O (500 mL) and H₂O (100 mL). The aqueous phase was extracted with Et₂O (3 x 250 mL), and the combined organics were washed with H₂O (100 mL) and brine (100 mL) and dried over MgSO₄. Evaporation of the solvent afforded a crude yellow oil, which was filtered over a plug of silica gel (4:1 pentane:Et₂O → 3:2 pentane:Et₂O eluent). After evaporating the solvent in vacuo, the residue was triturated with ice-cold pentane (40 mL). The white solid was filtered and washed with ice-cold pentane (2 x 2 mL). A second crop was collected from the filtrate after concentrating its volume to 15 mL. Drying the collected material in vacuo afforded methylene lactone **103** (22.1 g, 41% yield) as a white solid. *R*_f 0.59 (1:1 hexanes:EtOAc); mp 87-88 °C; ¹H NMR (300 MHz, CDCl₃): δ 5.25-5.23 (m, 1H), 5.13-5.10 (m, 1H), 5.07 (d, *J* = 6.0 Hz, 1H), 4.38-4.29 (m, 1H), 2.85 (s, 1H), 2.67-2.59 (m, 1H), 2.31-2.21 (m, 1H), 2.09 (d, *J* =

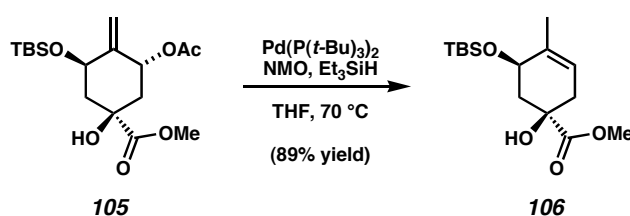
11.5 Hz, 1H), 1.86 (app. t, $J = 11.3$ Hz, 1H), 0.89 (s, 9H), 0.06 (s, 6H); ^{13}C NMR (75 MHz, CDCl_3): δ 178.1, 144.8, 111.0, 79.4, 73.1, 67.1, 44.7, 44.7, 26.0 (3C), 18.5, -4.5, -4.7; IR (film): 3426 (br), 2956, 2931, 2858, 1791, 1254, 1120, 1071 cm^{-1} ; HRMS-FAB (m/z): $[\text{M} + \text{H}]^+$ calc'd for $\text{C}_{14}\text{H}_{25}\text{O}_4\text{Si}$, 285.1522; found, 285.1519; $[\alpha]_D^{19}$ -101.71° (c 1.0, CHCl_3).



Methyl Ester 105. To lactone **103** (420 mg, 1.477 mmol) and activated oven-dried 4Å molecular sieves (100 mg) was added MeOH (15 mL). The reaction mixture was stirred at 23 °C for 5.5 h, then filtered over a short plug of Celite (EtOAc eluent). After evaporation of the reaction mixture under reduced pressure, the residue was purified by flash column chromatography (2:1 hexanes:EtOAc eluent) to afford starting material lactone **103** (82 mg, 20% yield) and siloxy diol **148** (345 mg, 74% yield, 92% yield based on recovered starting material), which was used directly in the subsequent reaction.

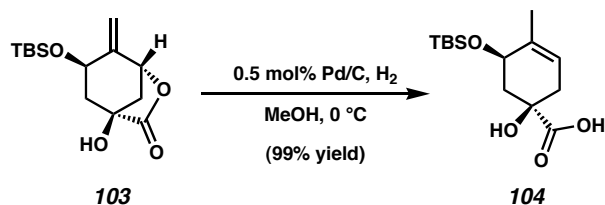
To siloxy diol **148** (80.0 mg, 0.253 mmol) in CH_2Cl_2 (1.5 mL) was added Et_3N (71 μL , 0.506 mmol), DMAP (3 mg, 0.0253 mmol), followed by Ac_2O (31 μL , 0.329 mmol). The reaction mixture was stirred at 23 °C for 10 min, quenched with saturated aq. NaHCO_3 (5 mL), and extracted with CH_2Cl_2 (3 x 15 mL). The combined organic layers were filtered over a plug of silica gel (CH_2Cl_2 eluent, then EtOAc eluent) and evaporated under reduced pressure. The crude product was purified by flash

chromatography (3:1 hexanes:EtOAc eluent) to afford methyl ester **105** (89.0 mg, 98% yield) as a colorless oil. R_f 0.50 (1:1 hexanes:EtOAc); ^1H NMR (300 MHz, CDCl_3): δ 5.90-5.81 (m, 1H), 4.96 (br s, 1H), 4.94 (br s, 1H), 4.91-4.89 (m, 1H), 4.67 (app. t, J = 3.2 Hz, 1H), 3.74 (s, 3H), 2.38 (ddd, J = 12.7, 5.2, 2.2 Hz, 1H), 2.19-2.03 (comp. m, 2H), 2.09 (s, 3H), 1.93 (app. t, J = 12.1 Hz, 1H), 0.87 (s, 9H), 0.09 (s, 3H), 0.08 (s, 3H); ^{13}C NMR (75 MHz, CDCl_3): δ 173.7, 169.6, 146.3, 108.5, 76.5, 75.1, 68.0, 52.9, 42.7, 41.2, 25.8 (3C), 21.1, 18.1, -4.6, -5.2; IR (film) 3464 (br), 2954, 2932, 2858, 2888, 1739 (br), 1369, 1233 (br), 1124, 1098, 1072, 1036 cm^{-1} ; HRMS-FAB (m/z): $[\text{M} + \text{H}]^+$ calc'd for $\text{C}_{17}\text{H}_{31}\text{O}_6\text{Si}$, 359.1890; found, 359.1900; $[\alpha]_D^{26}$ -26.61° (c 1.0, C_6H_6).



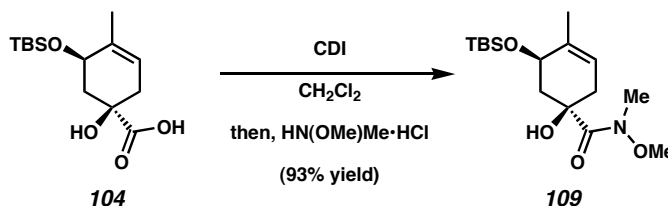
Siloxycyclohexene 106. Methyl ester **105** (94 mg, 0.262 mmol), $\text{Pd(P}(t\text{-Bu)}_3)_2$ (40.2 mg, 0.0786 mmol), anhydrous *N*-methylmorpholine *N*-oxide (307 mg, 2.52 mmol), THF (5.2 mL), and freshly distilled Et_3SiH (1.67 mL, 10.5 mmol) were combined under a glovebox atmosphere. The reaction mixture was immediately removed from the glovebox and placed in a 70 °C oil bath. After 3.5 h, the reaction mixture was cooled to 0 °C, and the volatiles were removed under reduced pressure. Saturated aq. NH_4Cl (15 mL) was added, and the mixture was extracted with Et_2O (3 x 25 mL). The combined organic layers were washed with brine (15 mL), dried over MgSO_4 , and evaporated under reduced pressure. The crude product was purified by flash chromatography (5:1 hexanes:EtOAc eluent) to afford siloxycyclohexene **106** (70 mg, 89% yield) as a pale

yellow oil. R_f 0.55 (2:1 hexanes:EtOAc); ^1H NMR (300 MHz, CDCl_3): δ 5.49-5.42 (m, 1H), 4.62 (s, 1H), 4.18-4.12 (m, 1H), 3.76 (s, 3H), 2.45-2.38 (comp. m, 2H), 2.16-2.10 (comp. m, 2H), 1.79-1.74 (m, 3H), 0.88 (s, 9H), 0.13 (s, 3H), 0.12 (s, 3H); ^{13}C NMR (75 MHz, CDCl_3): δ 175.3, 133.7, 120.9, 73.0, 68.7, 52.6, 38.4, 36.9, 25.9 (3C), 21.4, 18.0, -4.3, -4.7; IR (film) 3478 (br), 2955, 2858, 1740, 1451, 1253, 1217, 1111, 1065, 1037 cm^{-1} ; HRMS-FAB (m/z): $[\text{M} + \text{H}]^+$ calc'd for $\text{C}_{15}\text{H}_{19}\text{O}_4\text{Si}$, 301.1835; found, 301.1835; $[\alpha]_D^{24} +77.62^\circ$ (c 0.47, CHCl_3).

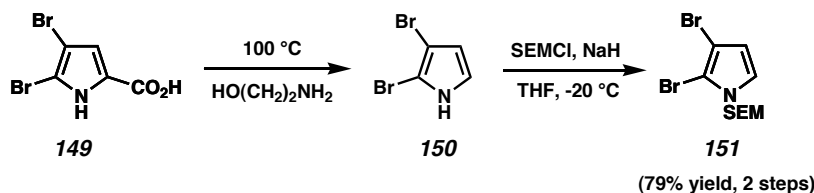


Acid 104. A mixture of methylene lactone **103** (4.0 g, 14.1 mmol) and 10% Pd/C (80 mg, 0.075 mmol) in methanol (120 mL) was cooled to 0 °C. The reaction vessel was evacuated and back-filled with H_2 (3x). After 7 h at 0 °C, the mixture was filtered over a pad of Celite (MeOH eluent), and the solvent was evaporated under reduced pressure to afford a colorless oil. Residual solvent was removed by holding the crude product under vacuum for 10 h, providing acid **104** (4.0 g, 99% yield), which was used immediately without further purification. R_f 0.28 (1:1 hexanes:EtOAc;1% acetic acid); ^1H NMR (300 MHz, CDCl_3): δ 5.88 (s, 1H), 5.53-5.48 (m, 1H), 4.16-4.11 (m, 1H), 2.71-2.60 (m, 1H), 2.36-2.22 (m, 1H), 2.18 (dd, $J = 14.3$ Hz, 3.9 Hz, 1H), 2.08-2.01 (m, 1H), 1.79-1.76 (m, 3H), 0.89 (s, 9H), 0.15-0.13 (comp. m, 6H); ^{13}C NMR (75 MHz, CDCl_3): δ 176.4, 133.2, 121.1, 73.6, 68.6, 37.9, 35.9, 25.8 (3C), 21.4, 18.0, -4.5, -4.7; IR (film): 3356 (br), 2956,

2931, 2858, 1768 (br), 1718 (br), 1255, 1063 cm^{-1} ; HRMS-FAB (m/z): $[\text{M} + \text{H}]^+$ calc'd for $\text{C}_{14}\text{H}_{27}\text{O}_4\text{Si}$, 287.1679; found, 287.1675; $[\alpha]_D^{19} +37.58^\circ$ (c 1.0, C_6H_6).



Weinreb Amide 109. To acid **104** (4.0 g, 14.1 mmol) in CH_2Cl_2 (70 mL) at 23 $^\circ\text{C}$ was added 1,1'-carbonyldiimidazole (3.65 g, 22.5 mmol) in equal portions over 15 min. After the final addition, stirring was continued for 10 min, then *N,O*-dimethylhydroxylamine \cdot HCl (3.43 g, 35.16 mmol) was added in one portion. The reaction was allowed to stir at 23 $^\circ\text{C}$ for 3 h. Et_2O was added (50 mL), and the reaction mixture was filtered. The filtrate was evaporated, diluted with Et_2O (125 mL), washed with 5% aq. citric acid (2 x 50 mL) and brine (50 mL), and dried over MgSO_4 . The crude product was purified by flash chromatography (3:1 hexanes: EtOAc) to afford Weinreb amide **109** (4.29 g, 93% yield) as a colorless oil. R_f 0.42 (2:1 hexanes: EtOAc); ^1H NMR (300 MHz, CDCl_3): δ 5.43 (m, 1H), 4.72 (s, 1H), 4.17-4.11 (m, 1H), 3.71 (s, 3H), 3.22 (s, 3H), 2.59-2.24 (comp. m, 3H), 2.03 (dd, $J = 14.6$ Hz, 4.1 Hz, 1H), 1.75-1.71 (m, 3H), 0.86 (s, 9H), 0.11 (s, 3H), 0.09 (s, 3H); ^{13}C NMR (75 MHz, CDCl_3 , 15/16 $^\circ\text{C}$): δ 133.5, 121.5, 74.3, 69.4, 61.2, 38.1, 35.9, 26.0, 25.9 (3C), 21.3, 18.1, -4.3, -4.7; IR (film): 3463 (br), 2956, 2932, 2858, 1655, 1362, 1254 cm^{-1} ; HRMS-EI (m/z): $[\text{M} + \text{H}]^+$ calc'd for $\text{C}_{16}\text{H}_{32}\text{NO}_4\text{Si}$, 330.2101; found, 330.2085; $[\alpha]_D^{19} +41.13^\circ$ (c 1.0, CHCl_3).

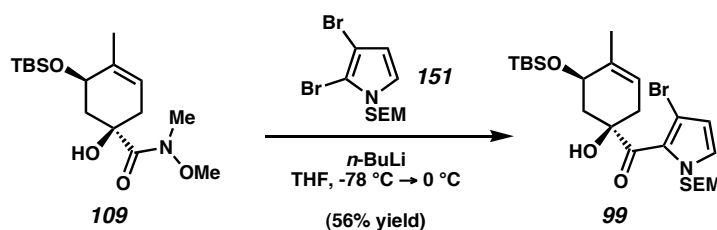


Dibromopyrrole 151. A solution of 4,5-dibromopyrrole carboxylic acid (**149**)⁵⁰ (6.05 g, 22.5 mmol) in ethanolamine (36 mL) was heated to $100\text{ }^\circ\text{C}$ for 2 h, cooled to $23\text{ }^\circ\text{C}$, and poured into a mixture of Et_2O (200 mL) and 0.5 N aq. HCl (300 mL). The layers were separated, and the aqueous layer was extracted with Et_2O (2 x 250 mL). The combined organic layers were washed with brine (200 mL), dried over MgSO_4 , and concentrated to 100 mL. The solution was diluted with hexanes (100 mL), filtered over a plug of silica gel (2:1 hexanes: Et_2O), and concentrated to 150 mL. THF (100 mL) was added, and the solution was concentrated to 100 mL. This solvent exchange procedure was repeated 2 additional times (2 x 100 mL THF) to afford 2,3-dibromopyrrole (**150**) as a solution in THF, which was used immediately in the subsequent reaction.

*CAUTION: Concentrating the above described solutions to dryness or near-dryness leads to rapid decomposition of 2,3-dibromopyrrole (**150**).²²*

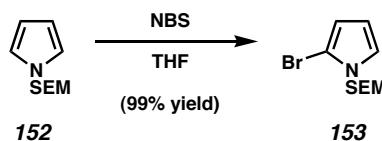
To 2,3-dibromopyrrole (**150**) in THF at $-20\text{ }^\circ\text{C}$ was added NaH (60% dispersion in mineral oil, 1.51 g, 37.8 mmol) in 3 equal portions over 3 min. After 10 min at $-20\text{ }^\circ\text{C}$, SEMCl (4.8 mL, 27.1 mmol) was added dropwise over 1 min. The reaction mixture was allowed to warm to $-8\text{ }^\circ\text{C}$ over 40 min and was then quenched with saturated aq. NH_4Cl (30 mL). After warming to $23\text{ }^\circ\text{C}$, the reaction mixture was diluted with Et_2O (75 mL) and H_2O (20 mL), and the layers were separated. The aqueous layer was further extracted with Et_2O (2 x 50 mL). The combined organic layers were washed with brine

(50 mL), dried over MgSO_4 , and evaporated under reduced pressure. The crude product was purified by flash chromatography (6:1 hexanes: CH_2Cl_2 , then 4:1 hexanes: CH_2Cl_2) to afford dibromopyrrole **151** (6.25 g, 79% yield) as a yellow oil. R_f 0.17 (6:1 hexanes: CH_2Cl_2); ^1H NMR (300 MHz, CDCl_3): δ 6.82 (d, J = 3.6 Hz, 1H), 6.25 (d, J = 3.3 Hz, 1H), 5.21 (s, 2H), 3.48 (t, J = 8.1 Hz, 2H), 0.88 (t, J = 8.1 Hz, 2H), -0.03 (s, 9H); ^{13}C NMR (75 MHz, CDCl_3): δ 123.1, 112.3, 103.7, 99.8, 77.8, 66.2, 17.9, -1.2 (3C); IR (film): 2953, 2896, 1514, 1470, 1279, 1250, 1109, 1084 cm^{-1} ; HRMS-EI (m/z): $[\text{M} + \text{H}]^+$ calc'd for $\text{C}_{10}\text{H}_{17}\text{NOSiBr}_2$, 352.9446; found, 352.9435.



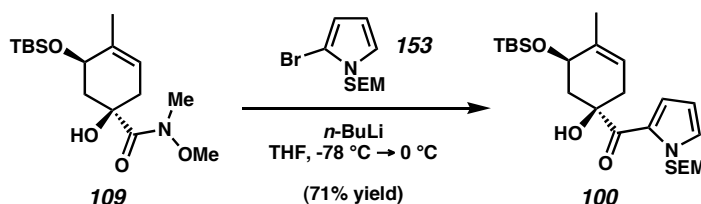
Bromo Acyl Pyrrole 99. To dibromopyrrole **151** (6.02 g, 17.06 mmol) in THF (114 mL) at $-78\text{ }^{\circ}\text{C}$ was added $n\text{-BuLi}$ (2.5 M in hexanes, 6.7 mL, 16.8 mmol) dropwise over 1 min. After 10 min at $-78\text{ }^{\circ}\text{C}$, Weinreb amide **109** (1.58 g, 4.80 mmol) in THF (15 mL) was added dropwise over 30 seconds. The reaction vessel was immediately warmed to $0\text{ }^{\circ}\text{C}$, stirred for 90 min, and cooled to $-78\text{ }^{\circ}\text{C}$. The reaction was quenched with saturated aq. NH_4Cl (15 mL), then warmed to $23\text{ }^{\circ}\text{C}$. The volatiles were removed in vacuo, and the residue was partitioned between Et_2O (75 mL) and H_2O (30 mL). The layers were separated, and the aqueous layer was further extracted with Et_2O (2 x 50 mL). The combined organic layers were washed with brine (50 mL), dried over MgSO_4 , and evaporated under reduced pressure. The crude product was purified by flash chromatography (11:9 CH_2Cl_2 :hexanes) to afford bromo acyl pyrrole **99** (1.47 g, 56%

yield) as a colorless oil. R_f 0.29 (11:9 hexanes: CH_2Cl_2); ^1H NMR (300 MHz, CDCl_3): δ 6.77 (d, $J = 2.9$ Hz, 1H), 6.20 (d, $J = 2.7$ Hz, 1H), 5.53-5.47 (m, 1H), 5.35 (d, $J = 10.4$ Hz, 1H), 5.29 (d, $J = 10.4$ Hz, 1H), 4.72 (s, 1H), 4.18-4.14 (m, 1H), 3.31 (t, $J = 8.2$ Hz, 2H), 2.65-2.53 (m, 1H), 2.53-2.41 (m, 1H), 2.32 (dt, $J = 14.3$ Hz, 1.7 Hz, 1H), 2.15 (dd, $J = 14.2$ Hz, 4 Hz, 1H), 1.79-1.76 (m, 3H), 0.87 (s, 9H), 0.81 (t, $J = 8.2$ Hz, 2H), 0.12 (s, 6H), -0.06 (s, 9H); ^{13}C NMR (75 MHz, CDCl_3): δ 201.9, 133.2, 129.6, 125.0, 121.6, 112.5, 101.8, 78.9, 78.6, 68.9, 66.2, 38.6, 37.4, 26.0 (3C), 21.5, 18.1, 17.8, -1.2 (3C), -4.1, -4.7; IR (film): 3477 (br), 2953, 1664 (br), 1400, 1253, 1101 cm^{-1} ; HRMS-EI (m/z): $[\text{M} + \text{H}]^+$ calc'd for $\text{C}_{24}\text{H}_{43}\text{NO}_4\text{Si}_2\text{Br}$, 544.1914; found, 544.1903; $[\alpha]_D^{19} +1.64^\circ$ (c 1.0, CHCl_3).



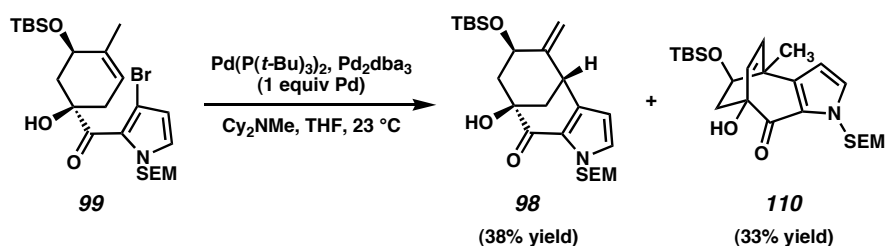
Bromopyrrole 153. To SEM pyrrole **152**¹⁴ (1.25 g, 6.33 mmol) in THF (125 mL) at 23 °C was added freshly recrystallized NBS (1.127 g, 6.33 mmol) in one portion. After stirring for 5 min, additional NBS was added (15 mg, 0.084 mmol), and the reaction was immediately judged complete by TLC. The reaction mixture was poured into saturated aq. NaHCO_3 (100 mL) and extracted with Et_2O (1 x 100 mL, 2 x 50 mL). The combined organic layers were washed with brine (75 mL), dried over MgSO_4 , and evaporated under reduced pressure. The crude product was purified by passage over a plug of silica gel (CH_2Cl_2 eluent) to afford bromopyrrole **153** (1.73 g, 99% yield) as a pale yellow oil. R_f 0.53 (1:1 CH_2Cl_2 :hexanes); ^1H NMR (300 MHz, CDCl_3): δ 6.83 (app. t, $J = 2.5$ Hz, 1H), 6.18-6.16 (comp. m, 2H), 5.22 (s, 2H), 3.53-3.46 (m, 2H), 0.92-0.85

(m, 2H), -0.03 (s, 9H); ^{13}C NMR (75 MHz, CDCl_3): δ 122.9, 111.9, 110.1, 102.0, 76.7, 66.0, 17.9, -1.2 (3C); IR (film): 2953, 2895, 1264, 1249, 1108, 1085 cm^{-1} ; HRMS-EI (m/z): $[\text{M} + \text{H}]^+$ calc'd for $\text{C}_{10}\text{H}_{18}\text{NOSiBr}$, 275.0341; found, 275.0331.



Acyl Pyrrole 100. To bromopyrrole **153** (1.73 g, 6.26 mmol) in THF (42 mL) at $-78\text{ }^{\circ}\text{C}$ was added $n\text{-BuLi}$ (2.25 M in hexanes, 2.7 mL, 6.16 mmol) dropwise over 1 min. After 10 min at $-78\text{ }^{\circ}\text{C}$, Weinreb amide **109** (655 mg, 1.99 mmol) in THF (5 mL) was added dropwise over 1 min. The reaction vessel was immediately warmed to $0\text{ }^{\circ}\text{C}$, stirred for 25 min, and cooled to $-78\text{ }^{\circ}\text{C}$. The reaction mixture was quenched with saturated aq. NH_4Cl (10 mL), then warmed to $23\text{ }^{\circ}\text{C}$. The volatiles were removed under reduced pressure. The residue was partitioned between Et_2O (75 mL) and H_2O (50 mL), and the layers were separated. The aqueous layer was further extracted with Et_2O (2 x 40 mL). The combined organic layers were washed with brine (50 mL), dried over MgSO_4 , and evaporated under reduced pressure. The crude product was purified by flash chromatography (23:1 hexanes: EtOAc , then 15:1 hexanes: EtOAc) to afford acyl pyrrole **100** (656 mg, 71% yield) as a colorless oil. R_f 0.30 (9:1 hexanes: EtOAc); ^1H NMR (300 MHz, CDCl_3): δ 7.66 (dd, $J = 4.0\text{ Hz}$, 1.7 Hz , 1H), 7.06 (dd, $J = 2.5\text{ Hz}$, 1.7 Hz , 1H), 6.19 (dd, $J = 4.0\text{ Hz}$, 2.5 Hz , 1H), 5.71 (d, $J = 10.4\text{ Hz}$, 1H), 5.67 (d, $J = 10.0\text{ Hz}$, 1H), 5.52-5.47 (m, 1H), 4.90 (s, 1H), 4.19 (app. t, $J = 3.1\text{ Hz}$, 1H), 3.51 (t, $J = 8.3\text{ Hz}$, 2H), 2.52-2.46 (comp. m, 2H), 2.19-2.16 (comp. m, 2H), 1.80-1.78 (m, 3H), 0.92-0.88 (comp. m,

11H), 0.13 (s, 6H), -0.06 (s, 9H); ^{13}C NMR (75 MHz, CDCl_3 , 22/24 °C): δ 193.7, 133.5, 129.9, 128.0, 123.8, 121.7, 109.0, 78.2, 69.4, 66.3, 38.6, 38.3, 26.0 (3C), 21.5, 18.1, -1.2 (3C), -4.2, -4.7; IR (film): 3476, 2954, 2931, 2859, 1639, 1412, 1310, 1251, 1085 cm^{-1} ; HRMS-EI (m/z): $[\text{M} + \text{H}]^+$ calc'd for $\text{C}_{24}\text{H}_{44}\text{NO}_4\text{Si}_2$, 466.2809; found, 466.2822; $[\alpha]_{\text{D}}^{19}$ +34.25° (c 1.0, C_6H_6).



[3.3.1] Bicycle 98. Bromo acyl pyrrole **99** (52.0 mg, 0.0955 mmol), Pd_2dba_3 (21.9 mg, 0.0239 mmol), $\text{Pd}(\text{P}(t\text{-Bu})_3)_2$ (24.4 mg, 0.0477 mmol), THF (1.2 mL), and Cy_2NMe (24.3 μL , 0.115 mmol) were combined under a glovebox atmosphere and stirred at 23 °C for 10 h. The reaction vessel was removed from the glovebox, diluted with 3:1 hexanes:EtOAc (2 mL), and filtered over a plug of silica gel topped with Celite (3:1 hexanes:EtOAc eluent). The solvent was removed under reduced pressure, and the residue was purified by flash chromatography (CH_2Cl_2 , then 3:1 hexanes:EtOAc). The crude product was further purified by flash chromatography (6:1 hexanes:EtOAc) to afford [3.3.1] bicycle **98** (16.7 mg, 38% yield) and [3.2.2] bicycle **110** (14.4 mg, 33% yield), both as pale yellow oils.

[3.3.1] Bicycle 98: R_f 0.20 (4:1 hexanes:EtOAc); ^1H NMR (300 MHz, CDCl_3): δ 7.07 (d, $J = 2.7$ Hz, 1H), 6.05 (d, $J = 2.7$ Hz, 1H), 5.71 (d, $J = 9.9$ Hz, 1H), 5.58 (d, $J = 9.9$ Hz, 1H), 5.09-5.05 (m, 2H), 4.00 (s, 1H), 3.99-3.90 (m, 1H), 3.84 (app. t, $J = 3.0$ Hz, 1H),

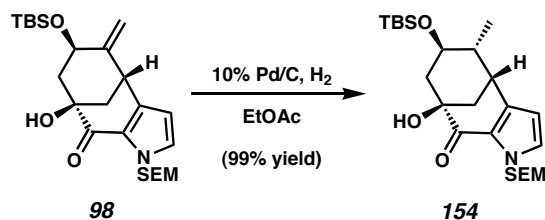
3.55-3.47 (m, 2H), 2.39 (app. dt, $J = 7.4$ Hz, 3.8 Hz, 1H), 2.13-2.03 (comp. m, 2H), 1.73 (app. t, $J = 11.8$ Hz, 1H), 0.98-0.76 (comp. m, 11H), -0.04 (s, 9H), -0.11 (s, 6H); ^1H NMR (300 MHz, C_6D_6): δ 6.53 (d, $J = 2.5$ Hz, 1H), 5.77 (d, $J = 2.8$ Hz, 1H), 5.55 (d, $J = 10.2$ Hz, 1H), 5.32 (app. t, $J = 1.9$ Hz, 1H), 5.26 (d, $J = 10.2$ Hz, 1H), 5.01-4.97 (m, 1H), 4.29 (s, 1H), 4.27-4.19 (m, 1H), 3.59-3.47 (comp. m, 3H), 2.45-2.31 (comp. m, 2H), 2.16 (dd, $J = 12.1$ Hz, 3.0 Hz, 1H), 2.07 (app. t, $J = 11.8$ Hz, 1H), 0.92-0.89 (comp. m, 11H), 0.01 (s, 9H), -0.06 (s, 3H), -0.07 (s, 3H); ^{13}C NMR (75 MHz, C_6D_6): δ 191.5, 149.4, 141.8, 132.0, 125.5, 108.5, 107.4, 76.8, 75.8, 68.4, 66.3, 48.9, 45.5, 40.7, 26.3 (3C), 18.8, 18.2, -0.8 (3C), -4.4, -4.7; IR (film): 3480, 2953, 2858, 1651, 1420, 1318, 1251, 1100, 1077 cm^{-1} ; HRMS-FAB (m/z): $[\text{M}]^+$ calc'd for $\text{C}_{24}\text{H}_{41}\text{NO}_4\text{Si}_2$, 463.2574; found, 463.2577; $[\alpha]_{\text{D}}^{23}$ -275.07° (c 1.0, CHCl_3).

[3.2.2] Bicycle 110: R_f 0.42 (5:1 hexanes:EtOAc); ^1H NMR (300 MHz, CDCl_3): δ 6.98 (d, $J = 2.7$ Hz, 1H), 6.15 (d, $J = 2.7$ Hz, 1H), 6.02 (d, $J = 9.3$ Hz, 1H), 5.98 (d, $J = 8.8$ Hz, 1H), 5.69 (d, $J = 9.9$ Hz, 1H), 5.62 (d, $J = 9.9$ Hz, 1H), 4.93 (s, 1H), 3.81 (d, $J = 7.7$ Hz, 1H), 3.50 (t, $J = 8.0$ Hz, 2H), 2.36 (dd, $J = 14.3$ Hz, 7.7 Hz, 1H), 1.94 (dd, $J = 14.3$ Hz, 1.6 Hz, 1H), 1.55 (s, 3H), 0.91-0.83 (comp. m, 11H), 0.02 (s, 3H), 0.01 (s, 3H), -0.07 (s, 9H); ^1H NMR (300 MHz, C_6D_6): δ 6.55 (d, $J = 2.7$ Hz, 1H), 6.23 (d, $J = 8.8$ Hz, 1H), 5.96 (d, $J = 3.3$ Hz, 1H), 5.94 (d, $J = 9.2$ Hz, 1H), 5.59 (d, $J = 10.4$ Hz, 1H), 5.40 (d, $J = 9.9$ Hz, 1H), 5.32 (s, 1H), 3.82-3.75 (m, 1H), 3.46 (t, $J = 7.7$ Hz, 2H), 2.46 (dd, $J = 13.7$ Hz, 7.7 Hz, 1H), 2.25 (dd, $J = 13.7$ Hz, 1.6 Hz, 1H), 1.52 (s, 3H), 0.92 (s, 9H), 0.82 (t, $J = 8.0$ Hz, 2H), -0.03 (s, 3H), -0.08 (s, 3H), -0.09 (s, 9H); ^{13}C NMR (75 MHz, CDCl_3): δ 188.7, 144.1, 139.4, 134.5, 129.1, 121.8, 107.7, 78.2, 77.8, 73.3, 66.4, 45.7, 45.0, 26.0 (3C),

22.2, 18.2, 18.0, -1.25 (3C), -4.1, -4.6; IR (film): 3432, 2955, 2858, 1645, 1250, 1081 cm^{-1} ; HRMS-EI (m/z): $[\text{M} + \text{H}]^+$ calc'd for $\text{C}_{24}\text{H}_{42}\text{NO}_4\text{Si}_2$, 464.2652; found, 464.2665; $[\alpha]_{\text{D}}^{19}$ +19.22° (c 1.0, C_6H_6).



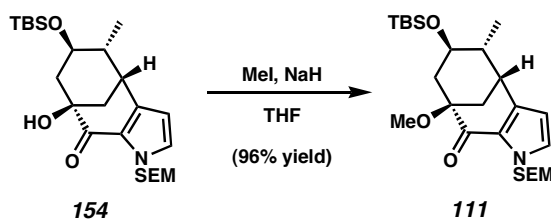
Alternate Procedure. To acyl pyrrole **100** (106.0 mg, 0.227 mmol) was added $\text{Pd}(\text{OAc})_2$ (51.1 mg, 0.227 mmol), DMSO (32.3 μL , 0.455 mmol), $t\text{-BuOH}$ (18.2 mL), and AcOH (4.5 mL). The mixture was heated to 60 °C for 10 h, cooled to 23 °C, and filtered over a plug of silica gel (3:1 hexanes:EtOAc). The solvent was evaporated, and the residue was again filtered over a plug of silica gel (3:1 hexanes:EtOAc). After removal of solvent in vacuo, the product was purified by flash chromatography on silica gel (6:1 hexanes:EtOAc) to afford [3.3.1] bicycle **98** (78.4 mg, 74% yield) as a pale yellow oil.



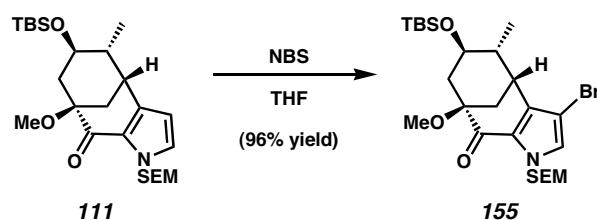
Reduced [3.3.1] Bicycle 154. [3.3.1] bicycle **98** (360 mg, 0.78 mmol), 10% Pd/C (130 mg, 0.12 mmol), and EtOAc (8 mL) were combined, and the reaction vessel was evacuated and back-filled with H_2 (1 atm). The reaction mixture was stirred under H_2 for 30 min, then filtered over a plug of silica gel topped with Celite (EtOAc eluent) to afford

reduced [3.3.1] bicycle **154** as a colorless oil (358 mg, 99% yield). R_f 0.28 (5:1 hexanes:EtOAc); ^1H NMR (300 MHz, C_6D_6): δ 6.55 (d, $J = 2.5$ Hz, 1H), 5.74 (d, $J = 2.5$ Hz, 1H), 5.56 (d, $J = 10.2$ Hz, 1H), 5.30 (d, $J = 10.2$ Hz, 1H), 4.27 (s, 1H), 3.59-3.45 (m, 2H), 3.19 (ddd, $J = 12.9$ Hz, 7.7 Hz, 3.3 Hz, 1H), 2.58 (dd, $J = 6.5$ Hz, 3.2 Hz, 1H), 2.37-2.20 (comp. m, 2H), 2.06-1.90 (comp. m, 2H), 1.63-1.50 (m, 1H), 1.00 (d, $J = 6.6$ Hz, 3H), 0.94-0.89 (comp. m, 11H), -0.02 (s, 9H), -0.06 (s, 3H), -0.09 (s, 3H); ^{13}C NMR (75 MHz, C_6D_6): δ 190.8, 140.4, 131.3, 125.2, 110.1, 76.6, 75.6, 71.8, 66.1, 46.8, 44.3, 40.0, 37.3, 25.9 (3C), 18.1, 17.9, 16.5, -1.2 (3C), -4.0, -4.6; IR (film): 3473 (br), 2953, 2931, 2857, 1651, 1420, 1249, 1079 cm^{-1} ; HRMS-EI (m/z): $[\text{M} + \text{H}]^+$ calc'd for $\text{C}_{24}\text{H}_{44}\text{NO}_4\text{Si}_2$, 466.2809; found, 466.2804; $[\alpha]_D^{19}$ -166.30° (c 1.0, C_6H_6).

*NOTE: In some instances, trace phosphine contaminants from the Heck reaction (i.e., **99** \rightarrow **98**) prevented the reduction from occurring. Simply working up the reaction and re-exposing it to the identical reaction conditions (as described above) allowed the reduction to proceed.*

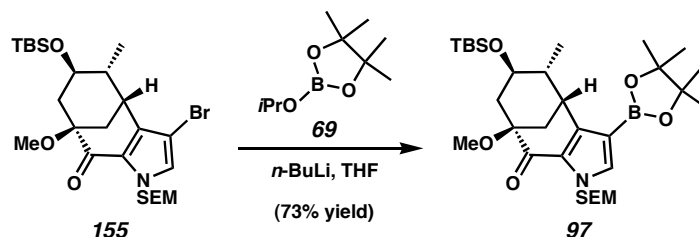


Methyl Ether 111. To reduced [3.3.1] bicycle **154** (358 mg, 0.77 mmol) in THF (7.7 mL) at 23 °C was added NaH (60% dispersion in mineral oil, 123 mg, 3.08 mmol). After stirring for 2 min at 23 °C, MeI was added (335 μL , 5.38 mmol). The resulting mixture was stirred for 1 h, cooled to 0 °C, and quenched with saturated aq. NH_4Cl (4 mL), then warmed to 23 °C. Et_2O (10 mL) and H_2O (5 mL) were added, and the layers



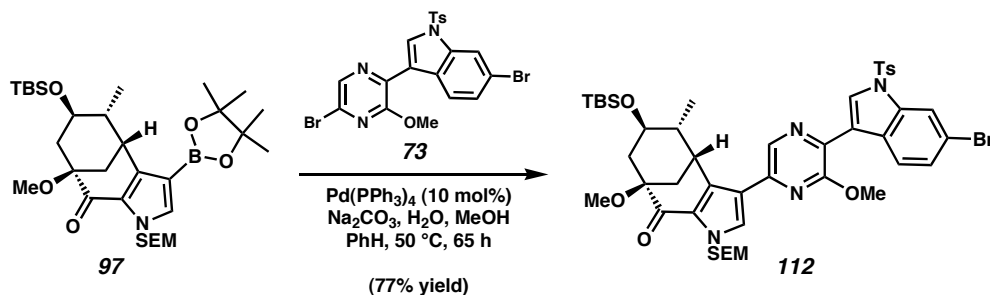
Bromide 155. To methyl ether **111** (305 mg, 0.64 mmol) in THF (6 mL) at 0 °C was added freshly recrystallized NBS (147 mg, 0.83 mmol). After stirring for 10 min at 0 °C, the reaction mixture was warmed to 23 °C, and additional NBS (30 mg, 0.17 mmol) was added. After 5 min, the reaction was quenched with saturated aq. Na₂S₂O₃, diluted with H₂O (15 mL), and extracted with Et₂O (3 x 15 mL). The combined organic layers

were washed with brine (15 mL), dried over MgSO_4 , and evaporated under reduced pressure. The crude product was purified by flash chromatography (5:1 hexanes:EtOAc) to afford bromide **155** (340 mg, 96% yield) as a colorless oil. R_f 0.55 (3:1 hexanes:EtOAc); ^1H NMR (300 MHz, C_6D_6): δ 6.57 (s, 1H), 5.46 (d, $J = 10.2$ Hz, 1H), 5.34 (d, $J = 10.2$ Hz, 1H), 3.57-3.41 (m, 2H), 3.32-3.20 (m, 4H), 2.88 (dd, $J = 6.5$ Hz, 3.2 Hz, 1H), 2.46 (ddd, $J = 12.2$ Hz, 5.1 Hz, 2.5 Hz, 1H), 2.28 (app. dt, $J = 7.4$ Hz, 4.0 Hz, 1H), 1.78 (app. t, $J = 11.8$ Hz, 1H), 1.69-1.57 (m, 1H), 1.52 (dd, $J = 11.8$ Hz, 3.0 Hz, 1H), 1.19 (d, $J = 6.9$ Hz, 3H), 0.91-0.80 (comp. m, 11H), -0.05 (s, 9H), -0.09 (s, 3H), -0.12 (s, 3H); ^{13}C NMR (75 MHz, C_6D_6): δ 189.6, 147.2, 137.2, 130.1, 98.4, 81.8, 77.0, 72.1, 66.6, 51.8, 45.8, 42.4, 41.0, 35.9, 26.3 (3C), 18.5, 18.3, 17.8, -0.9 (3C), -3.7, -4.3; IR (film): 2954, 2930, 1664, 1249, 1089 cm^{-1} ; HRMS-EI (m/z): $[\text{M} + \text{H}]^+ - \text{H}_2$ calc'd for $\text{C}_{25}\text{H}_{43}\text{NO}_4\text{Si}_2\text{Br}$, 556.1914; found, 556.1928; $[\alpha]_D^{19}$ -98.22° (c 1.0, C_6H_6).



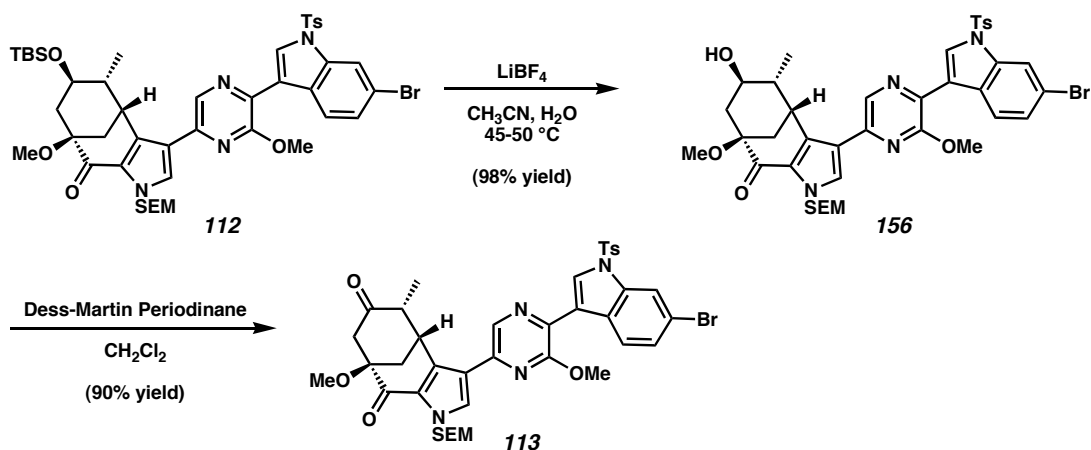
Boronic Ester 97. To bromide **155** (116 mg, 0.21 mmol) and 2-isopropoxy-4,4,5,5-tetramethyl-1,3,2-dioxaborolane (**69**) (847 μL , 4.15 mmol) in THF (10.4 mL) at -78 °C was added $n\text{BuLi}$ (2.3 M in hexanes, 1.35 mL, 3.11 mmol) dropwise over 2 min. After stirring for 15 min at -78 °C, the reaction mixture was quenched with saturated aq. NH_4Cl , warmed to 23 °C, and diluted with H_2O (10 mL). The mixture was extracted with Et_2O (3 x 15 mL). The combined organic layers were washed with brine (15 mL), dried over MgSO_4 , and evaporated under reduced pressure. The crude product was purified by

flash chromatography (4:1 hexanes:EtOAc with 0.5% Et₃N) to afford boronic ester **97** (92 mg, 73% yield) as a white powder, which was used immediately in the next step. *R*_f 0.50 (3:1 hexanes:EtOAc); mp 143–145 °C; ¹H NMR (300 MHz, C₆D₆): δ 7.42 (s, 1H), 5.55 (d, *J* = 10.1 Hz, 1H), 5.51 (d, *J* = 9.8 Hz, 1H), 3.74–3.68 (m, 1H), 3.60–3.50 (m, 2H), 3.43–3.36 (m, 1H), 3.33 (s, 3H), 2.65–2.53 (comp. m, 2H), 1.91 (app. t, *J* = 11.8 Hz, 1H), 1.89–1.80 (m, 1H), 1.68 (dd, *J* = 11.8 Hz, 2.8 Hz, 1H), 1.34 (d, *J* = 6.6 Hz, 3H), 1.15 (s, 6H), 1.14 (s, 6H), 0.94–0.81 (comp. m, 11H), -0.04 (s, 3H), -0.05 (s, 9H), -0.07 (s, 3H); ¹³C NMR (75 MHz, C₆D₆, 30/31 °C): δ 190.1, 145.1, 139.3, 130.2, 83.5 (2C), 82.0, 77.2, 72.6, 66.5, 51.7, 46.1, 42.0, 41.6, 36.8, 26.4 (3C), 25.4 (2C), 25.2 (2C), 18.5, 18.3, 16.9, -0.9 (3C), -3.6, -4.3; IR (film): 2953, 2931, 2858, 1658, 1543, 1249, 1141, 1085 cm⁻¹; HRMS-FAB (*m/z*): [*M* + *H*]⁺ calc'd for C₃₁H₅₇BNO₆Si₂, 606.3818; found, 606.3805; [*α*]_D¹⁹ -98.84° (*c* 1.0, C₆H₆).



Suzuki Adduct 112. Bromopyrazine **73** (46.5 mg, 0.087 mmol), boronic ester **97** (35 mg, 0.058 mmol), benzene (1.15 mL), methanol (231 μL), 2 M aq. Na₂CO₃ (96 μL), and tetrakis(triphenylphosphine)palladium(0) (6.7 mg, 0.0058 mmol) were combined and deoxygenated by sparging with argon for 5 min. The reaction vessel was evacuated, purged with N₂, sealed, heated to 50 °C for 65 h, cooled to 23 °C, then quenched by the addition of Na₂SO₄ (200 mg). Following filtration over a pad of silica gel (2:1

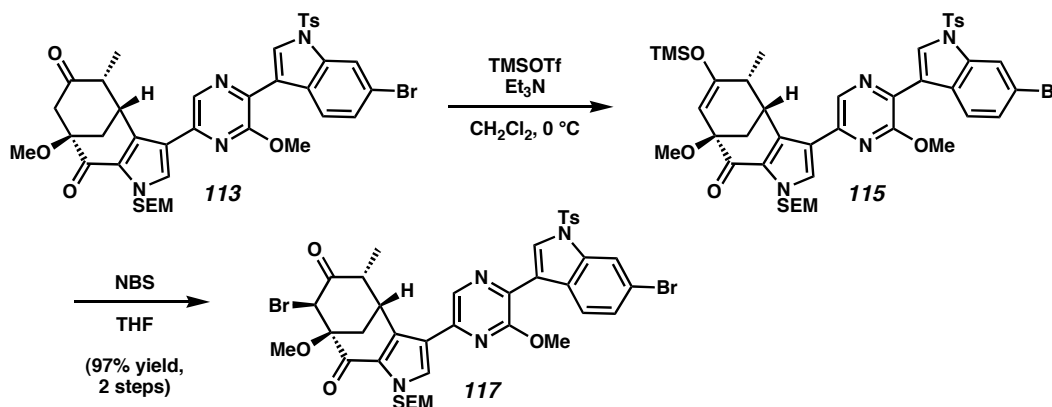
hexanes:EtOAc eluent) and evaporation to dryness under reduced pressure, the remaining residue was purified by flash chromatography (3:1 hexanes:EtOAc) to afford Suzuki adduct **112** (41.5 mg, 77% yield) as a yellow oil. R_f 0.43 (2:1 hexanes:EtOAc); ^1H NMR (300 MHz, CDCl_3): δ 8.61 (d, $J = 8.5$ Hz, 1H), 8.45 (s, 1H), 8.44 (s, 1H), 8.16 (d, $J = 1.5$ Hz, 1H), 7.80 (d, $J = 8.5$ Hz, 2H), 7.59 (s, 1H), 7.40 (dd, $J = 8.5$ Hz, 1.8 Hz, 1H), 7.23 (d, $J = 7.9$ Hz, 2H), 5.85 (d, $J = 10.0$ Hz, 1H), 5.78 (d, $J = 10.0$ Hz, 1H), 4.27-4.21 (m, 1H), 4.19 (s, 3H), 3.72-3.59 (m, 2H), 3.34 (s, 3H), 3.13-3.02 (m, 1H), 2.87-2.77 (m, 1H), 2.32 (s, 3H), 2.22-2.12 (m, 1H), 1.98-1.89 (m, 1H), 1.82-1.72 (m, 1H), 1.67 (app. t, $J = 11.7$ Hz, 1H), 1.04-0.83 (m, 2H), 0.78 (s, 9H), 0.72 (d, $J = 6.7$ Hz, 3H), -0.02 (s, 9H), -0.09 (s, 3H), -0.16 (s, 3H); ^{13}C NMR (75 MHz, CDCl_3 , 44/45 °C): δ 190.0, 156.2, 145.7, 143.6, 136.9, 135.7, 135.5, 135.0, 132.7, 130.3 (2C), 130.2, 129.3, 128.8, 128.5, 127.3, 127.1 (2C), 125.3, 120.5, 119.0, 116.9, 116.4, 81.3, 77.2, 71.4, 66.7, 54.3, 51.6, 44.8, 41.8, 40.2, 34.8, 25.9 (3C), 21.8, 18.1, 16.1, -1.1 (3C), -4.0, -4.7; IR (film): 2952, 1660, 1555, 1372, 1372, 1190, 1140, 1089 cm^{-1} ; HRMS-FAB (m/z): $[\text{M}]^+$ calc'd for $\text{C}_{45}\text{H}_{59}\text{N}_4\text{O}_7\text{Si}_2\text{SBr}$, 934.2826; found, 934.2829; $[\alpha]_D^{21} +51.73^\circ$ (c 1.0, CHCl_3).



Ketone 113. Suzuki adduct **112** (113 mg, 0.121 mmol), LiBF_4 (113 mg, 1.21 mmol), acetonitrile (6 mL), and water (600 μL) were heated to $45\text{--}50\text{ }^\circ\text{C}$. After 9 h, additional LiBF_4 (30 mg, 0.32 mmol) was introduced, and heating was continued. After 6 h, additional LiBF_4 (35 mg, 0.32 mmol) was introduced, and heating was continued for 16 h. The reaction mixture was cooled to $23\text{ }^\circ\text{C}$, quenched with 10% aq. citric acid (10 mL), and extracted with EtOAc (3 x 20 mL). The combined organic layers were dried over MgSO_4 and evaporated under reduced pressure. The crude product was purified by flash chromatography (3:1 EtOAc:hexanes) to yield alcohol **156** (96.9 mg, 98% yield) as a yellow oil, which was used in the subsequent step without further purification. $R_f = 0.44$ (3:1 EtOAc:hexanes).

To alcohol **156** (96 mg, 0.117 mmol) in CH_2Cl_2 (2.0 mL) at $23\text{ }^\circ\text{C}$ was added Dess-Martin Periodinane (74.3 mg, 0.175 mmol). The mixture was stirred for 3 min, quenched with a solution of saturated aq. NaHCO_3 and saturated aq. $\text{Na}_2\text{S}_2\text{O}_3$ (1:1, 5 mL), stirred for 5 min, and extracted with EtOAc (3 x 15 mL). The combined organic layers were washed with brine (15 mL), dried over MgSO_4 , and evaporated under reduced pressure. The crude product was purified by flash chromatography (1:1 hexanes:EtOAc) to yield ketone **113** (86 mg, 90% yield) as a yellow foam. $R_f = 0.48$ (1:1

hexanes:EtOAc); ^1H NMR (300 MHz, CDCl_3): δ 8.61 (d, $J = 8.5$ Hz, 1H), 8.45 (s, 1H), 8.42 (s, 1H), 8.18 (d, $J = 1.7$ Hz, 1H), 7.81 (d, $J = 8.5$ Hz, 2H), 7.56 (s, 1H), 7.42 (dd, $J = 8.7$ Hz, 1.8 Hz, 1H), 7.25 (d, $J = 7.7$ Hz, 2H), 5.77 (d, $J = 10.5$ Hz, 1H), 5.72 (d, $J = 10.2$ Hz, 1H), 4.62-4.56 (m, 1H), 4.20 (s, 3H), 3.57 (app. dt, $J = 8.2$ Hz, 1.8 Hz, 2H), 3.43 (s, 3H), 3.14-3.06 (m, 1H), 2.91-2.81 (m, 1H), 2.74 (s, 2H), 2.40 (dd, $J = 12.5$ Hz, 2.9 Hz, 1H), 2.34 (s, 3H), 0.96-0.88 (m, 2H), 0.78 (d, $J = 6.6$ Hz, 3H), -0.02 (s, 9H); ^{13}C NMR (75 MHz, CDCl_3 , 37/39 °C): δ 207.2, 188.0, 156.1, 145.7, 143.2, 136.3, 135.7, 134.9, 132.6, 130.7, 130.3 (2C), 128.8, 128.4, 127.3, 127.1 (2C), 125.4, 120.5, 119.0, 116.8, 116.3, 82.4, 77.1, 66.9, 54.3, 52.2, 52.0, 49.2, 40.2, 35.2, 21.8, 18.1, 12.2, -1.2 (3C); IR (film): 2950, 1716, 1664, 1557, 1373, 1190, 1178, 1090 cm^{-1} ; HRMS-FAB (m/z): $[\text{M}]^+$ calc'd for $\text{C}_{39}\text{H}_{43}\text{N}_4\text{O}_7\text{SiSBr}$, 818.1805; found, 818.1836; $[\alpha]_D^{21} +71.61^\circ$ (c 1.0, CHCl_3).

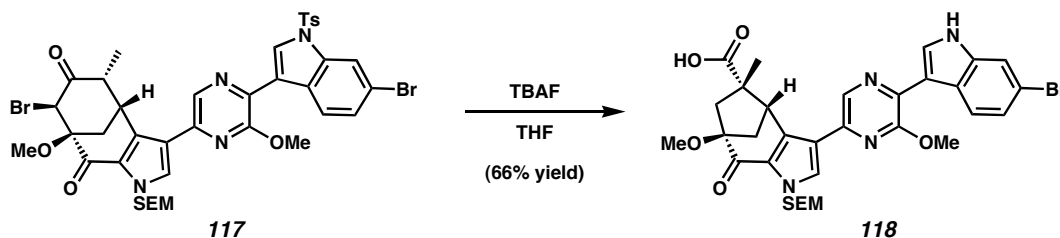
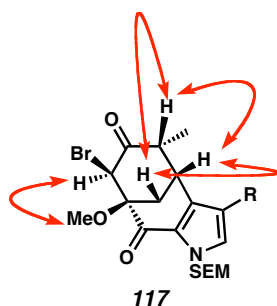


α -Bromoketone 117. To ketone **113** (5.0 mg, 0.0061 mmol) and triethylamine (160 μL , 1.15 mmol) in CH_2Cl_2 (1 mL) at 0 °C was added TMSOTf (70 μL , 0.350 mmol) dropwise over 1 min. The reaction mixture was stirred for 30 min, quenched with saturated aq. NaHCO_3 (2 mL), and extracted with EtOAc (5 x 1 mL). The combined organic layers were washed with brine (1.5 mL) and dried over Na_2SO_4 . Evaporation of

the solvent under reduced pressure afforded silyl enol ether **115** as an unstable yellow oil that was used immediately in the subsequent reaction.

To crude silyl enol ether product **115** in THF (1.5 mL) at 23 °C was added freshly recrystallized NBS (14 mg, 0.0786 mmol). The reaction mixture was stirred for 1 min, quenched with saturated aq. NaHCO₃ (2 mL), and extracted with EtOAc (5 x 1 mL). The combined organic layers were washed with brine (1.5 mL), dried by passage over a plug of silica gel (EtOAc eluent), and evaporated under reduced pressure to afford the crude product. Purification by preparative thin layer chromatography (1:1 hexanes:EtOAc eluent) afforded α -bromoketone **117** (5.3 mg, 97% yield, 2 steps) as a colorless oil. *R_f* 0.68 (1:1 hexanes:EtOAc); ¹H NMR (300 MHz, C₆D₆): δ 9.01 (d, *J* = 8.5 Hz, 1H), 8.87 (s, 1H), 8.69 (s, 1H), 8.15 (s, 1H), 7.70 (d, *J* = 8.3 Hz, 2H), 7.49 (d, *J* = 8.5 Hz, 1H), 7.10 (s, 1H), 6.40 (d, *J* = 8.0 Hz, 2H), 5.45 (d, *J* = 10.2 Hz, 1H), 5.36 (d, *J* = 10.2 Hz, 1H), 4.75 (s, 1H), 4.14-4.06 (m, 1H), 3.68 (s, 3H), 3.60-3.46 (comp. m, 3H), 3.44 (s, 3H), 2.64-2.55 (m, 1H), 2.52-2.43 (m, 1H), 1.58 (s, 3H), 0.89 (t, *J* = 8.0 Hz, 2H), 0.78 (d, *J* = 6.6 Hz, 3H), -0.03 (s, 9H); ¹³C NMR (125 MHz, C₆D₆, 38/39 °C): δ 202.4, 185.4, 156.6, 145.5, 143.2, 136.9, 136.7, 136.6, 135.8, 133.2, 131.8, 130.5 (2C), 129.8, 129.4, 128.0, 127.3 (2C), 126.5, 121.0, 120.0, 117.7, 117.3, 82.9, 77.3, 67.0, 58.4, 54.1, 53.0, 43.4, 36.7, 35.0, 21.3, 18.4, 12.4, -1.0 (3C); IR (film): 2950, 1719, 1662, 1557, 1374, 1190, 1178, 1141, 1089; HRMS-FAB (*m/z*): [M + H]⁺ calc'd for C₃₉H₄₃Br₂N₄O₇SSi, 899.0968; found, 899.0952; [α]_D²⁷ +10.23° (*c* 0.66, C₆H₆).

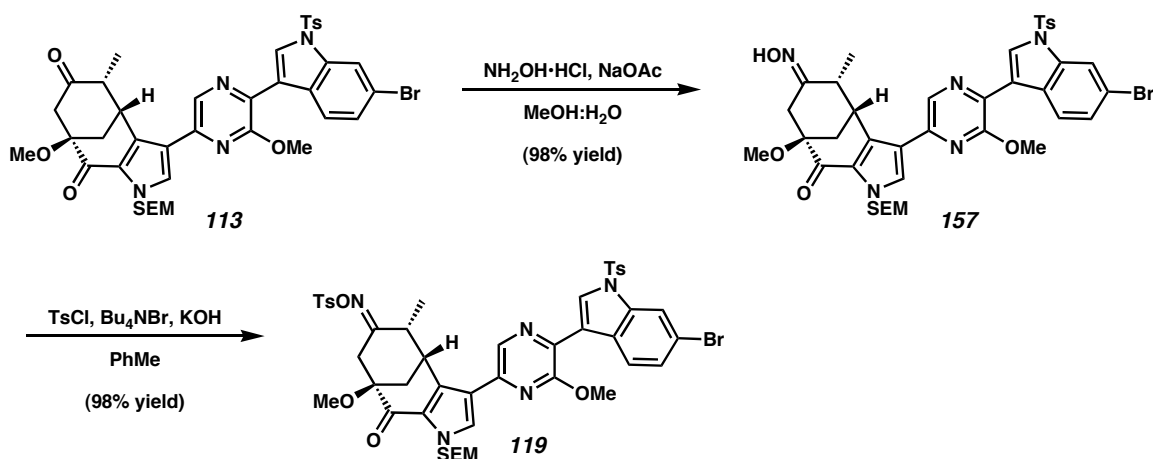
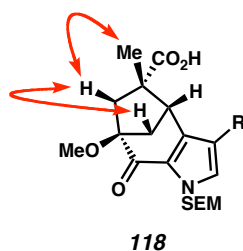
The relative stereochemistry of α -bromoketone **117** was determined by NOE experiments. Medium strength NOE interactions were observed as indicated below.⁵¹



Favorskii product 118. To α -bromoketone **117** (3.0 mg, 0.0033 mmol) in THF (1.0 mL) at 23 °C was added TBAF (1.0 M in THF, 20 μ L, 0.020 mmol). The reaction mixture was stirred for 15 min, quenched with 10% (w/v) aq. citric acid (1 mL), diluted with brine (500 μ L), and extracted with EtOAc (5 x 1 mL). The combined organic layers were dried by passage over a plug of silica gel (EtOAc eluent, then 5:1 CH_2Cl_2 :MeOH eluent) and evaporated under reduced pressure to afford the crude product. Purification by preparative thin layer chromatography (5:1 CH_2Cl_2 :MeOH eluent) afforded Favorskii product **118** (1.5 mg, 66% yield) as a yellow oil. R_f 0.53 (5:1 CH_2Cl_2 :MeOH); ^1H NMR (600 MHz, CD_3OD): δ 8.61 (d, J = 9.2 Hz, 1H), 8.59 (s, 1H), 8.21 (s, 1H), 7.97 (s, 1H), 7.60 (s, 1H), 7.25 (d, J = 8.2 Hz, 1H), 5.81 (d, J = 10.1 Hz, 1H), 5.76 (d, J = 10.1 Hz, 1H), 4.96 (app. d, J = 3.7 Hz, 1H), 4.24 (s, 3H), 3.65 (m, 2H), 3.42 (s, 3H), 2.98 (d, J =

14.7 Hz, 1H), 2.38 (d, $J = 11.0$ Hz, 1H), 2.30 (dd, $J = 11.0, 4.6$ Hz, 1H), 1.63 (d, $J = 14.7$ Hz, 1H), 1.07 (s, 3H), 0.94-0.88 (m, 2H), -0.02 (s, 9H); ^{13}C NMR (125 MHz, CD_3OD): δ 193.1, 170.2, 157.1, 142.4, 142.3, 139.5, 139.1, 133.1, 131.5, 130.6, 128.4, 126.9, 125.5, 124.4, 121.9, 116.8, 115.3, 112.8, 91.3, 77.8, 67.2, 55.1, 54.1, 46.2, 45.6, 44.7, 30.9, 25.0, 18.8, -1.1 (3C); IR (film): 3288 (br), 2927, 2855, 1711, 1659, 1553, 1535, 1449, 1409, 1367, 1250, 1198, 1093; HRMS-FAB (m/z): $[\text{M} + \text{H}]^+$ calc'd for $\text{C}_{32}\text{H}_{38}\text{BrN}_4\text{O}_6\text{Si}$, 683.1724; found, 683.1721; $[\alpha]_{\text{D}}^{23} -26.34^\circ$ (c 0.2, CH_3OH).

The relative stereochemistry of Favorskii product **118** was determined by NOE experiments. Medium strength NOE interactions were observed as indicated below.⁵¹

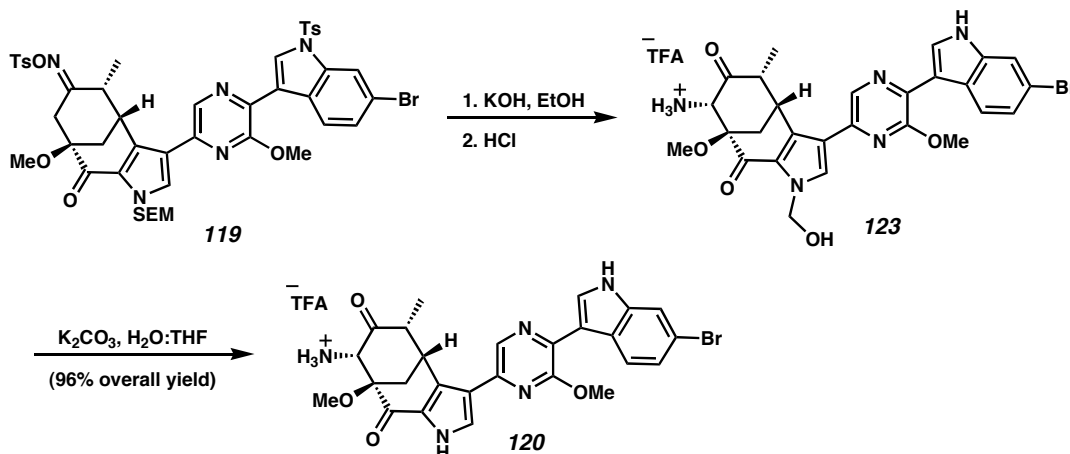


Tosyl Oxime 119. To ketone **113** (50.0 mg, 0.061 mmol), $\text{NH}_2\text{OH}\cdot\text{HCl}$ (85 mg, 1.22 mmol), and $\text{NaOAc}\cdot 3\text{H}_2\text{O}$ (125 mg, 0.915 mmol) was added methanol (2.5 mL),

followed by H₂O (350 μ L), then additional methanol (5 mL). The homogeneous solution was stirred at 23 °C for 8 h, and the solvent was removed under reduced pressure. H₂O (15 mL) was added, and the resulting mixture was extracted with EtOAc (3 x 15 mL). The combined organic layers were washed with brine (15 mL), dried over MgSO₄, and evaporated under reduced pressure. The crude product was further purified by filtration over a plug of silica gel (EtOAc eluent) to yield oxime **157** (50.1 mg, 98% yield) as a yellow foam, which was used without purification in the subsequent reaction. R_f = 0.46 (1:1 hexanes:EtOAc).

To a solution of oxime **157** (20.0 mg, 0.0240 mmol), TsCl (14.0 mg, 0.0734 mmol), and Bu₄NBr (1.0 mg, 0.0031 mmol) in toluene (2.0 mL) at 0 °C was added 50% aq. KOH (310 μ L). The reaction mixture was stirred at 0 °C for 2 h, quenched with ice-cold H₂O (1.5 mL) and extracted with ice-cold EtOAc (5 x 1 mL). The combined organic layers were washed with brine (1 mL), dried by passage over a plug of silica gel (EtOAc eluent), and evaporated under reduced pressure. The crude product was purified by flash chromatography (1:1 hexanes:EtOAc) to yield tosyl oxime **119** (23.3 mg, 98% yield) as a yellow foam. R_f = 0.48 (1:1 hexanes:EtOAc); ¹H NMR (300 MHz, CDCl₃): δ 8.63 (d, J = 8.5 Hz, 1H), 8.46 (s, 1H), 8.41 (s, 1H), 8.19 (d, J = 1.4 Hz, 1H), 7.81 (d, J = 8.3 Hz, 2H), 7.65 (d, J = 8.0 Hz, 2H), 7.51 (s, 1H), 7.44 (dd, J = 8.7 Hz, 1.5 Hz, 1H), 7.28-7.19 (comp. m, 4H), 5.87 (d, J = 10.2 Hz, 1H), 5.42 (d, J = 10.2 Hz, 1H), 4.45-4.43 (m, 1H), 4.20 (s, 3H), 3.67-3.53 (comp. m, 3H), 3.38 (s, 3H), 2.98-2.89 (m, 1H), 2.87-2.77 (m, 1H), 2.42 (s, 3H), 2.35 (s, 3H), 2.12 (d, J = 14.0 Hz, 2H), 1.05-0.85 (m, 2H), 0.78 (d, J = 6.6 Hz, 3H), -0.02 (s, 9H); ¹³C NMR (75 MHz, CDCl₃): δ 187.2, 165.8, 156.3, 145.8, 144.8, 143.5, 135.8, 135.7, 135.3, 135.0, 132.9, 132.6, 130.4 (2C), 129.9, 129.4 (2C), 129.1

(2C), 128.9, 128.4, 128.0, 127.5, 127.2 (2C), 125.3, 120.3, 119.2, 116.8, 116.5, 80.8, 77.4, 67.2, 54.4, 52.2, 42.5, 40.3, 36.5, 36.2, 21.9, 21.9, 18.1, 13.7, -1.1 (3C); IR (film): 2946, 1665, 1555, 1373, 1191, 1178, 1140 cm^{-1} ; HRMS-FAB (m/z): $[M]^+$ calc'd for $\text{C}_{46}\text{H}_{50}\text{N}_5\text{O}_9\text{SiS}_2\text{Br}$, 987.2002; found, 987.2038; $[\alpha]_D^{20} +139.01^\circ$ (c 1.0, CHCl_3).

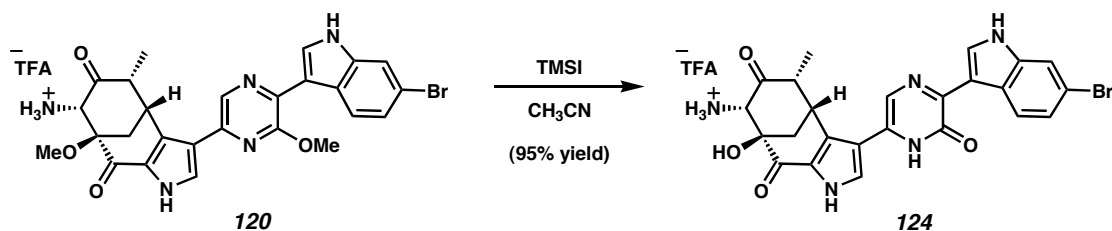
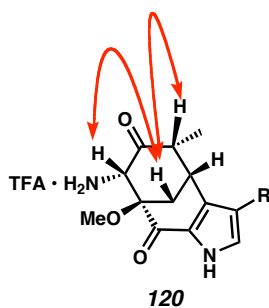


Aminoketone 120. To a stirred solution of tosyl oxime **119** (23.3 mg, 0.0236 mmol) in EtOH (3.5 mL) at 0 °C was added 50% aq. KOH (450 μL) dropwise over 1 min. The reaction mixture was stirred at 0 °C for 3 h, then 6 N aq. HCl (5 mL) was added. The reaction mixture was heated to 60 °C for 10 h, cooled to 23 °C, and purified by reversed-phase filtration through a Sep-Pak column: loaded with water containing 0.1% (w/v) TFA, washed with 15% acetonitrile:water containing 0.1% (w/v) TFA to remove salts, then 70% acetonitrile:water containing 0.1% (w/v) TFA to collect the crude product. The solvents were removed under reduced pressure to afford hemiaminal **123**, which was used immediately in the subsequent reaction. Although hemiaminal **123** is typically used in crude form, it has been observed by ^1H NMR. ^1H NMR (600 MHz, CD_3OD): δ 8.61 (d, J = 8.2 Hz, 1H), 8.52 (s, 1H), 8.24 (s, 1H), 7.94 (s, 1H), 7.60 (s, 1H), 7.25 (d, J = 9.2 Hz, 1H), 5.72 (d, J = 10.1 Hz, 1H), 5.65 (d, J = 10.1 Hz, 1H), 4.85-4.82

(m, 1H), 4.49 (s, 1H), 4.21 (s, 3H), 3.47 (s, 3H), 3.36-3.30 (m, 1H), 3.26 (dd, $J = 12.8$, 2.7 Hz, 1H), 2.61 (dd, $J = 12.8$, 2.7 Hz, 1H), 0.85 (d, $J = 7.3$ Hz, 3H).

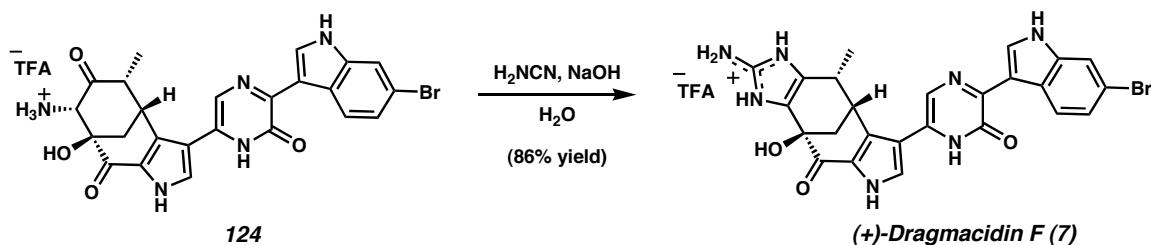
Hemiaminal **123** and K_2CO_3 (60 mg, 0.434 mmol) in THF (2 mL) at 23 °C was added H_2O (200 μ L). The reaction mixture was stirred for 10 min, then purified by reversed-phase filtration through a Sep-Pak column: loaded with water containing 0.1% (w/v) TFA, washed with 10% acetonitrile:water containing 0.1% (w/v) TFA to remove salts, then 70% acetonitrile:water containing 0.1% (w/v) TFA to collect the crude product. After removal of solvents under reduced pressure, the crude material was further purified by reversed-phased HPLC. Concentration under reduced pressure provided aminoketone **120** (15.0 mg, 96% yield) as an orange/red oil. 1H NMR (300 MHz, CD_3OD): δ 8.60 (d, $J = 8.5$ Hz, 1H), 8.53 (s, 1H), 8.23 (s, 1H), 7.81 (s, 1H), 7.61 (d, $J = 1.4$ Hz, 1H), 7.25 (dd, $J = 8.7$ Hz, 1.8 Hz, 1H), 4.82-4.78 (m, 1H), 4.46 (s, 1H), 4.21 (s, 3H), 3.47 (s, 3H), 3.41-3.30 (m, 1H), 3.26 (dd, $J = 12.9$ Hz, 3.9 Hz, 1H), 2.61 (dd, $J = 12.9$ Hz, 3.0 Hz, 1H), 0.88 (d, $J = 6.6$ Hz, 3H); ^{13}C NMR (75 MHz, CD_3OD , 25/26 C): δ 203.5, 183.3, 156.8, 142.4, 139.9, 139.1, 136.3, 133.4, 130.7, 129.9, 129.6, 126.9, 125.5, 124.5, 123.1, 116.9, 115.4, 112.6, 84.3, 66.0, 54.5, 52.9, 40.4, 36.6, 12.2; IR (film): 3156 (br), 2935, 1674, 1531, 1447, 1409, 1203, 1135 cm^{-1} ; HRMS-FAB (m/z): $[M + H]^+$ calc'd for $C_{26}H_{25}N_5O_4Br$, 550.1090; found, 550.1071; $[\alpha]_D^{20} +99.19^\circ$ (c 0.87, MeOH).

The relative stereochemistry of deprotected aminoketone **120** was determined by NOE experiments. Medium strength NOE interactions were observed as indicated below.⁵¹ Analogous NOE interactions were observed for hemiaminal **123** and deprotected aminoketone **124**.



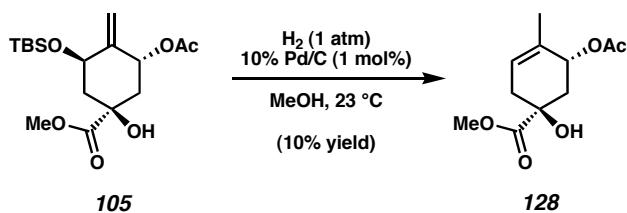
Deprotected Aminoketone 124. To a stirred solution of aminoketone **120** (7.5 mg, 0.0113 mmol) in MeCN (1 mL) at 0 °C was added TMSI (500 μ L, 3.51 mmol) dropwise over 30 sec. The reaction mixture was heated to 60 °C for 48 h, cooled to 0 °C, then transferred dropwise into a chilled solution (0 °C) of saturated aqueous sodium metabisulfite (5 mL). The mixture was diluted with 6 N HCl (15 mL), stirred at 0 °C for 20 min, then purified by reversed-phase filtration through a Sep-Pak column: loaded with water containing 0.1% (w/v) TFA, washed with 1 N HCl, 10% acetonitrile:water containing 0.1% (w/v) TFA to remove salts, then 60% acetonitrile:water containing 0.1% (w/v) TFA to collect the crude product. After removal of solvents under reduced

pressure, the crude material was further purified by reversed-phase HPLC. Concentration under reduced pressure provided deprotected aminoketone **124** (6.8 mg, 95% yield) as an orange/red oil. ^1H NMR (300 MHz, CD_3OD): δ 8.69 (s, 1H), 8.59 (d, J = 8.5 Hz, 1H), 7.69 (s, 1H), 7.61 (d, J = 1.7 Hz, 1H), 7.57 (s, 1H), 7.27 (dd, J = 8.5 Hz, 1.7 Hz, 1H), 4.40 (s, 1H), 4.06-3.98 (m, 1H), 3.31-3.21 (m, 1H), 2.87 (dd, J = 13.2 Hz, 3.3 Hz, 1H), 2.79 (dd, J = 13.1 Hz, 2.9 Hz, 1H), 0.85 (d, J = 6.6 Hz, 3H); ^{13}C NMR (75 MHz, CD_3OD , 23/24 $^\circ\text{C}$): δ 203.4, 186.0, 157.4, 139.1, 136.3, 132.5, 132.4, 130.2, 130.1, 128.2, 126.7, 126.7, 125.6, 124.9, 117.1, 115.4, 113.6, 79.3, 67.1, 49.6, 45.5, 36.7, 12.3; IR (film): 3164 (br), 2927, 1674, 1451, 1207, 1143 cm^{-1} ; HRMS-FAB (m/z): $[\text{M} + \text{H}]^+$ calc'd for $\text{C}_{24}\text{H}_{21}\text{N}_5\text{O}_4\text{Br}$, 522.0777; found, 522.0783; $[\alpha]_{\text{D}}^{22} +86.88^\circ$ (c 0.33, MeOH).



(+)-Dragmacidin F (7). To deprotected aminoketone **124** (3.6 mg, 0.0056 mmol) and cyanamide (120 mg, 2.86 mmol) in H_2O (2 mL, degassed by sparging with argon) at 23 $^\circ\text{C}$ was added 10% aq. NaOH (80 μL). The reaction mixture was heated to 60 $^\circ\text{C}$ for 2 h, cooled to 23 $^\circ\text{C}$, then purified by reversed-phase filtration through a Sep-Pak column: loaded with water containing 0.1% (w/v) TFA, washed with 10% acetonitrile:water containing 0.1% (w/v) TFA to remove salts, then 60% acetonitrile:water containing 0.1% (w/v) TFA to collect the crude product. After removal of solvents under reduced pressure, the product was further purified by reversed-phase HPLC. Concentration under reduced pressure afforded (+)-dragmacidin F (**7**, 3.2 mg,

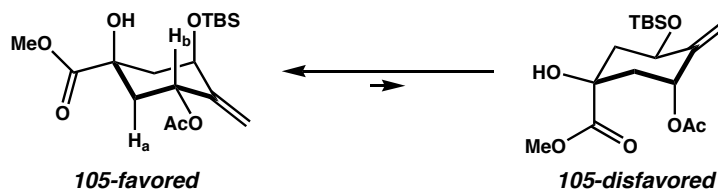
86% yield) as an orange/red oil. ^1H NMR (600 MHz, CD_3OD): δ 8.69 (s, 1H), 8.59 (d, J = 8.7 Hz, 1H), 7.68 (s, 1H), 7.60 (s, 1H), 7.47 (s, 1H), 7.26 (d, J = 8.7 Hz, 1H), 4.12 (br s, 1H), 3.40-3.34 (m, 1H), 2.73 (dd, J = 12.0 Hz, 2.9 Hz, 1H), 2.45 (d, J = 11.6 Hz, 1H), 0.92 (d, J = 7.0 Hz, 3H); ^{13}C NMR (125 MHz, CD_3OD , 22/25 °C): δ 188.5, 157.5, 149.6, 139.1, 132.6, 132.4, 128.5, 128.4, 126.7, 126.2, 125.6, 124.9, 124.8, 123.3, 117.1, 115.4, 113.7, 72.8, 45.3, 36.9, 33.3, 15.9; IR (film): 3175 (br), 2925, 1679, 1637, 1205, 1141 cm^{-1} ; UV (MeOH) λ_{max} 283, 389 nm; HRMS-FAB (m/z): $[\text{M} + \text{H}]^+$ calc'd for $\text{C}_{25}\text{H}_{21}\text{N}_7\text{O}_3\text{Br}$, 546.0889; found, 546.0883; $[\alpha]_{\text{D}}^{23}$ +146.21° (c 0.45, MeOH).



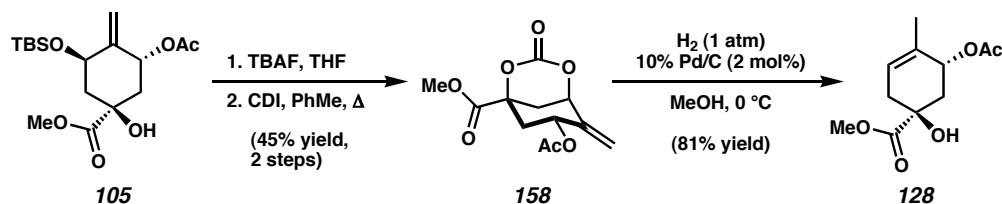
Acetoxycyclohexene 128. A mixture of methyl ester **105** (50.0 mg, 0.140 mmol) and 10% Pd/C (1.5 mg, 0.0014 mmol) in MeOH (1.3 mL) was stirred under an H_2 atmosphere at 23 °C. After 35 min, the reaction mixture was filtered over a Celite plug (MeOH eluent), and the solvent was evaporated in vacuo. ^1H NMR integration showed that acetoxycyclohexene **128** was formed in approximately 10% yield.

Alternate Procedure. A mixture of methyl ester **105** (21.4 mg, 0.06 mmol) and 10% Pd/C (0.3 mg, 0.0003 mmol) in MeOH (1.5 mL) was cooled to 0 °C. The reaction vessel was then evacuated and back-filled with H_2 (4x). After 1 h, the reaction mixture was filtered over a Celite plug (MeOH eluent), and the solvent was evaporated in vacuo. ^1H NMR integration showed that acetoxycyclohexene **128** was formed in approximately 3% yield.

The stable chair conformer of methyl ester **105** was determined using homodecoupling NMR experiments. The coupling constant between H_a and H_b was measured as $J_{ab} = 10.7$ Hz.



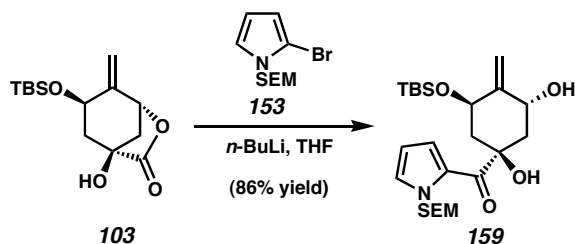
*An analytical sample of **105** was prepared via an alternate route as follows:*



Acetoxycarbonate 158. To a solution of methyl ester **105** (44.8 mg, 0.12 mmol) in THF (2 mL) was added TBAF (1.0 M in THF, 140 μ L, 0.14 mmol). After 3 min of stirring, the reaction was quenched by the addition of saturated aq. NH_4Cl (2 mL). EtOAc (4 mL) was added, and the phases were partitioned. The aqueous phase was further extracted with EtOAc (2 x 2 mL). The combined organic layers were successively washed with H_2O (1 mL) and brine (1 mL), and dried over MgSO_4 . The solvent was evaporated in vacuo, and the residue was dissolved in toluene (4 mL). 1,1'-carbonyldiimidazole (82.1 mg, 0.51 mmol) was added, and the mixture was heated at reflux for 2 h. After cooling to 23 $^\circ\text{C}$, the crude reaction mixture was directly purified by flash column chromatography (3:2 hexanes:EtOAc eluent) to afford pure

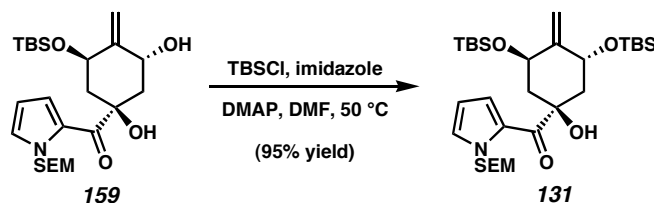
acetoxycarbonate **158** (16.9 mg, 45% yield, 2 steps). R_f 0.15 (1:1 hexanes:EtOAc); ^1H NMR (300 MHz, CDCl_3): δ 5.70-5.62 (m, 1H), 5.25 (app. d, $J = 2.5$ Hz, 1H), 5.19 (app. d, $J = 2.5$ Hz, 1H), 5.16 (dd, $J = 4.1, 1.9$ Hz, 1H), 3.81 (s, 3H), 2.84 (ddd, $J = 13.4, 6.4, 2.7$ Hz, 1H), 2.55-2.48 (m, 1H), 2.32-2.26 (m, 1H), 2.12 (s, 3H), 1.96 (dd, $J = 13.3, 11.1$ Hz, 1H); ^{13}C NMR (75 MHz, CDCl_3): δ 169.3, 168.3, 146.6, 140.2, 113.7, 81.6, 79.5, 66.4, 53.7, 39.3, 32.7, 20.9; IR (film) 1763 (br), 1230, 1180, 1120 cm^{-1} ; HRMS-FAB (m/z): $[\text{M} + \text{H}]^+$ calc'd for $\text{C}_{12}\text{H}_{15}\text{O}_7$, 271.0818; found, 271.0810; $[\alpha]_{\text{D}}^{25}$ -154.53° (c 1.0, C_6H_6).

Acetoxycyclohexene 128. A mixture of acetoxycarbonate **158** (18.5 mg, 0.07 mmol) and 10% Pd/C (1.4 mg, 0.001 mmol) in MeOH (1.3 mL) was cooled to 0 °C. The reaction vessel was then evacuated and back-filled with H_2 (3x). After 1 hr at 0 °C, the reaction mixture was filtered over a Celite plug (MeOH eluent), and the solvent was evaporated in vacuo. The residue was purified by flash chromatography (1:1 EtOAc:hexanes eluent) to afford acetoxycyclohexene **128** (12.6 mg, 81% yield) as a colorless oil. R_f 0.46 (2:1 EtOAc:hexanes); ^1H NMR (300 MHz, CDCl_3): δ 5.57-5.48 (comp. m, 2H), 3.77 (s, 3H), 3.06 (br s, 1H), 2.69-2.58 (m, 1H), 2.29-2.20 (m, 1H), 2.16-1.91 (comp. m, 2H), 2.05 (s, 3H), 1.69-1.66 (m, 3H); ^{13}C NMR (75 MHz, CDCl_3): δ 176.1, 170.9, 132.7, 122.0, 73.8, 70.7, 53.2, 37.1, 35.3, 21.3, 19.2; IR (film) 3477 (br), 2953, 1736, 1239 cm^{-1} ; HRMS-FAB (m/z): $[\text{M} + \text{H}]^+$ calc'd for $\text{C}_{11}\text{H}_{17}\text{O}_5$, 229.1076; found 229.1066; $[\alpha]_{\text{D}}^{25}$ -3.31° (c 0.6, CHCl_3).



Anti-diol 159. To 2-bromo SEM pyrrole (**153**, 4.66 g, 16.87 mmol) in THF (112 mL) at $-78\text{ }^{\circ}\text{C}$ was added *n*-BuLi (2.5 M in hexanes, 6.04 mL, 15.09 mmol) dropwise over 1 min. After 7 min at $-78\text{ }^{\circ}\text{C}$, lactone **103** (1.26 g, 4.44 mmol) in THF (10 mL) was added dropwise over 1 min. The reaction vessel was immediately warmed to $-42\text{ }^{\circ}\text{C}$, stirred for 30 min, and cooled to $-78\text{ }^{\circ}\text{C}$. The reaction mixture was quenched with saturated aq. NH_4Cl (50 mL), then warmed to $23\text{ }^{\circ}\text{C}$. The volatiles were removed under reduced pressure. The residue was partitioned between Et_2O (125 mL) and H_2O (100 mL), and the layers were separated. The aqueous layer was further extracted with Et_2O (2 x 125 mL). The combined organic layers were washed with brine (75 mL), dried over MgSO_4 , and evaporated under reduced pressure. The crude product was purified by flash chromatography (4:1 hexanes:EtOAc eluent) to afford *anti*-diol **159** (1.84 g, 86% yield) as a pale yellow foam. R_f 0.48 (2:1 hexanes:EtOAc); ^1H NMR (300 MHz, C_6D_6): δ 8.11 (dd, $J = 4.1, 1.7\text{ Hz}$, 1H), 6.78 (app. t, $J = 2.1\text{ Hz}$, 1H), 6.15 (dd, $J = 4.0, 2.6\text{ Hz}$, 1H), 5.71 (d, $J = 9.9\text{ Hz}$, 1H), 5.58 (d, $J = 10.2\text{ Hz}$, 1H), 5.26 (s, 1H), 5.17 (app. t, $J = 1.8\text{ Hz}$, 1H), 4.92-4.82 (m, 1H), 4.76-4.73 (m, 1H), 4.45 (app. t, $J = 3.0\text{ Hz}$, 1H), 3.47 (t, $J = 7.7\text{ Hz}$, 2H), 2.66 (ddd, $J = 12.4, 5.2, 2.5\text{ Hz}$, 1H), 2.39 (dd, $J = 14.4, 2.9\text{ Hz}$, 1H), 2.20 (app. dt, $J = 8.7, 4.8\text{ Hz}$, 1H), 1.92 (app. t, $J = 12.0\text{ Hz}$, 1H), 0.88-0.80 (comp. m, 12H), -0.04 (s, 3H), -0.06 (s, 3H), -0.06 (s, 9H); ^{13}C NMR (75 MHz, C_6D_6): δ 192.8, 151.6, 130.5, 128.6, 124.8, 109.3, 108.3, 83.0, 78.5, 76.7, 66.4, 66.2, 48.5, 42.1, 26.1 (3C), 18.4, 18.4, -0.9 (3C), -4.4, -5.1; IR (film): 3456 (br), 2953, 1637, 1406, 1250, 1091 cm^{-1} ; HRMS-FAB

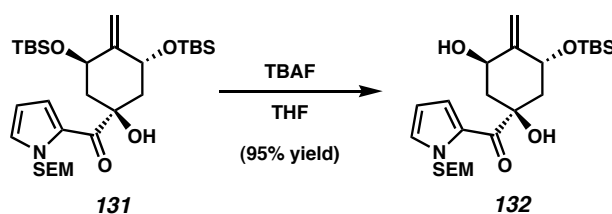
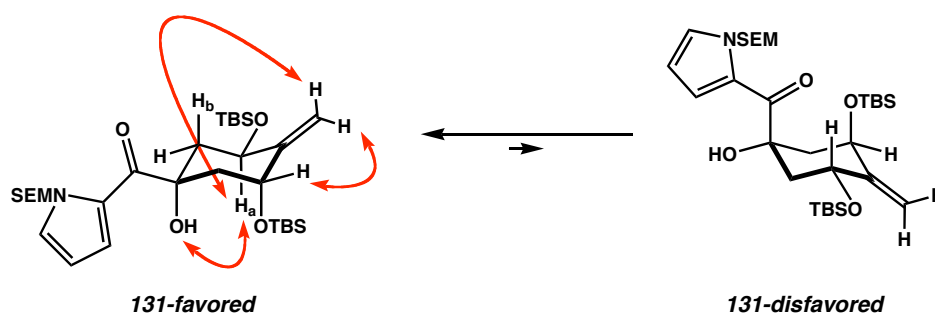
(m/z): $[M + H]^+$ calc'd for $C_{24}H_{44}NO_5Si_2$, 482.2758; found, 482.2751; $[\alpha]_D^{28}$ -21.18° (c 1.0, C_6H_6).



Bis(silylether) 131. To a solution of *anti*-diol **159** (253.1 mg, 0.53 mmol), imidazole (147.1 mg, 2.16 mmol), and DMAP (23.5 mg, 0.19 mmol) in DMF (5.0 mL), was added TBSCl (152.5 mg, 1.01 mmol). The solution was warmed to 50 °C for 70 min, cooled to 0 °C, then quenched by the addition of 10% (w/v) aq. citric acid (10 mL). Et₂O (40 mL) was added, and the layers were partitioned. The aqueous phase was further extracted with Et₂O (2 x 30 mL). The combined organic extracts were washed with brine (15 mL), dried over MgSO₄, and evaporated under reduced pressure. The crude product was purified by flash chromatography (9:1 hexanes:EtOAc eluent) to provide bis(silylether) **131** (296.0 mg, 95% yield) as a colorless oil that solidified under reduced pressure. R_f 0.61 (4:1 hexanes:EtOAc); ¹H NMR (300 MHz, C₆D₆): δ 8.17 (dd, J = 4.0, 1.8 Hz, 1H), 6.76 (dd, J = 2.5, 1.7 Hz, 1H), 6.14 (dd, J = 4.0, 2.6 Hz, 1H), 5.68 (d, J = 9.9 Hz, 1H), 5.62 (d, J = 10.2 Hz, 1H), 5.37 (s, 1H), 5.32 (app. t, J = 2.1 Hz, 1H), 5.22-5.14 (m, 1H), 4.77 (app. t, J = 1.9 Hz, 1H), 4.50 (app. t, J = 3.0 Hz, 1H), 3.47 (t, J = 7.8 Hz, 2H), 2.82 (ddd, J = 12.7, 5.1, 2.6 Hz, 1H), 2.45 (dd, J = 14.6, 2.8 Hz, 1H), 2.27-2.18 (comp. m, 2H), 0.99 (s, 9H), 0.88 (s, 9H), 0.82 (t, J = 7.8 Hz, 2H), 0.17 (s, 3H), 0.14 (s, 3H), 0.00 (s, 3H), -0.04 (s, 3H), -0.07 (s, 9H); ¹³C NMR (75 MHz, C₆D₆, 29/30 °C): δ 192.6, 151.6, 130.4, 124.5, 109.3, 108.6, 83.2, 78.5, 76.8, 67.4, 66.3, 49.3, 42.1, 26.4

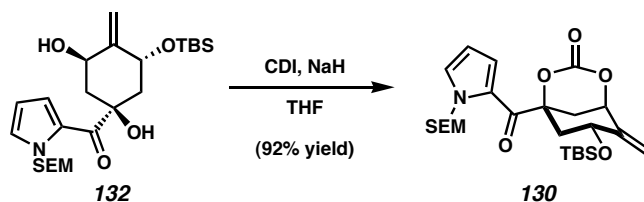
(3C), 26.1 (3C), 18.9, 18.4, 18.3, -0.9 (3C), -4.3, -4.4, -4.5, -5.1; IR (film): 3464 (br), 1953, 2929, 1640, 1405, 1309, 1251, 1094 cm^{-1} ; HRMS-FAB (m/z): $[\text{M} + \text{H}]^+$ calc'd for $\text{C}_{30}\text{H}_{58}\text{NO}_5\text{Si}_3$, 596.3623; found, 596.3594; $[\alpha]_{\text{D}}^{27} -7.16^\circ$ (c 1.0, C_6H_6).

The stable chair conformer of bis(silylether) **131** was determined using a combination of NOESY-1D, gCOSY, and homodecoupling NMR experiments. Medium strength NOE interactions were observed as indicated below.⁵¹ The coupling constant between H_a and H_b was measured as $J_{ab} = 11.0$ Hz.



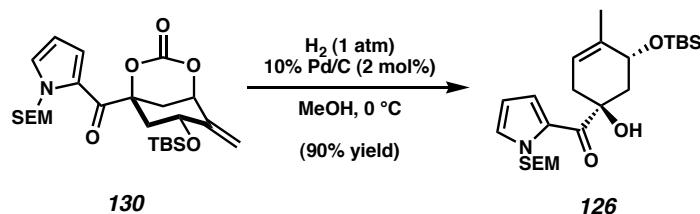
Syn-diol 132. To bis(silylether) **131** (113.9 mg, 0.19 mmol) in THF (10.0 mL) was added TBAF (1.0 M in THF, 195 μL , 0.20 mmol) in a dropwise fashion over 1 min. The reaction mixture was stirred for 2 min, quenched with saturated aq. NH_4Cl (15 mL), then poured into EtOAc (40 mL). The layers were partitioned, and the aqueous layer was further extracted with EtOAc (2 x 40 mL). The combined organic extracts were successively washed with H_2O (15 mL) and brine (15 mL), dried over MgSO_4 , and

evaporated under reduced pressure. The residue was purified by flash chromatography (7:1 hexanes:EtOAc eluent) to furnish *syn* diol **132** (87.5 mg, 95% yield) as a pale yellow oil. R_f 0.29 (4:1 hexanes:EtOAc); ^1H NMR (300 MHz, C_6D_6): δ 7.09 (dd, $J = 4.1, 1.4$ Hz, 1H), 6.63 (dd, $J = 2.3, 1.5$ Hz, 1H), 5.89 (dd, $J = 4.1, 2.5$ Hz, 1H), 5.51-5.39 (comp. m, 4H), 5.27-5.19 (m, 1H), 5.01 (app. t, $J = 2.1$ Hz, 1H), 4.52-4.46 (m, 1H), 3.86 (d, $J = 8.0$ Hz, 1H), 3.37 (t, $J = 7.7$ Hz, 2H), 2.45-2.23 (comp. m, 3H), 2.04 (app. dt, $J = 8.4, 4.9$ Hz, 1H), 0.99 (s, 9H), 0.79 (t, $J = 7.8$ Hz, 2H), 0.14 (s, 3H), 0.11 (s, 3H), -0.09 (s, 9H); ^{13}C NMR (75 MHz, C_6D_6): δ 191.6, 152.9, 131.4, 126.4, 124.0, 109.8, 108.5, 81.2, 78.8, 74.7, 67.4, 66.6, 49.0, 43.3, 26.4 (3C), 18.9, 18.3, -1.0 (3C), -4.5, -4.5; IR (film): 3363 (br), 2954, 1631, 1410, 1314, 1250, 1101 (br) cm^{-1} ; HRMS-FAB (m/z): $[\text{M} + \text{H}]^+$ calc'd for $\text{C}_{24}\text{H}_{44}\text{NO}_5\text{Si}_2$, 482.2758; found, 482.2780; $[\alpha]_D^{27}$ -27.06° (c 1.0, C_6H_6).



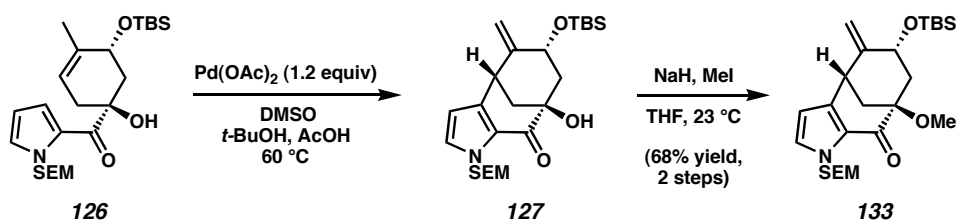
Carbonate 130. To *syn* diol **132** (68.2 mg, 0.14 mmol) and 1,1'-carbonyldiimidazole (37.0 mg, 0.23 mmol) in THF (2.6 mL) was added NaH (60% dispersion in mineral oil, 21.9 mg, 0.55 mmol) in one portion. The reaction was stirred for 20 min at 23 °C, then quenched by addition of saturated aq. NH_4Cl (20 mL). The reaction mixture was poured into EtOAc (30 mL), the layers were partitioned, and the aqueous layer was further extracted with EtOAc (2 x 30 mL). The combined organic extracts were successively washed with H_2O (10 mL) and brine (10 mL), dried over MgSO_4 , and evaporated under reduced pressure. Purification of the residue by flash

chromatography (6:1 hexanes:EtOAc eluent) afforded carbonate **130** (65.8 mg, 92% yield) as a colorless oil. R_f 0.29 (4:1 hexanes:EtOAc); ^1H NMR (300 MHz, C_6D_6): δ 7.91 (dd, $J = 4.1, 1.7$ Hz, 1H), 6.68 (dd, $J = 2.8, 1.7$ Hz, 1H), 6.02 (dd, $J = 4.3, 2.6$ Hz, 1H), 5.51 (d, $J = 9.9$ Hz, 1H), 5.43 (d, $J = 9.9$ Hz, 1H), 5.24 (app. t, $J = 1.9$ Hz, 1H), 4.84-4.75 (m, 1H), 4.69 (app. t, $J = 1.8$ Hz, 1H), 4.46 (dd, $J = 3.9, 1.9$ Hz, 1H), 3.39 (t, $J = 7.7$ Hz, 2H), 2.78 (ddd, $J = 13.5, 6.1, 2.5$ Hz, 1H), 2.12-1.98 (comp. m, 2H), 1.92-1.85 (m, 1H), 0.86 (s, 9H), 0.81 (t, $J = 7.8$ Hz, 2H), -0.07--0.08 (comp. m, 12H), -0.10 (s, 3H); ^{13}C NMR (75 MHz, C_6D_6): δ 185.9, 147.2, 146.4, 132.1, 126.7, 125.0, 112.2, 110.3, 87.9, 80.3, 78.8, 66.8, 66.5, 46.1, 33.7, 26.2 (3C), 18.6, 18.3, -1.0 (3C), -4.7, -5.0; IR (film): 2954, 1764, 1641, 1413, 1354, 1251, 1173, 1089 cm^{-1} ; HRMS-FAB (m/z): $[\text{M} + \text{H}]^+$ calc'd for $\text{C}_{25}\text{H}_{42}\text{NO}_6\text{Si}_2$, 508.2551; found, 508.2560; $[\alpha]_D^{27}$ -54.78° (c 1.0, C_6H_6).



Pyrrolocyclohexene 126. A mixture of carbonate **130** (40.0 mg, 0.08 mmol) and 10% Pd/C (1.7 mg, 0.002 mmol) in MeOH (1.0 mL) was cooled to 0 °C. The reaction vessel was then evacuated and back-filled with H_2 (3x). After 1.75 hr at 0 °C, the reaction mixture was filtered over a Celite plug (MeOH eluent), and the solvent was evaporated in vacuo. The residue was purified by flash chromatography (9:1 hexanes:EtOAc eluent) to afford pyrrolocyclohexene **126** (33.1 mg, 90% yield) as a colorless oil. R_f 0.53 (4:1 hexanes:EtOAc); ^1H NMR (300 MHz, C_6D_6): δ 6.94 (dd, $J = 4.1, 1.4$ Hz, 1H), 6.64 (dd, $J = 2.6, 1.5$ Hz, 1H), 5.89 (dd, $J = 4.0, 2.6$ Hz, 1H), 5.54 (d, J

= 10.2 Hz, 1H), 5.45 (d, J = 10.2 Hz, 1H), 5.39-5.33 (m, 1H), 4.87-4.78 (m, 1H), 4.78 (s, 1H), 3.40 (t, J = 7.8 Hz, 2H), 2.97-2.85 (m, 1H), 2.48 (dd, J = 12.5, 9.8 Hz, 1H), 2.34-2.26 (m, 1H), 2.21-2.08 (m, 1H), 1.95-1.90 (m, 3H), 0.96 (s, 9H), 0.81 (t, J = 7.8 Hz, 2H), 0.06 (s, 3H), 0.03 (s, 3H), -0.08 (s, 9H); ^{13}C NMR (75 MHz, C_6D_6): δ 193.8, 138.5, 131.0, 126.4, 123.1, 120.1, 109.7, 78.8, 78.2, 69.6, 66.5, 44.7, 38.9, 26.4 (3C), 20.6, 18.6, 18.3, -1.0 (3C), -3.8, -4.5; IR (film): 3431 (br), 2954, 1634, 1414, 1250, 1089 (br) cm^{-1} ; HRMS-FAB (m/z): $[\text{M} + \text{H}]^+$ calc'd for $\text{C}_{24}\text{H}_{44}\text{NO}_4\text{Si}_2$, 466.2809; found, 466.2804; $[\alpha]_{\text{D}}^{28} +26.19^\circ$ (c 1.0, C_6H_6).

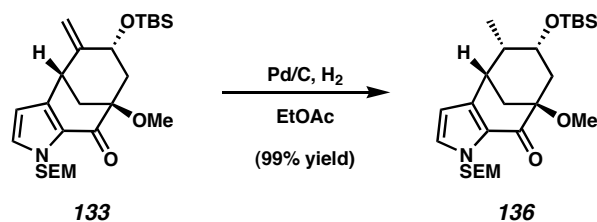


[3.3.1] Bicycle 127. To pyrrolocyclohexene **126** (40.0 mg, 0.0859 mmol) was added $\text{Pd}(\text{OAc})_2$ (23.0 mg, 0.103 mmol), DMSO (14.6 μL , 0.206 mmol), $t\text{-BuOH}$ (6.9 mL), and AcOH (1.7 mL). The mixture was heated to 60°C for 8 h, cooled to 23°C , and filtered over a plug of silica gel (2:1 hexanes:EtOAc eluent). The solvent was evaporated, and the product was purified by flash chromatography on silica gel (8:1 hexanes:EtOAc eluent) to afford [3.3.1] bicycle **127** contaminated with a trace amount of pyrrolocyclohexene **126**. Although this material was carried on to the subsequent step without further purification, an analytical sample of **127** was obtained by flash chromatography on silica gel (12:1 hexanes:EtOAc eluent) as a colorless oil. R_f 0.64 (3:1 hexanes:EtOAc); ^1H NMR (300 MHz, C_6D_6): δ 6.64 (d, J = 2.5 Hz, 1H), 6.25 (d, J = 10.2 Hz, 1H), 5.84 (d, J = 2.8 Hz, 1H), 5.07 (d, J = 9.9 Hz, 1H), 4.79 (br s, 1H), 4.66 (br s,

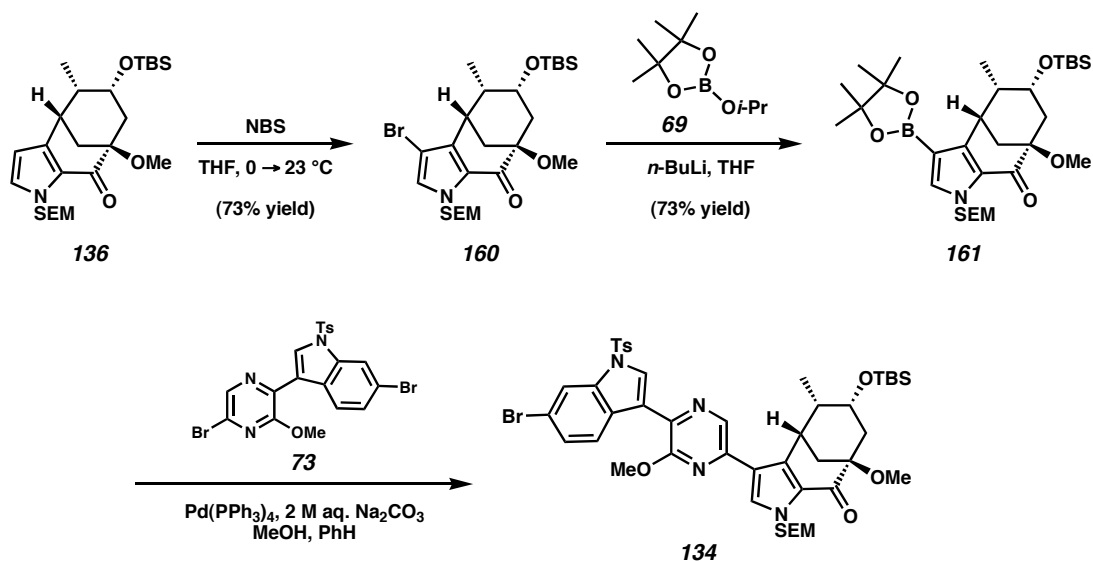
1H), 4.24-4.19 (m, 1H), 4.19 (s, 1H), 3.68-3.51 (m, 2H), 3.43-3.38 (m, 1H), 2.61 (app. dt, $J = 7.3, 3.9$ Hz, 1H), 2.21-2.10 (m, 2H), 2.06-1.98 (m, 1H), 0.99-0.77 (m, 2H), 0.72 (s, 9H), -0.04 (s, 9H), -0.11 (s, 3H), -0.24 (s, 3H); ^{13}C NMR (75 MHz, C_6D_6): δ 192.0, 148.6, 142.7, 130.5, 126.3, 113.2, 108.3, 77.0, 73.4, 73.0, 66.6, 48.5, 45.5, 40.2, 26.1 (3C), 18.4, 18.3, -1.0 (3C), -4.4, -5.1; IR (film): 3468 (br), 2951, 1648, 1422, 1250, 1094, 1062 cm^{-1} ; HRMS-FAB (m/z): $[\text{M} + \text{H}]^+$ calc'd for $\text{C}_{24}\text{H}_{42}\text{NO}_4\text{Si}_2$, 464.2652; found, 464.2661; $[\alpha]_{\text{D}}^{27} +319.22^\circ$ (c 1.0, C_6H_6).

Methyl Ether 133. The crude mixture of **126** and **127** obtained from the previous step was dissolved in THF (1.5 mL) at 23 °C, and NaH (60% dispersion in mineral oil, 17 mg, 0.429 mmol) was added. After stirring for 1 min at 23 °C, MeI was added (53 μL , 0.859 mmol). The resulting mixture was stirred for 1.5 h, quenched with saturated aq. NH_4Cl (1.5 mL), and extracted with Et_2O (4 x 1 mL). The combined organic layers were washed with brine (1 mL), dried by passage over a plug of silica gel (EtOAc eluent), and evaporated under reduced pressure. The crude product was purified by flash chromatography (10:1 hexanes:EtOAc eluent) to afford methyl ether **133** (28.2 mg, 68% yield, 2 steps) as a colorless oil. R_f 0.43 (5:1 hexanes:EtOAc); ^1H NMR (300 MHz, C_6D_6): δ 6.62 (d, $J = 2.6$ Hz, 1H), 6.43 (d, $J = 10.3$ Hz, 1H), 5.86 (d, $J = 2.6$ Hz, 1H), 5.06 (d, $J = 10.0$ Hz, 1H), 4.84 (d, $J = 1.5$ Hz, 1H), 4.69 (d, $J = 1.5$ Hz, 1H), 4.29-4.22 (m, 1H), 3.42-3.52 (m, 2H), 3.45 (app. t, $J = 2.8$ Hz, 1H), 3.39 (s, 3H), 2.79 (app. dt, $J = 7.4, 3.8$ Hz, 1H), 2.49 (app. dt, $J = 8.1, 4.4$ Hz, 1H), 1.96 (dd, $J = 13.8, 4.7$ Hz, 1H), 1.70 (dd, $J = 11.7, 3.2$ Hz, 1H), 0.96-0.82 (m, 2H), 0.73 (s, 9H), -0.06 (s, 9H), -0.11 (s, 3H), -0.23 (s, 3H); ^{13}C NMR (75 MHz, C_6D_6): δ 189.2, 149.2, 140.9, 129.6, 128.9, 112.9, 107.6, 79.0, 77.3, 72.7, 66.6, 51.5, 46.3, 41.7, 39.9, 26.1 (3C), 18.4, 18.4, -1.0 (3C), -4.4,

-5.1; IR (film): 2951, 1661, 1426, 1250, 1113, 1066; HRMS-FAB (m/z): $[M + H]^+$ calc'd for $C_{25}H_{44}NO_4Si_2$, 478.2809; found, 478.2815; $[\alpha]_D^{27} +312.37^\circ$ (c 1.0, C_6H_6).



Reduced Bicycle 136. Methyl ether **133** (23 mg, 0.0479 mmol), 10% Pd/C (15 mg, 0.014 mmol), and EtOAc (2.5 mL) were combined, and the reaction vessel was evacuated and back-filled with H_2 (1 atm). The reaction mixture was stirred under H_2 for 5 min, then filtered over a plug of silica gel topped with Celite (EtOAc eluent) to afford reduced bicycle **136** as a colorless oil (23 mg, 99% yield). R_f 0.28 (5:1 hexanes:EtOAc); 1H NMR (300 MHz, C_6D_6): 6.64 (d, $J = 2.5$ Hz, 1H), 6.52 (d, $J = 10.2$ Hz, 1H), 5.83 (d, $J = 2.5$ Hz, 1H), 5.05 (d, $J = 10.2$ Hz, 1H), 3.71-3.51 (comp. m, 3H), 3.42 (s, 3H), 2.78 (app. dt, $J = 7.4, 3.9$ Hz, 1H), 2.60 (app. q, $J = 3.1$ Hz, 1H), 2.40 (app. dt, $J = 8.1, 4.6$ Hz, 1H), 1.81 (dd, $J = 13.8, 4.4$ Hz, 1H), 1.58 (dd, $J = 11.4, 2.9$ Hz, 1H), 1.42-1.53 (m, 1H), 0.99-0.81 (m, 2H), 0.87 (d, $J = 7.2$ Hz, 3H), 0.72 (s, 9H), -0.06 (s, 9H), -0.10 (s, 3H), -0.21 (s, 3H); ^{13}C NMR (75 MHz, C_6D_6 , 24/25 $^\circ C$): δ 189.3, 140.3, 129.1, 109.2, 79.2, 77.2, 71.5, 66.5, 51.2, 45.4, 41.9, 38.3, 36.8, 26.1 (3C), 18.4, 18.4, 17.1, -1.0 (3C), -4.4, -5.0; IR (film): 2952, 1660, 1497, 1425, 1251, 1118, 1100, 1042 cm^{-1} ; HRMS-FAB (m/z): $[M + H]^+$ calc'd for $C_{25}H_{46}NO_4Si_2$, 480.2965; found, 480.2955; $[\alpha]_D^{25} +220.84^\circ$ (c 1.0, C_6H_6).



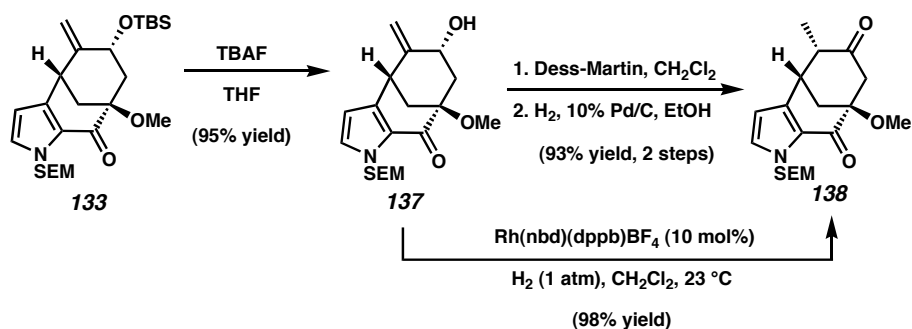
Pyrazine 134. To silyl ether **136** (10.0 mg, 0.0208 mmol) in THF (2 mL) at 0 °C was added freshly recrystallized NBS (4.8 mg, 0.0271 mmol) in THF (200 μ L). After 10 min at 0 °C, the reaction mixture was warmed to 23 °C, stirred for 40 min, then cooled to 0 °C. The reaction was quenched with saturated aq. Na₂S₂O₃ (1.5 mL), diluted with H₂O (1 mL), and extracted with EtOAc (5 x 1 mL). The combined organic layers were washed with brine (1 mL), dried by passage over a plug of silica gel (EtOAc eluent), and evaporated under reduced pressure to afford the crude product. Further purification by preparative thin layer chromatography (4:1 hexanes:EtOAc eluent) afforded bromide **160** (8.5 mg, 73% yield) as a colorless oil. *R_f* 0.4 (5:1 hexanes:EtOAc).

To bromide **160** (12.7 mg, 0.0227 mmol) and 2-isopropoxy-4,4,5,5-tetramethyl-1,3,2-dioxaborolane (**69**, 190 μ L, 0.932 mmol) in THF (2.3 mL) at -78 °C was added *n*-BuLi (2.5 M in hexanes, 273 μ L, 0.682 mmol) dropwise over 1 min. After stirring for 10 min at -78 °C, the reaction mixture was quenched with saturated aq. NH₄Cl (1.5 mL), warmed to 23 °C, diluted with H₂O (1 mL), and extracted with EtOAc (5 x 1 mL). The combined organic layers were washed with brine (1 mL), dried by passage over a plug of

silica gel (EtOAc eluent), and evaporated under reduced pressure to afford the crude product. Further purification by preparative thin layer chromatography (4:1 hexanes:EtOAc eluent) afforded boronic ester **161** (10.1 mg, 73% yield) as a colorless oil. R_f 0.38 (5:1 hexanes:EtOAc).

A vial charged with bromopyrazine **73** (12.4 mg, 0.0231 mmol), boronic ester **161** (10.0 mg, 0.0165 mmol), and tetrakis(triphenylphosphine)palladium(0) (2.9 mg, 0.00248 mmol) was evacuated and purged with N_2 . Deoxygenated benzene (330 μ L), deoxygenated methanol (65 μ L), and deoxygenated 2 M aq. Na_2CO_3 (28 μ L) were then added. The reaction vessel was sealed, heated to 50 $^{\circ}C$ for 82 h, cooled to 23 $^{\circ}C$, then quenched by the addition of Na_2SO_4 (100 mg). Following filtration over a pad of silica gel (1:1 hexanes:EtOAc eluent) and evaporation to dryness under reduced pressure, the residue was purified by preparative thin layer chromatography (2:1 hexanes:EtOAc eluent) to afford pyrazine **134** (4.4 mg, 28% yield) as a yellow foam. R_f 0.44 (2:1 hexanes:EtOAc); 1H NMR (500 MHz, C_6D_6): δ 9.02 (d, J = 8.8 Hz, 1H), 8.85 (s, 1H), 8.69 (d, J = 2.0 Hz, 1H), 8.35 (s, 1H), 7.71-7.68 (m, 2H), 7.48 (dd, J = 8.8 Hz, 2.0 Hz, 1H), 7.26 (s, 1H), 6.57 (d, J = 10.3 Hz, 1H), 6.40 (d, J = 8.3 Hz, 2H), 5.16 (d, J = 10.3 Hz, 1H), 3.92 (d, J = 3.4 Hz, 1H), 3.74 (s, 3H), 3.73-3.58 (comp. m, 3H), 3.45 (s, 3H), 2.91 (app. dt, J = 7.3, 3.6 Hz, 1H), 2.44 (app. t, J = 7.1 Hz, 1H), 1.86 (dd, J = 13.9, 4.2 Hz, 1H), 1.74 (dd, J = 11.7, 2.9 Hz, 1H), 1.64-1.55 (comp. m, 4H), 1.02-0.86 (m, 2H), 0.75 (s, 9H), 0.68 (d, J = 6.8 Hz, 3H), -0.05 (s, 9H), -0.09 (s, 3H), -0.23 (s, 3H); ^{13}C NMR (125 MHz, C_6D_6): δ 190.4, 156.7, 145.4, 145.0, 138.6, 136.7, 135.9, 135.8, 133.4, 131.0, 130.4 (2C), 129.5, 129.5, 129.1, 127.9, 127.4 (2C), 126.7, 120.8, 119.8, 118.0, 117.2, 79.0, 77.8, 72.1, 67.1, 53.9, 51.4, 45.4, 41.7, 39.8, 34.6, 26.2 (3C), 21.3, 18.6, 18.5, 17.3,

-1.0 (3C), -4.4, -5.0; IR (film): 2951, 1661, 1556, 1376, 1250, 1178, 1141, 1090, 1011 cm^{-1} ; HRMS-FAB (m/z): $[\text{M}]^+$ calc'd for $\text{C}_{45}\text{H}_{59}\text{BrN}_4\text{O}_7\text{SSi}_2$, 934.2826; found, 934.2872; $[\alpha]_D^{20}$ -91.02° (c 0.57, C_6H_6).



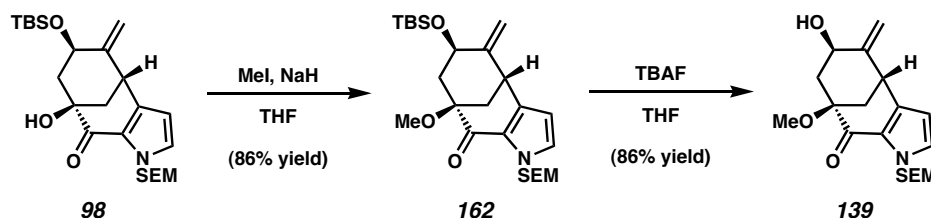
Ketone 138. To methyl ether **133** (120 mg, 0.25 mmol) in THF (12.5 mL) was added TBAF (1.0 M in THF, 750 μL , 0.75 mmol). The reaction mixture was stirred for 4 h, quenched with saturated aq. NH_4Cl (10 mL), diluted with H_2O (5 mL), and extracted with EtOAc (3 x 25 mL). The combined organic extracts were washed with brine (15 mL), dried over MgSO_4 , and evaporated under reduced pressure. The residue was purified by flash chromatography (1:1 hexanes:EtOAc eluent) to furnish allylic alcohol **137** (86 mg, 95% yield) as a pale yellow oil. R_f 0.12 (2:1 hexanes:EtOAc); ^1H NMR (300 MHz, C_6D_6): δ 6.60 (d, J = 2.8 Hz, 1H), 5.81 (d, J = 2.8 Hz, 1H), 5.64 (d, J = 10.2 Hz, 1H), 5.58 (d, J = 10.2 Hz, 1H), 4.80 (d, J = 1.7 Hz, 1H), 4.64 (d, J = 1.7 Hz, 1H), 4.15-4.09 (m, 1H), 3.68-3.59 (m, 2H), 3.42 (t, J = 3.2 Hz, 1H), 3.36 (s, 3H), 2.72 (app. dt, J = 7.4, 3.9 Hz, 1H), 2.58 (app. dt, J = 8.1, 4.9 Hz, 1H), 1.89 (dd, J = 14.2, 5.1 Hz, 1H), 1.65 (dd, J = 11.6, 3.0 Hz, 1H), 0.97-0.88 (m, 2H), 0.59 (d, J = 3.9 Hz, 1H), -0.03 (s, 9H); ^{13}C NMR (75 MHz, C_6D_6 , 18/19 °C): δ 189.4, 149.4, 140.6, 130.4, 113.8, 107.4, 78.9, 76.7, 72.0, 66.2, 51.6, 44.3, 41.1, 39.5, 18.4, -0.9 (3C); IR (film): 3460 (br), 2951, 1659, 1424,

1248, 1111, 1023 cm^{-1} ; HRMS-FAB (m/z): $[\text{M} + \text{H}]^+$ calc'd for $\text{C}_{19}\text{H}_{30}\text{NO}_4\text{Si}$, 364.1944; found, 364.1942; $[\alpha]_{\text{D}}^{24} +330.71^\circ$ (c 1.0, C_6H_6).

Allylic alcohol **137** (44.0 mg, 0.121 mmol) and freshly prepared $\text{Rh}(\text{nbd})(\text{dppb})\text{BF}_4$ (8.6 mg, 0.0121 mmol)⁴⁸ were combined under a glovebox atmosphere. The reaction vessel was carefully sealed and removed from the glovebox. CH_2Cl_2 (12.0 mL) was added, and a balloon of H_2 (1 atm) was applied without purging. After 3 h of stirring, the reaction mixture was filtered over a plug of silica gel (CH_2Cl_2 , then 2:1 hexanes:EtOAc eluent) to afford ketone **138** (43.0 mg, 98% yield) as a colorless oil.

Alternate Procedure. To allylic alcohol **137** (10.6 mg, 0.029 mmol) in CH_2Cl_2 (1.5 mL) at 23 °C was added Dess-Martin periodinane (50.0 mg, 0.118 mmol). The mixture was stirred for 10 min, quenched with a solution of saturated aq. NaHCO_3 and saturated aq. $\text{Na}_2\text{S}_2\text{O}_3$ (1:1, 2 mL), stirred for 10 min, and extracted with EtOAc (4 x 1 mL). The combined organic layers were washed with brine (1 mL), dried by passage over a plug of silica gel (EtOAc eluent), and evaporated under reduced pressure to afford the crude oxidized product, which was used in the subsequent reaction. R_f 0.31 (2:1, hexanes:EtOAc).

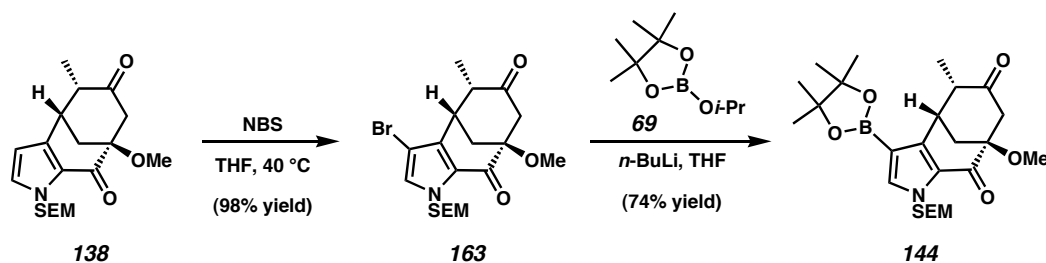
A flask containing the crude oxidized product and 10% Pd/C (10 mg, 0.0094 mmol) in EtOH (2.0 mL) at 23 °C was evacuated and back-filled with H_2 (3x). After 20 min, the reaction mixture was filtered over a Celite plug (EtOAc eluent), and the solvent was evaporated in vacuo. The residue was dissolved in EtOAc (2 mL), and then filtered over a short plug of silica gel (EtOAc eluent). After evaporation of solvent under reduced pressure, the crude material was further purified by preparative thin layer



Allylic Alcohol 139. To [3.3.1] bicycle **98** (45 mg, 0.097 mmol) in THF (3 mL) at 23 °C was added NaH (60% dispersion in mineral oil, 40 mg, 1.0 mmol). After stirring for 2 min at 23 °C, MeI was added (335 μ L, 1.6 mmol). The resulting mixture was stirred for 1 h, and then quenched with saturated aq. NH_4Cl (3 mL). EtOAc (3 mL) and H_2O (3 mL) were added, and the layers were separated. The aqueous layer was further extracted with EtOAc (3 x 4 mL). The combined organic layers were washed with brine (4 mL), dried by passage over a plug of SiO_2 (EtOAc eluent), and evaporated under reduced pressure. The crude product was purified by flash chromatography (7:1

hexanes:EtOAc) to afford methyl ether **162** (40 mg, 86% yield) as a colorless oil. R_f 0.38 (5:1 hexanes:EtOAc).

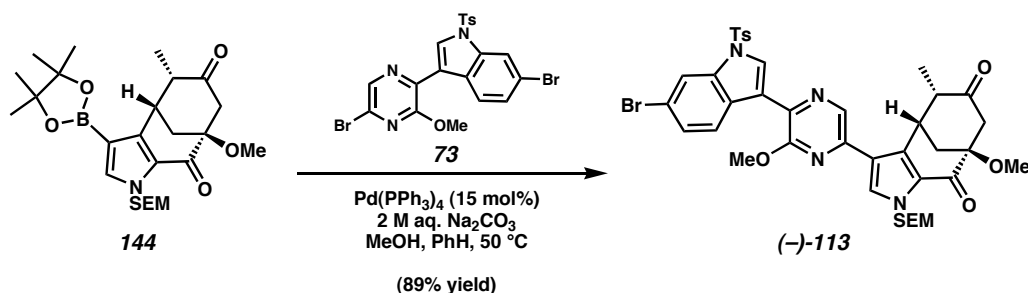
To methyl ether **162** (19 mg, 0.0396 mmol) in THF (1.5 mL) was added TBAF (1.0 M in THF, 75 μ L, 0.075 mmol). The reaction mixture was stirred for 45 min, quenched with saturated aq. NH_4Cl (1 mL), diluted with H_2O (1 mL), and extracted with EtOAc (5 x 1 mL). The combined organic extracts were washed with brine (1 mL), dried by passage over a plug of SiO_2 (EtOAc eluent), and evaporated under reduced pressure. The residue was purified by flash chromatography (1:1 hexanes:EtOAc eluent) to furnish allylic alcohol **139** (12.4 mg, 86% yield) as a pale yellow oil. R_f 0.16 (2:1 hexanes:EtOAc); ^1H NMR (300 MHz, C_6D_6): δ 6.57 (d, $J = 2.4$ Hz, 1H), 5.82 (d, $J = 2.4$ Hz, 1H), 5.58 (d, $J = 10.1$ Hz, 1H), 5.49 (d, $J = 10.1$ Hz, 1H), 5.23-5.18 (m, 1H), 5.00-4.95 (m, 1H), 4.03-3.90 (m, 1H), 3.60-3.51 (comp. m, 3H), 3.32 (s, 3H), 2.61-2.50 (comp. m, 2H), 1.73-1.61 (comp. m, 2H), 1.15 (br s, 1H), 0.87 (t, $J = 8.0$ Hz, 2H), -0.07 (s, 9H); ^{13}C NMR (75 MHz, C_6D_6 , 18/19 C): δ 189.2, 150.1, 139.9, 131.0, 107.9, 106.6, 81.4, 77.0, 67.0, 66.5, 52.0, 46.3, 41.7, 40.9, 18.3, -1.0 (3C); IR (film): 3452 (br), 2951, 1653, 1420, 1250, 1125, 1076 cm^{-1} ; HRMS-EI (m/z): $[\text{M}]^+$ calc'd for $\text{C}_{19}\text{H}_{29}\text{NO}_4\text{Si}$, 363.1866; found, 363.1857; $[\alpha]_{\text{D}}^{23}$ -410.29° (c 1.0, C_6H_6).



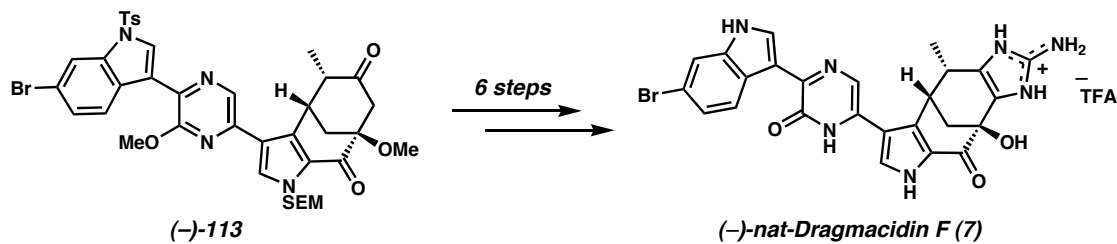
Boronic Ester 144. A flask wrapped in aluminum foil at 23 °C was charged with ketone **138** (25 mg, 0.0689 mmol), THF (5 mL), and freshly recrystallized NBS (37.5 mg, 0.211 mmol). The reaction vessel was placed in a 40 °C oil bath, stirred for 15 min, then cooled to 0 °C. The reaction was quenched with saturated aq. $\text{Na}_2\text{S}_2\text{O}_3$ (10 mL), diluted with H_2O (5 mL), and extracted with Et_2O (3 x 20 mL). The combined organic layers were washed with brine (15 mL), dried over MgSO_4 , and evaporated under reduced pressure to afford the crude product. Further purification by flash column chromatography (3:1 hexanes:EtOAc eluent) afforded bromide **163** (29.9 mg, 98% yield) as a colorless oil. R_f 0.45 (2:1 hexanes:EtOAc).

To bromide **163** (27 mg, 0.061 mmol) and 2-isopropoxy-4,4,5,5-tetramethyl-1,3,2-dioxaborolane (**69**, 510 μL , 2.5 mmol) in THF (7 mL) at -78 °C was added $n\text{-BuLi}$ (2.5 M in hexanes, 730 μL , 0.183 mmol) dropwise over 3 min. After stirring for an additional 10 min at -78 °C, the reaction mixture was quenched with saturated aq. NH_4Cl (7 mL), warmed to 23 °C, diluted with H_2O (10 mL), and extracted with EtOAc (3 x 20 mL). The combined organic layers were washed with brine (15 mL), dried over MgSO_4 and evaporated under reduced pressure to afford the crude product. Further purification by flash column chromatography (3:1 hexanes:EtOAc eluent) afforded boronic ester **144** (22 mg, 74% yield) as a colorless oil. R_f 0.42 (2:1 hexanes:EtOAc); ^1H NMR (300 MHz, C_6D_6): δ 7.37 (s, 1H), 5.46 (d, J = 10.2 Hz, 1H), 5.33 (d, J = 10.2 Hz, 1H), 3.77-3.72 (m,

1H), 3.49-3.38 (m, 2H), 3.31 (s, 3H), 3.03 (dd, $J = 14.0, 2.8$ Hz, 1H), 2.61-2.53 (m, 1H), 2.47 (d, $J = 13.8$ Hz, 1H), 2.36-2.25 (m, 1H), 1.78 (dd, $J = 12.4, 3.0$ Hz, 1H), 1.24 (d, $J = 6.6$ Hz, 3H), 1.12 (s, 12H), 0.84-0.77 (m, 2H), -0.05 (s, 9H); ^{13}C NMR (125 MHz, C_6D_6 , 23/25 °C): δ 206.4, 188.3, 144.6, 140.0, 83.6 (2C), 83.1, 77.1, 66.5, 52.9, 52.3, 49.0, 41.4, 37.1, 25.3 (2C), 25.2 (2C), 18.3, 13.0, -0.9 (3C); IR (film) 2977, 2951, 1718, 1664, 1543, 1399, 1322, 1263, 1145, 1092, 1074; HRMS-FAB (m/z): $[\text{M} + \text{H}]^+$ calc'd for $\text{C}_{25}\text{H}_{41}\text{NO}_6\text{SiB}$, 490.2796; found, 490.2800; $[\alpha]_{\text{D}}^{29} +50.77^\circ$ (c 0.4, C_6H_6).



Pyrazine (-)-113. A vial charged with bromopyrazine **73** (29.6 mg, 0.055 mmol), boronic ester **144** (18 mg, 0.0368 mmol), and tetrakis(triphenylphosphine)palladium(0) (6.4 mg, 0.0055 mmol) was evacuated and purged with N_2 . Deoxygenated benzene (735 μL), deoxygenated methanol (150 μL), and deoxygenated 2 M aq. Na_2CO_3 (61 μL) were then added. The reaction vessel was sealed, heated to 50 °C for 72 h, cooled to 23 °C, then quenched by the addition of Na_2SO_4 (200 mg). Following filtration over a pad of silica gel (3:1 EtOAc:hexanes eluent) and evaporation to dryness under reduced pressure, the residue was purified by flash column chromatography (2:1 \rightarrow 1:1 hexanes:EtOAc eluent) to afford pyrazine **(-)-113** (26.8 mg, 89% yield) as a yellow foam. R_f , ^1H NMR, ^{13}C NMR, HRMS, and IR characterization data for **(+)-113** are reported earlier in this section. $[\alpha]_{\text{D}}^{27} -72.92^\circ$ (c 1.0, CHCl_3).



(-)-Dragmacidin F (7). Pyrazine **(-)-113** was converted to **(-)-dragmacidin F (7)** by methods described earlier in this section. ^1H NMR, ^{13}C NMR, HRMS, and IR characterization data for **(+)-7** are also reported above. $[\alpha]_{\text{D}}^{29} -148.33^\circ$ (c 0.20, MeOH). For comparison, natural **(-)-dragmacidin F (7)**: $[\alpha]_{\text{D}}^{25} -159^\circ$ (c 0.40, MeOH).^{1b}

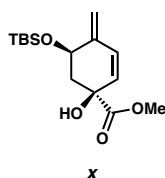
3.7 Notes and References

- (1) (a) Wright, A. E.; Pomponi, S. A.; Jacobs, R. S. PCT Int. Appl. WO 9942092 August 26, 1999. (b) Cutignano, A.; Bifulco, G.; Bruno, I.; Casapullo, A.; Gomez-Paloma, L.; Riccio, R. *Tetrahedron* **2000**, *56*, 3743-3748.
- (2) Portions of this work have been published, see: (a) Garg, N. K.; Caspi, D. D.; Stoltz, B. M. *J. Am. Chem. Soc.* **2004**, *126*, 9552-9553. (b) Garg, N. K.; Caspi, D. D.; Stoltz, B. M. *J. Am. Chem. Soc.* **2005**, *127*, *in press*.
- (3) For recent reviews of the Heck reaction, see: (a) Dounay, A. B.; Overman, L. E. *Chem. Rev.* **2003**, *103*, 2945-2963. (b) Beletskaya, I. P.; Cheprakov, A. V. *Chem. Rev.* **2000**, *100*, 3009-3066. (c) Amatore, C.; Jutand, A. *J. Organomet. Chem.* **1999**, *576*, 254-278.
- (4) For related examples of Pd-mediated carbocyclizations in natural product synthesis, see: (a) Baran, P. S.; Corey, E. J. *J. Am. Chem. Soc.* **2002**, *124*, 7904-7905. (b) Williams, R. M.; Cao, J.; Tsujishima, H.; Cox, R. J. *J. Am. Chem. Soc.* **2003**, *125*, 12172-12178.
- (5) (a) Stoltz, B. M. *Chem. Lett.* **2004**, *33*, 362-367. (b) Trend, R. M.; Ramtohl, Y. K.; Ferreira, E. M.; Stoltz, B. M. *Angew. Chem., Int. Ed.* **2003**, *42*, 2892-2895. (c)

- Ferreira, E. M.; Stoltz, B. M. *J. Am. Chem. Soc.* **2003**, *125*, 9578-9579. d) Zhang, H.; Ferreira, E. M.; Stoltz, B. M. *Angew. Chem., Int. Ed.* **2004**, *43*, 6144-6148.
- (6) For reviews and examples regarding the use of (–)-quinic acid in natural product synthesis, see: (a) Barco, A.; Benetti, S.; De Risi, C.; Marchetti, P.; Pollini, G. P.; Zanirato, V. *Tetrahedron: Asymmetry* **1997**, *8*, 3515-3545. (b) Huang, P.-Q. *Youji Huaxue* **1999**, *19*, 364-373. (c) Hanessian, S.; Pan, J.; Carnell, A.; Bouchard, H.; Lesage, L. *J. Org. Chem.* **1997**, *62*, 465-473. (d) Hanessian, S. In *Total Synthesis of Natural Products: The "Chiron" Approach*, Baldwin, E. J., Ed.; Pergamon Press: Oxford, 1983; pp 206-208.
- (7) (a) Philippe, M.; Sepulchre, A. M.; Gero, S. D.; Loibner, H.; Streicher, W.; Stutz, P. *J. Antibiot.* **1982**, *35*, 1507-1512. (b) Manthey, M. K.; González-Bello, C.; Abell, C. *J. Chem. Soc., Perkin Trans. I* **1997**, 625-628.
- (8) For a review, see: Tsuji, J.; Mandai, T. *Synthesis* **1996**, 1-24.
- (9) Greene, T. W.; Wuts, P. G. M. *Protective Groups in Organic Synthesis*, 3rd Ed.; Wiley-Interscience: New York, 1999.
- (10) Despite its widespread use in modern cross-coupling chemistry, to the best of our knowledge, this is the first report of Pd(P(*t*-Bu)₃)₂ being used for a π -allyl

palladium substitution reaction. For recent examples of $\text{Pd}(\text{P}(t\text{-Bu})_3)_2$ in cross-coupling reactions, see: Hills, I. D.; Fu, G. C. *J. Am. Chem. Soc.* **2004**, *126*, 13178-13179 and references therein.

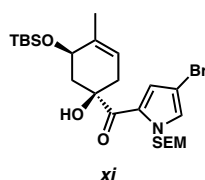
- (11) For the use of NMO as an additive in Stille couplings, see: Han, X.; Stoltz, B. M.; Corey, E. J. *J. Am. Chem. Soc.* **1999**, *121*, 7600-7605.
- (12) Under certain conditions, we were able to produce **108** as a mixture of diastereomers. However, upon exposure of **108** to Pd/C and H_2 in MeOH, no reaction took place.
- (13) Treatment of **105** under a variety of standard homogeneous π -allyl reduction conditions⁸ led to the formation of **106**, **107**, and **x**, all of which presumably arise from loss of OAc^- . In stark contrast, exposure of **105** to heterogeneous reductive isomerization conditions did not produce any of these compounds (see Scheme 3.4.2).



- (14) For the discovery and use of SEM pyrrole, see: (a) Edwards, M. P.; Ley, S. V.; Lister, S. G.; Palmer, B. D. *J. Chem. Soc., Chem. Commun.* **1983**, 630-633. (b)

Muchowski, J. M.; Solas, D. R. *J. Org. Chem.* **1984**, *49*, 203-205. (c) Edwards, M. P.; Ley, S. V.; Lister, S. G.; Palmer, B. D.; Williams, D. J. *J. Org. Chem.* **1984**, *49*, 3503-3516. (d) Edwards, M. P.; Doherty, A. M.; Ley, S. V.; Organ, H. M. *Tetrahedron* **1986**, *42*, 3723-3729.

- (15) During the conversion of **109** to **99**, pyrrole **xi** was formed as a byproduct.

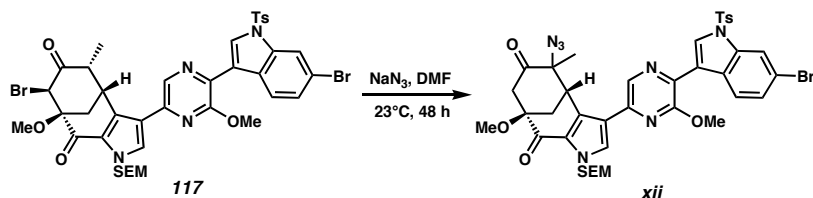


- (16) Littke, A. F.; Fu, G. C. *J. Am. Chem. Soc.* **2001**, *123*, 6989-7000.
- (17) By conducting reactions in THF-*d*₈, it was possible to monitor Heck reactions by ¹H NMR.
- (18) DMSO has commonly been employed in oxidative Pd(II) chemistry. See: (a) Larock, R. C.; Hightower, T. R. *J. Org. Chem.* **1993**, *58*, 5298-5300. (b) Van Benthem, R. A. T. M.; Hiemstra, H.; Michels, J. J.; Speckamp, W. N. *J. Chem. Soc., Chem. Commun.* **1994**, 357-359. (c) Rönn, M.; Bäckvall, J.-E.; Andersson, P. G. *Tetrahedron Lett.* **1995**, *36*, 7749-7752. (d) Chen, M. S.; White, M. C. *J. Am. Chem. Soc.* **2004**, *126*, 1346-1347. (e) Stahl, S. S. *Angew. Chem., Int. Ed.* **2004**, *43*, 3400-3420. See also references therein.

- (19) Gilow, H. M.; Hong, Y. H.; Millirons, P. L.; Snyder, R. C.; Casteel, W. J., Jr. *J. Heterocycl. Chem.* **1986**, *23*, 1475-1480.
- (20) Reactions conducted in the presence of acetic acid-*d* led to deuterium incorporation in the pyrrole ring of both **100** and **98**, mostly at C(4).
- (21) The instability of pyrroles to oxidants is well known. See: (a) Ciamician, G.; Silber, P. *Chem. Ber.* **1912**, *45*, 1842-1845. (b) Bernheim, F.; Morgan, J. E. *Nature* **1939**, *144*, 290. (c) Chierici, L.; Gardini, G. P. *Tetrahedron* **1966**, *22*, 53-56.
- (22) The Heck route required the use of 2,3-dibromopyrrole, an extremely unstable compound. For a discussion regarding the instability of bromopyrroles, see: Audebert, P.; Bidan, G. *Synthetic Metals* **1986**, *15*, 9-22.
- (23) In preliminary investigations, late-stage chemistry in the presence of a reactive 3° alcohol was unsuccessful.
- (24) (a) Rathore, R.; Kochi, J. K. *J. Org. Chem.* **1996**, *61*, 627-639. (b) Elfehail, F. E.; Zajac, W. W., Jr. *J. Org. Chem.* **1981**, *46*, 5151-5155. (c) Elfehail, F.; Dampawan, P.; Zajac, W. *Synth. Commun.* **1980**, *10*, 929-932. (d) Fischer, R. H.; Weitz, H. M. *Synthesis* **1980**, 261-282.

(25) Kreiser, W.; Körner, F. *Helv. Chim. Acta* **1999**, 82, 1610-1629.

(26) For example, upon treatment of bromoketone **117** with NaN_3 , azidoketone **xii** formed as the major product.



(27) (a) Favorskii, A. E. *J. Russ. Phys. Chem. Soc.* **1894**, 26, 559. (b) Chenier, P. J. *J. Chem. Ed.* **1978**, 55, 286-291.

(28) Neber, P. W.; Friedolsheim, A. V. *Justus Liebigs Ann. Chem.* **1926**, 449, 109-134.

(29) (a) For a review, see: O'Brien, C. *Chem. Rev.* **1964**, 64, 81-89. (b) For a recent study involving the Neber rearrangement, see: Ooi, T.; Takahashi, M.; Doda, K.; Maruoka, K. *J. Am. Chem. Soc.* **2002**, 124, 7640-7641.

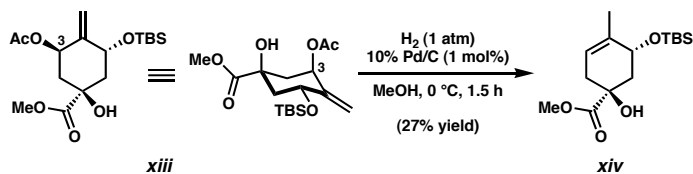
(30) (a) Purified by reversed-phase chromatography using trifluoroacetic acid in the eluent. (b) See Section 3.6 for details.

- (31) Derivatives of **119** bearing a free 3° alcohol or a TMS-protected 3° alcohol produced complex mixtures of products when subjected to Neber rearrangement conditions.
- (32) Acid-promoted dimerization of the aminoketone functionalities was not observed.
- (33) (a) Woodward reported a Neber rearrangement during synthetic studies involving lysergic acid. Unfortunately, the Neber rearrangement product could not be further utilized in the synthesis. See: Kornfeld, E. C.; Fornefeld, E. J.; Kline, G. B.; Mann, M. J.; Morrison, D. E.; Jones, R. G.; Woodward, R. B. *J. Am. Chem. Soc.* **1956**, 78, 3087-3114. (b) For the use of the Neber rearrangement in the synthesis of a pharmaceutical substance, see: Chung, J. Y. L.; Ho, G.-J.; Chartrain, M.; Roberge, C.; Zhao, D.; Leazer, J.; Farr, R.; Robbins, M.; Emerson, K.; Mathre, D. J.; McNamara, J. M.; Hughes, D. L.; Grabowski, E. J. J.; Reider, P. J. *Tetrahedron Lett.* **1999**, 40, 6739-6743.
- (34) The intermediacy of azirines in Neber rearrangements is well accepted. These azirines presumably arise from transient nitrenes. See: (a) House, H. O.; Berkowitz, W. F. *J. Org. Chem.* **1963**, 28, 307-311. (b) House, H. O.; Berkowitz, W. F. *J. Org. Chem.* **1963**, 28, 2271-2276.
- (35) Hemiaminal **123** has been isolated and characterized by ¹H NMR.

- (36) Boehm, J. C.; Gleason, J. G.; Pendrak, I.; Sarau, H. M.; Schmidt, D. B.; Foley, J. J.; Kingsbury, W. D. *J. Med. Chem.* **1993**, *36*, 3333-3340.
- (37) Dragmacidin numbering convention, see reference 1b.
- (38) (a) (+)-Quinic acid ((+)-**101**) is commercially available in limited quantities from Interbioscreen Ltd. (50 mg/\$305 USD). (b) (+)-Quinic acid ((+)-**101**) potentially could be prepared via multistep synthesis by applying methods used for the preparation of (–)-quinic acid (**101**). See: Rapado, L. P.; Bulugahapitiya, V.; Renaud, P. *Helv. Chim. Acta* **2000**, *83*, 1625-1632 and references therein.
- (39) Surprisingly, despite its widespread use in natural product synthesis and its near symmetry, (–)-quinic acid (**101**) has rarely been used in an enantiodivergent manner. For examples, see: (a) Ulibarri, G.; Nadler, W.; Skrydstrup, T.; Audrain, H.; Chiaroni, A.; Riche, C.; Grierson, D. S. *J. Org. Chem.* **1995**, *60*, 2753-2761. (b) Ulibarri, G.; Audrain, H.; Nadler, W.; Lhermitte, H.; Grierson, D. S. *Pure Appl. Chem.* **1996**, *68*, 601-604. (c) Barros, M. T.; Maycock, C. D.; Ventura, M. R. *J. Chem. Soc., Perkin Trans. 1* **2001**, 166-173.
- (40) If $R = R'$, **125** is considered to be pseudo- C_2 -symmetric. Pseudo- C_2 -symmetric molecules are those that would be C_2 -symmetric if they did not contain a central chirotopic, nonstereogenic center. For discussions, see: (a) Schreiber, S. L. *Chem.*

Scr. **1987**, 27, 563-566. (b) Poss, C. S.; Schreiber, S. L. *Acc. Chem. Res.* **1994**, 27, 9-17. (c) Magnuson, S. R. *Tetrahedron* **1995**, 51, 2167-2213. (d) Eliel, E. L.; Wilen, S. H.; Mander, L. N. *Stereochemistry of Organic Compounds*; Wiley-Interscience: New York, 1994.

- (41) Olefin **105** was also exposed to the reaction conditions used for the reductive isomerization of **103** to **104**. Only trace quantities of **128** were produced under those conditions.^{30b,42b}
- (42) (a) Yield determined based on ¹H NMR integration. (b) The material isolated was predominantly a mixture of diastereomeric olefin hydrogenation products.
- (43) The favored conformation of **105** depicted in Scheme 3.4.2 is consistent with NMR studies.^{30b}
- (44) Derivatives of **105** bearing C(3)-acetoxy groups (conformationally flexible and good leaving group) were also poor substrates in the reductive isomerization reaction as shown below (**xiii** → **xiv**).^{42a} The conformation of **xiii** was established by NMR studies.



- (45) NMR experiments show that the C(3) silyl ether of **131** is axially disposed.^{30b} For similar examples of axial-selective TBS cleavage promoted by TBAF, see: (a) Craig, B. N.; Janssen, M. U.; Wickersham, B. M.; Rabb, D. M.; Chang, P. S.; O'Leary, D. J. *J. Org. Chem.* **1996**, *61*, 9610-9613. (b) Meier, R.-M.; Tamm, C. *Helv. Chim. Acta*, **1991**, *74*, 807-818.
- (46) For a classic example involving the use of conformational analysis to solve stereochemical problems in total synthesis, see: Woodward, R. B.; Bader, F. E.; Bickel, H.; Frey, A. J.; Kierstead, R. W. *Tetrahedron* **1958**, *2*, 1-57.
- (47) Heating reactions above 50 °C led to mixtures of products involving partial and complete cleavage of the SEM and TBS groups.
- (48) (a) Brown, J. M. *Angew. Chem., Int. Ed. Engl.* **1987**, *26*, 190-203. (b) Bergens, S. H.; Bosnich, B. *J. Am. Chem. Soc.* **1991**, *113*, 958-967.
- (49) Xiao, W. *Huaxue Shiji* **1992**, *14*(6), 363-366.
- (50) Bailey, D. M.; Johnson, R. E. *J. Med. Chem.* **1973**, *16*, 1300-1302.
- (51) Claridge, T. D. W. In *High-Resolution NMR Techniques in Organic Chemistry*; Pergamon: Amsterdam, 1999; pp 320-326.

APPENDIX THREE

Synthetic Summary for (+)- and (-)-Dragmacidin F (7)

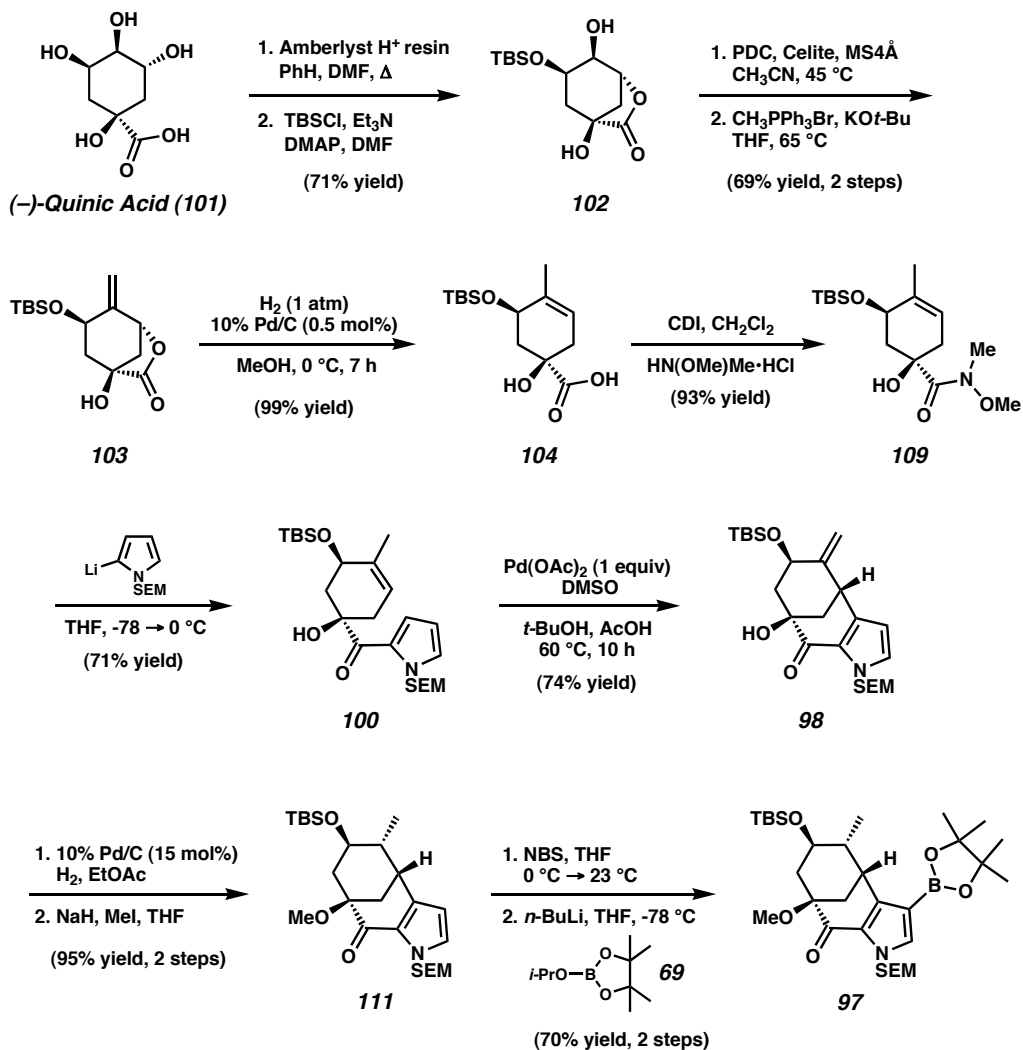
Figure A3.1 The synthesis of boronic ester **97**.

Figure A3.2 The synthesis of (+)-dragmacidin F (7).

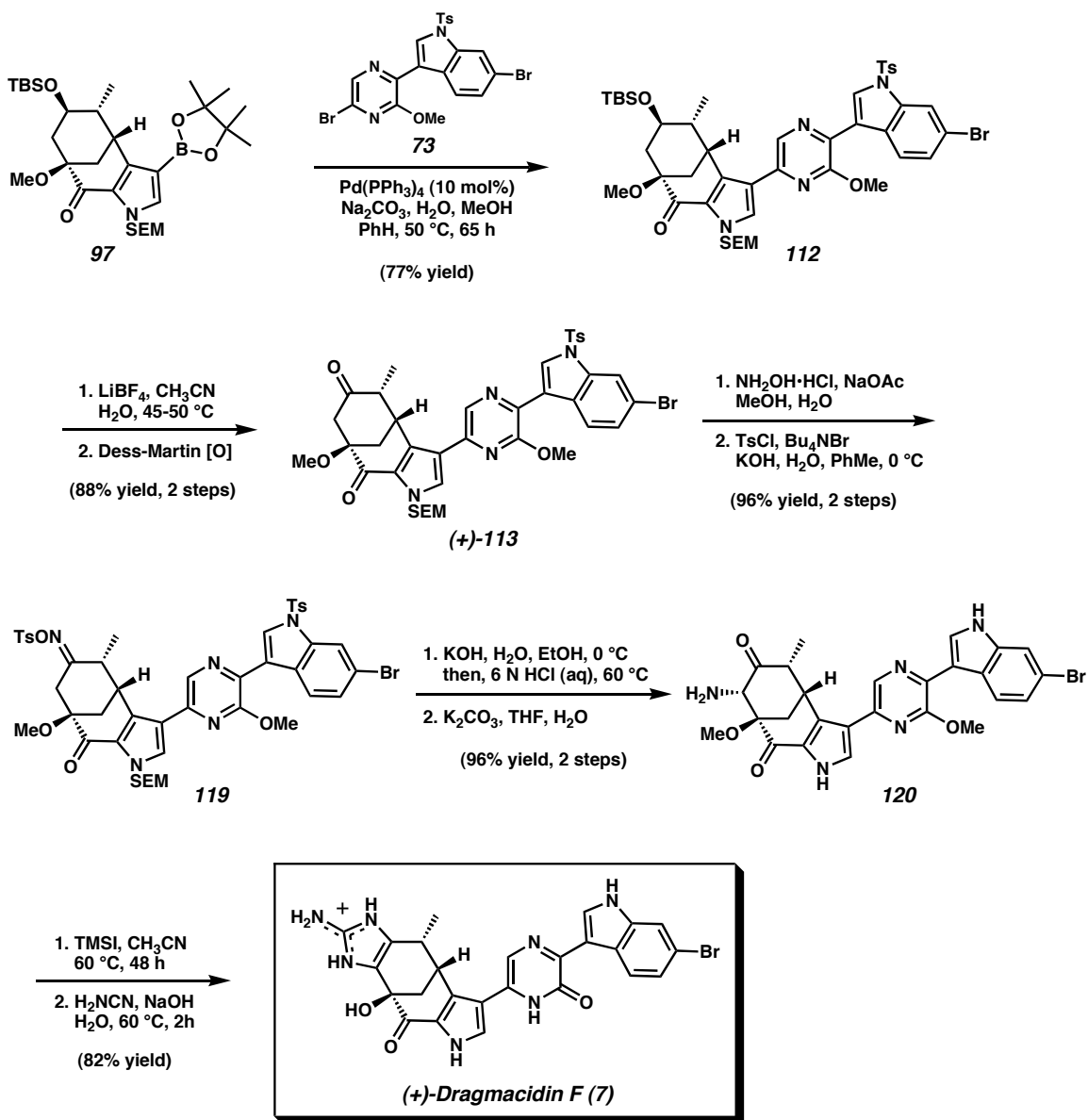
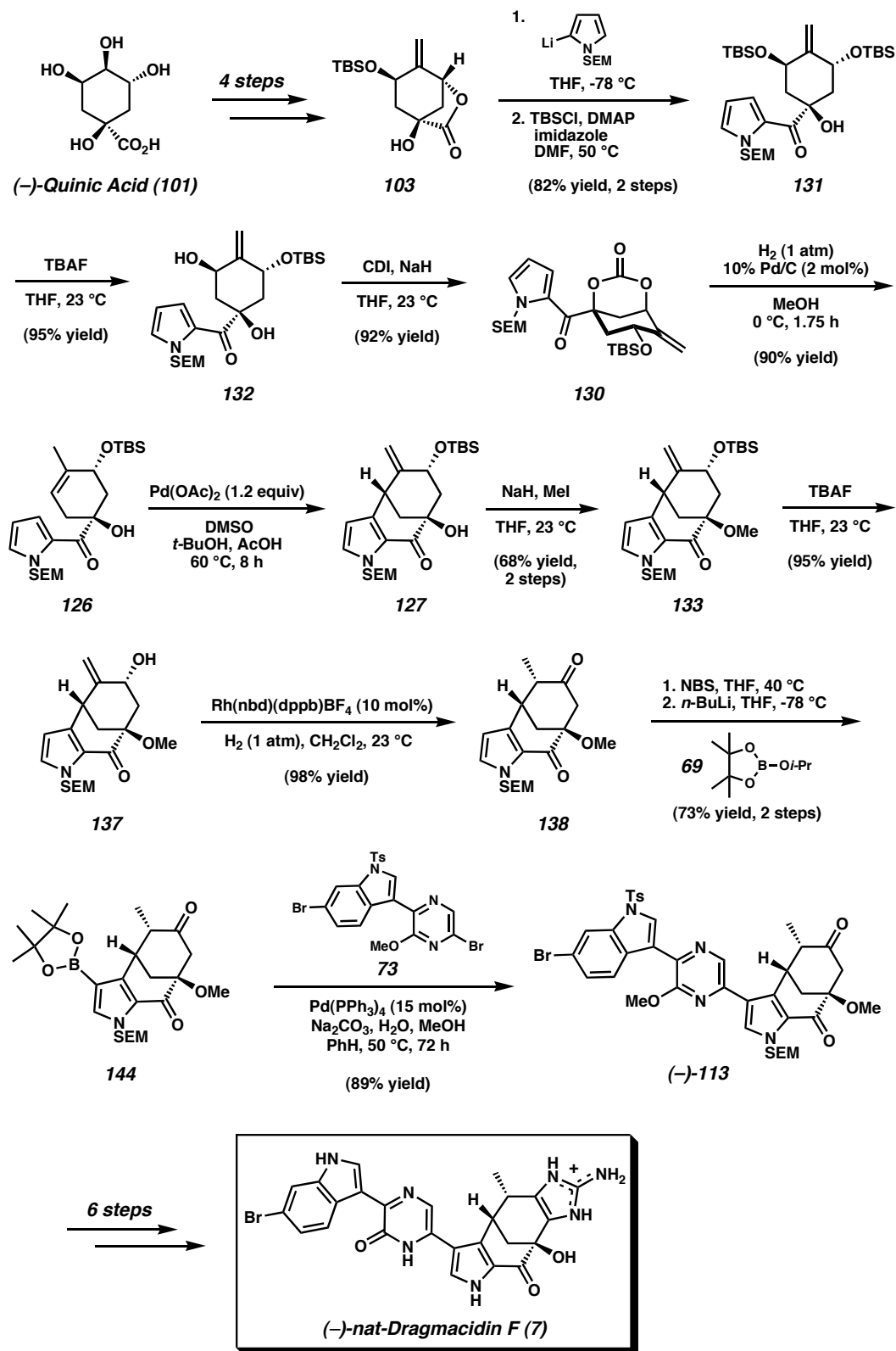


Figure A3.3 The synthesis of (–)-dragmacidin F (7).



APPENDIX FOUR

Spectra Relevant to Chapter Three:

The Total Synthesis of (+)- and (–)-Dragmacidin F



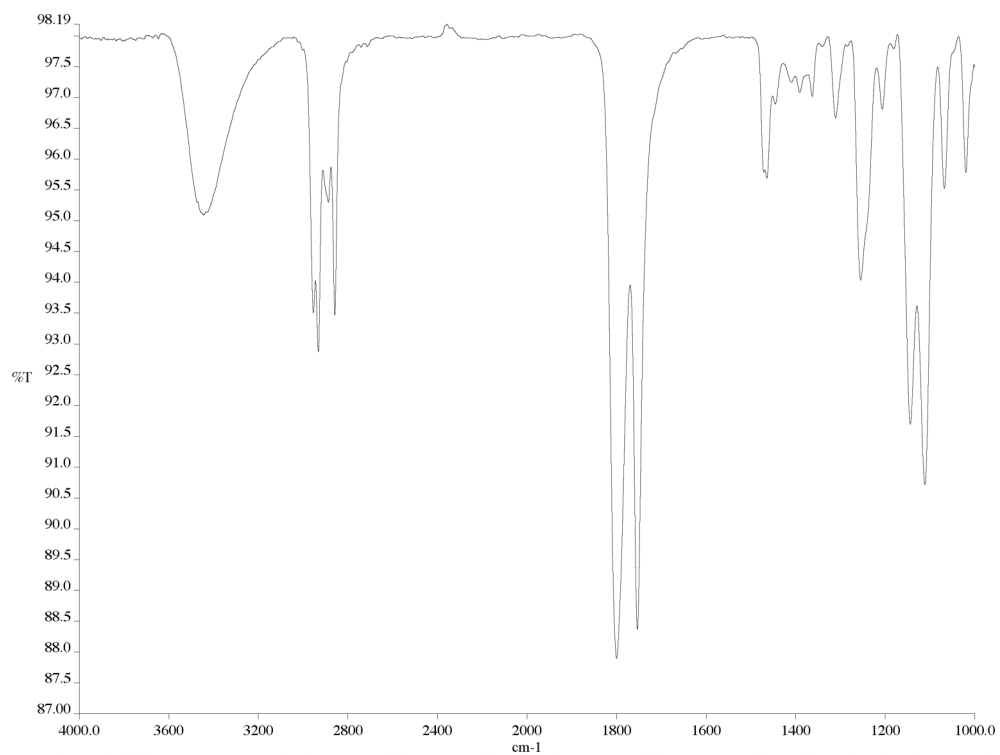


Figure A4.2 Infrared spectrum (thin film/NaCl) of compound **146**.

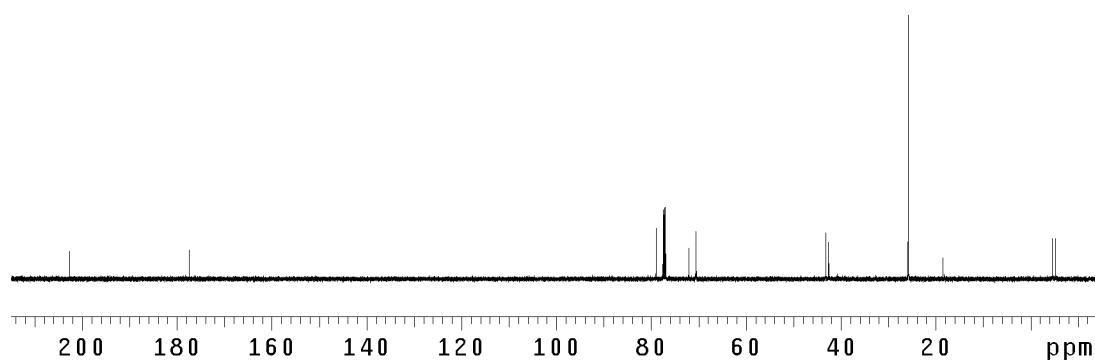


Figure A4.3 ¹³C NMR (75 MHz, CDCl₃) of compound **146**.

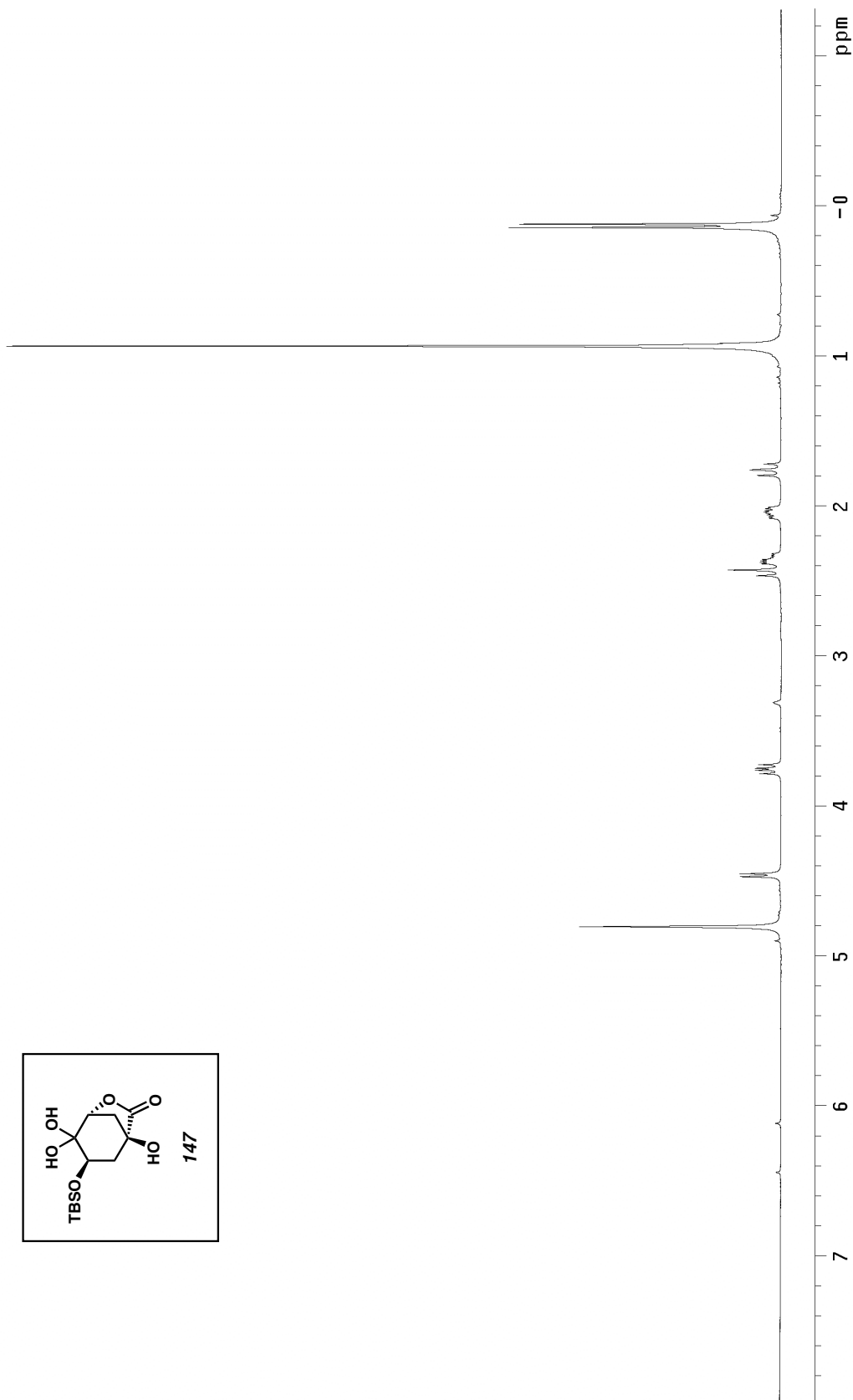


Figure A4.4 ^1H NMR (300 MHz, CD_3OD) of compound **147**.

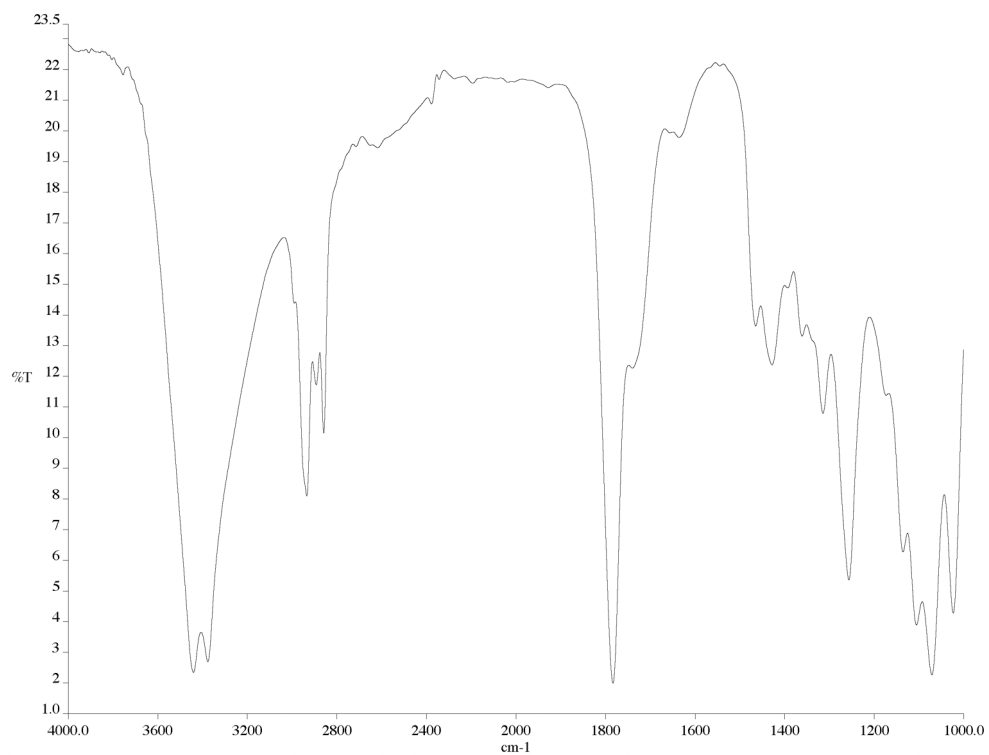


Figure A4.5 Infrared spectrum (thin film/NaCl) of compound **147**.

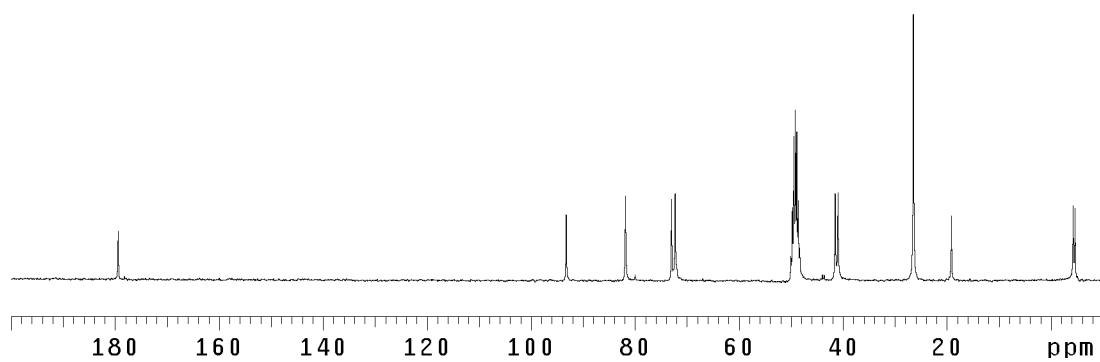


Figure A4.6 ¹³C NMR (75 MHz, CD₃OD) of compound **147**.

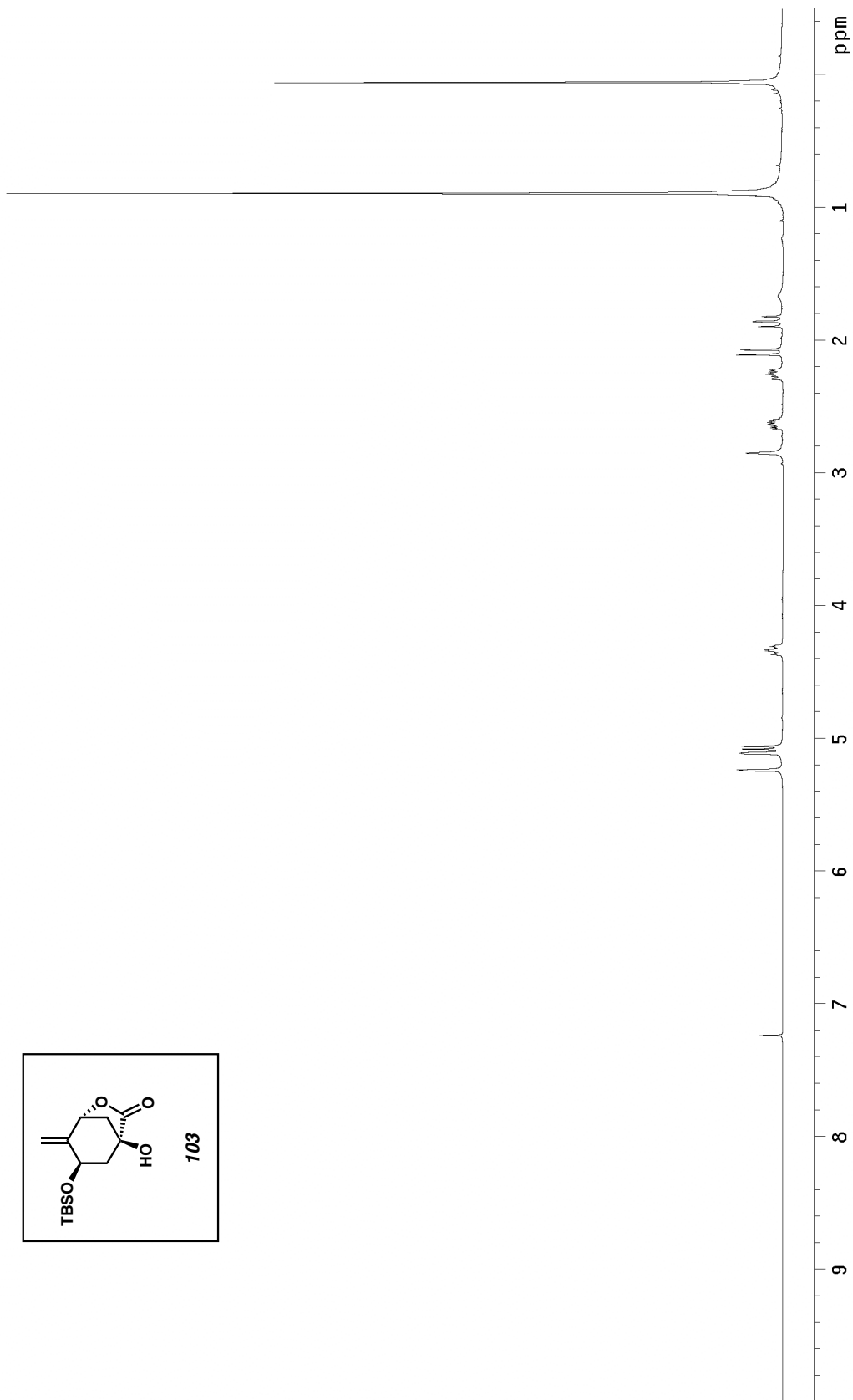
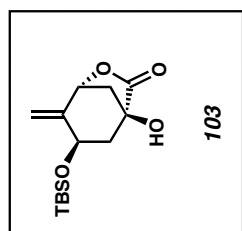


Figure A4.7 ^1H NMR (300 MHz, CDCl_3) of compound **103**.

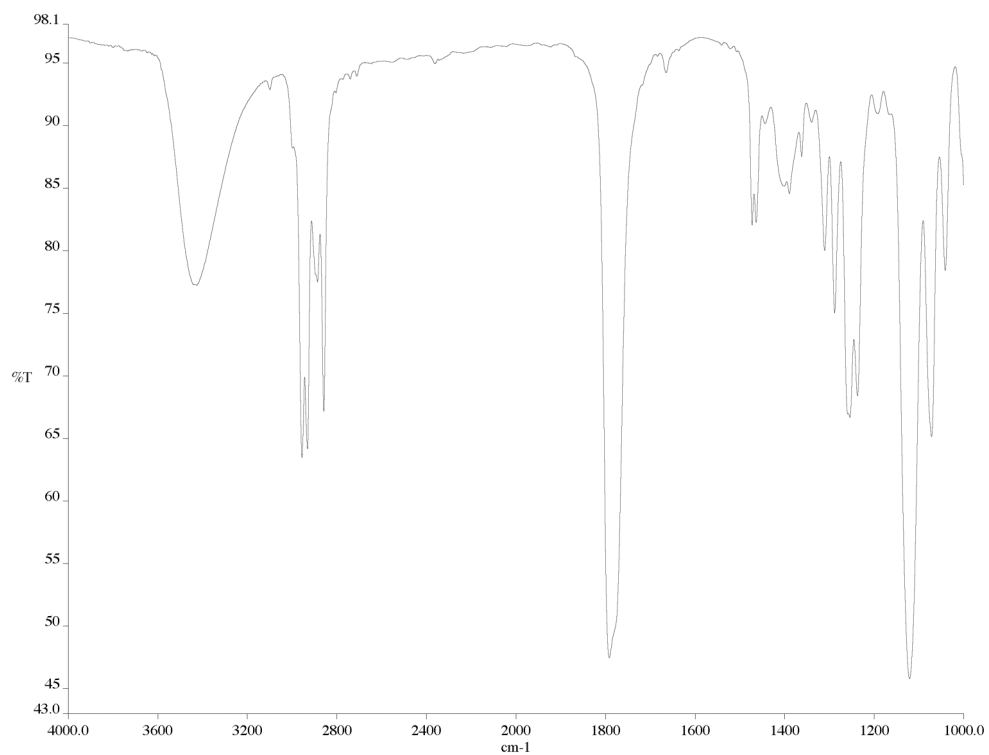


Figure A4.8 Infrared spectrum (thin film/NaCl) of compound **103**.

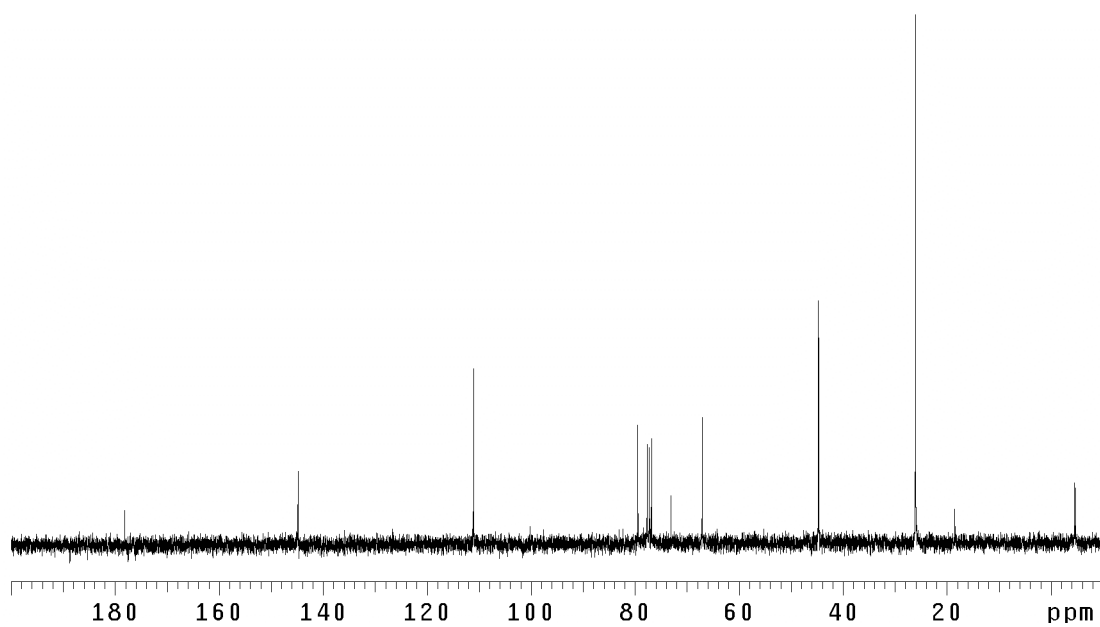


Figure A4.9 ¹³C NMR (75 MHz, CDCl₃) of compound **103**.

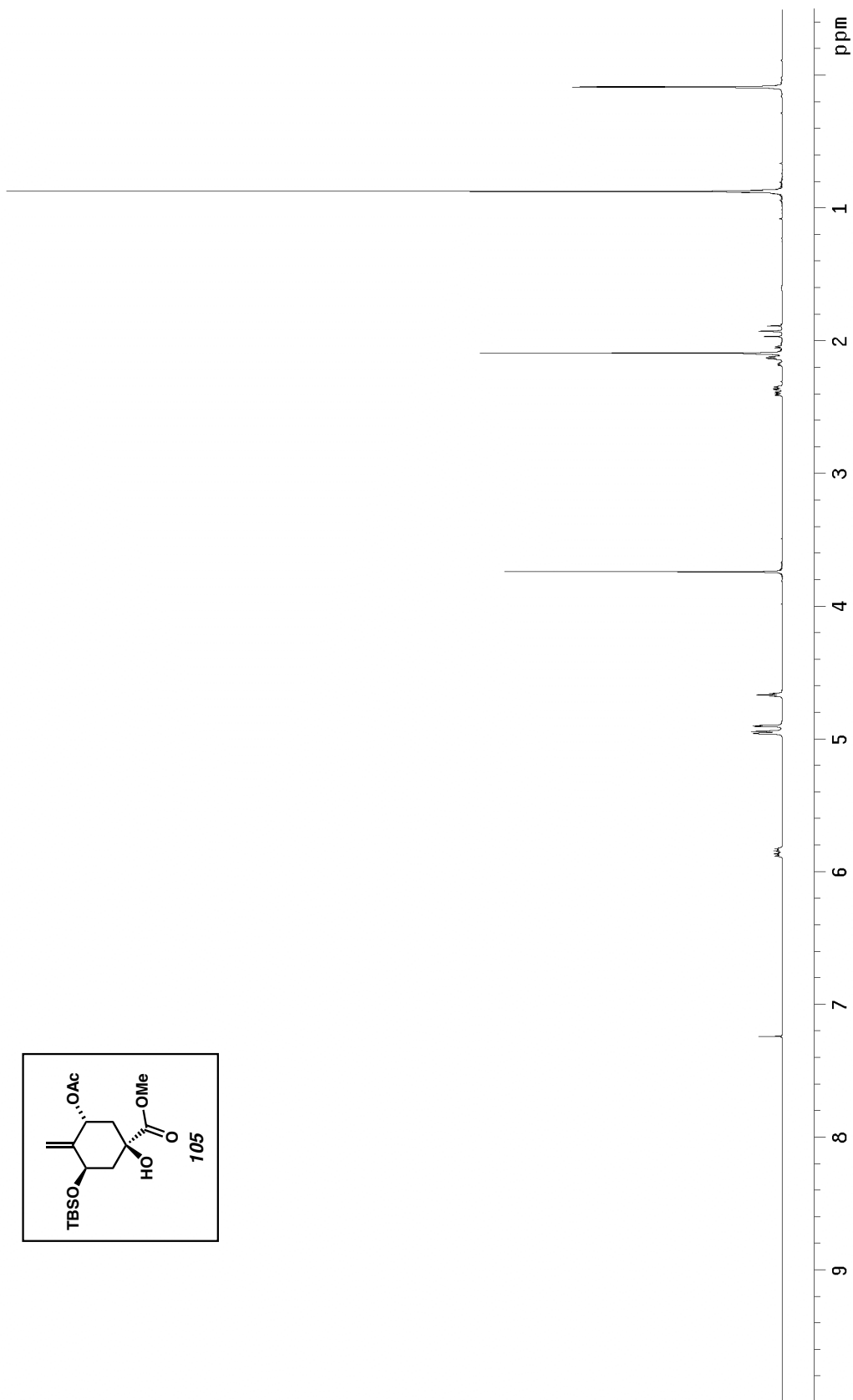
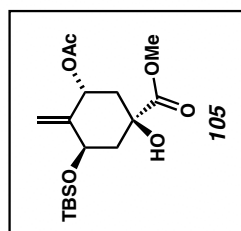


Figure A4.10 ¹H NMR (300 MHz, CDCl₃) of compound **105**.

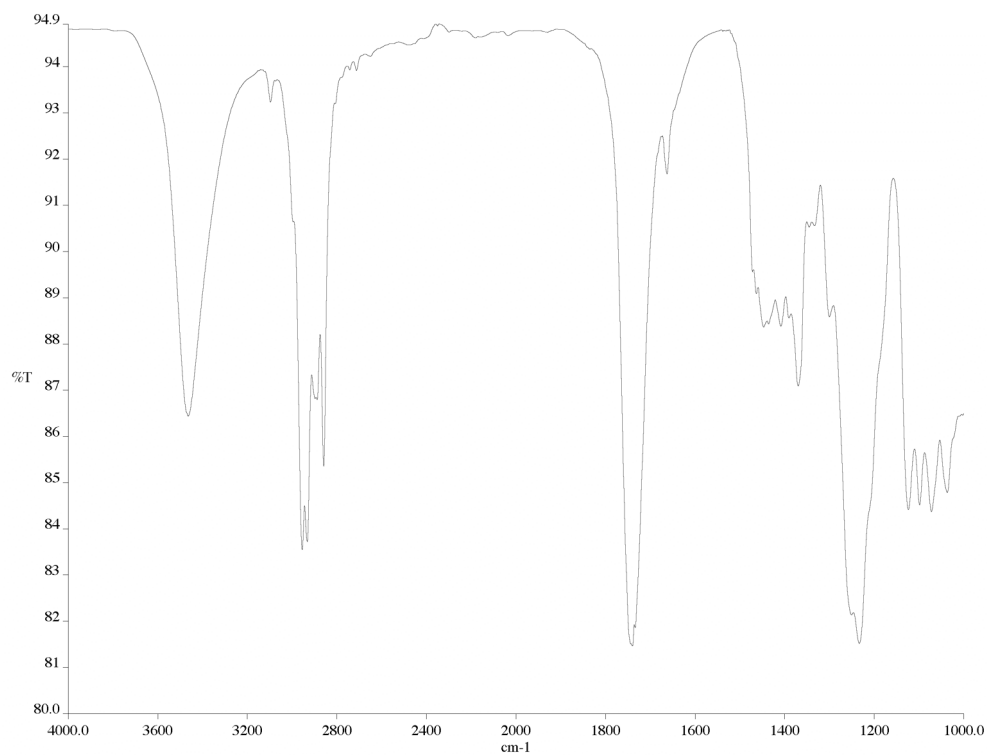


Figure A4.11 Infrared spectrum (thin film/NaCl) of compound **105**.

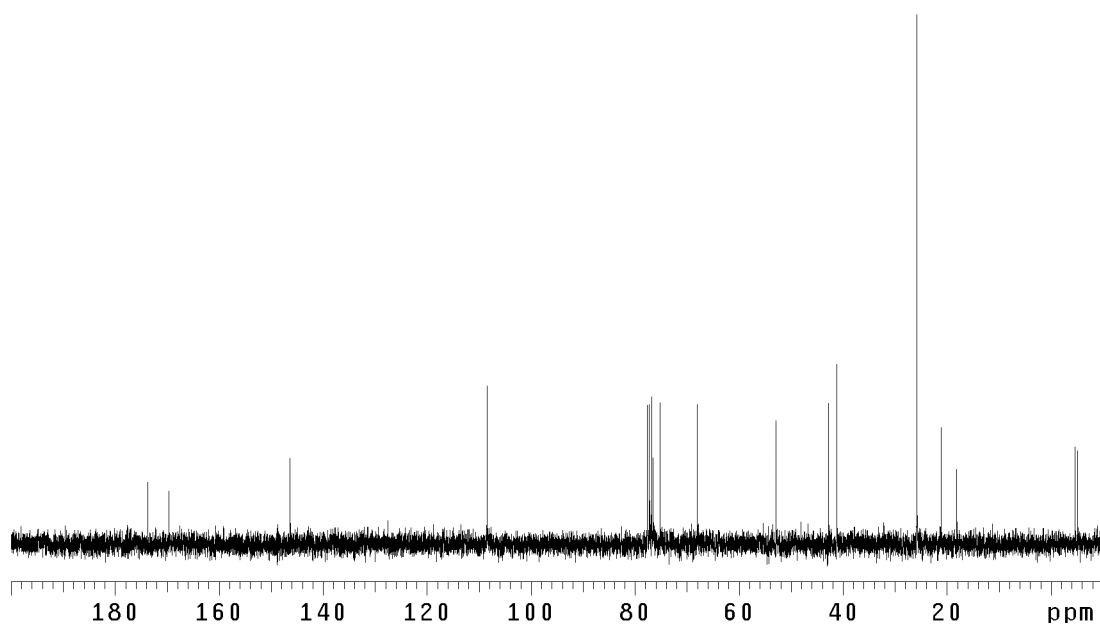


Figure A4.12 ¹³C NMR (75 MHz, CDCl₃) of compound **105**.

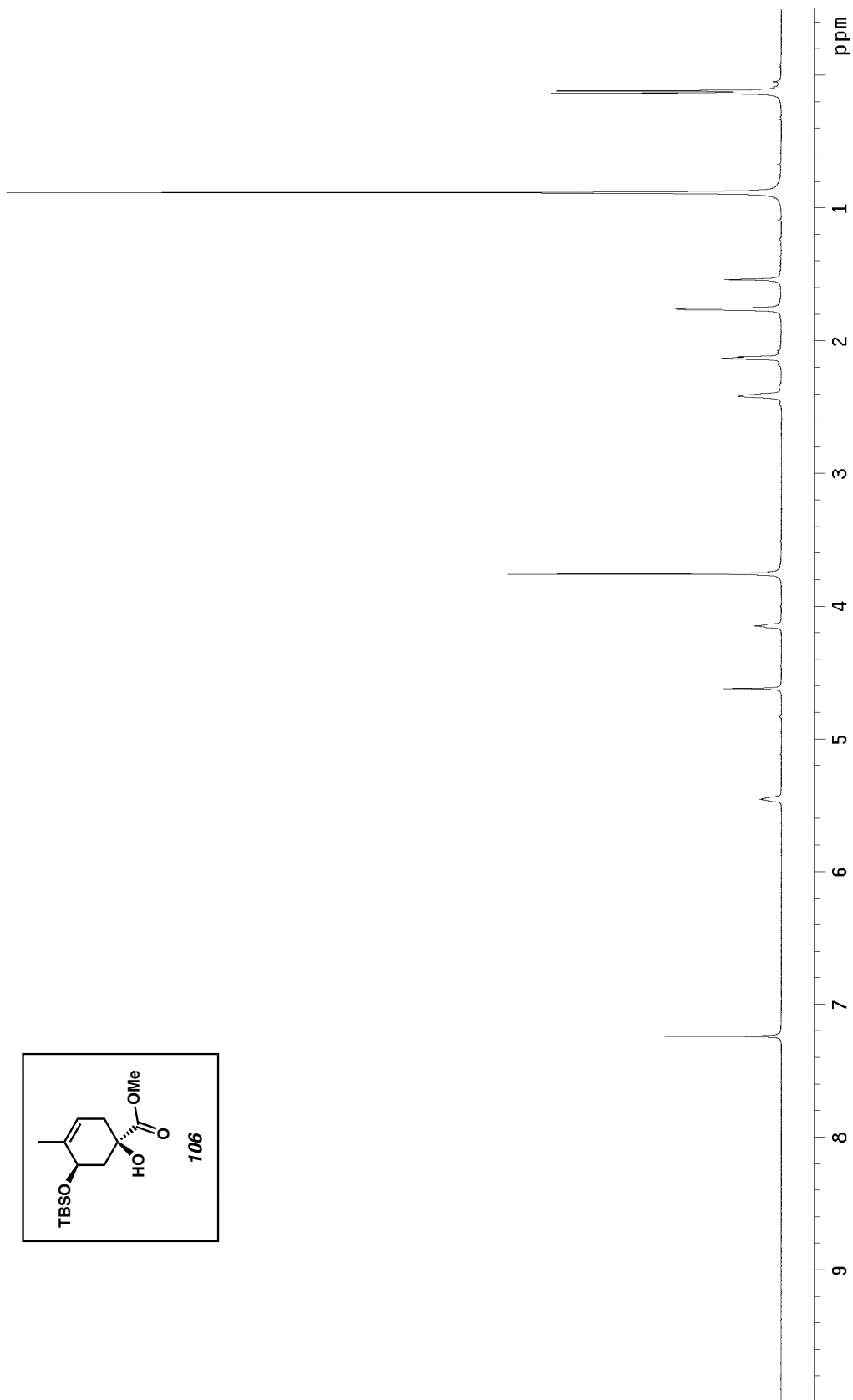
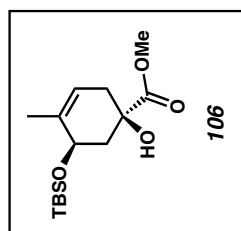


Figure A4.13 ¹H NMR (300 MHz, CDCl₃) of compound **106**.

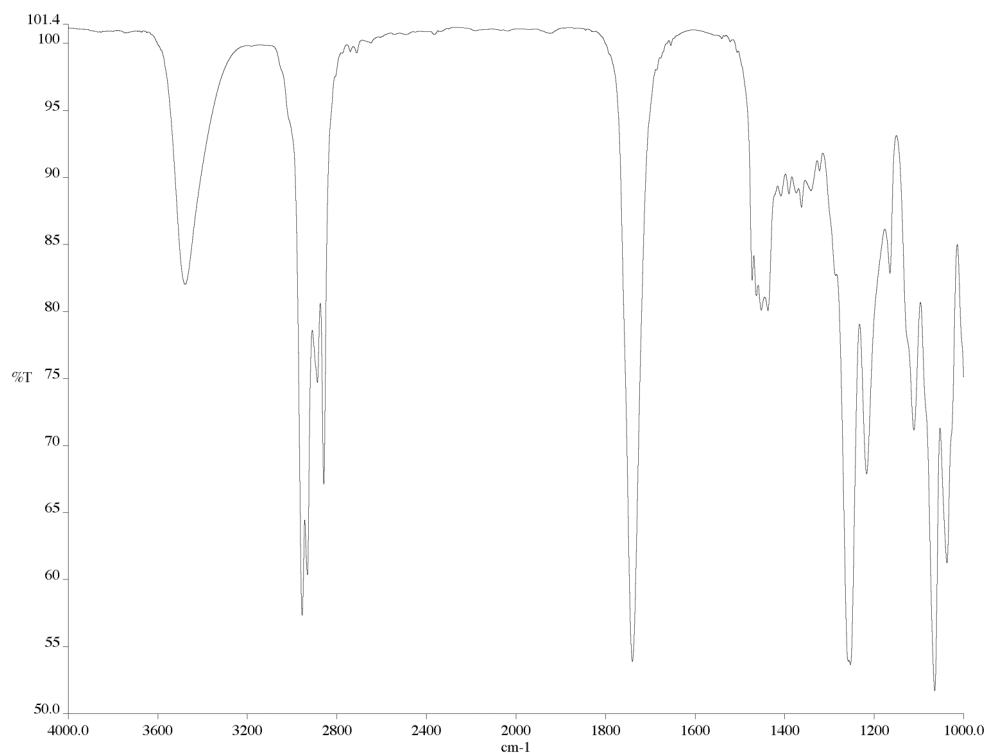


Figure A4.14 Infrared spectrum (thin film/NaCl) of compound **106**.

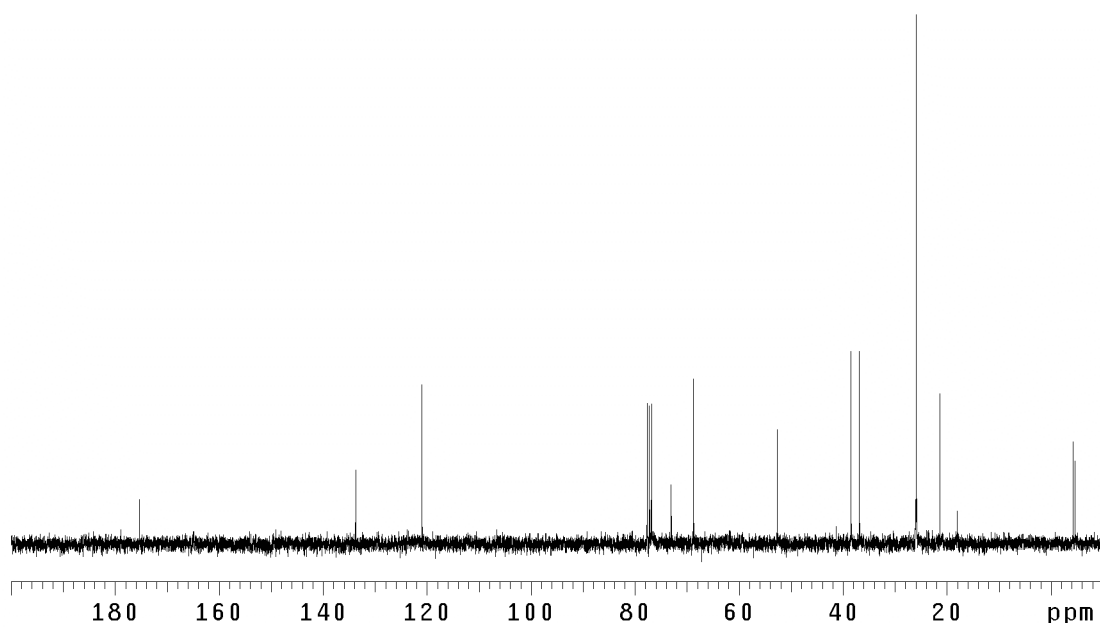


Figure A4.15 ¹³C NMR (75 MHz, CDCl₃) of compound **106**.

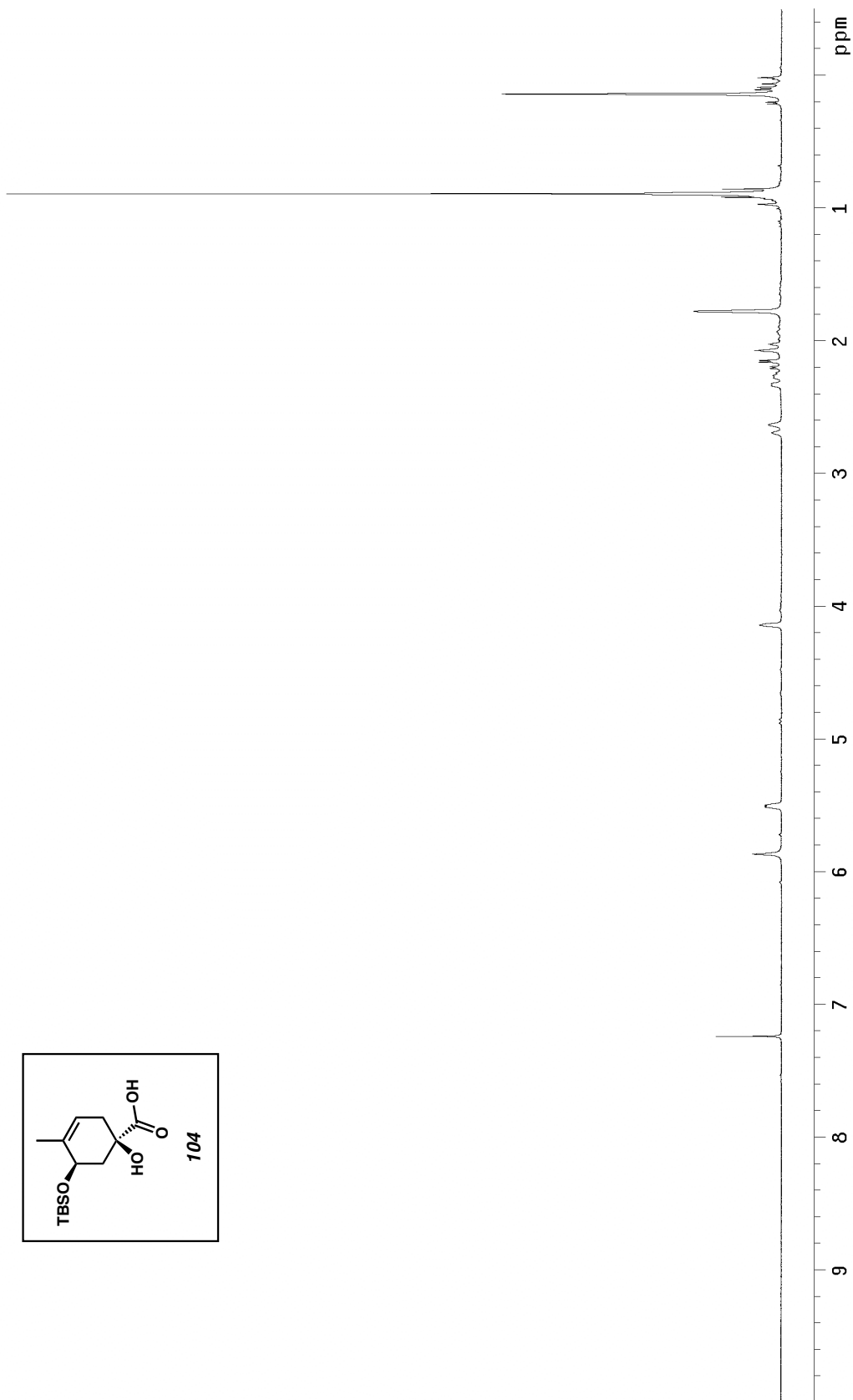
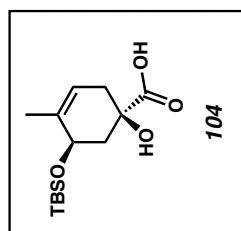


Figure A4.16 ¹H NMR (300 MHz, CDCl₃) of compound **104**.

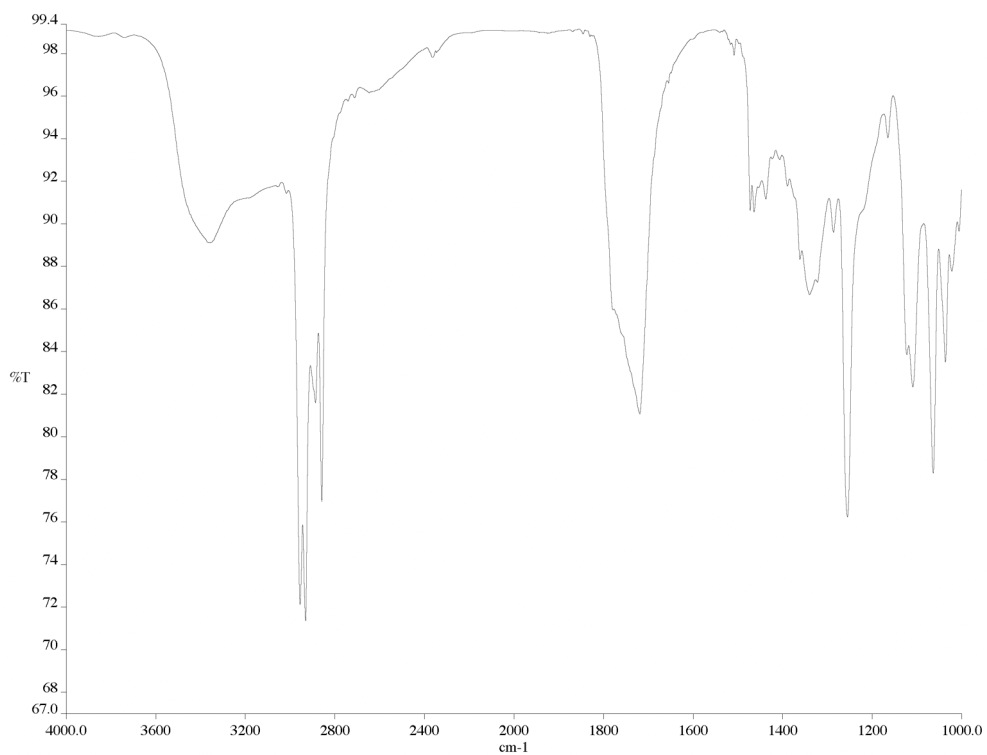


Figure A4.17 Infrared spectrum (thin film/NaCl) of compound **104**.

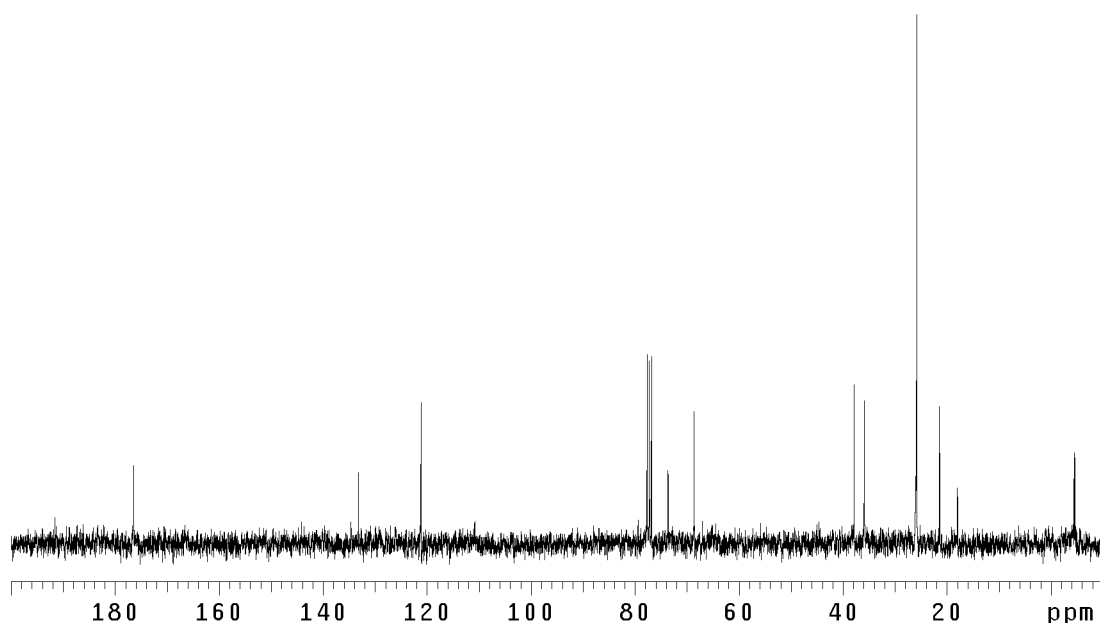


Figure A4.18 ¹³C NMR (75 MHz, CDCl₃) of compound **104**.

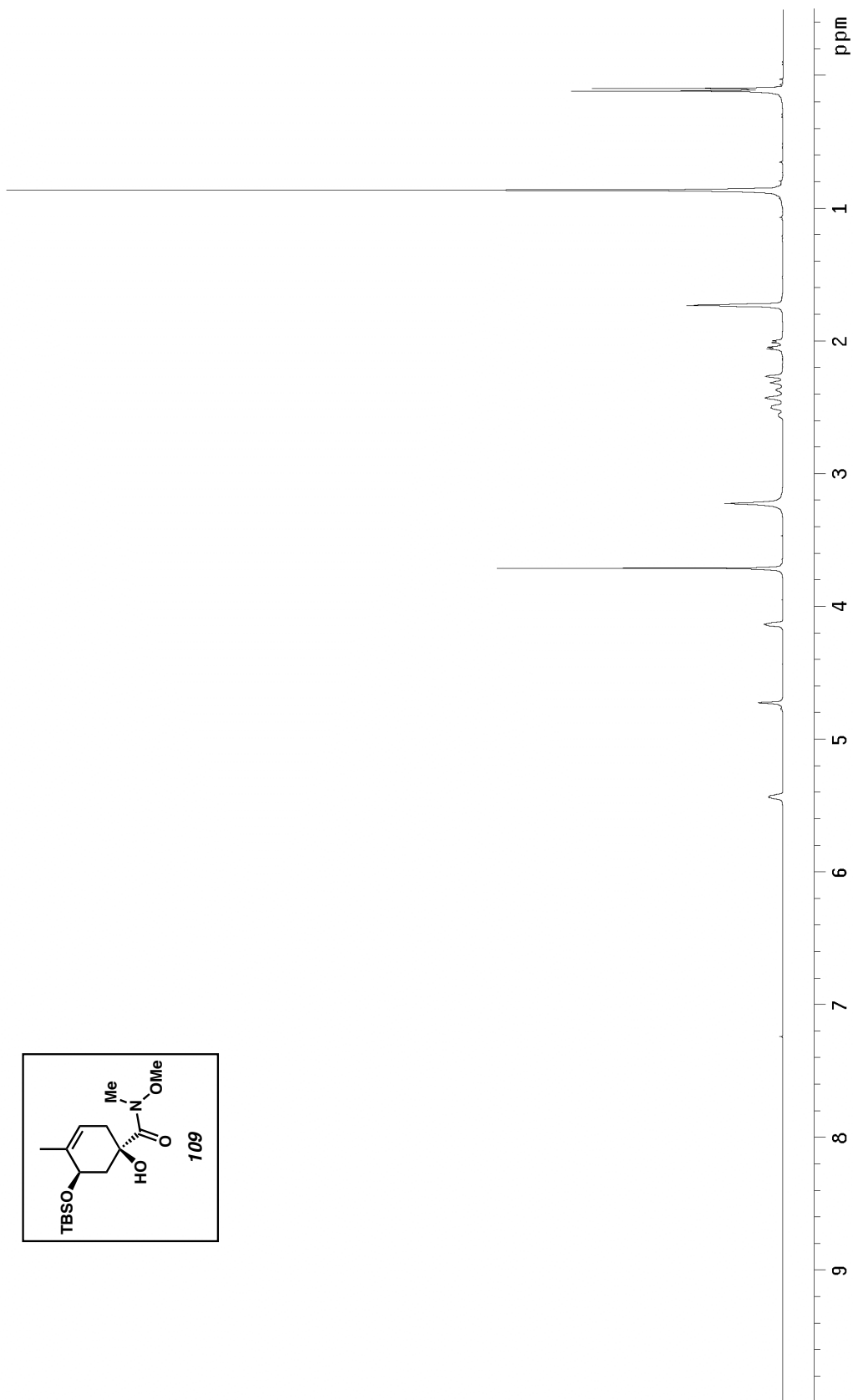
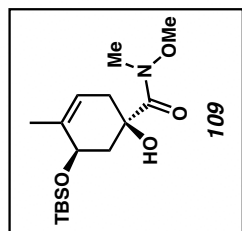


Figure A4.19 ¹H NMR (300 MHz, CDCl₃) of compound **109**.

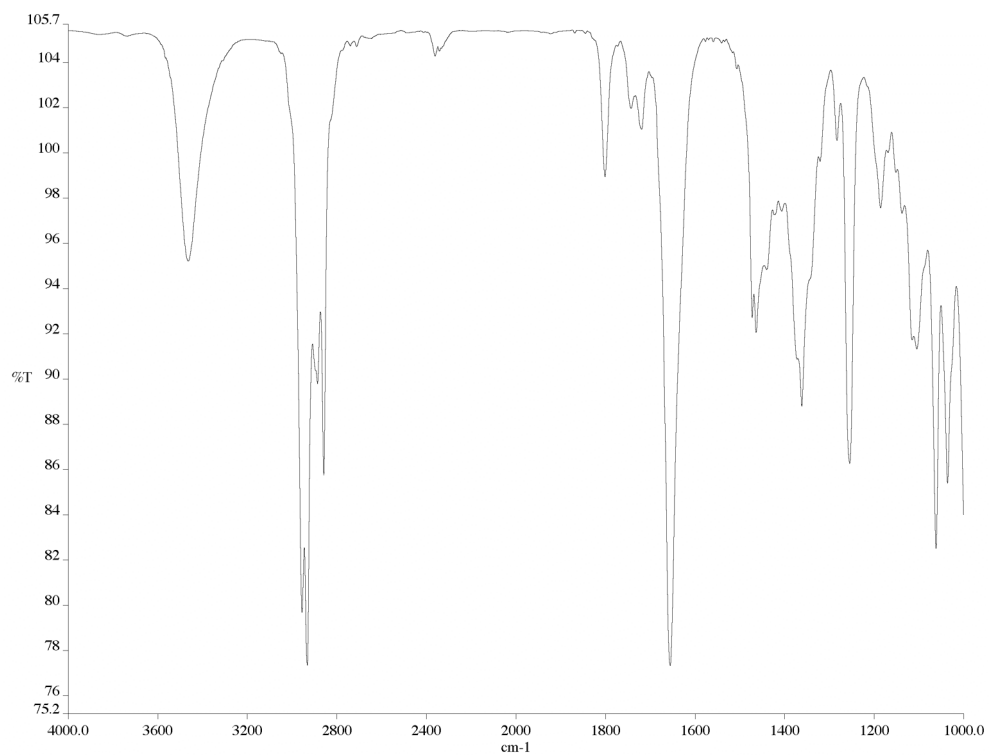


Figure A4.20 Infrared spectrum (thin film/NaCl) of compound **109**.

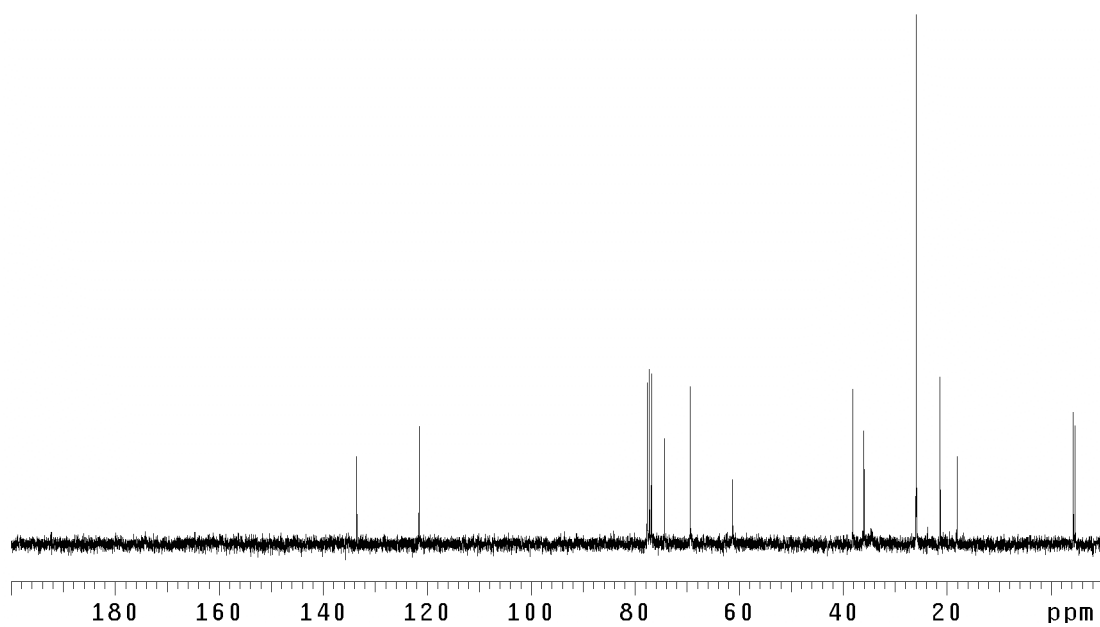


Figure A4.21 ¹³C NMR (75 MHz, CDCl₃) of compound **109**.

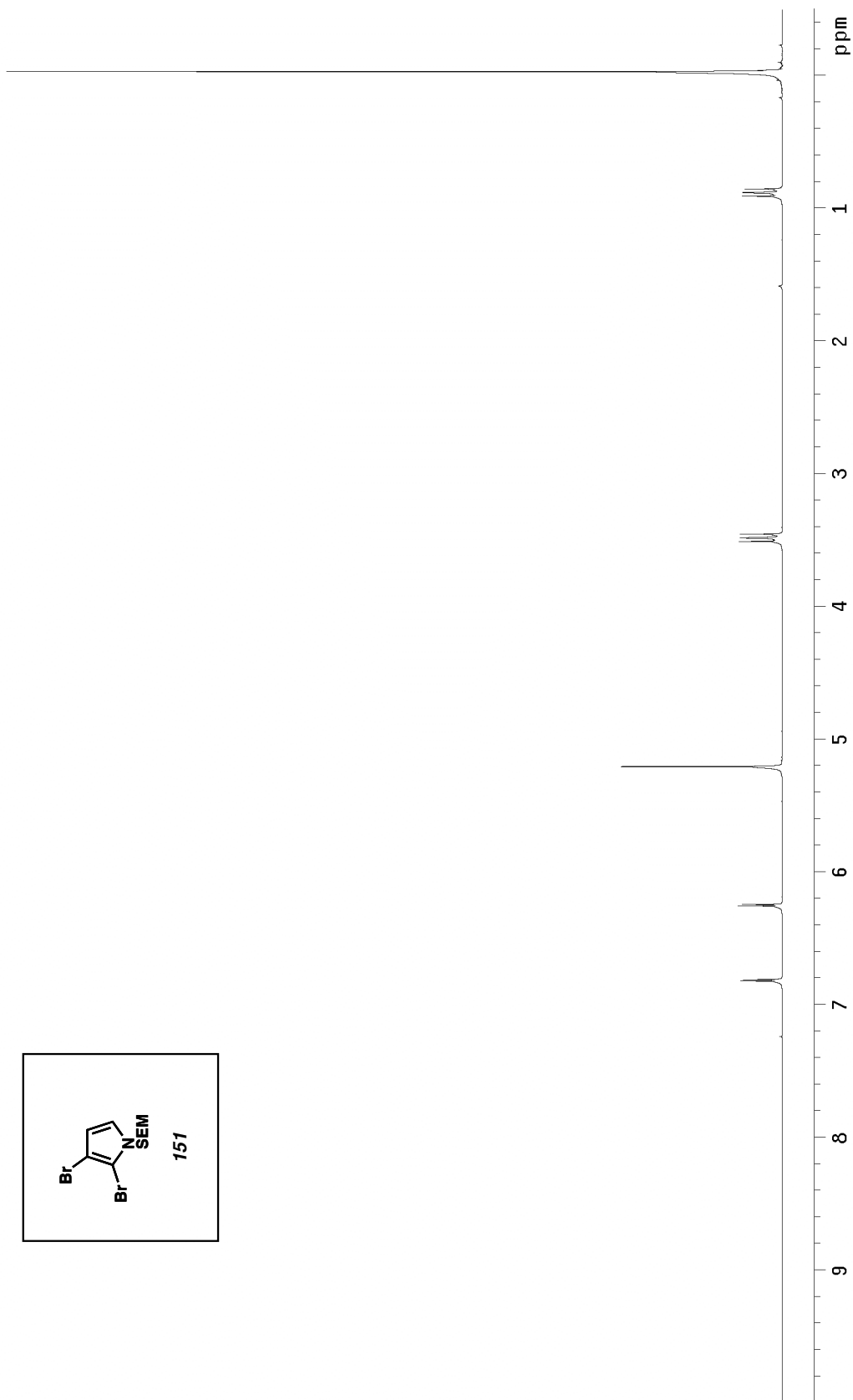
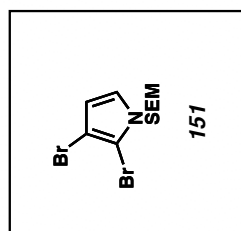


Figure A4.22 ^1H NMR (300 MHz, CDCl_3) of compound **151**.

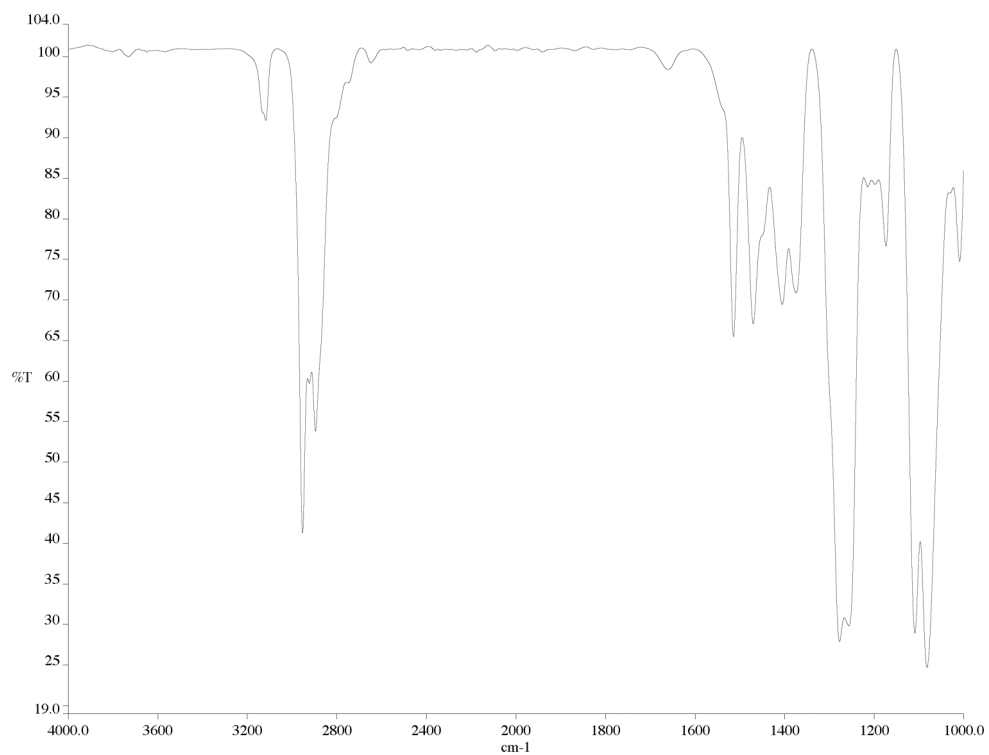


Figure A4.23 Infrared spectrum (thin film/NaCl) of compound **151**.

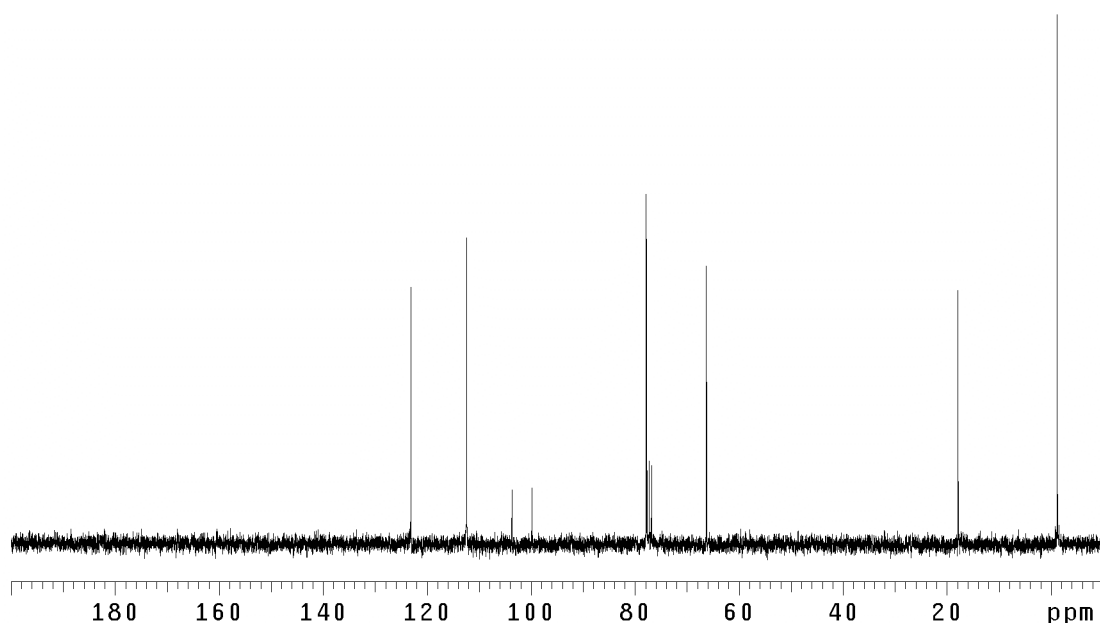


Figure A4.24 ¹³C NMR (75 MHz, CDCl₃) of compound **151**.

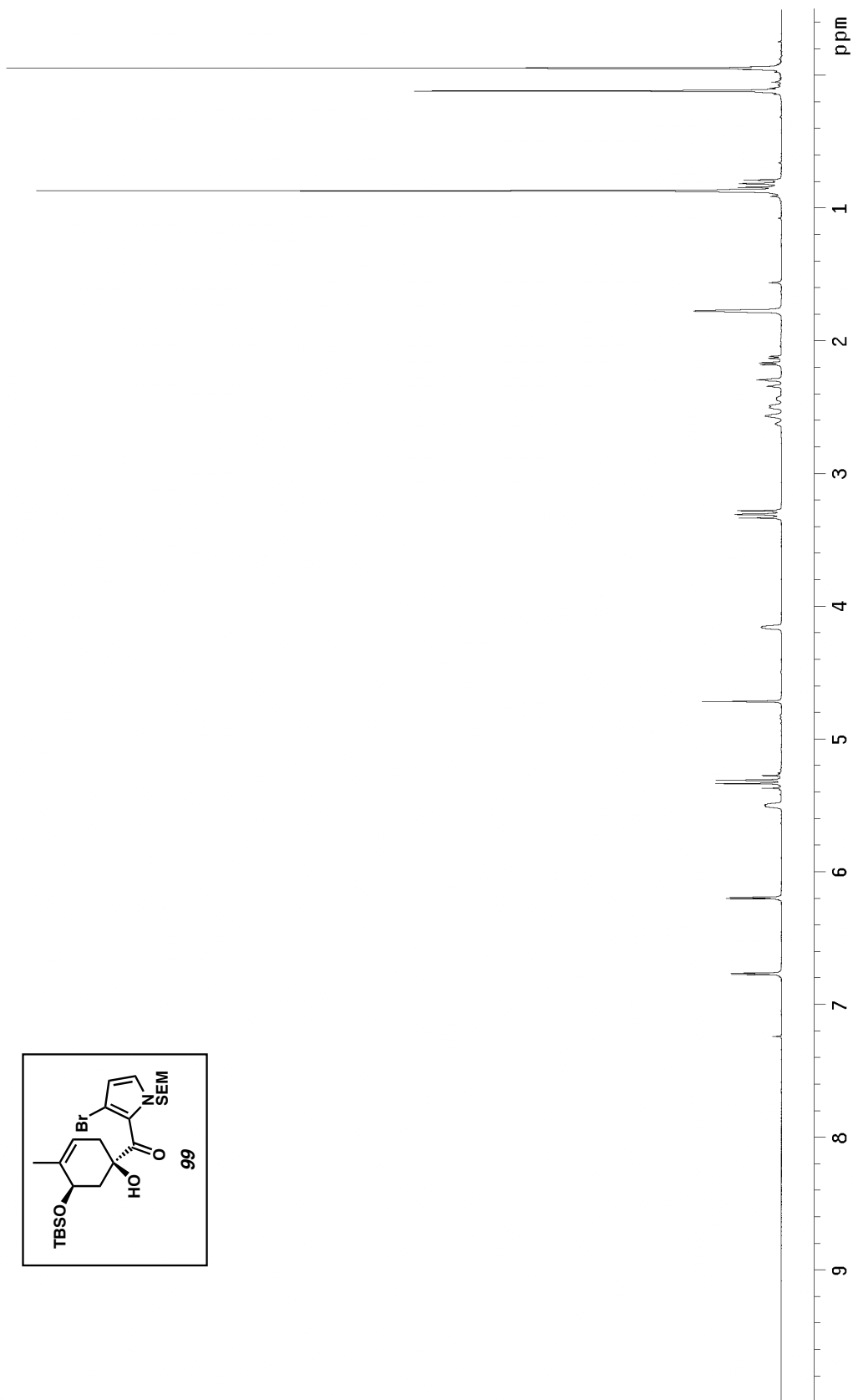
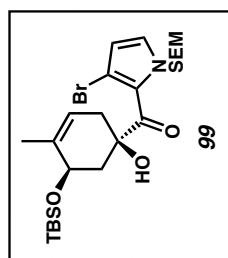


Figure A4.25 ^1H NMR (300 MHz, CDCl_3) of compound **99**.

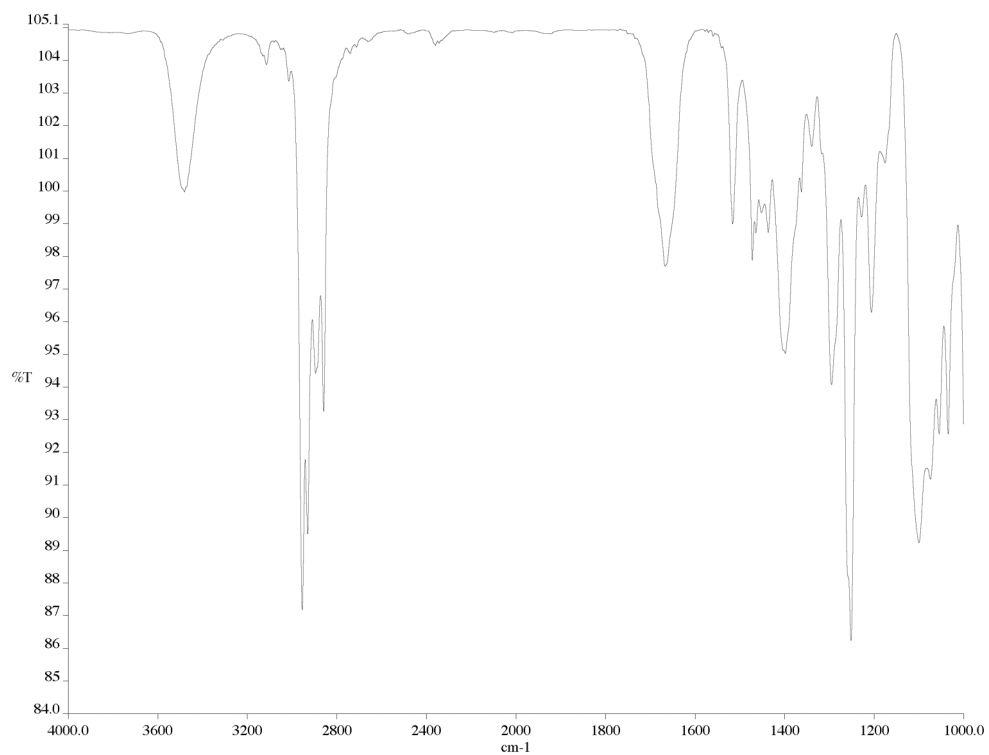


Figure A4.26 Infrared spectrum (thin film/NaCl) of compound **99**.

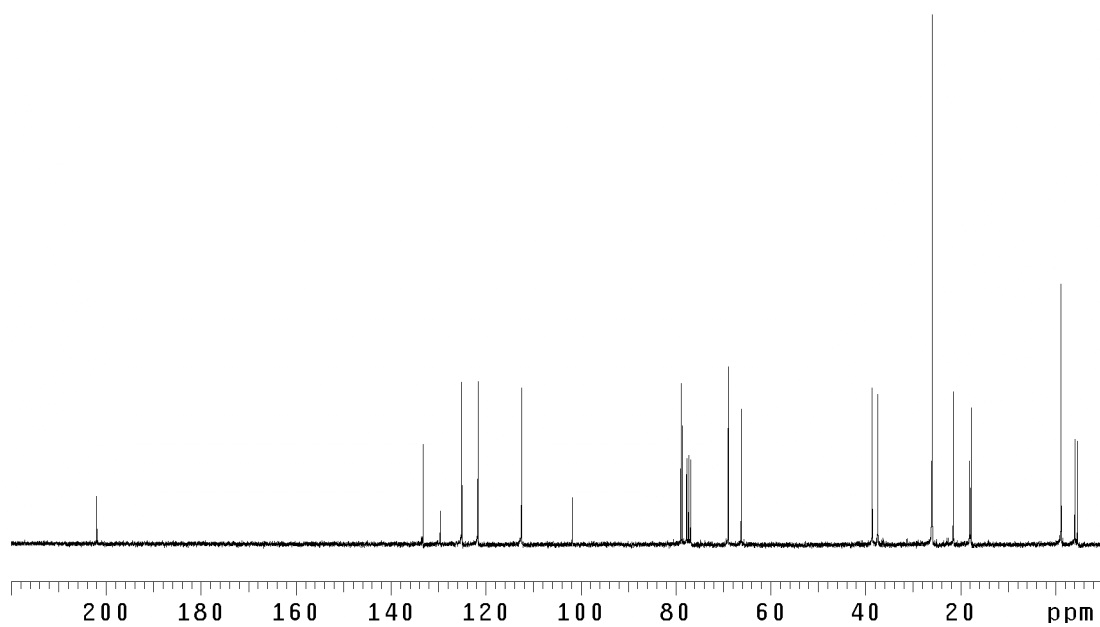


Figure A4.27 ¹³C NMR (75 MHz, CDCl₃) of compound **99**.

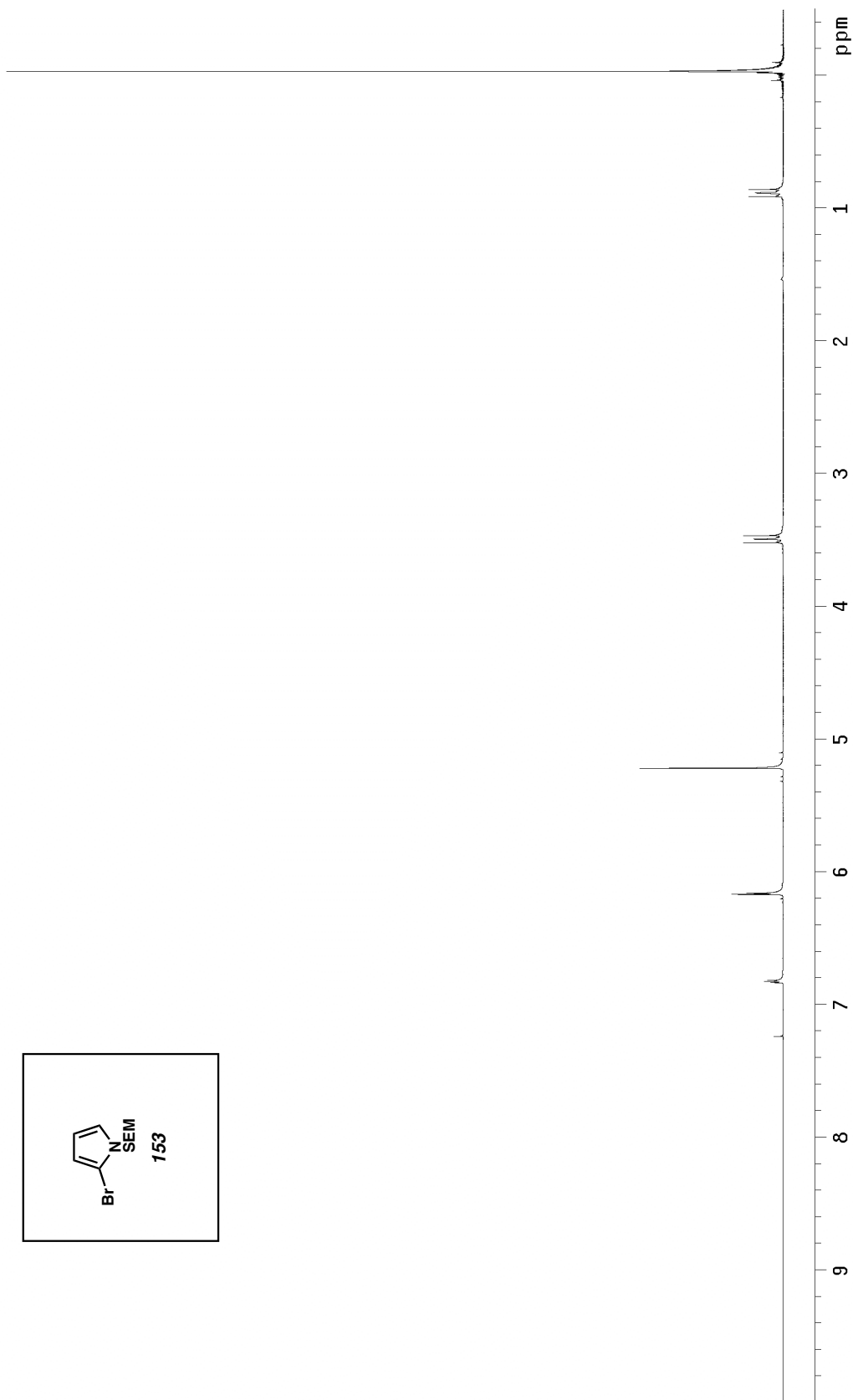


Figure A4.28 ^1H NMR (300 MHz, CDCl_3) of compound **153**.

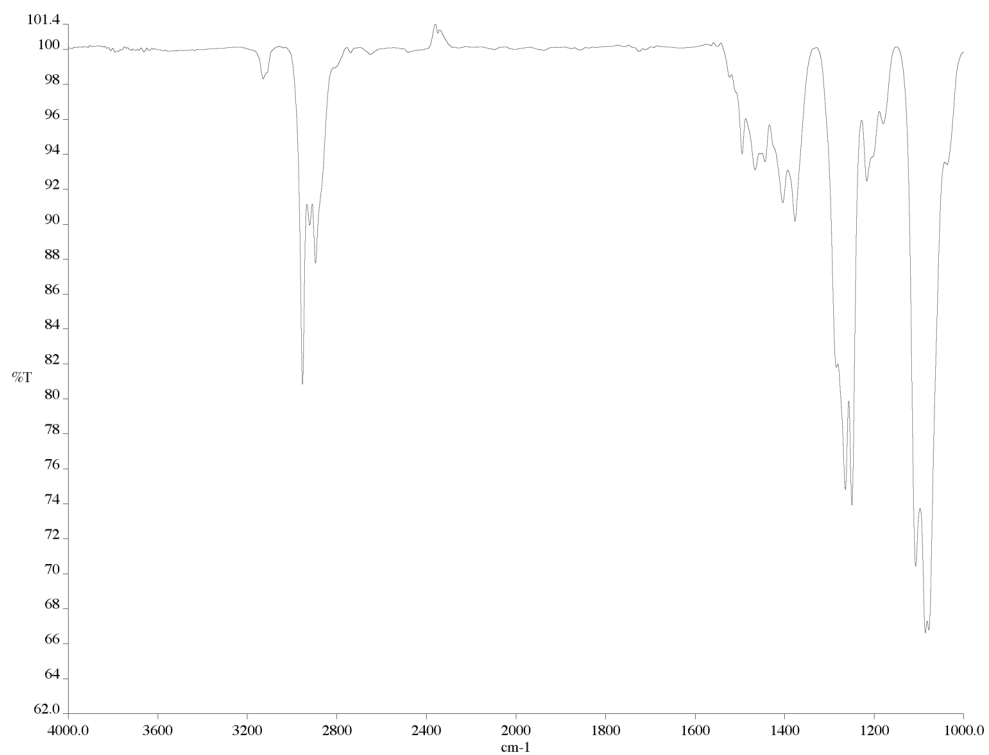


Figure A4.29 Infrared spectrum (thin film/NaCl) of compound **153**.

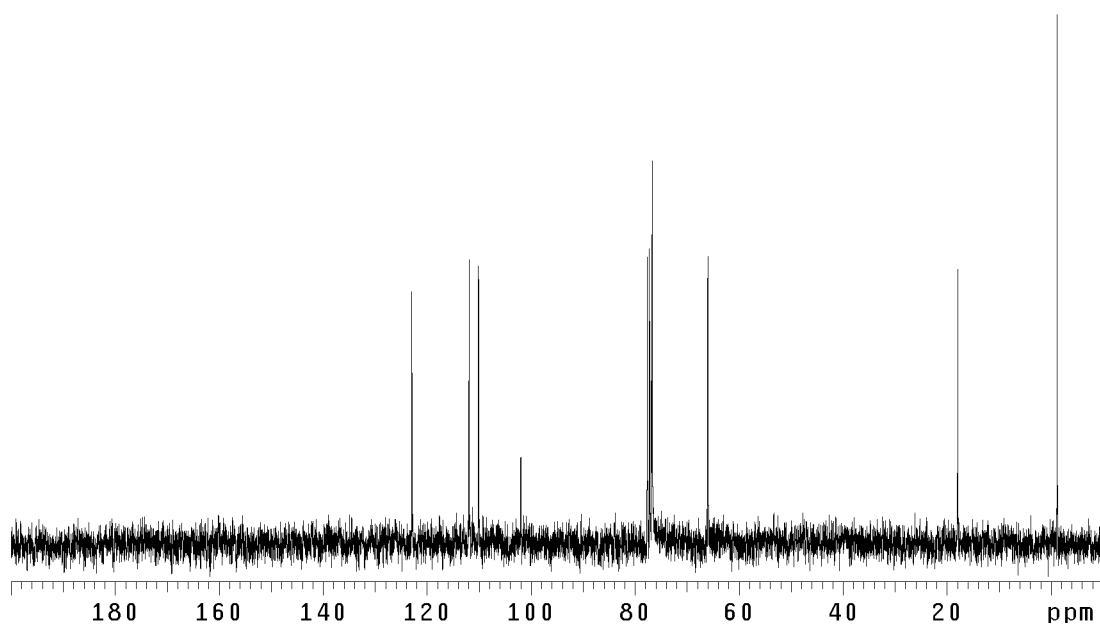


Figure A4.30 ¹³C NMR (75 MHz, CDCl₃) of compound **153**.

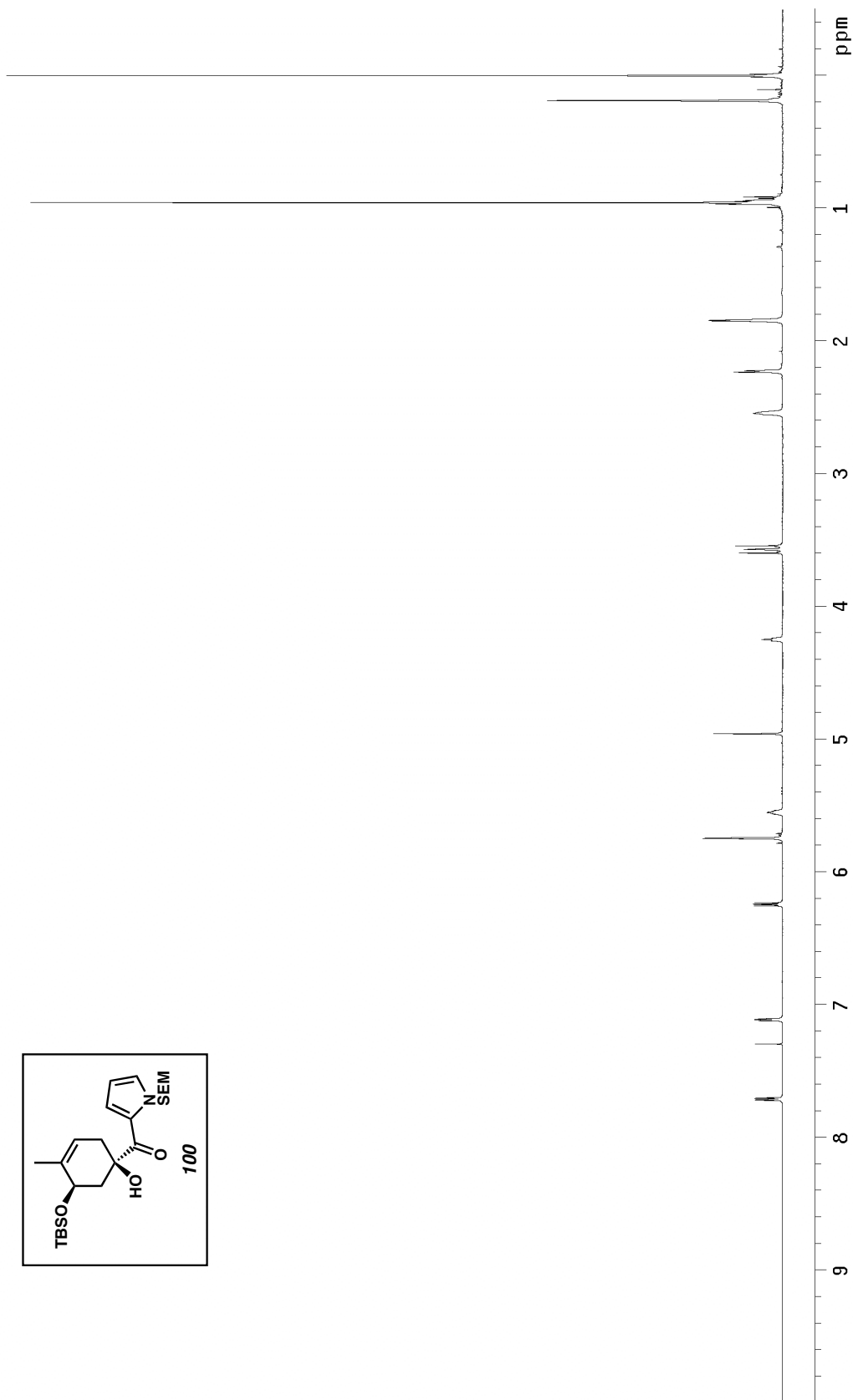


Figure A4.31 ^1H NMR (300 MHz, CDCl_3) of compound **100**.

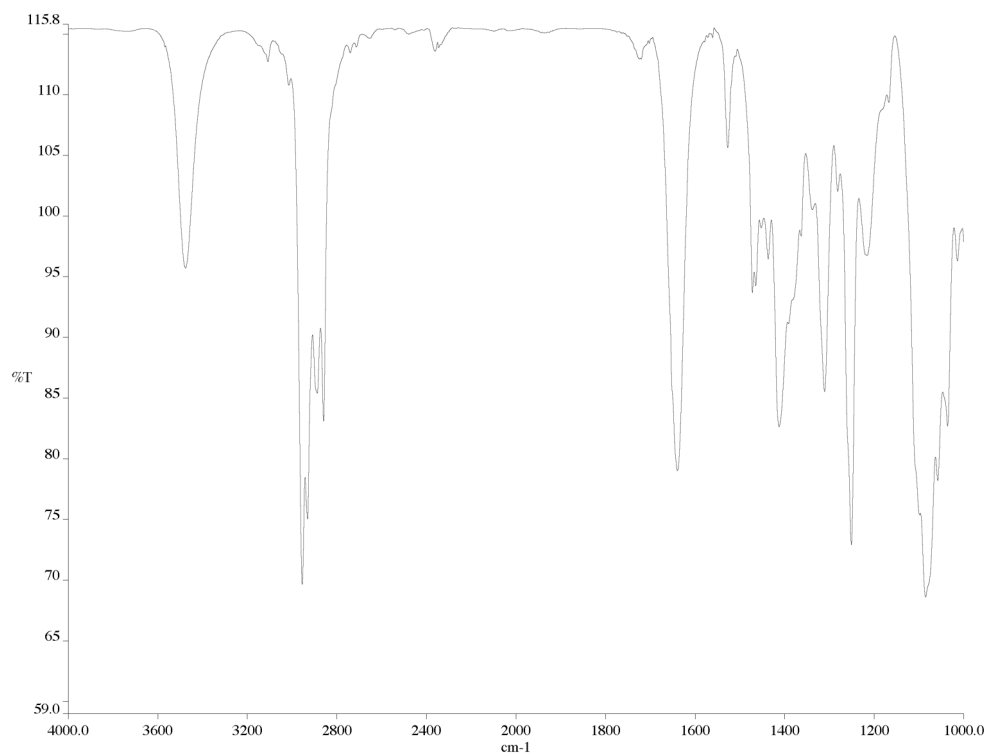


Figure A4.32 Infrared spectrum (thin film/NaCl) of compound **100**.

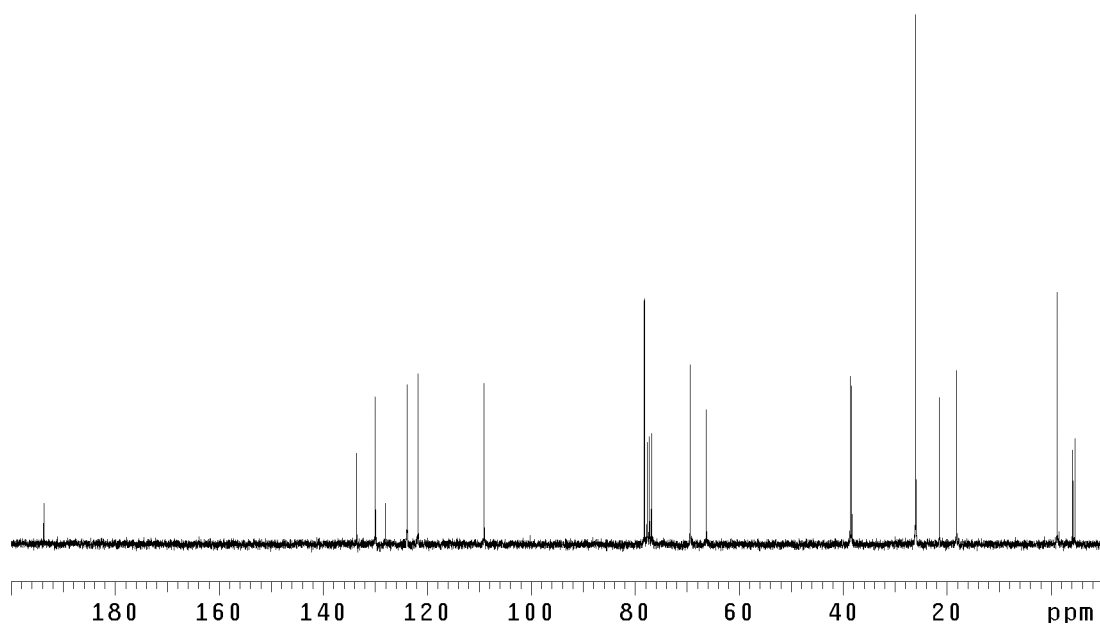


Figure A4.33 ¹³C NMR (75 MHz, CDCl₃) of compound **100**.

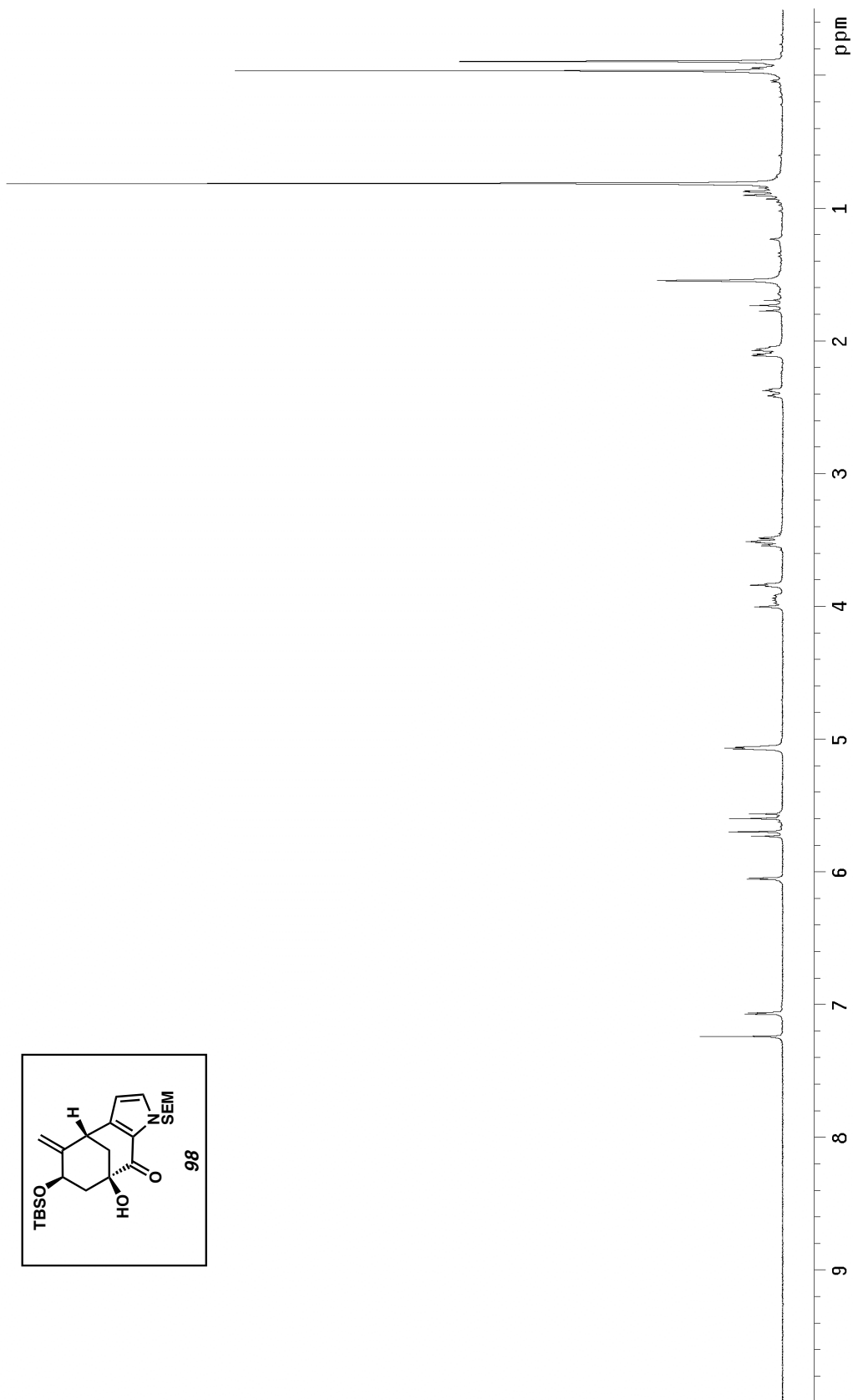
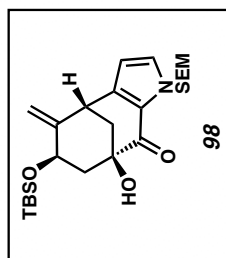


Figure A4.34 ^1H NMR (300 MHz, CDCl_3) of compound **98**.

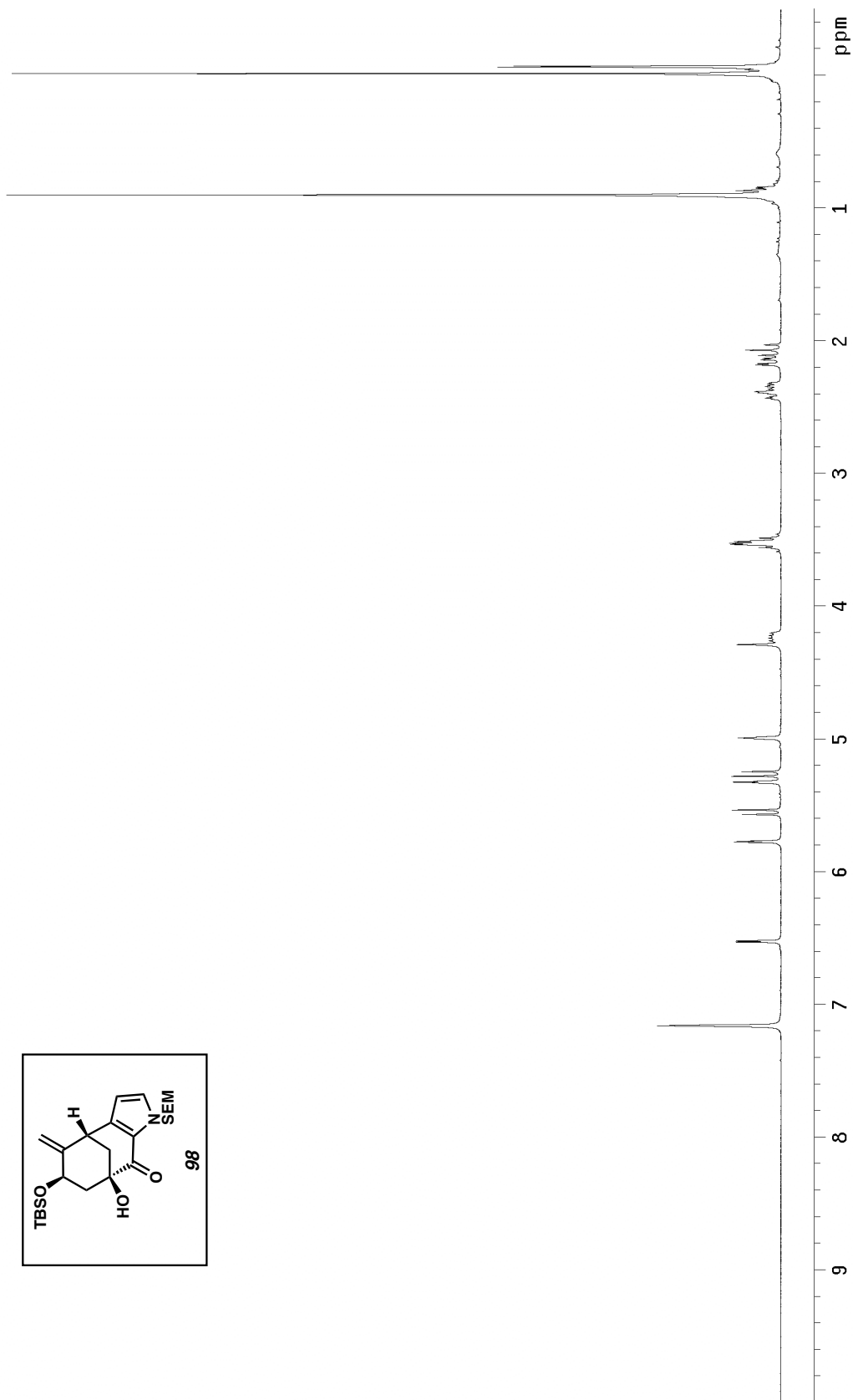
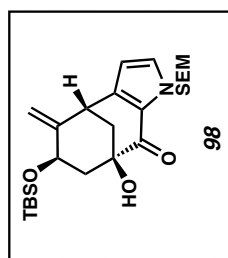


Figure A4.35 ^1H NMR (300 MHz, C_6D_6) of compound **98**.

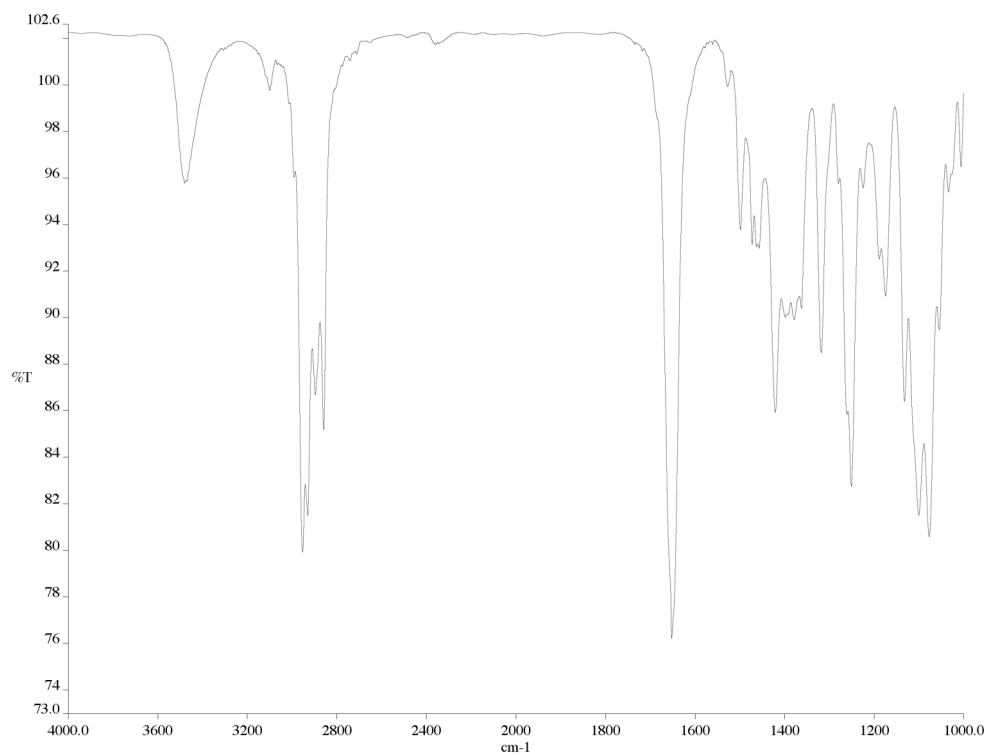


Figure A4.36 Infrared spectrum (thin film/NaCl) of compound **98**.

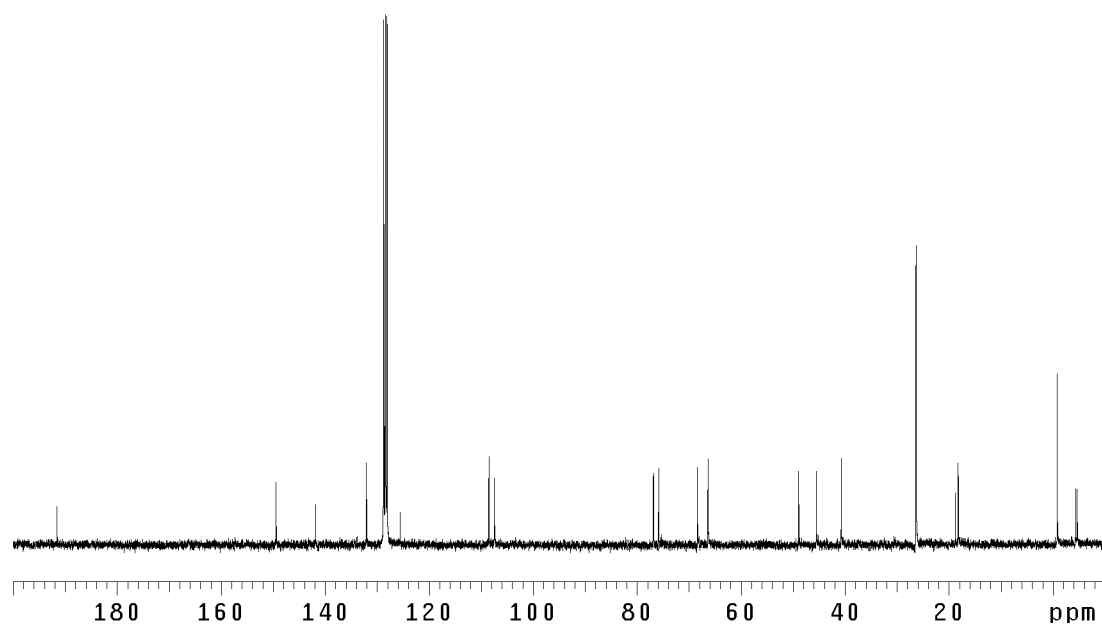


Figure A4.37 ¹³C NMR (75 MHz, C₆D₆) of compound **98**.

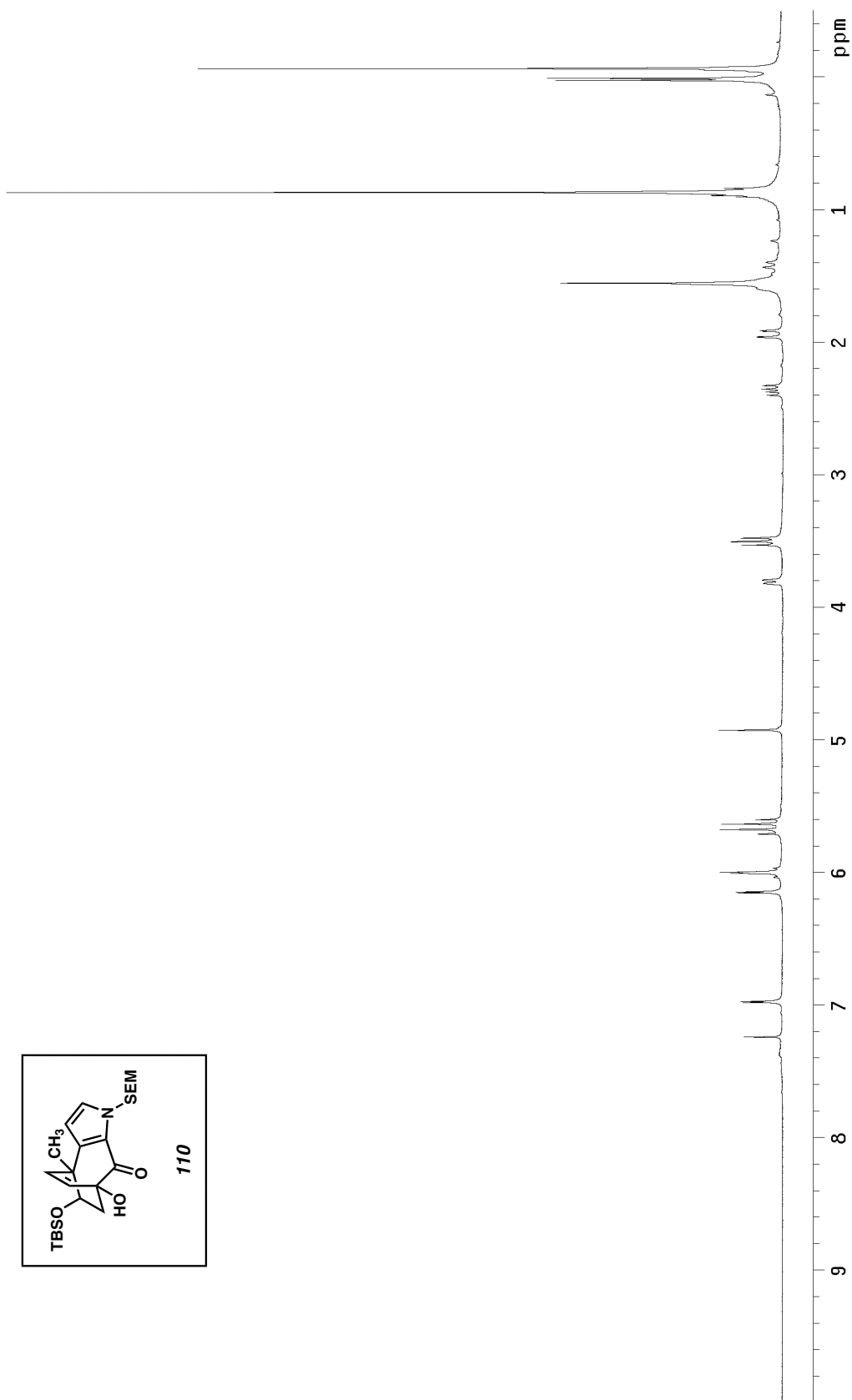
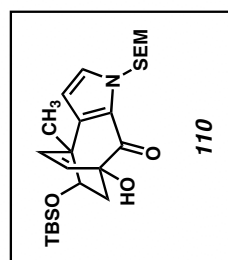
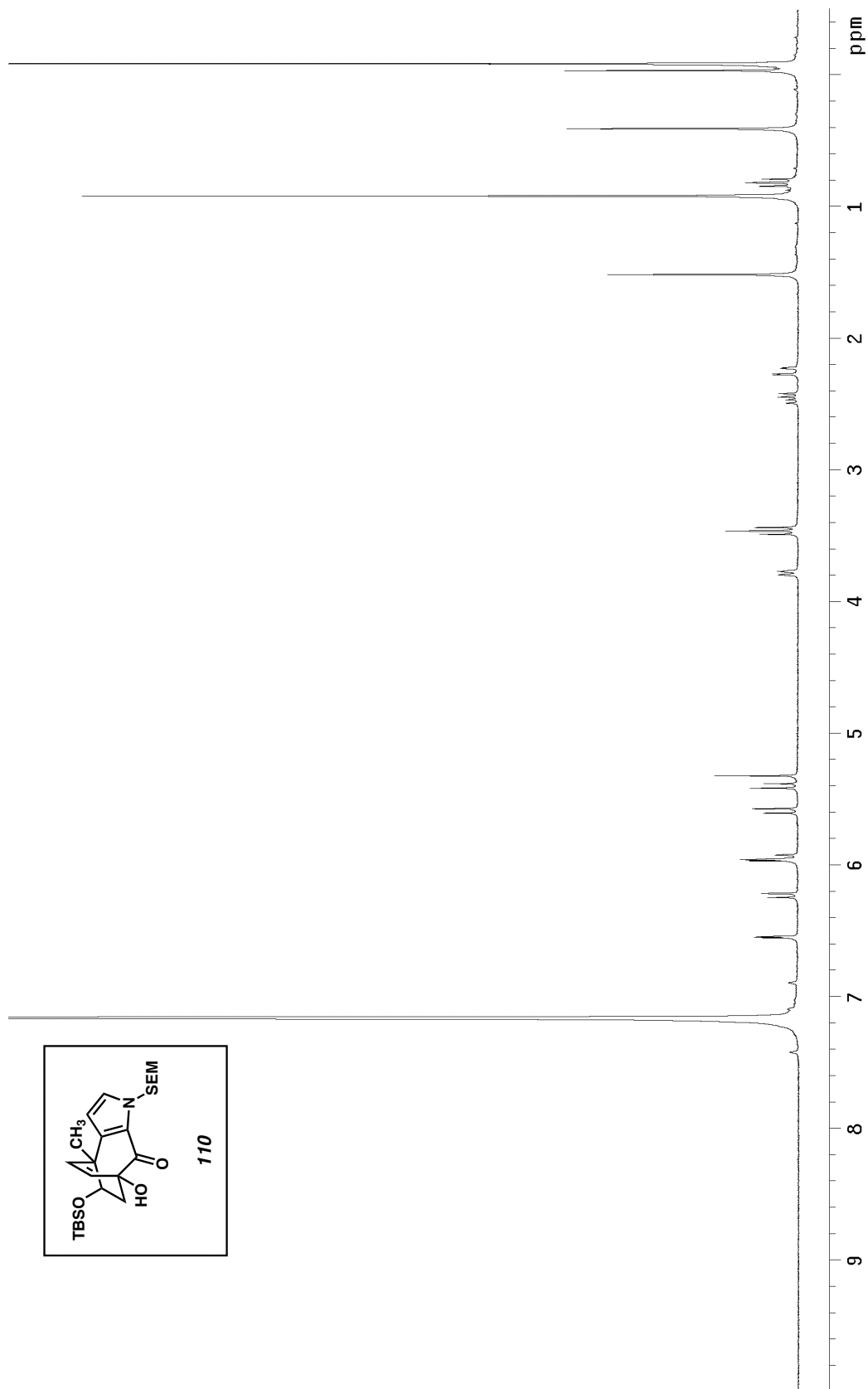


Figure A4.38 ^1H NMR (300 MHz, CDCl_3) of compound **110**.



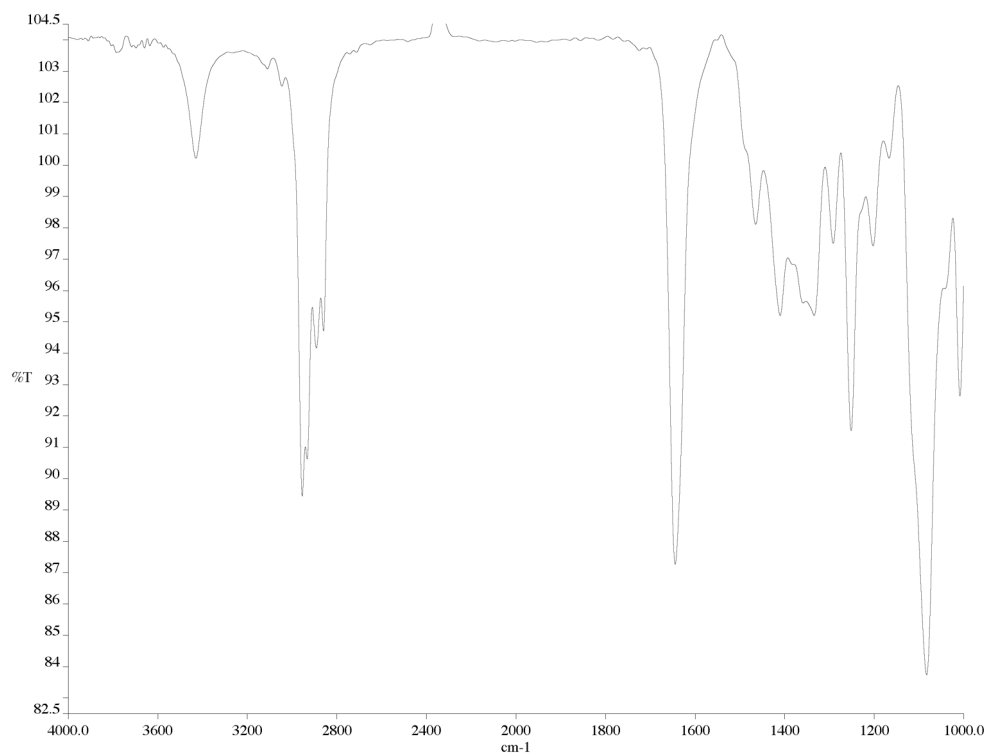


Figure A4.40 Infrared spectrum (thin film/NaCl) of compound **110**.

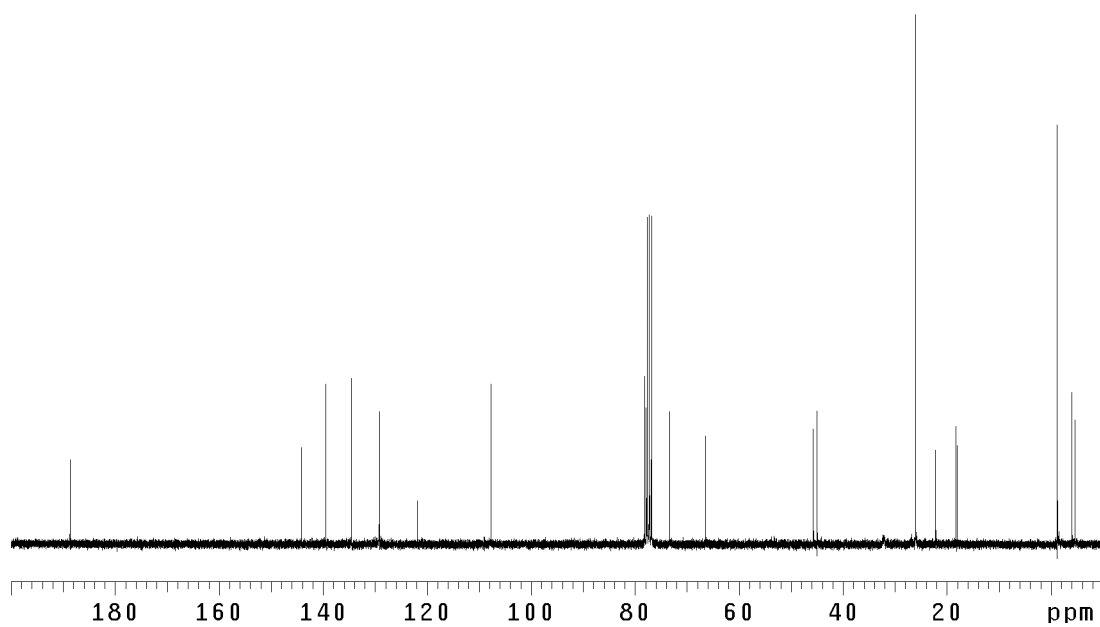


Figure A4.41 ¹³C NMR (75 MHz, CDCl₃) of compound **110**.

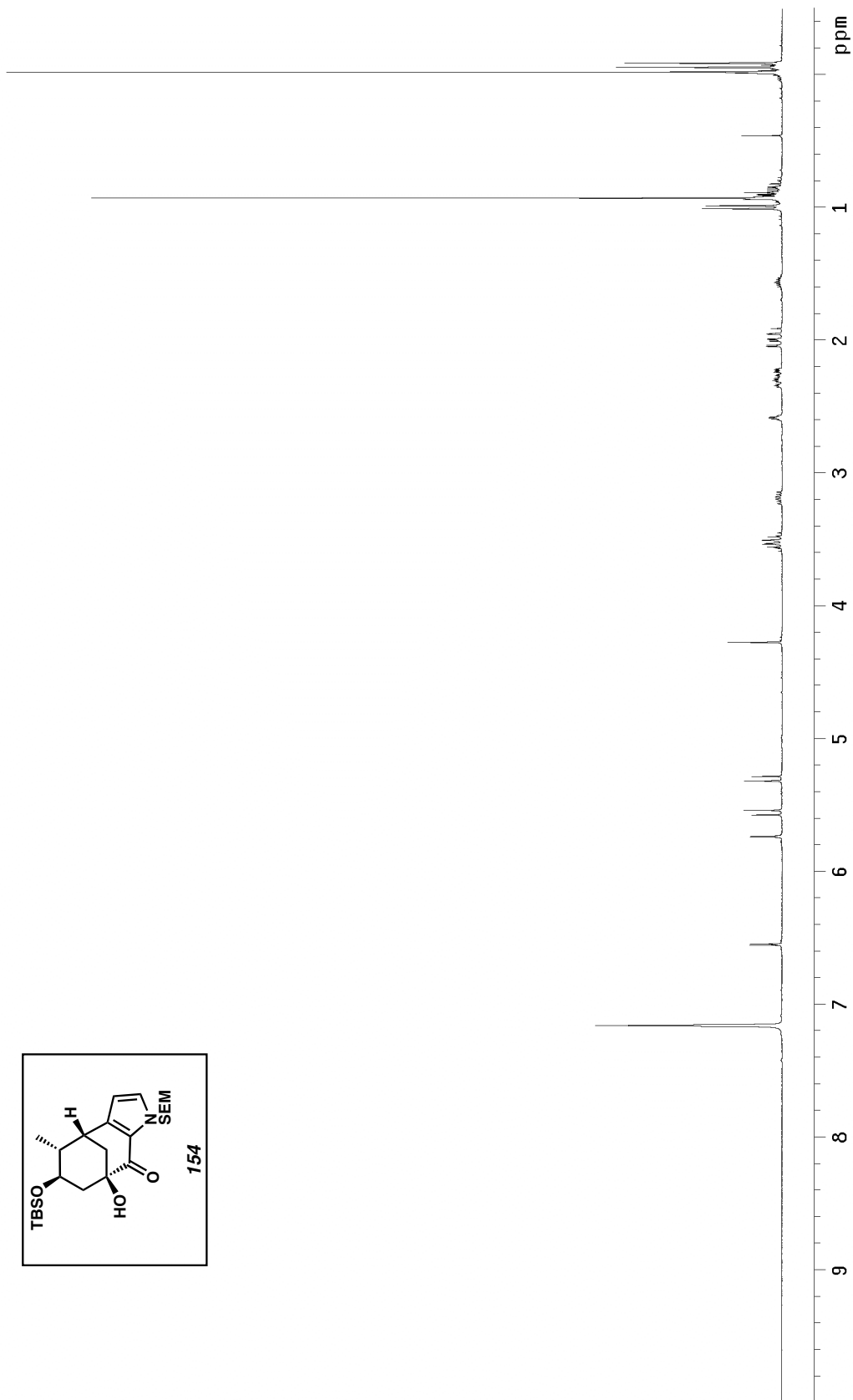
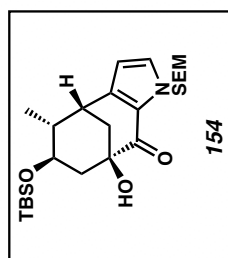


Figure A4.42 ^1H NMR (300 MHz, C_6D_6) of compound **154**.

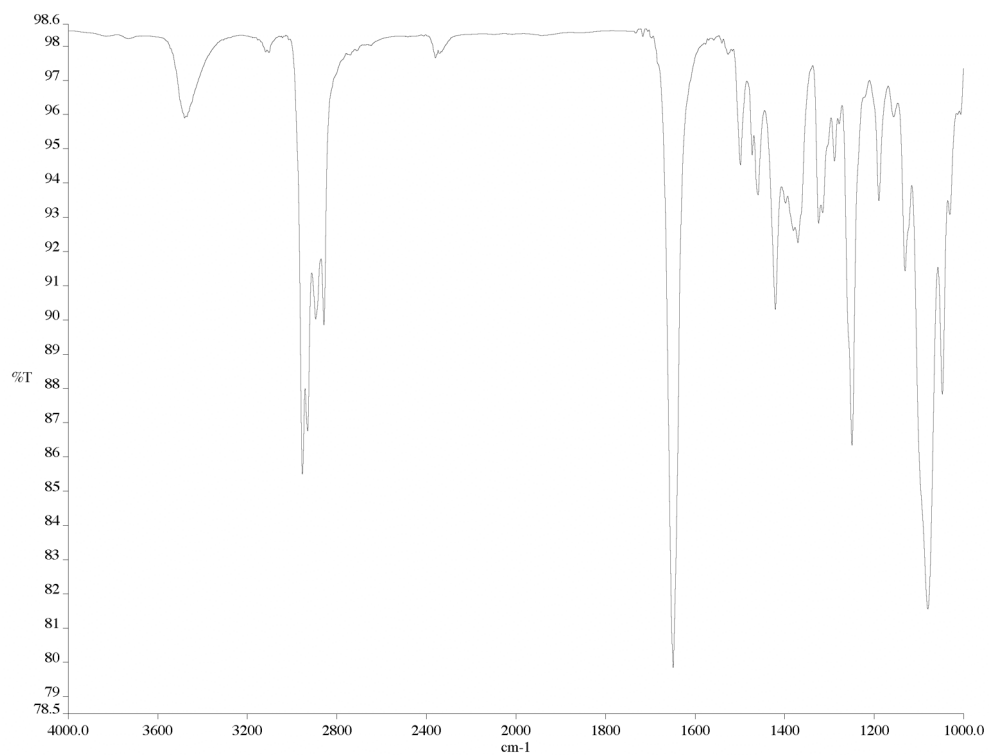


Figure A4.43 Infrared spectrum (thin film/NaCl) of compound **154**.

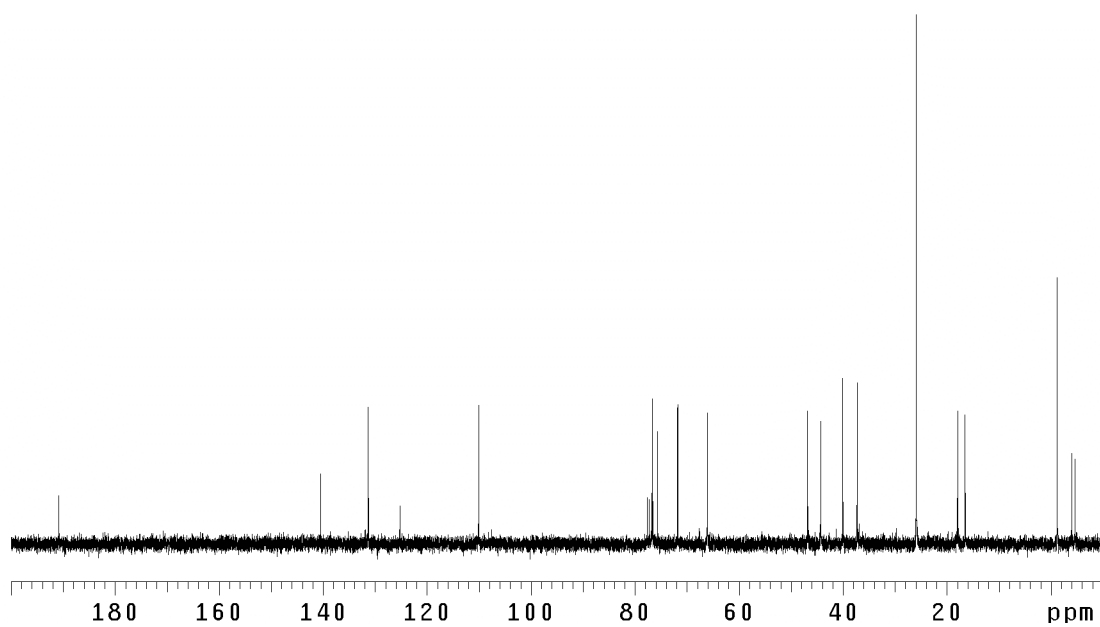


Figure A4.44 ¹³C NMR (75 MHz, C₆D₆) of compound **154**.

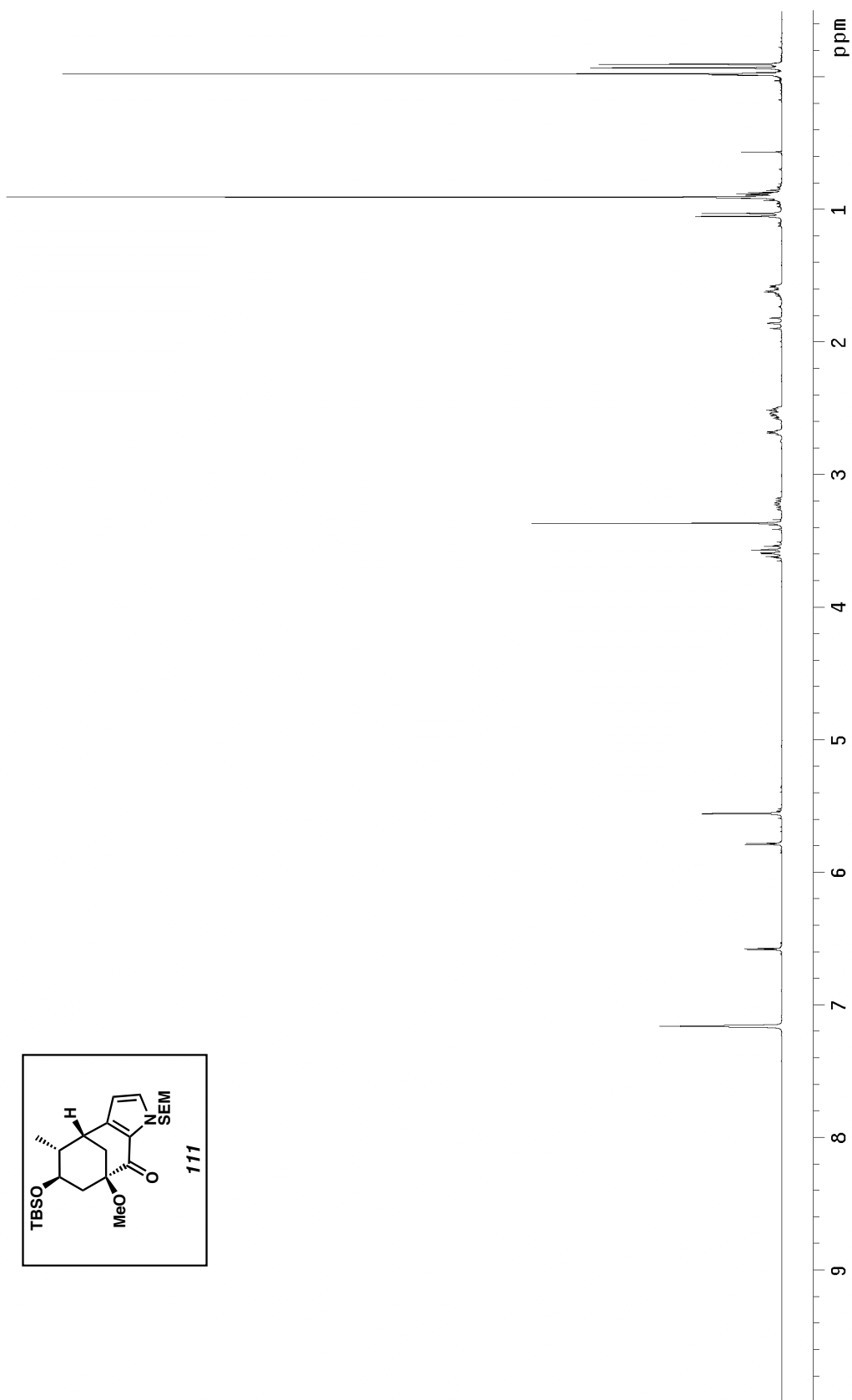
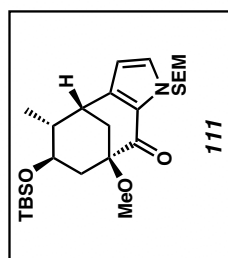


Figure A4.45 ^1H NMR (300 MHz, C_6D_6) of compound **111**.

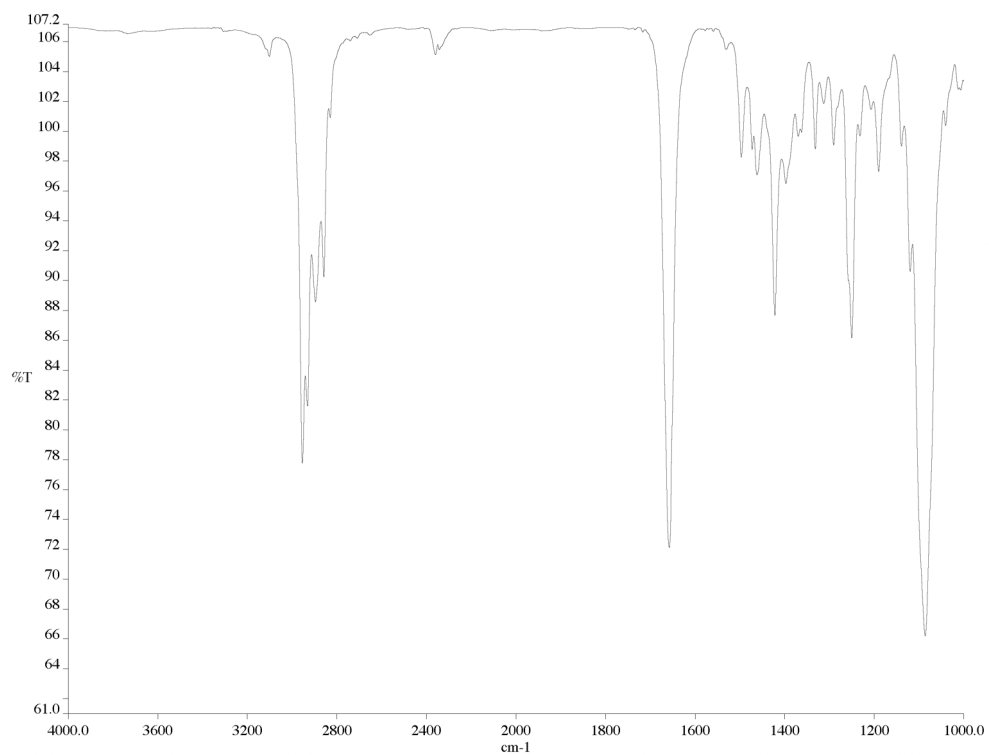


Figure A4.46 Infrared spectrum (thin film/NaCl) of compound **111**.

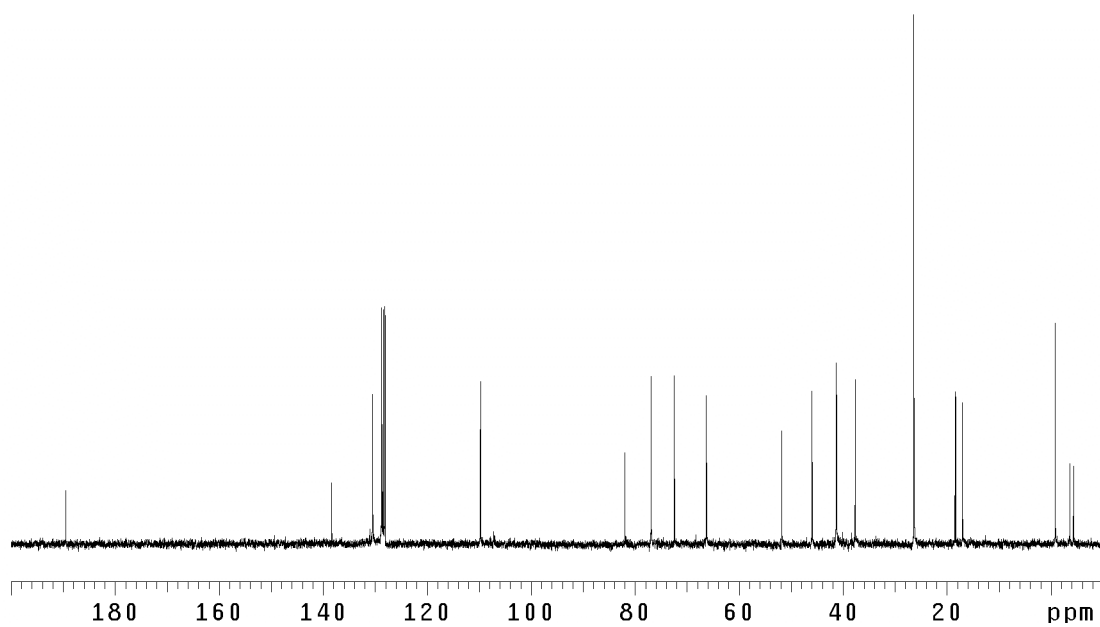


Figure A4.47 ¹³C NMR (75 MHz, C₆D₆) of compound **111**.

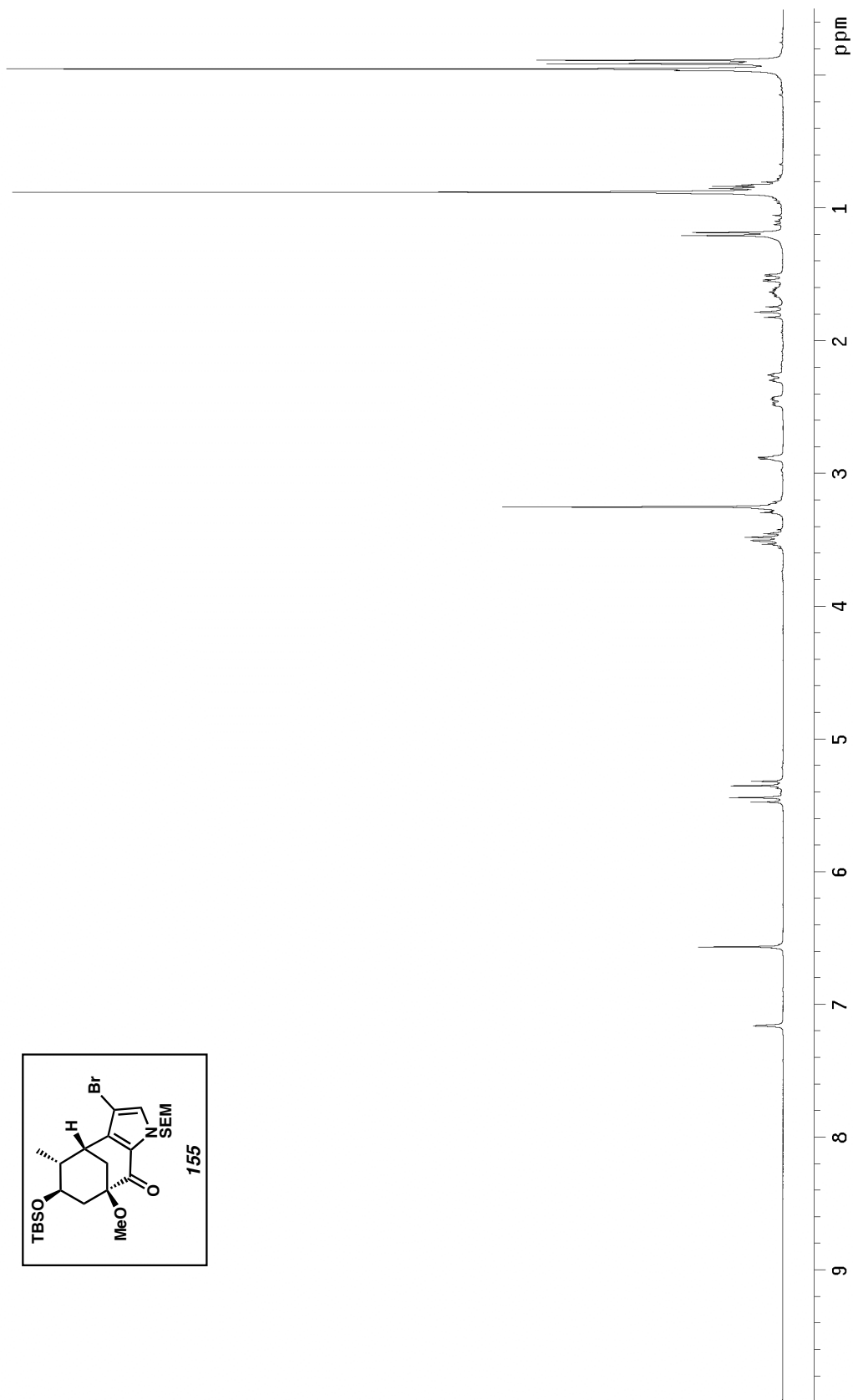
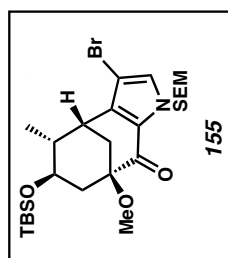


Figure A4.48 ^1H NMR (300 MHz, C_6D_6) of compound **155**.

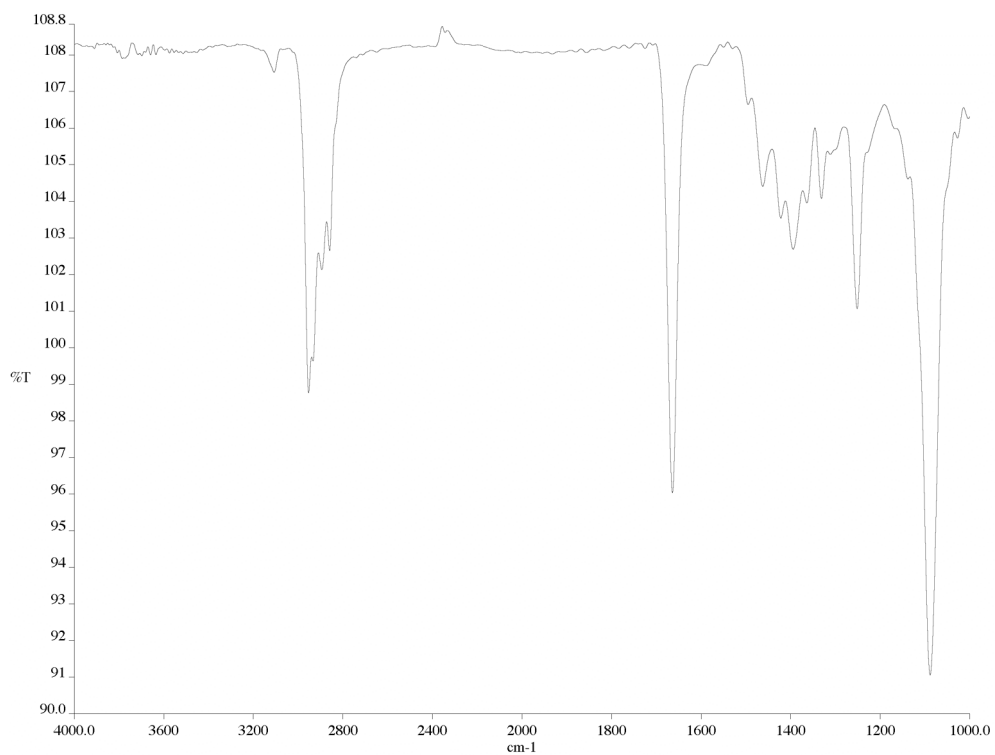


Figure A4.49 Infrared spectrum (thin film/NaCl) of compound **155**.

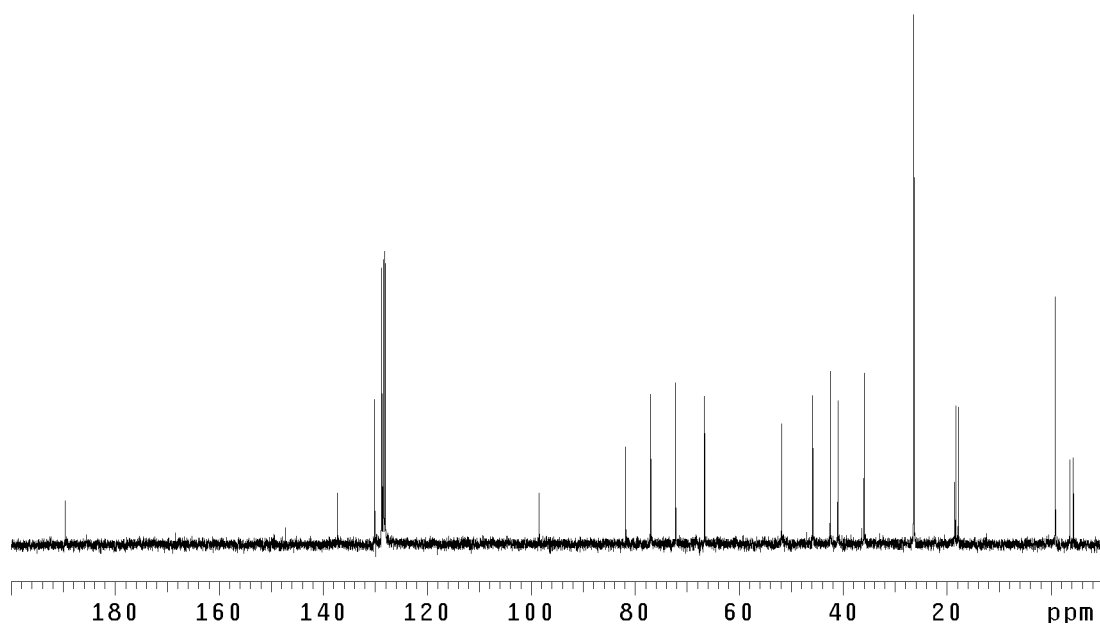


Figure A4.50 ¹³C NMR (75 MHz, C₆D₆) of compound **155**.

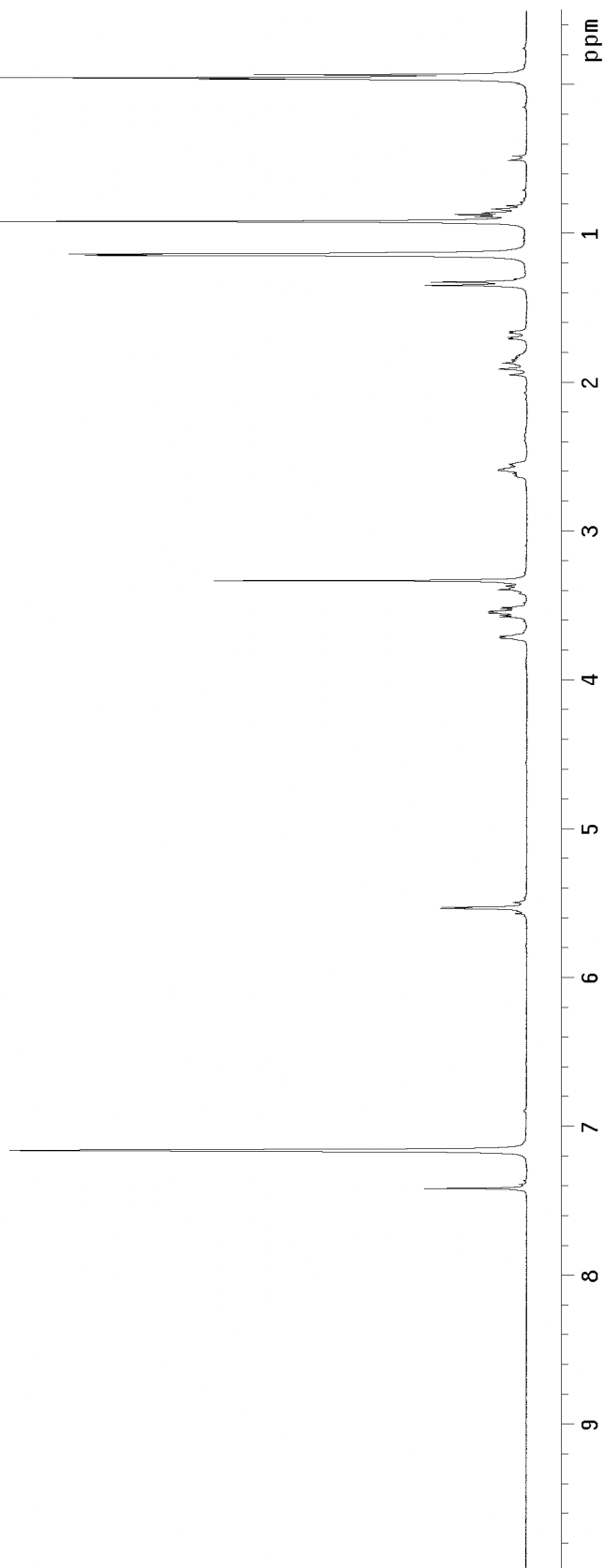
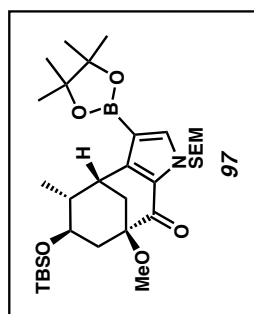


Figure A4.51 ^1H NMR (300 MHz, C_6D_6) of compound **97**.

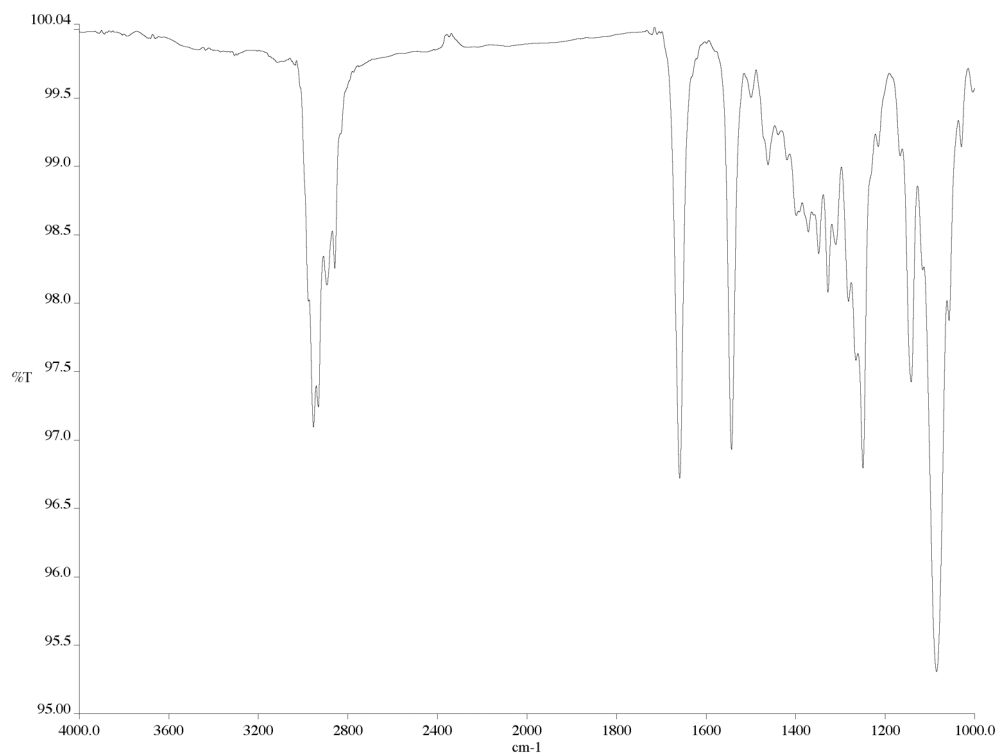


Figure A4.52 Infrared spectrum (thin film/NaCl) of compound **97**.

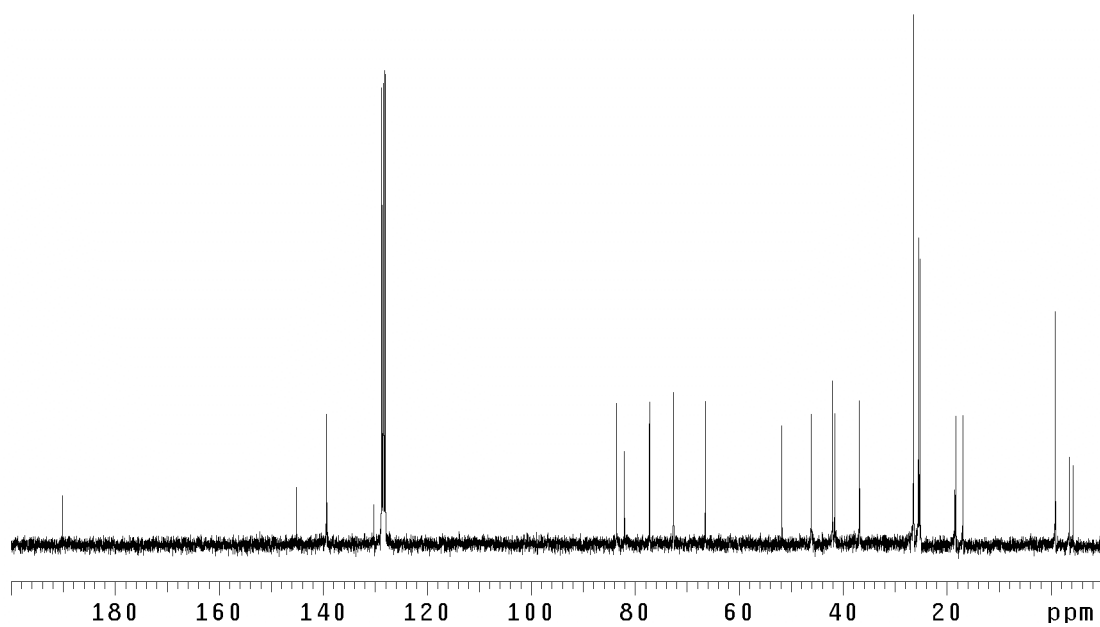


Figure A4.53 ¹³C NMR (75 MHz, C₆D₆) of compound **97**.

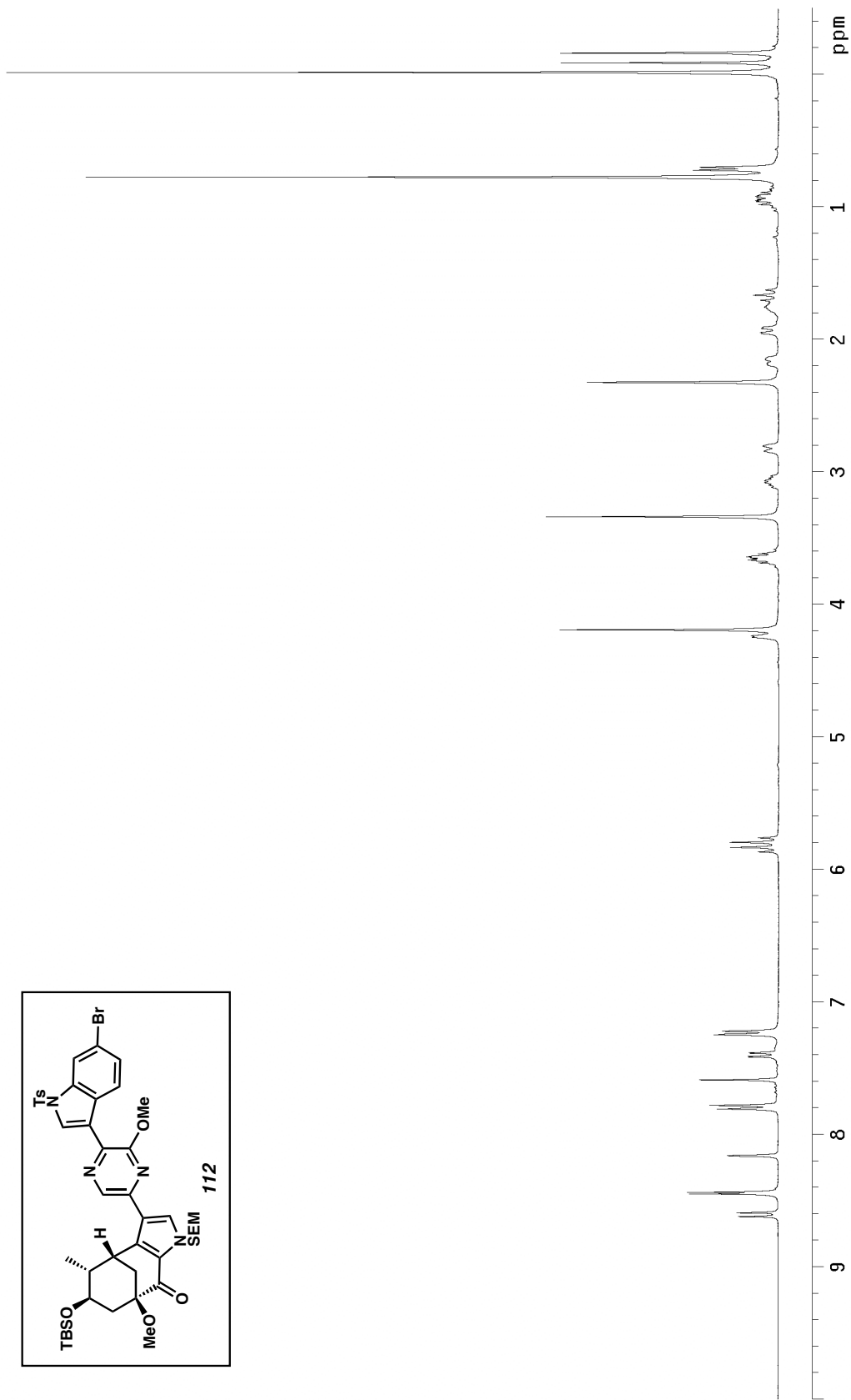
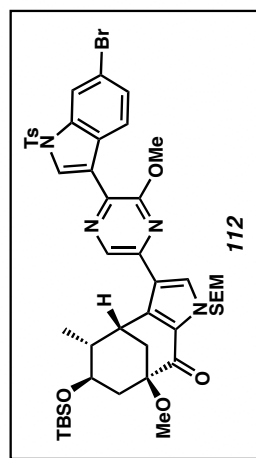


Figure A4.54 ^1H NMR (300 MHz, CDCl_3) of compound **112**.

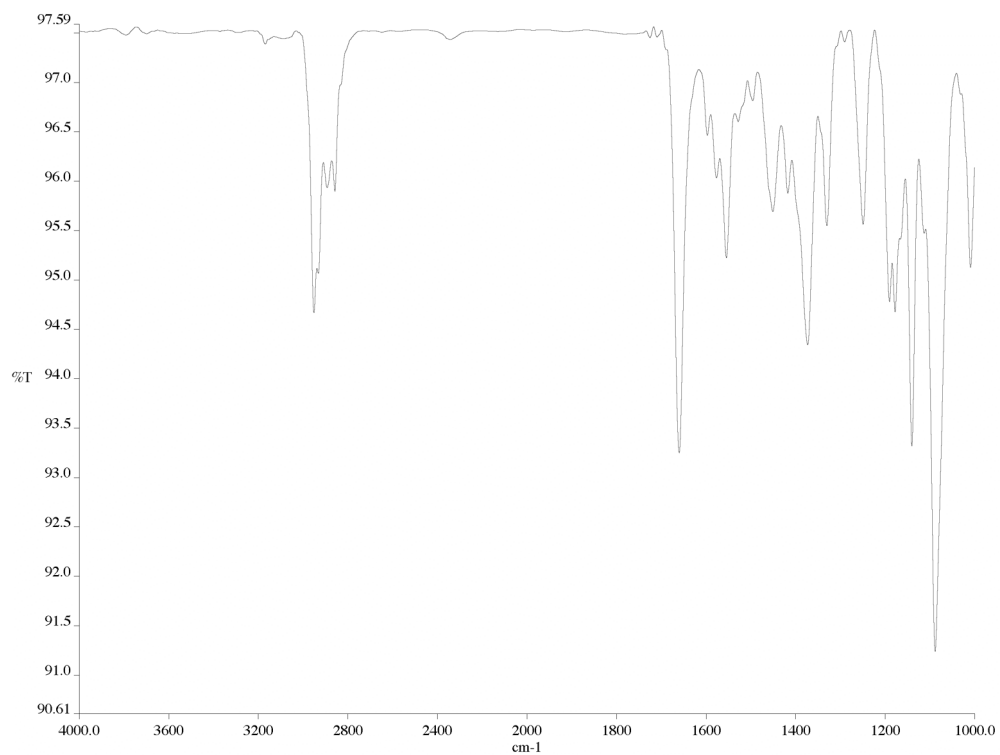


Figure A4.55 Infrared spectrum (thin film/NaCl) of compound **112**.

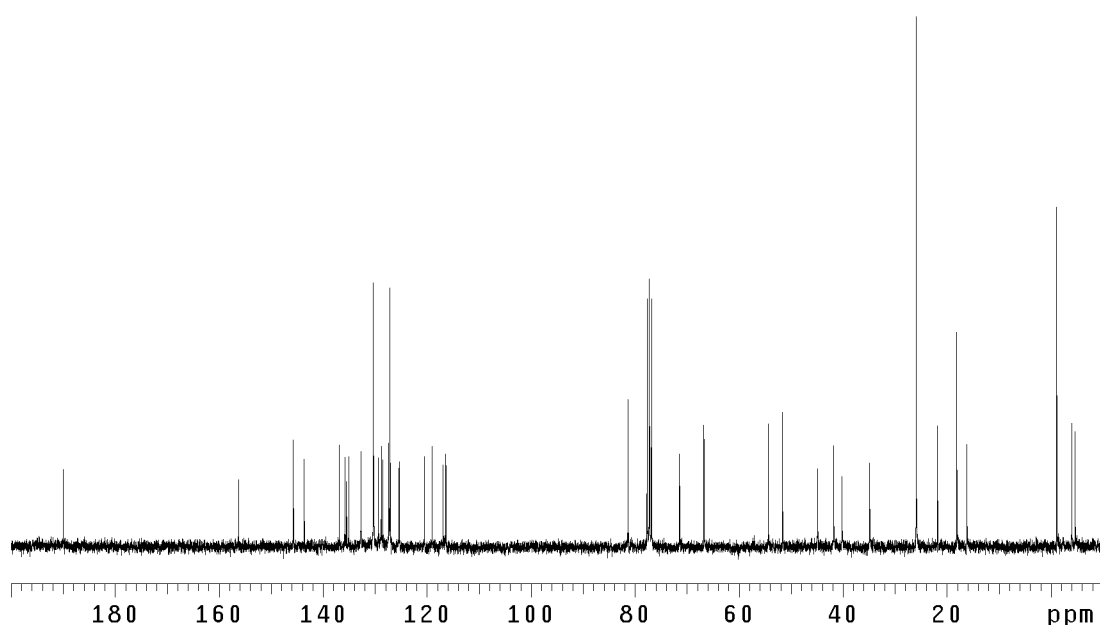


Figure A4.56 ¹³C NMR (75 MHz, CDCl₃) of compound **112**.

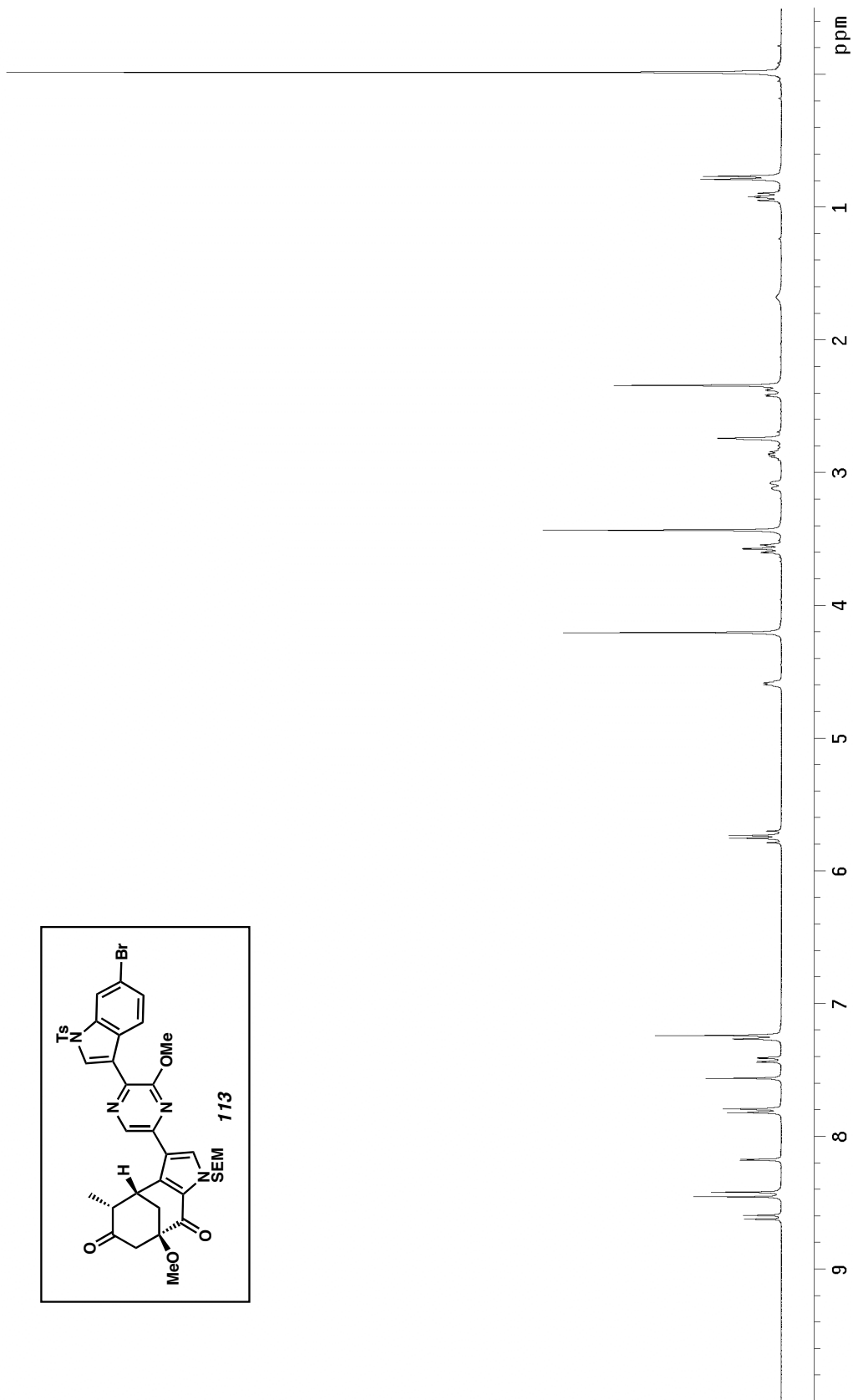
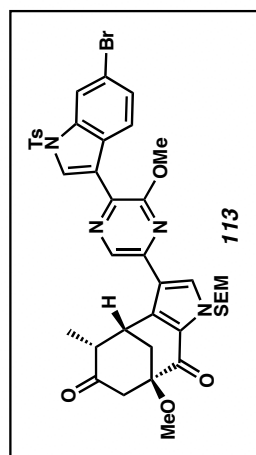


Figure A4.57 ¹H NMR (300 MHz, CDCl₃) of compound **113**.

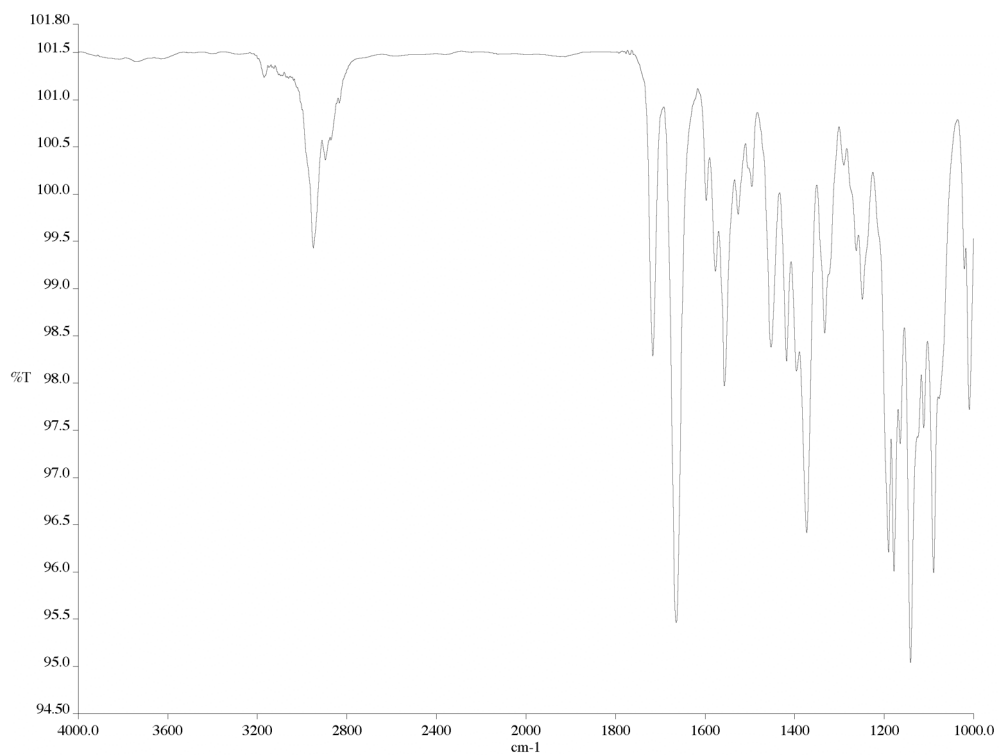


Figure A4.58 Infrared spectrum (thin film/NaCl) of compound **113**.

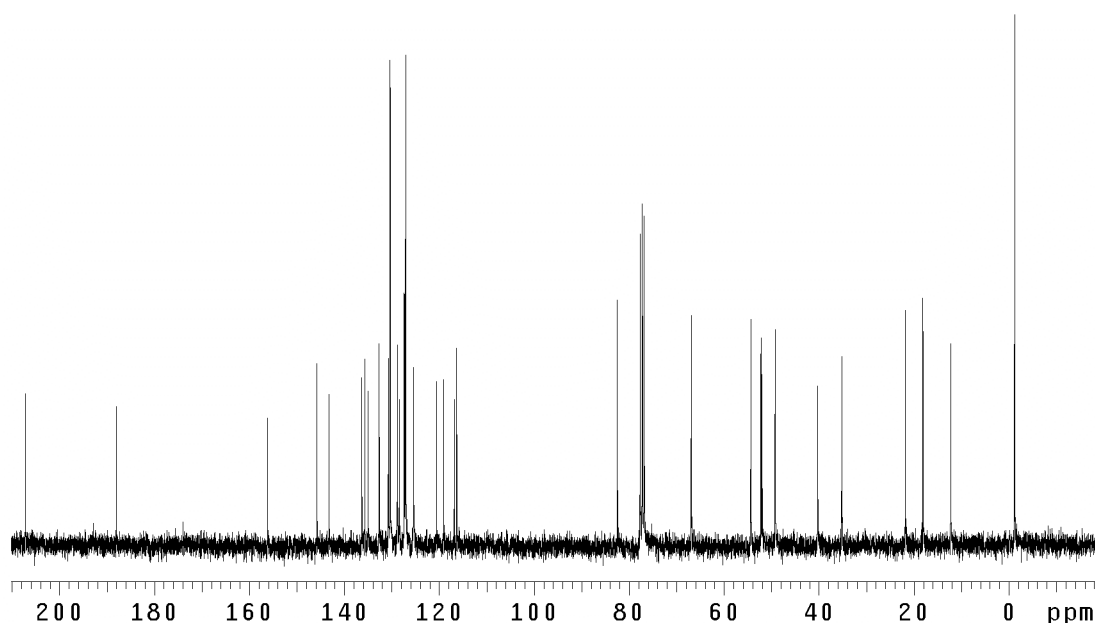


Figure A4.59 ^{13}C NMR (75 MHz, CDCl_3) of compound **113**.

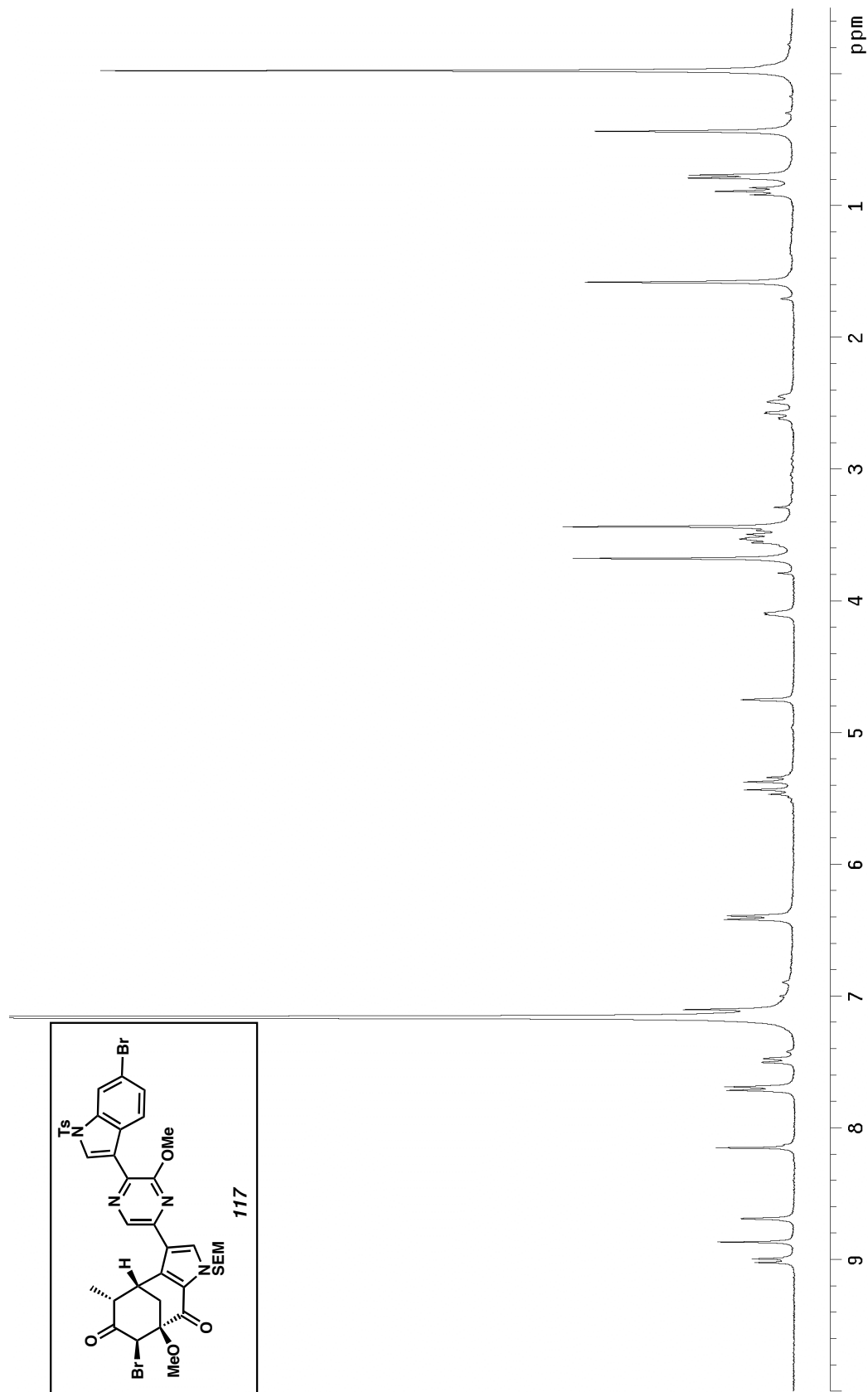


Figure A4.60 ^1H NMR (300 MHz, CDCl_3) of compound **117**.

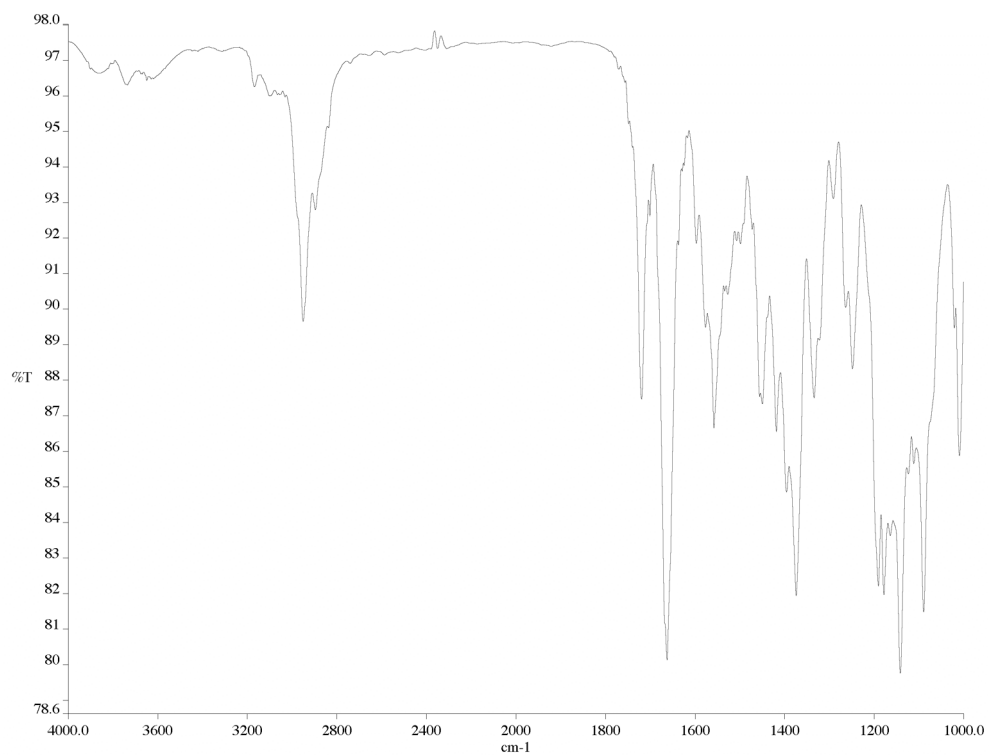


Figure A4.61 Infrared spectrum (thin film/NaCl) of compound **117**.

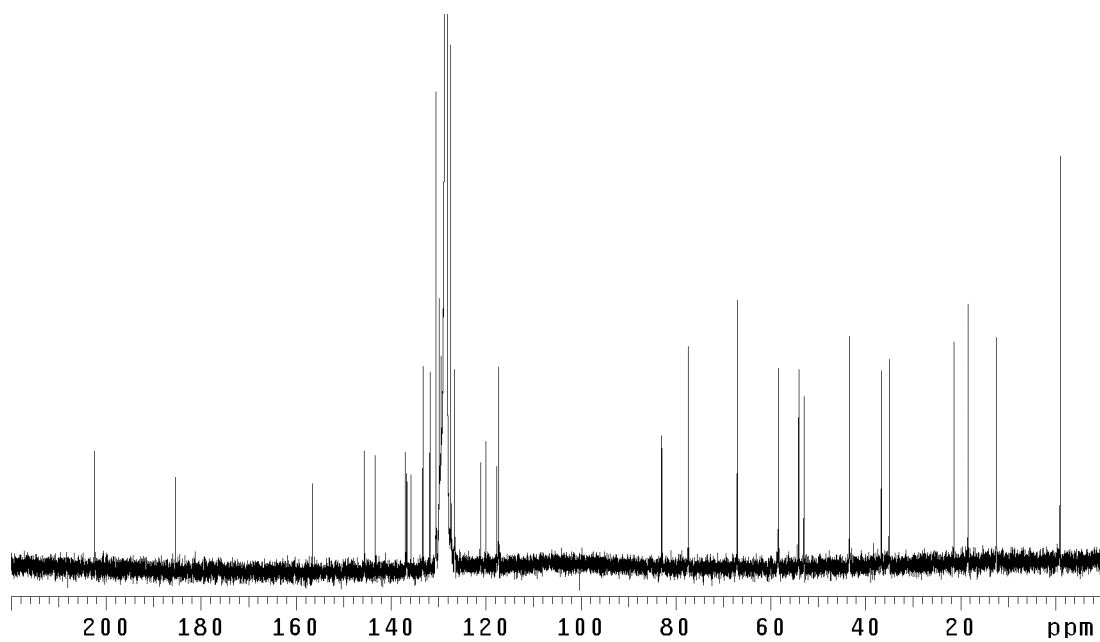


Figure A4.62 ¹³C NMR (125 MHz, C₆D₆) of compound **117**.

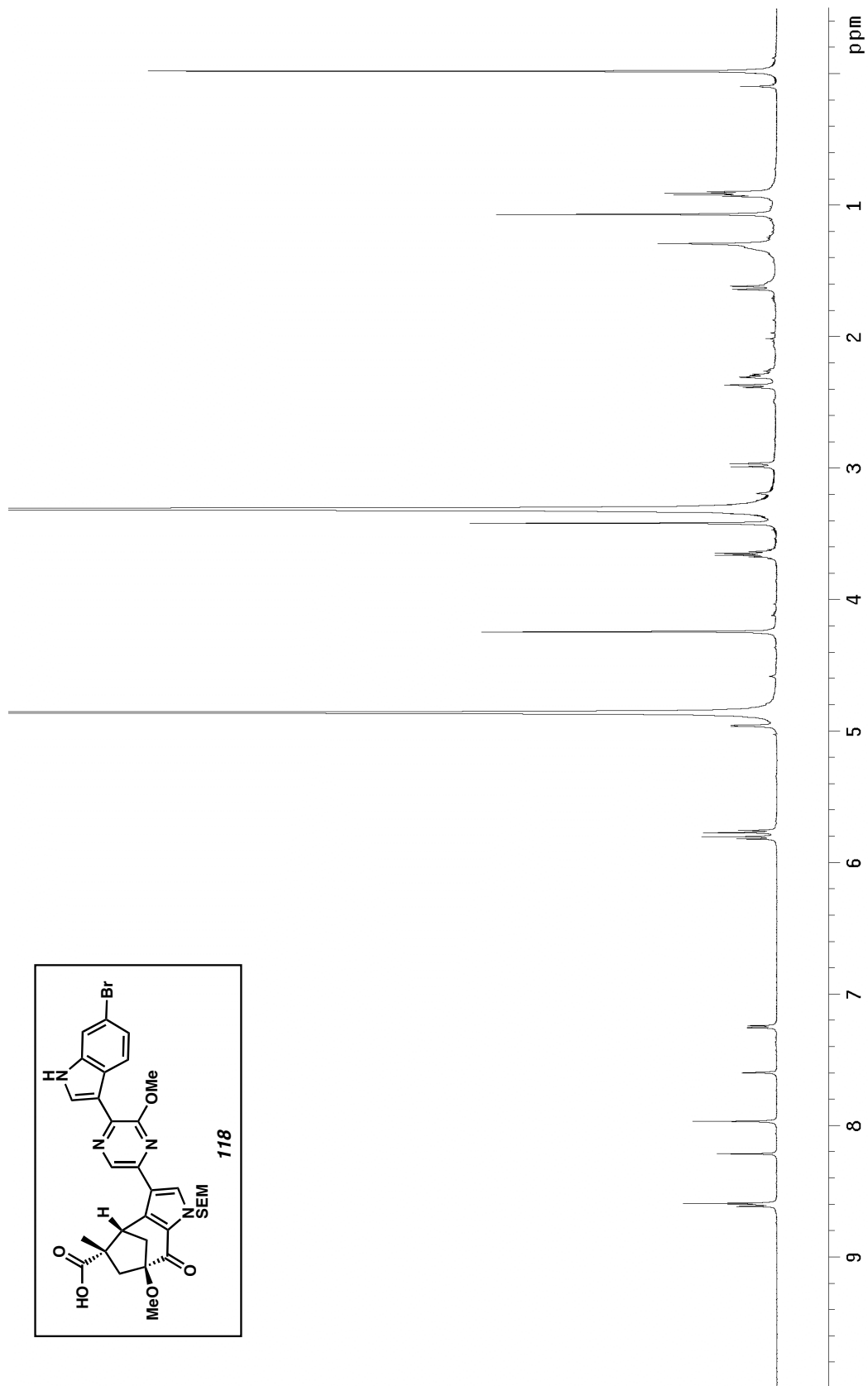


Figure A4.63 ^1H NMR (600 MHz, CD_3OD) of compound **118**.

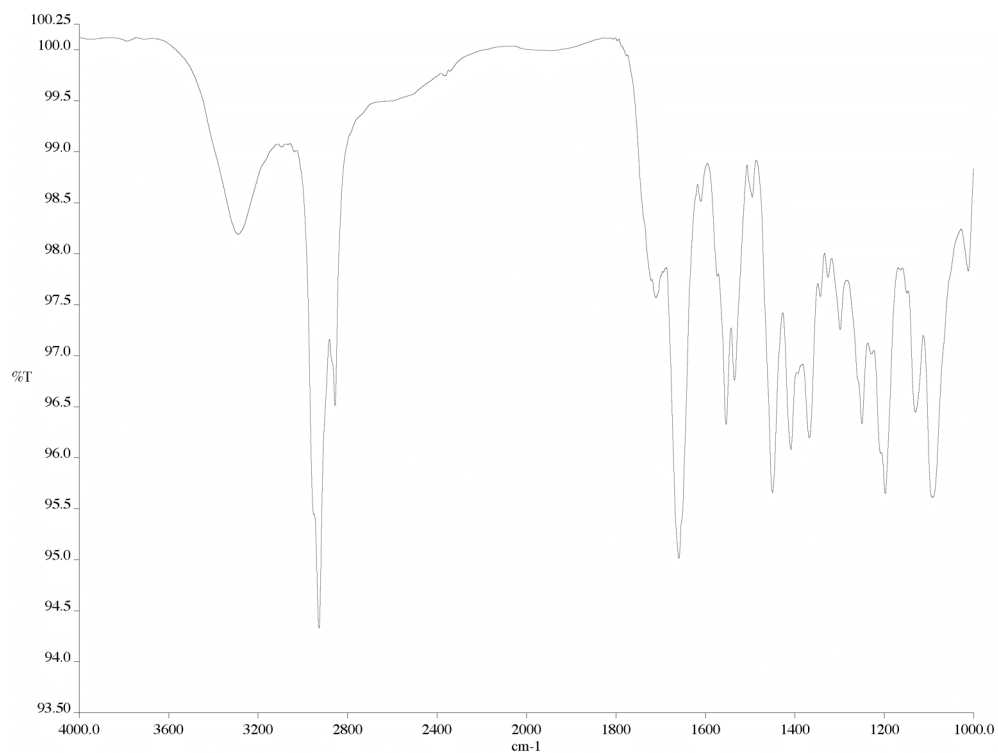


Figure A4.64 Infrared spectrum (thin film/NaCl) of compound **118**.

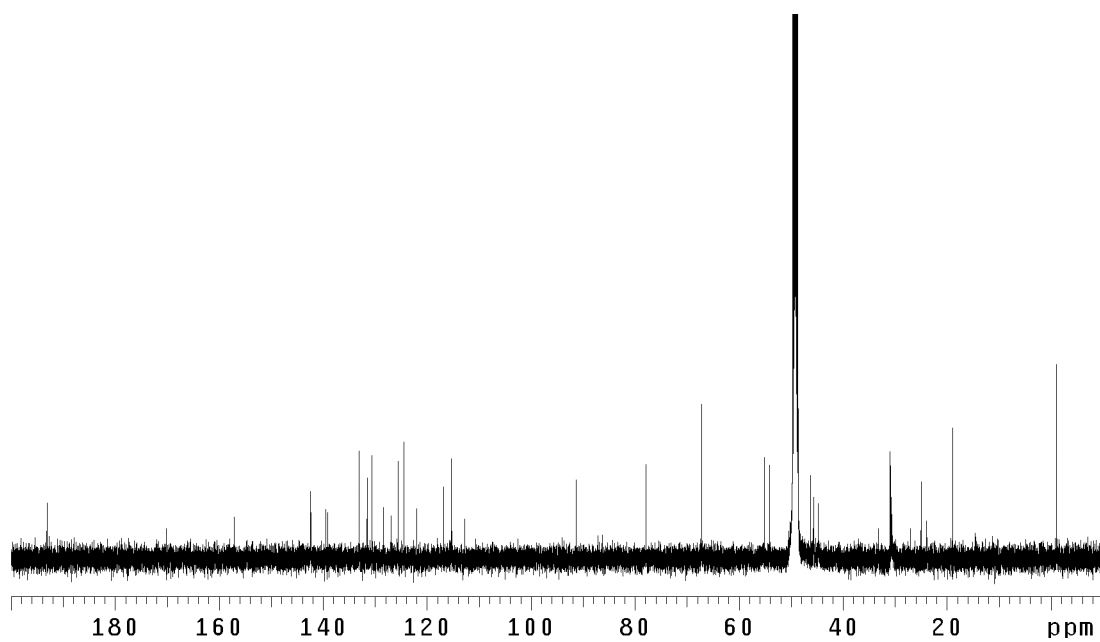


Figure A4.65 ¹³C NMR (125 MHz, CD₃OD) of compound **118**.

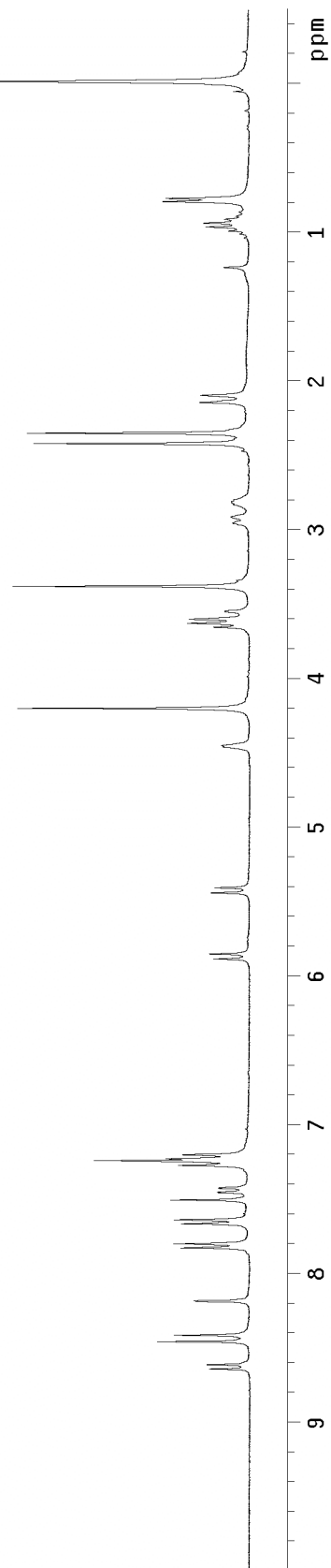
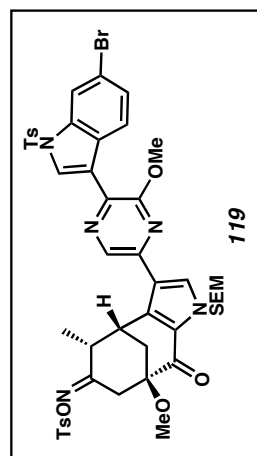


Figure A4.66 ^1H NMR (300 MHz, CDCl_3) of compound **119**.

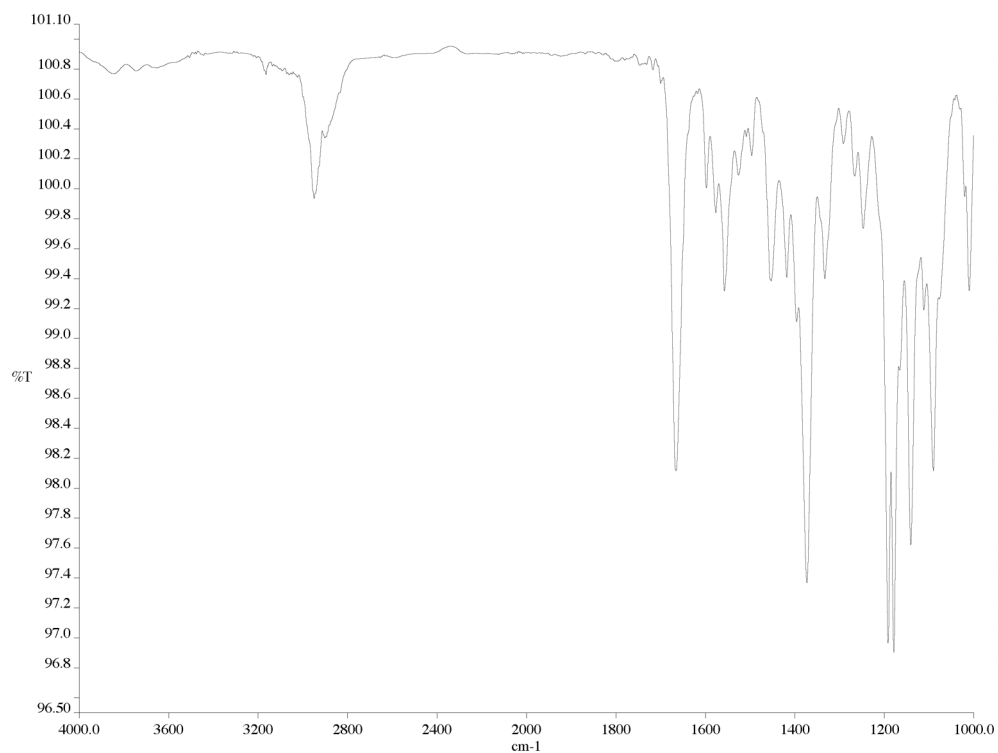


Figure A4.67 Infrared spectrum (thin film/NaCl) of compound **119**.

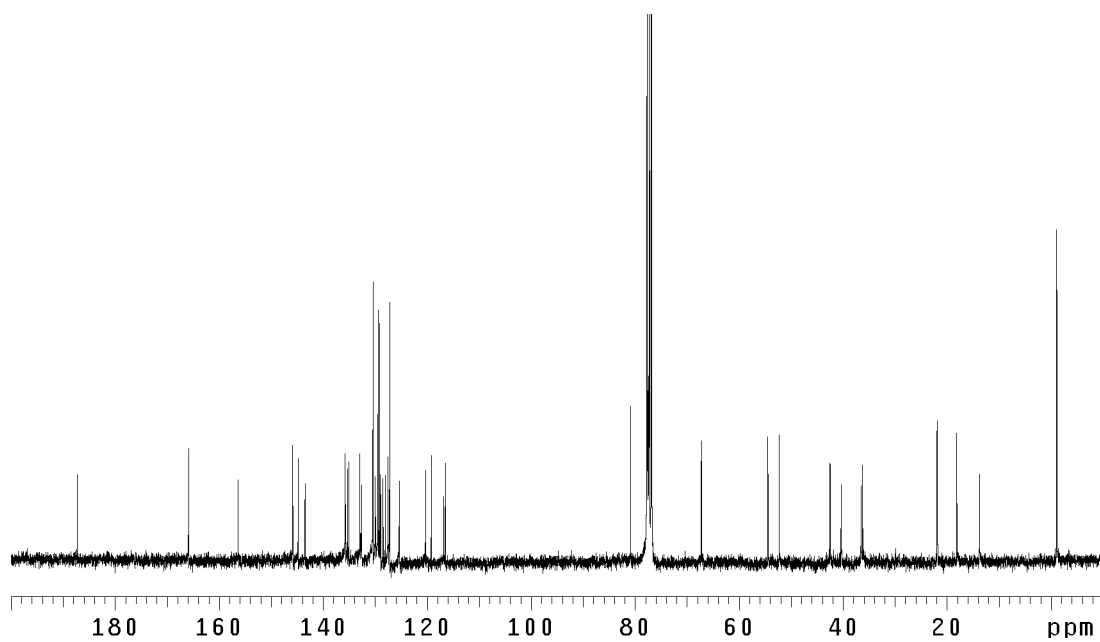


Figure A4.68 ¹³C NMR (75 MHz, CDCl₃) of compound **119**.

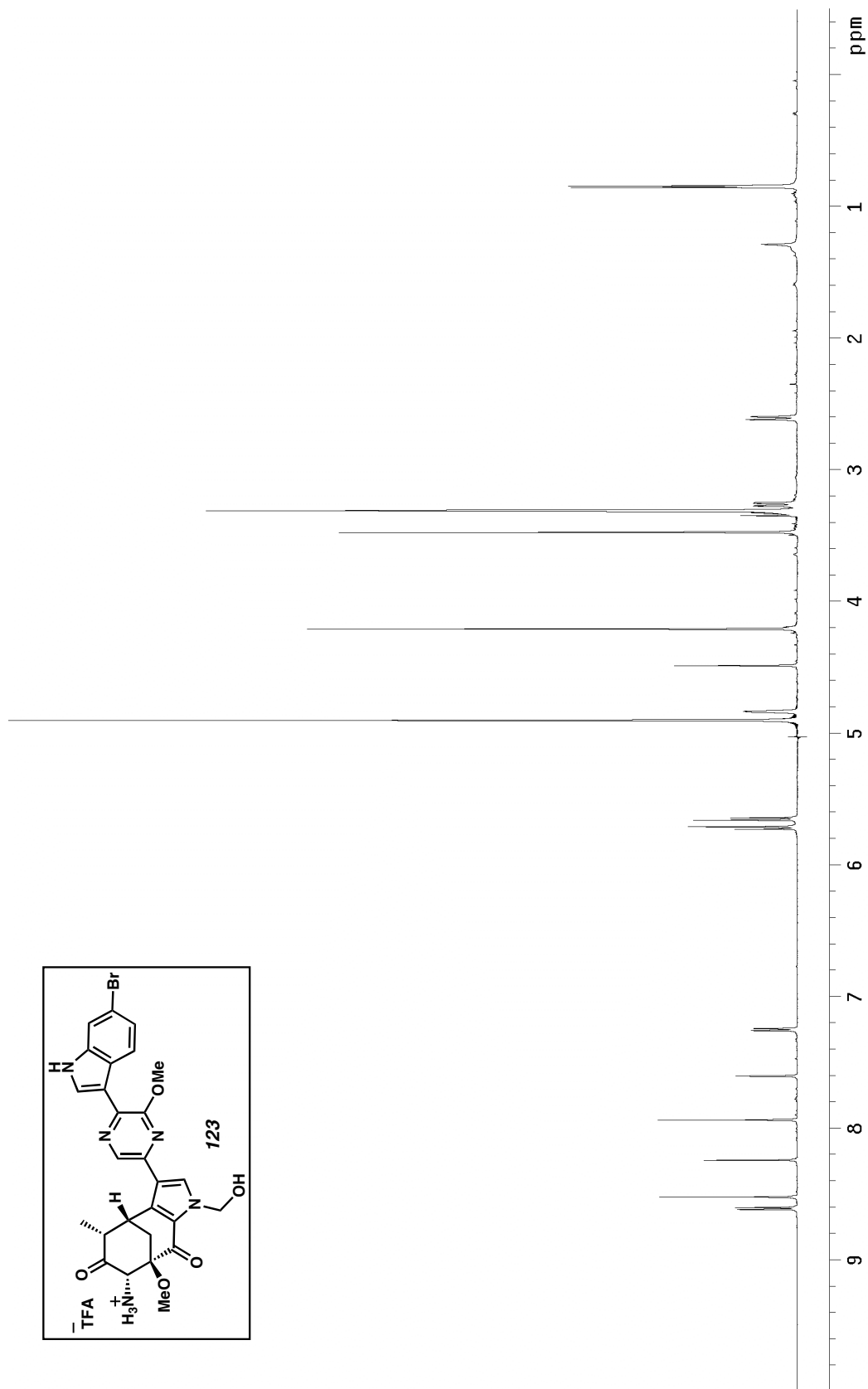


Figure A4.69 ^1H NMR (600 MHz, CD_3OD) of compound **123**.

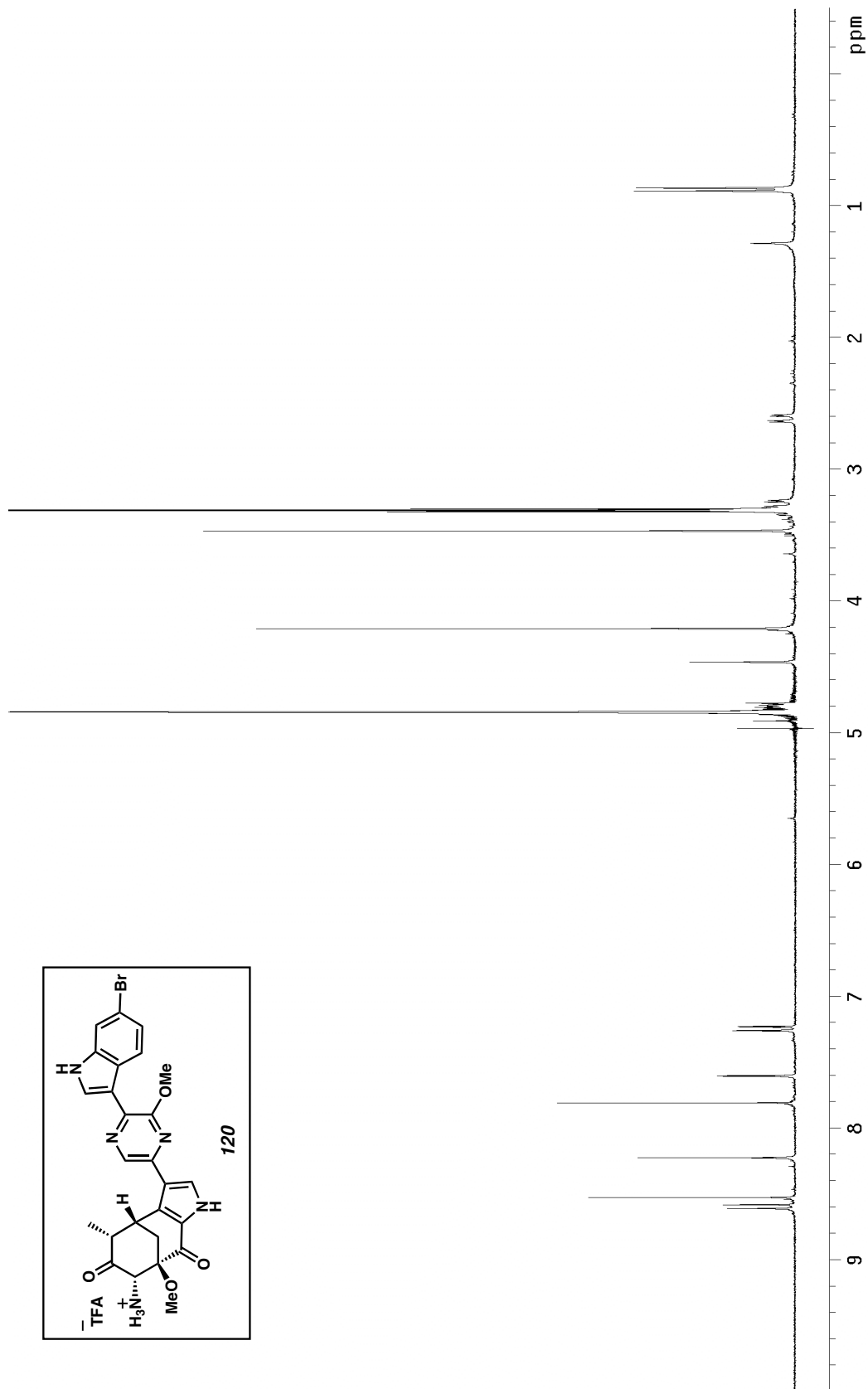


Figure A4.70 ^1H NMR (300 MHz, CD_3OD) of compound **120**.



Figure A4.71 Infrared spectrum (thin film/NaCl) of compound **120**.

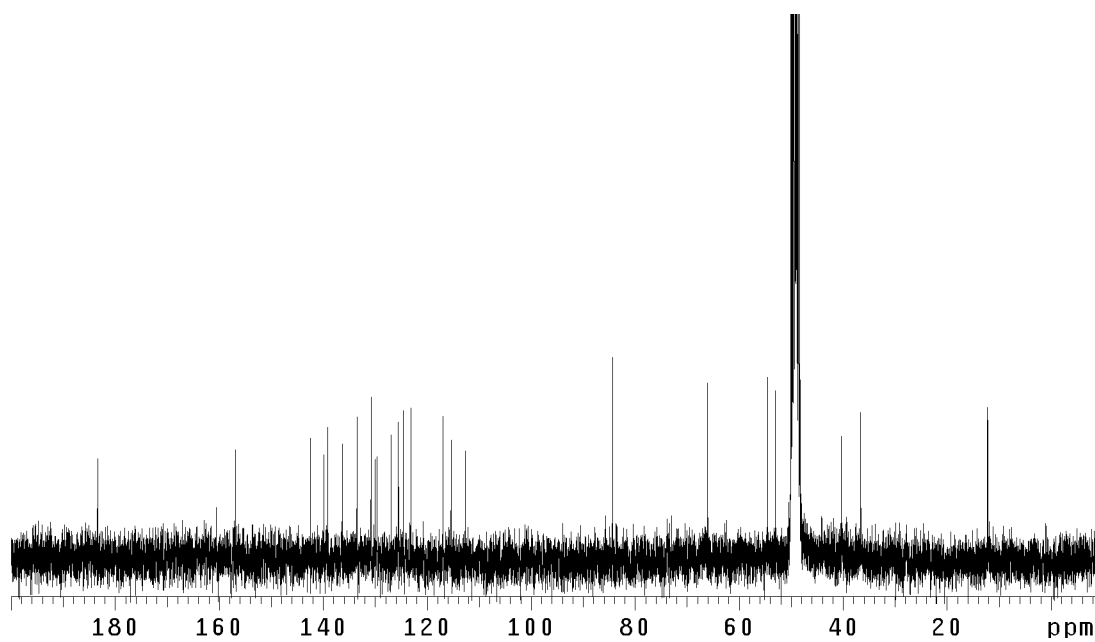


Figure A4.72 ¹³C NMR (75 MHz, CD₃OD) of compound **120**.

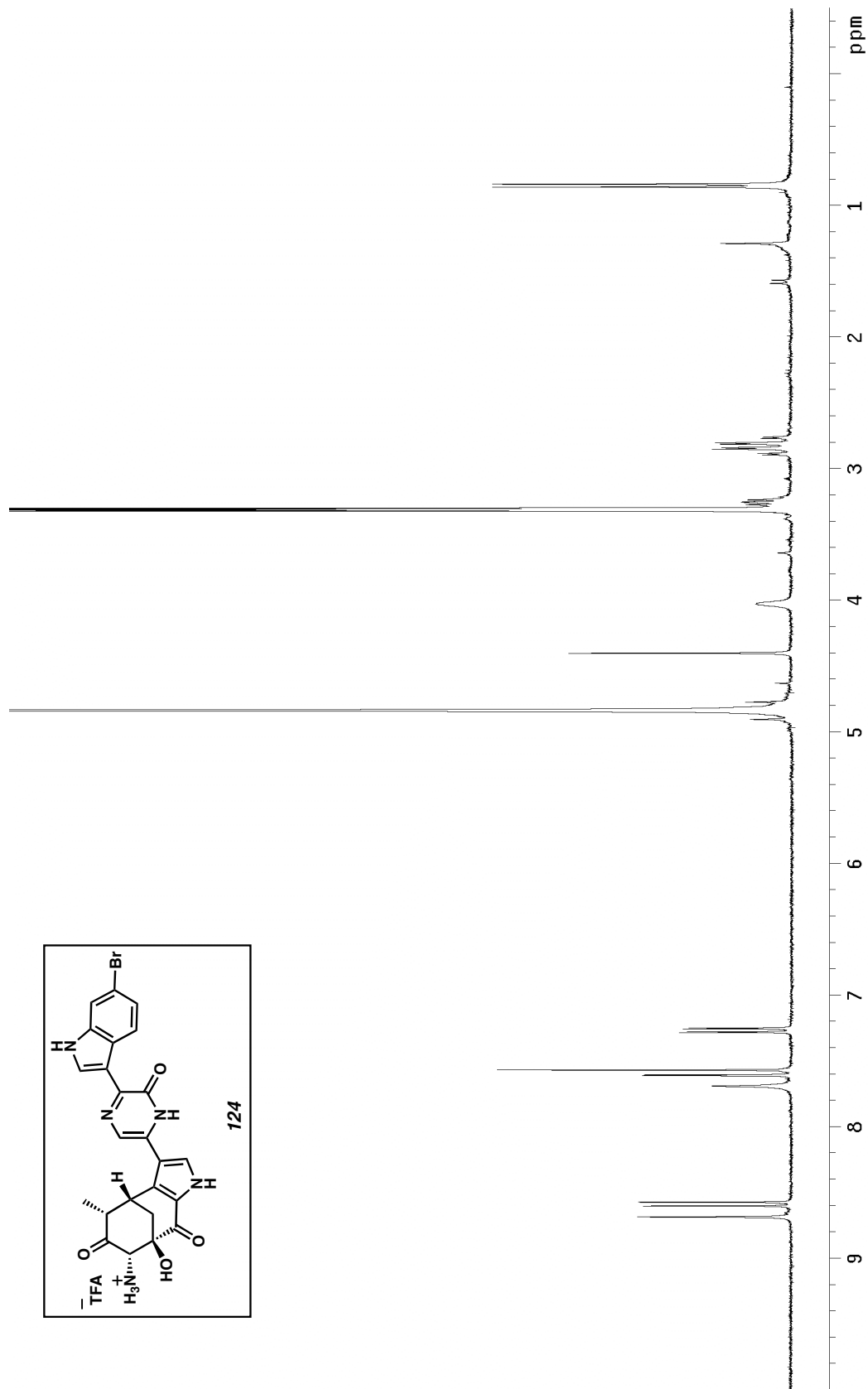


Figure A4.73 ^1H NMR (300 MHz, CD_3OD) of compound **124**.

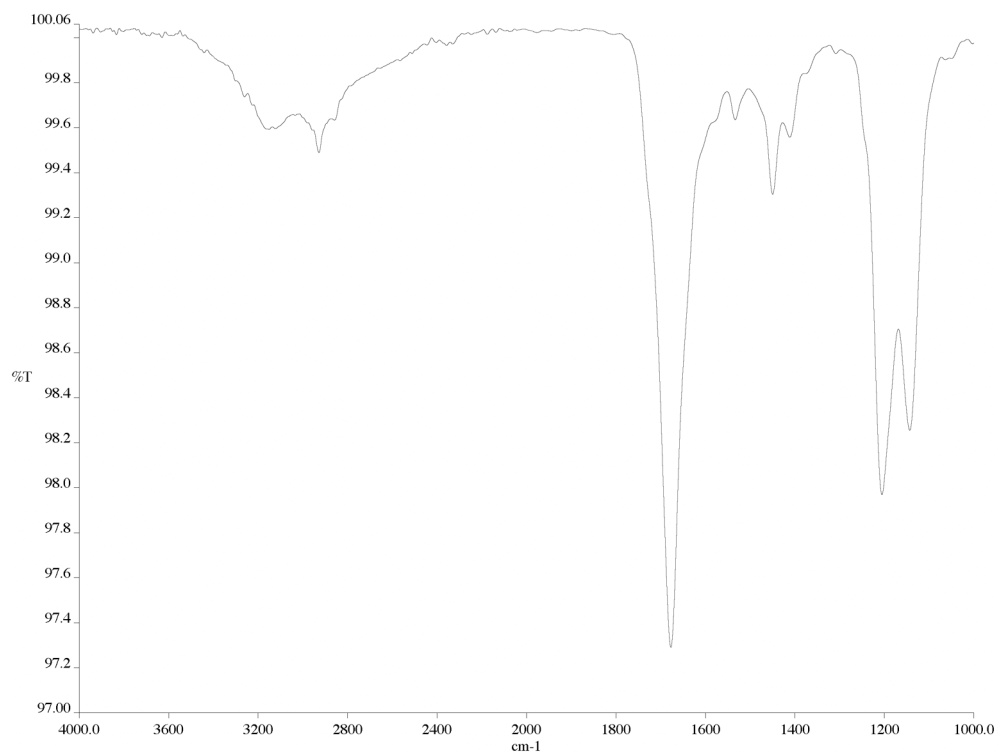


Figure A4.74 Infrared spectrum (thin film/NaCl) of compound **124**.

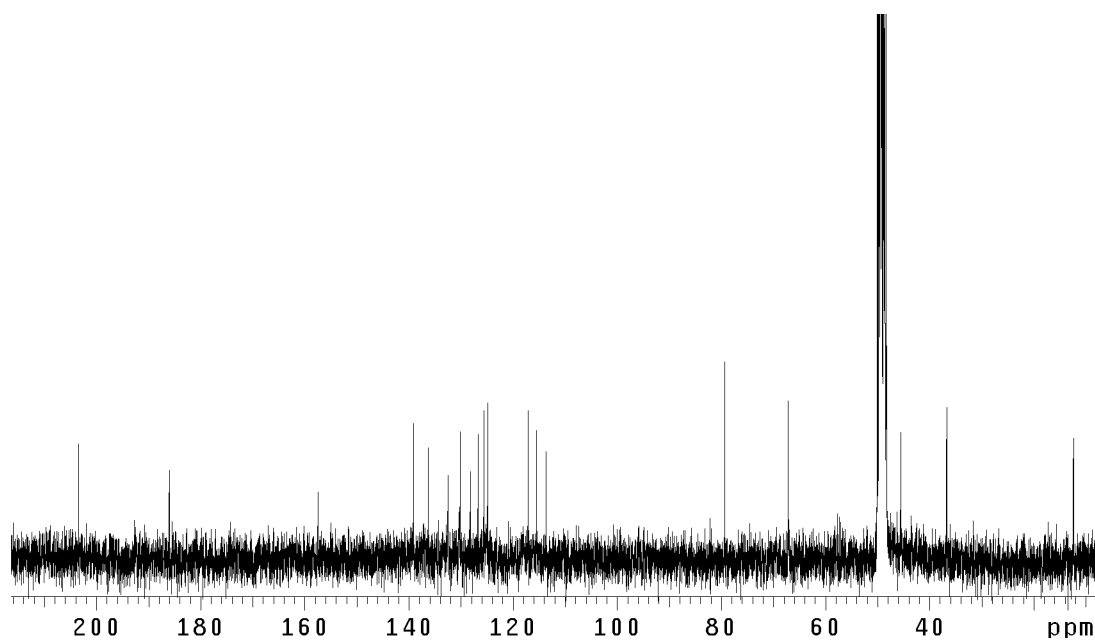


Figure A4.75 ¹³C NMR (75 MHz, CD₃OD) of compound **124**.

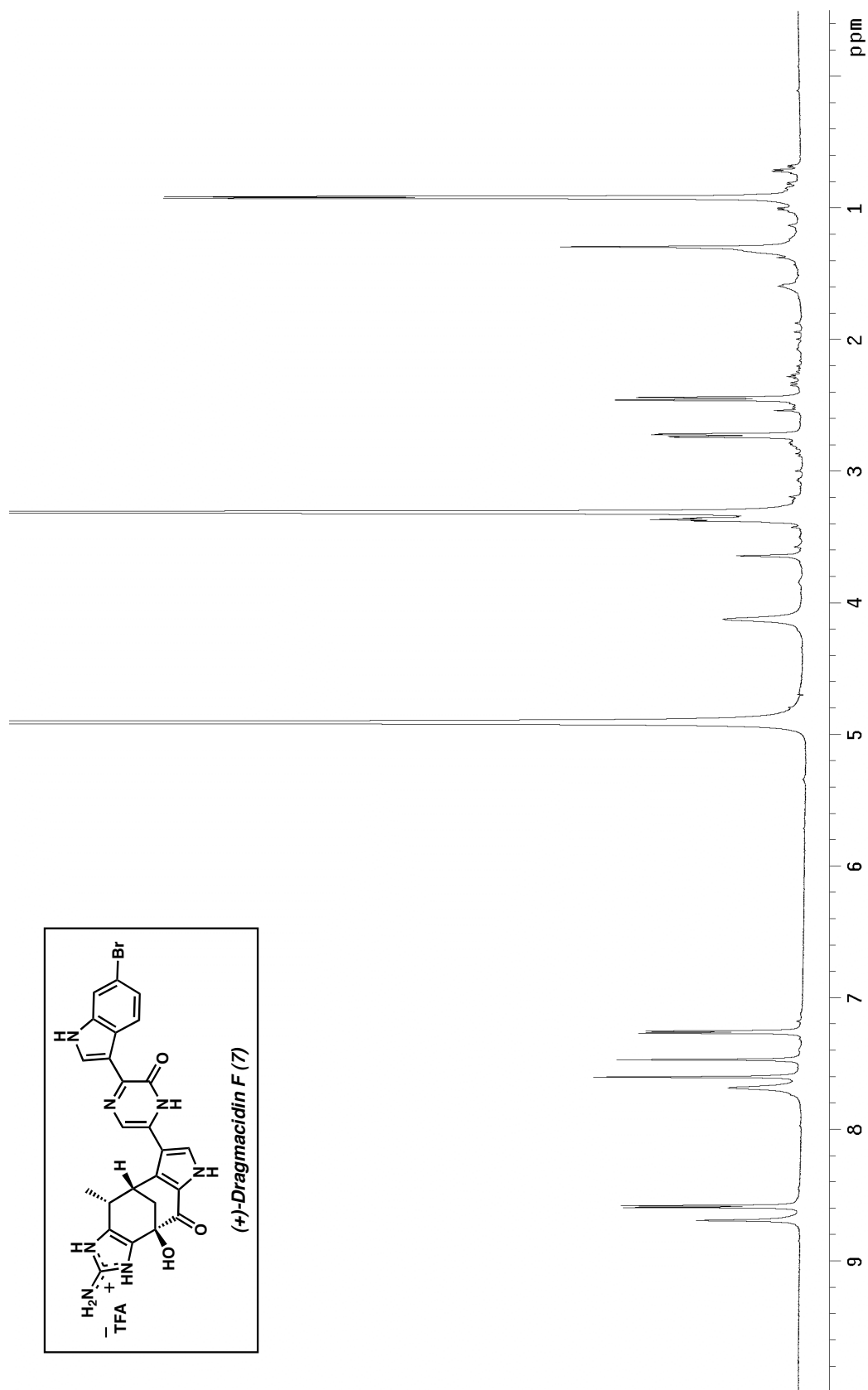


Figure A4.76 ^1H NMR (600 MHz, CD_3OD) of (+)-dragmacidin F (7).

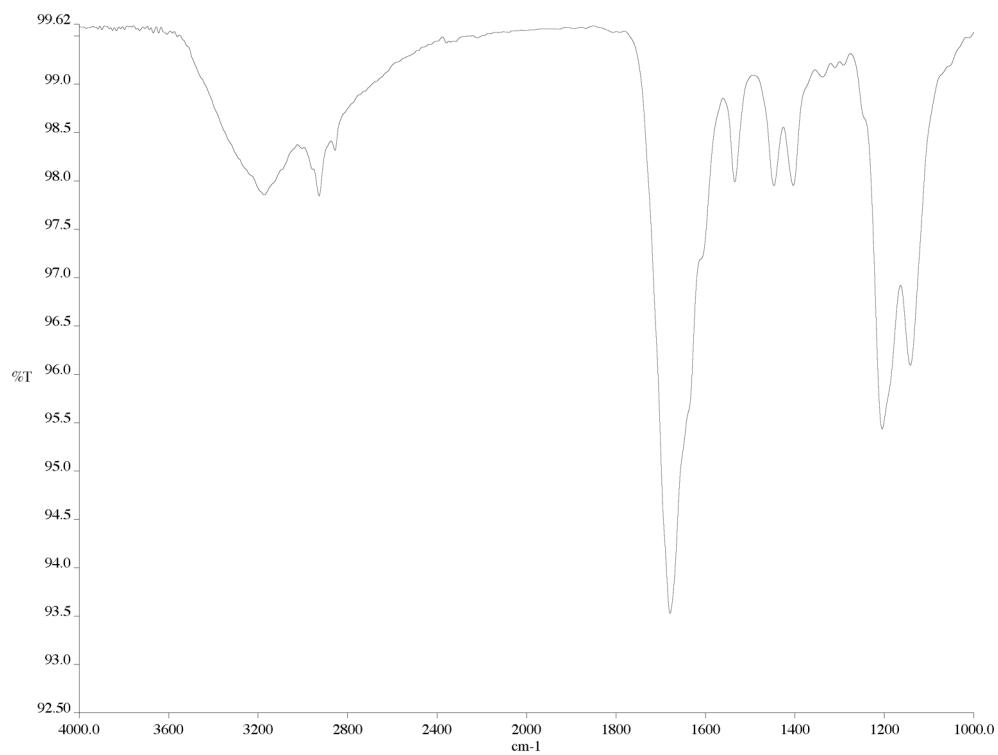


Figure A4.77 Infrared spectrum (thin film/NaCl) of (+)-dragmacidin F (**7**).

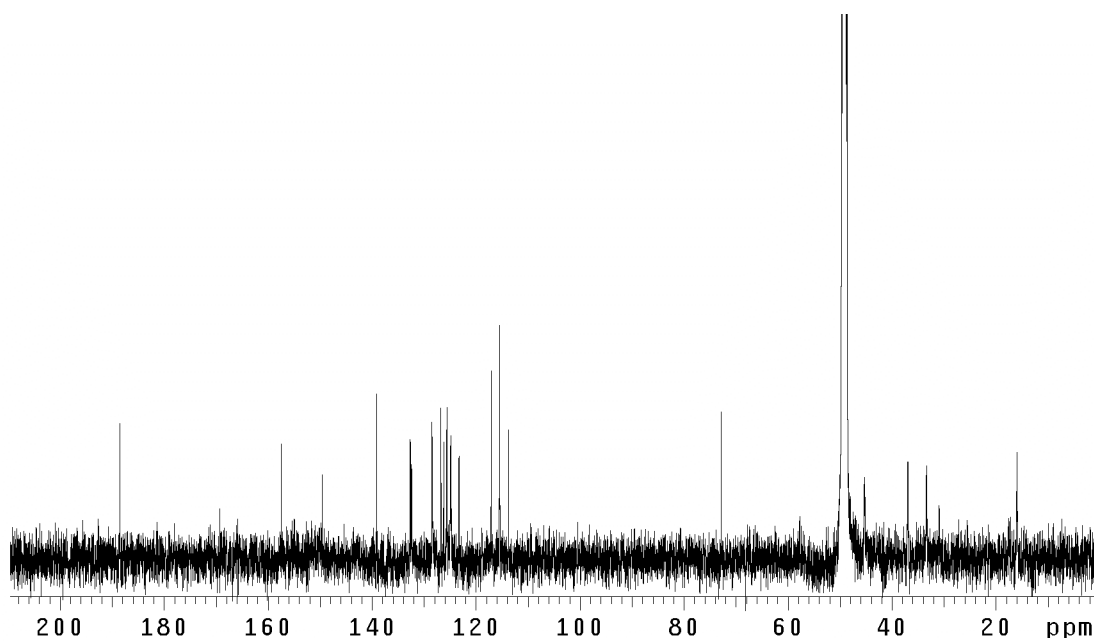


Figure A4.78 ¹³C NMR (125 MHz, CD₃OD) of (+)-dragmacidin F (**7**).

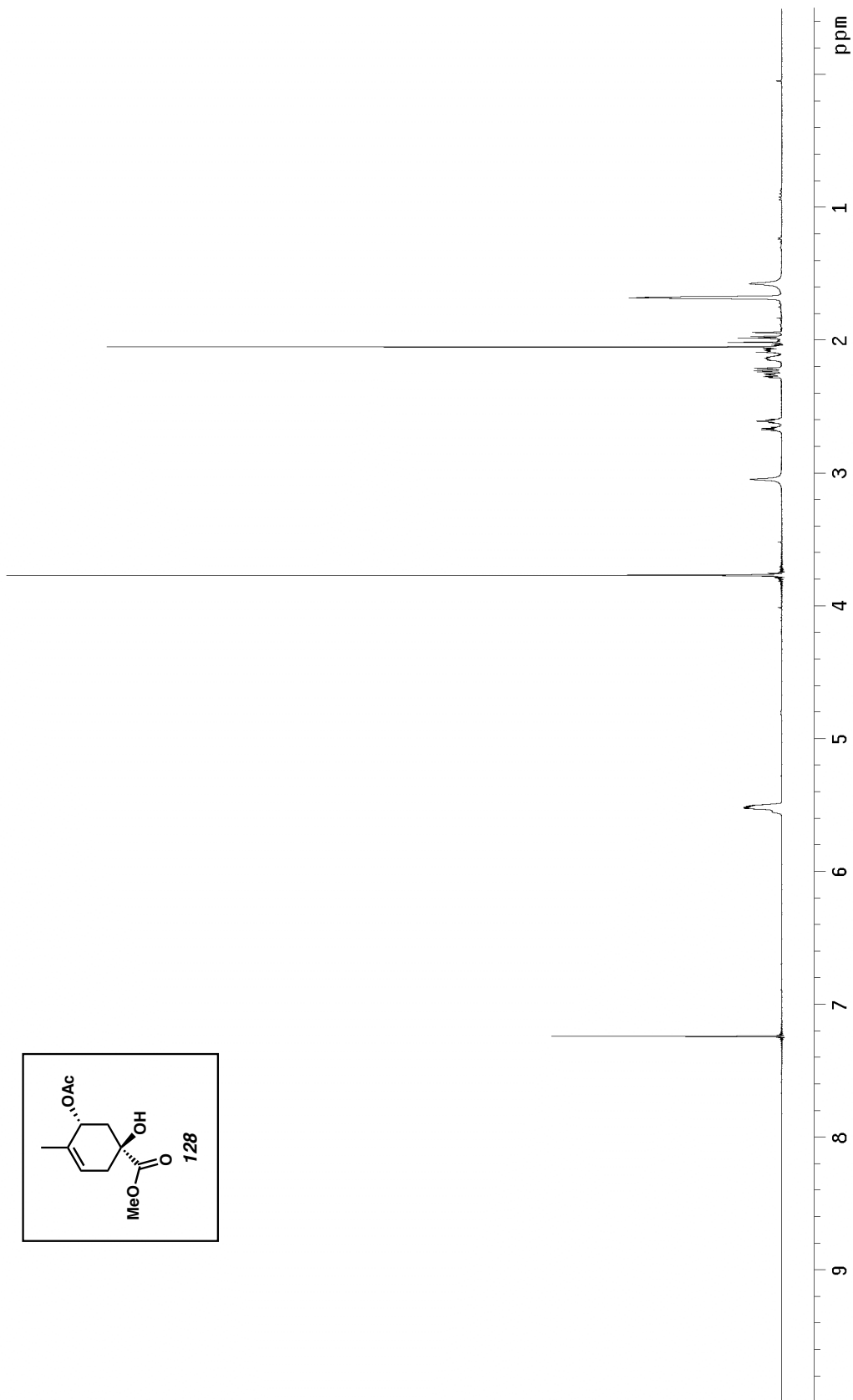
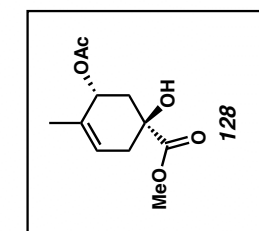


Figure A4.79 ¹H NMR (300 MHz, CDCl₃) of compound **128**.

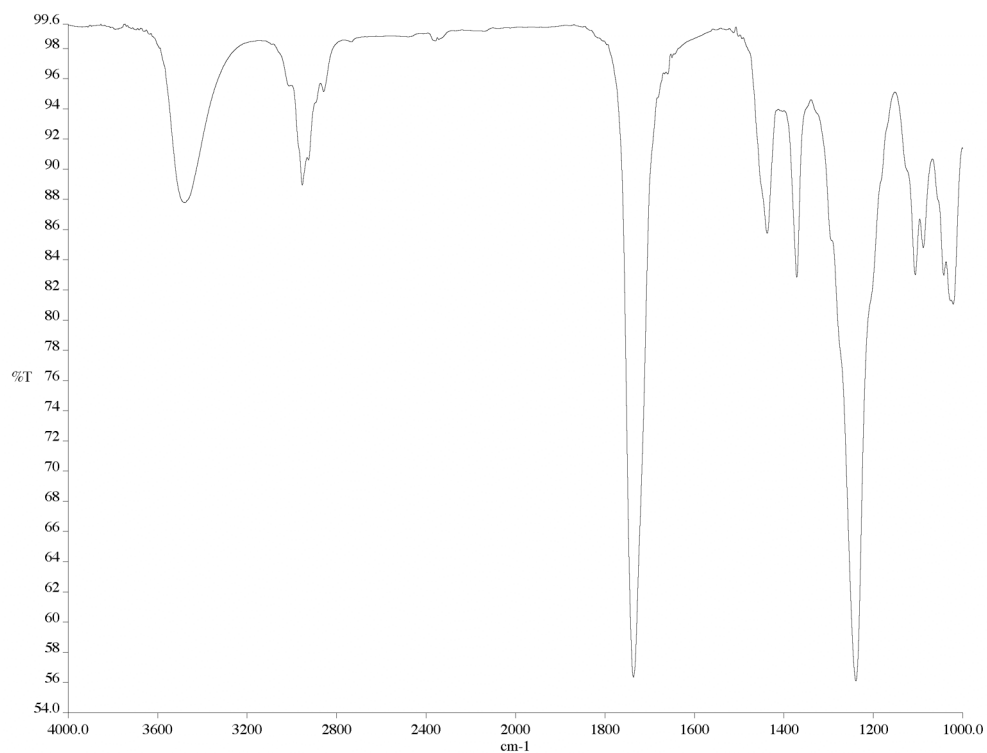


Figure A4.80 Infrared spectrum (thin film/NaCl) of compound **128**.

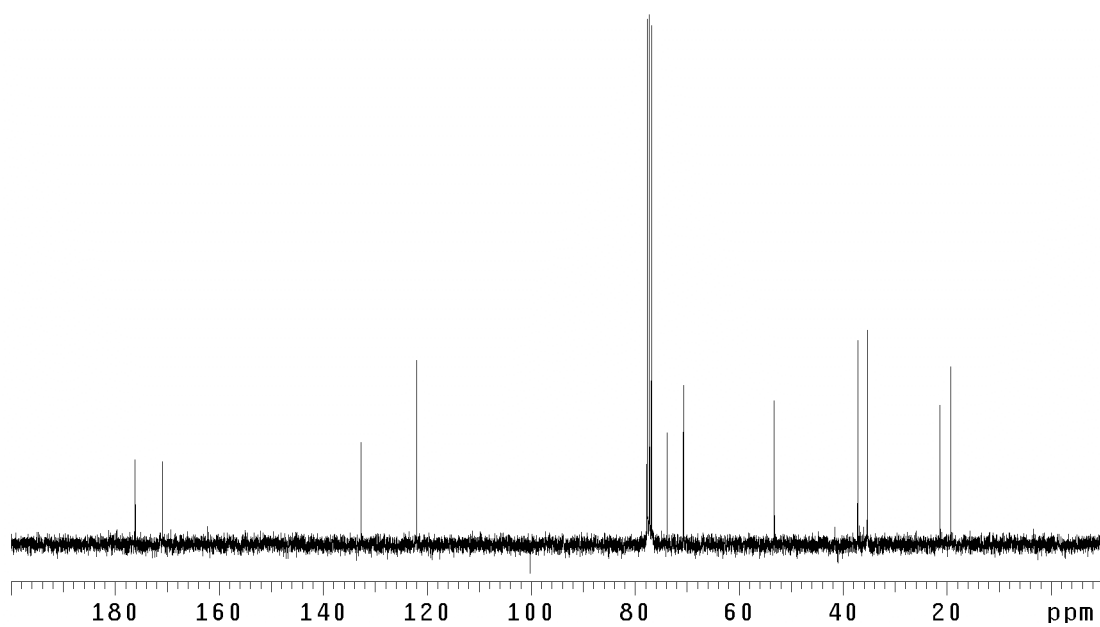


Figure A4.81 ¹³C NMR (75 MHz, CDCl₃) of compound **128**.

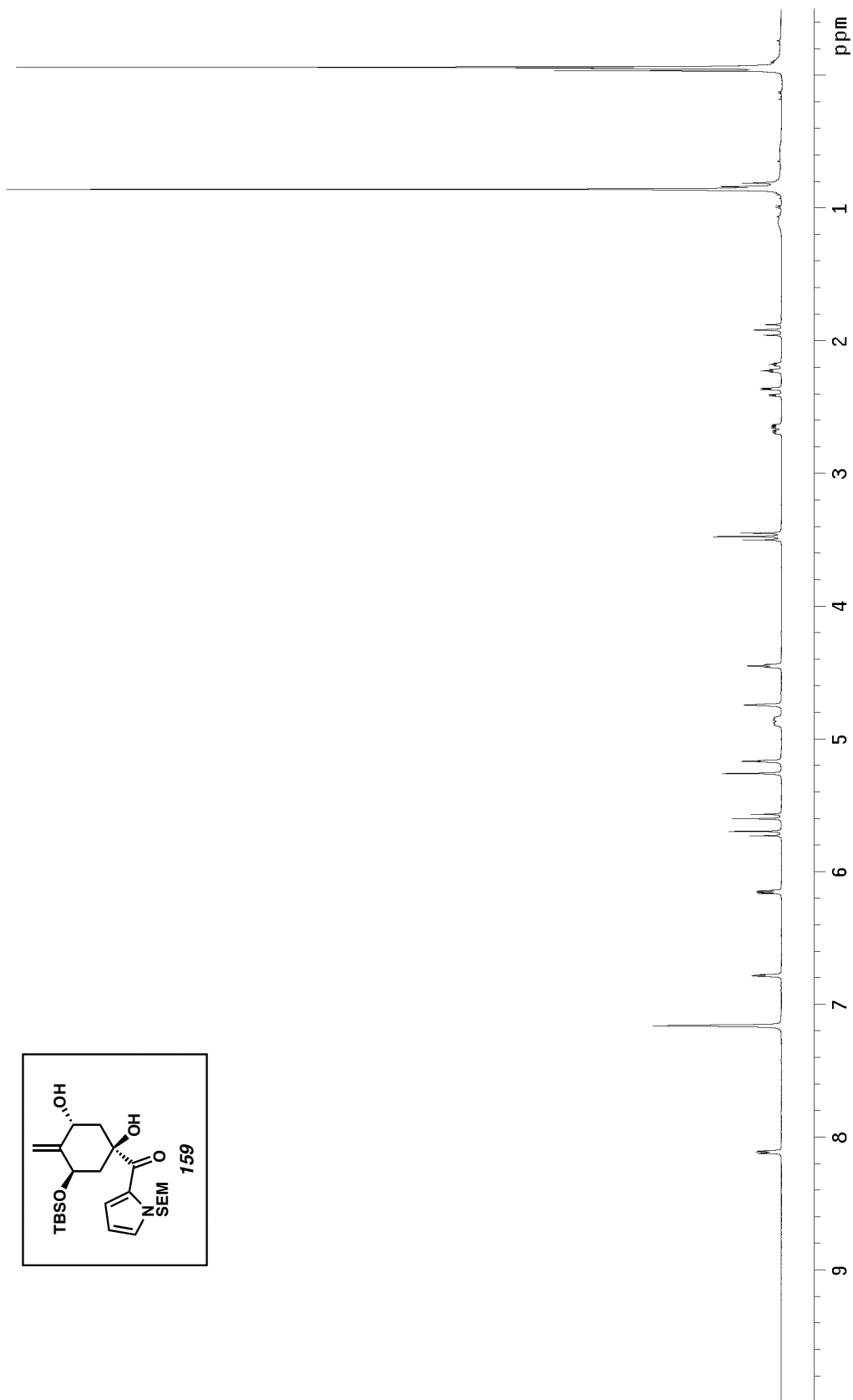
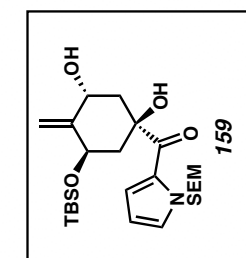


Figure A4.82 ^1H NMR (300 MHz, C_6D_6) of compound **159**.

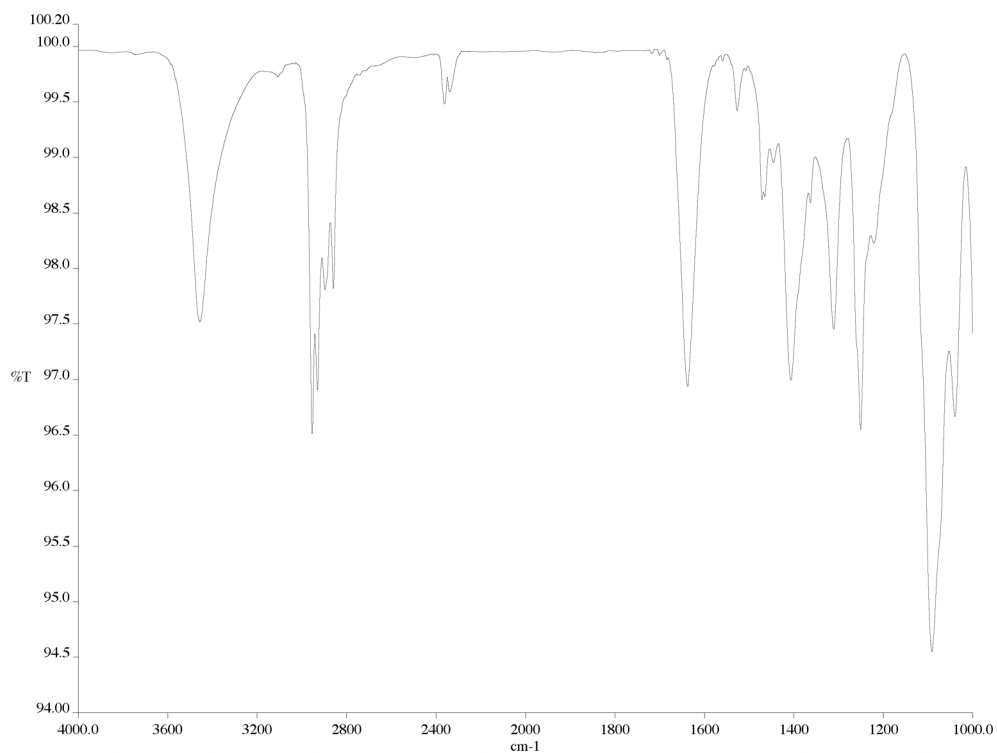


Figure A4.83 Infrared spectrum (thin film/NaCl) of compound **159**.

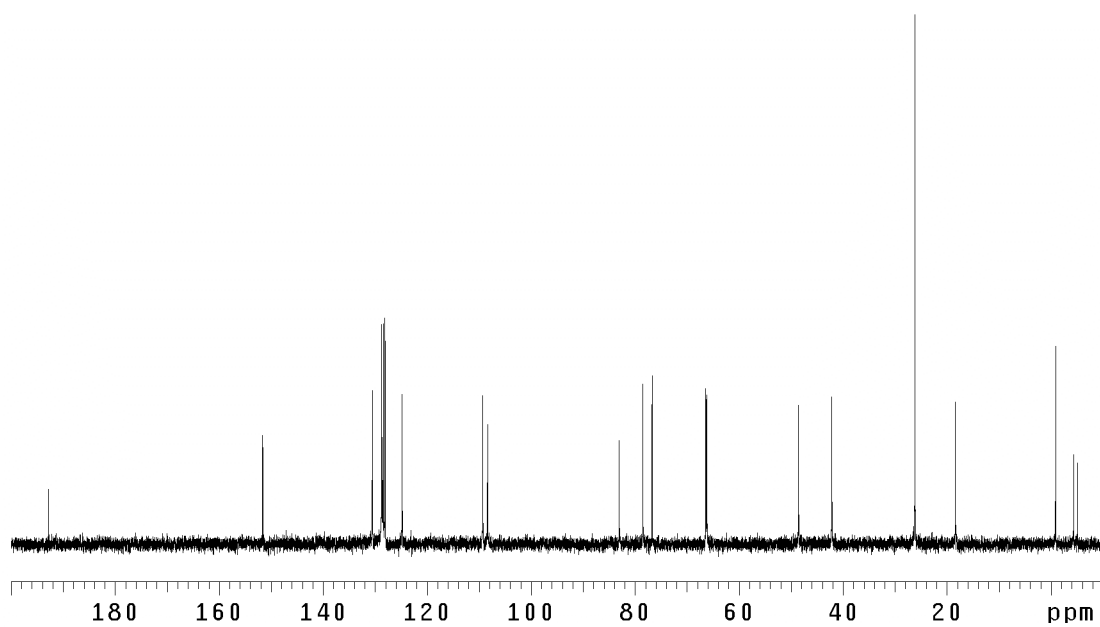


Figure A4.84 ¹³C NMR (75 MHz, C₆D₆) of compound **159**.

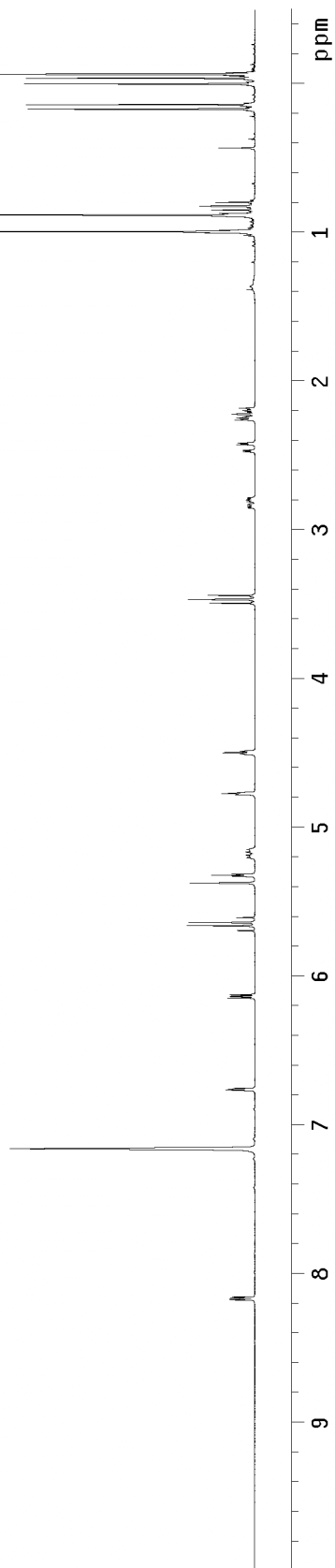
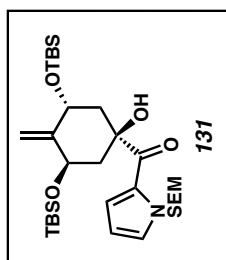


Figure A4.85 ^1H NMR (300 MHz, C_6D_6) of compound **131**.

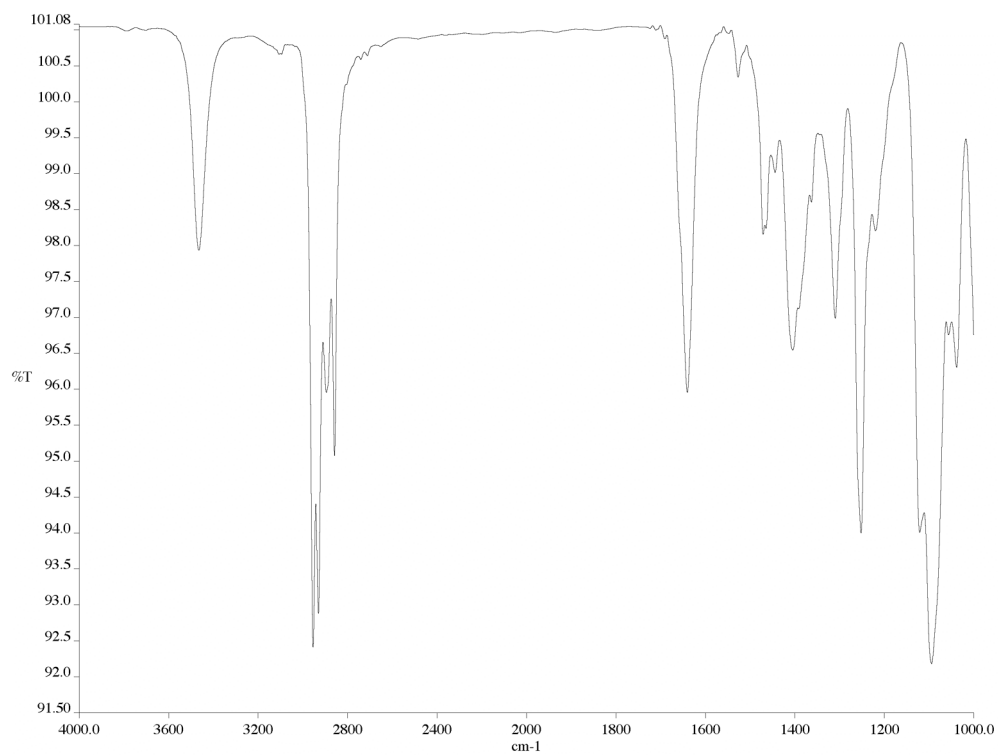


Figure A4.86 Infrared spectrum (thin film/NaCl) of compound **131**.

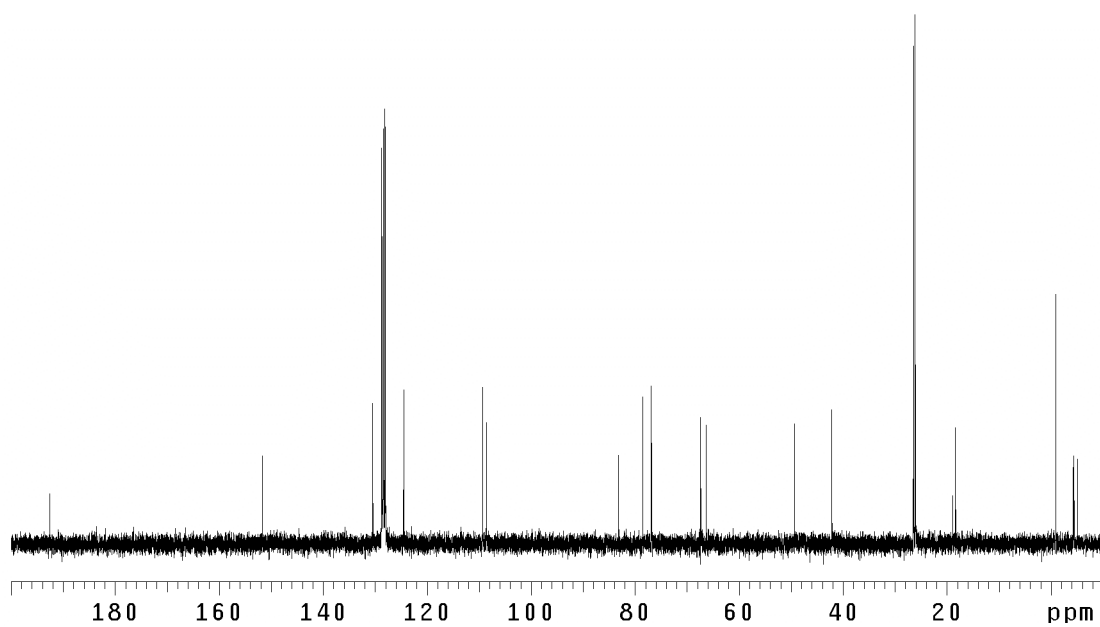


Figure A4.87 ¹³C NMR (75 MHz, C₆D₆) of compound **131**.

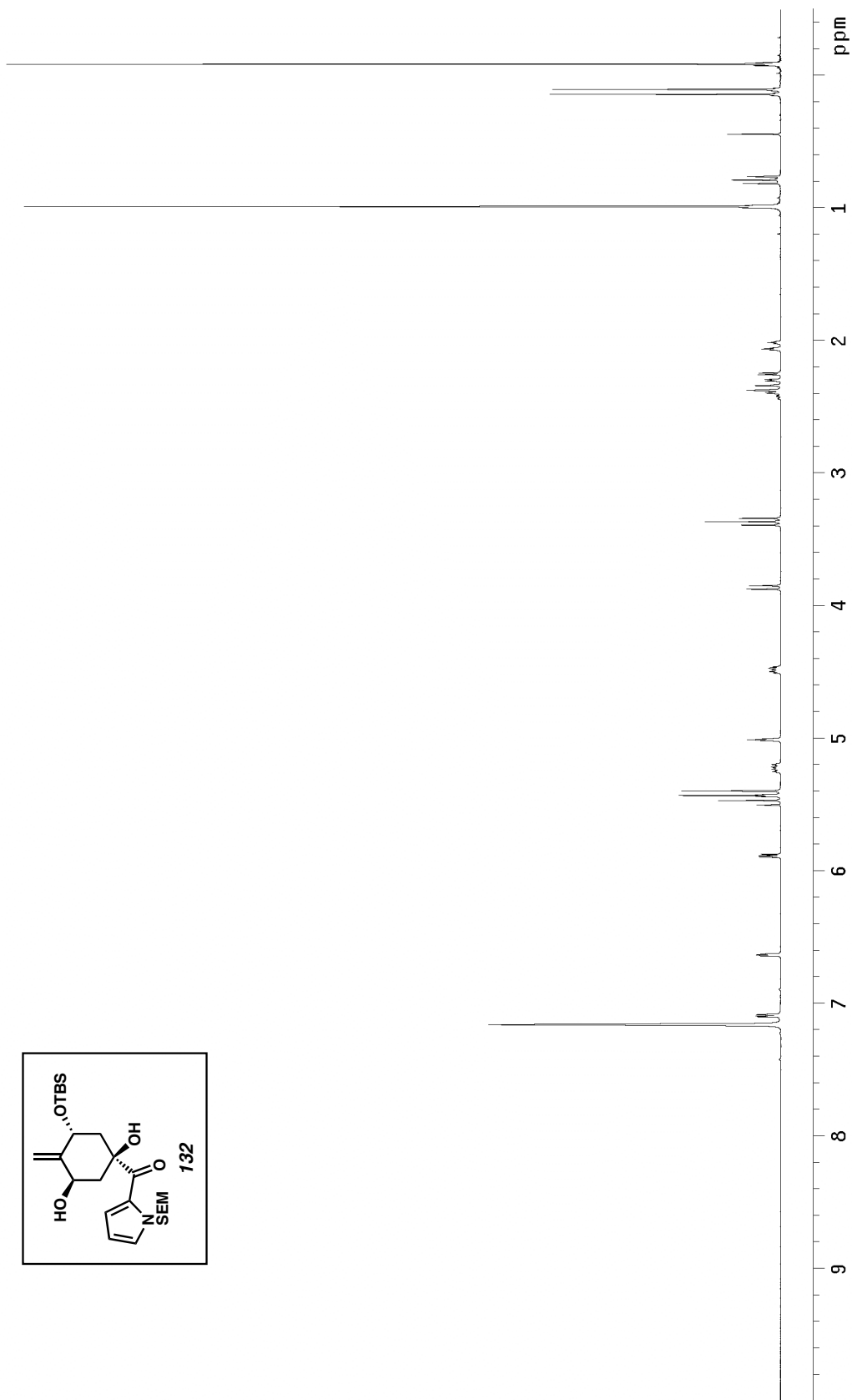
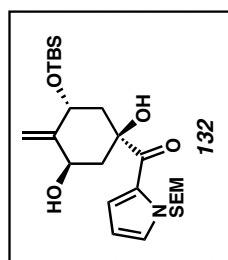


Figure A4.88 ^1H NMR (300 MHz, C_6D_6) of compound **132**.

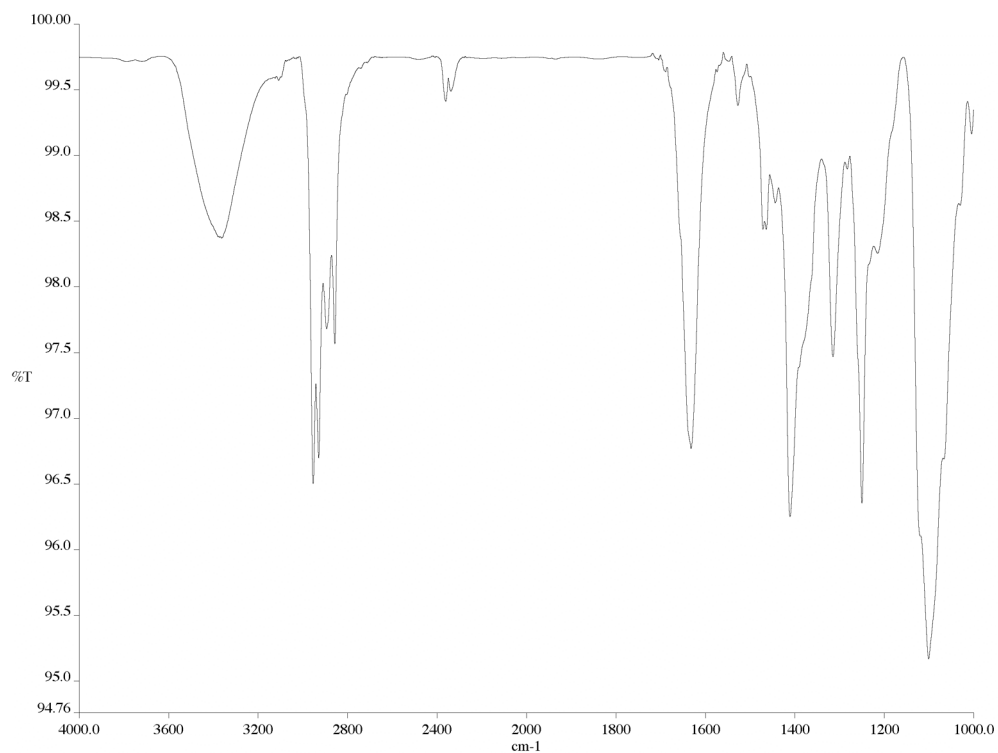


Figure A4.89 Infrared spectrum (thin film/NaCl) of compound **132**.

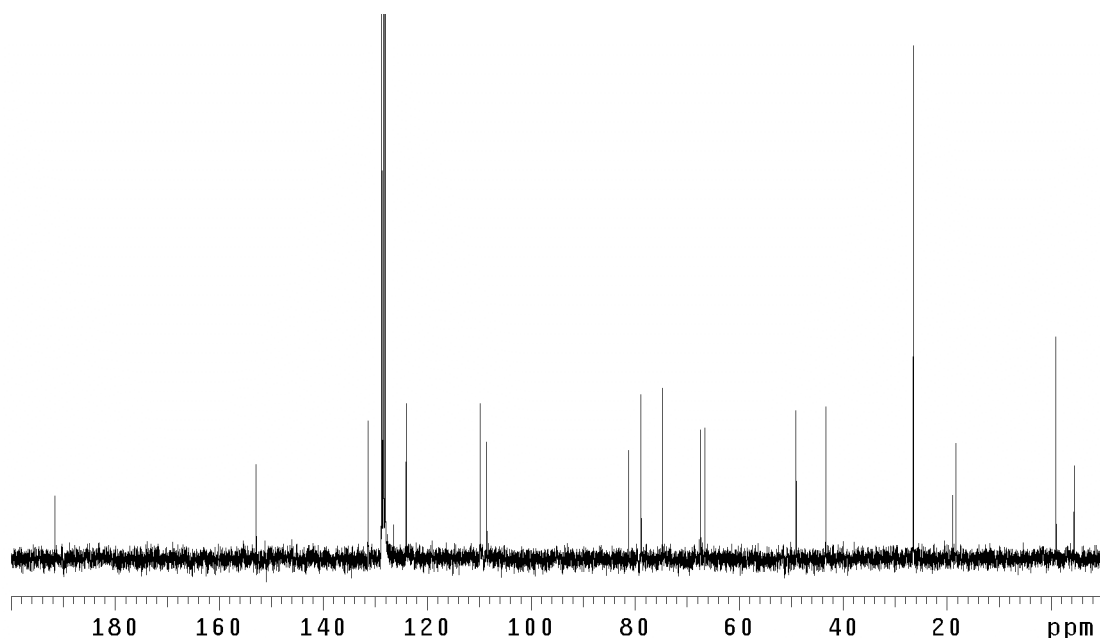


Figure A4.90 ¹³C NMR (75 MHz, C₆D₆) of compound **132**.

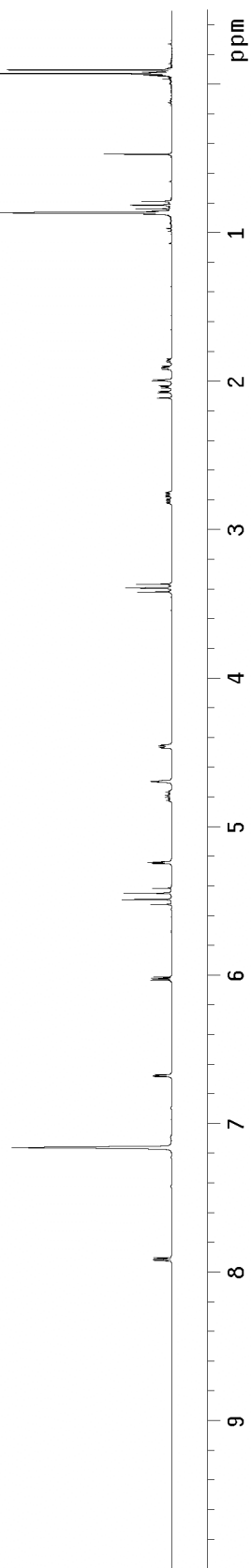
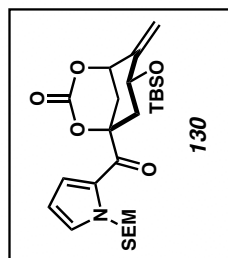


Figure A4.91 ^1H NMR (300 MHz, C_6D_6) of compound **130**.

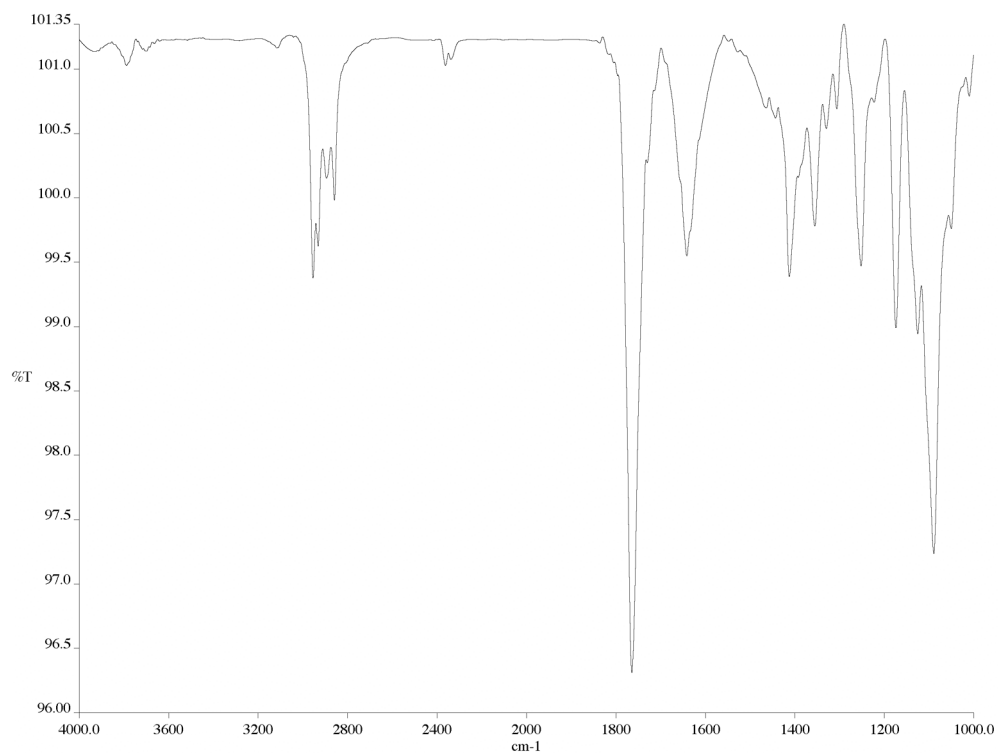


Figure A4.92 Infrared spectrum (thin film/NaCl) of compound **130**.

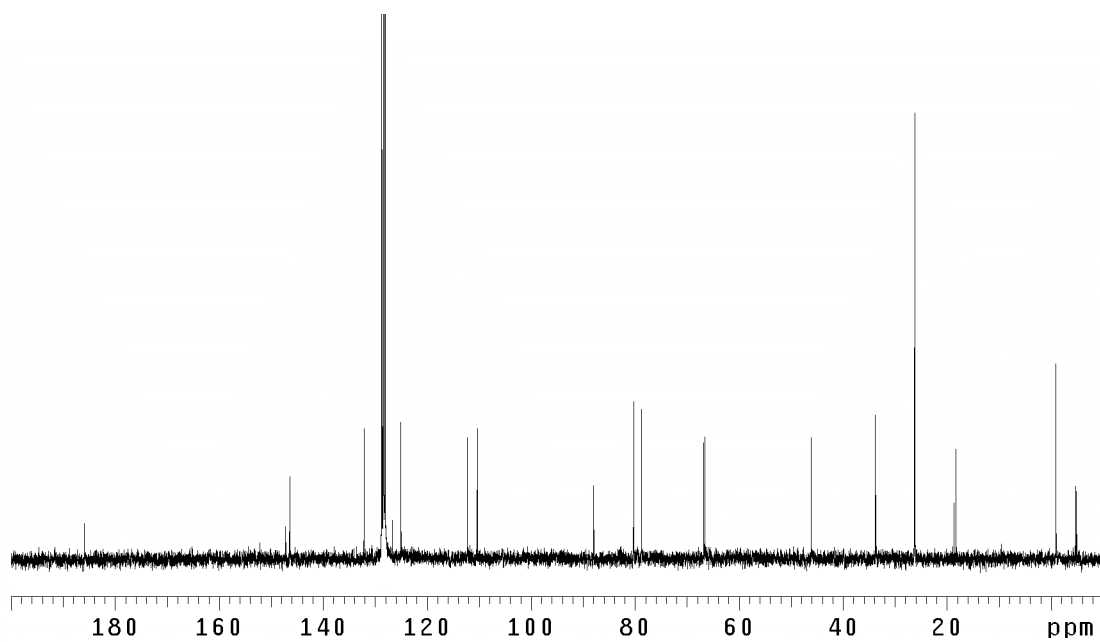


Figure A4.93 ¹³C NMR (75 MHz, C₆D₆) of compound **130**.

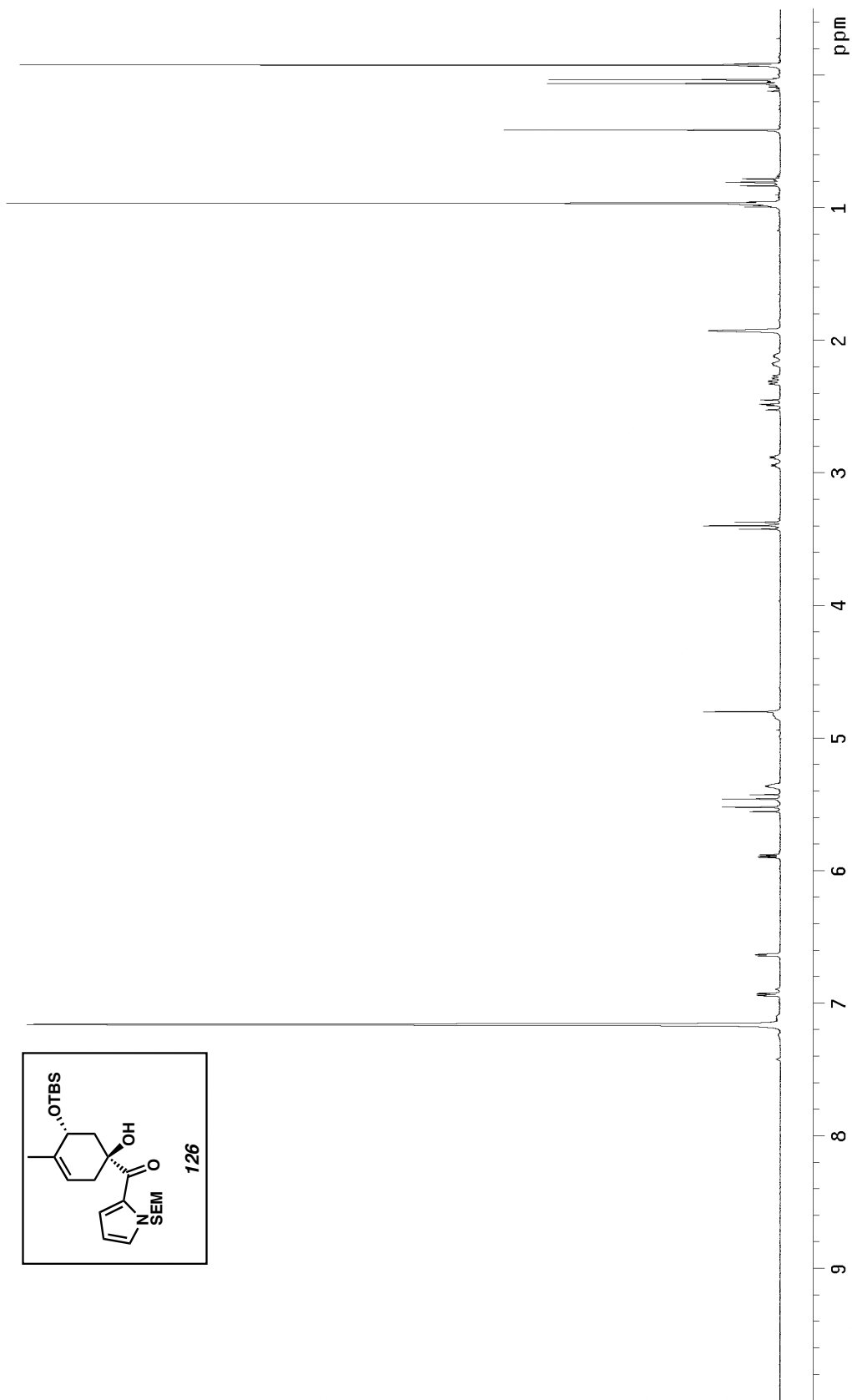


Figure A4.94 ^1H NMR (300 MHz, C_6D_6) of compound **126**.

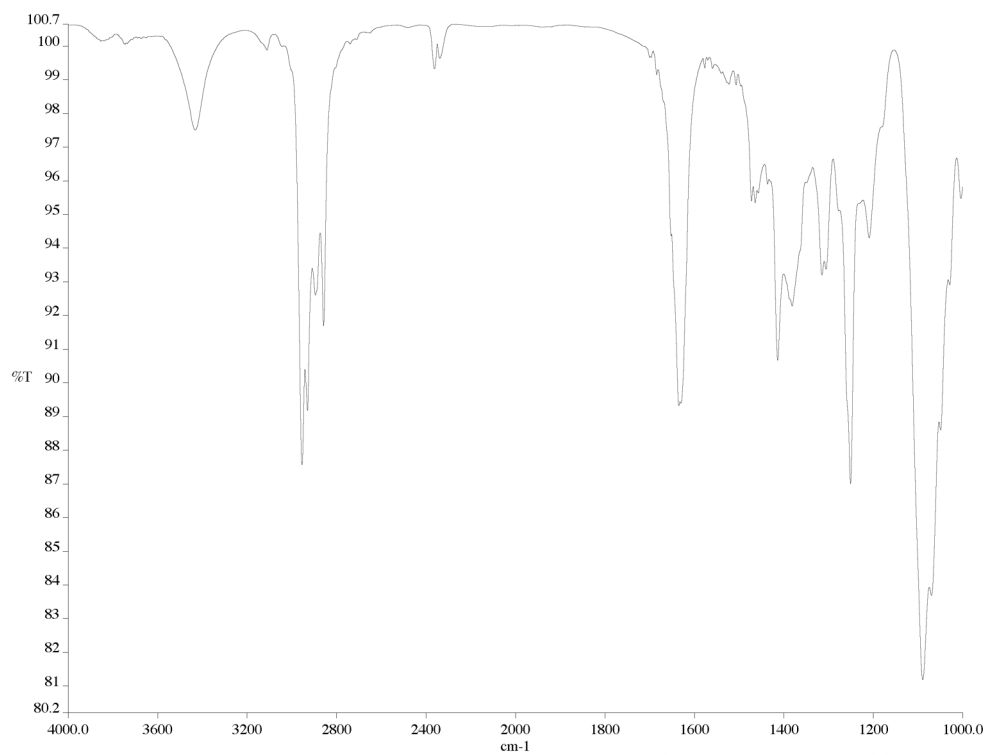


Figure A4.95 Infrared spectrum (thin film/NaCl) of compound **126**.

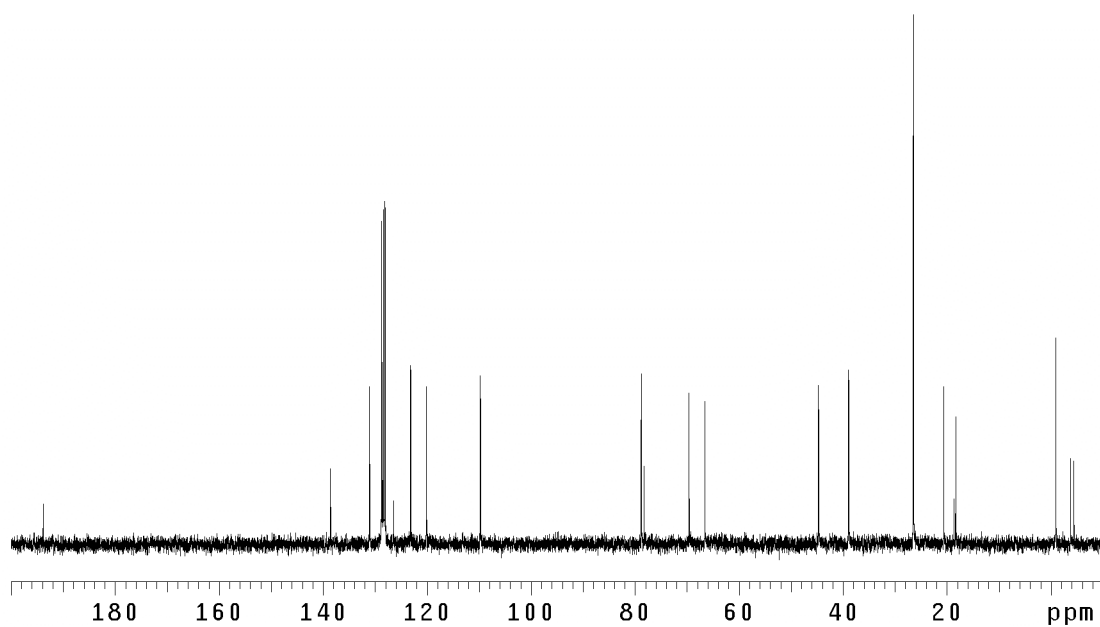


Figure A4.96 ¹³C NMR (75 MHz, C₆D₆) of compound **126**.

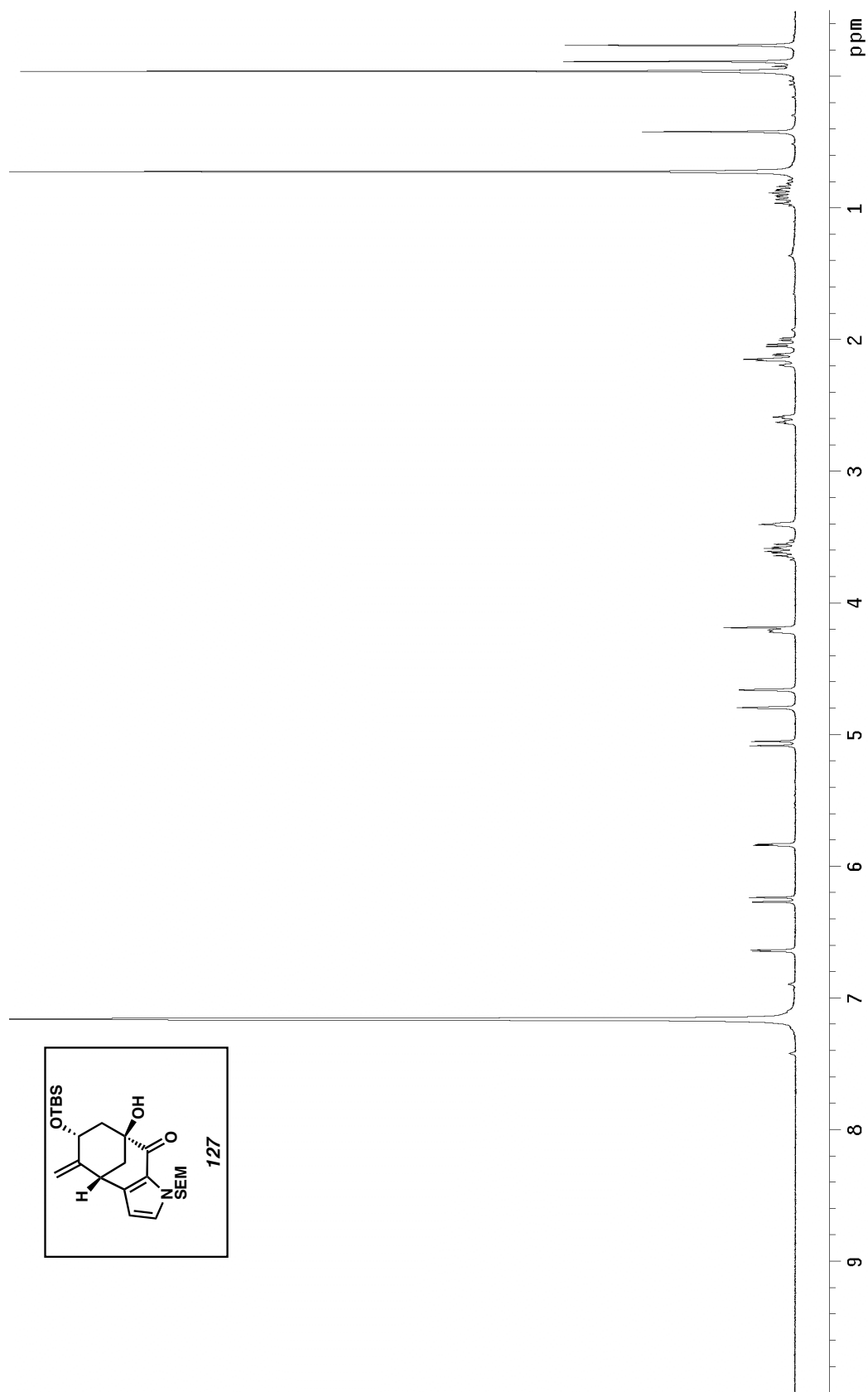


Figure A4.97 ^1H NMR (300 MHz, C_6D_6) of compound **127**.

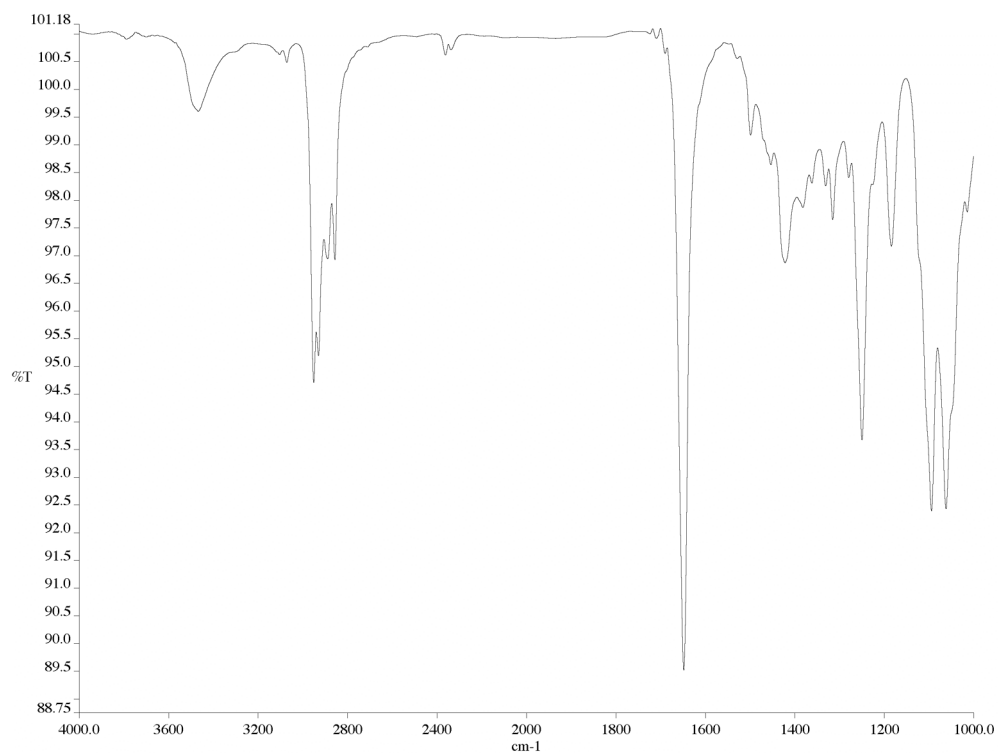


Figure A4.98 Infrared spectrum (thin film/NaCl) of compound **127**.

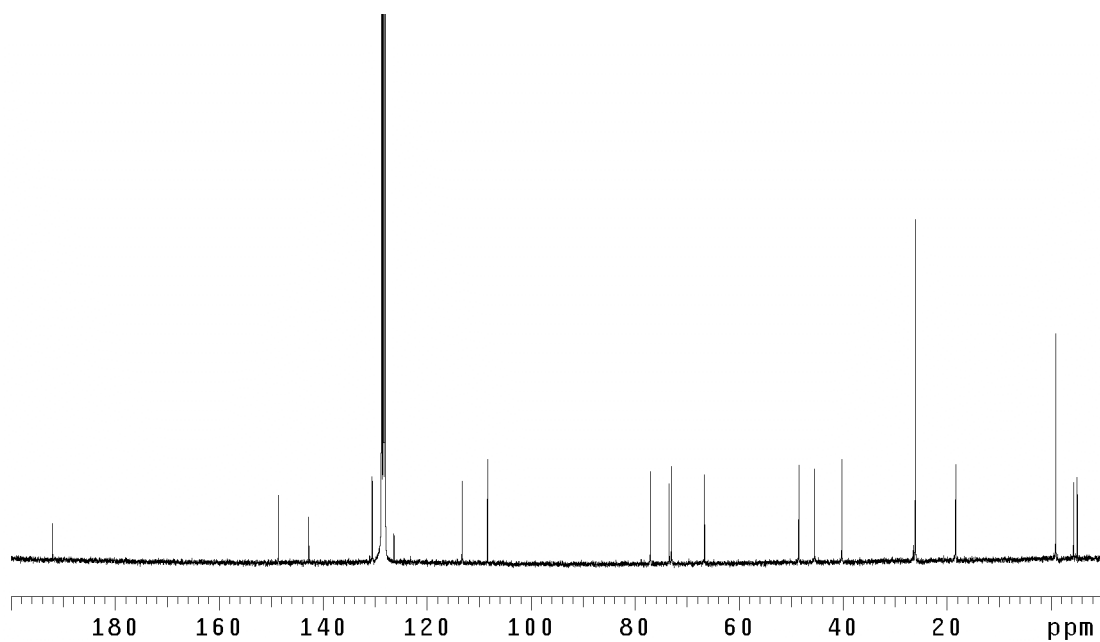


Figure A4.99 ¹³C NMR (75 MHz, C₆D₆) of compound **127**.

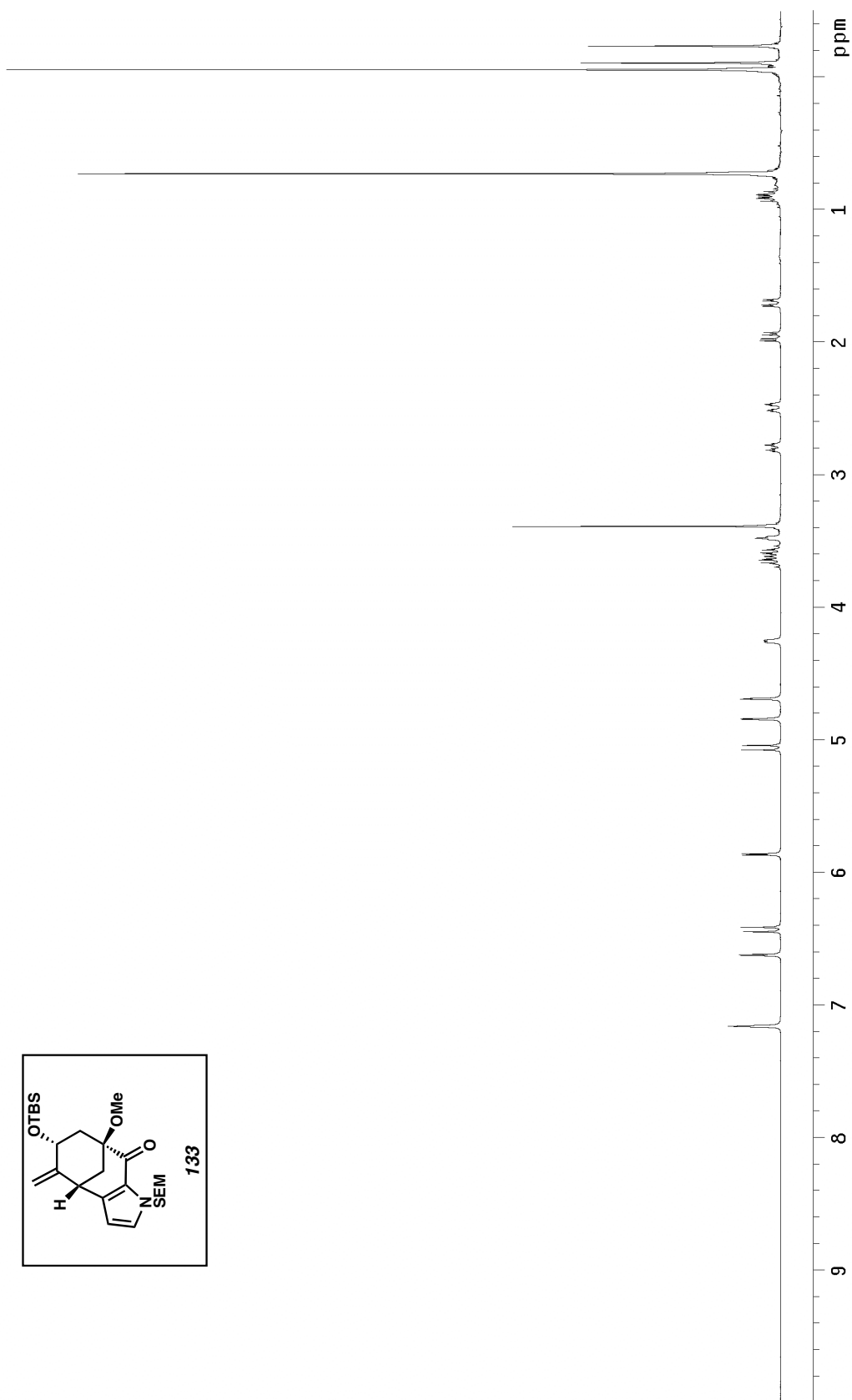
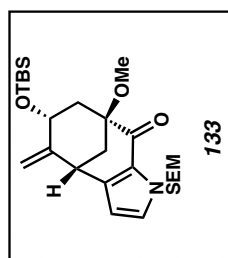


Figure A4.100 ¹H NMR (300 MHz, C₆D₆) of compound **133**.

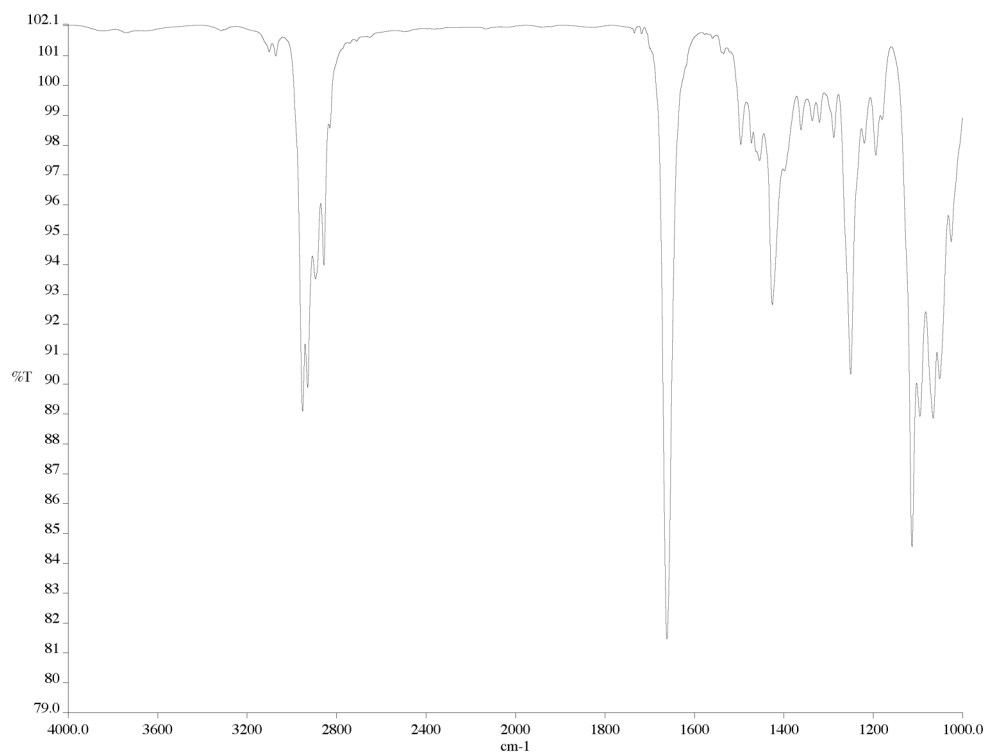


Figure A4.101 Infrared spectrum (thin film/NaCl) of compound **133**.

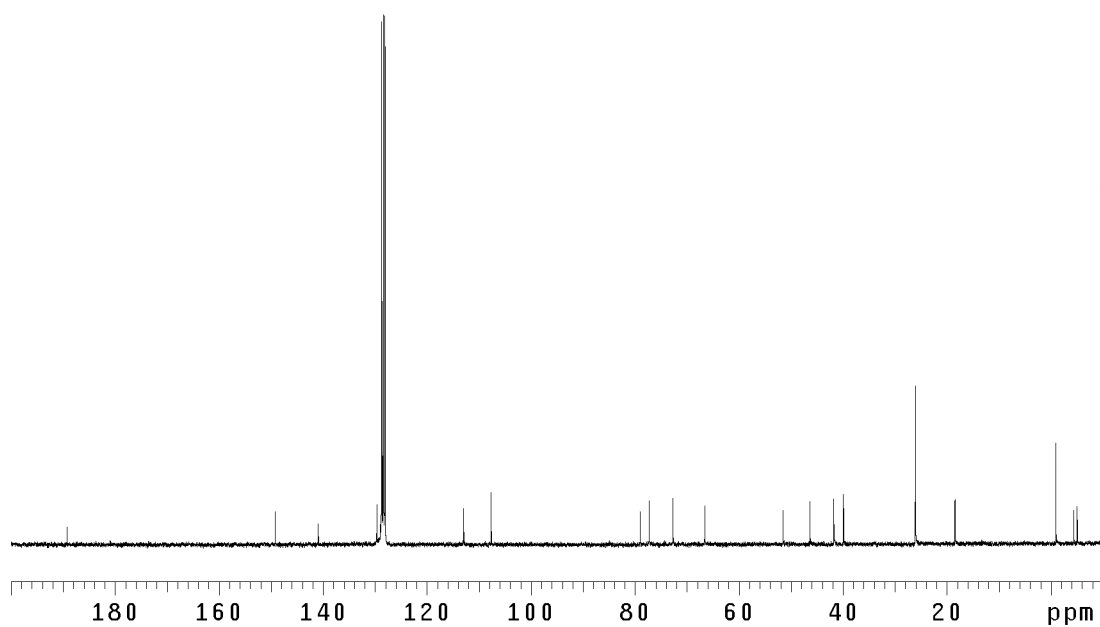


Figure A4.102 ¹³C NMR (75 MHz, C₆D₆) of compound **133**.

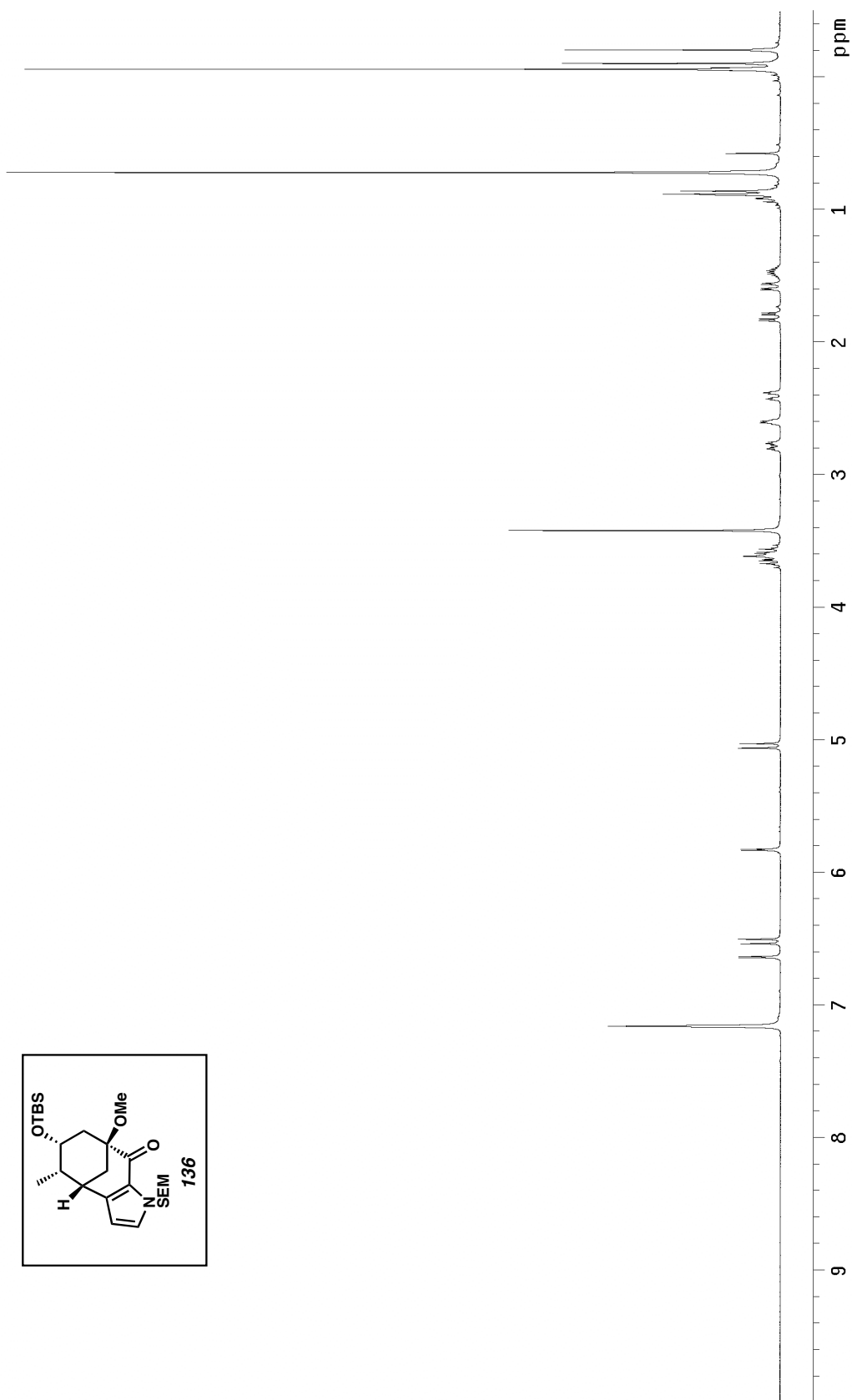
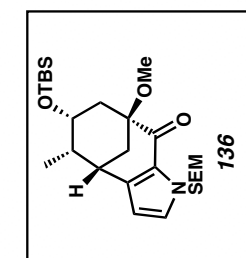


Figure A4.103 ^1H NMR (300 MHz, C_6D_6) of compound **136**.

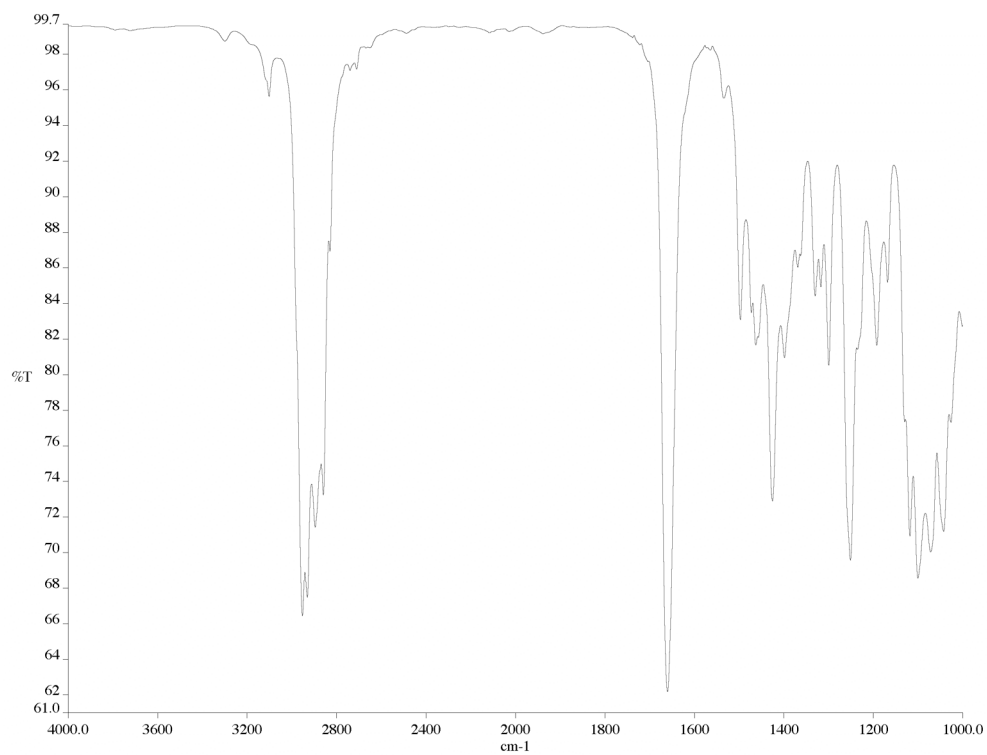


Figure A4.104 Infrared spectrum (thin film/NaCl) of compound **136**.

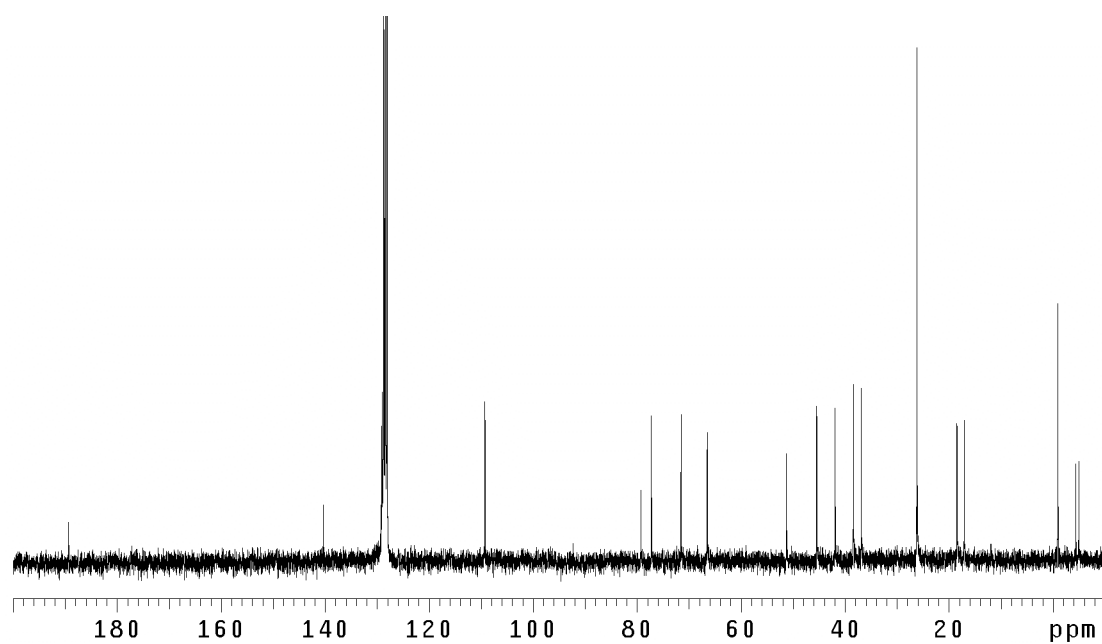


Figure A4.105 ¹³C NMR (75 MHz, C₆D₆) of compound **136**.

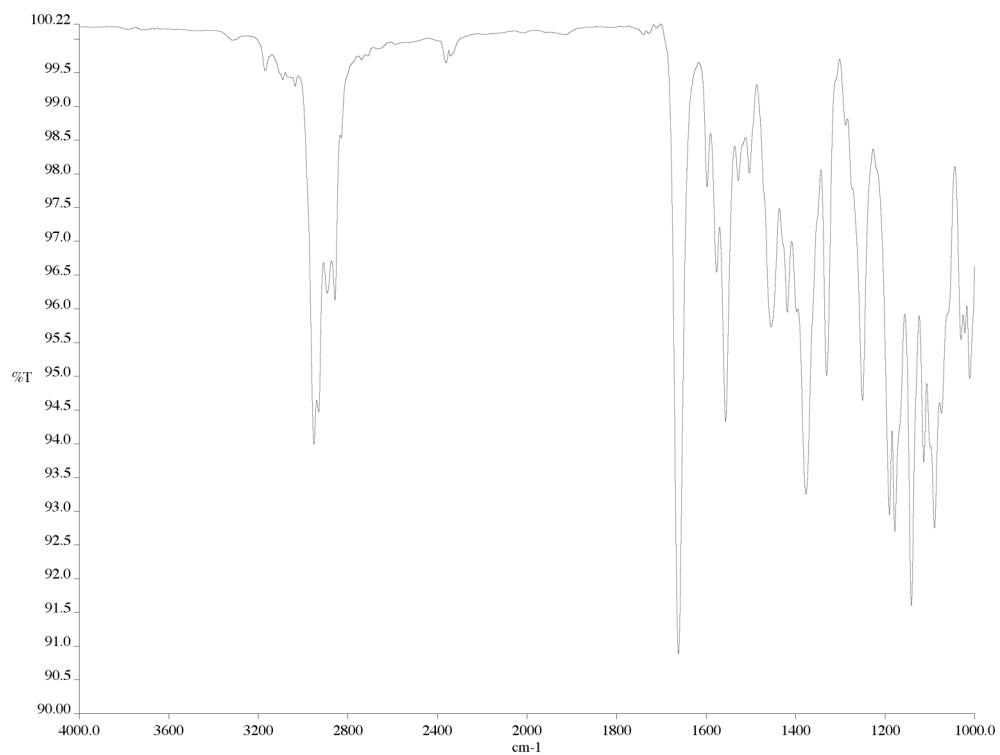


Figure A4.107 Infrared spectrum (thin film/NaCl) of compound **134**.

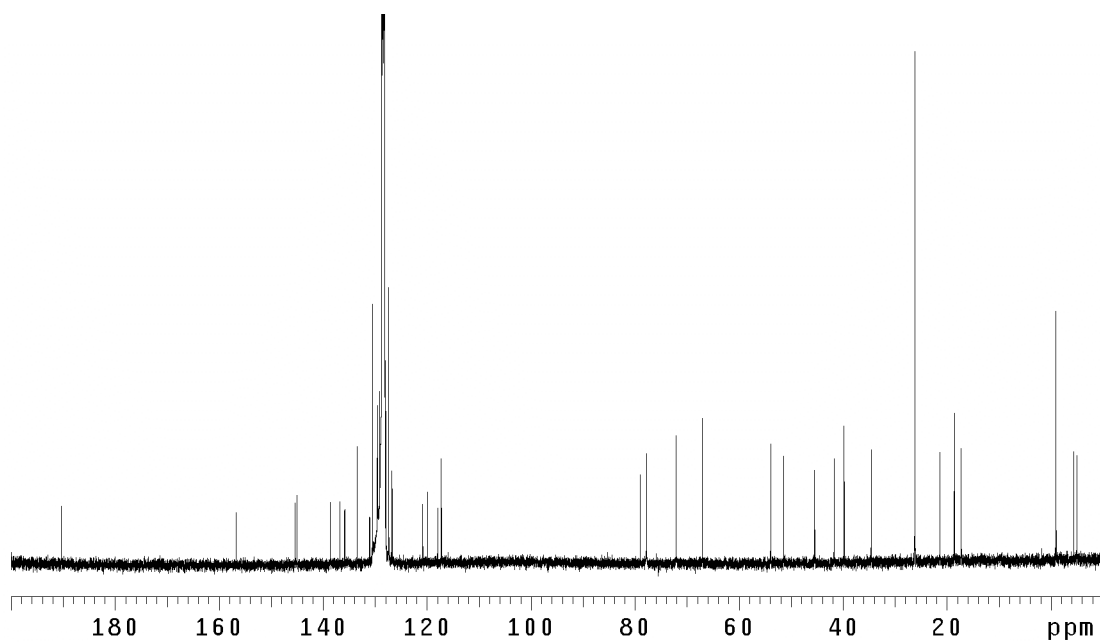


Figure A4.108 ^{13}C NMR (125 MHz, C_6D_6) of compound **134**.

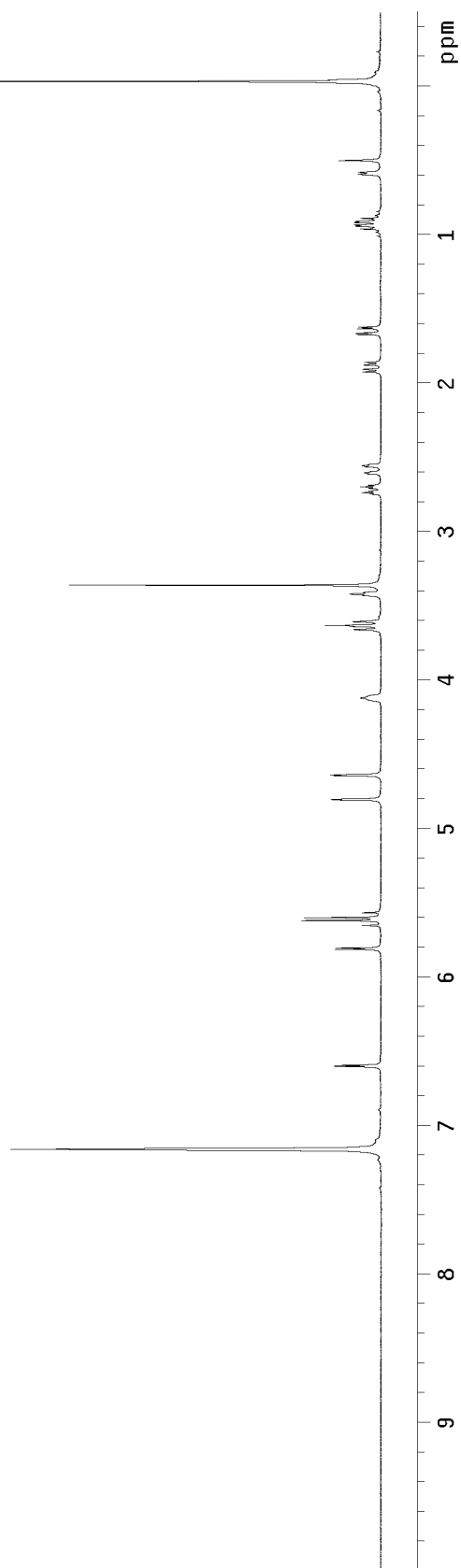
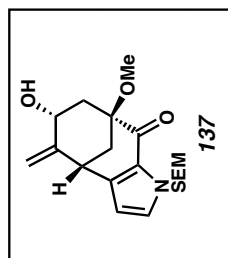


Figure A4.109 ^1H NMR (300 MHz, C_6D_6) of compound **137**.

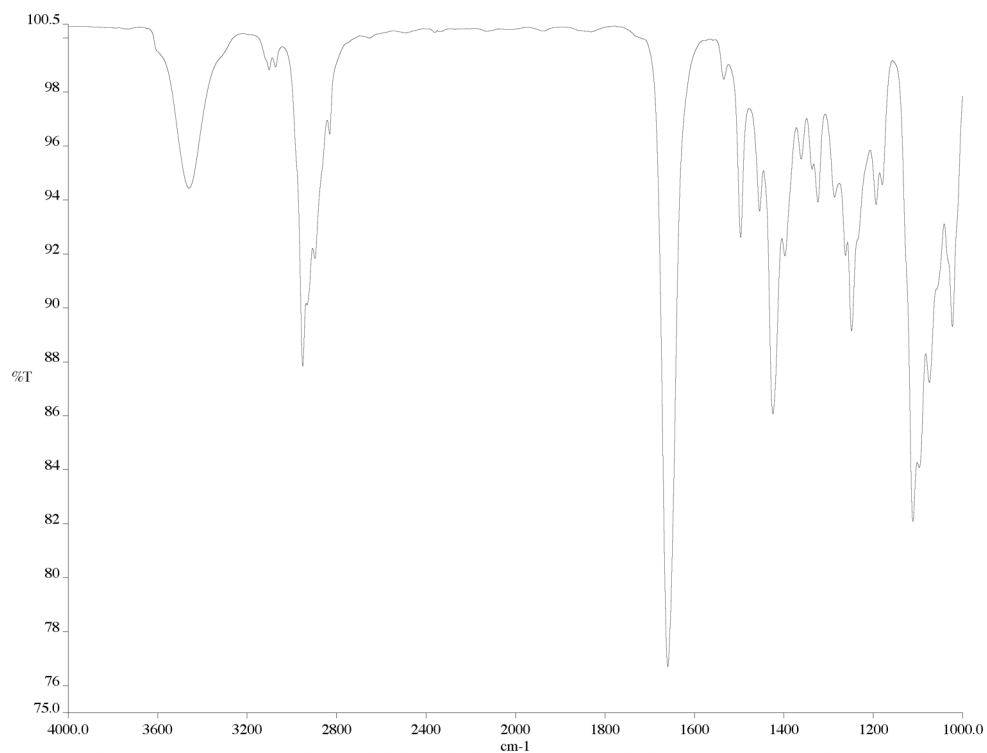


Figure A4.110 Infrared spectrum (thin film/NaCl) of compound **137**.

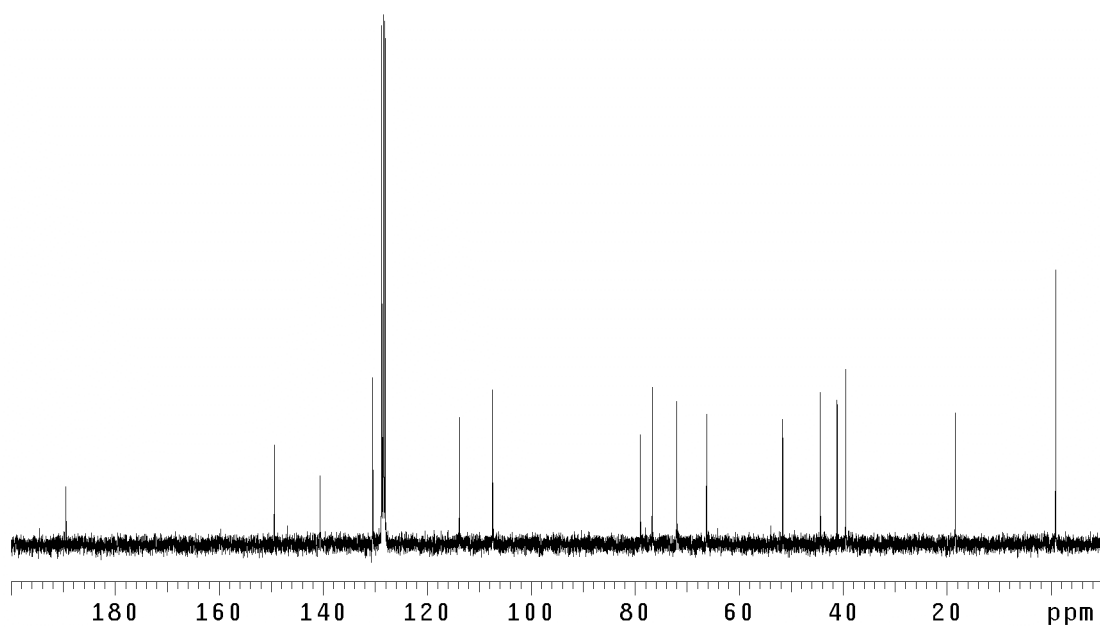


Figure A4.111 ¹³C NMR (75 MHz, C₆D₆) of compound **137**.

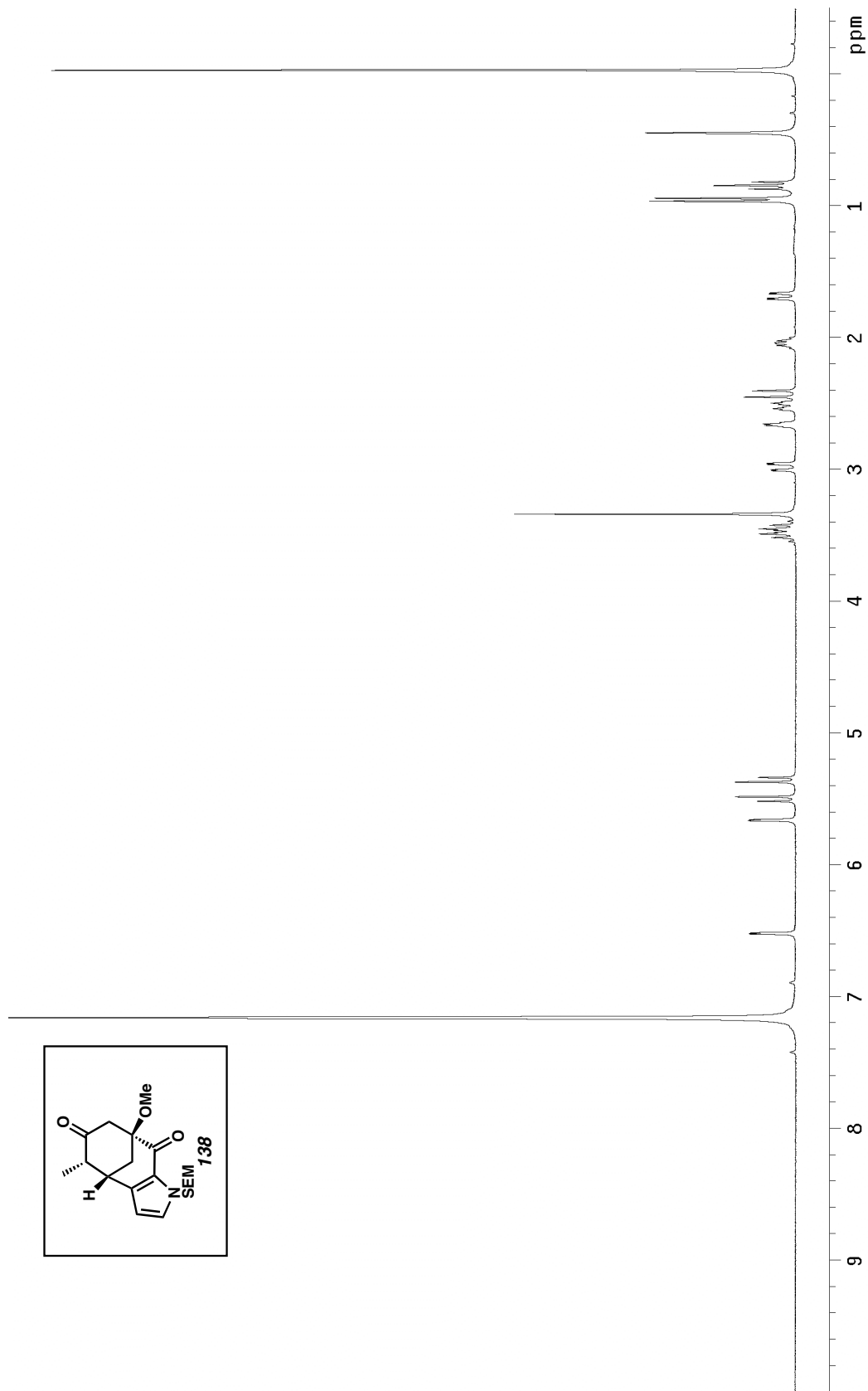


Figure A4.112 ¹H NMR (300 MHz, C₆D₆) of compound 138.

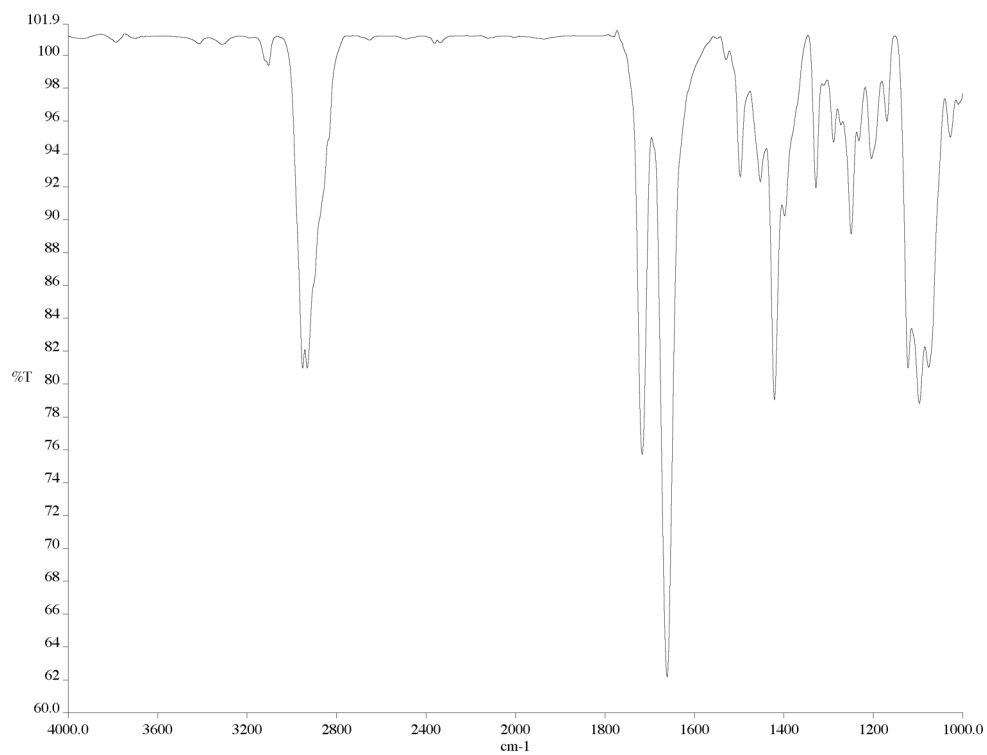


Figure A4.113 Infrared spectrum (thin film/NaCl) of compound **138**.

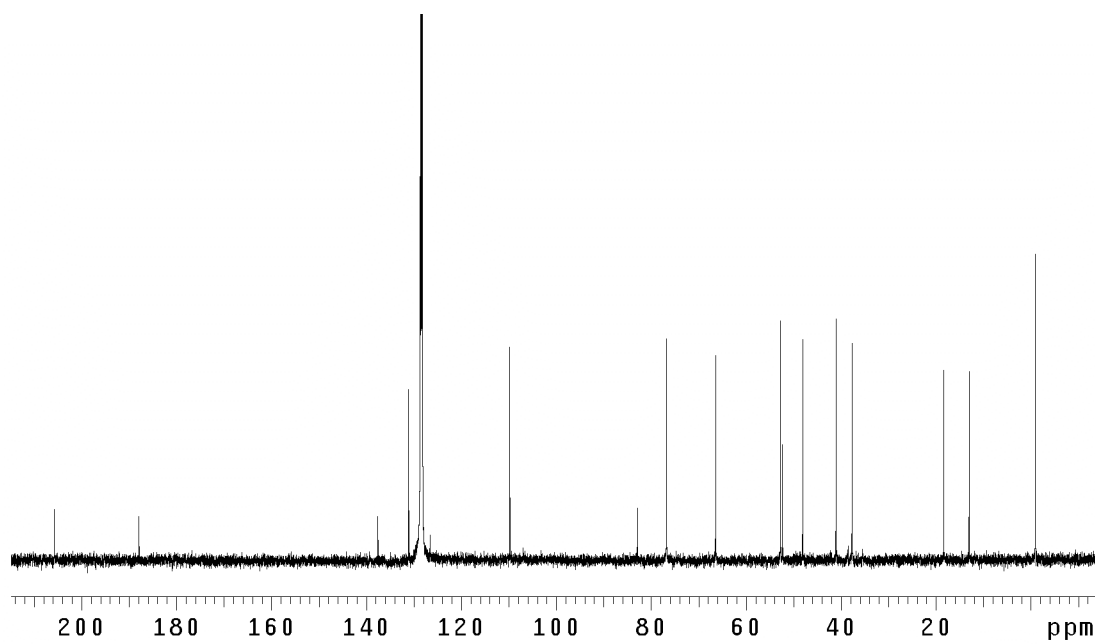


Figure A4.114 ¹³C NMR (125 MHz, C₆D₆) of compound **138**.

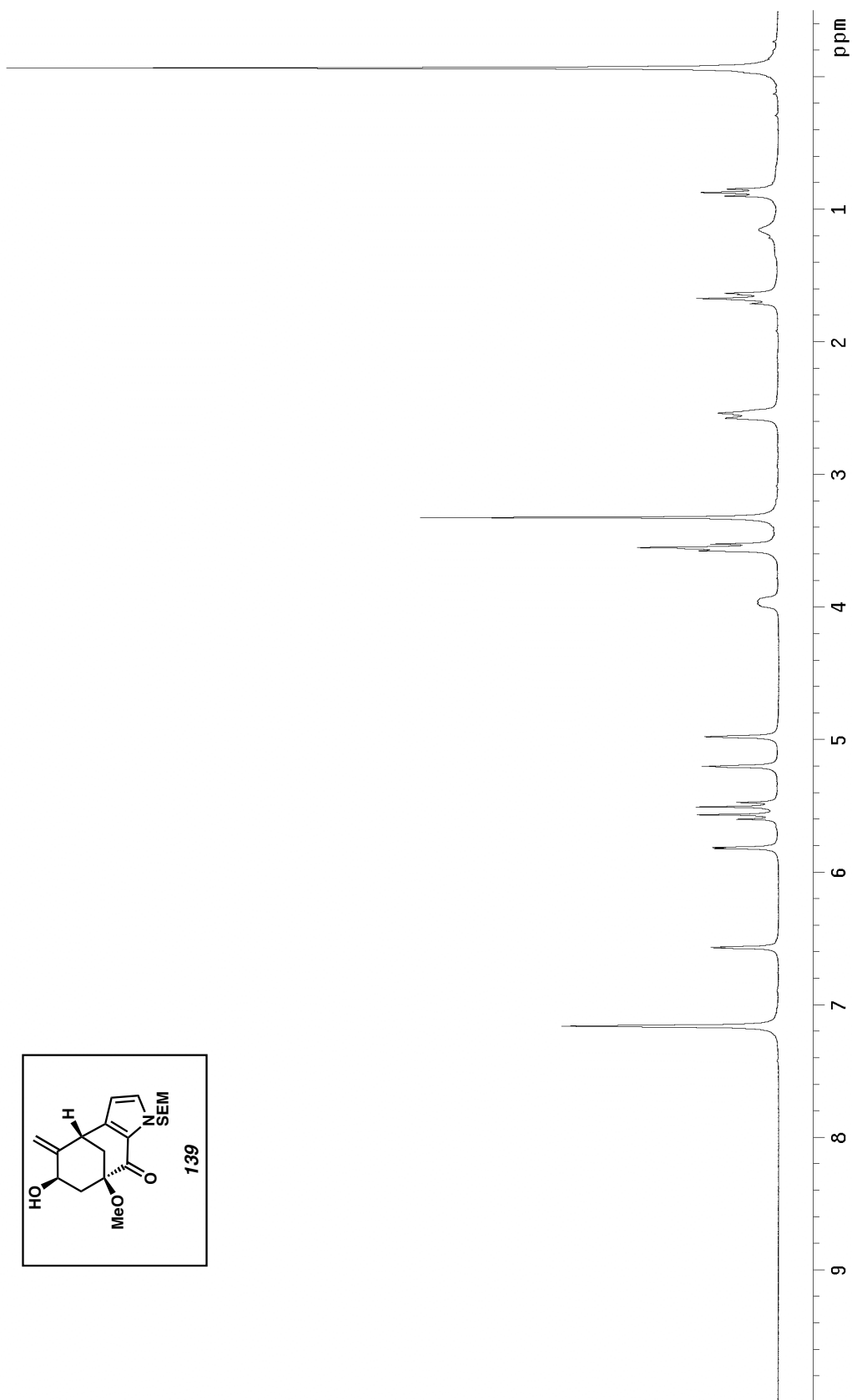
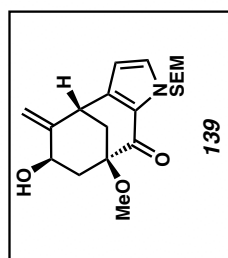


Figure A4.115 ^1H NMR (300 MHz, C_6D_6) of compound **139**.

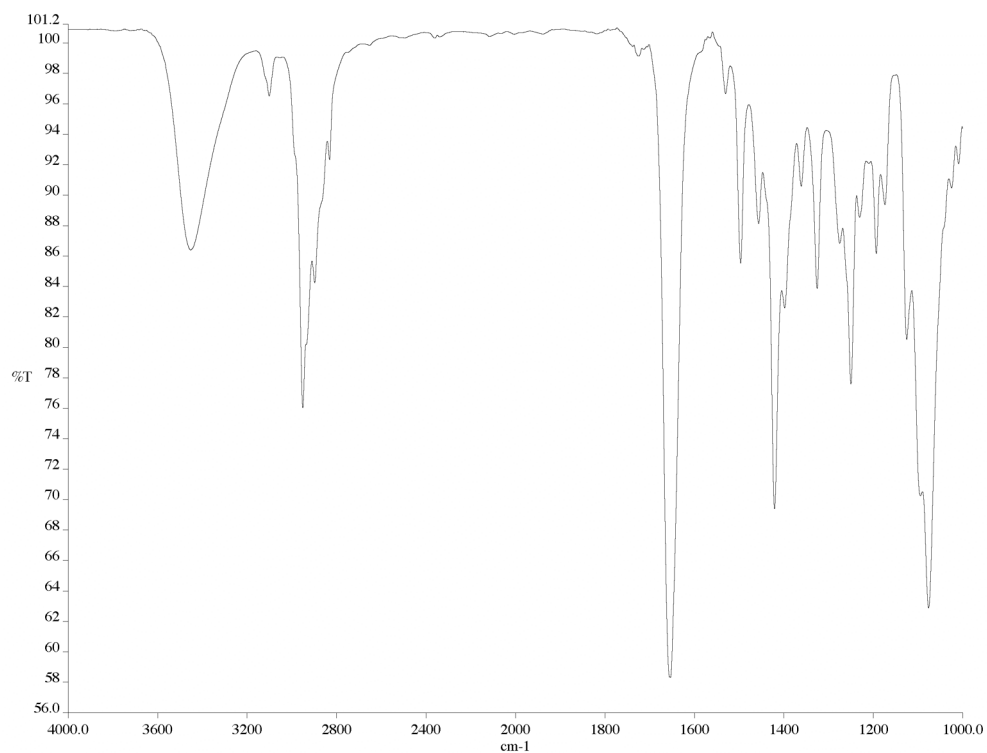


Figure A4.116 Infrared spectrum (thin film/NaCl) of compound **139**.

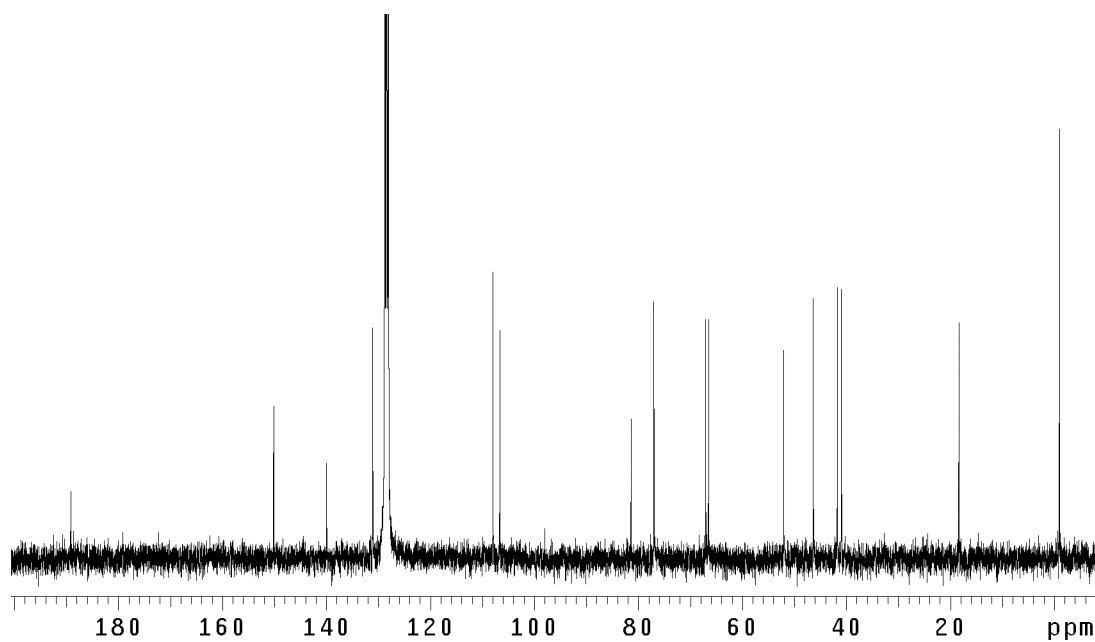


Figure A4.117 ¹³C NMR (75 MHz, C₆D₆) of compound **139**.

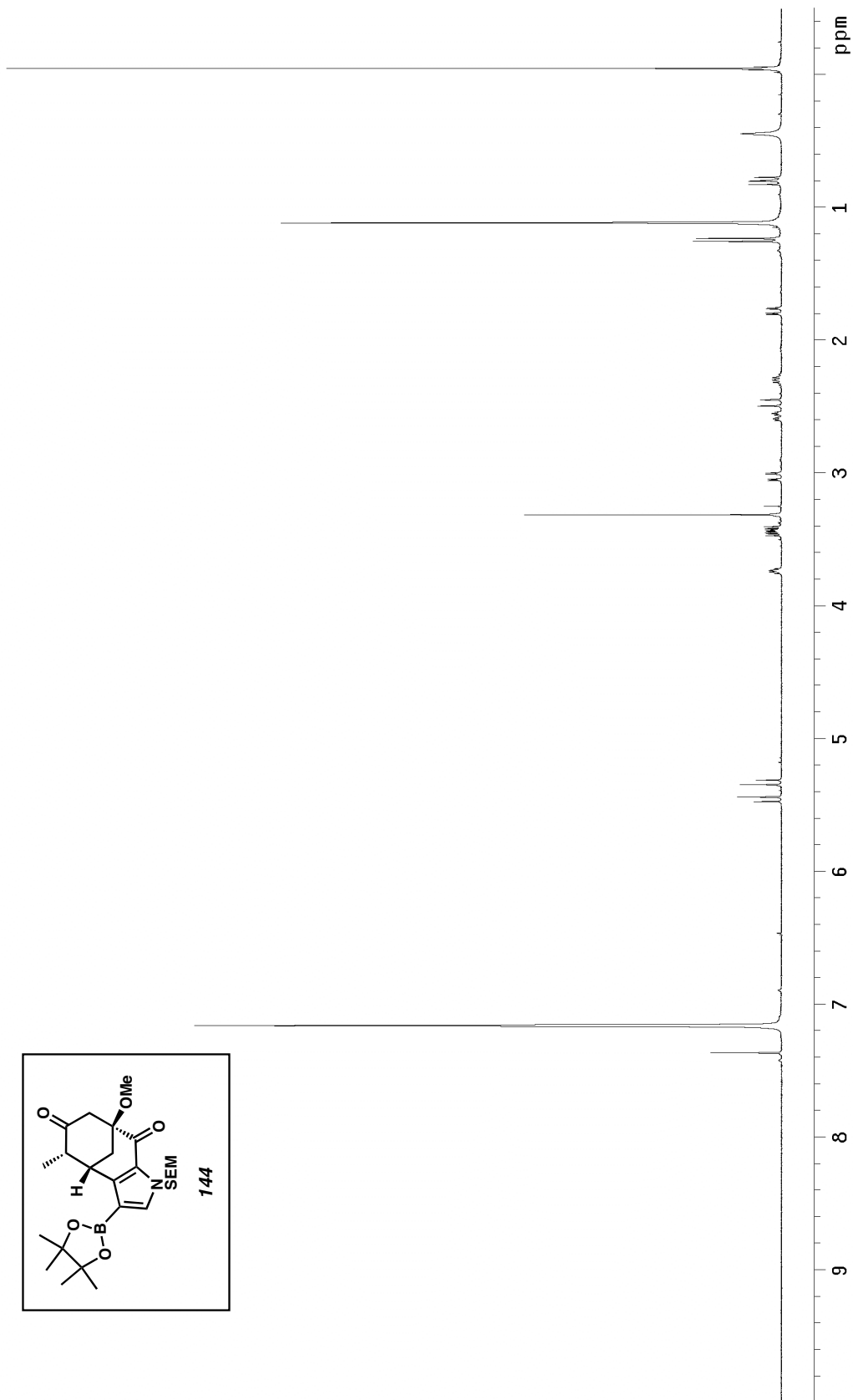


Figure A4.118 ¹H NMR (300 MHz, C₆D₆) of compound **144**.

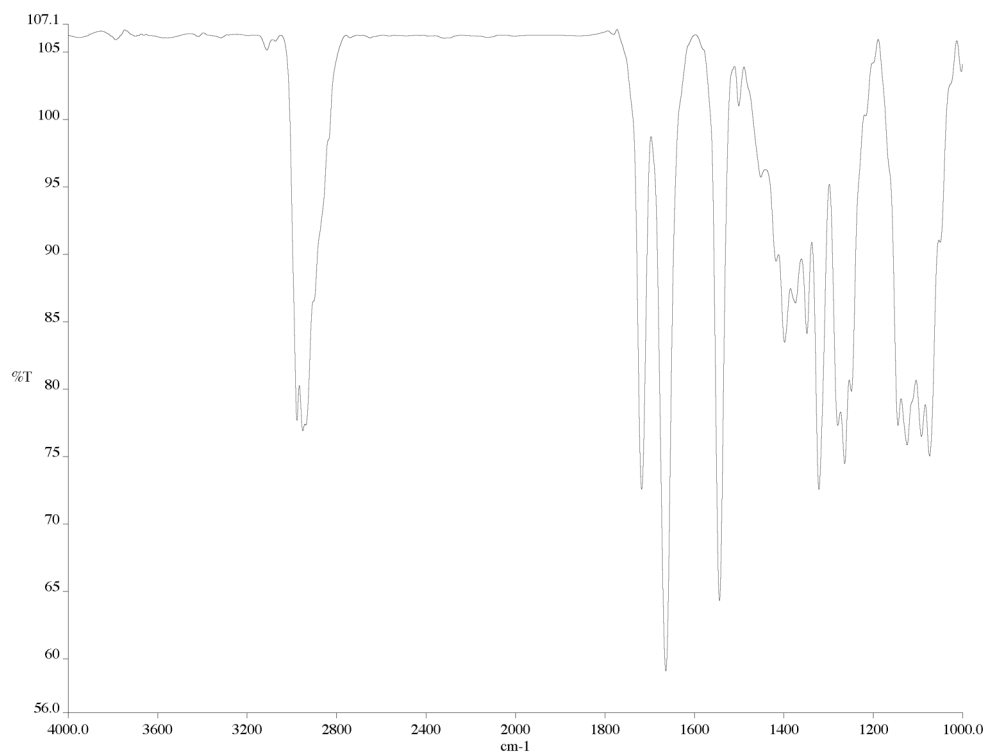


Figure A4.119 Infrared spectrum (thin film/NaCl) of compound **144**.

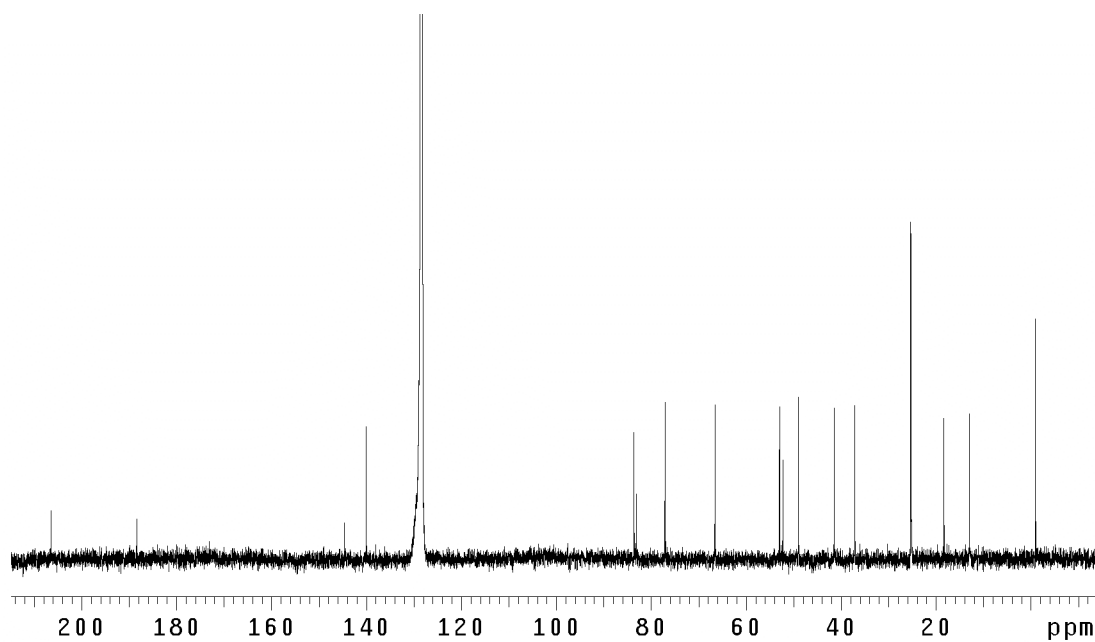
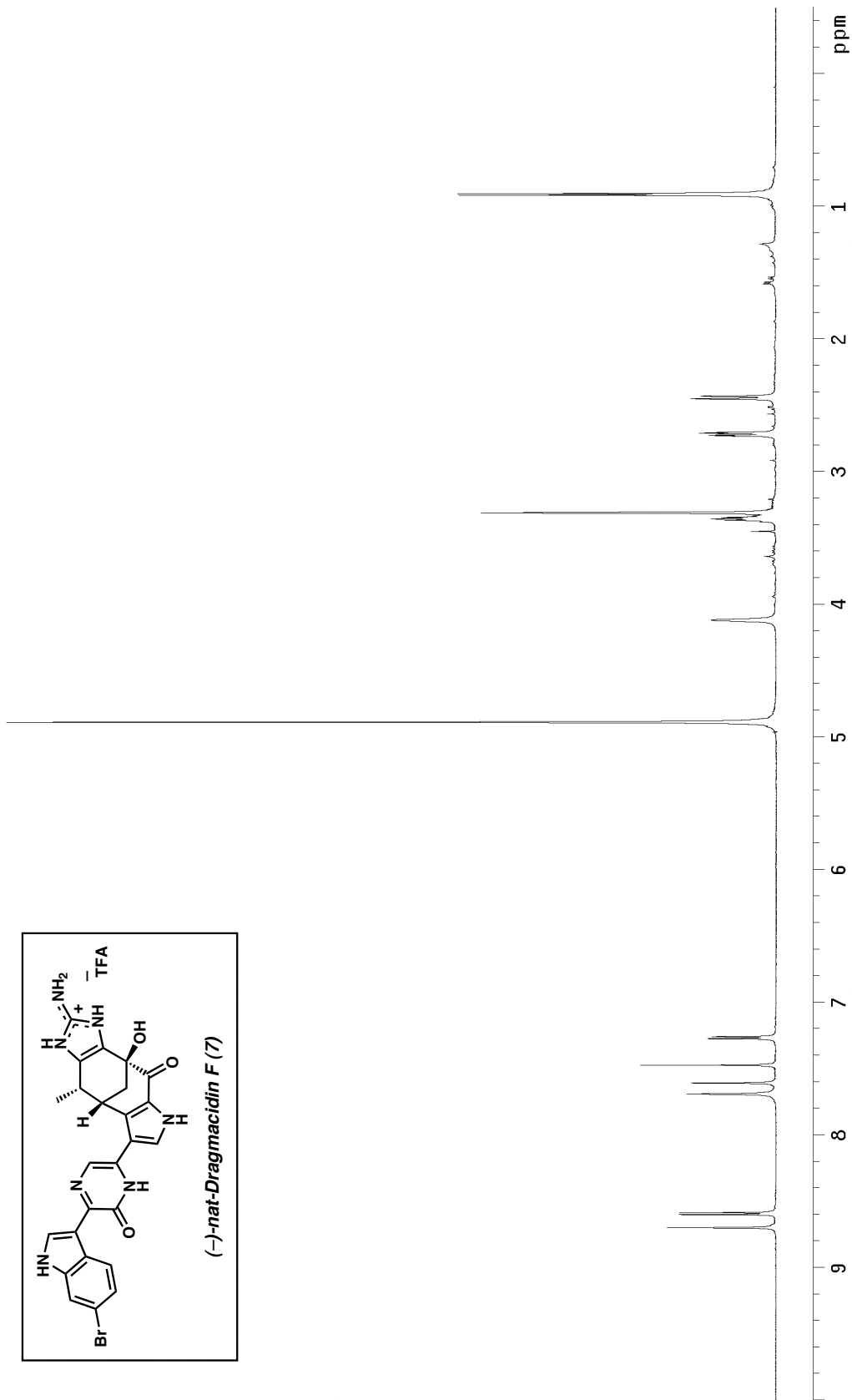
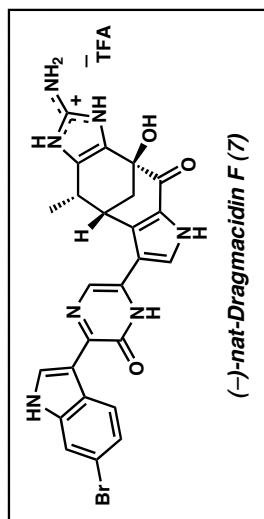


Figure A4.120 ¹³C NMR (125 MHz, C₆D₆) of compound **144**.

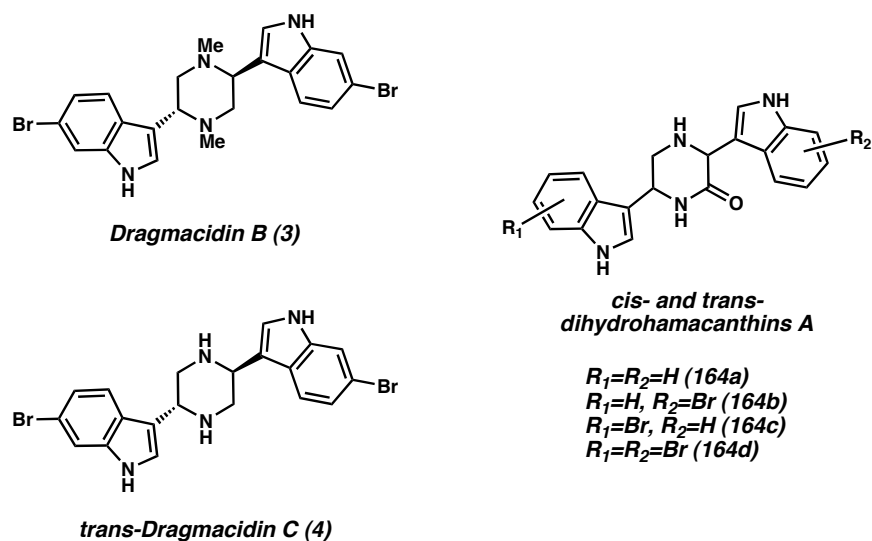


APPENDIX FIVE

**The Formal Total Synthesis of Dragmacidin B, *trans*-Dragmacidin C,
and *cis*- and *trans*-Dihydrohamacanthin A**

A5.1 Introduction

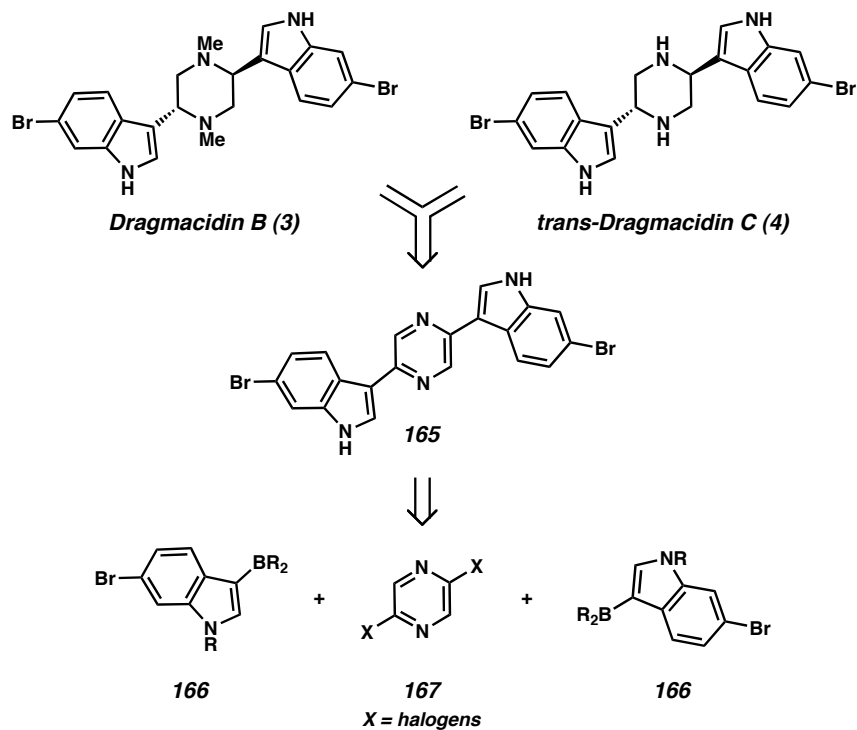
Having established that halogen-selective Suzuki couplings are a powerful method for constructing the carbon skeleton of the pyrazinone containing dragmacidins, we hypothesized that a similar strategy could be used to access the piperazine dragmacidins and related bis(indole) alkaloids. This appendix section describes the implementation of this approach to achieve the formal total synthesis of dragmacidin B (**3**),¹ *trans*-dragmacidin C (**4**),² and *cis*- and *trans*-dihydrohamacanthin A (**164b**)³ (Figure A5.1.1).⁴

Figure A5.1.1

A5.2 The Formal Total Synthesis of Dragmacidin B and *trans*-Dragmacidin C

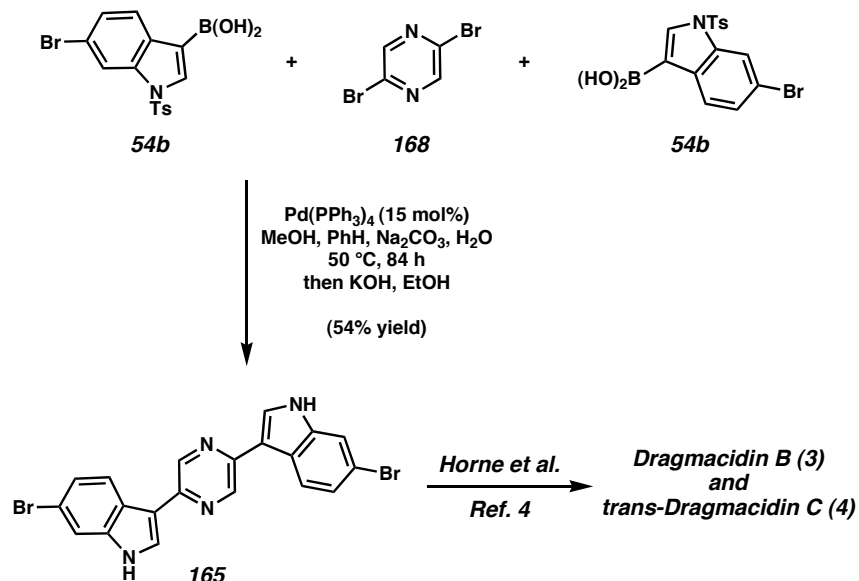
A retrosynthetic strategy for the preparation of dragmacidin B (**3**) and *trans*-dragmacidin C (**4**) is shown below in Scheme A5.2.1. Based on conditions reported by Horne, each of the bis(indole) alkaloids can be accessed from unsaturated derivative **165** in a single step.⁵ Pyrazine **165**, in turn, would be obtained from two halogen-selective Suzuki cross-coupling reactions of boronic acid **166** with a dihalogenated pyrazine (**167**). We anticipated that the boronic acid fragment employed in our synthesis of dragmacidin D (i.e., **54b**) could be utilized as a surrogate for **166** in order to achieve our current goals. However, the success of our plan would depend highly on the choice of halogens for pyrazine **167**.

Scheme A5.2.1



In order to probe the limits of our halogen-selective Suzuki cross-coupling methodology, we chose to use known dibromide **168**⁶ as the critical pyrazine fragment (Scheme A5.2.2). In a one-pot, 4-step transformation, an excess of 6-bromoindolylboronic acid (**54b**) was exposed to dibromopyrazine **168** under our standard cross-coupling conditions. Following quenching with KOH/ethanol, the deprotected pyrazine product (**165**) was obtained in 54% yield. Notably, although four bromides were introduced in the reaction mixture, only the two pyrazinyl bromides were reactive in the presence of Pd(0) at 50 °C. This rapid synthesis of bis(indole)pyrazine **165** constitutes a formal total synthesis of both dragmacidin B (**3**) and *trans*-dragmacidin C (**4**).^{5,7,8}

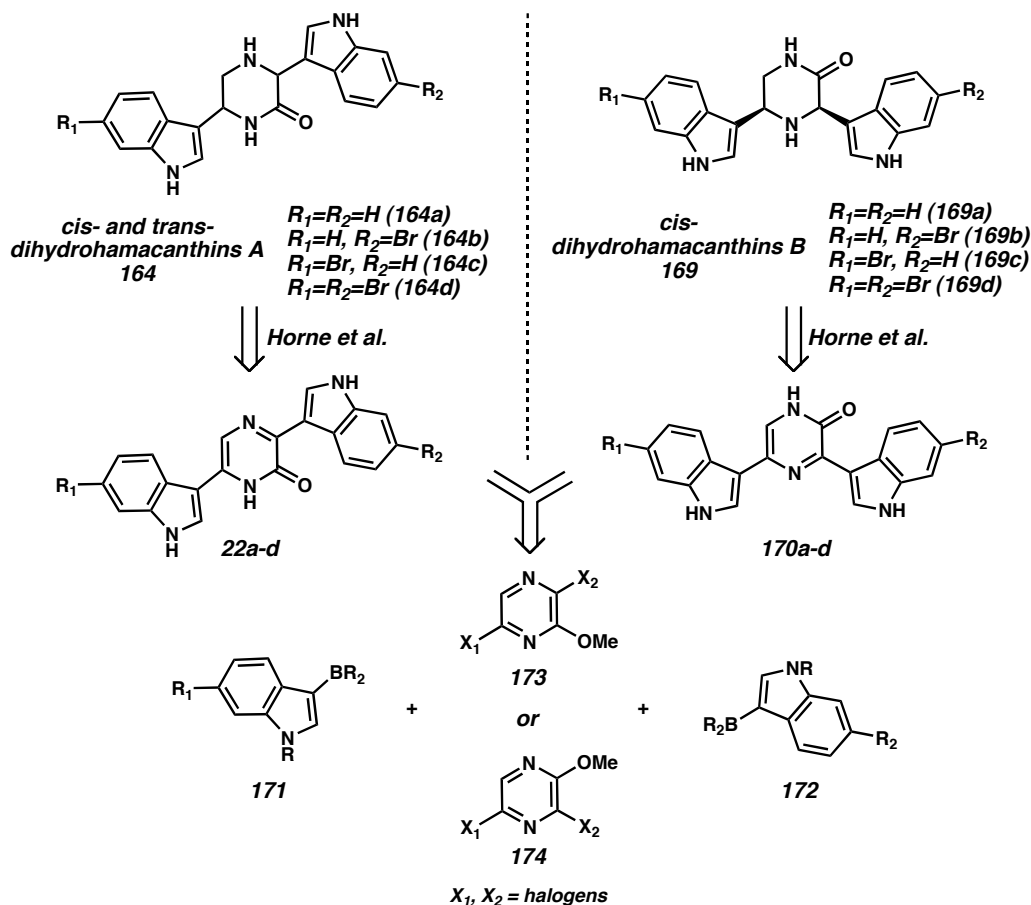
Scheme A5.2.2



A5.3 The Formal Total Synthesis of *cis*- and *trans*-Dihydrohamacanthin A

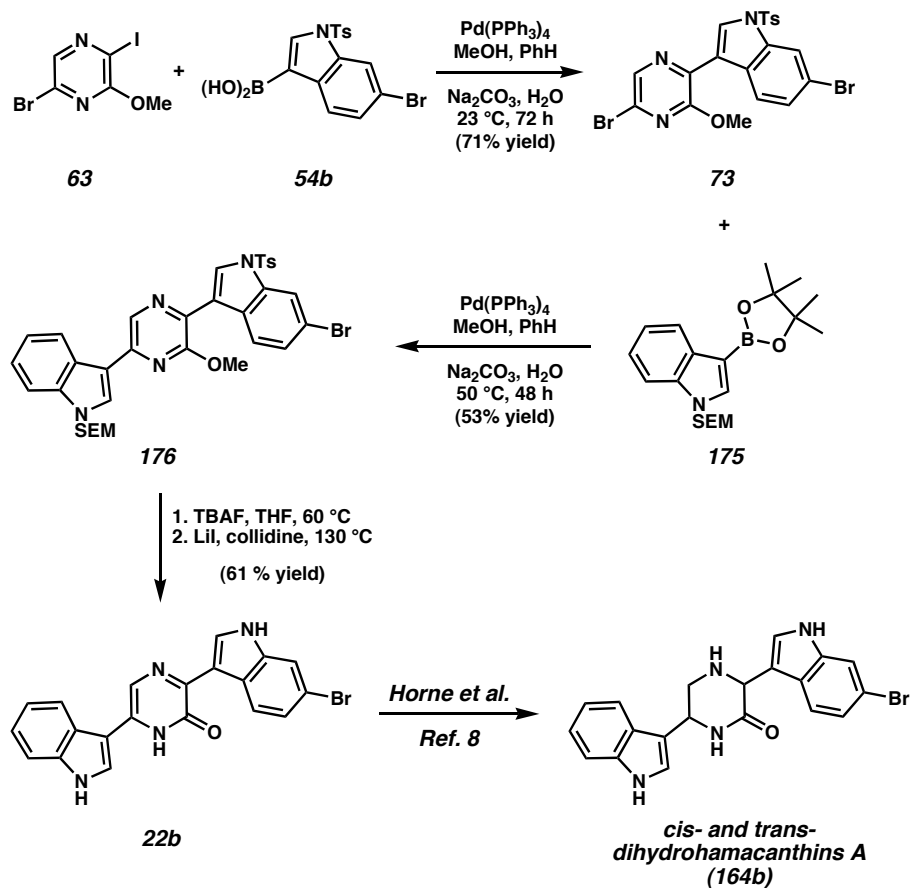
These halogen-selective Suzuki couplings also have great potential for assembling a related family of natural products, the dihydrohamacanthins (**164** and **169**, Scheme A5.3.1). In this scenario, the desired alkaloids (**164** and **169**) would be obtained from their pyrazinone counterparts (**22** and **170**), using the method established by Horne.⁹ Intermediates **22** and **170**, in turn, would arise via cross-coupling chemistry using indole fragments **171** and **172**, as well as pyrazine fragments **173** and **174**, in a manner similar to that described above. Halogen-selective cross-couplings will be crucial to prepare all of the halogenation patterns present in this series of natural products (**164a-d**, **169a-d**).

Scheme A5.3.1



To demonstrate the feasibility of this approach, we prepared one of the dihydrohamacanthin natural products (**164b**, Scheme A5.3.2). In the first Suzuki coupling, dihalopyrazine **63** and bromoindole **54b** were treated with Pd(0) at 23 °C to afford coupled indolylpyrazine **73**, as described in Chapter 2, Section 2.3.4. Dibromide **73**, in turn, was subjected to boronic ester **175** in the presence of Pd(0) at 50 °C to produce bis(indole)pyrazine **176** in 53% yield. In both cases, complete halogen-selectivity was observed. Subsequent removal of all protecting groups furnished pyrazinone **22b**, which has previously been converted to the natural product (**164b**) in a single step.^{9,10,11}

Scheme A5.3.2



A5.4 Conclusion

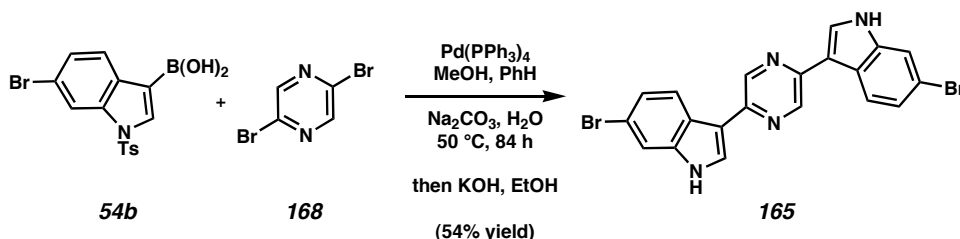
In summary, we have completed the formal total synthesis of dragmacidin B (**3**) and *trans*-dragmacidin C (**4**). Our route features a one-pot, 4-step halogen-selective cross-coupling/deprotection sequence to construct the bis(indole) scaffold of our targets. In addition, we have applied this methodology to the formal synthesis of a dihydrohamacanthin natural product (**164b**).

A5.5 Experimental Section

A5.5.1 Materials and Methods

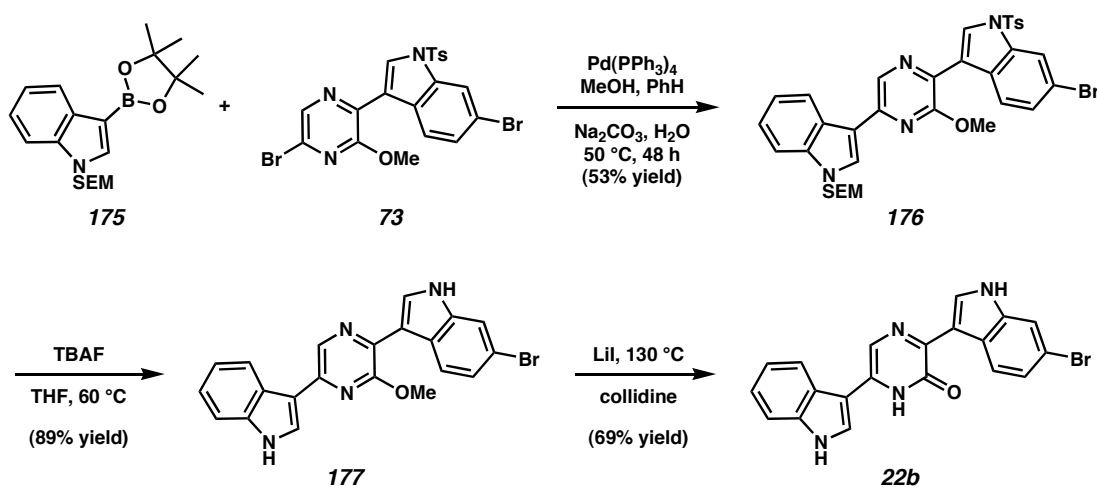
Unless stated otherwise, reactions were conducted in flame-dried glassware under an atmosphere of nitrogen using anhydrous solvents (either freshly distilled or passed through activated alumina columns). All commercially obtained reagents were used as received. Reaction temperatures were controlled using an IKAmag temperature modulator. Thin-layer chromatography (TLC) was conducted with E. Merck silica gel 60 F254 pre-coated plates (0.25 mm) and visualized using a combination of UV, anisaldehyde, and potassium permanganate staining. ICN silica gel (particle size 0.032-0.063 mm) was used for flash column chromatography.

A5.5.2 Preparative Procedures



Bis(indole)pyrazine 165. A vial charged with dibromopyrazine **168**⁶ (15.1 mg, 0.0635 mmol), boronic acid **54b** (75 mg, 0.190 mmol), and tetrakis(triphenylphosphine)palladium(0) (11 mg, 0.0095 mmol) was evacuated and purged with N₂. Deoxygenated benzene (1.2 mL), deoxygenated methanol (250 μ L), and deoxygenated 2 M aq. Na₂CO₃ (105 μ L) were added. The reaction mixture was sparged with argon for 3 min. The vial was then sealed, heated to 50 °C for 84 h, and cooled to 23 °C. EtOH (7 mL) and KOH (500 mg) were added. The reaction mixture was heated

to 50 °C for 20 h, cooled to 23 °C, then quenched by pouring into 10% (w/v) aq. citric acid (20 mL). EtOAc (30 mL) was added, and the layers were partitioned. The aqueous phase was further extracted with EtOAc (2 x 30 mL). The combined organic layers were washed with brine (15 mL), dried over MgSO₄, and evaporated under reduced pressure. The crude product was purified by flash chromatography (10:1 CH₂Cl₂:MeOH eluent), then further purified by preparative thin layer chromatography (2:1 EtOAc:hexanes eluent) to afford known bis(indole) **165**⁵ (16 mg, 54% yield) as a yellow powder.



Pyrazinone 22b. A reaction tube charged with indolylpyrazine **73**¹² (125 mg, 0.335 mmol), boronic ester **175** (90 mg, 0.168 mmol), and tetrakis(triphenylphosphine)palladium(0) (35 mg, 0.030 mmol) was evacuated and purged with N₂. Deoxygenated benzene (3.5 mL), deoxygenated methanol (690 μL), and deoxygenated 2 M aq. Na₂CO₃ (180 μL) were then added. The reaction mixture was sparged with argon for 2 min. The tube was then sealed, heated to 50 °C for 48 h, cooled to 23 °C, and quenched by the addition of Na₂SO₄ (200 mg). The reaction mixture was filtered over a plug of SiO₂ (CH₂Cl₂ eluent), and the solvent was evaporated under

reduced pressure. The crude product was purified by flash chromatography (2:1 CH₂Cl₂:hexanes eluent) to afford bis(indole) **176** (62 mg, 53% yield), which was used immediately in the subsequent reaction.

Bis(indole) **176** (30 mg, 0.043 mmol) was dissolved in 1.0 M TBAF in THF (1 mL, 1 mmol) and heated to 65 °C for 16 h. After cooling to 23 °C, the solvent was removed under reduced pressure, and CH₂Cl₂ (5 mL) was added. The organic layer was washed with H₂O (2 x 1 mL) and brine (1 mL), concentrated to dryness, then purified by flash chromatography (CH₂Cl₂ eluent) to give bis-*N*-deprotected intermediate **177** (16 mg, 89% yield). A mixture of crude **177** (1.5 mg, 0.0034 mmol), LiI (100 mg, 0.75 mmol), and collidine (1 mL) was heated to 130 °C for 4 days. After cooling to 23 °C, the reaction mixture was diluted with EtOAc (5 mL), washed with H₂O (3 x 5 mL) and brine (2 mL), then dried by passage over a plug of SiO₂ (EtOAc eluent). The solvent was removed under reduced pressure to afford known pyrazone **22b**⁹ (1.0 mg, 69% yield).

A5.6 Notes and References

- (1) Morris, S. A.; Andersen, R. J. *Tetrahedron* **1990**, *46*, 715-720.
- (2) Fahy, E.; Potts, B. C. M.; Faulkner, D. J.; Smith, K. *J. Nat. Prod.* **1991**, *54*, 564-569.
- (3) Casapullo, A.; Bifulco, G.; Bruno, I.; Riccio, R. *J. Nat. Prod.* **2000**, *63*, 447-451.
- (4) Portions of this work have been described in a communication, see: Garg, N. K.; Stoltz, B. M. *Tetrahedron Lett.* **2005**, *46*, 2423-2426.
- (5) Miyake, F. Y.; Yakushijin, K.; Horne, D. A. *Org. Lett.* **2000**, *2*, 3185-3187.
- (6) Ellingson, H. *J. Am. Chem. Soc.* **1949**, *71*, 2798-2800.
- (7) Treatment of **165** with NaBH₃CN in formic acid leads to the formation of dragmacidin B (**3**), while the analogous reaction conducted in acetic acid results in production of *trans*-dragmacidin C (**4**).⁵
- (8) Sakamoto et al. have shown that natural dragmacidin C is *cis*-fused. See: Kawasaki, T.; Ohno, K.; Enoki, H.; Umemoto, Y.; Sakamoto, M. *Tetrahedron Lett.* **2002**, *43*, 4245-4248.

- (9) Miyake, F. Y.; Yakushijin, K.; Horne, D. A. *Org. Lett.* **2002**, *4*, 941-943.
- (10) Reduction of **22b** with NaBH₃CN leads to the production of **164b**.
- (11) We have also prepared bromopyrazinone **22b** by an alternative cyclocondensation route. See Chapter 2, Section 2.2.
- (12) See Chapter 2, Section 2.7.2 for preparative procedure.

APPENDIX SIX

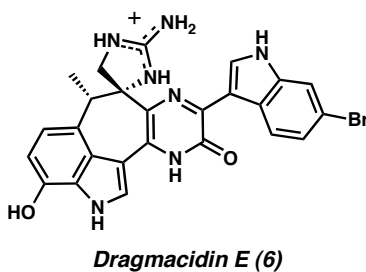
A Strategy for the Preparation of Dragmacidin E

A6.1 Background

A6.1.1 Introduction

To date, dragmacidin E (**6**) is the only member of the dragmacidin family that has not been synthesized (Figure A6.1.1). In 2000, when the Stoltz laboratory began, we developed a strategy to prepare this complex alkaloid. This appendix section describes our novel approach to the total synthesis of dragmacidin E and highlights our preliminary results involving the synthesis of model systems.¹

Figure A6.1.1

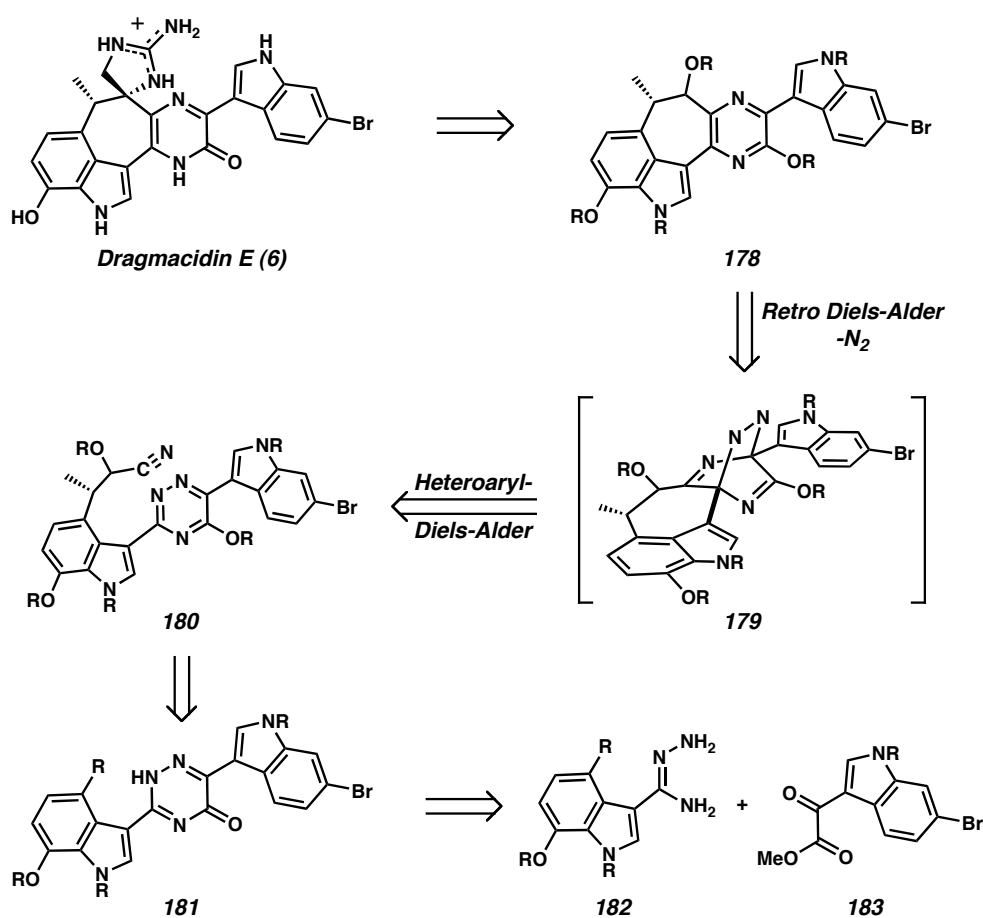


A6.1.2 Retrosynthetic Analysis of Dragmacidin E

Our retrosynthetic strategy for the preparation of dragmacidin E (**6**) is shown below in Scheme A6.1.1. We envisioned that the guanidinium unit could be installed at a late-stage in the synthesis, and the pyrazinone moiety could be masked as a pyrazine. Thus, the natural product (**6**) was disconnected to bis(indole)pyrazine **178**. The seven-

membered ring of dragmacidin E could then be installed from cyanotriazine **180** via a hetero-aryl Diels-Alder/Retro Diels-Alder sequence with concomitant loss of N₂ (**180** → **179** → **178**).^{2,3} Aromatic triazine **180** would be obtained from a non-aromatic triazinone (**181**), which in turn could be prepared via a cyclocondensation reaction of amidrazone **182** and ketoester **183**. Although indole-ketoesters are well known in the literature, indole-amidrazones are not. Therefore, our initial goal was to develop a simple synthesis of indole-amidrazones and then utilize those amidrazones to access bis(indole)triazinones.

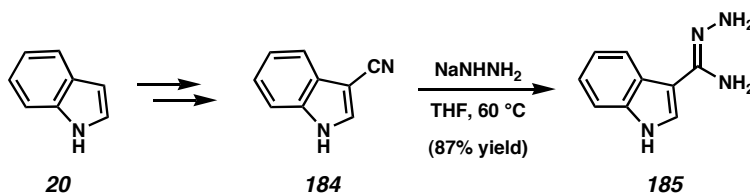
Scheme A6.1.1



A6.2 Model Systems: The Facile Synthesis of Bis(indole)-1,2,4-Triazinones

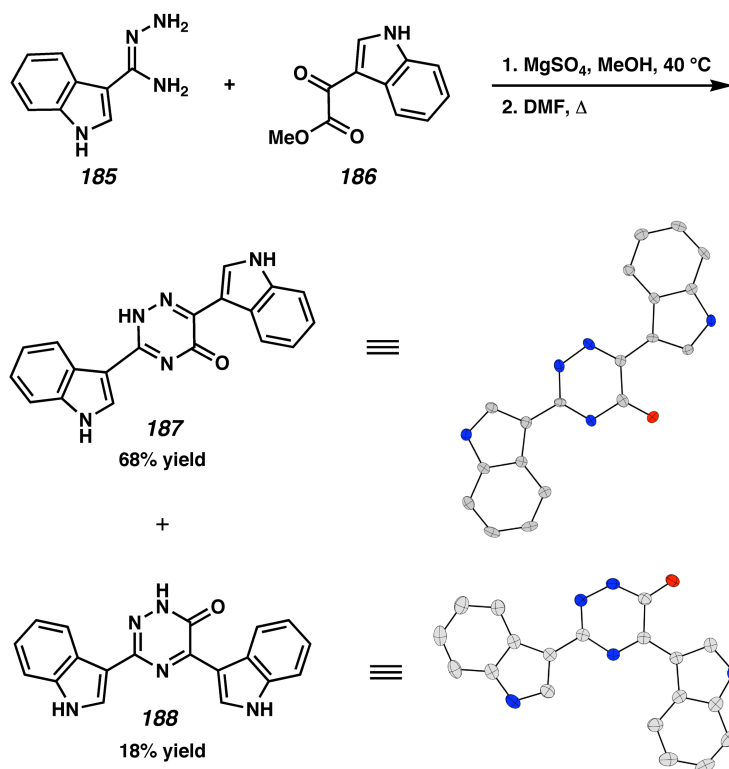
The preparation of unsubstituted indole-amidrazones turned out to be relatively straightforward (Scheme A6.2.1). Beginning from commercially available indole (**20**), we were able to access cyanoindole **184** in three steps using a known protocol.⁴ Then, simply treating **184** with sodium hydrazide in refluxing THF afforded the desired amidrazone (**185**) in good yield.⁵

Scheme A6.2.1



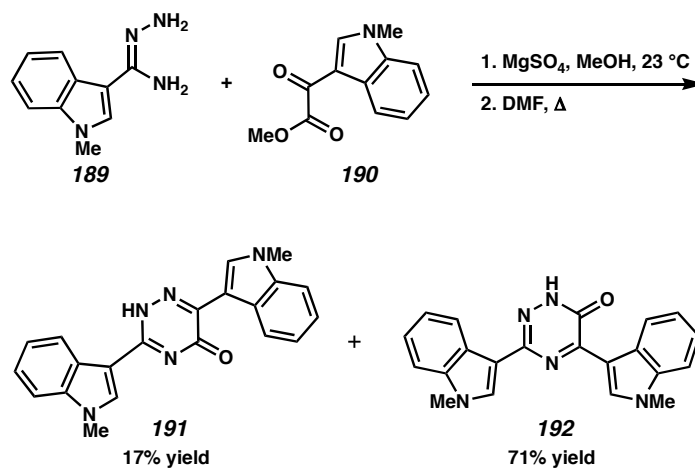
In the cyclocondensation reaction, exposure of amidrazone **185** to ketoester **186**⁶ in the presence of MgSO_4 in methanol,⁵ followed by reflux in DMF, afforded the desired *p*-triazinone product (**187**) in 68% yield (Scheme A6.2.2). *m*-Triazinone **188** was also formed, although in low yield. After separation by silica gel chromatography, the C-C connectivity of each of the triazinone products (**187** and **188**) was determined by single crystal X-ray diffraction studies.^{7a,b}

Scheme A6.2.2



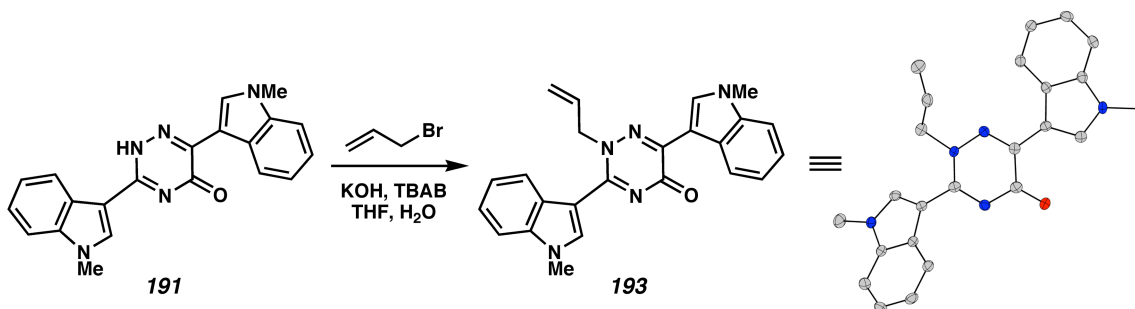
We also prepared the corresponding 1-methylated cyclization starting materials, methylamidrazone **189** and methylketoester **190**⁸ (Scheme A6.2.3). When these compounds were reacted under similar conditions to those described above, triazinone formation proceeded readily. However, the product distribution favored *m*-methyltriazinone **192** over *p*-methyltriazinone **191**. This reversal in selectivity is presumably due to the electron donating effect of the *N*-Me group on the ketone functionality of **190**, thereby altering its reactivity.

Scheme A6.2.3



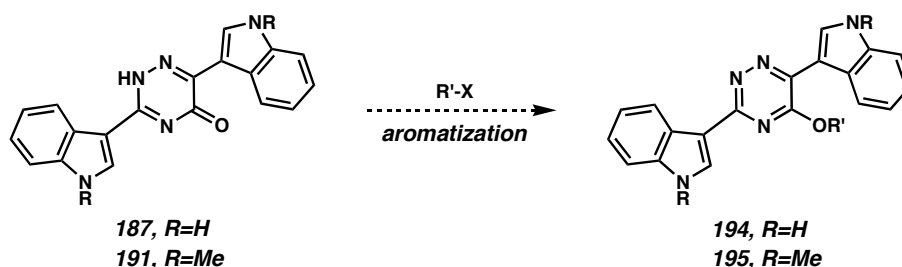
Structural assignments for *N*-methyl derivatives **191** and **192** were made by correlating ^1H NMR and TLC data with data for the corresponding *N*-H compounds (**187** and **188**, respectively). In addition, methyltriazinone **191** was treated with allyl bromide under phase transfer conditions to afford allyl derivative **193** (Scheme A6.2.4). X-ray diffraction analysis of a single crystal revealed the C-C connectivity of allyl species **193** and confirmed that triazinone **191** was *para*-substituted.^{7c}

Scheme A6.2.4



While the cyclocondensation strategy described above was effective for the preparation of *para*-substituted bis(indole)triazinones **187** and **191**, initial attempts to aromatize those compounds to their triazine counterparts (**194** and **195**) were met with limited success (Scheme A6.2.5).⁹ Although further work in this area has not been carried out, an alternative strategy to directly access bis(indole)triazines, rather than triazinones, would be attractive in order to access substrates suitable for the critical Diels-Alder/Retro Diels-Alder sequence en route to dragmacidin E (**6**).

Scheme A6.2.5

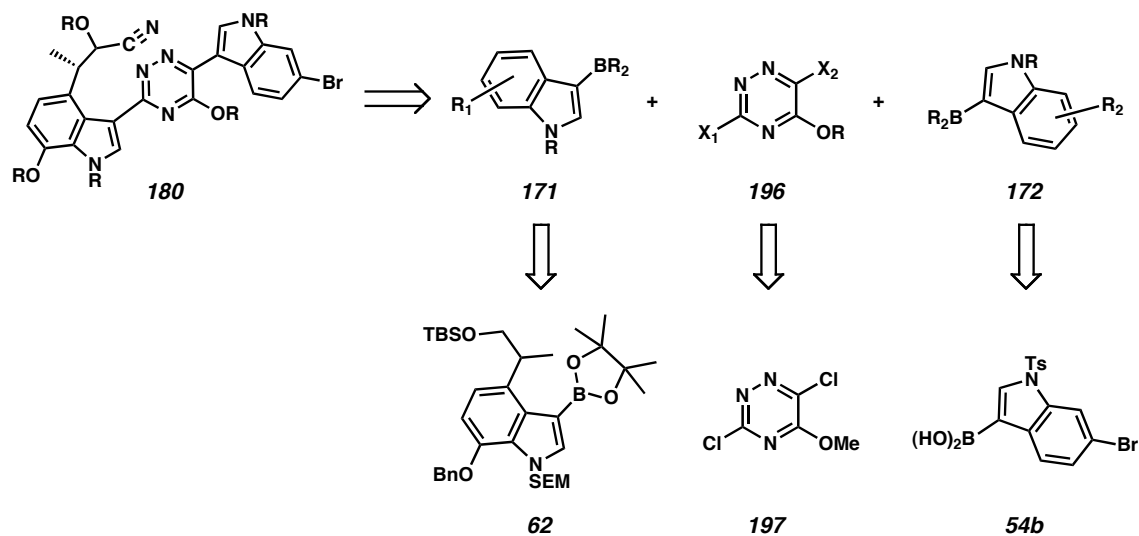


A6.3 An Alternative Strategy to Access Bis(indole)triazines

Based on our work related to the other dragmacidins (see Chapters 2 and 3), an alternative cross-coupling approach to access aromatic bis(indole)triazines (**180**) can also be envisioned (Scheme A6.3.1). In this scenario, **180** would be obtained by the sequential cross-coupling reactions of metalated indoles (**171** and **172**) and a dihalogenated triazine (**196**). Notably, it may be possible to utilize the same indole fragments (**62** and **54b**) that were employed in the total synthesis of dragmacidin D. The appropriate halogenated triazine (**196**) would likely be discovered after some experimentation; however, known dichloride **197**¹⁰ could serve as a starting point for

optimization. This promising cross-coupling strategy to access dragmacidin E (**6**) has not yet been explored.

Scheme A6.3.1



A6.4 Conclusion

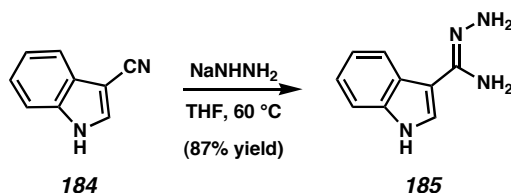
In summary, we have developed a facile method for the synthesis of bis(indole)triazinones involving a cyclocondensation reaction between amidrazone and ketoester functionalities. Although we have only prepared simple model systems thus far, more highly functionalized bis(indole)triazinones could potentially be used as intermediates en route to the total synthesis of dragmacidin E (**6**). Additionally, in future efforts, it may be possible to access substituted bis(indole)triazines via halogen-selective cross-coupling reactions.

A6.5 Experimental Section

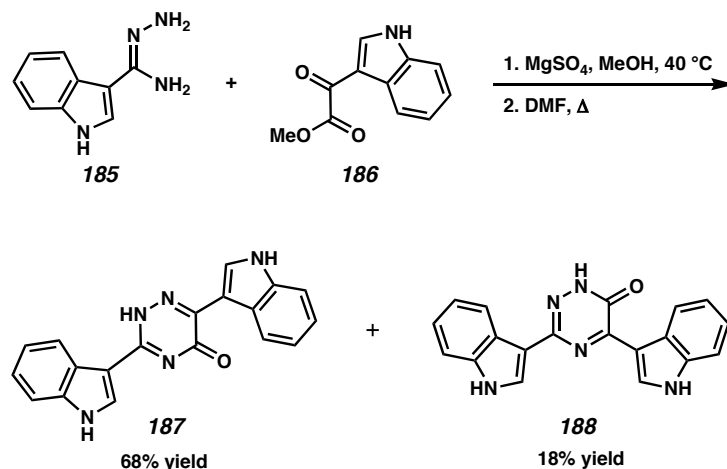
A6.5.1 Materials and Methods

Unless stated otherwise, reactions were conducted in flame-dried glassware under an atmosphere of nitrogen using anhydrous solvents (either freshly distilled or passed through activated alumina columns). All commercially obtained reagents were used as received. Reaction temperatures were controlled using an IKAmag temperature modulator. Thin-layer chromatography (TLC) was conducted with E. Merck silica gel 60 F254 pre-coated plates (0.25 mm) and visualized using a combination of UV, anisaldehyde, and potassium permanganate staining. ICN silica gel (particle size 0.032-0.063 mm) was used for flash column chromatography. ^1H NMR spectra were recorded on a Varian Mercury 300 (at 300 MHz) or a Varian Inova 500 (at 500 MHz) and are reported relative to Me_4Si (δ 0.0). Data for ^1H NMR spectra are reported as follows: chemical shift (δ ppm), multiplicity, coupling constant (Hz), and integration. ^{13}C NMR spectra were recorded on a Varian Mercury 300 (at 75 MHz) or a Varian Inova 500 (at 125 MHz) and are reported relative to Me_4Si (δ 0.0). Data for ^{13}C NMR spectra are reported in terms of chemical shift. IR spectra were recorded on a Perkin Elmer Paragon 1000 spectrometer and are reported in frequency of absorption (cm^{-1}). High resolution mass spectra were obtained from the California Institute of Technology Mass Spectral Facility. X-ray crystallographic structures were obtained by Mr. Larry M. Henling and Dr. Mike W. Day at the California Institute of Technology Beckman Institute X-Ray Crystallography Laboratory.

A6.5.2 Preparative Procedures



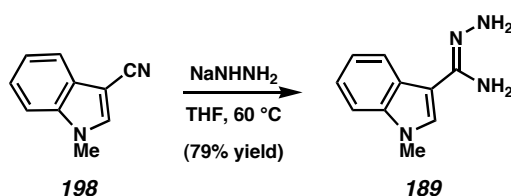
Amidrazone 185. To a suspension of NaH (60% dispersion in mineral oil, 167 mg, 4.16 mmol) in Et₂O (3.5 mL) at 0 °C was added anhydrous hydrazine (131 μL, 4.15 mmol). After stirring for 1 h, a solution of cyanoindole **184**⁴ (200 mg, 1.39 mmol) in THF (7 mL) was added dropwise over 10 min. The reaction mixture was heated to 60 °C for 6 h, cooled to 23 °C, quenched by the addition of H₂O (5 mL), and extracted with EtOAc (3 x 20 mL). The combined organic extracts were washed with brine (15 mL), dried over MgSO₄, and evaporated under reduced pressure. The residue was triturated with Et₂O (2 mL) and dried under vacuum to afford amidrazone **185** (213 mg, 87% yield), which was used immediately in the subsequent reaction. ¹H NMR (300 MHz, DMSO-*d*₆): δ 11.10 (br s, 1H), 8.15 (d, *J* = 7.7 Hz, 1H), 7.69 (s, 1H), 7.33 (d, *J* = 8.1 Hz, 1H), 7.10-7.03 (m, 1H), 7.01-6.93 (m, 1H), 5.48 (br s, 2H), 4.83 (br s, 2H). ¹³C NMR (75 MHz, DMSO-*d*₆): δ 145.3, 136.3, 124.8, 123.6, 122.2, 121.2, 119.0, 111.3, 111.1.



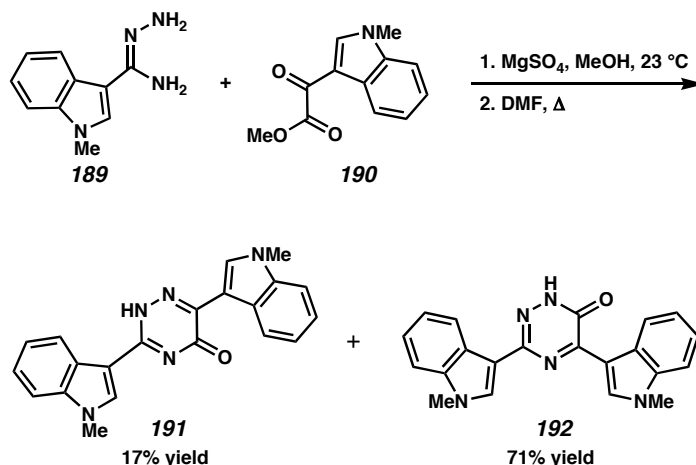
Triazinones 187 and 188. To crude amidrazone **185** (100 mg, 0.568 mmol) and MgSO₄ (171 mg, 1.42 mmol) in MeOH (2 mL) at 23 °C was added a solution of ester **186**⁶ (105 mg, 0.516 mmol) in MeOH (5 mL). The reaction mixture was heated to 40 °C for 24 h, then cooled to 23 °C. After removal of solvent under vacuum, DMF (5 mL) was added. The resulting suspension was refluxed for 24 h, then cooled to 23 °C. The solvent was removed under vacuum, and the crude product was purified by flash column chromatography (1:1 hexanes:EtOAc eluent) to afford *p*-triazinone **187** (115 mg, 68% yield) and *m*-triazinone **188** (30 mg, 18% yield) as yellow solids. For **187**, suitable crystals for X-ray diffraction were grown by the slow diffusion of hexanes into a saturated solution of **187** in 1:1 DMF:MeOH. For **188**, single crystals suitable for X-ray diffraction were obtained by the slow diffusion of hexanes into a saturated solution of **188** in MeOH. *p*-Triazinone **187**: R_f 0.28 (4:1 EtOAc:hexanes); mp >250 °C dec; ¹H NMR (500 MHz, DMSO-*d*₆): δ 13.66 (br s, 1H), 12.03 (s, 1H), 11.67 (s, 1H), 8.83 (s, 1H), 8.52 (d, *J* = 7.6 Hz, 1H), 8.50-8.45 (m, 1H), 8.44 (d, *J* = 2.5 Hz, 1H), 7.55-7.51 (comp. m, 2H), 7.28-7.17 (comp. m, 4H); ¹³C NMR (125 MHz, DMSO-*d*₆, 16/19 °C): δ 136.7, 136.3, 131.6, 129.0, 125.3, 125.2, 122.7, 122.3, 122.1, 121.9, 121.1, 120.5, 112.2, 112.0, 108.1, 106.2. CCDC deposition number 259291; IR (film) 3350, 1520, 1421,

1187 cm^{-1} ; HRMS-FAB (m/z): $[\text{M}+\text{H}]^+$ calc'd for $\text{C}_{19}\text{H}_{14}\text{N}_3\text{O}$, 328.1198; found, 328.1185.

m-Triazinone **188**: R_f 0.61 (4:1 EtOAc:hexanes); mp >250 °C dec; ^1H NMR (300 MHz, $\text{DMSO}-d_6$): δ 13.12 (s, 1H), 12.13 (s, 1H), 11.54 (s, 1H), 9.12 (d, $J = 2.9$ Hz, 1H), 8.77 (d, $J = 7.3$ Hz, 1H), 8.26 (d, $J = 7.7$ Hz, 1H), 8.14 (d, $J = 2.6$ Hz, 1H), 7.60-7.47 (comp. m, 2H), 7.39-7.26 (comp. m, 2H), 7.25-7.12 (comp. m, 2H). CCDC deposition number 161494.

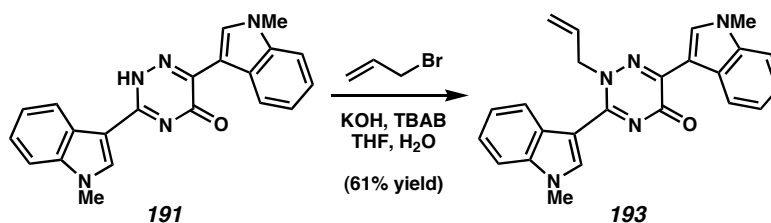


Methylamidrazone 189. Methylamidrazone **189** was prepared in a manner analogous to the preparation of **185**. To a suspension of NaH (60% dispersion in mineral oil, 779 mg, 19.48 mmol) in Et_2O (16.2 mL) at 0 °C was added anhydrous hydrazine (611 μL , 19.48 mmol). After stirring for 1 h, a solution of *N*-methyl-3-cyanoindole¹¹ (**198**, 910 mg, 6.49 mmol) in THF (32.5 mL) was added dropwise over 10 min. The reaction mixture was heated to 60 °C for 6 h, cooled to 23 °C, quenched by the addition of H_2O (17 mL), and extracted with EtOAc (4 x 25 mL). The combined organic extracts were washed with brine (2 x 25 mL), dried over MgSO_4 , and evaporated under reduced pressure to afford crude amidrazone **189** (880 mg, 79% yield), which was used immediately in the subsequent reaction without further purification. ^1H NMR (300 MHz, $\text{DMSO}-d_6$): δ 8.16 (d, $J = 8.0$ Hz, 1H), 7.65 (s, 1H), 7.39 (d, $J = 8.2$ Hz, 1H), 7.18-7.11 (m, 1H), 7.07-6.99 (m, 1H), 5.43 (br s, 2H), 4.81 (br s, 2H), 3.76 (s, 3H).



Bis(methyl)triazinones 191 and 192. To crude amidrazone **189** (65 mg, 0.378 mmol) and MgSO_4 (159 mg, 1.32 mmol) in MeOH (2 mL) at 23 °C was added a solution of ester **190**⁸ (75 mg, 0.343 mmol) in MeOH (3.4 mL). The reaction mixture was stirred at 23 °C for 24 h. After removal of solvent under vacuum, DMF (5 mL) was added. The resulting suspension was refluxed for 24 h, then cooled to 23 °C. The solvent was removed under vacuum, and the crude product was purified by flash chromatography (1:1 hexanes:EtOAc eluent) to afford *p*-bis(methyl)triazinone **191** (20 mg, 16% yield) as a yellow solid and impure *m*-bis(methyl)triazinone **192**. The crude *m*-triazinone was repurified by flash chromatography (1:1 hexanes:EtOAc eluent) to afford pure **192** (86 mg, 71% yield) as a yellow solid. *p*-Bis(methyl)triazinone **191**: R_f 0.10 (1:1 hexanes:EtOAc); mp >250 °C dec; ^1H NMR (500 MHz, $\text{DMSO-}d_6$): δ 13.60 (br s, 1H), 8.79 (s, 1H), 8.57–8.49 (comp. m, 2H), 8.34 (s, 1H), 7.60–7.52 (comp. m, 2H), 7.33–7.20 (comp. m, 4H), 3.91 (s, 3H), 3.90 (s, 3H); ^{13}C NMR (75 MHz, $\text{DMSO-}d_6$, 19/21 °C): δ 153.9, 137.2, 136.8, 135.1, 132.5, 125.9, 125.7, 122.6, 122.4, 122.2, 122.1, 121.1, 120.6, 110.5, 110.1, 107.6, 106.3, 33.3, 32.9; IR (film) 3600, 1567, 1539, 1370 cm^{-1} ; HRMS-FAB (m/z): $[\text{M} + \text{H}]^+$ calc'd for $\text{C}_{21}\text{H}_{18}\text{N}_5\text{O}$, 356.1511; found, 356.1520. *m*-Bis(methyl)triazinone **192**: R_f 0.43 (1:1 hexanes:EtOAc); mp >250 °C dec; ^1H NMR (300

MHz, DMSO- d_6): δ 13.15 (br s, 1H), 9.14 (s, 1H), 8.83 (d, J = 7.3 Hz, 1H), 8.28 (d, J = 7.8 Hz, 1H), 8.14 (s, 1H), 7.62 (d, J = 7.0 Hz, 1H), 7.54 (d, J = 7.7 Hz, 1H), 7.47-7.32 (comp. m, 2H), 7.31-7.16 (comp. m, 2H), 3.96 (comp. m, 6H); ^{13}C NMR (75 MHz, DMSO- d_6 , 20/21 °C): δ 157.7, 153.2, 148.0, 140.0, 137.6, 137.2, 131.4, 126.3, 124.9, 123.2, 122.4, 122.1, 121.6, 120.3, 111.2, 110.7, 110.3, 109.2, 33.3, 32.9; IR (film) 3600, 1646, 1465, 1373 cm^{-1} ; HRMS-FAB (m/z): $[\text{M} + \text{H}]^+$ calc'd for $\text{C}_{21}\text{H}_{18}\text{N}_5\text{O}$, 356.1511; found, 356.1521.



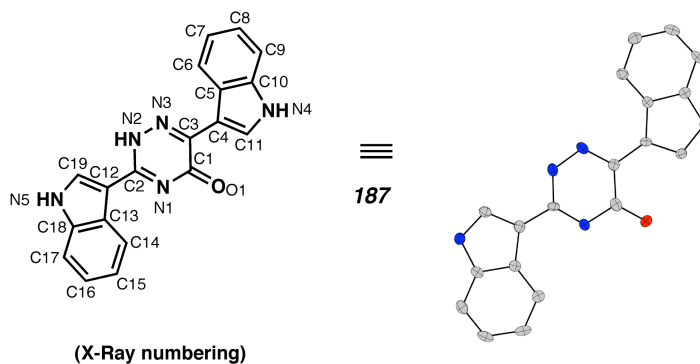
Allyl triazinone 193. To *p*-triazinone **191** (25 mg, 0.070 mmol) in THF at 23 °C, was added allyl bromide (6.7 μL , 0.078 mmol), H_2O (150 μL), powdered KOH (20 mg, 0.35 mmol), and tetrabutylammonium bromide (0.2 mg, 0.0007 mmol) in H_2O (10 μL). The resulting solution was stirred for 24 h, diluted with H_2O (5 mL), and extracted with EtOAc (3 x 15 mL). The combined organic layers were washed with brine (10 mL), dried over MgSO_4 , and evaporated under reduced pressure to afford allyl triazinone **193** (17 mg, 61% yield). Single crystals suitable for X-ray diffraction were obtained by the slow diffusion of hexanes into a saturated solution of **193** in acetone. ^1H NMR (300 MHz, DMSO- d_6): δ 8.85 (s, 1H), 8.42 (d, J = 7.7 Hz, 1H), 8.14 (d, J = 8.1 Hz, 1H), 8.02 (s, 1H), 7.62-7.51 (comp. m, 2H), 7.37-7.18 (comp. m, 4H), 6.30-6.15 (m, 1H), 5.40-5.28 (comp. m, 2H), 5.07 (d, J = 5.1 Hz, 2H), 3.92 (s, 3H), 3.91 (s, 3H). ^{13}C NMR (125 MHz, DMSO- d_6): δ 160.3, 154.4, 145.6, 136.9, 136.6, 136.0, 133.3, 133.2, 126.4, 125.8, 122.6,

122.5, 122.4, 121.2, 121.1, 121.0, 118.3, 110.6, 110.3, 106.4, 105.8, 58.3, 33.1, 33.0.

CCDC deposition number 259195.

A6.6 X-Ray Crystallography Reports

A6.6.1 X-Ray Crystallographic Report for *p*-Triazinone 187



Crystal data and structure refinement for 187 (CCDC 259291).

Empirical formula	$C_{19}H_{13}N_5O \cdot 2(C_3H_7NO)$
Formula weight	473.54
Crystallization Solvent	DMF/methanol/hexanes
Crystal Habit	Fragment
Crystal size	0.26 x 0.24 x 0.23 mm ³
Crystal color	Colorless

Data Collection

Type of diffractometer	Bruker SMART 1000	
Wavelength	0.71073 Å MoK α	
Data Collection Temperature	100(2) K	
θ range for 11276 reflections used in lattice determination	2.77 to 28.01°	
Unit cell dimensions	$a = 7.7516(6)$ Å	$\alpha = 115.3400(10)^\circ$
	$b = 12.8092(11)$ Å	$\beta = 90.9730(10)^\circ$
	$c = 13.5909(11)$ Å	$\gamma = 106.3430(10)^\circ$
Volume	1155.56(16) Å ³	
Z	2	
Crystal system	Triclinic	
Space group	P1	
Density (calculated)	1.361 Mg/m ³	

F(000)	500
Data collection program	Bruker SMART v5.630
θ range for data collection	1.68 to 28.01°
Completeness to $\theta = 28.01^\circ$	93.8 %
Index ranges	$-10 \leq h \leq 10$, $-16 \leq k \leq 16$, $-17 \leq l \leq 17$
Data collection scan type	ω scans at 7 ϕ settings
Data reduction program	Bruker SAINT v6.45A
Reflections collected	23339
Independent reflections	10181 [$R_{\text{int}} = 0.0447$]
Absorption coefficient	0.093 mm ⁻¹
Absorption correction	None
Max. and min. transmission	0.9789 and 0.9761

Structure solution program	Bruker XS v6.12
Primary solution method	Direct methods
Secondary solution method	Difference Fourier map
Hydrogen placement	Difference Fourier map
Structure refinement program	Bruker XL v6.12
Refinement method	Full matrix least-squares on F^2
Data / restraints / parameters	10181 / 3 / 847
Treatment of hydrogen atoms	Unrestrained
Goodness-of-fit on F^2	1.286
Final R indices [$I > 2\sigma(I)$, 8409 reflections]	$R1 = 0.0403$, $wR2 = 0.0678$
R indices (all data)	$R1 = 0.0509$, $wR2 = 0.0699$
Type of weighting scheme used	Sigma
Weighting scheme used	$w = 1/\sigma^2(F_o^2)$
Max shift/error	0.006
Average shift/error	0.001
Absolute structure parameter	1.2(7)
Largest diff. peak and hole	0.283 and -0.236 e. \AA^{-3}

Special Refinement Details

Refinement of F^2 against ALL reflections. The weighted R-factor (wR) and goodness of fit (S) are based on F^2 , conventional R-factors (R) are based on F , with F set to zero for negative F^2 . The threshold expression of $F^2 > 2\sigma(F^2)$ is used only for calculating R-factors(gt) etc. and is not relevant to the choice of reflections for refinement. R-factors based on F^2 are statistically about twice as large as those based on F , and R-factors based on ALL data will be even larger.

All esds (except the esd in the dihedral angle between two l.s. planes) are estimated using the full covariance matrix. The cell esds are taken into account individually in the estimation of esds in distances, angles and torsion angles; correlations between esds in cell parameters are only used when they are defined by crystal symmetry. An approximate (isotropic) treatment of cell esds is used for estimating esds involving l.s. planes.

Atomic coordinates ($\times 10^4$) and equivalent isotropic displacement parameters ($\text{\AA}^2 \times 10^3$) for 187 (CCDC 259291). $U(\text{eq})$ is defined as the trace of the orthogonalized U^{ij} tensor.

	x	y	z	U_{eq}
O(1A)	3192(2)	-1559(1)	2826(1)	24(1)
N(1A)	6162(3)	-358(2)	3238(2)	19(1)
N(2A)	6945(3)	1045(2)	2523(2)	20(1)
N(3A)	5230(3)	781(2)	2043(2)	20(1)
N(4A)	-879(3)	-1308(2)	1026(2)	18(1)
N(5A)	12261(3)	1932(2)	4134(2)	19(1)
C(1A)	4396(3)	-704(2)	2747(2)	19(1)
C(2A)	7389(3)	508(2)	3105(2)	15(1)
C(3A)	3952(3)	-75(2)	2149(2)	16(1)
C(4A)	2116(3)	-374(2)	1633(2)	15(1)
C(5A)	1508(3)	155(2)	994(2)	15(1)
C(6A)	2333(4)	1051(2)	674(2)	19(1)
C(7A)	1302(4)	1265(2)	-20(2)	22(1)
C(8A)	-547(4)	601(2)	-399(2)	24(1)
C(9A)	-1405(4)	-265(2)	-81(2)	21(1)
C(10A)	-371(3)	-474(2)	621(2)	17(1)
C(11A)	593(3)	-1247(2)	1630(2)	17(1)
C(12A)	9284(3)	889(2)	3592(2)	18(1)
C(13A)	10029(3)	414(2)	4228(2)	16(1)
C(14A)	9341(4)	-515(2)	4549(2)	19(1)
C(15A)	10492(4)	-662(2)	5222(2)	24(1)
C(16A)	12323(4)	58(2)	5580(2)	23(1)
C(17A)	13055(3)	933(2)	5233(2)	20(1)
C(18A)	11882(3)	1099(2)	4563(2)	17(1)
C(19A)	10709(3)	1797(2)	3556(2)	18(1)
O(1B)	-1098(2)	2912(1)	2152(1)	25(1)
N(1B)	1047(3)	4719(2)	3310(2)	16(1)
N(2B)	1604(3)	6308(2)	2815(2)	19(1)
N(3B)	386(3)	5665(2)	1871(2)	20(1)
N(4B)	-3939(3)	2243(2)	-750(2)	18(1)
N(5B)	5380(3)	8298(2)	5778(2)	19(1)
C(1B)	-217(3)	4002(2)	2370(2)	18(1)
C(2B)	1921(3)	5845(2)	3507(2)	15(1)
C(3B)	-528(3)	4517(2)	1627(2)	16(1)
C(4B)	-1796(3)	3816(2)	624(2)	15(1)
C(5B)	-2163(3)	4183(2)	-215(2)	14(1)
C(6B)	-1504(3)	5244(2)	-341(2)	19(1)
C(7B)	-2213(4)	5250(2)	-1283(2)	23(1)
C(8B)	-3533(4)	4241(2)	-2096(2)	25(1)
C(9B)	-4208(3)	3178(2)	-1997(2)	21(1)
C(10B)	-3498(3)	3167(2)	-1050(2)	18(1)
C(11B)	-2924(3)	2622(2)	240(2)	18(1)
C(12B)	3246(3)	6649(2)	4502(2)	17(1)
C(13B)	3677(3)	6366(2)	5376(2)	16(1)
C(14B)	3097(3)	5356(2)	5597(2)	18(1)
C(15B)	3867(4)	5445(2)	6562(2)	25(1)

C(16B)	5211(3)	6513(2)	7325(2)	21(1)
C(17B)	5794(3)	7497(2)	7123(2)	20(1)
C(18B)	5018(3)	7424(2)	6161(2)	16(1)
C(19B)	4315(3)	7825(2)	4797(2)	19(1)
O(1C)	5353(2)	7351(2)	472(2)	28(1)
N(1C)	4737(3)	5870(2)	1035(2)	20(1)
C(1C)	3747(4)	4604(2)	782(2)	24(1)
C(2C)	6150(4)	6563(2)	1997(2)	23(1)
C(3C)	4485(4)	6340(3)	367(2)	26(1)
O(1D)	6049(2)	3243(2)	4744(2)	29(1)
N(1D)	6737(3)	4699(2)	4134(2)	20(1)
C(1D)	7751(4)	5933(3)	4366(2)	24(1)
C(2D)	5339(4)	3990(3)	3159(2)	23(1)
C(3D)	6972(4)	4242(2)	4828(2)	24(1)
O(1E)	3755(2)	9886(2)	8020(2)	28(1)
C(1E)	2070(5)	7586(3)	8921(3)	29(1)
N(1E)	2176(3)	8266(2)	8272(2)	22(1)
C(2E)	769(4)	7800(3)	7344(3)	34(1)
C(3E)	3529(4)	9279(2)	8531(2)	22(1)
O(1F)	7626(2)	625(2)	7005(2)	30(1)
N(1F)	9359(3)	2310(2)	6890(2)	21(1)
C(1F)	9603(5)	3073(3)	6341(3)	31(1)
C(2F)	10667(4)	2687(3)	7848(3)	37(1)
C(3F)	7955(4)	1300(2)	6558(2)	23(1)

Bond lengths [Å] and angles [°] for 187 (CCDC 259291).

O(1A)-C(1A)	1.268(3)	N(4B)-H(4B)	0.94(3)
N(1A)-C(2A)	1.323(3)	N(5B)-C(19B)	1.348(3)
N(1A)-C(1A)	1.375(3)	N(5B)-C(18B)	1.388(3)
N(2A)-C(2A)	1.345(3)	N(5B)-H(5B)	0.97(2)
N(2A)-N(3A)	1.355(3)	C(1B)-C(3B)	1.471(3)
N(2A)-H(2A)	1.13(2)	C(2B)-C(12B)	1.453(3)
N(3A)-C(3A)	1.316(3)	C(3B)-C(4B)	1.428(3)
N(4A)-C(11A)	1.358(3)	C(4B)-C(11B)	1.386(3)
N(4A)-C(10A)	1.369(3)	C(4B)-C(5B)	1.459(3)
N(4A)-H(4A)	0.78(2)	C(5B)-C(6B)	1.396(3)
N(5A)-C(19A)	1.352(3)	C(5B)-C(10B)	1.411(3)
N(5A)-C(18A)	1.388(3)	C(6B)-C(7B)	1.388(3)
N(5A)-H(5A)	1.05(2)	C(6B)-H(6B)	0.97(2)
C(1A)-C(3A)	1.462(3)	C(7B)-C(8B)	1.390(4)
C(2A)-C(12A)	1.456(3)	C(7B)-H(7B)	1.03(3)
C(3A)-C(4A)	1.446(3)	C(8B)-C(9B)	1.379(3)
C(4A)-C(11A)	1.377(3)	C(8B)-H(8B)	0.94(2)
C(4A)-C(5A)	1.452(3)	C(9B)-C(10B)	1.398(3)
C(5A)-C(6A)	1.392(3)	C(9B)-H(9B)	0.98(2)
C(5A)-C(10A)	1.412(3)	C(11B)-H(11B)	0.949(15)
C(6A)-C(7A)	1.387(4)	C(12B)-C(19B)	1.372(3)
C(6A)-H(6A)	0.99(2)	C(12B)-C(13B)	1.442(3)
C(7A)-C(8A)	1.399(4)	C(13B)-C(14B)	1.406(3)
C(7A)-H(7A)	1.12(2)	C(13B)-C(18B)	1.409(3)
C(8A)-C(9A)	1.366(3)	C(14B)-C(15B)	1.377(4)
C(8A)-H(8A)	0.87(2)	C(14B)-H(14B)	0.97(2)
C(9A)-C(10A)	1.391(3)	C(15B)-C(16B)	1.406(4)
C(9A)-H(9A)	0.92(2)	C(15B)-H(15B)	0.97(2)
C(11A)-H(11A)	0.89(2)	C(16B)-C(17B)	1.359(3)
C(12A)-C(19A)	1.380(3)	C(16B)-H(16B)	1.00(2)
C(12A)-C(13A)	1.442(3)	C(17B)-C(18B)	1.385(3)
C(13A)-C(18A)	1.402(3)	C(17B)-H(17B)	0.92(3)
C(13A)-C(14A)	1.410(3)	C(19B)-H(19B)	1.11(3)
C(14A)-C(15A)	1.371(4)	O(1C)-C(3C)	1.224(3)
C(14A)-H(14A)	0.95(2)	N(1C)-C(3C)	1.323(3)
C(15A)-C(16A)	1.399(4)	N(1C)-C(2C)	1.452(3)
C(15A)-H(15A)	0.919(19)	N(1C)-C(1C)	1.467(3)
C(16A)-C(17A)	1.380(3)	C(1C)-H(1C1)	1.01(3)
C(16A)-H(16A)	1.02(2)	C(1C)-H(1C2)	0.95(2)
C(17A)-C(18A)	1.395(3)	C(1C)-H(1C3)	1.03(2)
C(17A)-H(17A)	1.04(2)	C(2C)-H(2C1)	0.96(3)
C(19A)-H(19A)	1.05(2)	C(2C)-H(2C2)	1.00(2)
O(1B)-C(1B)	1.267(3)	C(2C)-H(2C3)	0.99(2)
N(1B)-C(2B)	1.313(3)	C(3C)-H(3C)	1.12(3)
N(1B)-C(1B)	1.372(3)	O(1D)-C(3D)	1.233(3)
N(2B)-N(3B)	1.354(3)	N(1D)-C(3D)	1.340(3)
N(2B)-C(2B)	1.360(3)	N(1D)-C(1D)	1.443(3)
N(2B)-H(2B)	1.18(2)	N(1D)-C(2D)	1.457(3)
N(3B)-C(3B)	1.327(3)	C(1D)-H(1D1)	1.01(2)
N(4B)-C(11B)	1.362(3)	C(1D)-H(1D2)	0.93(3)
N(4B)-C(10B)	1.369(3)	C(1D)-H(1D3)	1.04(3)

C(2D)-H(2D1)	0.95(3)	C(7A)-C(6A)-H(6A)	120.1(13)
C(2D)-H(2D2)	1.05(3)	C(5A)-C(6A)-H(6A)	120.7(13)
C(2D)-H(2D3)	1.03(3)	C(6A)-C(7A)-C(8A)	121.2(2)
C(3D)-H(3D)	1.01(2)	C(6A)-C(7A)-H(7A)	121.7(12)
O(1E)-C(3E)	1.227(3)	C(8A)-C(7A)-H(7A)	117.1(12)
C(1E)-N(1E)	1.471(3)	C(9A)-C(8A)-C(7A)	121.0(2)
C(1E)-H(1E1)	0.96(3)	C(9A)-C(8A)-H(8A)	121.1(14)
C(1E)-H(1E2)	1.03(2)	C(7A)-C(8A)-H(8A)	117.8(14)
C(1E)-H(1E3)	1.04(2)	C(8A)-C(9A)-C(10A)	117.7(2)
N(1E)-C(3E)	1.319(3)	C(8A)-C(9A)-H(9A)	123.2(12)
N(1E)-C(2E)	1.442(4)	C(10A)-C(9A)-H(9A)	119.1(12)
C(2E)-H(2E1)	1.08(3)	N(4A)-C(10A)-C(9A)	129.2(2)
C(2E)-H(2E2)	1.07(3)	N(4A)-C(10A)-C(5A)	108.0(2)
C(2E)-H(2E3)	1.03(2)	C(9A)-C(10A)-C(5A)	122.7(2)
C(3E)-H(3E)	1.00(2)	N(4A)-C(11A)-C(4A)	110.1(2)
O(1F)-C(3F)	1.230(3)	N(4A)-C(11A)-H(11A)	122.8(13)
N(1F)-C(3F)	1.324(3)	C(4A)-C(11A)-H(11A)	126.9(13)
N(1F)-C(1F)	1.439(3)	C(19A)-C(12A)-C(13A)	106.6(2)
N(1F)-C(2F)	1.449(4)	C(19A)-C(12A)-C(2A)	126.5(2)
C(1F)-H(1F1)	0.99(3)	C(13A)-C(12A)-C(2A)	126.8(2)
C(1F)-H(1F2)	0.96(3)	C(18A)-C(13A)-C(14A)	118.3(2)
C(1F)-H(1F3)	1.00(3)	C(18A)-C(13A)-C(12A)	106.14(19)
C(2F)-H(2F1)	0.92(3)	C(14A)-C(13A)-C(12A)	135.6(2)
C(2F)-H(2F2)	0.91(2)	C(15A)-C(14A)-C(13A)	118.4(2)
C(2F)-H(2F3)	0.97(2)	C(15A)-C(14A)-H(14A)	124.9(14)
C(3F)-H(3F)	1.034(19)	C(13A)-C(14A)-H(14A)	116.3(14)
		C(14A)-C(15A)-C(16A)	122.5(2)
C(2A)-N(1A)-C(1A)	117.42(19)	C(14A)-C(15A)-H(15A)	115.8(13)
C(2A)-N(2A)-N(3A)	124.1(2)	C(16A)-C(15A)-H(15A)	121.6(13)
C(2A)-N(2A)-H(2A)	123.9(12)	C(17A)-C(16A)-C(15A)	120.3(2)
N(3A)-N(2A)-H(2A)	112.0(12)	C(17A)-C(16A)-H(16A)	117.6(12)
C(3A)-N(3A)-N(2A)	116.6(2)	C(15A)-C(16A)-H(16A)	122.1(12)
C(11A)-N(4A)-C(10A)	109.6(2)	C(16A)-C(17A)-C(18A)	117.4(2)
C(11A)-N(4A)-H(4A)	123.5(19)	C(16A)-C(17A)-H(17A)	125.1(13)
C(10A)-N(4A)-H(4A)	126.5(19)	C(18A)-C(17A)-H(17A)	117.2(14)
C(19A)-N(5A)-C(18A)	108.7(2)	N(5A)-C(18A)-C(17A)	128.7(2)
C(19A)-N(5A)-H(5A)	131.4(14)	N(5A)-C(18A)-C(13A)	108.3(2)
C(18A)-N(5A)-H(5A)	119.9(14)	C(17A)-C(18A)-C(13A)	123.0(2)
O(1A)-C(1A)-N(1A)	119.3(2)	N(5A)-C(19A)-C(12A)	110.2(2)
O(1A)-C(1A)-C(3A)	121.6(2)	N(5A)-C(19A)-H(19A)	121.5(13)
N(1A)-C(1A)-C(3A)	119.1(2)	C(12A)-C(19A)-H(19A)	128.2(13)
N(1A)-C(2A)-N(2A)	122.0(2)	C(2B)-N(1B)-C(1B)	117.96(18)
N(1A)-C(2A)-C(12A)	119.4(2)	N(3B)-N(2B)-C(2B)	123.8(2)
N(2A)-C(2A)-C(12A)	118.5(2)	N(3B)-N(2B)-H(2B)	111.8(10)
N(3A)-C(3A)-C(4A)	117.2(2)	C(2B)-N(2B)-H(2B)	124.4(10)
N(3A)-C(3A)-C(1A)	120.8(2)	C(3B)-N(3B)-N(2B)	116.68(19)
C(4A)-C(3A)-C(1A)	122.0(2)	C(11B)-N(4B)-C(10B)	109.2(2)
C(11A)-C(4A)-C(3A)	126.5(2)	C(11B)-N(4B)-H(4B)	125.0(15)
C(11A)-C(4A)-C(5A)	106.0(2)	C(10B)-N(4B)-H(4B)	124.3(15)
C(3A)-C(4A)-C(5A)	127.4(2)	C(19B)-N(5B)-C(18B)	108.5(2)
C(6A)-C(5A)-C(10A)	118.1(2)	C(19B)-N(5B)-H(5B)	127.4(14)
C(6A)-C(5A)-C(4A)	135.5(2)	C(18B)-N(5B)-H(5B)	124.1(14)
C(10A)-C(5A)-C(4A)	106.27(19)	O(1B)-C(1B)-N(1B)	120.0(2)
C(7A)-C(6A)-C(5A)	119.2(2)	O(1B)-C(1B)-C(3B)	120.9(2)

N(1B)-C(1B)-C(3B)	119.10(19)	C(12B)-C(19B)-H(19B)	125.5(15)
N(1B)-C(2B)-N(2B)	122.1(2)	C(3C)-N(1C)-C(2C)	120.5(2)
N(1B)-C(2B)-C(12B)	120.1(2)	C(3C)-N(1C)-C(1C)	122.0(2)
N(2B)-C(2B)-C(12B)	117.7(2)	C(2C)-N(1C)-C(1C)	117.2(2)
N(3B)-C(3B)-C(4B)	117.5(2)	N(1C)-C(1C)-H(1C1)	105.6(14)
N(3B)-C(3B)-C(1B)	120.4(2)	N(1C)-C(1C)-H(1C2)	106.9(14)
C(4B)-C(3B)-C(1B)	122.1(2)	H(1C1)-C(1C)-H(1C2)	120(2)
C(11B)-C(4B)-C(3B)	126.6(2)	N(1C)-C(1C)-H(1C3)	111.8(12)
C(11B)-C(4B)-C(5B)	105.5(2)	H(1C1)-C(1C)-H(1C3)	102.1(19)
C(3B)-C(4B)-C(5B)	127.9(2)	H(1C2)-C(1C)-H(1C3)	110.1(18)
C(6B)-C(5B)-C(10B)	118.8(2)	N(1C)-C(2C)-H(2C1)	113.8(17)
C(6B)-C(5B)-C(4B)	134.9(2)	N(1C)-C(2C)-H(2C2)	112.0(13)
C(10B)-C(5B)-C(4B)	106.3(2)	H(2C1)-C(2C)-H(2C2)	103(2)
C(7B)-C(6B)-C(5B)	118.1(2)	N(1C)-C(2C)-H(2C3)	108.3(13)
C(7B)-C(6B)-H(6B)	122.7(13)	H(2C1)-C(2C)-H(2C3)	118(2)
C(5B)-C(6B)-H(6B)	119.2(13)	H(2C2)-C(2C)-H(2C3)	100.3(18)
C(6B)-C(7B)-C(8B)	122.3(2)	O(1C)-C(3C)-N(1C)	126.0(3)
C(6B)-C(7B)-H(7B)	117.8(15)	O(1C)-C(3C)-H(3C)	124.0(13)
C(8B)-C(7B)-H(7B)	119.9(15)	N(1C)-C(3C)-H(3C)	109.5(13)
C(9B)-C(8B)-C(7B)	121.0(2)	C(3D)-N(1D)-C(1D)	121.5(2)
C(9B)-C(8B)-H(8B)	120.4(13)	C(3D)-N(1D)-C(2D)	120.5(2)
C(7B)-C(8B)-H(8B)	118.5(13)	C(1D)-N(1D)-C(2D)	117.8(2)
C(8B)-C(9B)-C(10B)	117.0(2)	N(1D)-C(1D)-H(1D1)	112.4(12)
C(8B)-C(9B)-H(9B)	125.5(13)	N(1D)-C(1D)-H(1D2)	113.0(19)
C(10B)-C(9B)-H(9B)	117.4(13)	H(1D1)-C(1D)-H(1D2)	113(2)
N(4B)-C(10B)-C(9B)	128.6(2)	N(1D)-C(1D)-H(1D3)	115.0(16)
N(4B)-C(10B)-C(5B)	108.5(2)	H(1D1)-C(1D)-H(1D3)	102(2)
C(9B)-C(10B)-C(5B)	122.8(2)	H(1D2)-C(1D)-H(1D3)	101(2)
N(4B)-C(11B)-C(4B)	110.5(2)	N(1D)-C(2D)-H(2D1)	110.4(16)
N(4B)-C(11B)-H(11B)	122.1(10)	N(1D)-C(2D)-H(2D2)	104.6(15)
C(4B)-C(11B)-H(11B)	127.4(10)	H(2D1)-C(2D)-H(2D2)	125(2)
C(19B)-C(12B)-C(13B)	106.9(2)	N(1D)-C(2D)-H(2D3)	110.6(14)
C(19B)-C(12B)-C(2B)	126.8(2)	H(2D1)-C(2D)-H(2D3)	97.8(19)
C(13B)-C(12B)-C(2B)	126.4(2)	H(2D2)-C(2D)-H(2D3)	108(2)
C(14B)-C(13B)-C(18B)	118.0(2)	O(1D)-C(3D)-N(1D)	125.5(3)
C(14B)-C(13B)-C(12B)	136.2(2)	O(1D)-C(3D)-H(3D)	121.1(11)
C(18B)-C(13B)-C(12B)	105.7(2)	N(1D)-C(3D)-H(3D)	113.3(11)
C(15B)-C(14B)-C(13B)	118.6(2)	N(1E)-C(1E)-H(1E1)	109.9(14)
C(15B)-C(14B)-H(14B)	118.6(13)	N(1E)-C(1E)-H(1E2)	109.0(11)
C(13B)-C(14B)-H(14B)	122.7(13)	H(1E1)-C(1E)-H(1E2)	109.7(18)
C(14B)-C(15B)-C(16B)	121.8(2)	N(1E)-C(1E)-H(1E3)	107.0(12)
C(14B)-C(15B)-H(15B)	117.8(13)	H(1E1)-C(1E)-H(1E3)	109.0(19)
C(16B)-C(15B)-H(15B)	120.3(12)	H(1E2)-C(1E)-H(1E3)	112.2(17)
C(17B)-C(16B)-C(15B)	120.4(2)	C(3E)-N(1E)-C(2E)	120.6(2)
C(17B)-C(16B)-H(16B)	117.9(12)	C(3E)-N(1E)-C(1E)	120.8(2)
C(15B)-C(16B)-H(16B)	121.5(12)	C(2E)-N(1E)-C(1E)	118.6(2)
C(16B)-C(17B)-C(18B)	118.4(2)	N(1E)-C(2E)-H(2E1)	107.6(13)
C(16B)-C(17B)-H(17B)	125.0(15)	N(1E)-C(2E)-H(2E2)	111.8(18)
C(18B)-C(17B)-H(17B)	116.5(15)	H(2E1)-C(2E)-H(2E2)	128(2)
C(17B)-C(18B)-N(5B)	129.0(2)	N(1E)-C(2E)-H(2E3)	107.9(13)
C(17B)-C(18B)-C(13B)	122.7(2)	H(2E1)-C(2E)-H(2E3)	107.4(18)
N(5B)-C(18B)-C(13B)	108.3(2)	H(2E2)-C(2E)-H(2E3)	91(2)
N(5B)-C(19B)-C(12B)	110.6(2)	O(1E)-C(3E)-N(1E)	125.3(3)
N(5B)-C(19B)-H(19B)	123.7(15)	O(1E)-C(3E)-H(3E)	118.7(13)

N(1E)-C(3E)-H(3E)	115.9(13)
C(3F)-N(1F)-C(1F)	121.7(2)
C(3F)-N(1F)-C(2F)	119.8(2)
C(1F)-N(1F)-C(2F)	118.5(2)
N(1F)-C(1F)-H(1F1)	111.1(15)
N(1F)-C(1F)-H(1F2)	106.9(16)
H(1F1)-C(1F)-H(1F2)	98(2)
N(1F)-C(1F)-H(1F3)	109.4(16)
H(1F1)-C(1F)-H(1F3)	116(2)
H(1F2)-C(1F)-H(1F3)	114(2)
N(1F)-C(2F)-H(2F1)	116.7(17)
N(1F)-C(2F)-H(2F2)	106.1(14)
H(2F1)-C(2F)-H(2F2)	126(2)
N(1F)-C(2F)-H(2F3)	108.5(13)
H(2F1)-C(2F)-H(2F3)	104(2)
H(2F2)-C(2F)-H(2F3)	91.6(19)
O(1F)-C(3F)-N(1F)	125.4(3)
O(1F)-C(3F)-H(3F)	122.7(11)
N(1F)-C(3F)-H(3F)	111.7(10)

Anisotropic displacement parameters ($\text{\AA}^2 \times 10^4$) for 187 (CCDC 259291). The anisotropic displacement factor exponent takes the form: $-2\pi^2 [h^2 a^{*2} U^{11} + \dots + 2h k a^* b^* U^{12}]$.

	U^{11}	U^{22}	U^{33}	U^{23}	U^{13}	U^{12}
O(1A)	227(8)	207(8)	297(8)	156(7)	9(6)	23(7)
N(1A)	150(10)	200(10)	197(10)	88(9)	2(8)	44(8)
N(2A)	143(10)	209(10)	230(11)	88(9)	19(8)	41(8)
N(3A)	179(11)	206(11)	180(11)	63(9)	-10(9)	76(9)
N(4A)	130(11)	193(11)	204(12)	92(10)	6(9)	13(9)
N(5A)	181(11)	191(11)	195(11)	91(9)	17(9)	33(9)
C(1A)	180(13)	226(13)	141(12)	49(10)	26(10)	70(11)
C(2A)	206(13)	123(11)	139(12)	51(10)	17(10)	91(10)
C(3A)	181(12)	166(12)	114(12)	47(10)	29(10)	46(10)
C(4A)	185(13)	153(12)	140(12)	76(10)	25(10)	87(10)
C(5A)	147(13)	162(12)	131(13)	48(11)	39(10)	72(10)
C(6A)	185(13)	177(12)	196(13)	79(11)	19(10)	70(10)
C(7A)	286(13)	187(12)	213(13)	97(11)	39(11)	83(11)
C(8A)	279(15)	281(14)	203(14)	115(12)	18(12)	167(12)
C(9A)	148(12)	265(14)	170(13)	61(11)	-27(10)	84(11)
C(10A)	191(14)	158(13)	152(13)	59(11)	48(11)	72(11)
C(11A)	188(13)	166(12)	172(13)	95(11)	11(10)	40(10)
C(12A)	189(13)	151(12)	146(13)	38(11)	12(10)	39(10)
C(13A)	194(14)	144(12)	132(13)	38(11)	20(11)	65(10)
C(14A)	222(14)	190(13)	171(13)	79(11)	51(11)	78(11)
C(15A)	379(16)	226(13)	201(13)	136(12)	79(12)	151(12)
C(16A)	305(15)	267(14)	145(13)	61(12)	-11(11)	176(12)
C(17A)	171(13)	225(13)	178(13)	48(11)	20(11)	81(11)
C(18A)	185(14)	189(13)	127(13)	43(11)	24(11)	94(11)
C(19A)	201(13)	191(13)	152(13)	69(11)	6(10)	73(10)
O(1B)	281(9)	189(9)	267(8)	130(7)	-10(6)	15(7)
N(1B)	147(10)	199(10)	155(11)	85(9)	32(8)	59(8)
N(2B)	162(10)	188(10)	167(11)	45(9)	-2(8)	20(8)
N(3B)	153(11)	256(11)	169(11)	93(10)	-1(9)	55(9)
N(4B)	149(10)	174(11)	179(10)	57(9)	-14(8)	23(9)
N(5B)	226(11)	130(10)	213(11)	82(9)	31(9)	39(9)
C(1B)	133(12)	234(13)	177(13)	80(11)	33(10)	83(10)
C(2B)	135(12)	195(12)	131(12)	75(10)	37(9)	68(10)
C(3B)	146(12)	174(12)	200(13)	100(10)	62(10)	85(10)
C(4B)	154(13)	171(12)	164(13)	98(11)	53(10)	61(10)
C(5B)	138(13)	179(13)	124(13)	63(11)	10(10)	68(10)
C(6B)	155(13)	195(13)	210(14)	91(12)	24(11)	42(11)
C(7B)	228(14)	261(14)	260(14)	154(12)	69(11)	86(11)
C(8B)	266(14)	340(15)	217(14)	167(12)	45(12)	151(12)
C(9B)	186(13)	253(14)	162(13)	53(12)	-5(11)	87(11)
C(10B)	176(13)	194(13)	214(14)	103(12)	77(11)	97(11)
C(11B)	193(13)	148(12)	195(13)	84(11)	26(10)	60(10)
C(12B)	144(13)	207(13)	192(13)	100(11)	40(11)	82(11)
C(13B)	143(13)	177(13)	184(14)	82(12)	68(11)	75(11)
C(14B)	162(13)	180(13)	235(14)	108(12)	28(11)	68(11)
C(15B)	258(15)	306(15)	315(16)	232(13)	85(12)	146(12)

C(16B)	214(13)	296(13)	145(13)	113(11)	28(10)	115(11)
C(17B)	177(13)	231(14)	161(13)	54(11)	24(11)	95(11)
C(18B)	152(13)	188(13)	150(13)	62(11)	62(10)	71(11)
C(19B)	157(12)	242(13)	205(13)	134(11)	48(10)	73(10)
O(1C)	190(10)	320(11)	365(12)	236(10)	-8(8)	12(8)
N(1C)	197(12)	220(11)	224(12)	132(10)	40(10)	70(9)
C(1C)	240(15)	188(14)	250(16)	91(13)	44(13)	33(12)
C(2C)	197(15)	208(15)	242(16)	79(13)	14(13)	63(12)
C(3C)	206(15)	294(15)	264(16)	126(14)	-2(12)	56(12)
O(1D)	245(10)	290(10)	333(11)	186(9)	-9(8)	25(8)
N(1D)	175(12)	208(11)	173(12)	62(10)	-1(9)	33(9)
C(1D)	228(16)	254(15)	281(16)	139(14)	71(13)	91(13)
C(2D)	233(15)	259(15)	210(15)	109(13)	11(12)	84(13)
C(3D)	147(14)	286(15)	271(16)	140(14)	16(12)	14(12)
O(1E)	300(11)	244(10)	257(10)	102(9)	74(8)	46(8)
C(1E)	381(18)	276(15)	279(16)	139(14)	113(15)	157(13)
N(1E)	185(12)	216(12)	205(12)	76(10)	23(10)	37(10)
C(2E)	260(17)	356(18)	298(18)	91(16)	-42(14)	28(14)
C(3E)	194(14)	212(14)	225(14)	64(12)	62(11)	77(11)
O(1F)	325(11)	220(10)	277(10)	92(9)	84(8)	24(8)
N(1F)	200(12)	172(11)	206(12)	58(10)	31(10)	21(9)
C(1F)	346(18)	230(15)	336(18)	121(14)	130(15)	85(13)
C(2F)	231(17)	386(19)	276(18)	23(15)	8(14)	2(14)
C(3F)	226(14)	237(14)	194(14)	42(12)	51(12)	101(12)

Hydrogen coordinates ($\times 10^4$) and isotropic displacement parameters ($\text{\AA}^2 \times 10^{-3}$) for 187 (CCDC 259291).

	x	y	z	U_{iso}
H(2A)	7960(30)	1770(20)	2381(19)	20(6)
H(4A)	-1870(30)	-1700(20)	990(20)	29(8)
H(5A)	13580(30)	2540(20)	4300(20)	35(7)
H(6A)	3630(30)	1540(20)	951(18)	26(7)
H(7A)	1900(30)	1990(20)	-280(20)	40(8)
H(8A)	-1140(30)	766(19)	-836(17)	16(6)
H(9A)	-2640(30)	-686(17)	-282(16)	9(5)
H(11A)	520(30)	-1685(18)	1995(16)	7(5)
H(14A)	8070(30)	-930(20)	4350(20)	28(7)
H(15A)	9970(30)	-1226(19)	5467(17)	11(6)
H(16A)	13160(30)	-29(19)	6107(18)	27(6)
H(17A)	14380(30)	1530(20)	5480(20)	40(8)
H(19A)	10670(30)	2380(20)	3200(19)	31(7)
H(2B)	2370(30)	7308(18)	2954(16)	3(5)
H(4B)	-4620(30)	1430(20)	-1230(20)	36(8)
H(5B)	6280(30)	9100(20)	6168(19)	30(7)
H(6B)	-600(30)	5950(20)	240(18)	21(6)
H(7B)	-1760(40)	6050(20)	-1360(20)	49(8)
H(8B)	-4010(30)	4313(19)	-2697(18)	23(6)
H(9B)	-5080(30)	2410(20)	-2557(19)	23(6)
H(11B)	-3050(20)	2115(14)	596(13)	-11(4)
H(14B)	2160(30)	4610(20)	5112(19)	18(6)
H(15B)	3430(30)	4747(19)	6714(17)	11(6)
H(16B)	5680(30)	6603(18)	8059(17)	19(6)
H(17B)	6720(30)	8200(20)	7560(20)	30(7)
H(19B)	4400(40)	8310(30)	4270(20)	71(10)
H(1C1)	2920(40)	4260(20)	60(20)	41(8)
H(1C2)	3250(30)	4620(20)	1421(19)	12(6)
H(1C3)	4590(30)	4070(19)	582(17)	12(6)
H(2C1)	7190(40)	6290(20)	1920(20)	44(9)
H(2C2)	5720(30)	6484(19)	2659(19)	18(6)
H(2C3)	6350(30)	7440(20)	2241(18)	16(6)
H(3C)	3480(40)	5630(20)	-380(20)	44(8)
H(1D1)	8810(30)	6310(20)	4984(19)	21(7)
H(1D2)	7010(40)	6420(30)	4470(30)	61(10)
H(1D3)	8390(40)	6030(20)	3730(20)	40(8)
H(2D1)	4910(40)	3160(20)	3020(20)	40(8)
H(2D2)	5850(40)	4290(20)	2580(20)	46(8)
H(2D3)	4150(40)	4180(20)	3330(20)	25(7)
H(3D)	8070(30)	4769(18)	5416(16)	3(5)
H(1E1)	3120(30)	7960(20)	9480(20)	26(7)
H(1E2)	2010(30)	6708(18)	8405(16)	10(5)
H(1E3)	920(30)	7620(20)	9295(19)	22(6)
H(2E1)	1120(30)	8390(20)	6950(20)	52(8)

H(2E2)	-540(50)	7400(30)	7500(30)	82(11)
H(2E3)	800(30)	6960(20)	6790(20)	45(7)
H(3E)	4450(30)	9540(20)	9178(19)	22(6)
H(1F1)	10710(40)	3080(20)	5990(20)	38(8)
H(1F2)	10010(40)	3900(30)	6900(20)	54(9)
H(1F3)	8450(40)	2850(20)	5850(20)	46(9)
H(2F1)	10320(40)	3040(20)	8530(20)	58(8)
H(2F2)	11780(30)	2930(20)	7668(18)	19(6)
H(2F3)	10880(30)	1970(20)	7832(18)	34(7)
H(3F)	7190(30)	1099(17)	5830(16)	1(5)

Hydrogen bonds for 187 (CCDC 259291) [\AA and $^\circ$].

D-H...A	d(D-H)	d(H...A)	d(D...A)	<(DHA)
N(2A)-H(2A)...O(1B)#1	1.13(2)	1.60(2)	2.700(2)	164(2)
N(4A)-H(4A)...O(1C)#2	0.78(2)	2.08(3)	2.836(3)	162(3)
N(5A)-H(5A)...O(1D)#1	1.05(2)	1.83(2)	2.842(3)	161(2)
N(2B)-H(2B)...O(1A)#3	1.18(2)	1.498(19)	2.656(2)	165.6(17)
N(4B)-H(4B)...O(1E)#4	0.94(3)	1.83(3)	2.765(3)	169(2)
N(5B)-H(5B)...O(1F)#3	0.97(2)	1.76(2)	2.725(3)	171(2)

Symmetry transformations used to generate equivalent atoms:

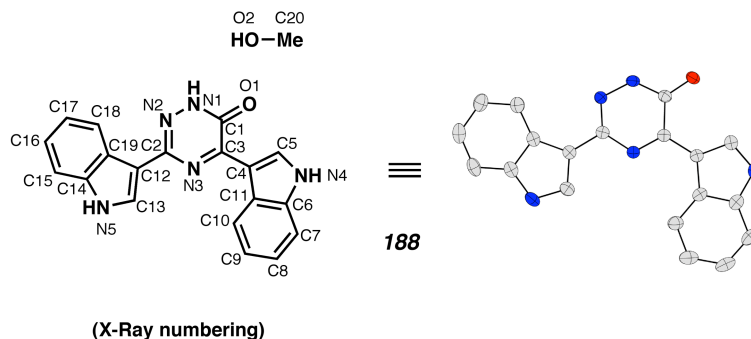
#1 x+1,y,z

#2 x-1,y-1,z

#3 x,y+1,z

#4 x-1,y-1,z-1

A6.6.2 X-Ray Crystallographic Report for *m*-Triazinone 188



Crystal data and structure refinement for 188 (CCDC 161494).

Empirical formula	C20 H17 N5 O2
Formula weight	359.39
Crystallization Solvent	Methanol
Crystal Habit	needle
Crystal size	0.33 x 0.14 x 0.09 mm ³
Crystal color	yellow

Data Collection

Preliminary Photos	none
Type of diffractometer	CCD
Wavelength	0.71073 Å MoK α
Data Collection Temperature	98(2) K
θ range for 7767 reflections used in lattice determination	2.20 to 27.35°
Unit cell dimensions	$a = 4.6579(4)$ Å $b = 18.5134(15)$ Å $c = 19.5156(16)$ Å
	$\alpha = 90^\circ$ $\beta = 90^\circ$ $\gamma = 90^\circ$
Volume	1682.9(2) Å ³
Z	4
Crystal system	Orthorhombic
Space group	P2(1)2(1)2(1)
Density (calculated)	1.418 Mg/m ³
F(000)	752

Data collection program	Bruker SMART
θ range for data collection	2.09 to 28.53°
Completeness to $\theta = 28.53^\circ$	95.9 %
Index ranges	$-6 \leq h \leq 6$, $-24 \leq k \leq 24$, $-25 \leq l \leq 25$
Data collection scan type	phi and omega scans
Data reduction program	Bruker SAINT 6.2
Reflections collected	20360
Independent reflections	4014 ($R_{\text{int}} = 0.0620$)
Absorption coefficient	0.096 mm^{-1}
Absorption correction	None
Structure solution program	SHELXS-97 (Sheldrick, 1990)
Primary solution method	direct
Secondary solution method	difmap
Hydrogen placement	geom
Structure refinement program	SHELXL-97 (Sheldrick, 1997)
Refinement method	Full-matrix least-squares on F^2
Data / restraints / parameters	4014 / 0 / 312
Treatment of hydrogen atoms	refall
Goodness-of-fit on F^2	0.903
Final R indices [$I > 2\sigma(I)$, 3238 reflections]	$R1 = 0.0367$, $wR2 = 0.0833$
R indices (all data)	$R1 = 0.0502$, $wR2 = 0.0890$
Type of weighting scheme used	calc
Weighting scheme used	$\text{calc } w = 1 / [\sigma^2(F_o^2) + (0.0569P)^2 + 0.0000P]$ where
$P = (F_o^2 + 2F_c^2) / 3$	
Max shift/error	0.010
Average shift/error	0.001
Absolute structure parameter	0.2(12)
Largest diff. peak and hole	0.200 and $-0.175 \text{ e. \AA}^{-3}$

Atomic coordinates ($\times 10^4$) and equivalent isotropic displacement parameters ($\text{\AA}^2 \times 10^3$) for 188 (CCDC 161494). $U(\text{eq})$ is defined as the trace of the orthogonalized U_{ij} tensor.

	x	y	z	U_{eq}
O(1)	8039(3)	8255(1)	10244(1)	29(1)
C(1)	6801(3)	8516(1)	9727(1)	24(1)
C(2)	3843(3)	9014(1)	8628(1)	22(1)
C(3)	7333(3)	9241(1)	9441(1)	22(1)
C(4)	9428(3)	9713(1)	9754(1)	22(1)
C(5)	11233(4)	9558(1)	10295(1)	27(1)
C(6)	12174(4)	10705(1)	10005(1)	29(1)
C(7)	13284(4)	11402(1)	9982(1)	36(1)
C(8)	12196(4)	11856(1)	9489(1)	40(1)
C(9)	10072(4)	11624(1)	9032(1)	39(1)
C(10)	8977(4)	10932(1)	9058(1)	32(1)
C(11)	10029(3)	10457(1)	9559(1)	25(1)
C(12)	2242(3)	9293(1)	8049(1)	24(1)
C(13)	2428(4)	9992(1)	7815(1)	29(1)
C(14)	-771(4)	9450(1)	7138(1)	29(1)
C(15)	-2803(4)	9291(1)	6634(1)	34(1)
C(16)	-3858(4)	8598(1)	6607(1)	38(1)
C(17)	-2948(4)	8074(1)	7078(1)	37(1)
C(18)	-961(4)	8231(1)	7582(1)	30(1)
C(19)	177(3)	8932(1)	7619(1)	25(1)
N(1)	4781(3)	8142(1)	9396(1)	26(1)
N(2)	3216(3)	8360(1)	8843(1)	25(1)
N(3)	5856(3)	9465(1)	8911(1)	22(1)
N(4)	12866(3)	10143(1)	10444(1)	31(1)
N(5)	634(3)	10087(1)	7271(1)	32(1)
C(20)	8632(6)	8407(1)	11949(1)	48(1)
O(2)	6379(4)	8685(1)	11542(1)	54(1)

Selected bond lengths [Å] and angles [°] for 188 (CCDC 161494).

O(1)-C(1)	1.259(2)	N(3)-C(3)-C(4)	119.81(13)
C(1)-N(1)	1.335(2)	N(3)-C(3)-C(1)	119.89(14)
C(1)-C(3)	1.474(2)	C(4)-C(3)-C(1)	120.29(13)
C(2)-N(2)	1.313(2)	C(5)-C(4)-C(3)	127.56(14)
C(2)-N(3)	1.373(2)	C(5)-C(4)-C(11)	106.19(14)
C(2)-C(12)	1.450(2)	C(3)-C(4)-C(11)	126.25(14)
C(3)-N(3)	1.309(2)	N(4)-C(5)-C(4)	109.93(14)
C(3)-C(4)	1.445(2)	N(4)-C(6)-C(7)	129.08(17)
C(4)-C(5)	1.379(2)	N(4)-C(6)-C(11)	107.66(14)
C(4)-C(11)	1.457(2)	C(7)-C(6)-C(11)	123.26(16)
C(5)-N(4)	1.355(2)	C(8)-C(7)-C(6)	116.94(18)
C(6)-N(4)	1.385(2)	C(7)-C(8)-C(9)	121.24(17)
C(6)-C(7)	1.390(2)	C(10)-C(9)-C(8)	121.55(18)
C(6)-C(11)	1.403(2)	C(9)-C(10)-C(11)	118.56(17)
C(7)-C(8)	1.376(3)	C(6)-C(11)-C(10)	118.44(15)
C(8)-C(9)	1.399(3)	C(6)-C(11)-C(4)	106.52(14)
C(9)-C(10)	1.379(2)	C(10)-C(11)-C(4)	135.04(16)
C(10)-C(11)	1.404(2)	C(13)-C(12)-C(19)	106.59(14)
C(12)-C(13)	1.374(2)	C(13)-C(12)-C(2)	124.22(15)
C(12)-C(19)	1.441(2)	C(19)-C(12)-C(2)	129.18(13)
C(13)-N(5)	1.362(2)	N(5)-C(13)-C(12)	109.97(15)
C(14)-N(5)	1.373(2)	N(5)-C(14)-C(15)	129.58(16)
C(14)-C(15)	1.396(2)	N(5)-C(14)-C(19)	107.96(14)
C(14)-C(19)	1.412(2)	C(15)-C(14)-C(19)	122.46(16)
C(15)-C(16)	1.374(3)	C(16)-C(15)-C(14)	117.76(16)
C(16)-C(17)	1.402(3)	C(15)-C(16)-C(17)	120.89(17)
C(17)-C(18)	1.382(2)	C(18)-C(17)-C(16)	121.47(17)
C(18)-C(19)	1.403(2)	C(17)-C(18)-C(19)	119.00(16)
N(1)-N(2)	1.364(2)	C(18)-C(19)-C(14)	118.41(15)
C(20)-O(2)	1.413(3)	C(18)-C(19)-C(12)	135.30(15)
		C(14)-C(19)-C(12)	106.29(14)
O(1)-C(1)-N(1)	120.81(14)	C(1)-N(1)-N(2)	127.30(13)
O(1)-C(1)-C(3)	125.10(14)	C(2)-N(2)-N(1)	114.03(13)
N(1)-C(1)-C(3)	114.08(13)	C(3)-N(3)-C(2)	118.98(12)
N(2)-C(2)-N(3)	125.72(13)	C(5)-N(4)-C(6)	109.69(15)
N(2)-C(2)-C(12)	117.63(14)	C(13)-N(5)-C(14)	109.19(14)
N(3)-C(2)-C(12)	116.64(13)		

Bond lengths [Å] and angles [°] for 188 (CCDC 161494).

O(1)-C(1)	1.259(2)	N(2)-C(2)-N(3)	125.72(13)
C(1)-N(1)	1.335(2)	N(2)-C(2)-C(12)	117.63(14)
C(1)-C(3)	1.474(2)	N(3)-C(2)-C(12)	116.64(13)
C(2)-N(2)	1.313(2)	N(3)-C(3)-C(4)	119.81(13)
C(2)-N(3)	1.373(2)	N(3)-C(3)-C(1)	119.89(14)
C(2)-C(12)	1.450(2)	C(4)-C(3)-C(1)	120.29(13)
C(3)-N(3)	1.309(2)	C(5)-C(4)-C(3)	127.56(14)
C(3)-C(4)	1.445(2)	C(5)-C(4)-C(11)	106.19(14)
C(4)-C(5)	1.379(2)	C(3)-C(4)-C(11)	126.25(14)
C(4)-C(11)	1.457(2)	N(4)-C(5)-C(4)	109.93(14)
C(5)-N(4)	1.355(2)	N(4)-C(5)-H(5)	120.6(10)
C(5)-H(5)	0.99(2)	C(4)-C(5)-H(5)	129.5(10)
C(6)-N(4)	1.385(2)	N(4)-C(6)-C(7)	129.08(17)
C(6)-C(7)	1.390(2)	N(4)-C(6)-C(11)	107.66(14)
C(6)-C(11)	1.403(2)	C(7)-C(6)-C(11)	123.26(16)
C(7)-C(8)	1.376(3)	C(8)-C(7)-C(6)	116.94(18)
C(7)-H(7)	0.96(2)	C(8)-C(7)-H(7)	122.3(11)
C(8)-C(9)	1.399(3)	C(6)-C(7)-H(7)	120.7(11)
C(8)-H(8)	0.96(2)	C(7)-C(8)-C(9)	121.24(17)
C(9)-C(10)	1.379(2)	C(7)-C(8)-H(8)	119.5(10)
C(9)-H(9)	0.98(2)	C(9)-C(8)-H(8)	119.2(10)
C(10)-C(11)	1.404(2)	C(10)-C(9)-C(8)	121.55(18)
C(10)-H(10)	0.99(2)	C(10)-C(9)-H(9)	118.4(13)
C(12)-C(13)	1.374(2)	C(8)-C(9)-H(9)	120.1(12)
C(12)-C(19)	1.441(2)	C(9)-C(10)-C(11)	118.56(17)
C(13)-N(5)	1.362(2)	C(9)-C(10)-H(10)	122.7(10)
C(13)-H(13)	1.03(2)	C(11)-C(10)-H(10)	118.7(10)
C(14)-N(5)	1.373(2)	C(6)-C(11)-C(10)	118.44(15)
C(14)-C(15)	1.396(2)	C(6)-C(11)-C(4)	106.52(14)
C(14)-C(19)	1.412(2)	C(10)-C(11)-C(4)	135.04(16)
C(15)-C(16)	1.374(3)	C(13)-C(12)-C(19)	106.59(14)
C(15)-H(15)	1.02(2)	C(13)-C(12)-C(2)	124.22(15)
C(16)-C(17)	1.402(3)	C(19)-C(12)-C(2)	129.18(13)
C(16)-H(16)	0.98(2)	N(5)-C(13)-C(12)	109.97(15)
C(17)-C(18)	1.382(2)	N(5)-C(13)-H(13)	120.9(9)
C(17)-H(17)	1.00(2)	C(12)-C(13)-H(13)	129.0(9)
C(18)-C(19)	1.403(2)	N(5)-C(14)-C(15)	129.58(16)
C(18)-H(18)	1.00(2)	N(5)-C(14)-C(19)	107.96(14)
N(1)-N(2)	1.364(2)	C(15)-C(14)-C(19)	122.46(16)
N(1)-H(1N)	0.93(2)	C(16)-C(15)-C(14)	117.76(16)
N(4)-H(4N)	0.87(2)	C(16)-C(15)-H(15)	122.6(11)
N(5)-H(5N)	0.90(2)	C(14)-C(15)-H(15)	119.5(11)
C(20)-O(2)	1.413(3)	C(15)-C(16)-C(17)	120.89(17)
C(20)-H(20A)	0.93(3)	C(15)-C(16)-H(16)	119.1(11)
C(20)-H(20B)	1.02(2)	C(17)-C(16)-H(16)	119.8(11)
C(20)-H(20C)	1.01(2)	C(18)-C(17)-C(16)	121.47(17)
O(2)-H(2O)	0.83(2)	C(18)-C(17)-H(17)	118.8(10)
		C(16)-C(17)-H(17)	119.7(10)
O(1)-C(1)-N(1)	120.81(14)	C(17)-C(18)-C(19)	119.00(16)
O(1)-C(1)-C(3)	125.10(14)	C(17)-C(18)-H(18)	121.2(11)
N(1)-C(1)-C(3)	114.08(13)	C(19)-C(18)-H(18)	119.8(11)

C(18)-C(19)-C(14)	118.41(15)
C(18)-C(19)-C(12)	135.30(15)
C(14)-C(19)-C(12)	106.29(14)
C(1)-N(1)-N(2)	127.30(13)
C(1)-N(1)-H(1N)	119.5(11)
N(2)-N(1)-H(1N)	113.2(11)
C(2)-N(2)-N(1)	114.03(13)
C(3)-N(3)-C(2)	118.98(12)
C(5)-N(4)-C(6)	109.69(15)
C(5)-N(4)-H(4N)	124.2(14)
C(6)-N(4)-H(4N)	125.9(14)
C(13)-N(5)-C(14)	109.19(14)
C(13)-N(5)-H(5N)	130.4(13)
C(14)-N(5)-H(5N)	120.2(13)
O(2)-C(20)-H(20A)	108.3(17)
O(2)-C(20)-H(20B)	105.9(15)
H(20A)-C(20)-H(20B)	108(2)
O(2)-C(20)-H(20C)	106.6(15)
H(20A)-C(20)-H(20C)	118(2)
H(20B)-C(20)-H(20C)	109.4(18)
C(20)-O(2)-H(2O)	103.1(17)

Anisotropic displacement parameters ($\text{\AA}^2 \times 10^4$) for 188 (CCDC 161494). The anisotropic displacement factor exponent takes the form: $-2\pi^2 [h^2 a^{*2} U^{11} + \dots + 2h k a^* b^* U^{12}]$.

	U^{11}	U^{22}	U^{33}	U^{23}	U^{13}	U^{12}
O(1)	380(7)	228(5)	264(6)	30(4)	-52(5)	27(5)
C(1)	272(9)	216(7)	226(8)	-6(6)	17(7)	32(6)
C(2)	225(8)	225(7)	215(7)	-11(6)	42(6)	26(6)
C(3)	212(8)	212(7)	224(7)	-14(6)	41(6)	27(6)
C(4)	215(8)	216(7)	243(7)	-22(6)	33(6)	27(6)
C(5)	247(8)	306(8)	248(8)	-7(6)	9(7)	12(7)
C(6)	258(8)	306(8)	295(8)	-57(6)	54(7)	-11(7)
C(7)	284(10)	343(9)	442(11)	-110(8)	65(8)	-83(8)
C(8)	381(10)	264(8)	557(12)	-69(8)	142(10)	-76(8)
C(9)	369(10)	274(8)	517(11)	48(8)	86(9)	8(8)
C(10)	293(9)	267(8)	386(10)	16(7)	16(8)	4(7)
C(11)	220(8)	232(7)	303(8)	-41(6)	55(7)	-1(6)
C(12)	215(8)	263(7)	229(7)	-2(6)	37(6)	20(6)
C(13)	303(9)	295(8)	270(8)	31(6)	16(7)	20(7)
C(14)	237(8)	377(9)	240(8)	15(7)	39(7)	40(7)
C(15)	246(9)	528(11)	248(8)	50(8)	9(7)	70(8)
C(16)	264(9)	598(12)	272(9)	-40(8)	-20(8)	-9(9)
C(17)	326(10)	451(10)	323(9)	-74(8)	15(8)	-50(9)
C(18)	292(9)	359(9)	262(8)	-19(7)	13(7)	14(7)
C(19)	200(8)	317(8)	223(8)	-5(6)	39(6)	34(6)
N(1)	322(8)	195(6)	255(6)	31(5)	-8(6)	-17(6)
N(2)	283(7)	242(6)	227(6)	15(5)	-17(6)	-12(5)
N(3)	221(7)	220(6)	224(6)	3(5)	23(5)	3(5)
N(4)	269(8)	368(8)	287(8)	-40(6)	-14(7)	-30(6)
N(5)	332(8)	337(7)	304(8)	97(6)	-21(6)	45(7)
C(20)	556(15)	440(11)	453(13)	-64(9)	-39(11)	-35(11)
O(2)	617(10)	608(9)	394(8)	-159(7)	12(8)	230(8)

Hydrogen coordinates ($\times 10^4$) and isotropic displacement parameters ($\text{\AA}^2 \times 10^{-3}$) for 188 (CCDC 161494).

	x	y	z	U_{iso}
H(5)	11440(40)	9105(9)	10561(8)	27(4)
H(7)	14790(50)	11546(10)	10287(9)	44(5)
H(8)	12950(40)	12339(9)	9447(8)	29(4)
H(9)	9280(50)	11960(11)	8692(10)	47(5)
H(10)	7450(40)	10762(9)	8746(8)	27(4)
H(13)	3570(40)	10417(9)	8014(8)	27(4)
H(15)	-3520(50)	9692(10)	6319(10)	45(6)
H(16)	-5350(40)	8481(10)	6275(9)	41(5)
H(17)	-3780(40)	7577(9)	7059(9)	33(5)
H(18)	-340(40)	7859(9)	7920(9)	32(5)
H(1N)	4290(40)	7686(10)	9549(8)	37(5)
H(4N)	14060(50)	10166(11)	10788(11)	52(6)
H(5N)	190(40)	10487(11)	7035(10)	48(6)
H(2O)	6840(50)	8561(12)	11147(13)	59(7)
H(20A)	10300(70)	8664(14)	11848(13)	83(9)
H(20B)	8070(60)	8513(13)	12446(12)	77(8)
H(20C)	8660(60)	7868(14)	11873(11)	72(7)

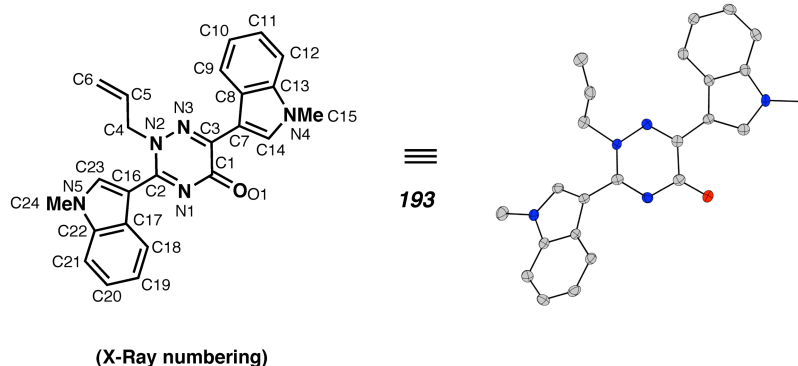
Hydrogen bonds for 188 (CCDC 161494) [\AA and $^\circ$].

D-H...A	d(D-H)	d(H...A)	d(D...A)	$\angle(\text{DHA})$
N(1)-H(1N)...O(1)#1	0.93(2)	1.88(2)	2.800(2)	173(2)
N(5)-H(5N)...O(2)#2	0.90(2)	1.95(2)	2.842(2)	171(2)
O(2)-H(2O)...O(1)	0.83(2)	1.93(3)	2.765(2)	178(2)

Symmetry transformations used to generate equivalent atoms:

#1 $x-1/2, -y+3/2, -z+2$ #2 $-x+1/2, -y+2, z-1/2$

A6.6.3 X-Ray Crystallographic Report for Allyl Triazinone 193



Crystal data and structure refinement for 193 (CCDC 259195).

Empirical formula	C ₂₄ H ₂₁ N ₃ O
Formula weight	395.46
Crystallization Solvent	hexanes/acetone
Crystal Habit	Fragment
Crystal size	0.21 x 0.11 x 0.11 mm ³
Crystal color	Colorless

Data Collection

Type of diffractometer	Bruker SMART 1000
Wavelength	0.71073 Å MoKα
Data Collection Temperature	100(2) K
θ range for 6305 reflections used in lattice determination	2.49 to 27.62°
Unit cell dimensions	a = 7.8852(8) Å b = 15.3322(15) Å c = 16.3273(16) Å
Volume	1973.9(3) Å ³
Z	4
Crystal system	Orthorhombic
Space group	P2 ₁ 2 ₁ 2 ₁
Density (calculated)	1.331 Mg/m ³
F(000)	832
Data collection program	Bruker SMART v5.630

θ range for data collection	1.82 to 28.45°
Completeness to $\theta = 28.45^\circ$	96.5 %
Index ranges	$-10 \leq h \leq 10$, $-20 \leq k \leq 20$, $-21 \leq l \leq 20$
Data collection scan type	ω scans at 6 ϕ settings
Data reduction program	Bruker SAINT v6.45A
Reflections collected	34532
Independent reflections	4712 [$R_{\text{int}} = 0.0963$]
Absorption coefficient	0.085 mm ⁻¹
Absorption correction	None
Max. and min. transmission	0.9907 and 0.9824

Structure solution program	Bruker XS v6.12
Primary solution method	Direct methods
Secondary solution method	Difference Fourier map
Hydrogen placement	Difference Fourier map
Structure refinement program	Bruker XL v6.12
Refinement method	Full matrix least-squares on F^2
Data / restraints / parameters	4712 / 0 / 355
Treatment of hydrogen atoms	Unrestrained
Goodness-of-fit on F^2	1.148
Final R indices [$I > 2\sigma(I)$, 3244 reflections]	$R1 = 0.0458$, $wR2 = 0.0560$
R indices (all data)	$R1 = 0.0824$, $wR2 = 0.0596$
Type of weighting scheme used	Sigma
Weighting scheme used	$w = 1/\sigma^2(F_o^2)$
Max shift/error	0.000
Average shift/error	0.000
Absolute structure parameter	2.8(14)
Largest diff. peak and hole	0.205 and -0.214 e. \AA^{-3}

Special Refinement Details

Refinement of F^2 against ALL reflections. The weighted R-factor (wR) and goodness of fit (S) are based on F^2 , conventional R-factors (R) are based on F , with F set to zero for negative F^2 . The threshold expression of $F^2 > 2\sigma(F^2)$ is used only for calculating R-factors(gt) etc. and is not relevant to the choice of reflections for refinement. R-factors based on F^2 are statistically about twice as large as those based on F , and R-factors based on ALL data will be even larger.

All esds (except the esd in the dihedral angle between two l.s. planes) are estimated using the full covariance matrix. The cell esds are taken into account individually in the estimation of esds in distances, angles and torsion angles; correlations between esds in cell parameters are only used when they are defined by crystal symmetry. An approximate (isotropic) treatment of cell esds is used for estimating esds involving l.s. planes.

Atomic coordinates ($\times 10^4$) and equivalent isotropic displacement parameters ($\text{\AA}^2 \times 10^3$) for 193 (CCDC 259195). $U(\text{eq})$ is defined as the trace of the orthogonalized U_{ij} tensor.

	x	y	z	U_{eq}
O(1)	13620(2)	2937(1)	622(1)	25(1)
N(1)	11116(2)	2895(1)	1314(1)	18(1)
N(2)	8961(2)	3837(1)	887(1)	18(1)
N(3)	9849(2)	4135(1)	230(1)	19(1)
N(4)	14226(2)	4330(1)	-1578(1)	19(1)
N(5)	6282(2)	2110(1)	2574(1)	19(1)
C(1)	12133(2)	3195(1)	694(1)	19(1)
C(2)	9552(2)	3205(1)	1384(1)	18(1)
C(3)	11387(2)	3830(1)	125(1)	18(1)
C(4)	7273(3)	4278(1)	968(1)	24(1)
C(5)	7379(3)	5204(1)	713(1)	25(1)
C(6)	6285(3)	5576(2)	212(1)	29(1)
C(7)	12267(2)	4154(1)	-586(1)	17(1)
C(8)	11604(2)	4759(1)	-1185(1)	16(1)
C(9)	10106(2)	5242(1)	-1268(1)	20(1)
C(10)	9911(3)	5772(1)	-1941(1)	21(1)
C(11)	11157(3)	5827(1)	-2547(1)	22(1)
C(12)	12653(3)	5360(1)	-2486(1)	20(1)
C(13)	12856(2)	4843(1)	-1796(1)	18(1)
C(14)	13867(3)	3927(1)	-855(1)	19(1)
C(15)	15833(3)	4284(2)	-2010(2)	26(1)
C(16)	8455(2)	2829(1)	2012(1)	16(1)
C(17)	8953(2)	2551(1)	2817(1)	17(1)
C(18)	10411(3)	2659(1)	3302(1)	20(1)
C(19)	10421(3)	2307(1)	4078(1)	23(1)
C(20)	9031(3)	1841(1)	4384(1)	27(1)
C(21)	7576(3)	1739(1)	3929(1)	24(1)
C(22)	7563(2)	2107(1)	3147(1)	19(1)
C(23)	6824(2)	2544(1)	1896(1)	18(1)
C(24)	4612(3)	1715(2)	2666(2)	27(1)

Bond lengths [Å] and angles [°] for 193 (CCDC 259195).

O(1)-C(1)	1.243(2)	C(23)-H(23)	0.996(15)
N(1)-C(2)	1.327(2)	C(24)-H(24A)	1.01(2)
N(1)-C(1)	1.371(2)	C(24)-H(24B)	1.05(2)
N(2)-C(2)	1.346(2)	C(24)-H(24C)	0.942(18)
N(2)-N(3)	1.361(2)		
N(2)-C(4)	1.499(2)	C(2)-N(1)-C(1)	119.13(16)
N(3)-C(3)	1.310(2)	C(2)-N(2)-N(3)	122.61(15)
N(4)-C(14)	1.363(2)	C(2)-N(2)-C(4)	125.35(16)
N(4)-C(13)	1.382(2)	N(3)-N(2)-C(4)	112.03(15)
N(4)-C(15)	1.452(2)	C(3)-N(3)-N(2)	117.33(16)
N(5)-C(23)	1.361(2)	C(14)-N(4)-C(13)	108.53(16)
N(5)-C(22)	1.378(2)	C(14)-N(4)-C(15)	125.45(18)
N(5)-C(24)	1.457(3)	C(13)-N(4)-C(15)	125.84(17)
C(1)-C(3)	1.468(2)	C(23)-N(5)-C(22)	108.93(16)
C(2)-C(16)	1.460(2)	C(23)-N(5)-C(24)	124.85(18)
C(3)-C(7)	1.441(2)	C(22)-N(5)-C(24)	126.23(18)
C(4)-C(5)	1.482(3)	O(1)-C(1)-N(1)	120.98(18)
C(4)-H(4A)	1.062(19)	O(1)-C(1)-C(3)	121.94(19)
C(4)-H(4B)	1.040(19)	N(1)-C(1)-C(3)	117.08(16)
C(5)-C(6)	1.319(3)	N(1)-C(2)-N(2)	121.85(17)
C(5)-H(5)	1.035(19)	N(1)-C(2)-C(16)	117.98(17)
C(6)-H(6A)	1.03(2)	N(2)-C(2)-C(16)	120.16(17)
C(6)-H(6B)	1.04(2)	N(3)-C(3)-C(7)	115.31(17)
C(7)-C(14)	1.380(3)	N(3)-C(3)-C(1)	121.65(18)
C(7)-C(8)	1.445(3)	C(7)-C(3)-C(1)	123.03(17)
C(8)-C(9)	1.401(3)	C(5)-C(4)-N(2)	110.94(17)
C(8)-C(13)	1.409(2)	C(5)-C(4)-H(4A)	112.2(10)
C(9)-C(10)	1.376(3)	N(2)-C(4)-H(4A)	111.4(10)
C(9)-H(9)	0.971(18)	C(5)-C(4)-H(4B)	110.6(10)
C(10)-C(11)	1.397(3)	N(2)-C(4)-H(4B)	103.3(10)
C(10)-H(10)	0.950(17)	H(4A)-C(4)-H(4B)	108.0(14)
C(11)-C(12)	1.383(3)	C(6)-C(5)-C(4)	123.5(2)
C(11)-H(11)	0.938(17)	C(6)-C(5)-H(5)	118.7(12)
C(12)-C(13)	1.388(3)	C(4)-C(5)-H(5)	117.5(12)
C(12)-H(12)	1.031(19)	C(5)-C(6)-H(6A)	123.8(11)
C(14)-H(14)	1.02(2)	C(5)-C(6)-H(6B)	124.7(12)
C(15)-H(15A)	1.00(2)	H(6A)-C(6)-H(6B)	111.3(16)
C(15)-H(15B)	0.977(19)	C(14)-C(7)-C(8)	106.12(17)
C(15)-H(15C)	1.01(2)	C(14)-C(7)-C(3)	127.52(18)
C(16)-C(23)	1.372(2)	C(8)-C(7)-C(3)	126.30(17)
C(16)-C(17)	1.437(2)	C(9)-C(8)-C(13)	118.32(19)
C(17)-C(22)	1.399(2)	C(9)-C(8)-C(7)	135.20(18)
C(17)-C(18)	1.406(2)	C(13)-C(8)-C(7)	106.48(16)
C(18)-C(19)	1.378(3)	C(10)-C(9)-C(8)	118.94(19)
C(18)-H(18)	0.979(17)	C(10)-C(9)-H(9)	120.8(12)
C(19)-C(20)	1.400(3)	C(8)-C(9)-H(9)	120.3(12)
C(19)-H(19)	0.994(16)	C(9)-C(10)-C(11)	121.5(2)
C(20)-C(21)	1.377(3)	C(9)-C(10)-H(10)	117.5(10)
C(20)-H(20)	0.900(19)	C(11)-C(10)-H(10)	120.9(10)
C(21)-C(22)	1.394(3)	C(12)-C(11)-C(10)	121.1(2)
C(21)-H(21)	1.016(19)	C(12)-C(11)-H(11)	120.9(12)

C(10)-C(11)-H(11)	117.8(12)
C(11)-C(12)-C(13)	116.94(19)
C(11)-C(12)-H(12)	123.7(11)
C(13)-C(12)-H(12)	119.4(11)
N(4)-C(13)-C(12)	128.58(18)
N(4)-C(13)-C(8)	108.33(17)
C(12)-C(13)-C(8)	123.09(18)
N(4)-C(14)-C(7)	110.52(18)
N(4)-C(14)-H(14)	122.0(11)
C(7)-C(14)-H(14)	127.4(11)
N(4)-C(15)-H(15A)	107.6(12)
N(4)-C(15)-H(15B)	109.0(11)
H(15A)-C(15)-H(15B)	110.0(16)
N(4)-C(15)-H(15C)	111.5(12)
H(15A)-C(15)-H(15C)	112.1(17)
H(15B)-C(15)-H(15C)	106.6(16)
C(23)-C(16)-C(17)	106.75(18)
C(23)-C(16)-C(2)	125.73(18)
C(17)-C(16)-C(2)	126.73(17)
C(22)-C(17)-C(18)	118.71(17)
C(22)-C(17)-C(16)	106.48(17)
C(18)-C(17)-C(16)	134.76(19)
C(19)-C(18)-C(17)	118.5(2)
C(19)-C(18)-H(18)	120.9(10)
C(17)-C(18)-H(18)	120.6(10)
C(18)-C(19)-C(20)	121.6(2)
C(18)-C(19)-H(19)	118.5(10)
C(20)-C(19)-H(19)	119.8(10)
C(21)-C(20)-C(19)	121.2(2)
C(21)-C(20)-H(20)	116.5(13)
C(19)-C(20)-H(20)	122.1(13)
C(20)-C(21)-C(22)	117.0(2)
C(20)-C(21)-H(21)	122.4(11)
C(22)-C(21)-H(21)	120.6(11)
N(5)-C(22)-C(21)	128.93(19)
N(5)-C(22)-C(17)	108.09(16)
C(21)-C(22)-C(17)	122.98(19)
N(5)-C(23)-C(16)	109.74(18)
N(5)-C(23)-H(23)	119.2(9)
C(16)-C(23)-H(23)	130.8(9)
N(5)-C(24)-H(24A)	106.0(12)
N(5)-C(24)-H(24B)	110.4(11)
H(24A)-C(24)-H(24B)	110.2(15)
N(5)-C(24)-H(24C)	110.4(11)
H(24A)-C(24)-H(24C)	112.0(16)
H(24B)-C(24)-H(24C)	107.9(16)

Anisotropic displacement parameters ($\text{\AA}^2 \times 10^4$) for 193 (CCDC 259195). The anisotropic displacement factor exponent takes the form: $-2\pi^2 [h^2 a^{*2} U^{11} + \dots + 2h k a^* b^* U^{12}]$.

	U^{11}	U^{22}	U^{33}	U^{23}	U^{13}	U^{12}
O(1)	166(8)	326(9)	248(8)	46(7)	23(7)	52(7)
N(1)	176(9)	198(10)	171(9)	14(8)	-9(8)	-10(8)
N(2)	150(9)	195(10)	200(9)	21(8)	33(8)	42(8)
N(3)	189(10)	232(10)	159(9)	10(8)	14(8)	13(8)
N(4)	142(9)	229(10)	210(10)	9(8)	47(8)	3(8)
N(5)	130(9)	209(10)	224(10)	30(8)	11(8)	-19(8)
C(1)	192(12)	199(12)	173(11)	-26(10)	-36(10)	-10(10)
C(2)	186(12)	167(12)	177(12)	-16(9)	-37(9)	-5(9)
C(3)	181(11)	179(11)	164(11)	-33(9)	-13(9)	-16(10)
C(4)	209(13)	258(13)	257(13)	9(11)	25(11)	43(11)
C(5)	243(13)	262(13)	235(12)	-25(11)	65(11)	35(11)
C(6)	275(14)	265(14)	315(13)	-17(12)	-21(12)	41(12)
C(7)	171(11)	147(11)	182(11)	-4(9)	-19(9)	9(9)
C(8)	152(11)	171(11)	164(11)	-9(9)	-1(9)	-35(9)
C(9)	176(12)	224(12)	190(12)	-4(10)	23(10)	5(10)
C(10)	164(12)	225(12)	243(12)	30(10)	1(10)	15(10)
C(11)	249(12)	206(12)	217(12)	62(11)	-19(11)	-17(11)
C(12)	204(12)	209(12)	197(12)	12(10)	35(11)	-41(10)
C(13)	180(11)	163(11)	191(11)	-9(10)	22(10)	-15(9)
C(14)	190(12)	193(12)	190(12)	-10(10)	-18(10)	-11(10)
C(15)	192(13)	296(15)	285(14)	29(12)	72(11)	5(12)
C(16)	165(11)	151(11)	173(11)	-1(9)	-12(9)	14(9)
C(17)	163(11)	165(11)	180(11)	1(9)	9(9)	28(9)
C(18)	178(12)	183(12)	235(12)	17(10)	18(10)	28(10)
C(19)	176(12)	288(13)	238(12)	3(10)	-67(10)	36(10)
C(20)	303(14)	328(14)	174(12)	67(11)	34(12)	68(11)
C(21)	238(13)	240(13)	239(13)	38(10)	42(11)	38(11)
C(22)	173(11)	196(11)	201(11)	4(10)	21(10)	47(10)
C(23)	216(12)	187(12)	146(11)	-14(10)	-6(10)	70(10)
C(24)	178(13)	255(15)	388(16)	44(13)	11(12)	-43(11)

Hydrogen coordinates ($\times 10^4$) and isotropic displacement parameters ($\text{\AA}^2 \times 10^3$) for 193 (CCDC 259195).

	x	y	z	U_{iso}
H(4A)	6310(20)	3933(12)	647(11)	35(6)
H(4B)	7010(20)	4231(12)	1591(12)	32(6)
H(5)	8290(20)	5589(13)	994(12)	49(7)
H(6A)	5310(20)	5246(13)	-77(12)	42(7)
H(6B)	6340(30)	6223(14)	20(12)	49(7)
H(9)	9210(20)	5190(12)	-862(11)	32(6)
H(10)	8910(20)	6114(11)	-1973(9)	12(5)
H(11)	10980(20)	6218(12)	-2980(10)	20(5)
H(12)	13600(20)	5380(13)	-2920(12)	41(6)
H(14)	14700(20)	3500(12)	-585(11)	39(6)
H(15A)	16560(30)	3843(14)	-1721(12)	49(7)
H(15B)	16380(20)	4857(13)	-1993(11)	28(6)
H(15C)	15670(30)	4135(14)	-2610(13)	44(7)
H(18)	11410(20)	2962(11)	3085(10)	16(5)
H(19)	11480(20)	2351(11)	4409(10)	23(5)
H(20)	9000(20)	1636(12)	4900(12)	32(7)
H(21)	6550(20)	1414(12)	4144(12)	31(6)
H(23)	6075(19)	2570(11)	1404(10)	12(5)
H(24A)	3910(30)	1938(13)	2193(12)	49(7)
H(24B)	4060(30)	1902(13)	3224(13)	49(7)
H(24C)	4700(20)	1102(12)	2664(10)	19(6)

A6.7 Notes and References

- (1) Portions of this work have been described in a communication, see: Garg, N. K.; Stoltz, B. M. *Tetrahedron Lett.* **2005**, 46, 1997-2000.
- (2) (a) Lipinska, T.; Branowska, D.; Rykowski, A. *Chem. Heterocycl. Compd.* **1999**, 35, 334-342. (b) Taylor, E. C.; Pont, J. L.; Warner, J. C. *Tetrahedron* **1987**, 43, 5159-5168. (c) Taylor, E. C.; French, L. G. *Tetrahedron Lett.* **1986**, 27, 1967-1970.
- (3) For the use of similar strategies in natural product synthesis, see: (a) Boger, D. L.; Baldino, C. M. *J. Am. Chem. Soc.* **1993**, 115, 11418-11425. (b) Wasserman, H. H.; DeSimon, R. W.; Boger, D. L.; Baldino, C. M. *J. Am. Chem. Soc.* **1993**, 115, 8457-8458. (c) Boger, D. L.; Coleman, R. S. *J. Am. Chem. Soc.* **1987**, 109, 2717-2727.
- (4) Shaw, K. N. F.; McMillan, A.; Gudmundson, A. G.; Armstrong, M. D. *J. Org. Chem.* **1958**, 23, 1171-1178.
- (5) Li, J.-H.; Snyder, J. K. *J. Org. Chem.* **1993**, 58, 516-519.
- (6) Faul, M. M.; Winneroski, L. L.; Krumrich, C. A. *J. Org. Chem.* **1999**, 64, 2465-2470.

- (7) Molecular structures are shown with 50% probability ellipsoids, and hydrogen atoms have been omitted for clarity. Crystallographic data have been deposited at the CCDC, 12 Union Road, Cambridge CB2 1EZ, UK, and copies can be obtained on request, free of charge, by quoting the publication citation and the deposition number; *p*-triazinone **187**: 259291; *m*-triazinone **188**: 161494; allyl triazinone **193**: 259195.
- (8) Faul, M. M.; Winneroski, L. L.; Krumrich, C. A. *J. Org. Chem.* **1998**, *63*, 6053-6058.
- (9) Attempted aromatization/protection of **187** or **191** resulted primarily in *N*-protection, rather than *O*-protection.
- (10) Sanemitsu, Y.; Nakayama, Y.; Tanabe, Y.; Matsumoto, H.; Hashimoto, S. *Agric. Biol. Chem.* **1990**, *54*, 3367-3369.
- (11) Pletnov, A. A.; Tian, Q.; Larock, R. C. *J. Org. Chem.* **2002**, *67*, 9276-9287.

APPENDIX SEVEN

Notebook Cross-Reference

The following notebook cross-reference has been included to facilitate access to the original spectroscopic data obtained for the compounds presented in this thesis. For each compound, both hardcopy and electronic characterization folders have been created that contain copies of the original ^1H NMR, ^{13}C NMR, and IR spectra. All notebooks and spectral data are stored in the Stoltz archives.

Table A7.1 Compounds Appearing in Chapter 2:

The Total Synthesis of Dragmacidin D

Compound	^1H NMR	^{13}C NMR	IR
52	NKGIV-73	NKGIV-73	NKGIV-73
53	NKGIV-45	NKGIV-45	NKGIV-45
22	NKGXI-73	NKGXI-73	NKGXIII-109
63	RSVI-205	RSVI-205	RSVI-205
91	NKGV-247	NKGV-247	NKGV-247
65	RSVI-279		
67	NKGVII-85	NKGVII-85	NKGVII-85
68	NKGVII-49	NKGVII-49	NKGVII-49
70	NKGVII-53	NKGVII-53	NKGVII-53
72	NKGVII-191	NKGVII-191	NKGVII-191
92	NKGVII-211	NKGVII-211	NKGVII-211
93	NKGVII-213	NKGVII-213	NKGVII-213
62	NKGVII-243		
73	NKGVII-193	NKGVII-193	NKGVII-193
74	NKGVII-217	NKGVII-217	NKGVII-217

Compound	¹ H NMR	¹³ C NMR	IR
75	RSVII-161	RSVII-161	RSVII-161
76	RSVII-201	RSVII-201	RSVII-201
77	RSVII-246	RSVII-246	RSVII-246
78	NKGVII-275	NKGVII-275	NKGVII-275
80	NKGVIII-241		
81	NKGVIII-273		
82	NKGX-243	NKGX-243	NKGX-243
83	NKGX-259	NKGX-259	NKGX-259
84	NKGX-241	NKGX-241	NKGX-241
5	NKGXXIII-221	NKGXI-37B	NKGX-253
86	RSX-107	RSX-107	RSX-157
88	RSX-167	RSX-167	RSX-167

Table A7.2 Compounds Appearing in Chapter 3:

The Total Synthesis of (+)- and (-)-Dragmacidin F

Compound	¹ H NMR	¹³ C NMR	IR
146	DDCIV-223	DDCIII-107	DDCIV-223
147	NKGXVI-105	NKGXVI-105	NKGXVI-105
103	DDCIII-121	DDCIII-121	DDCIII-121
105	DDCVIII-65	DDCVIII-65	DDCVIII-65
106	NKGXXIII-75	NKGXIX-133	NKGXXIII-75
104	NKGXIX-237	NKGXIX-131	NKGXIX-131
109	NKGXV-123	NKGXIX-103	NKGXIX-103
151	DDCIV-221	DDCIV-221	DDCIV-221
99	NKGXIX-107	NKGXIX-107	NKGXIX-107
153	DDCIV-217	DDCIV-217	DDCIV-217
100	DDCIV-61	DDCIV-61	NKGXVIII-63
98	NKGXIV-301P3 & NKGXXI-101	NKGXXI-101	NKGXIX-112

Compound	¹ H NMR	¹³ C NMR	IR
110	NKGXVI-295P1	NKGXVI-295P1	NKGXVI-295P1
154	NKGXIX-118	NKGXIX-118	NKGXIX-118
111	NKGXIX-119	NKGXIX-119	NKGXIX-119
155	NKGXIX-121	NKGXIX-121	NKGXIX-121
97	NKGXIX-123	NKGXIX-123	NKGXIX-123
112	NKGXIX-135	NKGXIX-135	NKGXIX-135
113	NKGXIX-143	NKGXIX-143	NKGXIX-143
117	NKGXXII-289	NKGXXII-289	NKGXXII-289
118	NKGXVIII-139	NKGXXIII-43	NKGXXIII-43
119	NKGXIX-139	NKGXIX-139	NKGXIX-139
123	NKGXIX-37		
120	NKGXIX-151	NKGXIX-151	NKGXIX-151
124	NKGXIX-163	NKGXIX-163	NKGXIX-155
(+)-7	NKGXIX-227B	NKGXIX-227	NKGXIX-227
128	DDCVIII-143	DDCVIII-143	DDCVIII-143
159	NKGXXII-53	NKGXXII-53	NKGXXII-53
131	DDCVII-201	DDCVII-195	DDCVII-195
132	DDCVII-207	DDCVII-227	DDCVII-207
130	DDCVII-217	DDCVII-213	DDCVII-213
126	DDCVIII-99	NKGXXII-81	NKGXXII-81
127	NKGXXII-116	NKGXXII-116	NKGXXII-116
133	NKGXXII-131	NKGXXII-131	NKGXXII-131
136	NKGXXIII-53	NKGXXIII-53	NKGXXIII-53
134	NKGXXIII-157	NKGXXIII-157	NKGXXIII-157
137	NKGXXIII-57	NKGXXIII-57	NKGXXIII-57
138	NKGXXIII-35	NKGXXII-209	NKGXXII-209
139	NKGXXIII-91	NKGXXIII-91	NKGXXIII-91
144	NKGXXII-213	NKGXXII-213	NKGXXII-213
(-)-7	NKGXXIII-179		

COMPREHENSIVE BIBLIOGRAPHY

Amat, M.; Hadida, S.; Sathyanarayana, S.; Bosch, J. *J. Org. Chem.* **1994**, *59*, 10-11.

Amatore, C.; Jutand, A. *J. Organomet. Chem.* **1999**, *576*, 254-278.

Aoki, S.; Ye, Y.; Higuchi, K.; Takashima, A.; Tanaka, Y.; Kitagawa, I.; Kobayashi, M. *Chem. Pharm. Bull.* **2001**, *49*, 1372-1374.

Arndt, F. *Org. Synth.*, **1943**, Coll. Vol. 2, 165.

Audebert, P.; Bidan, G. *Synthetic Metals* **1986**, *15*, 9-22.

Auwers, K. *Justus Liebigs Ann. Chem.* **1907**, *357*, 85-94.

Ayer, W. A.; Craw, P. A.; Ma, Y. T.; Miao, S. *Tetrahedron* **1992**, *48*, 2919-2924.

Ayerbe, M.; Arrieta, A.; Cossio, F. *J. Org. Chem.* **1998**, *63*, 1795-1805.

Aygün, A.; Pindur, U. *Curr. Med. Chem.* **2003**, *10*, 1113-1127.

Bailey, D. M.; Johnson, R. E. *J. Med. Chem.* **1973**, *16*, 1300-1302.

Baran, P. S.; Corey, E. J. *J. Am. Chem. Soc.* **2002**, *124*, 7904-7905.

Barco, A.; Benetti, S.; De Risi, C.; Marchetti, P.; Pollini, G. P.; Zanirato, V. *Tetrahedron: Asymmetry* **1997**, *8*, 3515-3545.

Barlin, G. B. *Aust. J. Chem.* **1983**, *36*, 983-992.

Barros, M. T.; Maycock, C. D.; Ventura, M. R. *J. Chem. Soc., Perkin Trans. 1* **2001**, 166-173.

Bartik, K.; Braekman, J.-C.; Daloze, D.; Stoller, C.; Huysecom, J.; Vendevyver, G.; Ottinger, R. *Can. J. Chem.* **1987**, *65*, 2118-2121.

Bartoli, G.; Palmieri, G.; Bosco, M.; Dalpozzo, R. *Tetrahedron Lett.* **1989**, *30*, 2129-2132.

Batcho, A. D.; Leimgruber, W. *Org. Synth.* **1985**, *63*, 214-225.

Beletskaya, I. P.; Cheprakov, A. V. *Chem. Rev.* **2000**, *100*, 3009-3066.

Belletete, M.; Beaupre, S.; Bouchard, J.; Blondin, P.; Leclerc, M.; Durocher, G. *J. Phys. Chem. B* **2000**, *104*, 9118-9125.

Bergens, S. H.; Bosnich, B. *J. Am. Chem. Soc.* **1991**, *113*, 958-967.

Bernheim, F.; Morgan, J. E. *Nature* **1939**, *144*, 290.

Blunt, J. W.; Copp, B. R.; Munro, M. H. G.; Northcote, P. T.; Prinsep, M. R. *Nat. Prod. Rep.* **2004**, *21*, 1-49.

Boehm, J. C.; Gleason, J. G.; Pendrak, I.; Sarau, H. M.; Schmidt, D. B.; Foley, J. J.; Kingsbury, W. D. *J. Med. Chem.* **1993**, *36*, 3333-3340.

Boger, D. L.; Coleman, R. S. *J. Am. Chem. Soc.* **1987**, *109*, 2717-2727.

Boger, D. L.; Baldino, C. M. *J. Am. Chem. Soc.* **1993**, *115*, 11418-11425.

Bosco, M.; Dalpozzo, R.; Bartoli, G.; Palmieri, G.; Petrini, M. *J. Chem. Soc., Perkin Trans. 2* **1991**, *5*, 657-663.

Brown, J. M. *Angew. Chem., Int. Ed. Engl.* **1987**, *26*, 190-203.

Brown, J. M. In *Comprehensive Asymmetric Catalysis*; Jacobsen, E. N.; Pfaltz, A.; Yamamoto, H., Eds.; Springer: Berlin, 1999; Vol. 1, pp 121-195.

Burke, T. R.; Zhang, Z.-Y. *Biopolymers* **1998**, *47*, 225-241.

Butler, A.; Carter-Franklin, J. N. *Nat. Prod. Rep.* **2004**, *21*, 180-188.

Capon, R. J.; Rooney, F.; Murray, L. M.; Collins, E.; Sim, A. T. R.; Rostas, J. A. P.; Butler, M. S.; Carroll, A. R. *J. Nat. Prod.* **1998**, *61*, 660-662.

Casapullo, A.; Bifulco, G.; Bruno, I.; Riccio, R. *J. Nat. Prod.* **2000**, *63*, 447-451.

Chen, M. S.; White, M. C. *J. Am. Chem. Soc.* **2004**, *126*, 1346-1347.

Chenier, P. J. *J. Chem. Ed.* **1978**, *55*, 286-291.

Chierici, L.; Gardini, G. P. *Tetrahedron* **1966**, *22*, 53-56.

Chung, J. Y. L.; Ho, G.-J.; Chartrain, M.; Roberge, C.; Zhao, D.; Leazer, J.; Farr, R.; Robbins, M.; Emerson, K.; Mathre, D. J.; McNamara, J. M.; Hughes, D. L.; Grabowski, E. J. J.; Reider, P. J. *Tetrahedron Lett.* **1999**, *40*, 6739-6743.

Ciamician, G.; Silber, P. *Chem. Ber.* **1912**, *45*, 1842-1845.

Claridge, T. D. W. In *High-Resolution NMR Techniques in Organic Chemistry*; Pergamon: Amsterdam, 1999; pp 320-326.

Craig, B. N.; Janssen, M. U.; Wickersham, B. M.; Rabb, D. M.; Chang, P. S.; O'Leary, D. J. *J. Org. Chem.* **1996**, *61*, 9610-9613.

Cutignano, A.; Bifulco, G.; Bruno, I.; Casapullo, A.; Gomez-Paloma, L.; Riccio, R. *Tetrahedron* **2000**, *56*, 3743-3748.

Dess, D. B.; Martin, J. C. *J. Org. Chem.* **1983**, *48*, 4155-4156.

Diederich, F.; Stang, P. J.; Eds.; *Metal-Catalyzed Cross-Coupling Reactions*; Wiley-VCH: Weinheim, 1998.

Dounay, A. B.; Overman, L. E. *Chem. Rev.* **2003**, *103*, 2945-2963.

Edwards, M. P.; Ley, S. V.; Lister, S. G.; Palmer, B. D. *J. Chem. Soc., Chem. Commun.* **1983**, 630-633.

Edwards, M. P.; Ley, S. V.; Lister, S. G.; Palmer, B. D.; Williams, D. J. *J. Org. Chem.* **1984**, *49*, 3503-3516.

Edwards, M. P.; Doherty, A. M.; Ley, S. V.; Organ, H. M. *Tetrahedron* **1986**, *42*, 3723-3729.

Elfehail, F.; Dampawan, P.; Zajac, W. *Synth. Commun.* **1980**, *10*, 929-932.

Elfehail, F. E.; Zajac, W. W., Jr. *J. Org. Chem.* **1981**, *46*, 5151-5155.

Eliel, E. L.; Wilen, S. H.; Mander, L. N. *Stereochemistry of Organic Compounds*; Wiley-Interscience: New York, 1994.

Ellingson, H. *J. Am. Chem. Soc.* **1949**, *71*, 2798-2800.

Fahy, E.; Potts, B. C. M.; Faulkner, D. J.; Smith, K. *J. Nat. Prod.* **1991**, *54*, 564-569.

Faul, M. M.; Winneroski, L. L.; Krumrich, C. A. *J. Org. Chem.* **1998**, *63*, 6053-6058.

Faul, M. M.; Winneroski, L. L.; Krumrich, C. A. *J. Org. Chem.* **1999**, *64*, 2465-2470.

Faulkner, D. J. *Nat. Prod. Rep.* **2002**, *19*, 1-48.

Favorskii, A. E. *J. Russ. Phys. Chem. Soc.* **1894**, *26*, 559.

Ferreira, E. M.; Stoltz, B. M. *J. Am. Chem. Soc.* **2003**, *125*, 9578-9579.

Fischer, R. H.; Weitz, H. M. *Synthesis* **1980**, 261-282.

Garg, N. K.; Sarpong, R.; Stoltz, B. M. *J. Am. Chem. Soc.* **2002**, *124*, 13179-13184.

Garg, N. K.; Caspi, D. D.; Stoltz, B. M. *J. Am. Chem. Soc.* **2004**, *126*, 9552-9553.

Garg, N. K.; Stoltz, B. M. *Tetrahedron Lett.* **2005**, *46*, 1997-2000.

Garg, N. K.; Stoltz, B. M. *Tetrahedron Lett.* **2005**, *46*, 2423-2426.

Garg, N. K.; Caspi, D. D.; Stoltz, B. M. *J. Am. Chem. Soc.* **2005**, *127*, *in press*.

Geissler, H. In *Transition Metals for Organic Synthesis*; Beller, M.; Bolm, C., Eds.; Wiley-VCH: Weinheim, 1998; Chapter 2.10, p 158.

Gilbert, E. J.; Chisholm, J. D.; Van Vranken, D. L. *J. Org. Chem.* **1999**, *64*, 5670-5676.

Gilow, H. M.; Hong, Y. H.; Millirons, P. L.; Snyder, R. C.; Casteel, W. J., Jr. *J. Heterocycl. Chem.* **1986**, *23*, 1475-1480.

Greene, T. W.; Wuts, P. G. M. *Protective Groups in Organic Synthesis*, 3rd Ed.; John Wiley-Interscience: New York, 1999.

Gunasekera, S. P.; McCarthy, P. J.; Kelly-Borges, M. *J. Nat. Prod.* **1994**, *57*, 1437-1441.

Gushin, V. V.; Alper, H. *Chem. Rev.* **1994**, *94*, 1047-1062.

Han, X.; Stoltz, B. M.; Corey, E. J. *J. Am. Chem. Soc.* **1999**, *121*, 7600-7605.

Hanessian, S. In *Total Synthesis of Natural Products: The "Chiron" Approach*, Baldwin, E. J., Ed.; Pergamon Press: Oxford, 1983; pp 206-208.

Hanessian, S.; Pan, J.; Carnell, A.; Bouchard, H.; Lesage, L. *J. Org. Chem.* **1997**, *62*, 465-473.

Hashem, M. A.; Sultana, I.; Hai, M. A. *Indian J. Chem. Sect. B* **1999**, *38*, 789-794.

Hibino, S.; Choshi, T. *Nat. Prod. Rep.* **2002**, *19*, 148-180.

Hills, I. D.; Fu, G. C. *J. Am. Chem. Soc.* **2004**, *126*, 13178-13179.

House, H. O.; Berkowitz, W. F. *J. Org. Chem.* **1963**, *28*, 307-311.

House, H. O.; Berkowitz, W. F. *J. Org. Chem.* **1963**, *28*, 2271-2276.

Howes, P. D.; Cleasby, A.; Evans, D. N.; Feilden, H.; Smith, P. W.; Sollis, S. L.; Taylor, N.; Wonacott, A. J. *Eur. J. Med. Chem.* **1999**, *34*, 225-234.

Huang, P.-Q. *Youji Huaxue* **1999**, *19*, 364-373.

Jacobs, R. S.; Pomponi, S.; Gunasekera, S.; Wright, A. PCT Int. Appl. WO 9818466, May 7, 1998.

Jiang, B.; Smallheer, J. M.; Amaral-Ly, C.; Wuonola, M. A. *J. Org. Chem.* **1994**, *59*, 6823-6827.

Jiang, B.; Gu, X.-H. *Bioorg. Med. Chem.* **2000**, *8*, 363-371.

Jiang, B.; Gu, X.-H. *Heterocycles* **2000**, *53*, 1559-1568.

Jin, Z. *Nat. Prod. Rep.* **2003**, *20*, 584-605.

Kam, T.-S.; Pang, H.-S.; Lim, T.-M. *Org. Biomol. Chem.* **2003**, *1*, 1292-1297.

Kawasaki, T.; Enoki, H.; Matsumura, K.; Ohyama, M.; Inagawa, M.; Sakamoto, M. *Org. Lett.* **2000**, *2*, 3027-3029.

Kawasaki, T.; Ohno, K.; Enoki, H.; Umemoto, Y.; Sakamoto, M. *Tetrahedron Lett.* **2002**, *43*, 4245-4248.

Kerwin, J. F., Jr.; Lancaster, J. R., Jr.; Feldman, P. L. *J. Med. Chem.* **1995**, *38*, 4343-4362.

Kharasch, M. S.; Kane, S. S.; Brown, H. C. *J. Am. Chem. Soc.* **1940**, 62, 2242-2243.

Kohmoto, S.; Kashman, Y.; McConnell, O. J.; Rinehart, K. L., Jr.; Wright, A.; Koehn, F. *J. Org. Chem.* **1988**, 53, 3116-3118.

Kong, Y. C.; Cheng, K. F.; Cambie, R. C.; Waterman, P. G. *J. Chem. Soc., Chem. Commun.* **1985**, 47-48.

Kornfeld, E. C.; Fornefeld, E. J.; Kline, G. B.; Mann, M. J.; Morrison, D. E.; Jones, R. G.; Woodward, R. B. *J. Am. Chem. Soc.* **1956**, 78, 3087-3114.

Kreiser, W.; Körner, F. *Helv. Chim. Acta* **1999**, 82, 1610-1629.

Kuivila, H. G. *J. Org. Chem.* **1960**, 25, 284-285.

Kutney, J. P. *Nat. Prod. Rep.* **1990**, 7, 85-103.

Lancini, G. C.; Lazzari, E.; Sartori, G. *J. Antibiot.* **1968**, 21, 387-392.

Larock, R. C.; Hightower, T. R. *J. Org. Chem.* **1993**, 58, 5298-5300.

Leete, E.; Bjorklund, J. A.; Reineccius, G. A.; Chen, T.-B. *Spec. Publ.-R. Soc. Chem.* **1992**, 95, 75-95.

Li, J. J.; Gribble, G. W. In *Palladium in Heterocyclic Chemistry: A Guide for the Synthetic Chemist*; Pergamon: Amsterdam, 2000; pp 355-373.

Li, J.-H.; Snyder, J. K. *J. Org. Chem.* **1993**, 58, 516-519.

Li, K.; Du, W.; Que, N. L.; Liu, H. *J. Am. Chem. Soc.* **1996**, 118, 8763-8764.

Lipinska, T.; Branowska, D.; Rykowski, A. *Chem. Heterocycl. Compd.* **1999**, 35, 334-342.

Littke, A. F.; Fu, G. C. *J. Am. Chem. Soc.* **2001**, 123, 6989-7000.

Littke, A. F.; Schwarz, L.; Fu, G. C. *J. Am. Chem. Soc.* **2002**, 124, 6343-6348.

Little, T. L.; Webber, S. E. *J. Org. Chem.* **1994**, 59, 7299-7305.

Longley, R. E.; Isbrucker, R. A.; Wright, A. E. U.S. Patent 6,087,363, July 11, 2000.

Lott, R. S.; Chauhan, V. S.; Virander, S.; Stammer, C. H. *J. Chem. Soc., Chem. Commun.* **1979**, 495-496.

Luzzio, F. A. *Tetrahedron* **2001**, 57, 915-945.

MacDonald, J. C. *J. Biol. Chem.* **1961**, 236, 512-514.

Maehr, H.; Smallheer, J. *J. Am. Chem. Soc.* **1985**, 107, 2943-2945.

Magnuson, S. R. *Tetrahedron* **1995**, 51, 2167-2213.

Maki, S.; Okawa, M.; Matsui, R.; Hirano, T.; Niwa, H. *Synlett* **2001**, 10, 1590-1592.

Manthey, M. K.; González-Bello, C.; Abell, C. *J. Chem. Soc., Perkin Trans. 1* **1997**, 625-628.

Marletta, M. A. *J. Med. Chem.* **1994**, 37, 1899-1907.

McCluskey, A.; Sim, A. T. R.; Sakoff, J. A. *J. Med. Chem.* **2002**, 45, 1151-1175.

McIntire, W. S.; Wemmer, D. E.; Chistoserdov, A.; Lidstrom, M. E. *Science* **1991**, 252, 817-824.

Meier, R.-M.; Tamm, C. *Helv. Chim. Acta*, **1991**, 74, 807-818.

Miyake, F. Y.; Yakushijin, K.; Horne, D. A. *Org. Lett.* **2000**, 2, 3185-3187.

Miyake, F. Y.; Yakushijin, K.; Horne, D. A. *Org. Lett.* **2002**, 4, 941-943.

Miyake, H.; Yamamura, K. *Chem. Lett.* **1989**, 6, 981-984.

Miyaura, N.; Suzuki, A. *Chem. Rev.* **1995**, 95, 2457-2483.

Mocada, S.; Palmer, R. M. J.; Higgs, E. A. *Pharmacol. Rev.* **1991**, 43, 109-142.

Molina, J. A.; Jimenez-Jimenez, F. J.; Orti-Pareja, M.; Navarro, J. A. *Drugs Aging* **1998**, 12, 251-259.

Morris, S. A.; Andersen, R. J. *Tetrahedron* **1990**, 46, 715-720.

Muchowski, J. M.; Solas, D. R. *J. Org. Chem.* **1984**, 49, 203-205.

Murray, L. M.; Lim, T. K.; Hooper, J. N. A.; Capon, R. J. *Aust. J. Chem.* **1995**, 48, 2053-2058.

Neber, P. W.; Friedolsheim, A. *Justus Liebigs Ann. Chem.* **1926**, 449, 109-134.

Nicolaou, K. C.; Webber, S. E. *Synthesis* **1986**, 6, 453-461.

Noble, R. L.; Beer, C. T.; Cutts, J. H. *Ann. N.Y. Acad. Sci.* **1958**, 76, 882-894.

Noyori, R. In *Asymmetric Catalysis in Organic Synthesis*; Wiley: New York, 1994; pp 16-94.

O'Brien, C. *Chem. Rev.* **1964**, *64*, 81-89.

Omura, S.; Iwai, Y.; Hirano, A.; Nakagawa, A.; Awaya, J.; Tsuchiya, H.; Takahashi, Y.; Masuma, R. *J. Antibiot.* **1977**, *30*, 275-289.

Ooi, T.; Takahashi, M.; Doda, K.; Maruoka, K. *J. Am. Chem. Soc.* **2002**, *124*, 7640-7641.

Philippe, M.; Sepulchre, A. M.; Gero, S. D.; Loibner, H.; Streicher, W.; Stutz, P. *J. Antibiot.* **1982**, *35*, 1507-1512.

Piers, E.; Britton, R.; Andersen, R. J. *J. Org. Chem.* **2000**, *65*, 530-535.

Pindur, U.; Lemster, T. *Curr. Med. Chem.* **2001**, *8*, 1681-1698.

Pletnov, A. A.; Tian, Q.; Larock, R. C. *J. Org. Chem.* **2002**, *67*, 9276-9287.

Plieninger, H.; Suhr, K. *Chem. Ber.* **1956**, *89*, 270-278.

Poss, C. S.; Schreiber, S. L. *Acc. Chem. Res.* **1994**, *27*, 9-17.

Rapado, L. P.; Bulugahapitiya, V.; Renaud, P. *Helv. Chim. Acta* **2000**, 83, 1625-1632.

Rathore, R.; Kochi, J. K. *J. Org. Chem.* **1996**, 61, 627-639.

Rönn, M.; Bäckvall, J.-E.; Andersson, P. G. *Tetrahedron Lett.* **1995**, 36, 7749-7752.

Sakowski, J.; Bohn, M.; Sattler, I.; Dahse, H.; Schlitzer, M. *J. Med. Chem.* **2001**, 44, 2886-2899.

Sanemitsu, Y.; Nakayama, Y.; Tanabe, Y.; Matsumoto, H.; Hashimoto, S. *Agric. Biol. Chem.* **1990**, 54, 3367-3369.

Sasaki, S.; Ehara, T.; Sakata, I.; Fujino, Y.; Harada, N.; Kimura, J.; Nakamura, H.; Maeda, M. *Bioorg. Med. Chem. Lett.* **2001**, 11, 583-585.

Schmidt, H. H. W.; Walter, U. *Cell* **1994**, 78, 919-925.

Schreiber, S. L. *Chem. Scr.* **1987**, 27, 563-566.

Schumacher, R. W.; Davidson, B. S. *Tetrahedron* **1999**, 55, 935-942.

Shaw, K. N. F.; McMillan, A.; Gudmundson, A. G.; Armstrong, M. D. *J. Org. Chem.* **1958**, 23, 1171-1178.

Sheppeck, J. E.; Gauss, C.-M.; Chamberlin, A. R. *Bioorg. Med. Chem.* **1997**, *5*, 1739-1750.

Shin, J.; Seo, Y.; Cho, K. W.; Rho, J.-R.; Sim, C. J. *J. Nat. Prod.* **2000**, *62*, 647-649.

Stahl, S. S. *Angew. Chem., Int. Ed.* **2004**, *43*, 3400-3420.

Stoltz, B. M. *Chem. Lett.* **2004**, *33*, 362-367.

Sundberg, R. J., Ed.; *Indoles*; Academic Press: San Diego, 1996.

Suzuki, A. J. *Organomet. Chem.* **1999**, *576*, 147-168.

Takaya, H.; Ohta, T.; Noyori, R. In *Catalytic Asymmetric Synthesis*; Ojima, I., Ed.; VCH Publishers: New York, 1994; pp 1-39.

Taylor, E. C.; French, L. G. *Tetrahedron Lett.* **1986**, *27*, 1967-1970.

Taylor, E. C.; Pont, J. L.; Warner, J. C. *Tetrahedron* **1987**, *43*, 5159-5168.

Thorns, V.; Hansen, L. M. *Exp. Neurol.* **1998**, *150*, 14-20.

Trend, R. M.; Ramtohul, Y. K.; Ferreira, E. M.; Stoltz, B. M. *Angew. Chem., Int. Ed.* **2003**, *42*, 2892-2895.

Tsuiji, J. In *Transition Metal Reagents and Catalysts*; Wiley: Chichester, U.K., 2000; Chapter 3, p 27.

Tsuiji, J.; Mandai, T. *Synthesis* **1996**, 1-24.

Tsujii, S.; Rinehart, K. L.; Gunasekera, S. P.; Kashman, Y.; Cross, S. S.; Lui, M. S.; Pomponi, S. A.; Diaz, M. C. *J. Org. Chem.* **1988**, *53*, 5446-5453.

Turck, A.; Ple, N.; Dognon, D.; Harmoy, C.; Queguiner, G. *J. Heterocycl. Chem.* **1994**, *31*, 1449-1454.

Ulhaq, S.; Naylor, M. A.; Chinje, E. C.; Threadgill, M. D.; Stratford, I. J. *Anti-Cancer Drug Des.* **1997**, *12*, 61-65.

Ulibarri, G.; Audrain, H.; Nadler, W.; Lhermitte, H.; Grierson, D. S. *Pure Appl. Chem.* **1996**, *68*, 601-604.

Ulibarri, G.; Nadler, W.; Skrydstrup, T.; Audrain, H.; Chiaroni, A.; Riche, C.; Grierson, D. S. *J. Org. Chem.* **1995**, *60*, 2753-2761.

Van Benthem, R. A. T. M.; Hiemstra, H.; Michels, J. J.; Speckamp, W. N. *J. Chem. Soc., Chem. Commun.* **1994**, 357-359.

Vereshchagin, A. L.; Branskii, O. V.; Semenov, A. A. *Chem. Heterocycl. Compd. (Engl. Transl.)* **1983**, *19*, 40-42.

Wasserman, H. H.; DeSimon, R. W.; Boger, D. L.; Baldino, C. M. *J. Am. Chem. Soc.* **1993**, *115*, 8457-8458.

Wenkert, E.; Moeller, P. D.; Piettre, S. R.; McPhail, A. T. *J. Org. Chem.* **1988**, *53*, 3170-3178.

Whitlock, C. R.; Cava, M. P. *Tetrahedron Lett.* **1994**, *35*, 371-374.

Williams, R. M.; Cao, J.; Tsujishima, H.; Cox, R. J. *J. Am. Chem. Soc.* **2003**, *125*, 12172-12178.

Woodward, R. B.; Bader, F. E.; Bickel, H.; Frey, A. J.; Kierstead, R. W. *Tetrahedron* **1958**, *2*, 1-57.

Wright, A. E.; Pomponi, S. A.; Cross, S. S.; McCarthy, P. *J. Org. Chem.* **1992**, *57*, 4772-4775.

Wright, A. E.; Pomponi, S. A.; Jacobs, R. S. PCT Int. Appl. WO 9942092, August 26, 1999.

Xiao, W. *Huaxue Shiji* **1992**, 14(6), 363-366.

Yang, C.-G.; Huang, H.; Jiang, B. *Curr. Org. Chem.* **2004**, 8, 1691-1720.

Yang, C.-G.; Liu, G.; Jiang, B. *J. Org. Chem.* **2002**, 67, 9392-9396.

Yang, C.-G.; Wang, J.; Jiang, B. *Tetrahedron Lett.* **2002**, 43, 1063-1066.

Yang, C.-G.; Wang, J.; Tang, X.-X.; Jiang, B. *Tetrahedron: Asymmetry* **2002**, 13, 383-394.

Yaylayan, V. A. *J. Agric. Food. Chem.* **1996**, 44, 2511-2516.

Zhang, H.; Ferreira, E. M.; Stoltz, B. M. *Angew. Chem., Int. Ed.* **2004**, 43, 6144-6148.

Zheng, Q.; Yang, Y.; Martin, A. R. *Heterocycles* **1994**, 37, 1761-1772.

Zhu, Z.; Moore, J. S. *J. Org. Chem.* **2000**, 65, 116-123.

INDEX

Alkaloid	1, 2, 13, 17, 36, 310, 311, 313, 321
Alzheimer's disease	5
Amidrazone	322, 323, 324, 327
Amino Acid	7
Aminoimidazole	6, 9, 11, 20, 29, 30, 31, 32, 34, 74, 132, 140
Antifungal.....	3
Anti-inflammatory.....	7
Antipode	145, 159
Antiviral.....	3, 7, 131
Arginine	5, 6
Arndt-Eistert.....	29, 31
Aromatic	9, 20, 24, 27, 322, 326, 365
Asymmetric hydrogenation.....	35, 76
Bartoli indole synthesis.....	27, 72
Bicycle	131, 132, 133, 137, 138, 139, 142, 148, 151, 152, 153, 155
Biosynthesis.....	7, 8, 17
Biosynthetic.....	8, 19, 145

Bis(indole)	1, 2, 3, 6, 10, 12, 18, 20, 21, 23, 24, 28, 34, 36, 131, 310, 311, 312 314, 315, 321, 322, 323, 326, 327
Boronic acid	12, 27, 132, 311, 312
Boronic ester.....	24, 28, 132, 139, 156, 314
Bromination.....	27, 139, 156
Bromoindole.....	23, 26, 27, 71, 132, 312, 314
Brown's Rh Catalyst	154
Cancer.....	1, 6
Conformation	149, 150, 151, 221, 222
Cross-coupling	12, 20, 23, 24, 69, 70, 132, 156, 159, 214, 215, 311, 312, 313, 315, 326, 327
Cyclization.....	9, 18, 132, 133, 136, 137, 138, 148, 149, 151, 152, 153, 159, 213, 324
Cyclocondensation	11, 20, 21, 22, 23, 69, 320, 322, 323, 326, 327
Cytotoxicity	3, 5, 6
Decomposition	5, 31, 34, 138
Diels-Alder reaction	322, 326
Diazo.....	26, 29
Dihydrohamacanthin.....	16, 310, 313, 314, 315
Dragmacidin	1, 2, 8, 13
Dragmacidin A	2, 8, 13

Dragmacidin B	2, 8, 13, and Appendix 5
Dragmacidin C	2, 8, 13, and Appendix 5
Dragmacidin D	2, 3, 5, 6, 7, 8, 10, 11, 12, 131, 131, 132, 139, 140, 141, 145, 147, 311, and Chapter 2
Dragmacidin E.....	2, 3, 6, 8, 9, 10, 13, 19, 145, 147, and Appendix 6
Dragmacidin F.....	2, 3, 6, 7, 8, 9, 13, 19, and Chapter 3
Enantiodivergent	147, 159, 220
Favorskii rearrangment	142
Friedel-Crafts.....	9
Fluorescence.....	34
Guanidine	11, 29, 30, 321
Halogen.....	17, 24, 26, 27, 36, 131, 132, 133, 139, 156, 159, 310, 311, 312, 313, 314, 315, 326, 327
Hamacanthin.....	2, 16
Heck reaction.....	132, 133, 136, 137, 138, 213, 216, 217
Heterocycle.....	132, 143
HIV	7
HSV	7
Huntington's disease	5
Isomerization	135, 149, 150, 151, 154, 155, 159, 215, 221
Kinase	1, 4
Leimgruber-Batcho indole synthesis	11, 18, 71, 72

	391
Marine sponge	3, 8
Neber rearrangement	142, 143, 144, 159, 218, 219
Neurodegenerative disorders	5
Nitration	141
Nitric oxide	5, 6
Oxidation	8, 9, 11, 24, 29, 32, 132, 133, 136, 138, 140, 148, 154, 159, 216, 217
Palladium	13, 22, 24, 25, 28, 29, 35, 132, 133, 134, 135, 136, 137, 138, 139, 140, 148, 149, 150, 151, 152, 153, 155, 157, 159, 213, 214, 215, 216, 221, 312, 314
Parkinson's disease	5
π -Allyl	133, 134, 135, 136, 155, 214, 215
Phosphorylation	4
Piperazine	3, 7, 8, 13, 14, 15, 310
Plieninger	73
Protecting groups	11, 12, 23, 24, 25, 26, 27, 28, 31, 32, 34, 72, 139, 140, 143, 151, 152, 214, 219, 312, 314, 315, 365
Protein phosphatase	3, 4, 16
Pyrazine	12, 24, 26, 28, 34, 70, 132, 153, 311, 312, 313, 314, 321
Pyrazinone	3, 9, 10, 12, 13, 15, 18, 19, 20, 21, 22, 28, 34, 69, 70, 131, 144, 145, 310, 313, 314, 320, 321

	392
Pyrrole	132, 136, 137, 138, 139, 148, 151, 152, 156, 215, 216, 217
Quinic acid	132, 133, 135, 144, 145, 147, 148, 151, 152, 159, 214, 220
Reduction.....	22, 32, 34, 35, 36, 134, 135, 136, 149, 150, 151, 154, 155, 159, 215, 221, 320
Rhodium	154, 155, 156
Ruthenium	35
Silyl.....	24, 29, 74, 133, 140, 149, 151, 152, 153, 222
Stereochemistry	3, 132, 142, 145, 222
Stille coupling.....	35, 215
Suzuki coupling.....	24, 25, 27, 28, 36, 73, 131, 132, 133, 139, 156, 159, 310, 311, 312, 313, 314
Symmetry	147, 151, 220
Topsentin	2, 16
Triazine.....	322, 326, 327
Triazinone.....	322, 323, 324, 325, 326, 327, 365
Tryptamine	8
Tryptophan	8, 9
Weinreb amide	136
Wittig olefination	133
X-ray.....	323, 325

ABOUT THE AUTHOR

Neil K. Garg was born on December 18, 1978, in White Plains, NY. His immediate family consists of an older brother, Bobby, and two loving parents, Desh and Neena. Neil's childhood years were spent living in Fishkill, NY, a suburb 90 miles north of New York City. He attended John Jay Senior High School and pursued several extracurricular activities including tennis, soccer, and playing the trombone in a jazz band.

After graduating from high school in 1996, Neil began undergraduate studies at New York University. His early years at NYU were spent learning about a broad range of topics including psychology, writing, chemistry, biology, capitalism, and African culture. The sciences were undoubtedly his forte, and he began working in a chemistry research laboratory with Professor Marc Walters during his sophomore year. Neil also grew fond of teaching chemistry and continued both research and teaching until he graduated with a B.S. in chemistry in 2000. During his college years, Neil spent several months living in Strasbourg, France, and conducted research with Professor Mir Wais Hosseini at Université Louis Pasteur. While in France, Neil enjoyed exploring the French countryside on bike and hiking in the Vosges Mountains.

In 2000, Neil moved to Pasadena, CA, to pursue doctoral studies with Professor Brian M. Stoltz at the California Institute of Technology. In 2005, he earned his Ph.D. in chemistry for investigations involving the total synthesis of the dragmacidin alkaloids. Neil will marry his fiancée, Lindsey Bogard, in April 2005, and then begin postdoctoral studies under the direction of Professor Larry E. Overman at UC Irvine soon afterwards.